

Development of a Scaled Quantum Mechanical Force Field for Peptides in Aqueous Solution

by

Alan F. Weir, B. A., M. S.

Dissertation

Presented to the Faculty of the Graduate School of

The Uniformed Services University of the Health Sciences

in Partial Fulfillment

of the Requirements

for the Degree of

Doctor of Philosophy

**The Uniformed Services University of the Health
Sciences**

March 1996

To my family:

Without their patience, understanding, and help this would not have been possible.

This mind dances not
to a barbaric tune
but steeped in cadences
found by some
forgotten bard
long before grandfather
or even great-great-grandfather
Would that I could
throw off convention
with my clothes
This mind would grow
as vines

Bruce Weir

Acknowledgments

Uniformed Services University of the Health Sciences provided T-Grants (graduate student research funding) and faculty support

The Bioinstrumentation Center, especially Mike Flora for polypeptide synthesis

Edgewood Research, Development, and Engineering Center

National Cancer Institute Super Computer Center

US Army Medical Research Institute of Chemical Defense

Lucy Shanaman, Laboratory Technician

Dr. Robert W. Williams

Dr. Alfred Lowrey

Dr. Mark Roseman

Dr. David Grahame

Dr. Willem van de Mere

ALAN F. WEIR

The Uniformed Services University of the Health Sciences

March 1996

ABSTRACT

Development of a Scaled Quantum Mechanical Force Field for Peptides in Aqueous Solution

Alan F. Weir

Doctor of Philosophy, 1996

Dissertation Directed

By

Robert W. Williams, PhD

Associate Professor

Department of Biochemistry

Infrared and Raman vibrational spectroscopies have been useful tools for the study of biomolecules. However, only by normal mode analysis can detailed structural information be obtained from these techniques. Normal mode analysis calculates a vibrational spectrum for comparison with experimental data. The calculation requires an accurate set of force constants, which describe the forces between the atoms in the molecule. Empirical methods were the only means of determining force constants until recently, when the scaled quantum mechanical force field (SQMFF) method was developed [Fogarasi and Pulay, 1985]. The SQMFF method determines scale factors to correct *ab initio* force constants by fitting calculated frequencies to experimentally measured spectra. These corrections are necessary because *ab initio* force constants contain systematic errors due to assumptions and simplifications made in solving Schrödinger's equation. The scale factors are useful because they are transferable between molecules [Fogarasi and Pulay, 1985; Williams and Lowrey, 1991].

I have built a set of solution phase scale factors and force constants starting from small molecules and moving up in complexity to the alanyl-alanine peptide [Weir *et al*, 1996]. Different hydrogen bonded structures were included to model the intramolecular hydrogen bonding patterns observed in protein secondary structures. The solution phase scale factors demonstrate good transferability. They provide the basis for calculating vibrational spectra of larger molecules and for understanding the accuracy that can be expected from those calculations. The set of force constants I developed predict the amide I and III frequencies with an average error of 8 cm^{-1} . This is an improvement of more than 12 cm^{-1} over the best empirical force field [Williams *et al*, 1990].

Along with the development of the scale factors, vibrational modes were assigned to all observed frequencies for every structure. The assignments and scale factors are internally consistent, making this the most systematic and comprehensive set of vibrational assignments to date, including the first complete assignment of vibrational modes for alanyl-alanine. Reference to this set of assignments will simplify the development of improved force fields.

Contents

Acknowledgments	iii
Abstract	iv
List of Tables	ix
List of Figures	xv
Chapter 1 INTRODUCTION	1
1.1 Vibrational Spectroscopy	3
Isotopic Labeling and Difference Spectroscopy	7
1.2 Computational Chemistry	10
Empirical vs <i>ab initio</i> Methods	10
Ab initio calculations	11
1.3 The Secular Equation and Normal Mode Analysis	17
1.4 SQMFF, Combining Theory and Experiment	18
1.5 Solvation	22
1.6 Potential Applications of a Force Field	24
Limitations	26
1.7 Progress in Building a SQMFF up to 1993	26
Experimental Observation	26
Testing the Implications	27

Development of a New Force Field	29
1.8 Definition of Problem Investigated	31
Future Work	33
1.9 Historical Perspective	34
Spectroscopy	34
Computational Chemistry	36
Chapter 2 METHODS	39
2.1 Experimental Methods	39
Sample Preparation	39
Infrared Spectroscopy	40
Raman Spectroscopy	40
Difference Spectra	41
2.2 Computational Chemistry	41
<i>ab initio</i> Calculations–Determination of the Force Constants	45
Water–Excluded Configurations	47
Normal mode calculations–Development of the Scale Factors	48
2.3 Fermi Resonance Calculations	49
Chapter 3 RESULTS	51
3.1 Outline of Results Presented	51
3.2 Methanol and Ethanol–Testing Hydration Models	52
3.3 Small Molecules–Water Excluded Scale Factors	82
3.4 Alanine–Development of C α Coordinates	159
3.5 Alanyl-alanine–Peptide Coordinates and Defined Hydrogen Bonds	330
Chapter 4 DISCUSSION	494
4.1 Comparison of Hydration Models	494
4.2 Water–Excluded Scale Factors	498

Transferability of Water-Excluded Scale Factors	499
Retention of Electronic Effects of Hydrogen Bonding	500
4.3 C ^α Coordinates	503
4.4 Peptide Bond Coordinates	507
Chapter 5 CONCLUSIONS	511
Bibliography	513

List of Tables

1.1	Amide Frequencies ^a	7
3.1	Redundant Internal Coordinates for Methanol and Ethanol	64
3.2	Symmetry Coordinate Definitions for Methanol and Ethanol	65
3.3	Optimized Internal Coordinates for Methanol and Ethanol.	66
3.4	Scale factors for Methanol and Ethanol; Different Hydration Models.	69
3.5	Scaled 4-31G Frequencies and Potential Energy Distribution for Methanol Using Self Consistent Reaction Field Theory.	70
3.6	Scaled 4-31G Frequencies and Potential Energy Distribution for Iso- lated Ethanol	72
3.7	Scaled 4-31G Frequencies and Potential Energy Distributions for Ethanol two-water supermolecule, water included.	75
3.8	Scaled 4-31G Frequencies and Potential Energy Distribution for Ethanol Using Self Consistent Reaction Field Theory	79
3.9	Redundant Internal Coordinates for Methylamine in Base and Acid .	94
3.10	Symmetry Coordinate Definitions for Methylamine in Base and Acid	95
3.11	Optimized Internal Coordinates for Methylamine in Acid and Base .	96
3.12	Redundant Internal Coordinates for Acetate	97
3.13	Symmetry Coordinate Definitions for Acetate.	97
3.14	Optimized Internal Coordinates for Acetate One Water Supermolecule in Base	99

3.15	Redundant Internal Coordinates for Glycine in Base and Acid	101
3.16	Symmetry Coordinate Definitions for Glycine in Base and Acid . . .	102
3.17	Optimized Internal Coordinates for Glycinate and Glycine.	104
3.18	Scale factors for methylamine, acetate and glycine	106
3.19	Scaled 4-31G Frequencies and Potential Energy Distribtion for Water- Excluded Methylamine One-water Supermolecule in Base.	108
3.20	Scaled 4-31G Frequencies and Potential Energy Distribution for Water- Excluded Methylamine Three-water Supermolecule in Acid.	111
3.21	Scaled 4-31G Frequencies and Potential Energy Distributions for One- Water Acetic Acid Supermolecule Water-Excluded in Base.	113
3.22	Scaled 4-31G Frequencies and Potential Energy Distribution for One- Water Glycine Supermolecule Water-Excluded in Base.	115
3.23	Scaled 4-31G Frequencies and Potential Energy Distribution for Two- Water Glycine Supermolecule Water-Excluded in Base.	120
3.24	Scaled 4-31G Frequencies and Potential Energy Distribution for Four- Water Glycine Supermolecule Water-Excluded in Base.	124
3.25	Scaled 4-31G Frequencies and Potential Energy Distribution for One- water Glycine Supermolecule Water-Excluded in Acid.	128
3.26	Redundant Internal Coordinates for <i>trans</i> N-Methylacetamide	140
3.27	Symmetry Coordinate Definitions for <i>trans</i> N-Methylacetamide . . .	141
3.28	Optimized Internal Coordinates for <i>trans</i> N-Methylacetamide	142
3.29	Scale factors for <i>trans</i> N-Methylacetamide in different hydration states	143
3.30	Scaled 4-31G Frequencies and Potential Energy Distributions for <i>trans</i> N-methylacetamide Two-water Supermolecule.	145
3.31	Scaled 4-31G Frequencies and Potential Energy Distribution for Water- Excluded <i>trans</i> N-Methylacetamide One-water on the Amide Hydro- gen Supermolecule.	149

3.32	Scaled 4-31G Frequencies and Potential Energy Distribution for Water- Excluded <i>trans</i> <i>N</i> -methylacetamide One-water on the Amide Carbonyl Oxygen Supermolecule.	151
3.33	Scaled 4-31G Frequencies and Potential Energy Distribution for Water- Excluded <i>trans</i> <i>N</i> -methylacetamide Two-Water, One Water on the Amide Hydrogen, One Water on the Carbonyl Oxygen, Supermolecule.	153
3.34	Scaled 4-31G Frequencies and Potential Energy Distribution for Water- Excluded <i>trans</i> <i>N</i> -methylacetamide Two-Water, Both on the Amide Carbonyl Oxygen, Supermolecule.	155
3.35	Scaled 4-31G Frequencies and Potential Energy Distribution for Water- Excluded <i>trans</i> <i>N</i> -methylacetamide Three-water Supermolecule. . . .	157
3.36	Redundant Internal Coordinates for Alanine in Base and Acid.	167
3.37	Symmetry Coordinate Definitions for Alanine in Base	169
3.38	Symmetry Coordinate Definitions for Alanine in Acid.	170
3.39	Optimized Internal Coordinates for Isolated Structures of Alaninate Using Several different Basis Sets.	172
3.40	Optimized Internal Coordinates for One-water Supermolecule Struc- tures of Alaninate Using Several different Basis Sets and Structures .	174
3.41	Optimized Internal Coordinates for Supermolecule Structures of Ala- nine in Acid Using Several different Basis Sets	176
3.42	Scale factors for Methylamine and Acetate using the 6-31G** basis set	179
3.43	Scaled 6-31G** Frequencies and Potential Energy Distribution for Iso- lated Methylamine in Base.	180
3.44	Scaled 6-31G** Frequencies and Potential Energy Distribution for Iso- lated Acetate.	181
3.45	Frequencies and Potential Energy Distribution for Alanine in base, 6- 31G** basis set, scale factors from methylamine and acetate transfered without change: Placement of CCOO wag coordinate.	182

3.46	Scale factors for isolated alaninate structures using several basis sets.	184
3.47	Scaled 4-31G Frequencies and Potential Energy Distribution for Isolated Alaninate.	185
3.48	Scaled 4-31G* Frequencies and Potential Energy Distribution for Isolated Alaninate.	195
3.49	Scaled 6-31G** Frequencies and Potential Energy Distribution for Isolated Alaninate.	205
3.50	Scaled 6-31+G** Frequencies and Potential Energy Distribution for Isolated Alaninate.	215
3.51	Scale factors for alanine in base one-water supermolecule and water-excluded structures using different basis sets.	225
3.52	Scaled 4-31G Frequencies and Potential Energy Distribution for Alaninate One-water Supermolecule.	226
3.53	Scaled 4-31G Frequencies and Potential Energy Distribution for Water-Excluded Alaninate One-water Supermolecule.	238
3.54	Scaled 4-31G* Frequencies and Potential Energy Distribution for Water-Excluded Alaninate One-water Supermolecule.	247
3.55	Scaled 6-31G** Frequencies and Potential Energy distribution for Water-Excluded Alaninate One-water Supermolecule.	257
3.56	Scaled 6-31+G** Frequencies and Potential Energy Distribution for Water-Excluded Alaninate One-water Supermolecule.	267
3.57	Scaled 4-31G Frequencies and Potential Energy Distribution for Water-Excluded Alaninate One-water Supermolecule, bridging one carboxyl oxygen and an amine hydrogen.	277
3.58	Scale factors for alanine in acid, one-water water-excluded geometries using several basis sets.	288
3.59	Scaled 4-31G Frequencies and Potential Energy Distribution for Water-Excluded Alanine One-water Supermolecule in Acid.	290

3.60	Scaled 4-31G* Frequencies and Potential Energy Distribution for Water-Excluded Alanine One-water Supermolecule in Acid.	300
3.61	Scaled 6-31G** Frequencies and Potential Energy Distribution for Water-Excluded Alanine One-water Supermolecule in Acid.	310
3.62	Scaled 6-31+G** Frequencies and Potential Energy Distribution for Water-Excluded Alanine One-water Supermolecule in Acid.	320
3.63	Redundant Internal Coordinates for Dialanine in Base.	332
3.64	Redundant Internal Coordinates for Dialanine Zwitterion.	333
3.65	Redundant Internal Coordinates for Dialanine in Acid.	334
3.66	Symmetry Coordinate Definitions for Dialanine in Base.	336
3.67	Symmetry Coordinate Definitions for Dialanine Zwitterion.	338
3.68	Symmetry Coordinate Definitions for Dialanine in Acid.	340
3.69	Optimized internal coordinates calculated for dialanine isolated and supermolecule structures in base.	342
3.70	Optimized internal coordinates calculated for dialanine isolated and supermolecule structures in neutral and acid solutions.	345
3.71	Alanyl-alanine scale factors for isolated and two-water water-excluded structures.	358
3.72	Scaled 4-31G Frequencies and Potential Energy Distributions for Isolated Alanyl-alanine Structure in Base Conformation.	361
3.73	Scaled 4-31G Frequencies and Potential Energy Distribution for Water-Excluded Alanyl-alanine Two-water Supermolecule in Base.	370
3.74	Scaled 4-31G Frequencies and Potential Energy Distribution for Zwitterionic Alanyl-alanine Isolated Structure.	379
3.75	Scaled 4-31G Frequencies and Potential Energy Distribution for Water-Excluded Zwitterionic Alanyl-alanine Two-water Supermolecule. . .	398
3.76	Scaled 4-31G Frequencies and Potential Energy Distribution for Isolated Alanyl-alanine in acid.	417

3.77	Scaled 4-31G Frequencies and Potential Energy Distribution for Water-Excluded Alanyl-alanine Two-water Supermolecule in Acid.	427
3.78	Water-Excluded Alanyl-alanine One- and Three-water Supermolecule Scale Factors.	437
3.79	Scaled 4-31G Frequencies and Potential Energy Distribution for Water-Excluded Alanyl-alanine One-water Supermolecule, the Water Hydrogen Bonded to the Amide Hydrogen in Base.	439
3.80	Scaled 4-31G Frequencies and Potential Energy Distribution for Water-Excluded Alanyl-alanine One-water Supermolecule, The Water Hydrogen Bonded to the Carbonyl Oxygen, in Base.	448
3.81	Scaled 4-31G Frequencies and Potential Energy Distribution for Water-Excluded Alanyl-alanine Three-water Supermolecule, Two Waters Hydrogen Bonded to the Carbonyl Oxygen, in Base.	457
3.82	Alanyl-alanine Two-water Supermolecule Structure with the CO Stretch Coordinate Increased 10%, Water-Excluded Force Constants and Scale Factors used for the Normal Mode Analysis.	467
3.83	Alanyl-alanine Two-water Supermolecule Structure with the NH Stretch Coordinate Increased 10%, Water-Excluded Force Constants and Scale Factors used in the Normal Mode Analysis.	476
3.84	Alanyl-alanine Isolated Structure, Two-water Water-Excluded Force Constants and Scale Factors used for the Normal Mode Analysis. . .	485

List of Figures

1.1	Comparison of Raman spectra of Alanine (bottom) and $^{13}\text{C}^{me}$ Alanine (top).	9
1.2	Flow chart depicting the steps involved in the development of a Scaled Quantum Mechanical Force Field.	19
2.1	Programs for processing data generated for input to and output from Gaussian.	42
3.1	Optimized Structure of Methanol using SCRF (top), Isolated Ethanol (upper middle), Ethanol two-water supermolecule (lower middle), and Ethanol using SCRF (bottom).	53
3.2	Raman spectra of aqueous solutions of methanol. From top to bottom, CD_3OD , line with two dashes, 50% v/v in D_2O ; CD_3OH , line with dot, 10% v/v in H_2O ; CH_3OD , line with one dash, 10% v/v in D_2O ; and CH_3OH , solid line 50% v/v in H_2O .	54
3.3	Raman spectrum of 50% ethanol in H_2O (200-1600 cm^{-1}).	55
3.4	Raman spectrum of the hydrogen stretching region for 50% ethanol in H_2O .	56
3.5	Infrared spectrum of 50% ethanol in H_2O .	57
3.6	Raman spectrum of 50% ethanol in D_2O .	58
3.7	Raman spectrum of the hydrogen stretching region of 50% ethanol in D_2O .	59

3.8	Infrared spectrum of 50% ethanol in D ₂ O.	60
3.9	Raman spectrum of CD ₃ substituted ethanol, 50% in H ₂ O.	61
3.10	Raman spectrum of the hydrogen stretching region of CD ₃ substituted ethanol, 50% in H ₂ O.	62
3.11	Infrared spectrum of CD ₃ substituted ethanol in H ₂ O.	63
3.12	Small molecule supermolecule optimized geometries. Methylamine in base with one water (top), methylamine in acid with three waters (middle), and acetate with one water (bottom).	83
3.13	Raman spectra of methylamine and protonated methylamine in H ₂ O and D ₂ O. Top, CH ₃ ND ₃ ⁺ 10% (w/w) in D ₂ O, pD 6.4: second from top, CH ₃ NH ₃ ⁺ 10% (w/w) in H ₂ O, pH 6.4; third from top, CH ₃ ND ₂ 10% (w/w) in D ₂ O, pD 13.5; bottom, CH ₃ NH ₂ 10% (w/w) in H ₂ O pH 13.5.	84
3.14	Raman spectra of methylamine-3- <i>d</i> ₃ in D ₂ O (top) and H ₂ O (bottom).	85
3.15	Raman spectra of acetic acid: Top, CH ₃ COOD 50% (w/w) in D ₂ O; middle, CH ₃ COOH 50% in H ₂ O; bottom, CH ₃ COONa 50% in H ₂ O. The pH of the acid samples was adjusted to below 1. The pH of the sodium salt was adjusted to above 11.	86
3.16	Raman spectra of ¹³ C labeled acetic acid: Top, ¹³ CD ₃ ¹³ COOD 50% (w/w) in D ₂ O, pD 1; middle, ¹³ CH ₃ ¹³ COOH 50% in H ₂ O, pH 1; bottom, ¹³ CH ₃ ¹³ COONa 50% in D ₂ O pD 11.	87
3.17	Optimized structures for glycine supermolecules. Glycine in acid with one water (top), glycine in base with one water (upper middle), glycine in base with two waters (lower middle), and glycine in base with four waters (bottom).	88
3.18	Raman spectra for acidic glycine in H ₂ O. Solid line, ⁺ NH ₃ CH ₂ COOH pH 0.5; and dotted line, ⁺ NH ₃ CD ₂ COOH pH 0.8.	89
3.19	Raman spectra for acidic glycine in D ₂ O. Solid line, ⁺ ND ₃ CH ₂ COOD pD 0.5; and dotted line, ⁺ ND ₃ CD ₂ COOD pD 0.7.	90

3.20	Raman spectra for basic glycine in H ₂ O. Solid line, NH ₂ CH ₂ COO ⁻ pH 12.5; dotted line, NH ₂ CH ₂ ¹³ COO ⁻ pH 13; dashed line, NH ₂ ¹³ CH ₂ COO ⁻ pH 13.	91
3.21	Raman spectra for basic glycine in D ₂ O. Solid line, ND ₂ CH ₂ COO ⁻ pD 12.5; dotted line, ND ₂ CH ₂ ¹³ COO ⁻ pD 13; and dashed line, ND ₂ ¹³ CH ₂ COO ⁻ pD 13.	92
3.22	Raman spectra for basic glycine-2- <i>d</i> ₂ in H ₂ O, pH 12.5 (solid line) and D ₂ O, pD 13 (dotted line).	93
3.23	NMA one water supermolecules, with the water hydrogen bonded to the carbonyl oxygen (top), and with the water hydrogen bonded to the amide hydrogen (bottom).	137
3.24	NMA two water supermolecule, one water hydrogen bonded to the amide hydrogen, the other to the carbonyl oxygen (top), NMA two water supermolecule, both waters hydrogen bonded with the carbonyl oxygen (middle), and the NMA three water supermolecule (bottom).	138
3.25	Raman spectra of <i>N</i> -Methylacetamide. Dotted line, top, 50% v/v in H ₂ O; solid line, bottom, 50% v/v in D ₂ O.	139
3.26	Optimized structures of the Alaninate one water supermolecules (bottom CO ₂ bridged, middle NH-CO bridged) and Alanine at pH=1 one water supermolecule (top). Covalent bonds are solid, hydrogen bonds are outlined.	160
3.27	Raman spectra of alaninate in H ₂ O pH 13 (bottom), alanine(3,3,3- <i>d</i> ₃) pH 13 (middle), and alanine(2,3,3,3- <i>d</i> ₄) pH 13 (top).	161
3.28	Raman spectra of alaninate in D ₂ O pD 13 (bottom), alanine(3,3,3- <i>d</i> ₃) in D ₂ O pD 13 (middle), and alanine(2,3,3,3- <i>d</i> ₄) in D ₂ O pD 13 (top).	162
3.29	Raman spectra of alanine at pH=1 in H ₂ O (bottom), alanine(3,3,3- <i>d</i> ₃) pH 1 (middle), and alanine(2,3,3,3- <i>d</i> ₄) pH 1 (top).	163

3.30	Raman spectra of alanine at pHD1 in D ₂ O (bottom), alanine(3,3,3- <i>d</i> ₃) pD 1 (middle), and alanine(2,3,3,3- <i>d</i> ₄) pD 1 (top).	164
3.31	Difference spectra of alaninate and alaninate(3- ¹³ C) (top) and alaninate and alaninate(¹⁵ N) (bottom).	165
3.32	Difference spectra of alanine and alanine(3- ¹³ C) (top) and alanine and alanine(¹⁵ N) (bottom), all at pH=1.	166
3.33	Optimized structures of alanyl-alanine base three water and one water supermolecules. Three water supermolecule (top), one water supermolecule with the water hydrogen bonded to the carbonyl oxygen (middle), and the one water supermolecule with the water hydrogen bonded to the amide hydrogen (bottom).	348
3.34	Optimized structures of alanyl-alanine base isolated (top) and two water supermolecule (bottom).	349
3.35	Raman spectra of alanyl-alanine in H ₂ O at pH=13 (top), alanyl-alanine in D ₂ O at pD=13 (upper middle), alanyl-alanine labelled at the amine α-carbon with deuterium in H ₂ O at pH=13 (lower middle), and alanyl-alanine labelled with ¹³ C at the carbonyl carbon in H ₂ O at pH=13 (bottom).	350
3.36	Infrared spectra of alanyl-alanine in H ₂ O at pH=13 (top), alanyl-alanine in D ₂ O at pD=13 (middle), and alanyl-alanine labelled with ¹³ C at the carbonyl carbon in H ₂ O at pH=13 (bottom).	351
3.37	Optimized structures of alanyl-alanine zwitterion isolated and two-water supermolecules.	352

3.38	Raman spectra of alanyl-alanine in H ₂ O at pH=7 (top), alanyl-alanine in D ₂ O at pD=7 (second from top), alanyl-alanine labelled at the amine α -carbon with deuterium in H ₂ O at pH=7 (third from top), alanyl-alanine labelled with ¹³ C at the carbonyl carbon in H ₂ O at pH=7 (fourth from top), and alanyl-alanine labelled with ¹³ C at the carbonyl carbon in D ₂ O at pD=7 (bottom).	353
3.39	Infrared spectra of alanyl-alanine in H ₂ O at pH=7 (top), and alanyl-alanine in D ₂ O at pD=7 (bottom).	354
3.40	Optimized structures of alanyl-alanine at pH=1 isolated and two water supermolecules.	355
3.41	Raman spectra of alanyl-alanine in H ₂ O at pH=1 (top), alanyl-alanine in D ₂ O at pD=1 (upper middle), alanyl-alanine labelled at the amine α -C with deuterium in H ₂ O at pH=1 (lower middle), and alanyl-alanine labelled with ¹³ C at the carbonyl carbon in H ₂ O at pH=1 (bottom).	356
3.42	Infrared spectra of alanyl-alanine in H ₂ O at pH=1 (top), alanyl-alanine in D ₂ O at pD=1 (upper middle), alanyl-alanine labelled at the amine α -C with deuterium in H ₂ O at pH=1 (lower middle), and alanyl-alanine labelled with ¹³ C at the carbonyl carbon in H ₂ O at pH=1 (bottom).	357

Chapter 1

INTRODUCTION

The ultimate goal of modern molecular biology is to understand biological function at the level of molecular structure. One means of investigating molecular structure is through Raman and Infrared (IR) vibrational spectroscopies. However, there is currently no way to interpret the spectra of polypeptides and proteins beyond estimating the average secondary structure. The only method capable of fully evaluating the structural content of vibrational spectra is through normal mode analysis—testing hypothetical structures by comparing predicted spectra of specific secondary structures with experimental spectra [Krimm and Bandekar, 1986]. Details about molecular structure cannot be directly deduced from the vibrational spectrum.

In addition to specific secondary structure information, normal mode analysis requires a reliable set of force constants. Force constants describe the forces between the atoms of a molecule. Until recently the only methods available for the development of force constants were empirical. Empirical force constants have been used with a great deal of success for small molecules [Krimm and Bandekar, 1986], however, their usefulness is limited [Fogarasi and Pulay, 1985; Williams *et al*, 1990]: the predicted amide I and III frequencies for four diamino acid peptides using the best available empirical force field had an average error of greater than 20 cm^{-1} [Williams *et al*, 1990].

Quantum mechanical methods allow the calculation of force constants, which are the second derivatives of the molecular energy with respect to nuclear position. Only recently have means become generally available for the routine *ab initio* calculation of force constants for small molecules. Compared to empirical force constants, advantages of calculated force constants are that all of the interaction force constants are calculated and they are the most reliable interaction force constants [Fogarasi and Pulay, 1985]. (Interaction force constants describe the interactions between pairs of interatomic forces and are, at best, difficult to determine empirically.) However, calculated force constants contain inaccuracies due to neglect of electron correlation and to limitations in the basis sets (mathematical descriptions of molecular orbitals) used in their determination. These inaccuracies were shown to be consistent for isolated (vapor phase) geometries [Fogarasi and Pulay, 1985]. Force constants for the same chemical group in different molecules contain the same degree of error. These consistent, systematic errors can be corrected. The scaled quantum mechanical force field (SQMFF) method [Pulay *et al*, 1979; Fogarasi and Pulay, 1985] does this by adjusting calculated *ab initio* force constants with scale factors until the calculated vibrational spectra match experimental spectra. The isolated structure scale factors proved to be transferable, demonstrating the consistency of the *ab initio* calculations and the ability of the SQMFF method to correct the errors [Fogarasi and Pulay, 1985]. Investigation of different models of solution phase geometries has shown that the SQMFF method can be applied to aqueous phase spectra [Williams and Lowrey, 1991; Lowrey and Williams, 1992a and b; Williams, 1992; Lowrey *et al*, 1993; Williams *et al*, 1993]. Therefore, the development of a reliable set of force constants for the study of large molecules in aqueous solution is possible.

The goal of my thesis research was to use the SQMFF method to further the development of a set of scale factors and force constants for accurate prediction of vibrational spectra of peptides and proteins in solution. My contributions include:

- A study of the usefulness of the Self Consistent Reaction Field technique in

modeling hydration.

- A systematic development of scale factors using the water-excluded model to study the transferability, and therefore general applicability, of water-excluded scale factors.
- Development of force constants, scale factors, and vibrational assignments for the C^α coordinates of alanine, the simplest chiral amino acid, including a comparison of several hydration models (isolated, supermolecule, and water-excluded) and basis sets.
- Development of scale factors and vibrational assignments for peptide bond coordinates, using dialanine as a model, in a variety of hydrogen bonded configurations to model hydrogen bonding patterns observed in protein secondary structures.

The results have yielded a set of scale factors that predict the amide I and III frequencies for differently hydrogen bonded and protonated structures of dialanine with an average error of only 8 cm^{-1} . This is an improvement of more than 12 cm^{-1} over the best empirical force field. The scale factors and vibrational assignments have been built by slowly increasing the molecular and spectral complexity. They are the most systematic and comprehensive set of vibrational assignments to date, including the first complete set of vibrational assignments for dialanine. Future force fields, incorporating improvements in theory and computational techniques, will be easier to develop because of the vibrational mode assignments that I determined for dialanine.

1.1 Vibrational Spectroscopy

Raman and IR vibrational spectroscopies are particularly well suited to the study of biomolecules. The techniques can be applied to molecules in many different

states: solid, aqueous, liquid, gas, or even intact biological samples [Yu, 1977]. Methods have been developed for determination of average secondary structure content of proteins [Williams, 1983]. Potentially, much more structural information can be deduced.

When a beam of visible light passes through a medium, portions of it are transmitted, absorbed, or scattered. The scattered light can be either of the same wavelength, which is elastic scattering or Rayleigh light, or (less frequently) the wavelength may be altered, which is inelastic scattering or the Raman effect. The change in wavelength is due to absorption of (Stokes) or addition to (antistokes) the energy of the incident light. In the Raman effect, Stokes scattering is much more frequent and is usually measured. The ratio of Stokes to anti-Stokes intensities is expressed:

$$\frac{I(Stokes)}{I(anti - Stokes)} = \left(\frac{\nu_o - \nu_{mn}}{\nu_o + \nu_{mn}} \right)^4 \cdot e^{h\nu_{mn}/kT} \quad (1.1)$$

where ν_o is the incident frequency, ν_{mn} is the vibrational frequency, h is Planck's constant, and k is Boltzman's constant [Yu, 1977].

Raman spectroscopy measures the changes in wavelength due to molecular absorption during the inelastic scattering phenomenon. Spectra are recorded in units of $\Delta \text{ cm}^{-1}$, a measure of vibrational frequency, measured as the difference between incident and observed absolute frequencies. The 514.5 nm argon green laser line, which was used as the excitation source for all of the studies in this thesis, has a frequency of $19,436 \text{ cm}^{-1}$. Raman intensity is proportional to polarizability.

The electric field of the incident light induces a dipole moment, $\vec{\mu}$ in the molecule. The induced dipole is related to the electric field by the relationship $\vec{\mu} = \vec{\alpha} \vec{E}$. Where $\vec{\alpha}$ is the polarizability (or scattering) tensor. The x, y, and z components of the induced dipole moment can be expressed as:

$$\mu_x = \alpha_{xx}E_x + \alpha_{xy}E_y + \alpha_{xz}E_z \quad (1.2)$$

$$\mu_y = \alpha_{yx}E_x + \alpha_{yy}E_y + \alpha_{yz}E_z \quad (1.3)$$

$$\mu_z = \alpha_{zx}E_x + \alpha_{zy}E_y + \alpha_{zz}E_z \quad (1.4)$$

The components, μ_x , μ_y , and μ_z , are responsible for the Raman emission in each direction. The intensities of the emissions are proportional to the square of the component dipole moments: $|\mu_x|^2$, $|\mu_y|^2$, and $|\mu_z|^2$. An oscillating dipole does not emit in the direction of its axis, so if the detector is on the z axis, there is no contribution from μ_z and the measured intensity is due to the x and y components. In a typical experiment the laser light travels in the x direction and is polarized in the y direction so that $E_y \neq 0$, $E_x = 0$, and $E_z = 0$. Then $\mu_x = \alpha_{xy}E_y$ and $\mu_y = \alpha_{yy}E_y$. Finally, the total intensity is the sum of the component intensities and is proportional to the square of the induced dipoles,

$$I_T \propto (\alpha_{xy}^2 + \alpha_{yy}^2)E_y^2 \quad (1.5)$$

Where I_T is the total intensity [Yu, 1977]. Water is a poor Raman scatterer making the Raman technique especially useful for aqueous solution studies.

IR spectroscopy is an absorption phenomenon; the incident light must be the same energy as the molecular vibration for a photon to be absorbed. Frequencies at which absorption occurs are equal to the energy of vibration. Spectra are a measure of the difference between incident and transmitted intensities. IR intensity, the amount of absorption of the incident light, is proportional to the molecular dipole moment.

$$A_a = \frac{N\pi}{3c^2} \left(\frac{\partial \mu}{\partial Q_a} \right)^2 \quad (1.6)$$

where A_a is the absorbance for the a^{th} normal coordinate, N is Avagadro's number, c is the speed of light, μ is the dipole moment vector, and Q_a is the a^{th} normal mode vibration. The derivative of the dipole moment with respect to the normal mode vibration can be calculated from the sum of the contributions by the internal coordinates,

$$\frac{\partial \mu}{\partial Q_a} = \sum_i \left(\frac{\partial \mu}{\partial S_i} \right) L_{ia} \quad (1.7)$$

where S_i are the symmetry coordinates contributing to the normal mode vibration, and L_{ia} is the eigenvector for the normal mode vibration. It describes the percent

contributions of each of the symmetry coordinates to the normal mode. L is defined by $S = LQ$ and is obtained from a normal mode calculation [Cheam and Krimm, 1985]. The changes in dipole moment derivatives with respect to symmetry coordinates, $\frac{\partial \mu}{\partial S_i}$, are determined from *ab initio* calculations. Calculations are performed on geometries that are slightly distorted about a symmetry coordinate. The calculations yield dipole moments in the x, y, and z directions. The changes in the dipole moment derivatives are calculated by subtracting the dipole moment at $S_i + \delta S$ from $S_i - \delta S$ and dividing by $2\delta S$ for each direction:

$$\frac{\partial \mu}{\partial S_i} \simeq \left(\frac{(\mu_{x+\delta S}) - (\mu_{x-\delta S})}{2\delta S_i}, \frac{(\mu_{y+\delta S}) - (\mu_{y-\delta S})}{2\delta S_i}, \frac{(\mu_{z+\delta S}) - (\mu_{z-\delta S})}{2\delta S_i} \right) \quad (1.8)$$

The equation is approximate because of the inexact nature of numerical differentiation. The value of the dipole moment change is then calculated by combining the dipole moment derivatives for each direction:

$$\left\| \frac{\partial \mu}{\partial S_i} \right\| = \sqrt{(\partial \mu_x)^2 + (\partial \mu_y)^2 + (\partial \mu_z)^2} \quad (1.9)$$

IR intensities have been calculated, Raman have not [Krimm and Bandekar, 1986]. Water strongly absorbs IR radiation in frequency ranges of interest for protein structural determination making it more difficult to use IR techniques to study aqueous solutions of peptides and proteins.

Since polarizability (Raman) and dipole moments (IR) are different, the intensities of the various molecular vibrations measured by Raman and IR techniques will differ. Raman and IR techniques are complimentary which helps in assignment of observed vibrational modes.

As described in beginning organic chemistry texts [Morrison and Boyd, 1983], chemical groups within molecules vibrate at characteristic frequencies. Variations in the frequency of vibration for a particular chemical group are due to the local electronic environment. Amide groups have several characteristic frequencies (Table 1) [Krimm and Bandekar, 1986; Bandekar, 1992]. The vibrations of different structural components in proteins are sufficiently consistent and distinct so that spectra can be

Table 1.1: Amide Frequencies^a

Amide Vibration	Frequency Range	Contributing Internal Coordinates
I	1625–1695	CO <i>s</i> , CN <i>s</i> , C ^α CN <i>d</i> , C ^α C <i>s</i> , CNC ^α <i>d</i> , H ^α <i>b</i> , NH <i>ib</i>
II	1510–1560	NH <i>ib</i> , CN <i>s</i> , C ^α C <i>s</i> , CO <i>ib</i> , NC ^α <i>s</i>
II' ^b	1460–1490	CN <i>s</i>
III	1200–1400	NH <i>ib</i> , CN <i>s</i> , C ^α C <i>s</i> , CO <i>ib</i> , NC ^α <i>s</i> , CO <i>s</i>
III'	900–1000	ND <i>ib</i>
Skeletal	880– 960	C ^α C <i>s</i> , CN <i>s</i> , CO <i>s</i> , CNC ^α <i>d</i> , C ^α CN <i>d</i> , NC ^α C <i>d</i> , CO <i>ib</i> , CH ₃ <i>r</i>
V	620– 740	CN <i>t</i> , NH <i>ob</i>

^aAdapted from Krimm and Bandekar, 1986.

^bThe prime, ', designates D₂O solutions.

used to characterize the amount of secondary structure (α -helix, β -sheet, turns, and undefined) present in a protein [Williams, 1983]. If the frequency of vibration of a particular peptide bond can be determined, the secondary structure at that point in the protein can be deduced.

Each observed frequency is called a vibrational or normal mode, this is at a distinct energy where all the atoms in the molecule are moving with the same frequency and phase. The individual atomic motions of a normal mode are described by internal symmetry coordinates, a set of easily visualized local group motions: stretches between pairs of atoms, bending of angles, and rotations about bonds. The specific molecular structure defines the local groups present, the symmetry coordinates used to describe the motions of the molecule, and the energies of the various normal mode vibrations. A list of the symmetry coordinates contributing to each molecular normal mode and their percent contributions is called a potential energy distribution (PED).

Isotopic Labeling and Difference Spectroscopy

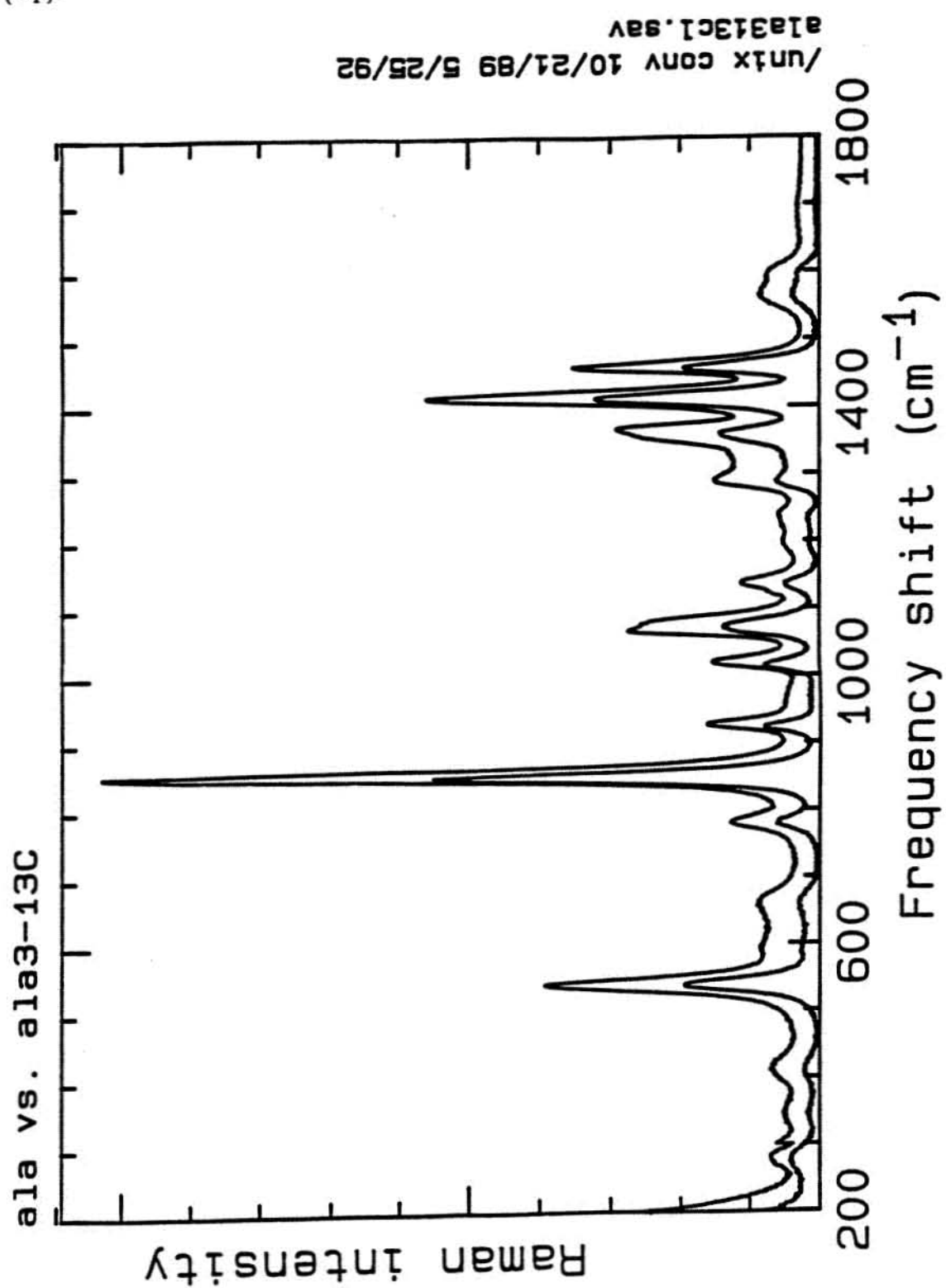
While chemical groups have characteristic vibrations, different groups may have frequency ranges which overlap. A particular group's vibrational frequency will vary depending on the local environment (for example, the presence or absence

of a nearby electron withdrawing or donating group). Large molecules may have several similar chemical groups (e.g. peptide bonds) whose frequencies vary only slightly making distinction between specific contributions difficult. A vibrational label, such as a stable isotopic substitution (a change in atomic mass), can be used to determine the frequencies to which a particular chemical group contributes. In a protein, substitution of ^{13}C at the carbonyl carbon of a peptide bond shifts the amide I frequency of that group. This provides information about the frequency and structure at that particular bond since the amide I frequency is dependent upon the local peptide conformation [Tadesse *et al*, 1991; Haris *et al*, 1992].

Substituting ^{13}C at the methyl carbon of alanine causes shifts that are difficult to detect even when the spectra are overlayed (see figure 1.1). However, difference spectroscopy makes even small shifts obvious (see figure 3.31 top;)[Tadesse *et al*, 1991; Williams, 1994]; spectra of normal and substituted molecules are subtracted from each other using simple arithmetic [Tadesse *et al*, 1991]. Frequencies unaffected by the isotopic substitution disappear, only shifted frequencies are observed. Those shifted vibrations contain contributions from coordinates influenced by the change in atomic mass.

Difference spectra can also be used to monitor changes in protein conformation as the protein goes through a reaction cycle, such as those recorded by Ludlam *et al* [1995]. When spectra of two intermediates in the reaction cycle are subtracted, observed frequencies are due to protein structure changes. Combining isotopic labeling and conformational difference spectroscopy allowed Ludlam *et al* to observe structural changes related to protein function at a single amino acid during the bacteriorhodopsin (bR) photocycle [Ludlam *et al*, 1995]. The observed peaks in the difference spectra of normal isotopic bR were due to changes in protein structure. Those difference peaks that shifted when a vibrational label was added at a particular amino acid were due to protein structural changes at that particular amino acid.

Figure 1.1: Comparison of Raman spectra of Alanine (bottom) and $^{13}\text{C}^{\text{me}}$ Alanine (top).



1.2 Computational Chemistry

Vibrational spectra of large biomolecules are complex; the number of fundamental vibrations, their often overlapping energies, and overtones of the fundamental vibrations combine to make interpretation difficult. Deciphering the experimental spectra requires extensive effort to include theoretical modeling and computational analysis.

Determination of protein structure from its vibrational spectrum cannot be done directly beyond the determination of average secondary structural content [Williams, 1983]. The Frequency-structure correlation is determined from a normal mode analysis: solving the secular equation, $GF = L\Lambda L^{-1}$ [Krimm and Bandekar, 1986]. Solution of the secular equation is dependent upon knowledge of the force field, F . The goal of our computational efforts is to determine a set of force constants, which together constitute a force field, that can be used in normal mode analyses for the evaluation of model structures for proteins in solution.

Empirical vs *ab initio* Methods

There are three computational techniques generally used for molecular structure analysis: molecular mechanics, semi-empirical, and *ab initio*. Molecular mechanics techniques use classical mechanical equations to describe molecular motion. The equations describe the motions only of nuclei, not electrons, and therefore large molecular systems can be described efficiently. These methods depend on empirical parameters for each atom type (sp^2 or sp^3 hybridized carbon, for example) and results depend on the chemical environment. If the environmental conditions for the system of interest are different from the conditions used to define the molecular mechanics parameters the results may not be accurate.

Semi-empirical and *ab initio* (from first principles) methods take into account motions of electrons. Electronic motion is described using the Schrödinger

equation which requires far greater computational resources than classical mechanical equations. Use of the Schrödinger equation limits the size of the system that can be studied. In order to reduce the time required to solve the Schrödinger equation, semi-empirical methods do not calculate long-range electronic interactions and differential overlap. Instead, empirical parameters, originally derived from experimental data such as heats of formation and ionization energies, are used. Because of the dependence on empirical parameters, accuracy of these methods are still dependent on the chemical environment used to define the parameters, limiting their applicability.

Ab initio methods do not neglect any of the integral calculations required to solve the Schrödinger equation. They are the most widely applicable techniques; there is no dependence on the chemical environment, no atom types to define and describe, and no dependence upon empirical parameters to define nuclear or electronic motions. They are, however, the most computationally resource intensive and most limited in the size of the system that can be studied. The advantage of *ab initio* methods is their ability to reliably determine off diagonal terms of the force constant matrix [Hamada *et al*, 1982; Fogarasi and Pulay, 1985], at least some of which are important in frequency determinations [Palmö *et al*, 1991]. The force constant matrix contains diagonal terms, which describe forces between atoms, and off-diagonal terms which describe the more subtle interactions between groups of atoms. The diagonal terms are large compared to the off-diagonal terms and so affect frequency calculations to a greater extent. While empirical methods are able to very accurately determine the diagonal force constants, *ab initio* methods determine the more subtle off-diagonal terms more consistently and reliably [Pulay, 1969; Fogarasi and Pulay, 1985].

Ab initio calculations

“Ab initio molecular orbital theory is concerned with predicting the properties of atomic and molecular systems. It is based upon the fundamental laws of quantum mechanics and uses a variety of mathematical transfor-

mation and approximation techniques to solve its fundamental equations.”

[Foresman and Frisch, 1993].

Ab initio calculations are performed using commercially available programs such as Gaussian [reference Gaussian92] or DeFT. They solve Schrödinger’s wave equation for the energy of a structure:

$$\nabla^2\Psi + \frac{8\pi^2m}{h^2}(E - U)\Psi = 0 \quad (1.10)$$

While the Schrödinger equation is exact, solutions to the equation require approximations. These lead to systematic errors in the calculated force constants and vibrational spectra for which corrections can be made.

Finding the molecular conformation with the minimum energy is the first step in calculating a vibrational spectrum. Once a minimum energy structure is determined, the second step, calculation of the force constants, which are the second derivatives of the energy with respect to Cartesian coordinates, is performed on that minimum energy structure. Force constants may not be exchanged between basis sets or levels of theory.

There is debate about what is the best geometry for use in force field calculations: calculated, experimental, or corrected [Pulay *et al*, 1979, Fogarasi *et al*, 1992, Allen and Császár, 1993]. Calculated geometries contain errors largely due to the approximations in solving the Schrödinger equation. Geometries can be corrected based on experimental data [Pulay *et al*, 1979] or by empirical correction of bond lengths using offset forces during initial calculations [Fogarasi *et al*, 1992], or used without correction. The minimum energy structure determined by Gaussian may not be an exact representation of the solution structure. Modeling the effects of solvent is difficult. Explicit incorporation of solvent molecules (a supermolecule structure) is computationally expensive. Other models tested show that modeling solvent as a bulk phase (self-consistent reaction field) does not incorporate specific hydrogen bonding effects [Williams *et al*, 1995]. The geometry used in these studies has been

the isolated minimal energy conformation. Explicit incorporation of water is used to model specific hydrogen bonding observed in protein structures. The effects of solvation are implicitly incorporated in the scale factors which correct for the inaccuracies in structure.

Two variables need to be specified in the solution of the Schrödinger equation, U , the potential energy, and Ψ . In the harmonic oscillator approximation (the simplest model of atomic motion), the potential energy assumes the form of a parabola:

$$U = \frac{1}{2}\kappa r^2 \quad (1.11)$$

$$\kappa = 4\pi^2\nu^2\mu \quad (1.12)$$

where r is the displacement from the equilibrium position, μ is the reduced mass ($m_1m_2/(m_1 + m_2)$) and ν is the frequency of vibration [Moore, 1955]. This approximation is valid only for small perturbations from the equilibrium geometry since the restoring force, in the harmonic oscillator approximation, $f = -(\delta U/\delta r) = -\kappa r$, is directly proportional to the displacement, r . In actual systems, the restoring force is not proportional to the displacement; the harmonic approximation does not account for dissociation.

There are two limiting factors in determining Ψ : the basis set and the level of theory used. The basis set is the mathematical description of molecular orbitals. It places limits on the space available to the electrons, unlike real orbitals where the electrons have a probability of being found anywhere in space. The larger the basis set, the more accurately molecular orbitals are described, however, it is at the expense of computational time. (The following description of the molecular orbitals and Hartree-Fock theory are derived largely from Foresman and Frisch, 1993.) Molecular orbitals are linear combinations of basis functions:

$$\phi_i = \sum_{\mu=1}^N c_{\mu i} \chi_{\mu} \quad (1.13)$$

where $c_{\mu i}$ are the molecular orbital expansion coefficients and χ_{μ} are basis functions. The basis functions are linear combinations of primitive Gaussian functions:

$$\chi_{\mu} = \sum_p d_{\mu p} g_p \quad (1.14)$$

where the $d_{\mu p}$ are fixed constants defined by the basis set.

Minimal basis sets use the smallest number of basis functions necessary to describe molecular orbitals. Split valence basis sets use differently sized functions to describe molecular orbitals; this allows the orbitals to change size. Addition of polarization functions (designated with *) allows the molecular orbitals to change shape by the addition of atomic orbitals with higher angular momenta than required for the ground state. Finally, diffuse functions can be incorporated into basis sets (designated with a +) to add electronic density far from the nucleus. Diffuse functions are especially useful for molecules with significant negative charge, including lone pairs of electrons. In most of the studies in this thesis the split-valence 4-31G basis set is used, which has been determined to predict spectra of small molecules as accurately as larger basis sets [Latajka *et al*, 1989; Lowrey and Williams, 1992b].

The level of theory refers to the simplifications and assumptions made to define the wave function, Ψ . Ψ is defined as a combination of molecular orbitals; each level of theory uses different combinations of orbitals in defining Ψ . As with basis sets, different levels of theory require different amounts of computational time.

At the Hartree-Fock level of theory, Ψ is defined as a single determinant of molecular orbitals representing all combinations of an electron in the molecular orbitals. The molecular orbitals are defined by the basis set used. In the definition of molecular orbitals (equation 1.13), ϕ_i , the molecular orbital expansion coefficients, $c_{\mu i}$, were not defined. The problem in solving Schrödinger's equation becomes one of finding the expansion coefficients that minimize the energy, E . This comes from the variational principle which states that for any non-exact wavefunction the calculated energy will always be greater than the exact energy. An iterative method, self-consistent field (SCF), is used to minimize the energy. (Symbols and the following

explanation of the self-consistent field method are derived from Roothaan, 1951.)

Given a set of orbitals (a set of $c_{\mu i}$), a new set can be generated from

$$F\phi = \epsilon\phi \quad (1.15)$$

where F (not to be confused with the force constant matrix F from the secular equation) is the Hartree-Fock Hamiltonian operator, ϕ is the collection of molecular orbitals and ϵ are eigenvalues representing orbital energies. The equation is solved for the n lowest energy ϵ_i and their corresponding ϕ_i , where n is the number of ground state orbitals describing the molecule. The calculated ϕ_i are compared with the original ones; if they differ a new set is chosen, based on this comparison, and the process repeated. If the original and calculated ϕ_i 's are the same, the iterations stop and that set of orbitals represents the set of orbitals with the lowest energy. The method is called self-consistent because F , the Hartree-Fock Hamiltonian operator, is calculated from the original ϕ 's, and is then used to calculate the new ϕ 's. When the original and new ϕ 's agree, the orbitals cannot be improved.

Determination of F from a set of orbitals begins with the calculation of the coulomb and exchange operators, J_i and K_i , respectively:

$$\left. \begin{aligned} J_i^\mu \phi^\mu &= e^2 \left(\int \frac{\phi_i^\nu \phi_i^\nu}{r^{\mu\nu}} dv^\nu \right) \phi^\mu, \\ K_i^\mu \phi^\mu &= e^2 \left(\int \frac{\phi_i^\nu \phi_i^\nu}{r^{\mu\nu}} dv^\nu \right) \phi^\mu \end{aligned} \right\} \quad (1.16)$$

where $r^{\mu\nu}$ is the distance between the μ^{th} and ν^{th} electrons. From these the total electron interaction operator G (not to be confused with the kinetic energy matrix of the secular equation) and F are calculated,

$$G = \sum_i (2J_i - K_i), \quad (1.17)$$

$$F = H + G \quad (1.18)$$

The newly calculated F is used in the determination of the new ϕ_i 's using equation 1.15. The comparison of original and new ϕ_i 's is made and the cycle restarted

with a new set of ϕ_i 's or it is terminated. When the cycle is complete, the final set of orbitals represents the lowest energy molecular geometry. This geometry is used to calculate the force constants, the second derivative of the energy with respect to Cartesian coordinates.

Hartree-Fock theory does not include consideration of electron correlation in the determination of the wave function, which is part of the systematic error in the calculated geometry and force constants. There are several theories that do incorporate electron correlation into the wave function. Configuration interaction theory begins by noting, in contrast to Hartree-Fock theory, that a single determinant is not sufficient to express the exact wavefunction, Ψ ; additional determinants are constructed that replace one or more occupied orbitals with virtual orbitals, equivalent to exciting electrons to higher energy orbitals. Møller-Plesset perturbation theory [Møller and Plesset, 1934] adds excitations non-iteratively based on many body perturbation theory. Both of these methods add computational expense to the calculations making them less appealing for studies of large molecules. Density functional theory (DFT) methods are based on theories of electron gasses which define the electronic energy, a portion of the E of the Schrödinger equation, differently than does Hartree-Fock theory, incorporating correlation effects implicitly. DFT methods have the potential advantage of being less computationally intense than Hartree-Fock theory. Programming to calculate analytical derivatives using DFT methods is not available (numerical derivations are performed) so that the potential for faster calculations has not been fully realized. The use of these higher levels of theory or basis sets larger than 4-31G does not completely eliminate errors in calculated force constants [Lowrey and Williams, 1992b].

1.3 The Secular Equation and Normal Mode Analysis

Once a set of force constants have been determined they can be used in a normal mode analysis. Normal mode analyses are based on the secular equation,

$$GF = L\Lambda L^{-1} \quad (1.19)$$

which relates molecular structure to vibrational frequencies. G is the inverse kinetic energy matrix containing information about atomic coordinates and masses, the optimized geometry. F is the force constant matrix or force field. The diagonal terms of the F matrix are force constants for each bond stretch, angle bend, and torsional bend while the off-diagonal terms are force constants describing interactions between the bonds (the force constants are analogous to spring constants in a mechanical system). L contains the eigenvectors of GF which describe the directions and relative magnitudes of motions contributing to each vibration, and Λ is a diagonal matrix containing the allowed energy levels from which are calculated the vibrational frequencies.

G and F are used to solve the secular equation for the eigenvectors, contained in L , which describe the contributions of each coordinate to the allowed vibrations, and for Λ , which contains the allowed vibrational energies, the eigenvalues. Λ is a diagonal matrix, whose terms, λ_i , are the allowed vibrational energies. The energies are converted to frequencies using

$$\nu_i = \frac{\sqrt{\lambda_i}}{2\pi c} \quad (1.20)$$

where ν_i are the frequencies, λ_i are the individual eigenvalues, and c is the speed of light. Calculated frequencies are compared to experimental spectra. Either known or hypothesized structures can be incorporated into the G matrix. Incorporation of a known structure into the G matrix tests or helps develop a force field, F . Interpretation of the validity of a hypothesized structure requires an accurate force field.

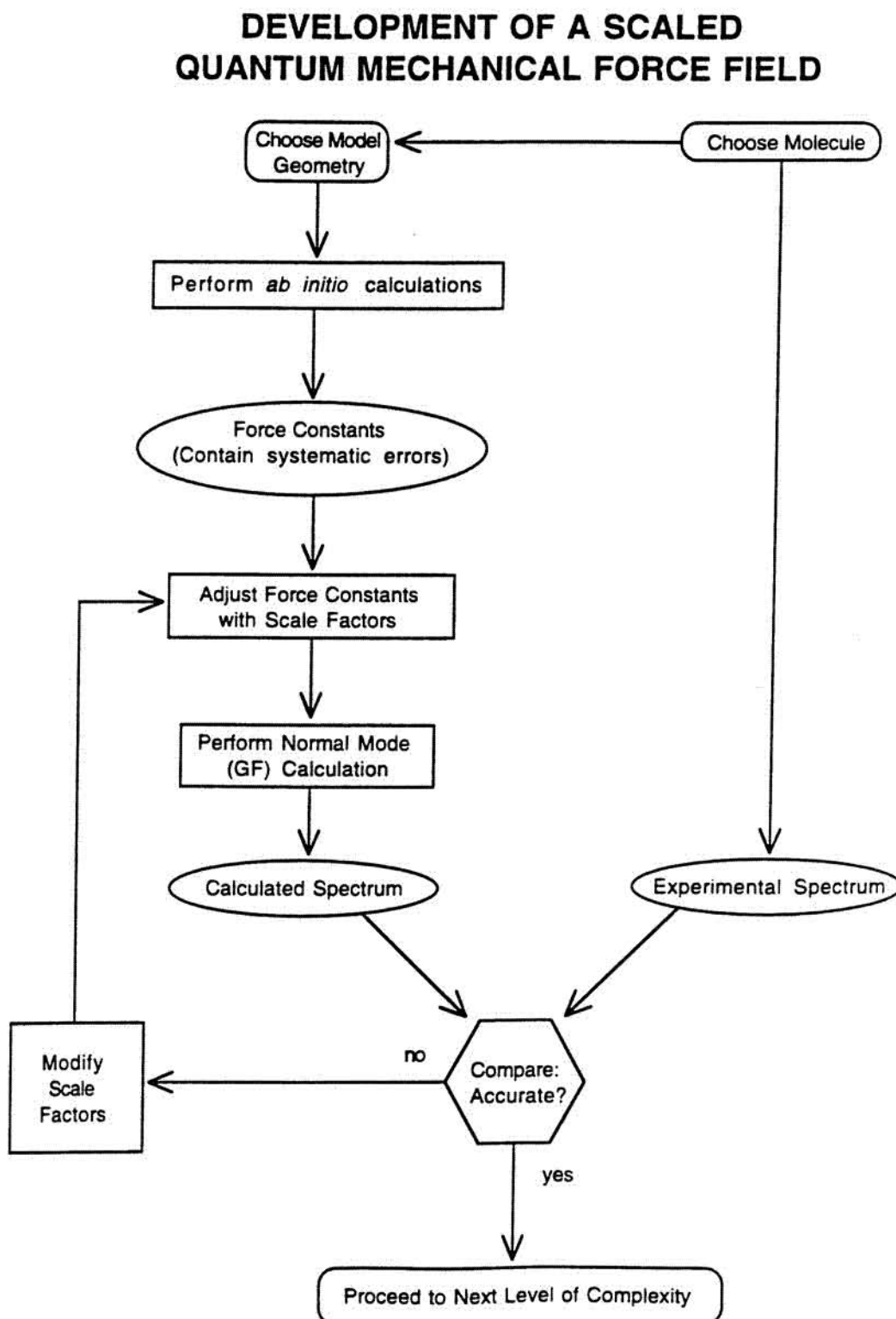
1.4 SQMFF, Combining Theory and Experiment

The SQMFF method is a technique for combining the information in experimental data with that derived from theoretical computational studies to create an accurate set of force constants for use in normal mode analysis. Calculated *ab initio* force constants at the Hartree–Fock level of theory contain systematic errors that lead to errors of about 5 to 15% in calculated frequencies [Fogarasi and Pulay, 1985]. *Ab initio* force fields, when properly scaled, are transferable to other molecules too large for direct *ab initio* calculations and reproduce experimental data very accurately [Fogarasi and Pulay, 1985]. Cheam and Krimm [1989a, 1989b] have used the SQMFF approach with glycyl- and alanyl-dipeptides to obtain detailed information about the effects of hydrogen bonding and conformation on changes in force constants and dipole moment derivatives. SQMFF can provide a significant improvement over empirically derived force fields in terms of the quality of information obtained [Fogarasi and Pulay, 1985, Cheam and Krimm, 1989a]. This methodology is currently the most successful approach to the development of force fields for the interpretation of vibrational spectra of larger peptides. “Scaled Quantum Mechanical (SQM) force fields represent the highest accuracy which can be achieved in the harmonic approximation [Fogarasi and Pulay, 1985].”

The SQMFF procedure (see Figure 1.2) begins with a choice of the system to be studied: the molecule and its environment. Since vibrational spectra can be taken of substances in vapor, solution, liquid, or solid states, choice of environment is important. Environment also influences the geometry of the model based on environmental effects such as hydrogen bonding. Experimental spectra are recorded and interpreted for coordinate group assignments. Spectra of molecules with isotopic substitutions (isotopic labeling) help in determination of coordinate assignments.

Large molecules are difficult to study, their spectra are complex. However, since scale factors can be transferred from smaller to larger molecules [Fogarasi and Pulay, 1985], small molecules that contain chemical groups similar to those present

Figure 1.2: Flow chart depicting the steps involved in the development of a Scaled Quantum Mechanical Force Field.



in large systems can be studied and the results applied to the larger system.

The next step is to choose the model and starting geometry for the *ab initio* calculations. The model includes the basis set, the level of theory, and solvent modeling (if necessary).

After the choices of system and model are made the *ab initio* calculations can be performed. The results of the *ab initio* calculations are an optimized geometry and a set of force constants in a Cartesian coordinate representation. The force constants in Cartesian coordinates are converted to internal symmetry coordinates (a functional grouping of atoms). Molecular motions are more easily visualized in symmetry coordinates than in Cartesian coordinates and allow transfer between molecules [Fogarasi and Pulay, 1985]. Each internal symmetry group coordinate is associated with one diagonal force constant, the off-diagonal force constants are associated with interactions between the internal symmetry coordinates (e.g. a C=O stretch interacting with a C=O in-plane bend).

The internal symmetry coordinate force constants, which still contain the systematic errors from the *ab initio* calculations, can be adjusted empirically with a scale factor for each internal symmetry coordinate. The calculated internal symmetry coordinate force matrix, F_{ij}^{calc} , is multiplied by the square root of the product of the diagonal scale factors [Pulay *et al*, 1983; Williams, 1992]:

$$F_{ij}^{scaled} = (c_i c_j)^{\frac{1}{2}} F_{ij}^{calc} \quad (1.21)$$

Thus the off-diagonal force constants are scaled to the same extent that the diagonal force constants are.

The scaled force constants are used in a normal mode calculation of the vibrational spectrum which is compared to the experimental spectrum. Differences are due to inaccuracies in the scaled force constants. To correct these differences, the scale factors are modified and the normal mode calculation repeated. The scale factors are adjusted until the agreement between calculated and experimental spectra can no longer be improved.

Scaling requires molecules with a defined geometry, calculated force constants, and measured frequencies so that the only unknowns in the secular equation are the scale factors. However, any number of sets of scale factors could simply match calculated to experimental frequencies. In order to insure accurate interpretation of experimental spectra in terms of molecular motion three criteria must be met:

1. The potential energy distribution (PED) must reflect what is known about coordinate vibrations, i.e. the C=O amide stretch (*s*) should be found in the frequency range 1625–1695 cm^{-1} [Krimm and Bandekar, 1986].
2. PED assignments determined from frequency shifts due to isotopic substitution and the correct magnitude of the shift must be accurately predicted. For example, substitution of the amide carbon with ^{13}C shifts the C=O *s* downward by more than 40 cm^{-1} [Williams, 1994]. This should be reflected in any predicted spectra.
3. The agreement between calculated and experimental frequencies is optimized from a least squares fit of the calculated frequencies to the experimental spectra.

Spectra calculated using the scaled force constants then match experimental data.

A scale factor for a symmetry group coordinate can be transferred from one molecule to another [Fogarasi and Pulay, 1985], so that once a scale factor is determined it can be used in any molecule. Larger molecules can be interpreted using combinations of scale factors from smaller molecules, making interpretation of spectra or evaluation of new coordinates easier. Other factors that influence protein vibrational spectra, like shifts and splittings in the amide I region due to transition dipole coupling (TDC) effects, can be investigated only after accurate scale factors for the chemical groups, in the absence of these effects, are determined. By proceeding in a step-wise fashion, where only one more complexity is added per iteration, a set of force constants can be developed for large systems, like proteins in solution.

When a force field is complete it can be applied to the investigation of proteins in either of two ways. First, by direct application in the secular equation, which is called a normal mode calculation [Krimm and Bandekar, 1986]. Second, by conversion to molecular mechanics potential functions, which describe the potential energy functions, for molecular mechanics calculations [Palmö *et al*, 1991].

1.5 Solvation

Fogarasi and Pulay [1985] found that the SQMFF scale factors developed for vapor phase molecules were transferable. Extension of this method to molecules in solution involves investigation of whether or not the effects of solvation on force constants can be modeled with transferable scale factors.

The effect of bulk solvent on molecular structure is difficult to model. Several schemes have been developed for modeling solvent effects on vibrational frequencies:

- Self consistent reaction field theory models the solvent as a uniform dielectric with the solute occupying a hole in the dielectric then uses a self-consistent method to optimize the wave equation, including solvent terms [Tapia, 1991]. Results on methanol using SCRF theory gave unsatisfactory modeling of hydrogen bonding effects [Williams *et al*, 1995] at least in part due to the lack of explicit hydrogen bond formation.
- Force constants determined from isolated geometries can be scaled to aqueous frequencies [Williams and Lowrey, 1991; Lowrey and Williams, 1992b]. These structures require the least computation time for geometry optimization. The isolated structure is not an exact replica of solvated molecular structures. It has been shown, however, that force constants calculated from isolated structures can be scaled so that calculated frequencies match measured aqueous frequencies [Williams and Lowrey, 1991; Williams, 1992; Lowrey *et al*, 1993]. Changes in

frequency due to solvation are not explicitly calculated, but are incorporated into the scale factors.

- To model solvation explicitly would require incorporation of many water molecules into a supermolecular structure which would be prohibitively resource intense at the *ab initio* level; the water molecules add considerable time to the geometry optimization. Rings formed in supermolecules add redundancies to definitions of coordinates which are not easily resolved. Artifacts not present in the *ab initio* calculations are introduced in normal mode calculations by the vibrational coupling of statically bound water molecule coordinates with solute coordinates [Williams *et al*, 1995]. Supermolecules are relatively hard to optimize because choice of scale factors for water coordinates, which are not well defined, can affect scale factors for the rest of the molecule.
- Water-excluded scale factors avoid some of the difficulties with scaling supermolecules. The Cartesian coordinates and force constants associated with water are removed after the *ab initio* force constant calculations are completed and prior to conversion of the force constants into internal coordinates. Scale factors for molecular coordinates no longer depend on those chosen for water and ring redundancies are avoided. Water coordinates are eliminated and can no longer couple with those of the solute. However, the electronic effects due to explicit formation of hydrogen bonds is maintained. Water-excluded supermolecule structures only model explicit hydrogen bonds, not the structural effects of solvation. Solvation effects are modeled by scaling to aqueous frequencies.

The water-excluded model is used in the work presented in this thesis. The explicit incorporation of water molecules in some models is used to mimic intramolecular hydrogen bonds of known geometry found in protein structures such as alpha helices and beta sheets. The bulk water effects on these intramolecular hydrogen bonds is incorporated into the force constants by scaling the calculated force con-

stands for the hydrogen bonded structures to aqueous frequencies.

1.6 Potential Applications of a Force Field

The potential usefulness of a force field capable of accurately predicting vibrational spectra is illustrated by considering two recently published papers. The published observations clearly demonstrate the power and limitations of vibrational spectroscopy as a probe of small but important structural changes. While small conformational changes were detected, at best only empirical interpretations and speculations can be made to explain, on a molecular level, the changes observed in the respective spectra.

Zhang *et al*, 1995, Peptide Models of Helical Hydrophobic Trans-membrane Segments of Membrane Proteins. 2. Differential Scanning Calorimetric and FTIR Spectroscopic Studies of the Interaction of Ac-K₂-(LA)₁₂-K₂-Amide with Phosphatidylcholine Bilayer

Interactions between lipid bilayers and intramembrane domains of membrane proteins are not fully understood but are known to contribute to conformation and functioning of both membrane and proteins. The authors used infrared spectroscopy to monitor the structure of an artificial membrane helix, Ac-K₂-(LA)₁₂-K₂-amide, which had been incorporated into defined phosphatidyl-choline membranes. The membrane changed phase from a liquid-crystal to a gel as the temperature was lowered. The infrared spectrum of the polypeptide imbedded in liquid crystal phase membranes had an amide I peak centered near 1656 cm⁻¹, suggestive of a regular α -helical conformation [Zhang *et al*, 1995]. As the membrane was induced to transition to the gel phase, a new peak appeared in the amide I region of the IR spectrum at 1665 cm⁻¹, along with a decrease in the intensity of the 1656 cm⁻¹ peak. This change in the spectrum indicates that the polypeptide changed its conformation. The authors

speculate that the regular α -helix was distorted into an α_{II} -helix by the change in phase of the membrane.

Ludlam *et al*, 1995, Site-Directed Isotope Labeling and ATR-FTIR Difference Spectroscopy of Bacteriorhodopsin: The Peptide Carbonyl Group of Tyr 185 is Structurally Active During the bR \rightarrow N Transition

In this study, the authors observed secondary structural changes at tyrosine 185 during the bacteriorhodopsin (bR) photo-cycle. Conformational changes between the ground state and N intermediate structures in the bR photocycle lead to subtle changes in the bR vibrational spectrum. Difference spectroscopy was used to monitor the changes in the bR structure between the ground state and N intermediate. ^{13}C was incorporated at each of the tyrosine residues in bR in turn and difference spectra of the same transition recorded. If the labeled tyrosine undergoes a conformational change during the transition from the ground state to the N intermediate, the labeled difference spectrum would be different from the unlabeled difference spectrum. Changes in the difference spectra of the bR to N intermediate transition were observed when Tyr 185 was labeled, but not when any other tyrosine residues were specifically labeled. By combining difference spectroscopy with isotopic labeling Ludlam *et al* were able to observe changes in conformation at a single amino acid. The authors concluded “that the amide I region of the bR \rightarrow N difference spectrum includes significant contributions from the Tyr 185 carbonyl group.”

Site-directed mutagenesis and electron diffraction studies had suggested that the region around Tyr 185–Pro 186 acts as a hinge [referenced in Ludlam *et al*, 1995]. This, combined with their spectral data, led Ludlam *et al* to postulate that a rotation of about 30° around the Tyr 185 ψ angle would be sufficient to reorient the F helix and cause the changes observed in the difference spectra.

Limitations

These studies clearly demonstrate how subtle changes in structure at specific sites can be observed using vibrational spectroscopy. However, the methods are limited with respect to interpretation. In both studies interpretation would be enhanced if vibrational spectra could be predicted for the proposed structures for comparison to the experimental spectra. Consistency between the model calculations and experimental spectra would support the proposed structures.

Normal mode analyses can predict vibrational spectra for a given structure. These analyses require, in addition to the structure, a force field. There is no force field currently available capable of accurately predicting vibrational spectra of proteins in solution [Williams *et al.*, 1990]. As stated earlier, the goal of my thesis research is to further the development of a SQMFF which would be capable of predicting vibrational spectra of polypeptides and proteins in solution. Development of this force field requires the analysis of known biomolecular structures.

1.7 Progress in Building a SQMFF up to 1993

Dr. Williams' lab has been engaged in the development of a SQMFF for peptides since 1989 by building up from small molecules a set of scale factors that are transferable to larger molecules and peptides [Weaver and Williams, 1990; Williams *et al.*, 1990; Williams and Lowrey, 1991; Lowrey *et al.*, 1993; Williams, 1992, 1994; Lowrey and Williams 1992a, 1992b, 1992c]. These small molecules have included formic and acetic acids, methylamine, N-methylacetamide, and glycine.

Experimental Observation

Interest in development of this force field began with the experimental observation of a trend in the amide III frequencies of a series of ala-X peptides in solution: as the molecular weight of the X side chain increased the amide III fre-

quency decreased [Weaver and Williams, 1990]. The investigation of this series of ala-X peptides had been prompted by two observations:

1. Sengupta and Krimm's [1985] observation that "despite the identical backbone α -helical structures, significantly different frequencies are calculated, and observed, in the Amide III and backbone stretch regions of α -poly(L-glutamic acid), as compared with α -poly(L-alanine)."
2. Diem and his co-workers, using Raman and vibrational CD measurements of L-alanine-L-alanine and D-alanine-L-alanine and their deuterated isotopomers, provided evidence that the N-H bend of the amide III band is coupled to the methine C-H bending coordinates [Diem *et al*, 1984; Oboodi *et al*, 1984; Roberts *et al*, 1988]. This suggested a relationship between changing amide III frequencies and peptide conformations.

The results of the investigation of the ala-X peptides [Weaver and Williams, 1990] imply that peptides with only two amino acids have side chain dependent conformational preferences in aqueous solutions which can be measured using vibrational spectroscopy. Weaver and Williams postulated several phenomena that could contribute to this effect: changes in conformation due to larger side chains, new vibrational couplings in the peptides without regard to changes in conformation, changes in the force field of the molecules, or simply change in mass.

Testing the Implications

To test these postulated mechanisms, a computational study was performed [Williams *et al*, 1990] using molecular mechanics (CHARMm), semiempirical (MOPAC), and *ab initio* (Gaussian 86) techniques. CHARMm and MOPAC calculations did not show any trends in the optimized structures of the ala-X peptides. The Gaussian86 (G86) optimized geometries predict the angle ϕ to become smaller as the X side chain mass increases [Williams *et al*, 1990].

The predicted geometries were tested by calculating spectra, based on the geometries, for comparison to the experimental data. Five sets of frequencies, based on the best available force fields, were calculated:

1. CHARMM (molecular mechanics),
2. MOPAC (semi-empirical),
3. MOPAC geometries with a force field determined by Krimm and Bandekar [1986],
4. the G86 geometries with a set of differential scale factors from Cheam and Krimm [1989a and 1989b],
5. the G86 geometries and force field with a single scale factor (81.06% , chosen to give good agreement between the calculated amide I frequency of the β -sheet geometry for ala-ala and the experimental band at 1680 cm^{-1}).

The CHARMM and MOPAC amide I and III calculated frequencies did not show any systematic trends in the amide III frequencies and were calculated to be about 130 cm^{-1} and 200 cm^{-1} too high, respectively. The results using MOPAC optimized geometries and the Krimm and Bandekar force field [1986] predicted the amide I frequencies with a correlation to experiment of 0.81 but did not predict any systematic variations in the amide III frequencies. The set of differential scale factors [Cheam and Krimm, 1989a and 1989b] with the G86 geometry predicted the amide III modes well, but not the amide I or the carboxylic acid C=O stretch (*s*) modes. Finally, the *ab initio* (G86) force field predicted the amide I, III, and the carboxylic acid C=O *s* frequencies well [Williams *et al*, 1990]; other modes were not well predicted with this single scale factor model. This evaluation of current force fields indicated that there was no force field capable of interpreting the complete vibrational spectrum of peptides.

While good fits to some frequencies were achieved, any conclusions from the study regarding trends contributing to the shift in amide III frequencies can not be considered certain, the good fit achieved may be an artifact of the computation and not due to actual changes in the ϕ angle preference. Therefore, to ascertain the nature of the shift in the amide III frequencies, a better force field is required. Once a complete *ab initio* force field is generated, it can also be converted to molecular mechanics potentials and used to interpret spectra of larger systems [Palmö *et al*, 1991].

Development of a New Force Field

The work completed prior to my working on the project included development of scaled force fields for isolated and supermolecule structures of formic acid, formate, acetic acid, acetate, and acetone [Williams and Lowrey, 1991, Lowrey and Williams, 1992b], methylamine [Lowrey and Williams, 1992a], N-methylacetamide [Williams, 1992], glycine [Lowrey *et al*, 1993], and glycinate [Williams *et al*, 1993]. In these studies it was determined that force fields calculated from isolated molecular structures could be scaled to provide good agreement with aqueous solution frequencies [Williams, 1992], the 4-31G basis set could predict spectra as well as larger basis sets and basis sets that also included polarization functions and diffuse functions [Lowrey and Williams, 1992a], basis set superposition error was not a factor in these calculations [Williams and Lowrey, 1991; Lowrey and Williams, 1992a], and higher levels of theory (MP2) did not provide better results [Lowrey and Williams, 1992b]. These results indicate that scaling can correct for deficiencies in the theory and basis sets used.

Several problems were found with the use of supermolecules. When hydrogen bonded ring structures were formed with the water molecule, redundant coordinates were required to completely describe the structure. In order to avoid the problem, the redundant coordinates were deleted. To determine if this had an adverse affect

on the frequency calculations, several calculations were performed where the deleted coordinates were varied. In most instances the only frequencies affected were those of water [Williams and Lowrey, 1991; Lowrey *et al*, 1993; Williams *et al*, 1993]. In studies investigating the effects of hydration on force constants, an artifact was noted [Williams and Lowrey, 1991; Williams *et al*, 1995]; coordinates for water coupled with solute coordinates. The choice of redundant coordinates which were ignored strongly affected the predicted frequencies for some methanol coordinates [Williams *et al*, 1995]. To eliminate this coupling the Cartesian coordinates and force constants for water were removed prior to the conversion of the coordinates and force constants into internal coordinates. This eliminated the coupling artifact and the problems with redundant coordinates in the rings formed in the supermolecules. However, the structural changes associated with the formation of hydrogen bonded structures was preserved. [Williams *et al*, 1995].

In building the SQMFF, the strategy has been to start with small molecules and work up to larger molecules. Assignments are more certain with smaller molecules, there are not as many fundamental vibrational modes to assign. The number of fundamental vibrations, and force constants, is equal to $3N - 6$, where N is the number of atoms in the molecule. Isotopic substitutions were also used to confirm assignments. The optimized scale factors were then applied to larger molecules to verify and refine the initial scale factors and to enable interpretation of more complex spectra. The assignments of coordinates previously scaled in smaller molecules provided preliminary PED assignments for those coordinates in the larger structures. Assignments of previously unscaled coordinates became easier because fewer modes were unassigned. New coordinate assignments were made based on data from isotopic substitution or the literature. The scale factors developed showed consistency as larger molecules were scaled and for different isotopic species. This verified the general usefulness of the scale factors.

1.8 Definition of Problem Investigated

The overall goal of this research is to develop a set of scale factors and force constants that can be used for the study of the secondary structure of polypeptides and proteins in solution. It is difficult to build a set of scale factors for proteins directly. Therefore, the research began with the study of small molecules in solution. The ability of the SQMFF method to correct for solvent effects had not been previously demonstrated, though it had been shown to be effective in correcting deficiencies in vapor phase force constants [Fogarasi and Pulay, 1985]. The scale factors are useful only if they can be transferred. The transferability of scale factors developed for molecules in solution reflects the ability of the SQMFF method to correct for systematic effects of solvation.

One of the problems under continuing investigation by Williams and co-workers is an examination of the effects of solvation on force constants. To build on this, a comparison of three methods, using methanol and ethanol as solutes, was performed: SCRF, isolated structures scaled to aqueous frequencies, and supermolecules. In that study [Williams *et al*, 1995] problems with redundant coordinates from hydrogen bonded ring structures could no longer be satisfactorily solved by simple exclusion of redundant coordinates, varying the excluded coordinates affected predicted frequencies and scale factors for methanol coordinates. To eliminate these artifacts the water-excluded scale factor method was developed.

Water-excluded scale factors were determined for methylamine, acetic acid, N-methylacetamide, and glycine in acidic and basic solutions, based on previously completed work, so that a consistent set would be built for polypeptides and proteins in solution. Scaling water-excluded supermolecule structures containing different numbers of water molecules for each solute helped verify that electronic effects due to hydrogen bonding were preserved using this model. The scale factors for the larger molecules were built using scale factors determined for the smaller molecules to help insure their transferability.

Prior to the application of scale factors developed for glycine and glycinate to dialanine structures, the coordinates for the chiral C^α coordinates of alanine (C^α rock^{1,2}, C^α deformation^{1,2,3}, and $C^\alpha C^{me}$, $C^\alpha N^{ter}$, $C^\alpha C^{ter}$, and $C^\alpha H$ stretches) had to be determined. Scale factors using all three solvation models (isolated geometries scaled to aqueous frequencies, supermolecules, and water-excluded) were developed for alaninate and alanine at pH=1.

Several problems were encountered in the interpretation of the experimental spectra of alaninate. In acetic acid and glycinate the COO *wag* coordinate was assigned to an experimental peak near 600 cm^{-1} . However, the transferred scale factor predicted the COO *wag* in alaninate to be assigned to an observed peak at 785 cm^{-1} even though there was another observed peak closer to 600 cm^{-1} , similar to those in acetate and glycinate. In order to determine the location of the COO *wag* coordinate, a set of calculations using the 6-31G** basis set was performed on methylamine and acetic acid. These scale factors were transferred to alaninate optimized using the 6-31G** basis set. The calculation using the transferred scale factors was consistent with the COO *wag* assignment at 785 cm^{-1} .

In the $500\text{--}900\text{ cm}^{-1}$ frequency range more peaks were observed in the experimental spectra of alaninate than were predicted by normal mode analysis. The predicted peak at about 620 cm^{-1} in the alaninate normal isotopic species could not be easily scaled to either nearby peak (590 or 654 cm^{-1}) in the experimental spectrum. A Fermi resonance calculation suggested that a fundamental vibration at 622 cm^{-1} was resonating with a combination of the 279 and 343 cm^{-1} peaks to produce the observed 590 and 654 cm^{-1} peaks.

Two different supermolecule geometries for alaninate were scaled, one using the same hydrogen bonding pattern as had been optimized for glycinate (the water forming a hydrogen bonded ring between the two carboxyl oxygens), the other modeling single hydrogen bonds to amine and carboxyl groups (with the water forming a hydrogen bonded ring between one of the carboxyl oxygens and one of the amine

hydrogens). Isolated basic and water-excluded basic and acidic structures were scaled using four basis sets (4-31G, 4-31G**, 6-31G**, 6-31+G**) to verify that limitations in the 4-31G basis set was not a factor in correcting the systematic errors due to solvation using the SQMFF method.

Dialanine was the first peptide to be scaled with this set of scale factors, providing additional scale factors for peptide group coordinates. Isolated and two-water water-excluded basic, neutral, and acidic solution structures and one-water and three-water water-excluded basic structures were scaled. The different supermolecule structures represent different internal hydrogen bonded states of peptide bonds in a protein. The set of supermolecules scaled represent amino acids present in all positions of a helix, where one or two internal hydrogen bonds of known geometry are present. The one-water supermolecules represent peptide bonds at the beginning and ends of α -helices where single hydrogen bonds are formed (either the C=O or the N-H participates). The two-water supermolecules represent peptide bonds deep in an α -helix and in β sheets where both the C=O and N-H groups participate in intramolecular hydrogen bonds. The three-water supermolecule structure is similar to the hydrogen bonding seen in the tri-alanine crystal structure [Qian *et al*, 1991]. All structures were scaled to aqueous frequencies to model solvated groups.

The effect of changing the molecular geometry on the predicted frequencies and PED was tested by incorporating an altered geometry into the normal mode analysis while using the scaled force constant matrix.

Future Work

The solution structures of small molecules do not contain multiple peptide bonds and so are not influenced by transition dipole coupling (TDC). A set of scale factors that can accurately predict frequencies in the absence of TDC can be applied to known structures that do contain TDC to determine the specific effect TDC has on vibrations; the differences between calculated and experimental frequencies are

due to TDC. The effects of TDC are incorporated into the force field by calculating a force constant using the equation [Krimm and Abe, 1972]:

$$F_{jk} = \left(\frac{0.1}{\epsilon} \right) \left\| \frac{\partial \vec{\mu}_j}{\partial S_j} \right\| \left\| \frac{\partial \vec{\mu}_k}{\partial S_k} \right\| \frac{[\vec{n}_j \cdot \vec{n}_k - 3(\vec{n}_j \cdot \vec{n}_{jk})(\vec{n}_k \cdot \vec{n}_{jk})]}{R_{jk}^3} \quad (1.22)$$

Where ϵ is the dielectric constant (assumed to be 1 in the internal environment of the protein), $\left\| \frac{\partial \vec{\mu}}{\partial S_j} \right\|$ and $\left\| \frac{\partial \vec{\mu}}{\partial S_k} \right\|$ are the Euclidean lengths of the dipole moment derivatives with respect to the symmetry coordinates for each dipole in debyes per angstrom (for stretches), \vec{n}_j and \vec{n}_k are unit vectors along the bonds j and k , respectively, \vec{n}_{jk} is the unit vector between the dipoles, and R is the distance between the dipoles. Assumptions about the dielectric constant, location, and angle of the vectors can only be tested with an accurate set of scale factors. Once these variables are understood the size of the sphere of influence can be determined, i.e., what is the greatest distance at which one bond will influence another?

1.9 Historical Perspective

Spectroscopy

In 1928 C. V. Raman and K. S. Krishnan published their finding of a “Compton effect” for visible radiation; using a focused beam of sunlight they were able to demonstrate a shift in wavelength of scattered radiation [Raman and Krishnan, 1928a]. They improved the method by substituting a mercury arc lamp [Raman 1928] for the light source. Taking photographs of the scattered radiation allowed them to measure the increase in wavelength which they determined was the same order of magnitude as the frequency of infrared absorption [Raman and Krishnan, 1928b,c]. For his discovery of the raman effect, Raman received the Nobel prize in 1930.

The first IR analysis of proteins was done by Vles and Heintz in 1937 [Sutherland, 1952]. Sutherland [1952] noted that “much valuable structural information can be derived from the partial interpretations now possible.” For instance, Ambrose

and Elliot had shown that α helical C=O amide I bands had a strong vibration at 1660 cm^{-1} while β sheet vibrations were centered at 1630 cm^{-1} [Elliot and Ambrose, 1950]. Isotopic substitution studies began in 1949 with the use of D_2O by Gore *et al* [Sutherland, 1952]. However, it was still difficult to assign bands in single amino acids, calculations could not be performed to help. The development of modern FTIR in the early 1980's allowed "dramatic improvements ... in the sensitivity of infrared spectroscopy" [Rothschild, 1992] now capable of investigating proton pump mechanisms of bacteriorhodopsin.

The first raman spectrum of a protein was that of lysozyme in 1958 [Spiro and Gaber, 1977]. The first use of lasers in raman spectrometers in 1968 produced spectra of sufficient quality for application on crystalline proteins [Tobin, 1968]. The method was of sufficient accuracy to distinguish between different proteins. Tobin noted, however, that "the low solubility of proteins is expected to be a difficulty." [Tobin, 1968]. Just two years later Wallach [1970] showed that dilute solutions could be used with as much success as solid or concentrated solutions. In 1970, Lord and Yu's pioneering papers emphasizing structural interpretation appeared [Spiro and Gaber, 1977]. Also in 1970, the first resonance raman spectra were taken [Spiro and Gaber, 1977]. Spiro and Gaber were optimistic about the use of raman spectroscopy, claiming that "the potential is high" for providing information on structure [Spiro and Gaber, 1977]. In 1973 raman spectra taken in D_2O did not use background solvent subtraction. By 1980, subtraction of water allowed the prediction of five types of secondary structure [Williams *et al*, 1980].

In 1988 Lugtenberg noted "that spectroscopy of isotopically labeled biomolecules will become increasingly important in studies of biological structure and function" which will help in assignments for extracting "the detailed structural information inherent in the spectra." [Lugtenberg, 1988]. Williams pointed out the usefulness of this approach in assigning secondary structure motifs in proteins; the amide I shift of 30 to 40 cm^{-1} in ^{13}C difference spectra makes frequency assignment in a partic-

ular amino acid obvious [Williams, 1994]. As noted, isotopic labeling has also been used to study structural changes in bacteriorhodopsin (bR) [Takei *et al*, 1994, Ludlam *et al*, 1995]. These studies determined specific amino acids involved in protein backbone changes as bR goes through its photo-cycle. However, neither study was able to determine the specific changes in terms of bond length or angle changes. A force field capable of predicting protein vibrational spectra is required to structurally characterize the findings.

The amide frequencies (Table 1) have been established based on the vibrational modes and frequencies of N-Methylacetamide beginning with work by Miyazawa and co-workers in the late 1950's and by normal mode analyses performed by Krimm's group [Krimm and Bandekar, 1986]. These are frequencies specifically associated with peptide bonds. The specific frequencies of the amide modes are related to the molecular environment of a peptide bond and so are indicative of the secondary structure about each bond.

As noted, in 1950 Ambrose and Elliot noted the difference in amide I frequencies of synthetic esters. Similarly, the Amide III band has been correlated with helical and sheet structures, Lord [1977] reports that right-handed α helix vibrates at about 1275 cm^{-1} while sheet vibrates at about 1230 cm^{-1} . Lord predicts that the amide III will be a more sensitive indicator of the ψ angle since that is "the one parameter most indicative of the α and β regions." Work by Williams *et al*, indicate that this frequency may also be sensitive to the ϕ angle. These correlations to structure have been utilized in linear combination methods of protein structure determination [Williams *et al*, 1980, Williams, 1986].

Computational Chemistry

The Schrödinger wave equation was introduced in 1926 [Schrödinger, 1926], the Hartree-Fock method for solving it for a many electron system was introduced in 1930. Møller and Plesset introduced a system for improving the accuracy of the

Hartree-Fock method in 1934 [Møller and Plesset, 1934]. Thirty-five years later Pulay stated, "it seems probable that the Hartree-Fock approximation can predict values of these force constants accurately enough to provide help to molecular spectroscopists" [Pulay, 1969]. This was demonstrated in 1975 "Recently it has been shown that *ab initio* Hartree-Fock calculations yield better force constants than thought" and off-diagonal force constants are just as accurate as the diagonal terms [Pulay and Török, 1975]. Scale factors, correcting the force constants to more accurately predict spectra, were first introduced by Pulay and Meyer in 1974 and expanded to include several scale factors for smaller groups of coordinates by Blom and Altona in 1976 [Blom and Altona, 1976a,b]. It was about this time that computers powerful enough to routinely solve these equations became available [Fogarasi and Balázs, 1985]. Fogarasi and Pulay noted that "It was the emergence of analytical derivative techniques which revolutionized the quantum chemical calculation of force constants" [Fogarasi and Pulay, 1985]. By 1986 "normal-mode analyses have only been applied to the infinite anti-parallel chain sheet structures" [Krimm and Bandekar, 1986]. They noted that normal mode calculations of a very large non-regular molecule presents formidable computational problems but "it is now possible to provide a detailed prediction of the effects of structural changes on the normal modes" [Krimm and Bandekar, 1986]. That same year studies on Gramicidin A, an anti-parallel β -sheet type protein, were published [Naik and Krimm, 1986].

Transition dipole coupling was introduced by Krimm and Abe in 1972 [Krimm and Abe, 1972]. They had noted a splitting in the amide I band of infrared spectra that was not explained with the perturbation theory of Miyazawa [Miyazawa, 1960]. In order to explain the splitting, they proposed inclusion of the " D_{11} " term, which describes interchain coupling between nearby peptide groups, previously assumed unimportant, to perturbation theory. They were able to show that transition dipole coupling interactions, calculated independently, gave the same sign and size force constant as perturbation theory required for the D_{11} term. They have since shown

that couplings within a radius of about 30 Å must be included in the calculations for accurate modeling of the amide I splittings [Krimm and Bandekar, 1986]. TDC was used by Torii and Tasumi to calculate amide I spectra for eight large proteins [Torii and Tasumi, 1992]. In order to help make normal mode calculations on molecules of this size feasible, the off-diagonal terms in the F matrix must be minimized. They had hypothesized that the amide I band could be modeled by assigning only one degree of freedom to each peptide group. All of the off-diagonal terms for the amide I band were determined from TDC calculations. In general, they were able to predict amide I band intensities with good success, calculated spectra looked similar to measured spectra. The eight proteins had quite different spectra in the amide I region [Torii and Tasumi, 1992].

The ability to measure vibrational spectra of proteins has improved tremendously since the first spectra were taken in 1937 and 1958. Our ability to calculate spectra for structures has also improved in the last decade. Tools have been developed that allow the probing of structure, and changes of structure, of individual amino acids in proteins [Ludlam *et al.*, 1995] but we have not yet reached the state, however, of being able to fully interpret the structural changes measured. The work I have completed is but a step along the path leading to this understanding.

Chapter 2

METHODS

2.1 Experimental Methods

Sample Preparation

All normal isotopic species (methylamine, methanol, acetic acid, *N*-methylacetamide, glycine, alanine, and alanyl-alanine) were purchased from Aldrich or Sigma. All stable isotopically substituted species ($^{13}\text{CD}_3\text{NH}_2$, $^{13}\text{CD}_3(^{13}\text{C})\text{O}_2\text{H}$, $\text{NH}_2\text{CH}_2(^{13}\text{C})\text{O}_2\text{H}$, $\text{NH}_2(^{13}\text{C})\text{H}_2\text{CO}_2\text{H}$, $\text{NH}_2\text{CD}_2\text{CO}_2\text{H}$, $\text{NH}_2\text{CDCD}_3\text{CO}_2\text{H}$, $\text{NH}_2\text{CHCD}_3\text{CO}_2\text{H}$, $\text{NH}_2\text{CH}^{13}\text{CH}_3\text{CO}_2\text{H}$, $^{15}\text{NH}_2\text{CHCH}_3\text{CO}_2\text{H}$, $\text{FMOC-NH}_2\text{CDCH}_3\text{CO}_2\text{H}$, and $\text{FMOC-NH}_2\text{CHCH}_3(^{13}\text{C})\text{O}_2\text{H}$), except those whose exchangeable protons were deuterated, were obtained from Cambridge Isotope Laboratories. Alcoholic, amine, amide, and acid hydrogens were exchanged for deuterium by repetitive refluxing of small samples (1-2 mls or 10-20 mgs) in 2-3 mls D_2O (Sigma, 99.8% pure).

The pH of sample solutions was measured using pHydrion brand pH indicator papers with ranges of 0.0 to 1.5, 1.0 to 2.5, 10.2 to 12.0, and 12.0 to 14.0 or with a micro pH electrode and adjusted with NaOH, NaOD, HCl, or DCl.

Synthesis of Alanyl-alanine Isotopic Species

Synthesis of the labeled alanyl-alanine species 2-d Ala-ala ($\text{NH}_2\text{CDCH}_3\text{CO-NHCHCH}_3\text{CO}_2\text{H}$) and Ala- ^{13}C -ala ($\text{NH}_2\text{CHCH}_3(^{13}\text{C})\text{ONHCHCH}_3\text{CO}_2\text{H}$), was by the F-MOC method [Chang and Meienhofer, 1978] by Mike Flora in the university's biomedical instrumentation center. Following synthesis, the alanyl-alanine species were purified, by Dr. Williams, using a DEAE column, to remove excess trifluoroacetic acid, followed by silica gel thin layer chromatography.

Infrared Spectroscopy

Fourier-transform infrared spectra were recorded using a Nicolet 60SX spectrometer equipped with a KBr/Ge beamsplitter and a liquid-nitrogen-cooled mercury cadmium telluride (MCT) detector. Samples were prepared at a concentration of 10% by weight in H_2O or D_2O . Samples were held in cells with a 0.06 mm pathlength using ZnSe and BaF_2 windows from Harrick Scientific. Interferograms were signal-averaged (128 scans each), then transformed using a Happ-Genzel apodization function to provide spectra with a nominal resolution of 4 cm^{-1} . Background spectra of ZnSe or the BaF_2 windows and water were used in generating transmittance spectra.

Raman Spectroscopy

Raman instrumentation and calibration are described elsewhere [Williams, 1986]. The spectrometer was calibrated daily using the 546.074 nm (18312.3 cm^{-1}) Hg vapor line. The laser was operated at 514.5 nm with typically 200 mW of light power focused at the sample to a beam with a diameter of about 0.1 mm. Samples, typically about 5 μl in melting point capillaries, were held thermostated at 20° . The concentration of water in each sample was 50% by volume.

Difference Spectra

It is often difficult to distinguish differences between two spectra of similar molecules. One means of accentuating the differences between spectra is by taking the difference of the two spectra. The result is called a difference spectrum. Difference spectra are generated by digitally subtracting one spectrum from another. The subtraction is complete when identical peaks in the two spectra cancel, leaving a zero baseline. Only peaks whose frequencies shift or intensities change remain (see figure 3.31). Difference spectra are helpful for different isotopic species of a single molecule, or, like in Ludlam *et al* [1995], between intermediates in a reaction pathway. Difference spectra of ^{13}C and ^{15}N labelled alanines versus normal isotopic alanine were made using the “sub” routine on the Cromemco computer.

2.2 Computational Chemistry

An outline of the programs used to run the calculations is shown in Figure 2.1. Calculations begin after choice of a model (Figure 1.2). Included in the model are the molecule to be studied, and the theoretical level and basis set to be used for the *ab initio* calculations. An initial geometry (input as filename.com) is input to GAUSSIAN which optimizes the geometry. This procedure relaxes the input geometry to a point on the potential energy surface where all the forces on the nuclei are zero. This is the equilibrium geometry; thermal energy of the system is not incorporated into this structure. Then an *ab initio* frequency job (input is filenamef.com) is run. The “filenamef” is our lab protocol, the “f” signifying a frequency job has been performed, it will be abbreviated to “fnf.” During the frequency calculation force constants are derived. If negative frequencies are calculated, the force constants are not used in later normal mode calculations, negative frequencies are an indication that the geometry was not completely relaxed. All of our *ab initio* calculations were performed using GAUSSIAN, a commercially available program.

Normal mode (GF) calculations (see Figure 1.2) are performed using programs designed to implement the scaled quantum mechanical force field (SQMFF, the term “SQMFF” refers to a set of corrected force constants originally derived from quantum mechanical calculations, in contrast to empirically derived force constants) methodology [Fogarasi and Pulay, 1985] and a general vibrational analysis system distributed by the Quantum Chemistry Program Exchange (QCMP # 012). Part of this SQMFF program package is a series of related programs developed by Peter Pulay and co-workers in the 1970s at the Etvös University, Budapest. They include the BMAT program which handles internal coordinates written by Peter Pulay, and the SCALE2 program written by Gabor Pongor. These programs have been extensively modified by Dr. Williams (thesis advisor) to use the Basic Linear Algebra Subroutines (BLAS) and LAPACK packages, and to produce input for the \TeX typesetting program to facilitate interpretation of the output.

This suite of programs requires three inputs:

1. The *ab initio* (Gaussian) results (fnf.log) provide the force constants, atomic masses, and geometry of the atoms in the molecule.
2. A file defining the local symmetry coordinates (fnf.ici). The symmetry coordinates we use are those suggested by Pulay *et al* [1979] with inclusion of the optional symmetrized combinations for CH, NH, and CO stretches [Fogarasi and Pulay, 1985]. The local symmetry coordinates are a description of the relationships between the atoms: stretches, bends, and torsions. The symmetry coordinate representation of the molecule has several advantages: it eliminates redundancy found in internal representations, it is defined in terms of nearby atoms which facilitates transferability [Fogarasi and Pulay, 1984, 1985; Krimm and Bandekar, 1986], and the coordinates are easy to visualize [Wilson, 1939].
3. A file listing experimental frequencies and scale factors (fnf.sca). Experimental frequencies for all isotopic species can be incorporated into this file. Only one

set of scale factors is used for all isotopic species.

The suite of programs is managed by *vibscaler*, which runs each program in turn and extracts and combines data and files in preparation for the next program.

Gausstofct extracts the force constant data from the G92 *fnf.log* file creating the *fnf.fci* file. *Icrdef* combines data from the G92 *fnf.log* file with the symmetry coordinates in the *fnf.ici* file to create *fnf.ico* and *fnf.geo*. The *fnf.fci* and *fnf.ico* files are combined and are input to *fct*. *Fct* creates several files, *fnf.fct* for input into the graphics programs, *fnf.mas* which lists the masses of the atoms in the molecule for use in calculating the G matrix, and *fnf.fma*, the force matrix.

The *fnf.mas* file from *fct* and the *fnf.geo* file from *icrdef* are combined to make a *fnf.gei* file for input to *geometc*. *Geometc* creates the G matrix. The *fnf.gei* file can be modified to incorporate isotopic substitutions in the masses for direct input into *geometc* to create modified G matrices. These modified G matrices are incorporated into the final *fnf.sci* file separately. The G matrix is written to the *fnf.gep* file.

The *fnf.fma* file from *fct*, the *fnf.gep* file from *geometc* and the *fnf.sca* input file are combined to create the *fnf.sci* file for input to *scaletex* (a modified version of SCALE2). The *fnf.sci* file can be appended to contain the modified G matrices along with the normal isotopic G matrix. Each GF calculation is run separately, the modified G matrix calculations use the same F matrix as the normal isotopic species. *Scaletex* performs a least squares analysis and adjusts the scale factors to a "best fit" between the experimental and calculated frequencies. The output compares the experimental to calculated frequencies and lists the potential energy distribution (PED, the PED is a description of each vibration in terms of the symmetry coordinates). Least squares calculations do not always provide the best PED interpretations of the data. Modifications to the original scale factors can be made in the *fnf.sci* file and *scaletex* can be rerun using *scaleta*.

Other programs in the package written by Dr. Williams (*sca2vib*, *vib2*, *vib2ortep*, and *gauss2ortep*) convert data formats and provide for graphical repre-

sensation of the results using ORTEP-II [Johnson, 1976, obtained from Oak Ridge National Laboratory] and other molecular graphics packages.

***ab initio* Calculations—Determination of the Force Constants**

We use the Hartree-Fock level of theory with the 4-31G basis set [Ditchfield, *et al*, 1971], which have been determined to predict spectra of small molecules as accurately as other levels of theory and larger basis sets [Latajka *et al*, 1989; Lowrey and Williams, 1992b]. The use of higher levels of theory and larger basis sets does not eliminate the need for scaling [Lowrey and Williams, 1992b]. Calculation of force constants begins by optimizing an input structure. The input structure is specified in either Cartesian coordinates or Z-matrix format. For small molecules the Z-matrix format is relatively simple. There are seven columns and as many rows as there are atoms. The first column specifies new atoms. The second column identifies an atom to which the new atom is attached. The third column gives the interatomic distance, the bond length. The fourth column identifies an atom which forms an angle with the first two, the angle being given next. Then a fourth atom is identified which forms a dihedral angle with the first three and the final column assigns a value for the dihedral angle.

The input geometry is optimized by energy minimization. Use of non-minimized structures often yield imaginary frequencies in the calculation of a spectrum because there are non-zero forces acting on the structure. The optimized structure is then used to calculate the second derivative of the energy with respect to displacements, which is the force field.

GAUSSIAN 90 and GAUSSIAN 92 (G92) [referenced under Gaussian 92] are commercially available programs for performing *ab initio* calculations. They were executed on the CRAY X-MP at the National Cancer Institute Supercomputer Center (NCISC), and a DEC Alpha at the USUHS. All geometry optimizations were performed to stationary points. The restricted Hartree-Fock (RHF) level and 4-31G

basis set were used for all models, additional calculations using larger basis sets are noted below. One set of unrestricted Hartree-Fock (UHF) calculations was performed on alaninate using the 4-31G basis set to check the RHF results. There were no differences, in calculated frequencies or PED assignments, from the RHF calculations (data not shown). UHF calculations must be used in systems containing unpaired electrons. UHF calculations are performed on each electron, as opposed to RHF calculations where all orbitals are doubly occupied and calculations are performed on pairs of electrons (one spin up, one spin down) [Foresman and Frisch, 1993].

Optimizations were performed for both isolated and supermolecule alanine at pH = 13 and supermolecule alanine at pH = 1 with the standard 4-31G*, 6-31G**, and 6-31+G** basis sets. Optimizations were also performed on acetate and methylamine, both in base, with the 6-31G** basis set. These are all double zeta basis sets, this means that valence orbitals are represented by two differently sized basis functions. This allows the orbital to change size. The ** in a basis set designation indicates that polarization functions have been added to all nuclei. Polarization functions give orbitals the ability to change shape by adding atomic orbitals with higher angular momenta than required for the ground state. The + refers to the addition of diffuse functions to the orbitals. These functions provide added electronic probability far from the nuclei. Diffuse functions are good for lone pairs of electrons, unpaired electrons, or molecules with significant negative charge [Foresman and Frisch, 1993]. All geometries were optimized to stationary points.

All *ab initio* force constant and frequency calculations were performed using the calculated reference geometries to obtain force constants. No force constants were used that gave negative frequencies. All frequency calculations were performed at the same level of theory and using the same basis sets as the corresponding geometry optimizations. The G92 Cartesian force matrix in units of Hartrees·Bohr⁻² was converted to mdyne·Å⁻¹ by multiplying the matrix by a factor of 15.56919. Cartesian coordinate force matrices from G92 were transformed into complete internal coordinate

force matrices. (This allows a direct comparison of FCs for specific functional groups in different molecules.) Hydrogen bonded rings in supermolecules lead to ring redundancies in the definitions of several of the hydrogen-bond related coordinates. These extra coordinates were simply omitted from the calculations of symmetry coordinates for the supermolecule calculations. In alaninate, the choice of coordinates omitted was based on results of previous calculations where the coordinates omitted were varied. These calculations demonstrated that, in most cases, the only frequencies that change were those related to the hydrogen bonded water molecules. Internal coordinate force matrices were differentially scaled with a least squares method (Scaletex) to fit the calculated frequencies to the experimental frequencies. Each coordinate was scaled independently.

Water-Excluded Configurations

To avoid artifacts related to vibrational coupling of statically bound water in supermolecules and the redundant coordinates in hydrogen bonded rings, Cartesian coordinates and force constants related to water molecules were removed, for water-excluded normal mode analyses. The electronic effects due to the hydrogen bonds present in the supermolecule representation is preserved. The Cartesian coordinates and force constants for water were removed following the *ab initio* calculation of the force constants, but prior to the transformation of the representation into internal coordinates. The resulting geometries are no longer stationary with respect to the 4-31G basis set, they are not equilibrium geometries. They do still retain the hydrogen bond structure. However, the practice of performing normal mode frequency calculations on non-stationary, corrected [Fogarasi and Pulay, 1985; Pulay *et al*, 1979], or model geometries is standard [Krimm and Bandekar, 1986]. Normal mode scale factor calculations were performed on the water-excluded structures only after the force constants were determined from the stationary reference geometries of the complete supermolecules.

Normal mode calculations—Development of the Scale Factors

Following determination of reference geometries and force constants, normal mode calculations can be performed. Isolated and supermolecule normal mode calculations were performed on the respective reference geometries and sets of force constants. The water-excluded calculations were performed using force constants and geometries derived from the supermolecule calculations, only the force constants and Cartesian coordinates for water were removed.

The removal of water from optimized supermolecule geometries results in a molecular geometry that is no longer the lowest energy structure, which was indicated as being the reference structure for use in building the set of scale factors; the lowest energy structure would be the isolated geometry. However, the goal in developing the water-excluded geometry was to model hydrogen bonding effects while eliminating the problems of ring coordinate redundancies and the artificially calculated vibrational coupling of statically bound water molecules with the solute. The structure used represents the geometries of hydrogen bonded polar groups, not an isolated structure. The problem with using a non-optimized geometry is that imaginary, or negative, frequencies are predicted. The G92 frequency calculations, from which the force constants were determined, did not produce imaginary frequencies on the supermolecule geometries used. This demonstrates that the input geometries were valid structures. It was only after the *ab initio* calculations were completed that the Cartesian coordinates and force constants for water were removed. Normal mode frequency calculations can be performed on any input geometry.

For proteins, *ab initio* optimized geometries are impossible. However, experimental data, like that found in the protein data bank (PDB), can be used. The usefulness of the force field being developed is that model geometries, based on many kinds of data, could be incorporated into normal mode analyses. The bacteriorhodopsin ground state structure is well-understood [Henderson *et al*, 1990]. A geometry reflecting the changes postulated by Ludlam *et al* could readily be deter-

mined for incorporation into a normal mode calculation.

In the alaninate calculations, two supermolecule structures were optimized. The starting geometry for the carboxylate oxygen to carboxylate oxygen bridged structure (bottom of Figure 3.26) was based on previous work performed on acetate [Williams and Lowrey, 1991] and glycinate [Lowrey *et al*, 1993]. The other hydrogen bonded geometries (top and middle of Figure 3.26) are not based on previous work and optimizations were begun with geometries very similar to those finally obtained. Differences between the model and actual geometries are compensated for in the scaling procedure. The actual geometry of molecules in solution is not well defined and is a mixture of structures. Thus we do not know exactly what the effects of solvation are on structure. Compensation for these errors are made in the scaling process.

After the initial calculation, adjustments to the scale factors are made to optimize the force constants. These adjustments can do two things, they can change the PED by shifting coordinates from one frequency to another, and they can alter the calculated frequencies. Data from isotopic substitutions provides insight into the PED assignments. Calculated PEDs must reflect what is known from experimental data. Judgment must be used to adjust the scale factors so that the PEDs reflect what is known about the vibrational modes of the molecule as well as minimize the differences between calculated and observed frequencies. Coordinate assignments can be determined using isotopic substitutions, the literature, or empirical data. Shifts in frequencies due to isotopic substitution must also be reflected in the calculated frequencies.

2.3 Fermi Resonance Calculations

A Fermi resonance is the enhancement of an overtone vibration (which is not usually observed) by resonance with a nearby fundamental. Both the overtone

and fundamental vibrations contributing to the resonance shift frequency. Overtone vibrations are either a doubling of a fundamental or a combination of two nearby fundamentals. Unperturbed vibrational frequencies can be determined from the observed vibrational frequencies and the intensities of the observed peaks using a combination of equations [Krimm and Dwivedi, 1982]:

$$\nu_A = \frac{1}{2}[(\nu_A^0 + \nu_B^0) + s] \quad (2.1)$$

$$\nu_B = \frac{1}{2}[(\nu_A^0 + \nu_B^0) - s] \quad (2.2)$$

where $s = \nu_A - \nu_B$ and

$$I_R \equiv \frac{I_B}{I_A} = \frac{s - \delta}{s + \delta} \quad (2.3)$$

where $\delta = \nu_A^0 - \nu_B^0$. Experimental determination of ν_A , ν_B , and the intensity ratio I_R allows the calculation of the unperturbed fundamental, ν_B^0 , and the unperturbed overtone, ν_A^0 . The calculated overtone should be nearly equal to twice the frequency of a fundamental, or the sum of two nearby fundamentals.

Chapter 3

RESULTS

3.1 Outline of Results Presented

For each molecule, several results are presented: the calculated optimized structure used to calculate the force constants; the symmetry and internal coordinate definitions used; the experimental IR and Raman spectra for all isotopic species studied; and, from the normal mode analysis, the calculated potential energy distribution (PED) and a comparison of experimental and calculated frequencies.

The experiments completed are separated into sections. The first section shows results for the study of different hydration models using methanol and ethanol as examples. Isolated geometries optimized to aqueous frequencies, supermolecules, and self consistent reaction field models are compared.

The second section shows results of calculations for small molecules using the water-excluded model. These results built a consistent set of scale factors for the water-excluded model for application to larger molecules. Scaling was completed using PED information from previous studies. Molecules studied in this section are methylamine (acid and base structures), acetate, glycine in acid and base conformations, and *N*-methylacetamide.

The scale factors from the second section were used to build scale factors for

alanine. The results from alanine provide scale factors for the unique C^α coordinates. This was new work. Results were obtained for several hydration models and basis sets. Both acidic and basic conformations were scaled.

Finally, the last section gives the results for alanyl-alanine. Acidic, neutral, and basic conformations were modeled. Isolated and two-water water-excluded models were scaled for all three conformations. In addition, two one-water structures for the basic conformation were scaled. These results provide scale factors for the peptide bond coordinates, and for hydrogen bonded peptide bonds.

3.2 Methanol and Ethanol—Testing Hydration Models

Optimized structures for methanol and ethanol are shown in Figure 3.1. Raman spectra of aqueous solutions of the four isotopic species of methanol used in the frequency optimization are shown in Figure 3.2. The spectra are from Williams *et al* [1995]. Raman spectra for ethanol are shown in Figures 3.3, 3.6, and 3.9. The hydrogen stretching frequencies for ethanol are shown in Figures 3.4, 3.7, and 3.10. Infrared spectra of ethanol are shown in Figures 3.5, 3.8, and 3.11 for the three isotopic species used.

Definitions for internal coordinates and symmetry coordinates for both methanol and ethanol are listed in Tables 3.1 and 3.2. The atomic numbering schemes used in these tables is the same as those for the figures. Optimized internal coordinates are listed in Table 3.3. Internal and symmetry coordinate definitions were kept constant for all hydration models examined. Calculations performed in support of my thesis were methanol SCRF, isolated ethanol, two water ethanol supermolecule, and ethanol SCRF. Other hydration models examined for methanol are from Williams *et al*, 1995.

Figure 3.1: Optimized Structure of Methanol using SCRF (top), Isolated Ethanol (upper middle), Ethanol two-water supermolecule (lower middle), and Ethanol using SCRF (bottom).

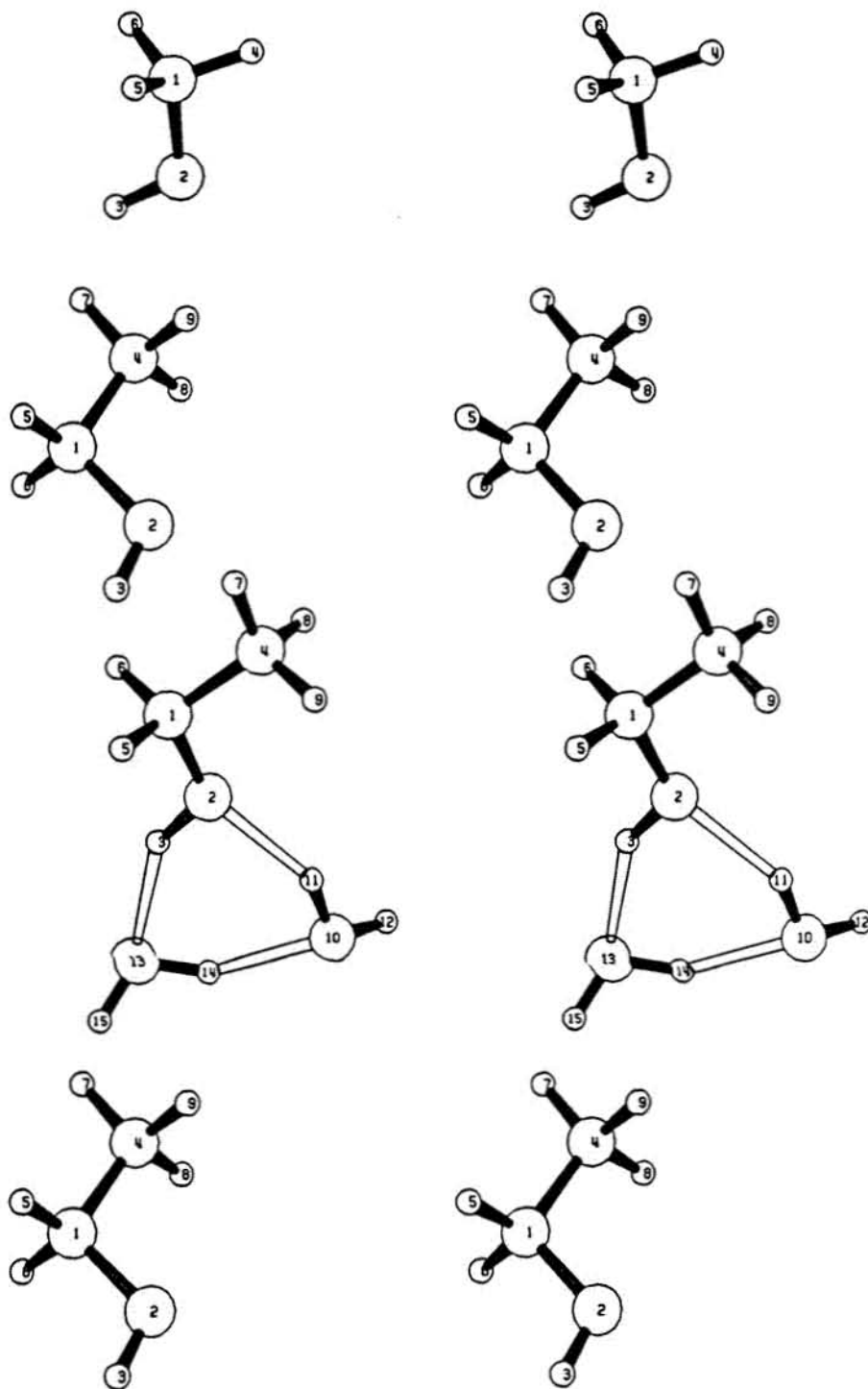


Figure 3.2: Raman spectra of aqueous solutions of methanol. From top to bottom, CD_3OD , line with two dashes, 50% v/v in D_2O ; CD_3OH , line with dot, 10% v/v in H_2O ; CH_3OD , line with one dash, 10% v/v in D_2O ; and CH_3OH , solid line 50% v/v in H_2O .

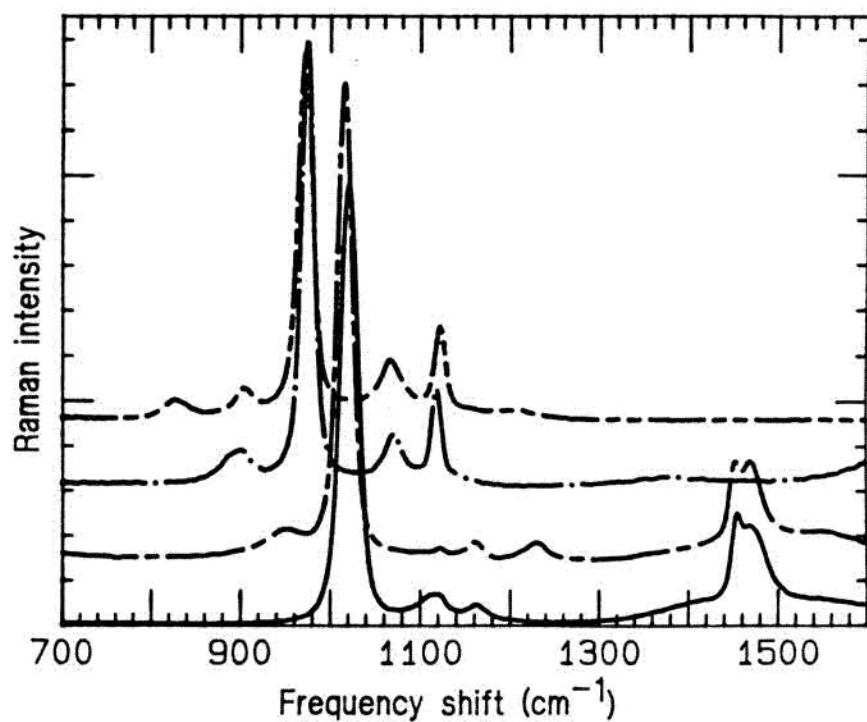


Figure 3.3: Raman spectrum of 50% ethanol in H₂O (200–1600 cm⁻¹).

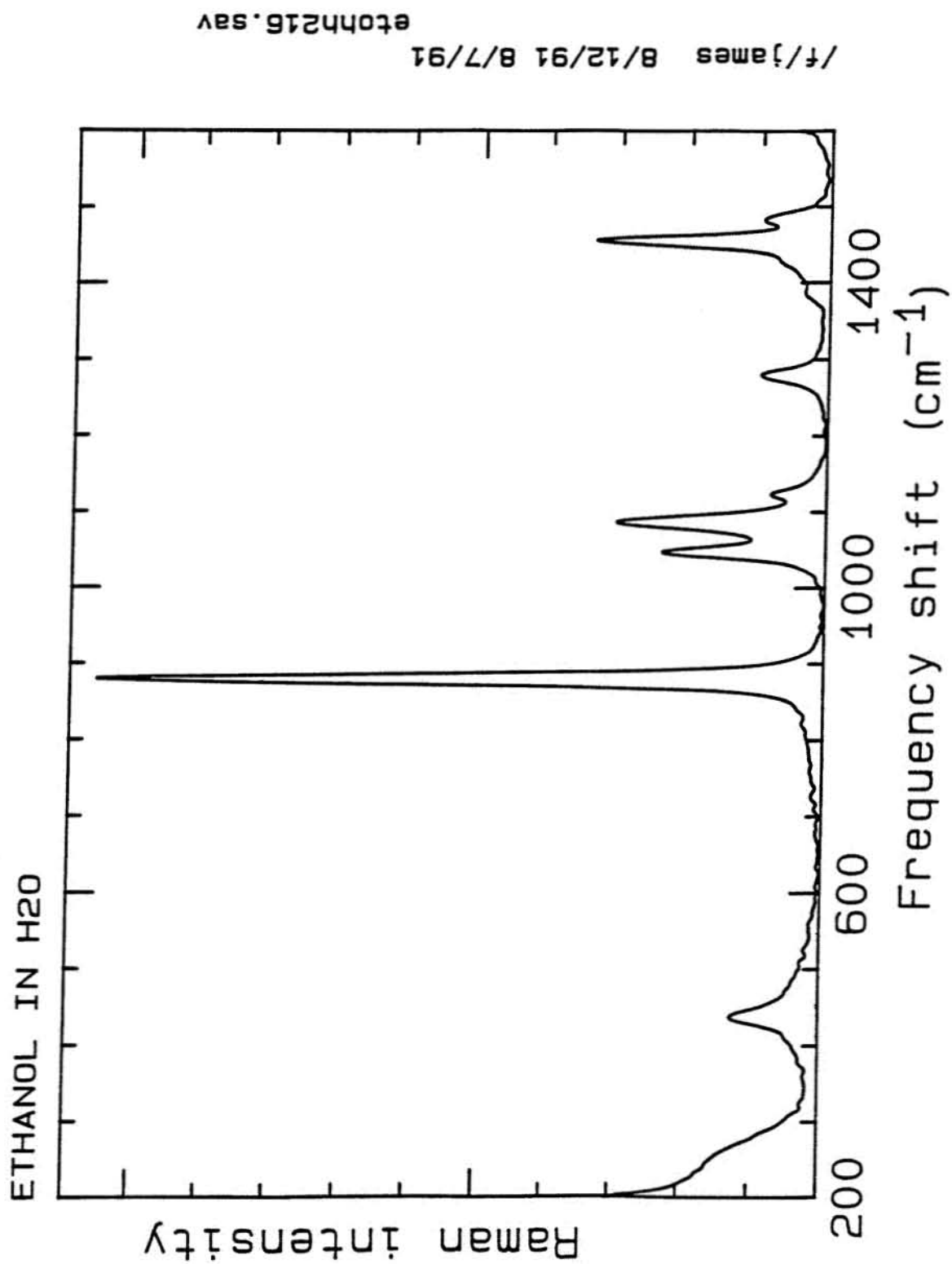


Figure 3.4: Raman spectrum of the hydrogen stretching region for 50% ethanol in H_2O .

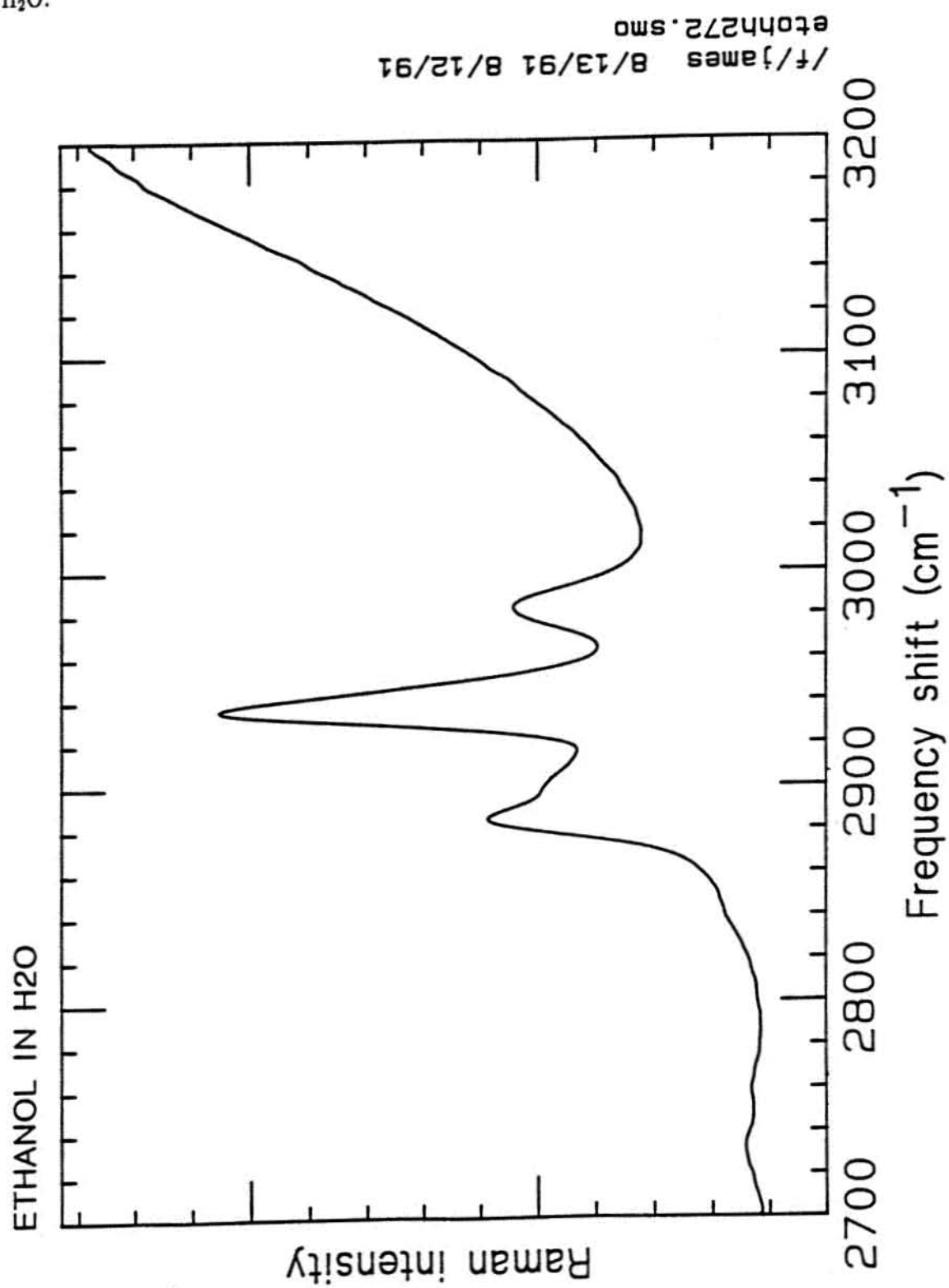


Figure 3.5: Infrared spectrum of 50% ethanol in H₂O.

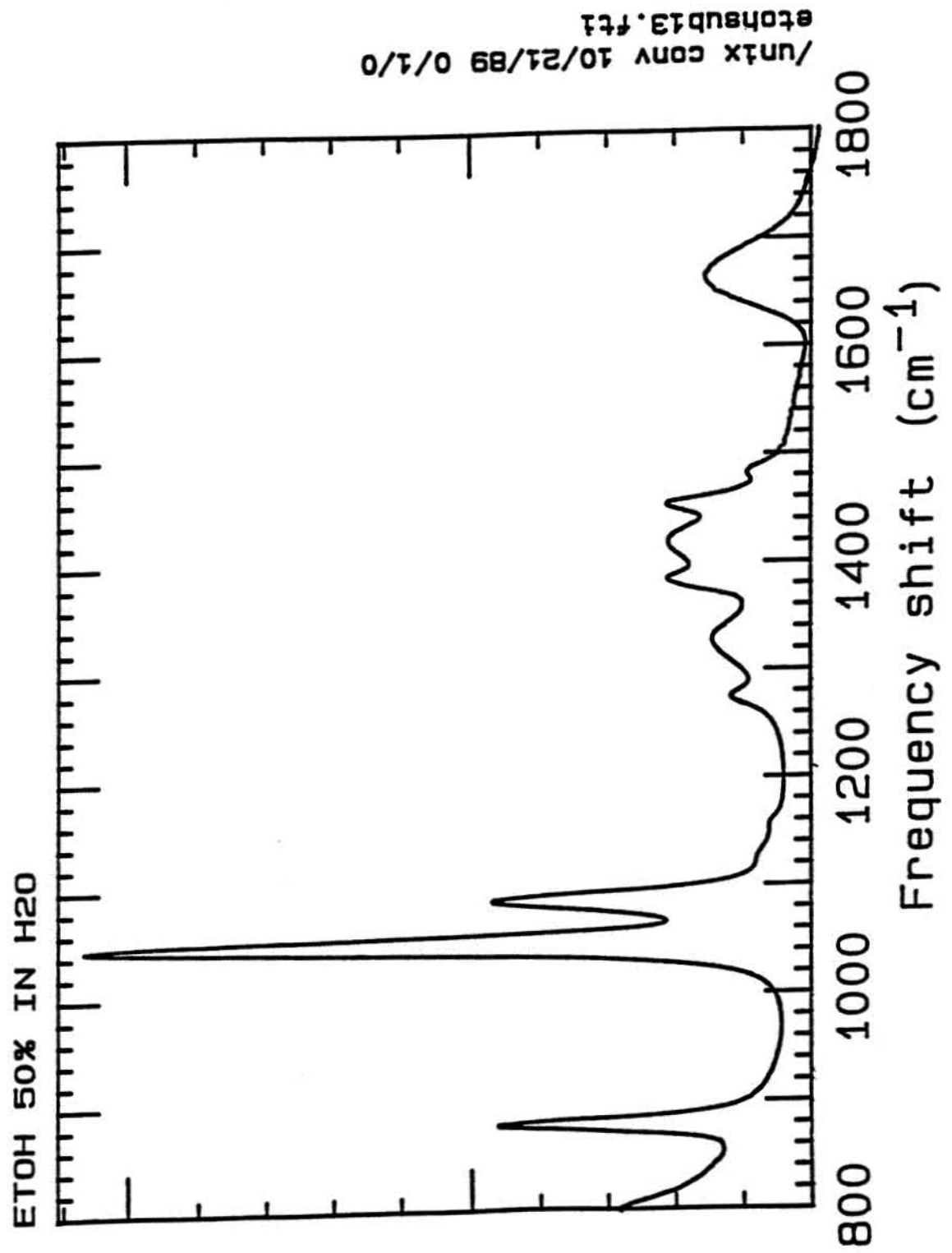


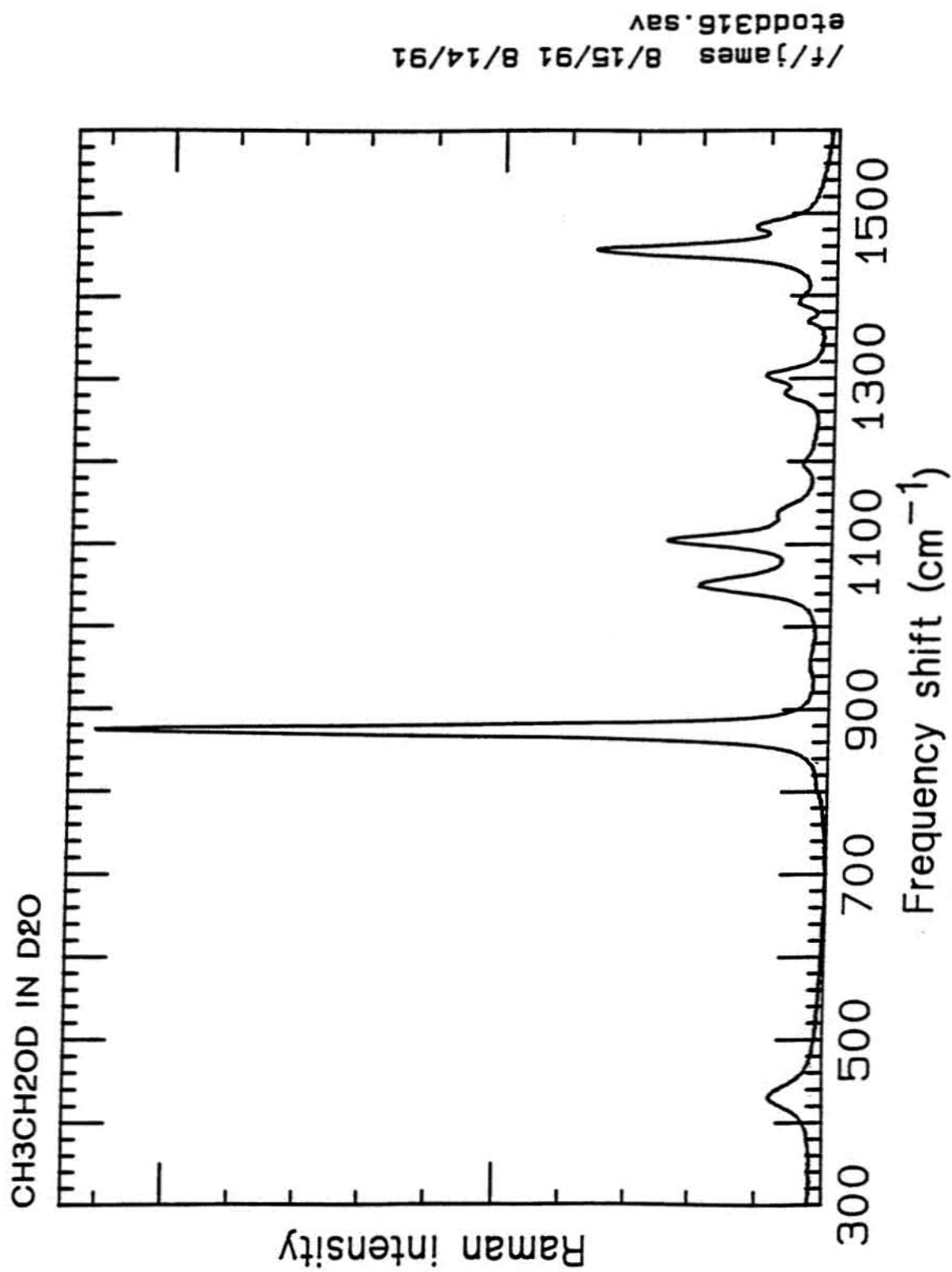
Figure 3.6: Raman spectrum of 50% ethanol in D₂O.

Figure 3.7: Raman spectrum of the hydrogen stretching region of 50% ethanol in D_2O .

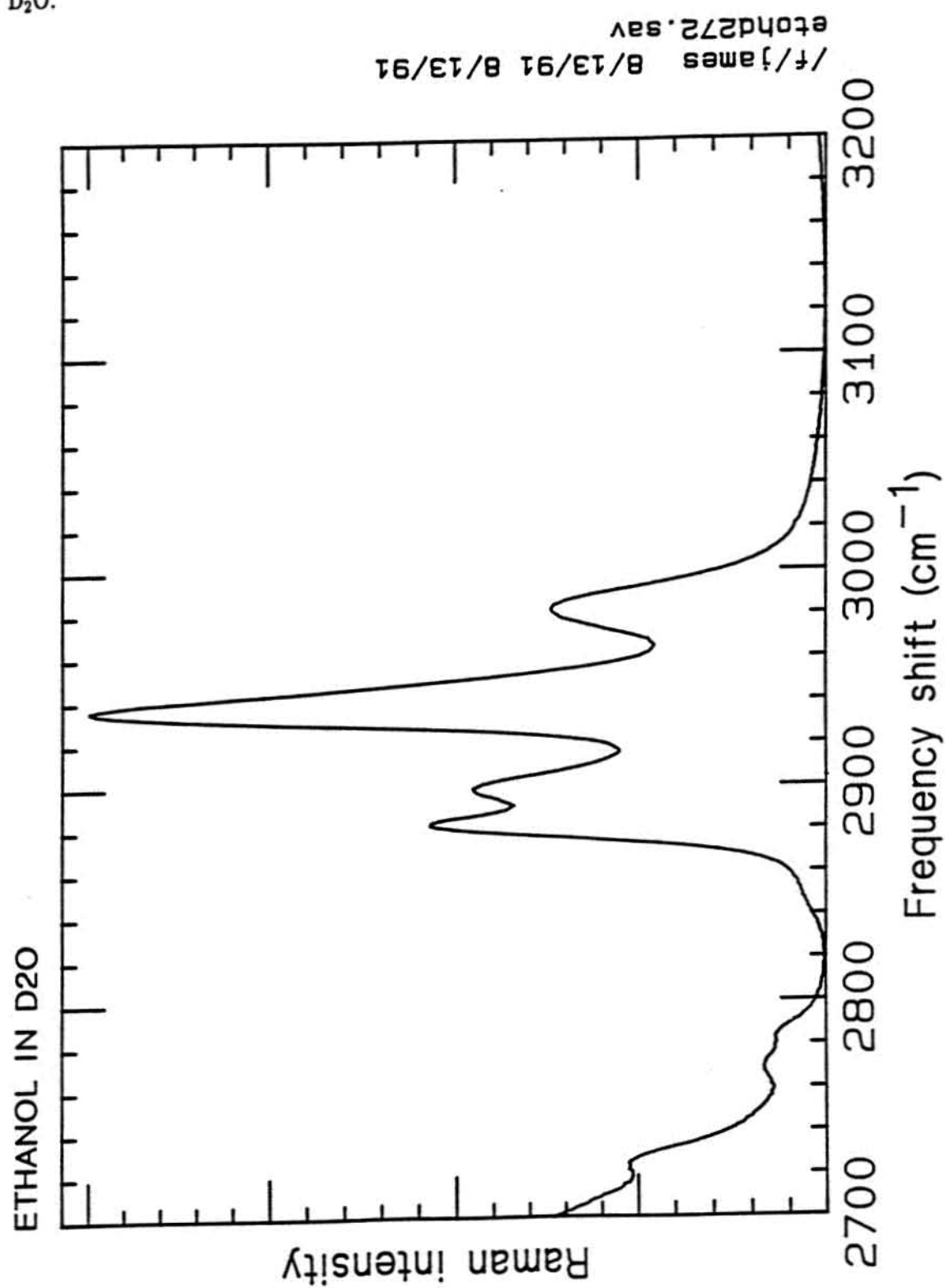


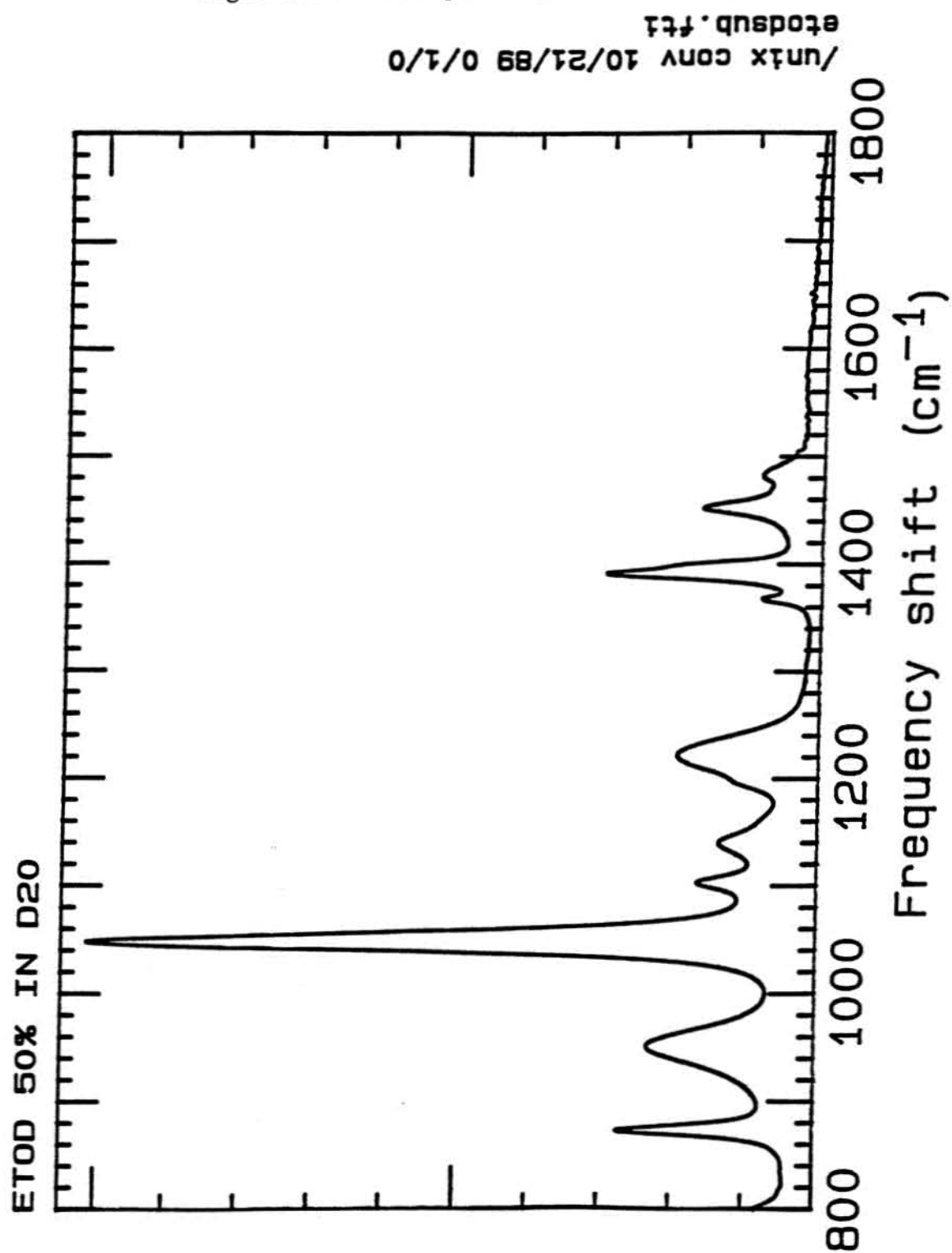
Figure 3.8: Infrared spectrum of 50% ethanol in D₂O.

Figure 3.9: Raman spectrum of CD_3 substituted ethanol, 50% in H_2O .

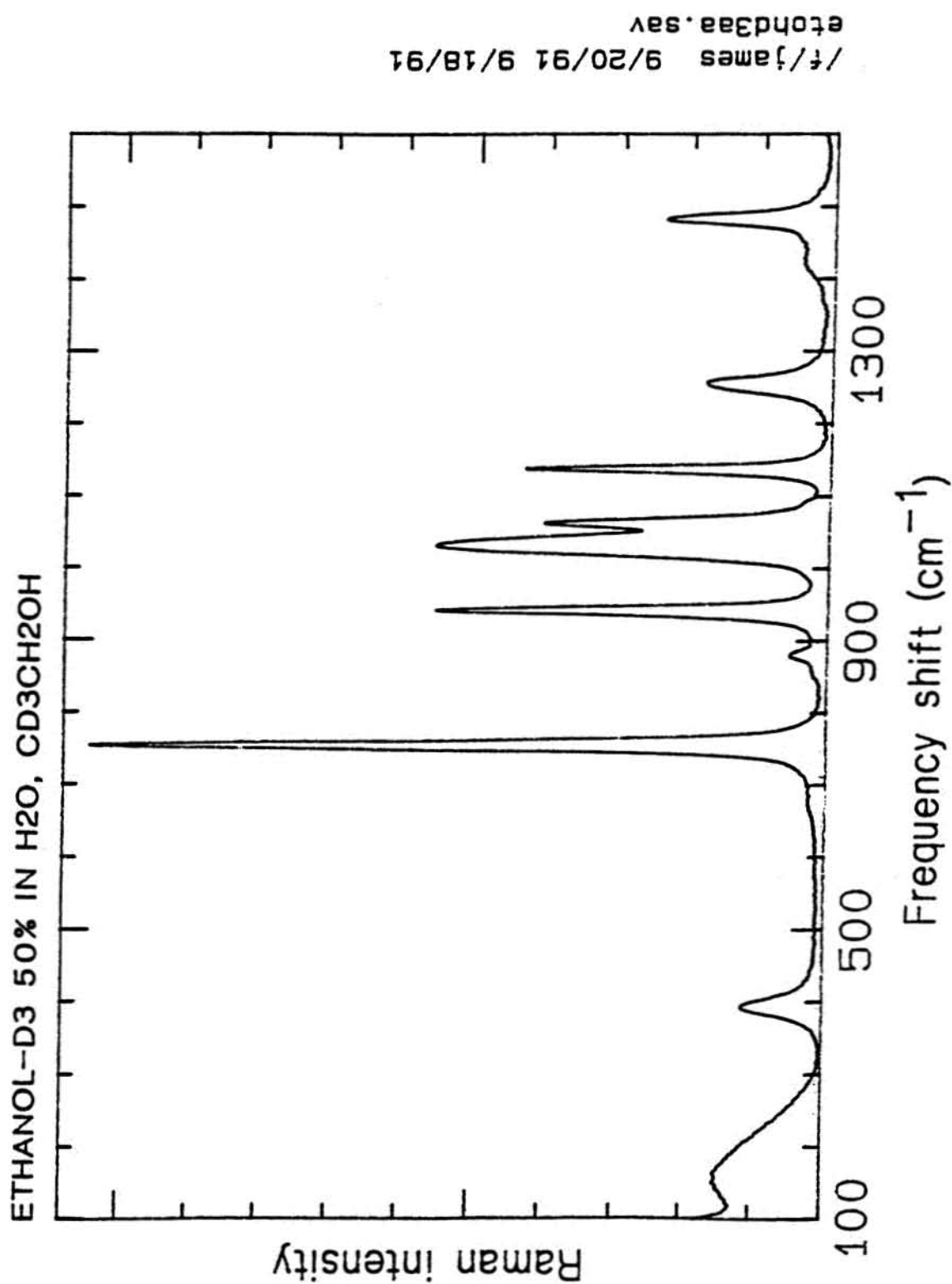


Figure 3.10: Raman spectrum of the hydrogen stretching region of CD₃ substituted ethanol, 50% in H₂O.

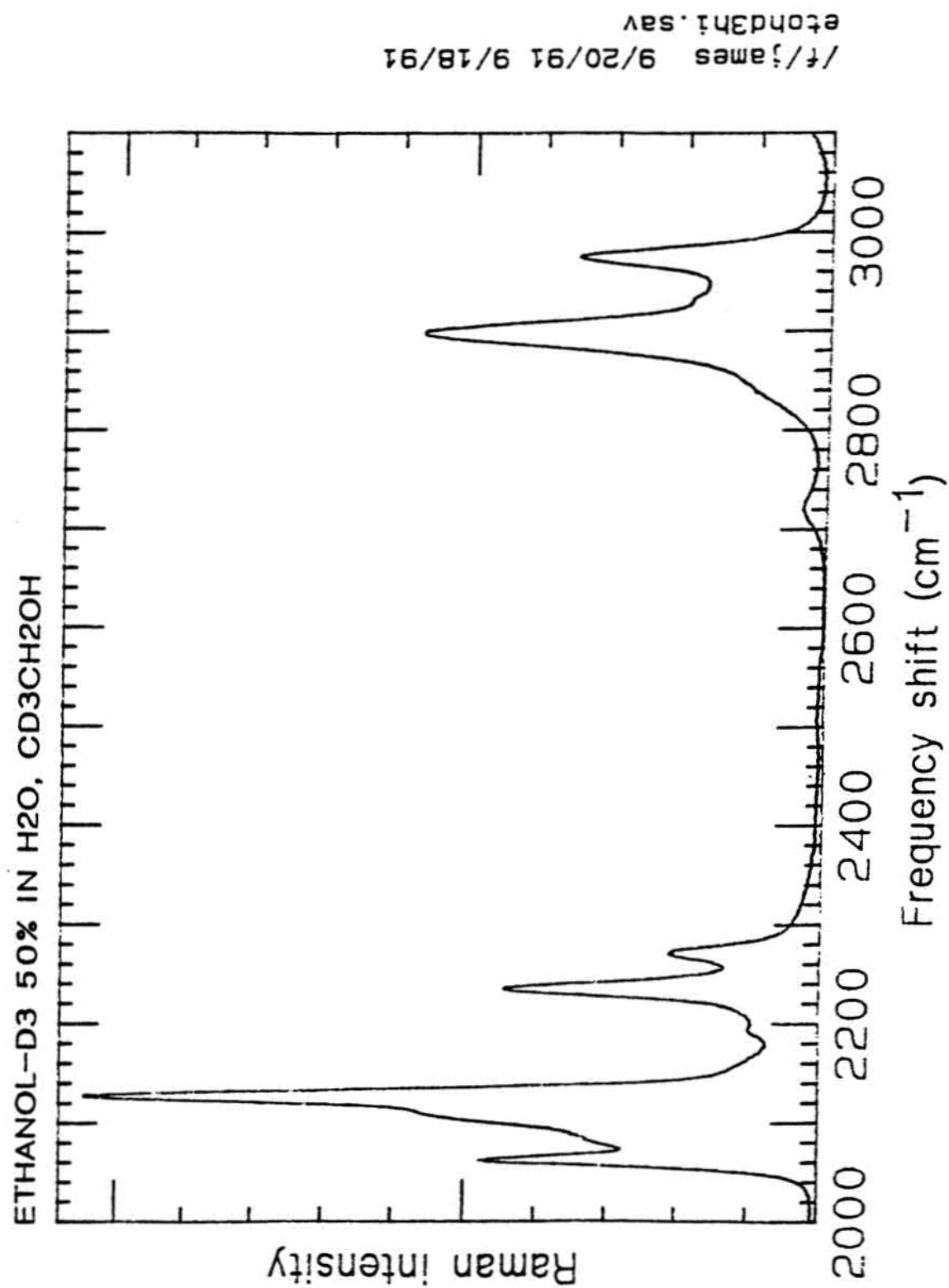


Figure 3.11: Infrared spectrum of CD_3 substituted ethanol in H_2O .

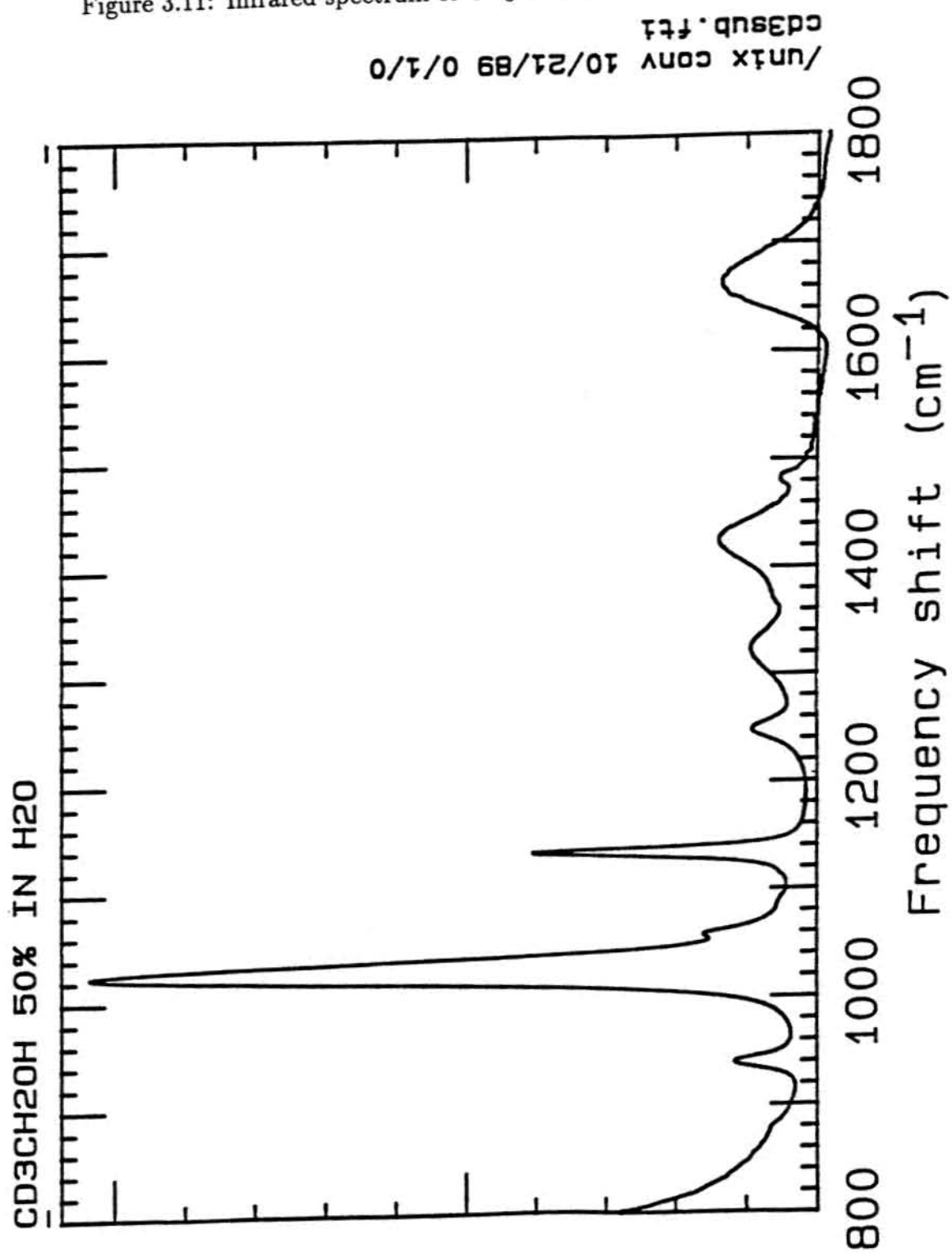


Table 3.1: Redundant Internal Coordinates for Methanol and Ethanol

Methanol ^a	
$R_1 = \Delta\gamma(\text{O}^2\text{-C}^1)$	$R_8 = \Delta\theta(\text{H}^5\text{-C}^1\text{-O}^2)$
$R_2 = \Delta\gamma(\text{H}^3\text{-O}^2)$	$R_9 = \Delta\theta(\text{H}^6\text{-C}^1\text{-O}^2)$
$R_3 = \Delta\gamma(\text{H}^4\text{-C}^1)$	$R_{10} = \Delta\theta(\text{H}^5\text{-C}^1\text{-H}^6)$
$R_4 = \Delta\gamma(\text{H}^5\text{-C}^1)$	$R_{11} = \Delta\theta(\text{H}^5\text{-C}^1\text{-H}^4)$
$R_5 = \Delta\gamma(\text{H}^6\text{-C}^1)$	$R_{12} = \Delta\theta(\text{H}^6\text{-C}^1\text{-H}^4)$
$R_6 = \Delta\theta(\text{H}^3\text{-O}^2\text{-C}^1)$	$R_{13} = \Delta\tau(\text{O}^2\text{-C}^1)$
$R_7 = \Delta\theta(\text{H}^4\text{-C}^1\text{-O}^2)$	
Ethanol	
$R_1 = \Delta\gamma(\text{O}^2\text{-C}^1)$	$R_{13} = \Delta\theta(\text{H}^5\text{-C}^1\text{-O}^2)$
$R_2 = \Delta\gamma(\text{H}^3\text{-O}^2)$	$R_{14} = \Delta\theta(\text{H}^6\text{-C}^1\text{-C}^4)$
$R_3 = \Delta\gamma(\text{C}^4\text{-C}^1)$	$R_{15} = \Delta\theta(\text{H}^6\text{-C}^1\text{-O}^2)$
$R_4 = \Delta\gamma(\text{H}^5\text{-C}^1)$	$R_{16} = \Delta\theta(\text{H}^8\text{-C}^4\text{-H}^9)$
$R_5 = \Delta\gamma(\text{H}^6\text{-C}^1)$	$R_{17} = \Delta\theta(\text{H}^8\text{-C}^4\text{-H}^7)$
$R_6 = \Delta\gamma(\text{H}^7\text{-C}^4)$	$R_{18} = \Delta\theta(\text{H}^9\text{-C}^4\text{-H}^7)$
$R_7 = \Delta\gamma(\text{H}^8\text{-C}^4)$	$R_{19} = \Delta\theta(\text{H}^7\text{-C}^4\text{-C}^1)$
$R_8 = \Delta\gamma(\text{H}^9\text{-C}^4)$	$R_{20} = \Delta\theta(\text{H}^9\text{-C}^4\text{-C}^1)$
$R_9 = \Delta\theta(\text{H}^3\text{-O}^2\text{-C}^1)$	$R_{21} = \Delta\theta(\text{H}^8\text{-C}^4\text{-C}^1)$
$R_{10} = \Delta\theta(\text{H}^6\text{-C}^1\text{-H}^5)$	$R_{22} = \Delta\tau(\text{O}^2\text{-C}^1)$
$R_{11} = \Delta\theta(\text{C}^4\text{-C}^1\text{-O}^2)$	$R_{23} = \Delta\tau(\text{C}^4\text{-C}^1)$
$R_{12} = \Delta\theta(\text{H}^5\text{-C}^1\text{-C}^4)$	

^aSymbols: γ = stretch, θ = bend, ω = out of plane bend, τ = torsion.

Table 3.2: Symmetry Coordinate Definitions for Methanol and Ethanol

Methanol	
CO s ^a	$S_1 = R_1$
OH s	$S_2 = R_2$
CH ₃ ss	$S_3 = (R_3 + R_4 + R_5)/\sqrt{3}$
CH ₃ as ¹	$S_4 = (2R_3 - R_4 - R_5)/\sqrt{6}$
CH ₃ as ²	$S_5 = (R_4 - R_5)/\sqrt{2}$
OH b	$S_6 = R_6$
CH ₃ sd	$S_7 = (R_{10} + R_{11} + R_{12} - R_7 - R_8 - R_9)/\sqrt{6}$
CH ₃ ad ¹	$S_8 = (2R_{10} - R_{11} - R_{12})/\sqrt{6}$
CH ₃ ad ²	$S_9 = (R_{11} - R_{12})/\sqrt{2}$
CH ₃ r ¹	$S_{10} = (2R_7 - R_8 - R_9)/\sqrt{6}$
CH ₃ r ²	$S_{11} = (R_8 - R_9)/\sqrt{2}$
CO ^H t	$S_{12} = R_{13}$
Ethanol	
CO s	$S_1 = R_1$
OH s	$S_2 = R_2$
CC s	$S_3 = R_3$
CH s ¹	$S_4 = R_4$
CH s ²	$S_5 = R_5$
CH ₃ ss	$S_6 = (R_6 + R_7 + R_8)/\sqrt{3}$
CH ₃ as ¹	$S_7 = (2R_6 - R_7 - R_8)/\sqrt{6}$
CH ₃ as ²	$S_8 = (R_7 - R_8)/\sqrt{2}$
OH b	$S_9 = R_9$
CH ₂ scissor	$S_{10} = (5R_{10} + R_{11})/\sqrt{26}$
OCC scissor	$S_{11} = R_{11}$
CH ₂ r	$S_{12} = (R_{12} - R_{13} + R_{14} - R_{15})/2$
CH-2 wag	$S_{13} = (R_{12} - R_{13} - R_{14} + R_{15})/2$
CH ₂ twist	$S_{14} = (R_{12} + R_{13} - R_{14} - R_{15})/2$
CH ₃ sd	$S_{15} = (R_{16} + R_{17} + R_{18} - R_{19} - R_{20} - R_{21})/\sqrt{6}$
CH ₃ ad ¹	$S_{16} = (2R_{16} - R_{17} - R_{18})/\sqrt{6}$
CH ₃ ad ²	$S_{17} = (R_{17} - R_{18})/\sqrt{2}$
CH ₃ r ¹	$S_{18} = (2R_{19} - R_{20} - R_{21})/\sqrt{6}$
CH ₃ r ²	$S_{19} = (R_{20} - R_{21})/\sqrt{2}$
CO ^H t	$S_{20} = R_{22}$
CC t	$S_{21} = R_{23}$

^aAbbreviations: s = stretch, t = torsion, ss = symmetric stretch,

Table 3.2: (continued)

as = antisymmetric stretch, sd = symmetric deformation, ad = anti-symmetric deformation, r = rock, b = bend.

Table 3.3: Optimized Internal Coordinates for Methanol and Ethanol.

Internal Coordinate	Methanol	Ethanol		
	SCRF ^a	Isolated ^b	Two Water	SCRF
Bond Stretches				
O ² -C ¹	1.4341	1.4352	1.4299	1.4354
H ³ -O ²	0.9514	0.9511	0.9629	0.9512
H ⁴ -C ¹	1.0763			
H ⁵ -C ¹	1.0816	1.0841	1.0838	1.0841
H ⁶ -C ¹	1.0816	1.0841	1.0834	1.0841
C ⁴ -C ¹		1.5123	1.5136	1.5123
H ⁷ -C ⁴		1.0833	1.0832	1.0834
H ⁸ -C ⁴		1.0811	1.0817	1.0811
H ⁹ -C ⁴		1.0811	1.0818	1.0811
Angle bends				
H ³ -O ² -C ¹	112.44	113.51	115.60	113.52
H ⁴ -C ¹ -O ²	106.33			
H ⁵ -C ¹ -O ²	111.51	110.14	109.88	110.15
H ⁶ -C ¹ -O ²	111.51	110.15	109.73	110.16
C ⁴ -C ¹ -O ²		117.08	107.92	107.10
H ⁷ -C ⁴ -C ¹		110.76	110.82	110.78
H ⁸ -C ⁴ -C ¹		110.11	110.18	110.11
H ⁹ -C ⁴ -C ¹		110.11	110.24	110.09
Torsions				
H ⁴ -C ¹ -O ² -H ³	180.00			
H ⁵ -C ¹ -O ² -H ³	61.21	59.60	59.34	59.69
H ⁶ -C ¹ -O ² -H ³	-61.21	-59.58	-59.39	-59.49
C ⁴ -C ¹ -O ² -H ³		180.01	-179.98	180.09
H ⁷ -C ⁴ -C ¹ -O ²		180.00	-180.12	180.14
H ⁸ -C ⁴ -C ¹ -O ²		59.60	59.65	59.73
H ⁹ -C ⁴ -C ¹ -O ²		-59.62	-59.88	-59.48

^aSelf Consistent Reaction Field Theory.

Table 3.3: (continued)

Internal Coordinate	Methanol	Ethanol		
	SCRF	Isolated	Two Water	SCRF

^bIsolated geometry scaled to aqueous frequencies.

These optimized geometries were used for calculations of force constants using Gaussian [reference Gaussian]. The calculated force constants were scaled to the spectra in Figures 3.2 and 3.3 using the scheme outlined in Figure 1.2. The scale factors for both methanol and ethanol in various states of hydration are listed in Table 3.4. The methanol scale factors are based on spectra of four isotopic species and those for ethanol on three isotopic species.

Potential energy distributions and frequency predictions from normal mode analyses, using the scaled force constants, are shown for methanol using SCRF theory in Table 3.5, for isolated ethanol scaled to aqueous frequencies in Table 3.6, for the two water ethanol supermolecule in Table 3.7, and using SCRF theory in Table 3.8. All models were scaled to aqueous frequencies for methanol and ethanol.

.52, $p < .01$). Student's t-tests did not show a significant difference between the frequency of use of intrusion (sessions 1 and 2 added together) and the frequency of use of avoidance. Avoidance and intrusion were significantly positively correlated for both individual sessions and the two sessions combined ($r = .69$, $p < .01$ in all cases. Additionally, when paired t-tests were used to examine differences in responding between the two sessions, there were no significant changes in the use of intrusion across the two sessions, nor were there significant changes in the use of avoidance across the two sessions.

Total IES scores (intrusion and avoidance added across the two sessions) accounted for 26% of the variance in total SCL-90R scores, $F(1,57) = 19.77$, $p < .001$. Additionally, total avoidance and total intrusion accounted for significant variance in SCL-90R scores. Avoidance accounted for 20% of the variance, $F(1,57) = 14.34$, $p < .001$ and intrusion accounted for 24% of the variance in SCL-90R scores, $F(1,57) = 18.03$, $p < .001$. Increases in intrusion and avoidance were associated with increases in SCL-90R scores but no significant findings emerged for the physiological or behavioral variables.

Interactions

In addition to their main effects, two different interaction effects were posited, the first being that support and exposure should interact such that low levels of support and high exposure will be associated with greater symptom reporting, poorer task performance and increased blood pressure. However, if support

Table 3.5: Scaled 4-31G Frequencies and Potential Energy Distribution for Methanol Using Self Consistent Reaction Field Theory.

frequency (cm^{-1})			CH ₃ OH (mean deviation = 11 cm^{-1})
obs.	calc.	dev.	Potential Energy Distribution
—	280	—	CO ^H t(100)
1021	1022	1	CO ^H s(98)
1113	1103	-10	CCH ₃ r ¹ (66), OH b(25)
1167	1167	0	CCH ₃ r ² (94)
1416	1433	17	OH b(56), CCH ₃ ad ^{1,2} (21), CCH ₃ sd(13), CCH ₃ r ¹ (12)
1454	1448	-6	CCH ₃ sd(85), CCH ₃ ad ^{1,2} (13)
1471	1470	-1	CCH ₃ ad ^{1,2} (94)
1471	1489	18	CCH ₃ ad ^{1,2} (62), CCH ₃ r ¹ (20), OH b(13)
2845	2869	24	CH ₃ ss(97)
2978	2981	3	CH ₃ as ^{1,2} (99)
3003	3025	22	CH ₃ as ^{1,2} (97)
3390	3394	4	OH s(100)

frequency (cm^{-1})			CH ₃ OD (mean deviation = 23 cm^{-1})
obs.	calc.	dev.	Potential Energy Distribution
—	222	—	CO ^H t(100)
950	917	-33	OH b(77), CCH ₃ r ¹ (23)
1019	1022	3	CO ^H s(103)
1158	1167	9	CCH ₃ r ² (94)
1231	1280	49	CCH ₃ r ¹ (67), OH b(24), CCH ₃ ad ^{1,2} (9)
1454	1447	-7	CCH ₃ sd(97)
1472	1470	-2	CCH ₃ ad ^{1,2} (94)
1472	1480	8	CCH ₃ ad ^{1,2} (85), CCH ₃ r ¹ (10)
2490	2471	-19	OH s(100)
2847	2869	22	CH ₃ ss(97)
2982	2981	-1	CH ₃ as ^{1,2} (99)
2998	3026	28	CH ₃ as ^{1,2} (97)

frequency (cm^{-1})			CD ₃ OH (mean deviation = 14 cm^{-1})
obs.	calc.	dev.	Potential Energy Distribution

Table 3.5: (continued)

frequency (cm^{-1})			Potential Energy Distribution
obs.	calc.	dev.	
—	267	—	CO^H t(100)
889	873	−16	CCH_3 r^1 (88), OH b(9)
901	898	−3	CCH_3 r^2 (99)
974	972	−2	CO^H s(78), CCH_3 sd(22)
1073	1063	−10	CCH_3 $\text{ad}^{1,2}$ (99)
1073	1067	−6	CCH_3 $\text{ad}^{1,2}$ (97)
1118	1116	−2	CCH_3 sd(77), CO^H s(21)
1381	1393	12	OH b(90), CCH_3 r^1 (8)
2081	2056	−25	CH_3 ss(99)
2236	2211	−25	CH_3 $\text{as}^{1,2}$ (99)
2250	2246	−4	CH_3 $\text{as}^{1,2}$ (97)
3350	3393	43	OH s(100)

frequency (cm^{-1})			CD ₃ OD (mean deviation = 16 cm^{-1}) Potential Energy Distribution
obs.	calc.	dev.	
—	205	—	CO^H t(100)
831	802	−29	CCH_3 r^1 (61), OH b(38)
904	898	−6	CCH_3 r^2 (99)
972	966	−6	CO^H s(78), CCH_3 sd(23)
1067	1062	−5	CCH_3 $\text{ad}^{1,2}$ (60), CCH_3 $\text{ad}^{1,2}$ (27), CCH_3 r^1 (8)
1067	1063	−4	CCH_3 $\text{ad}^{1,2}$ (72), CCH_3 $\text{ad}^{1,2}$ (23)
1086	1103	17	CCH_3 sd(37), OH b(26), CCH_3 $\text{ad}^{1,2}$ (14), CCH_3 r^1 (12), CO^H s(11)
1122	1137	15	CCH_3 sd(38), OH b(32), CCH_3 r^1 (16), CO^H s(10)
2079	2056	−23	CH_3 ss(99)
2230	2211	−19	CH_3 $\text{as}^{1,2}$ (99)
2255	2245	−10	CH_3 $\text{as}^{1,2}$ (97)
2501	2472	−29	OH s(100)

Table 3.6: Scaled 4-31G Frequencies and Potential Energy Distribution for Isolated Ethanol

frequency (cm^{-1})			CH ₃ CH ₂ OH (mean deviation = 17 cm^{-1})
obs.	calc.	dev.	Potential Energy Distribution
—	254	—	CC t(88), CO t(9)
—	308	—	CO t(89), CC t(9)
436	437	1	OCC scis(82), CH ₃ r ^{1,2} (10)
—	799	—	CH ₂ twist(48), CH ₃ r ^{1,2} (39), CH ₂ wag(7)
881	864	-17	CC s(41), CO s(35), CH ₃ r ^{1,2} (22)
1047	1009	-38	CC s(50), CO s(36), CH ₃ r ^{1,2} (7)
1087	1093	6	CH ₃ r ^{1,2} (43), CO s(30), OCC scis(10), OH b(7), CH ₂ r(7)
1126	1126	0	CH ₂ twist(48), CH ₃ r ^{1,2} (35), CH ₂ wag(14)
1280	1281	1	CH ₂ wag(78), CH ₃ r ^{1,2} (17)
1331	1302	-29	CH ₂ r(51), OH b(33), CH ₃ r ^{1,2} (10)
1386	1396	10	CH ₃ sd(97)
1456	1439	-17	CH ₃ ad ^{1,2} (92), CH ₃ r ^{1,2} (8)
1456	1451	-5	CH ₃ ad ^{1,2} (54), OH b(22), CH ₂ r(11), CH ₂ scis(7)
1421	1457	36	CH ₃ ad ^{1,2} (35), OH b(28), CH ₂ r(28)
1486	1484	-2	CH ₂ scis(91)
2884	2870	-14	CH s ¹ (50), CH s ¹ (49)
2902	2899	-3	CH s ¹ (49), CH s ¹ (49)
2936	2936	0	CH ₃ ss(94)
2982	2986	4	CH ₃ as(94)
2982	3001	19	CH ₃ as(99)
3390	3398	8	OH s(100)

frequency (cm^{-1})			CH ₃ CH ₂ OD (mean deviation = 17 cm^{-1})
obs.	calc.	dev.	Potential Energy Distribution
—	221	—	CO t(91), CC t(9)
—	263	—	CC t(88), CO t(8)
431	426	-5	OCC scis(82), CH ₃ r ^{1,2} (10)
—	799	—	CH ₂ twist(48), CH ₃ r ^{1,2} (39), CH ₂ wag(7)
875	846	-29	CC s(49), CO s(30), OH b(10), CH ₃ r ^{1,2} (10)
951	934	-17	OH b(51), CH ₃ r ^{1,2} (28), CO s(11)
1051	1041	-10	CO s(53), CC s(31), OH b(7)
1104	1126	22	CH ₂ twist(48), CH ₃ r ^{1,2} (35), CH ₂ wag(14)

Table 3.6: (continued)

frequency (cm^{-1})			Potential Energy Distribution
obs.	calc.	dev.	
1136	1174	38	CH_3 $r^{1,2}$ (39), OH b(23), OCC scis(18), CC s(8)
1282	1281	-1	CH_2 wag(78), CH_3 $r^{1,2}$ (17)
1369	1383	14	CH_2 r(79), CH_3 sd(11)
1392	1399	7	CH_3 sd(87), CH_2 r(8)
1455	1439	-16	CH_3 $ad^{1,2}$ (92), CH_3 $r^{1,2}$ (8)
1455	1454	-1	CH_3 $ad^{1,2}$ (87), CH_3 $r^{1,2}$ (7)
1486	1483	-3	CH_2 scis(95)
2490	2475	-15	OH s(100)
2879	2870	-9	CH s^1 (50), CH s^1 (49)
2898	2899	1	CH s^1 (49), CH s^1 (49)
2935	2936	1	CH_3 ss(94)
2984	2986	2	CH_3 as(94)
2984	3001	17	CH_3 as(99)

frequency (cm^{-1})			CD ₃ CH ₂ OH (mean deviation = 16 cm^{-1})
obs.	calc.	dev.	
—	195	—	CC t(95)
—	303	—	CO t(97)
392	389	-3	OCC scis(73), CH_3 $r^{1,2}$ (20)
—	670	—	CH_3 $r^{1,2}$ (67), CH_2 twist(22)
753	751	-2	CH_3 $r^{1,2}$ (45), CC s(25), CO s(20)
941	921	-20	CC s(39), CH_3 sd(22), CH_3 $r^{1,2}$ (17), OCC scis(12)
1022	1036	14	CO s(63), CH_3 $ad^{1,2}$ (18), CH_3 $r^{1,2}$ (9), OCC scis(8)
1032	1037	5	CH_3 $ad^{1,2}$ (97)
1032	1052	20	CH_3 $ad^{1,2}$ (80), CO s(13)
1061	1052	-9	CH_2 twist(74), CH_3 $r^{1,2}$ (25)
1135	1113	-22	CH_3 sd(67), CC s(27)
1255	1252	-3	CH_2 wag(94)
1320	1285	-35	CH_2 r(58), OH b(38)
1423	1454	31	OH b(50), CH_2 r(40)
1480	1483	3	CH_2 scis(94)
2112	2110	-2	CH_3 ss(99)
2237	2210	-27	CH_3 as(99)

Table 3.6: (continued)

frequency (cm^{-1})			Potential Energy Distribution
obs.	calc.	dev.	
2237	2222	-15	CH_3 as(100)
2852	2871	19	$\text{CH s}^1(50)$, $\text{CH s}^1(50)$
2897	2901	4	$\text{CH s}^1(50)$, $\text{CH s}^1(50)$
3390	3398	8	$\text{OH s}(100)$

Table 3.7: Scaled 4-31G Frequencies and Potential Energy Distributions for Ethanol two-water supermolecule, water included.

frequency (cm^{-1})			CH ₃ CH ₂ OH·2H ₂ O (mean deviation = 8 cm^{-1})
obs.	calc.	dev.	
—	22	—	wat39(74), wat37(14), wat29(12)
—	48	—	CO t(98), wat29(7)
—	76	—	wat35(43), wat28(28), wat32(9), wat37(9)
—	150	—	wat31(28), wat30(26), wat22(25), wat23(25)
—	162	—	wat23(47), wat31(23), wat28(10)
—	193	—	wat32(32), wat31(31), wat28(22), wat30(14)
—	210	—	wat30(31), wat28(25), wat31(19), wat23(13), wat32(9)
—	230	—	wat32(46), wat37(21), wat35(18), wat23(9), wat28(8), wat31(7)
—	271	—	CC t(95)
—	379	—	wat37(26), wat39(22), wat22(16), wat38(13)
—	433	—	wat29(48), OCC sis(27), wat26(11), wat35(10), wat37(9)
436	441	5	OCC sis(46), wat29(16), wat26(10), wat22(8)
—	624	—	wat29(95), wat26(23), wat38(19)
—	767	—	wat38(69), wat22(25), wat39(7)
—	796	—	CH ₂ twist(41), CH ₃ r ^{1,2} (38)
—	821	—	wat22(66), wat26(35), wat39(15), wat30(12), wat37(8), wat35(7)
881	872	-9	CC s(41), CO s(31), CH ₃ r ^{1,2} (24)
1047	1040	-7	CC s(48), CO s(40)
1087	1092	5	CH ₃ r ^{1,2} (48), CO s(26), OCC sis(12)
1126	1125	-1	CH ₂ twist(51), CH ₃ r ^{1,2} (36), CH ₂ wag(11)
1280	1280	0	CH ₂ wag(82), CH ₃ r ^{1,2} (15)
1331	1318	-13	CH ₂ r(50), OH b(34)
1386	1391	5	CH ₃ sd(95)
1421	1429	8	OH b(44), CH ₂ r(39)
1456	1441	-15	CH ₃ ad(93)
1456	1455	-1	CH ₃ ad(88)
1486	1484	-2	CH ₂ sis(96)
1630	1623	-7	wat27(55), wat36(39)
1630	1639	9	wat36(47), wat27(36)
2884	2869	-15	CH s ^{1,2} (57), CH s ^{1,2} (42)
2902	2900	-2	CH s ^{1,2} (56), CH s ^{1,2} (42)

Table 3.7: (continued)

frequency (cm^{-1})			Potential Energy Distribution
obs.	calc.	dev.	
2936	2937	1	CH_3 ss(98)
2982	2988	6	CH_3 as(98)
2982	2999	17	CH_3 as(98)
3370	3371	1	OH s(43), wat24(29), wat33(28)
—	3420	—	OH s(55), wat33(34), wat24(9)
—	3439	—	wat24(58), wat33(35)
—	3718	—	wat25(51), wat34(44)
—	3719	—	wat34(51), wat25(44)

frequency (cm^{-1})			CH ₃ CH ₂ OD·2D ₂ O (mean deviation = 11 cm^{-1})
obs.	calc.	dev.	
—	21	—	wat39(72), wat29(15), wat37(15)
—	47	—	CO t(96), wat29(7)
—	71	—	wat35(39), wat28(30), wat37(10), wat32(9)
—	112	—	wat31(47), wat30(30), wat22(29)
—	147	—	wat31(49), wat30(27), wat23(18), wat22(8)
—	158	—	wat23(48), wat35(14), wat30(12), wat31(10), wat28(8)
—	193	—	wat28(50), wat32(35), wat23(17)
—	219	—	wat32(48), wat37(28), wat35(13), wat23(10)
—	270	—	CC t(91)
—	283	—	wat39(22), wat37(19), wat38(16), wat22(15), wat35(8), wat30(7)
—	318	—	wat29(60), wat26(22), wat37(11), wat35(9)
431	417	-14	OCC sis(59), wat38(18), wat29(13), CH_3 r ^{1,2} (7)
—	456	—	wat29(84), wat26(18), OCC sis(16), wat38(8)
—	568	—	wat38(69), wat22(37), wat39(11)
—	605	—	wat22(52), wat26(40), wat35(15), wat39(12), wat30(11), wat37(8)
—	794	—	CH_2 twist(46), CH_3 r ^{1,2} (42), CH_2 wag(7)
875	857	-18	CC s(41), CO s(33), CH_3 r ^{1,2} (17)
951	957	6	OH b(53), CH_3 r ^{1,2} (23), wat26(7)
1051	1045	-6	CO s(53), CC s(39)
1104	1124	20	CH_2 twist(50), CH_3 r ^{1,2} (35), CH_2 wag(10)

Table 3.7: (continued)

frequency (cm^{-1})			Potential Energy Distribution
obs.	calc.	dev.	
1136	1136	0	CH_3 $r^{1,2}$ (41), OH b(18), OCC sis(14), CO s(9), CC s(8)
1200	1189	-11	wat27(60), wat36(35)
1200	1198	-2	wat36(51), wat27(32)
1282	1280	-2	CH_2 wag(82), CH_3 $r^{1,2}$ (15)
1369	1377	8	CH_2 r(87)
1392	1393	1	CH_3 sd(92)
1455	1441	-14	CH_3 ad(94)
1455	1455	0	CH_3 ad(89)
1486	1484	-2	CH_2 sis(96)
—	2446	—	wat24(37), wat33(37), OH s(19)
—	2482	—	wat33(52), OH s(22), wat24(17), wat34(7)
2490	2488	-2	OH s(59), wat24(35)
—	2718	—	wat34(54), wat25(36)
—	2720	—	wat25(53), wat34(35), wat24(7)
2879	2870	-9	CH $s^{1,2}$ (57), CH $s^{1,2}$ (42)
2898	2900	2	CH $s^{1,2}$ (57), CH $s^{1,2}$ (42)
2935	2937	2	CH_3 ss(98)
2984	2988	4	CH_3 as(98)
2984	2999	15	CH_3 as(98)

frequency (cm^{-1})			Potential Energy Distribution
obs.	calc.	dev.	
—	21	—	wat39(69), wat37(13), wat29(10)
—	44	—	CO t(92), wat29(8)
—	73	—	wat35(44), wat28(26), wat37(10), wat32(8)
—	149	—	wat23(31), wat22(24), wat30(24), wat31(24)
—	160	—	wat23(42), wat31(26), wat28(11)
—	193	—	wat32(33), wat31(29), wat28(23), wat30(12)
—	203	—	CC t(72), wat30(9), wat31(7)
—	212	—	wat30(24), CC t(23), wat28(20), wat31(16), CO t(7), wat32(7)
—	229	—	wat32(46), wat37(21), wat35(16), wat28(10), wat23(9)
—	374	—	OCC sis(22), wat37(22), wat39(17), wat22(12), wat38(7)

Table 3.7: (continued)

frequency (cm^{-1})			Potential Energy Distribution
obs.	calc.	dev.	
392	400	8	OCC sis(44), CH ₃ r ^{1,2} (13), wat35(11), wat38(10)
—	436	—	wat29(62), wat26(22), wat37(13)
—	622	—	wat29(91), wat26(22), wat38(18)
—	662	—	CH ₃ r ^{1,2} (66), CH ₂ twist(20)
753	744	-9	CH ₃ r ^{1,2} (45), CO s(16), CC s(13), wat38(11)
—	771	—	wat38(60), wat22(24), CC s(11), wat39(7)
—	821	—	wat22(65), wat26(34), wat39(14), wat30(12), wat37(8)
941	941	0	CC s(29), CH ₃ sd(28), CH ₃ r ^{1,2} (17), OCC sis(12)
1022	1038	16	CO s(63), CH ₃ ad(21)
1032	1039	7	CH ₃ ad(93)
1032	1054	22	CH ₃ ad(77), CO s(14)
1061	1054	-7	CH ₂ twist(74), CH ₃ r ^{1,2} (21)
1135	1122	-13	CH ₃ sd(58), CC s(34)
1255	1255	0	CH ₂ wag(95)
1320	1309	-11	CH ₂ r(55), OH b(34)
1423	1428	5	OH b(46), CH ₂ r(43)
1480	1483	3	CH ₂ sis(99)
1630	1623	-7	wat27(54), wat36(39)
1630	1639	9	wat36(46), wat27(37)
2112	2110	-2	CH ₃ ss(99)
2237	2212	-25	CH ₃ as(99)
2237	2220	-17	CH ₃ as(100)
2852	2870	18	CH s ^{1,2} (57), CH s ^{1,2} (43)
2897	2902	5	CH s ^{1,2} (57), CH s ^{1,2} (43)
3370	3371	1	OH s(43), wat24(29), wat33(28)
—	3420	—	OH s(55), wat33(34), wat24(9)
—	3439	—	wat24(58), wat33(35)
—	3718	—	wat25(51), wat34(44)
—	3719	—	wat34(51), wat25(44)

Table 3.8: Scaled 4-31G Frequencies and Potential Energy Distribution for Ethanol Using Self Consistent Reaction Field Theory

frequency (cm^{-1})			CH ₃ CH ₂ OH (mean deviation = 16 cm^{-1})
obs.	calc.	dev.	Potential Energy Distribution
—	170	—	CO t(95)
—	249	—	CC t(92)
436	437	1	OCC sis(82), CH ₃ r ^{1,2} (10)
—	795	—	CH ₂ twist(50), CH ₃ r ^{1,2} (39), CH ₂ wag(7)
881	863	-18	CC s(41), CO s(35), CH ₃ r ^{1,2} (22)
1047	1006	-41	CC s(50), CO s(36), CH ₃ r ^{1,2} (7)
1087	1092	5	CH ₃ r ^{1,2} (43), CO s(29), OCC sis(11)
1126	1125	-1	CH ₂ twist(48), CH ₃ r ^{1,2} (36), CH ₂ wag(13)
1280	1281	1	CH ₂ wag(79), CH ₃ r ^{1,2} (17)
1331	1300	-31	CH ₂ r(54), OH b(31), CH ₃ r ^{1,2} (10)
1386	1398	12	CH ₃ sd(96)
1456	1435	-21	CH ₃ ad ^{1,2} (92), CH ₃ r ^{1,2} (7)
1421	1449	28	CH ₃ ad ^{1,2} (78), OH b(8)
1456	1456	0	OH b(43), CH ₂ r(34), CH ₃ ad ^{1,2} (11)
1486	1484	-2	CH ₂ sis(90)
2884	2869	-15	CH s ^{1,2} (50), CH s ^{1,2} (50)
2902	2900	-2	CH s ^{1,2} (49), CH s ^{1,2} (49)
2936	2937	1	CH ₃ ss(96)
2982	2987	5	CH ₃ as ^{1,2} (96)
2982	3000	18	CH ₃ as ^{1,2} (99)
3370	3383	13	OH s(100)

frequency (cm^{-1})			CH ₃ CH ₂ OD (mean deviation = 17 cm^{-1})
obs.	calc.	dev.	Potential Energy Distribution
—	127	—	CO t(99)
—	247	—	CC t(96)
431	426	-5	OCC sis(81), CH ₃ r ^{1,2} (10)
—	795	—	CH ₂ twist(50), CH ₃ r ^{1,2} (39), CH ₂ wag(7)
875	845	-30	CC s(49), CO s(31), CH ₃ r ^{1,2} (11), OH b(10)
951	933	-18	OH b(50), CH ₃ r ^{1,2} (27), CO s(12)
1051	1039	-12	CO s(53), CC s(29), OH b(7)

Table 3.8: (continued)

frequency (cm^{-1})			Potential Energy Distribution
obs.	calc.	dev.	
1104	1125	21	CH_2 twist(48), CH_3 $r^{1,2}$ (36), CH_2 wag(13)
1136	1174	38	CH_3 $r^{1,2}$ (38), OH b(23), OCC sis(18), CC s(8)
1282	1281	-1	CH_2 wag(79), CH_3 $r^{1,2}$ (17)
1369	1379	10	CH_2 r(83)
1392	1400	8	CH_3 sd(92)
1455	1435	-20	CH_3 $ad^{1,2}$ (92), CH_3 $r^{1,2}$ (7)
1455	1450	-5	CH_3 $ad^{1,2}$ (87), CH_3 $r^{1,2}$ (7)
1486	1482	-4	CH_2 sis(96)
2490	2464	-26	OH s(100)
2879	2869	0	CH $s^{1,2}$ (50), CH $s^{1,2}$ (50)
2898	2900	2	CH $s^{1,2}$ (49), CH $s^{1,2}$ (49)
2935	2937	2	CH_3 ss(96)
2984	2987	3	CH_3 $as^{1,2}$ (96)
2984	3000	16	CH_3 $as^{1,2}$ (99)

frequency (cm^{-1})			CD ₃ CH ₂ OH (mean deviation = 16 cm^{-1})
obs.	calc.	dev.	
—	164	—	CO t(71), CC t(28)
—	195	—	CC t(68), CO t(29)
392	388	-4	OCC sis(72), CH_3 $r^{1,2}$ (20)
—	666	—	CH_3 $r^{1,2}$ (67), CH_2 twist(23)
753	750	-3	CH_3 $r^{1,2}$ (45), CC s(25), CO s(21)
941	919	-22	CC s(40), CH_3 sd(22), CH_3 $r^{1,2}$ (16), OCC sis(12)
1022	1033	11	CO s(59), CH_3 $ad^{1,2}$ (23), OCC sis(8), CH_3 $r^{1,2}$ (8)
1032	1034	2	CH_3 $ad^{1,2}$ (96)
1032	1049	17	CH_3 $ad^{1,2}$ (74), CO s(17), CH_3 $r^{1,2}$ (7)
1061	1050	-11	CH_2 twist(74), CH_3 $r^{1,2}$ (25)
1135	1114	-21	CH_3 sd(68), CC s(27)
1255	1253	-2	CH_2 wag(94)
1320	1284	-36	CH_2 r(61), OH b(36)
1423	1454	31	OH b(51), CH_2 r(37)
1480	1483	3	CH_2 sis(92)
2112	2110	-2	CH_3 ss(99)

Table 3.8: (continued)

frequency (cm^{-1})			Potential Energy Distribution
obs.	calc.	dev.	
2237	2212	-25	CH_3 as ^{1,2} (99)
2237	2221	-16	CH_3 as ^{1,2} (100)
2852	2870	18	CH s ^{1,2} (50), CH s ^{1,2} (50)
2897	2902	5	CH s ^{1,2} (50), CH s ^{1,2} (50)
3370	3383	13	OH s(100)

3.3 Small Molecules–Water Excluded Scale Factors

The scale factors determined for small molecules using the water-excluded model were based on results from previous studies: for both acidic and basic solutions of methylamine: Lowrey and Williams [1992a]; for acetate: Williams and Lowrey [1991]; for glycine and glycinate Williams *et al* [1993] and Lowrey *et al* [1993], respectively; and for N-methylacetamide (NMA): Williams [1992]. These previous studies provided optimized geometries, unscaled force constants, experimental frequencies for aqueous spectra, and guides for PED assignments. One new NMA structure was optimized and force constants calculated for this study: the two-water supermolecule with one water on the amide hydrogen and the other on the carbonyl oxygen. The experimental aqueous frequencies and PED assignments were not changed for this new structure.

The optimized geometries for the methylamine one water basic and three water acidic conformations and the acetate one water supermolecule are shown in Figure 3.12. The optimized geometries for the glycine supermolecules are shown in Figure 3.17.

Internal coordinate definitions for acidic and basic methylamine structures are listed in Table 3.9. Symmetry coordinate definitions, based on those recommended by Fogarasi and Pulay [1985], are listed in Table 3.10. Optimized internal coordinates are provided in Table 3.11. Raman spectra for the various methylamine species examined are shown in Figure 3.13. Spectra are from Lowrey and Williams [1992a].

Figure 3.12: Small molecule supermolecule optimized geometries. Methylamine in base with one water (top), methylamine in acid with three waters (middle), and acetate with one water (bottom).

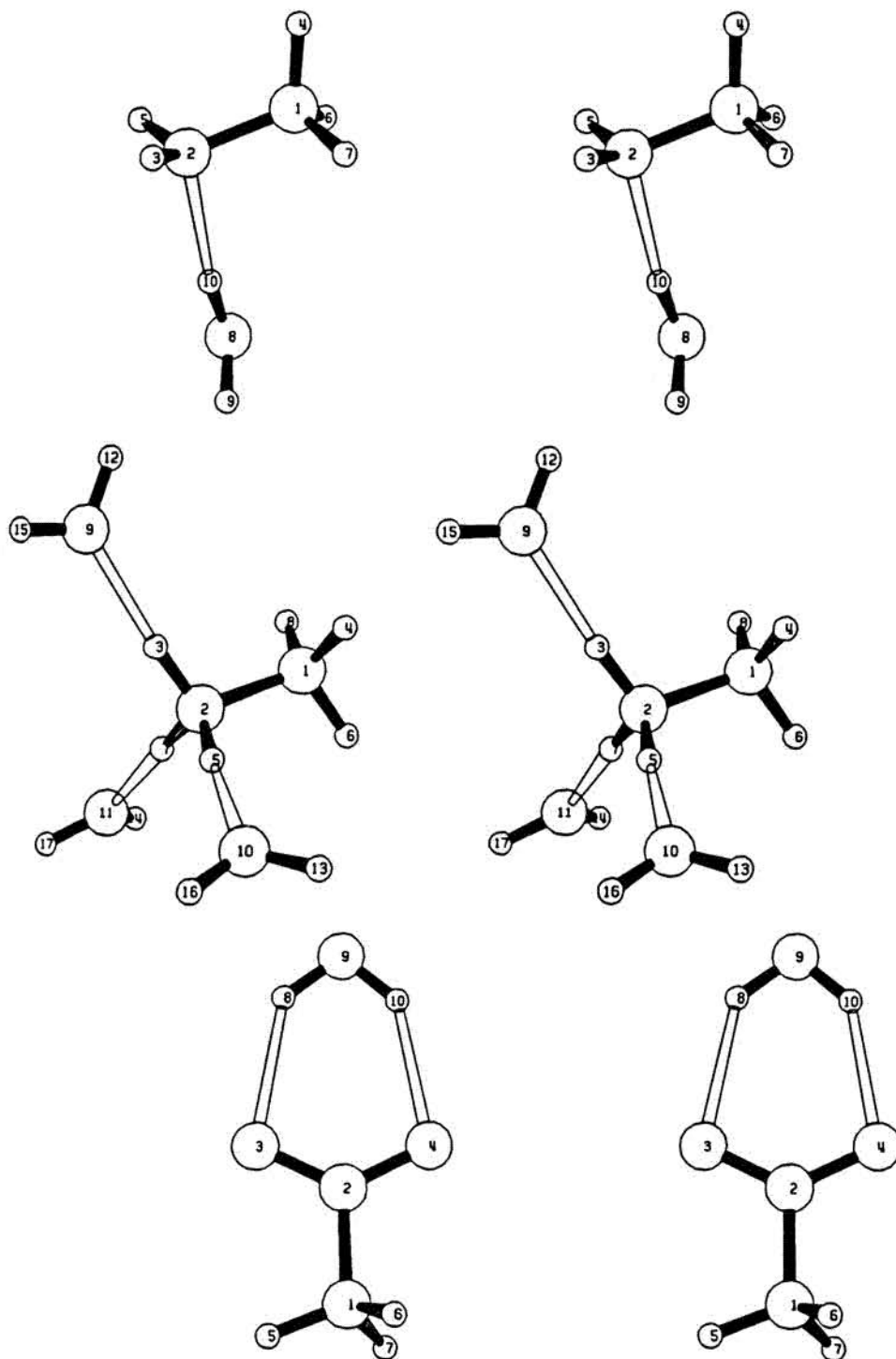


Figure 3.13: Raman spectra of methylamine and protonated methylamine in H_2O and D_2O . Top, CH_3ND_3^+ 10% (w/w) in D_2O , pD 6.4; second from top, CH_3NH_3^+ 10% (w/w) in H_2O , pH 6.4; third from top, CH_3ND_2 10% (w/w) in D_2O , pD 13.5; bottom, CH_3NH_2 10% (w/w) in H_2O pH 13.5.

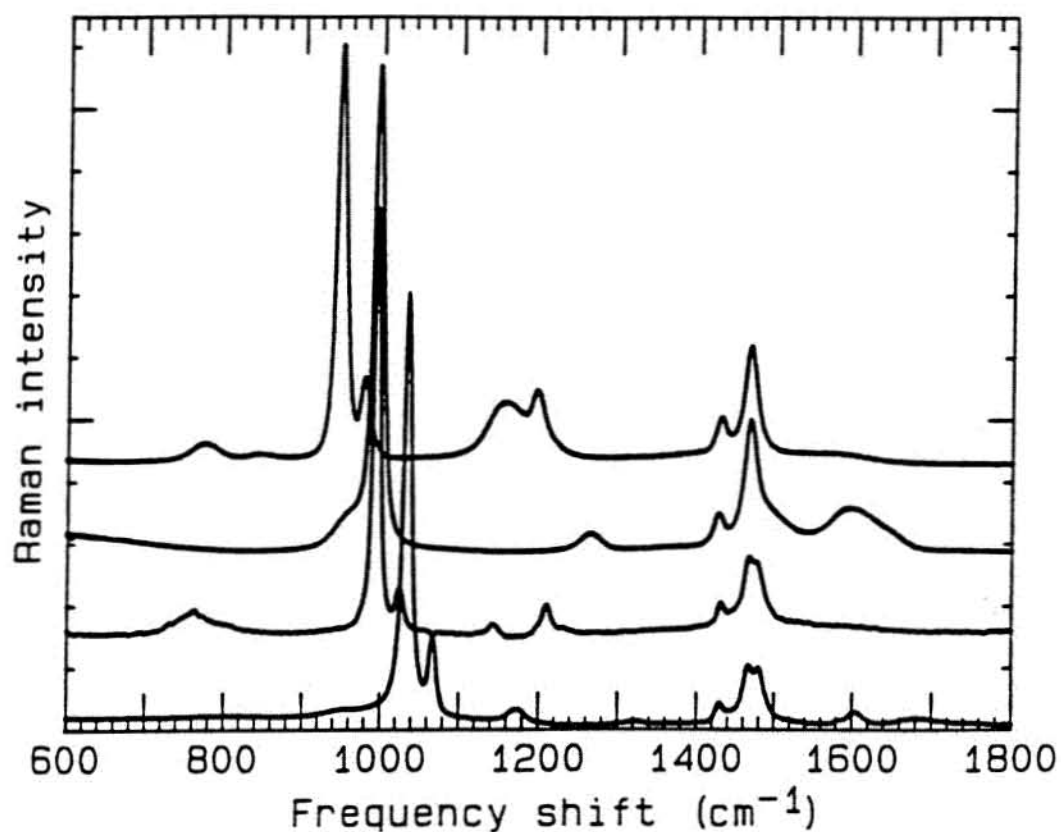


Figure 3.14: Raman spectra of methylamine-3- d_3 in D_2O (top) and H_2O (bottom).

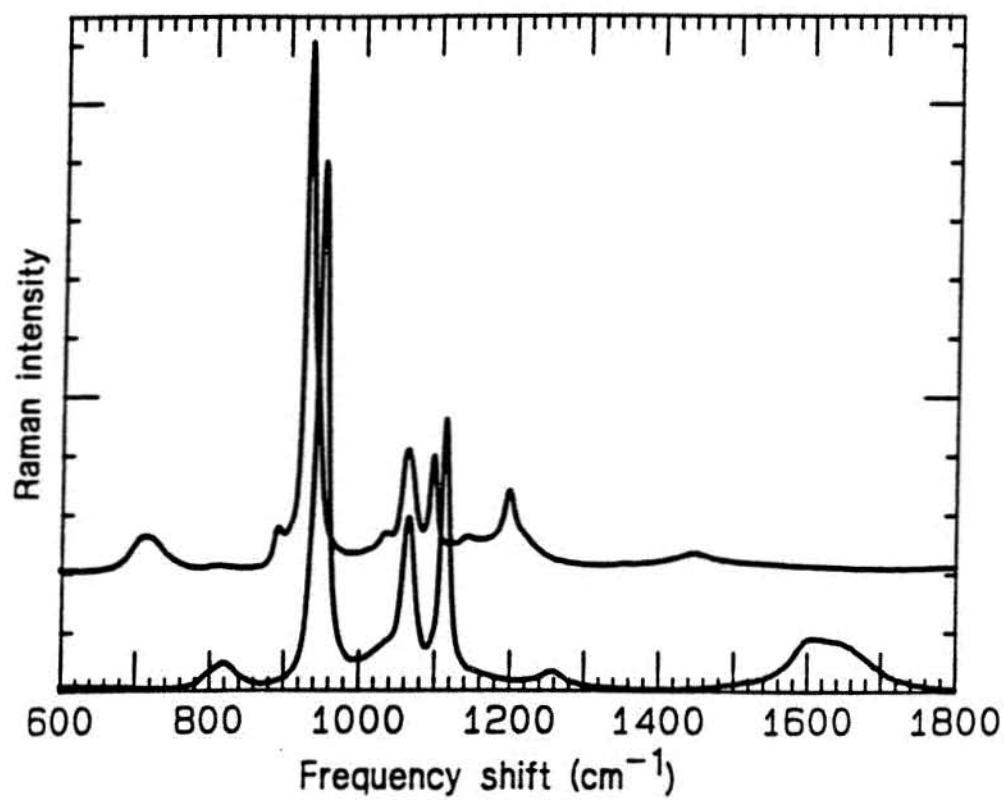


Figure 3.15: Raman spectra of acetic acid: Top, CH_3COOD 50% (w/w) in D_2O ; middle, CH_3COOH 50% in H_2O ; bottom, CH_3COONa 50% in H_2O . The pH of the acid samples was adjusted to below 1. The pH of the sodium salt was adjusted to above 11.

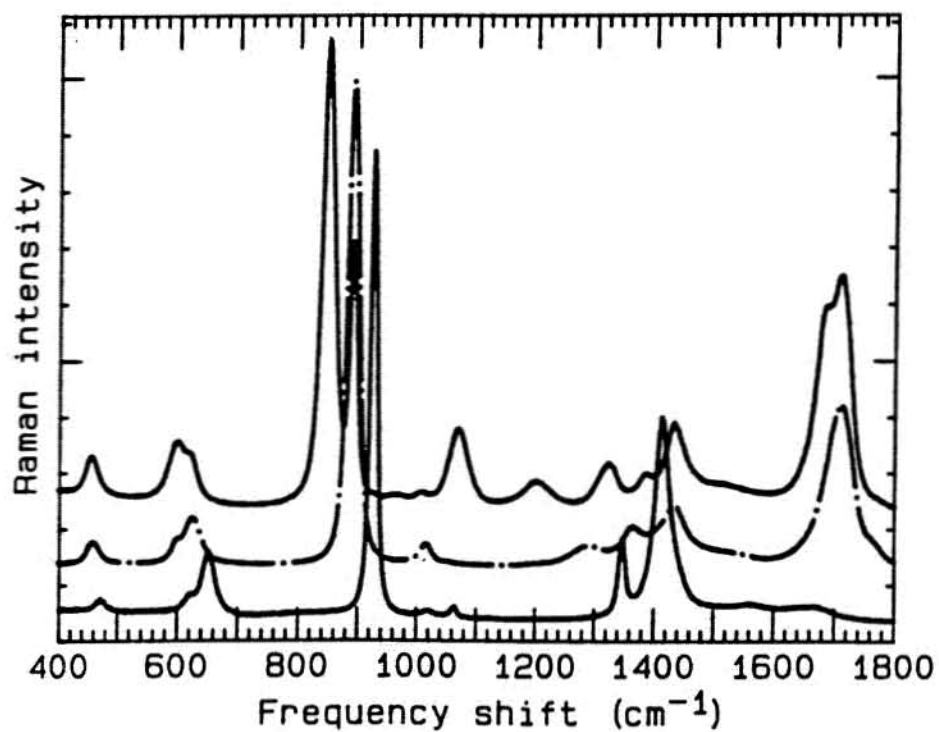


Figure 3.16: Raman spectra of ^{13}C labeled acetic acid: Top, $^{13}\text{CD}_3^{13}\text{COOD}$ 50% (w/w) in D_2O , pD less than 1; middle, $^{13}\text{CH}_3^{13}\text{COOH}$ 50% in H_2O , pH less than 1; bottom, $^{13}\text{CH}_3^{13}\text{COONa}$ 50% in D_2O pD greater than 11.

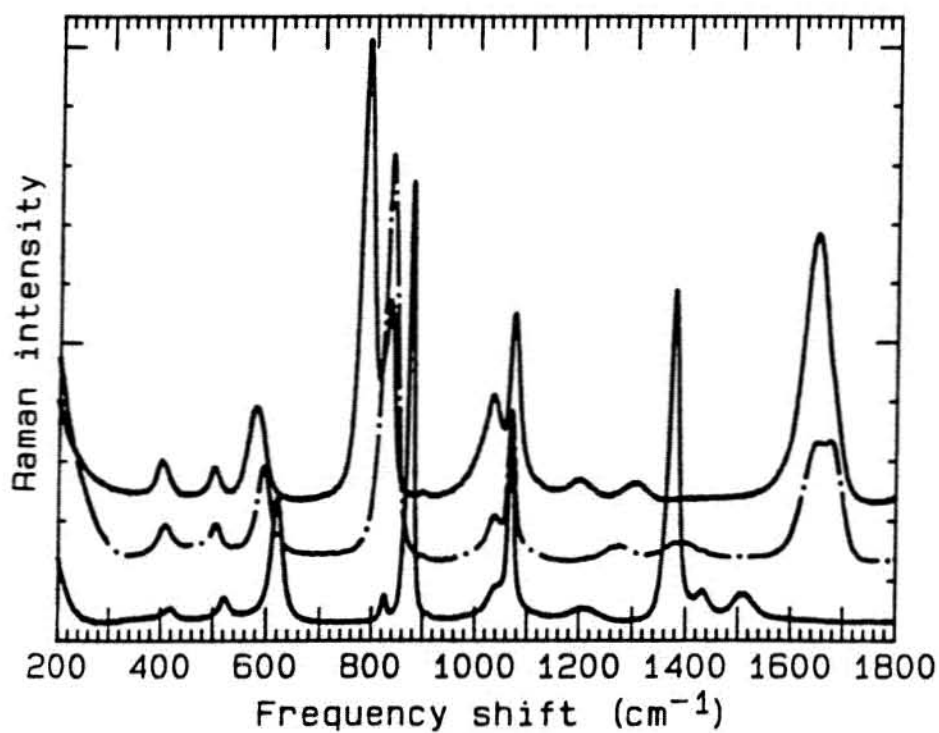


Figure 3.17: Optimized structures for glycine supermolecules. Glycine in acid with one water (top), glycine in base with one water (upper middle), glycine in base with two waters (lower middle), and glycine in base with four waters (bottom).

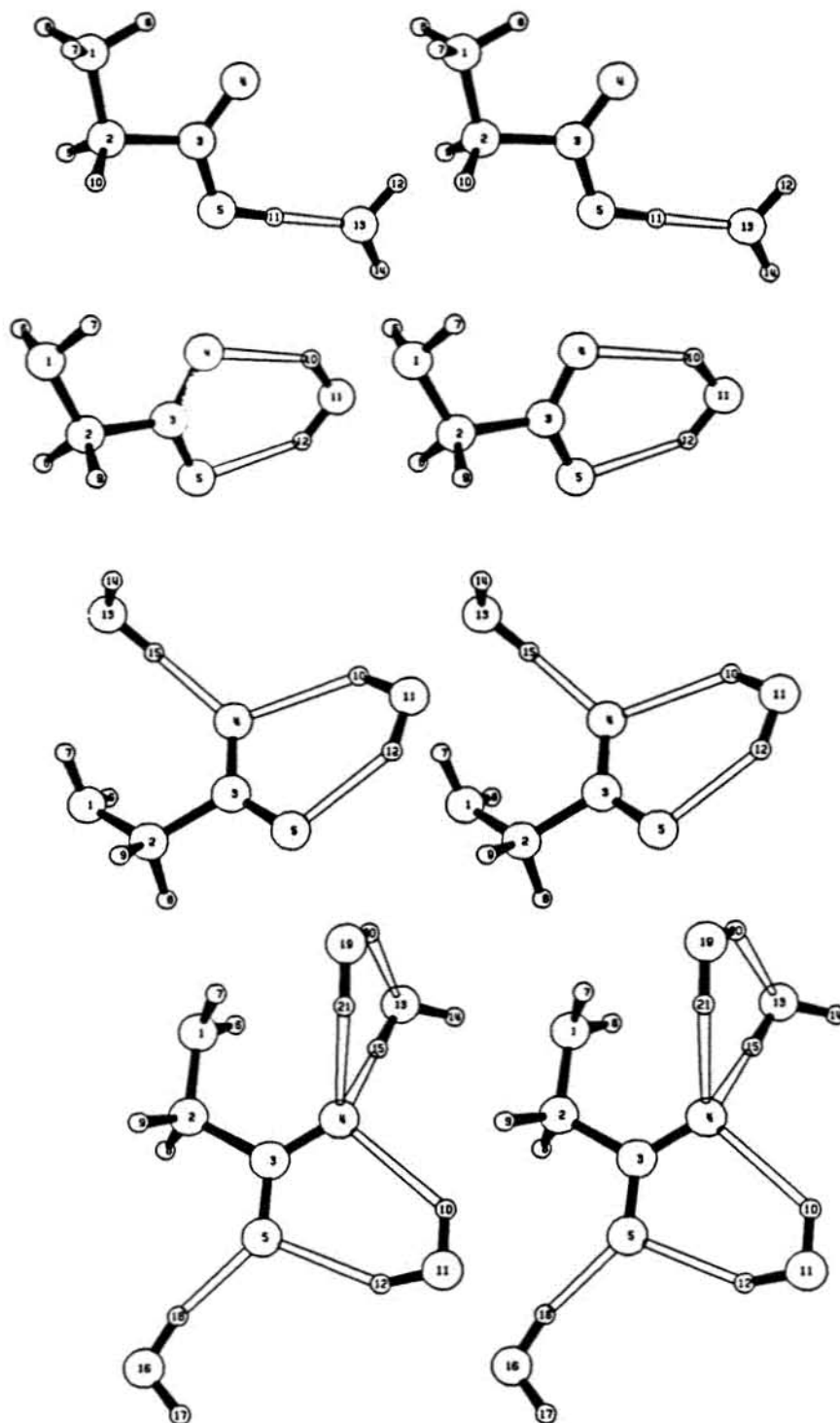


Figure 3.18: Raman spectra for acidic glycine in H_2O . Solid line, $^+\text{NH}_3\text{CH}_2\text{COOH}$ pH 0.5; and dotted line, $^+\text{NH}_3\text{CD}_2\text{COOH}$ pH 0.8.

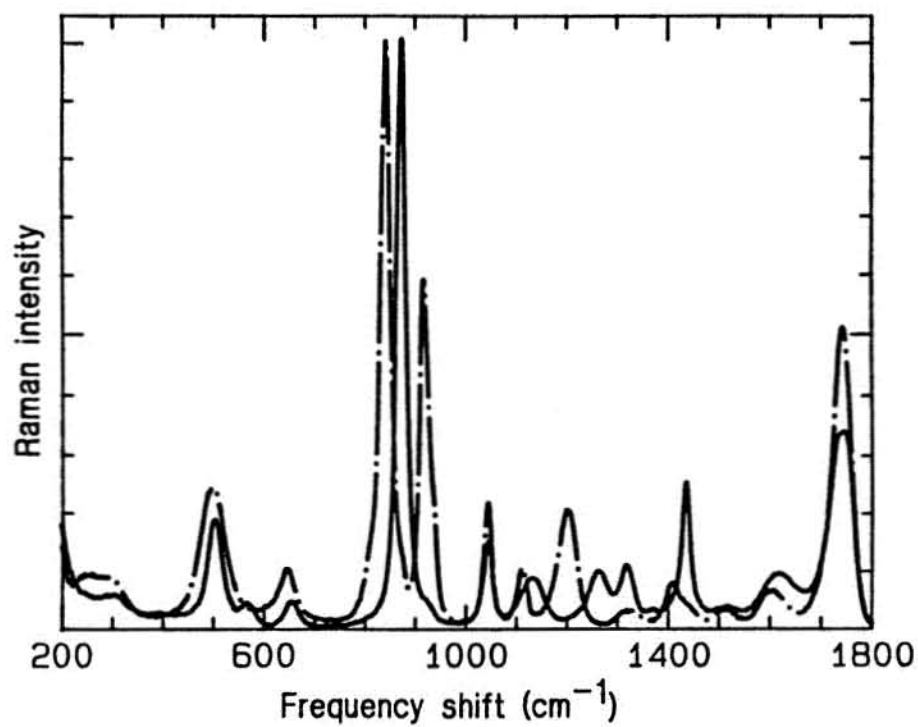


Figure 3.19: Raman spectra for acidic glycine in D_2O . Solid line, $^+ND_3CH_2COOD$ pD 0.5; and dotted line, $^+ND_3CD_2COOD$ pD 0.7.

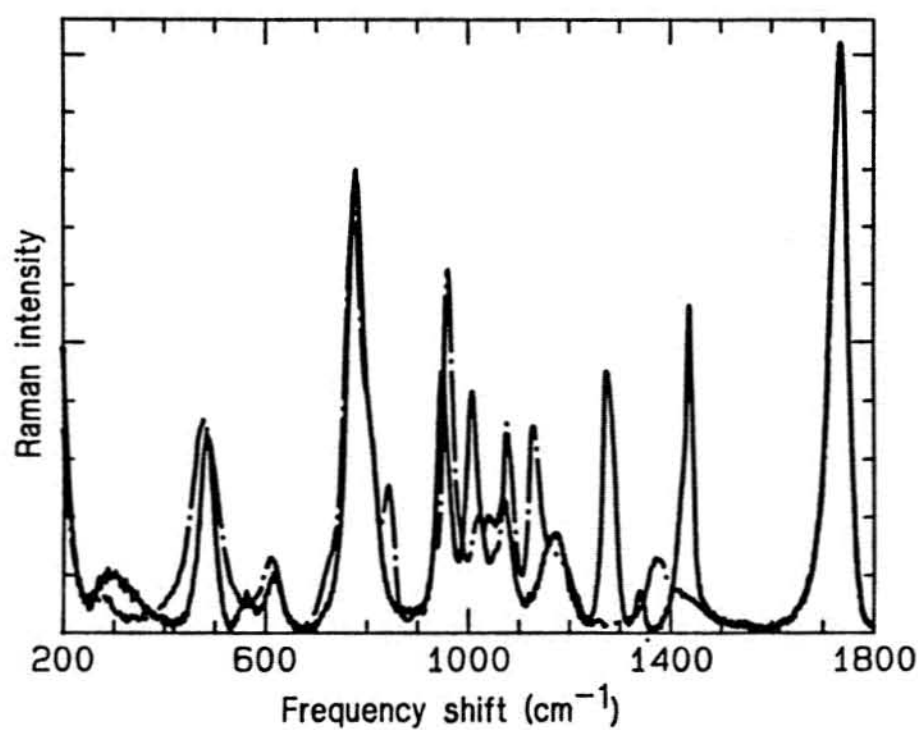


Figure 3.20: Raman spectra for basic glycine in H_2O . Solid line, $\text{NH}_2\text{CH}_2\text{COO}^-$ pH 12.5; dotted line, $\text{NH}_2\text{CH}_2^{13}\text{COO}^-$ pH 13; dashed line, $\text{NH}_2^{13}\text{CH}_2\text{COO}^-$ pH 13.

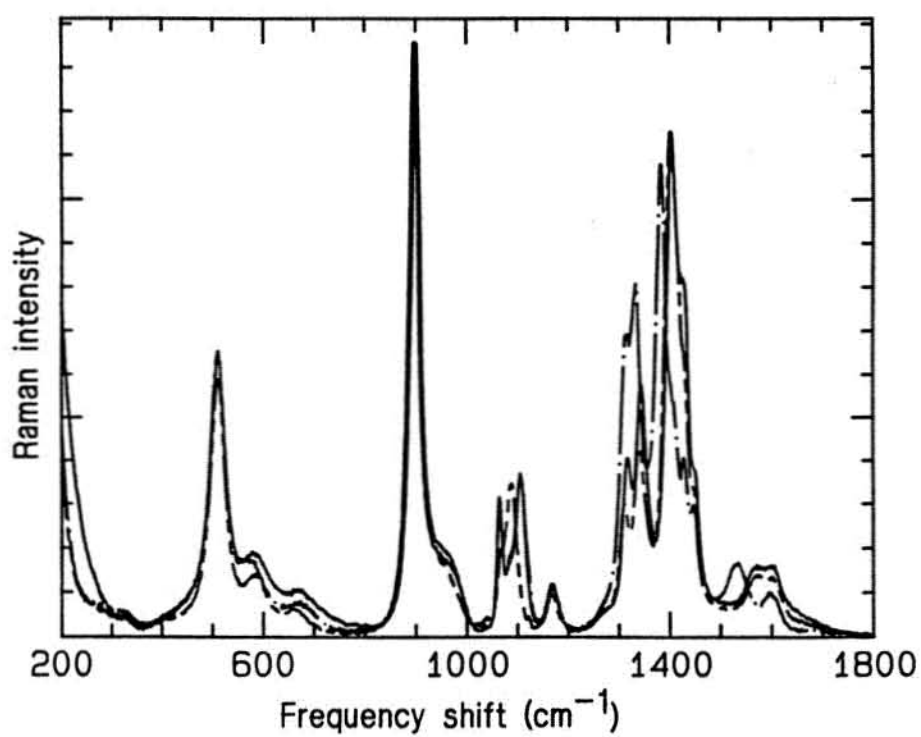


Figure 3.21: Raman spectra for basic glycine in D_2O . Solid line, $ND_2CH_2COO^-$ pD 12.5; dotted line, $ND_2CH_2^{13}COO^-$ pD 13; and dashed line, $ND_2^{13}CH_2COO^-$ pD 13.

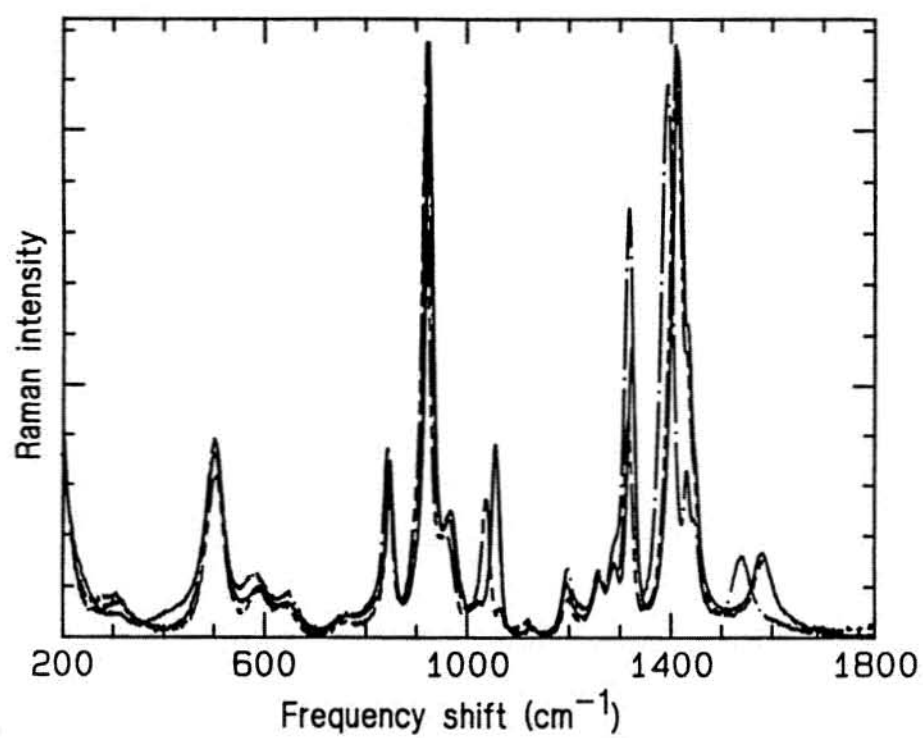


Figure 3.22: Raman spectra for basic glycine-2- d_2 in H_2O , pH 12.5 (solid line) and D_2O , pD 13 (dotted line).

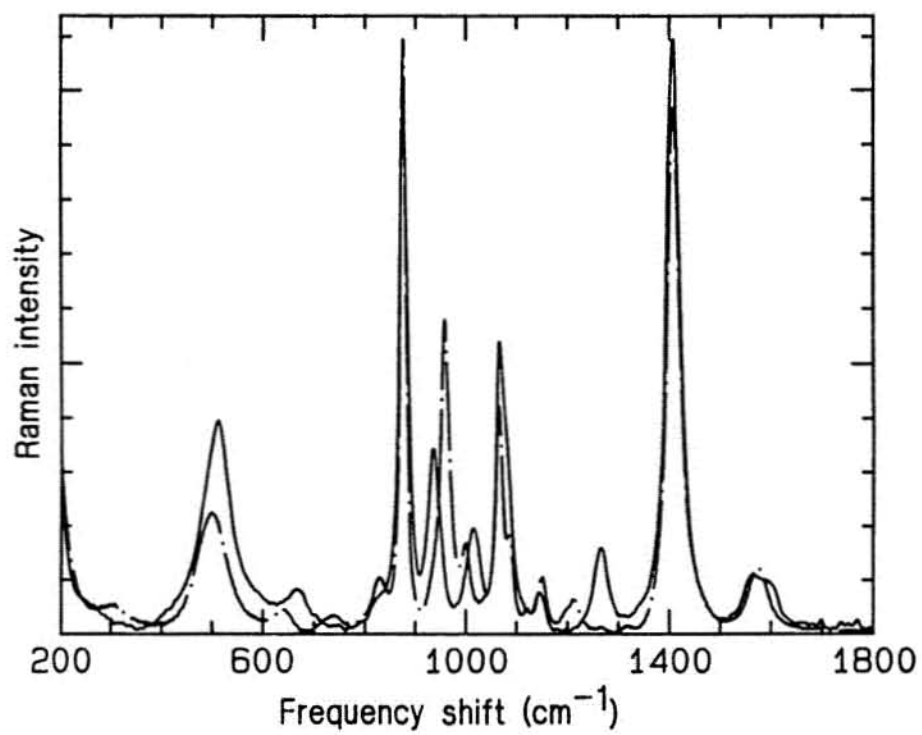


Table 3.9: Redundant Internal Coordinates for Methylamine in Base and Acid

Base ^a	Acid
$R_1 = \Delta\gamma(\text{N}^2\text{-C}^1)$	$R_1 = \Delta\gamma(\text{N}^2\text{-C}^1)$
$R_2 = \Delta\gamma(\text{H}^4\text{-C}^1)$	$R_2 = \Delta\gamma(\text{H}^6\text{-C}^1)$
$R_3 = \Delta\gamma(\text{H}^6\text{-C}^1)$	$R_3 = \Delta\gamma(\text{H}^4\text{-C}^1)$
$R_4 = \Delta\gamma(\text{H}^7\text{-C}^1)$	$R_4 = \Delta\gamma(\text{H}^8\text{-C}^1)$
$R_5 = \Delta\gamma(\text{H}^3\text{-N}^2)$	$R_5 = \Delta\gamma(\text{H}^3\text{-N}^2)$
$R_6 = \Delta\gamma(\text{H}^5\text{-N}^2)$	$R_6 = \Delta\gamma(\text{H}^5\text{-N}^2)$
$R_7 = \Delta\theta(\text{H}^4\text{-C}^1\text{-H}^7)$	$R_7 = \Delta\gamma(\text{H}^7\text{-N}^2)$
$R_8 = \Delta\theta(\text{H}^4\text{-C}^1\text{-H}^6)$	$R_8 = \Delta\theta(\text{H}^4\text{-C}^1\text{-H}^8)$
$R_9 = \Delta\theta(\text{H}^7\text{-C}^1\text{-H}^6)$	$R_9 = \Delta\theta(\text{H}^4\text{-C}^1\text{-H}^6)$
$R_{10} = \Delta\theta(\text{H}^6\text{-C}^1\text{-N}^2)$	$R_{10} = \Delta\theta(\text{H}^8\text{-C}^1\text{-H}^6)$
$R_{11} = \Delta\theta(\text{H}^7\text{-C}^1\text{-N}^2)$	$R_{11} = \Delta\theta(\text{H}^6\text{-C}^1\text{-N}^2)$
$R_{12} = \Delta\theta(\text{H}^4\text{-C}^1\text{-N}^2)$	$R_{12} = \Delta\theta(\text{H}^8\text{-C}^1\text{-N}^2)$
$R_{13} = \Delta\theta(\text{H}^5\text{-N}^2\text{-H}^3)$	$R_{13} = \Delta\theta(\text{H}^4\text{-C}^1\text{-N}^2)$
$R_{14} = \Delta\theta(\text{H}^5\text{-N}^2\text{-C}^1)$	$R_{14} = \Delta\theta(\text{H}^7\text{-N}^2\text{-H}^5)$
$R_{15} = \Delta\theta(\text{H}^3\text{-N}^2\text{-C}^1)$	$R_{15} = \Delta\theta(\text{H}^7\text{-N}^2\text{-H}^3)$
$R_{16} = \Delta\omega(\text{C}^1\text{-H}^5\text{-H}^3\text{-N}^2)$	$R_{16} = \Delta\theta(\text{H}^5\text{-N}^2\text{-H}^3)$
$R_{17} = \Delta\tau(\text{N}^2\text{-C}^1)$	$R_{17} = \Delta\theta(\text{H}^3\text{-N}^2\text{-C}^1)$
	$R_{18} = \Delta\theta(\text{H}^5\text{-N}^2\text{-C}^1)$
	$R_{19} = \Delta\theta(\text{H}^7\text{-N}^2\text{-C}^1)$
	$R_{20} = \Delta\tau(\text{N}^2\text{-C}^1)$

^aSymbols: γ = stretch, θ = bend, ω = out of plane bend, τ = torsion.

Table 3.10: Symmetry Coordinate Definitions for Methylamine in Base and Acid

Base	
CN s ^a	$S_1 = R_1$
NCH ₃ ss	$S_2 = (R_2 + R_3 + R_4)/\sqrt{3}$
NCH ₃ as ¹	$S_3 = (2R_2 - R_3 - R_4)/\sqrt{6}$
NCH ₃ as ²	$S_4 = (R_3 - R_4)/\sqrt{2}$
NH ₂ ss	$S_5 = (R_5 + R_6)/\sqrt{2}$
NH ₂ as	$S_6 = (R_5 - R_6)/\sqrt{2}$
NCH ₃ sd	$S_7 = (R_7 + R_8 + R_9 - R_{10} - R_{11} - R_{12})/\sqrt{6}$
NCH ₃ ad ¹	$S_8 = (2R_7 - R_8 - R_9)/\sqrt{6}$
NCH ₃ ad ²	$S_9 = (R_8 - R_9)/\sqrt{2}$
NCH ₃ r ¹	$S_{10} = (2R_{10} - R_{11} - R_{12})/\sqrt{6}$
NCH ₃ r ²	$S_{11} = (R_{11} - R_{12})/\sqrt{2}$
NCH ₂ scissor	$S_{12} = (2R_{13} - R_{14} - R_{15})/\sqrt{6}$
NCH ₃ r	$S_{13} = (R_{14} - R_{15})/\sqrt{2}$
NCH ₃ ob	$S_{14} = R_{16}$
CN t	$S_{15} = R_{17}$
Acid	
CN s	$S_1 = R_1$
CH ₃ ss	$S_2 = (R_2 + R_3 + R_4)/\sqrt{3}$
CH ₃ as ¹	$S_3 = (2R_2 - R_3 - R_4)/\sqrt{6}$
CH ₃ as ²	$S_4 = (R_3 - R_4)/\sqrt{2}$
NH ₃ ss	$S_5 = (R_5 + R_6 + R_7)/\sqrt{3}$
NH ₃ as ¹	$S_6 = (2R_5 - R_6 - R_7)/\sqrt{6}$
NH ₃ as ²	$S_7 = (R_6 - R_7)/\sqrt{2}$
CH ₃ sd	$S_8 = (R_8 + R_9 + R_{10} - R_{11} - R_{12} - R_{13})/\sqrt{6}$
CH ₃ ad ¹	$S_9 = (2R_8 - R_9 - R_{10})/\sqrt{6}$
CH ₃ ad ²	$S_{10} = (R_9 - R_{10})/\sqrt{2}$
CH ₃ r ¹	$S_{11} = (2R_{11} - R_{12} - R_{13})/\sqrt{6}$
CH ₃ r ²	$S_{12} = (R_{12} - R_{13})/\sqrt{2}$
NH ₃ sd	$S_{13} = (R_{14} + R_{15} + R_{16} - R_{17} - R_{18} - R_{19})/\sqrt{6}$
NH ₃ ad ¹	$S_{14} = (2R_{14} - R_{15} - R_{16})/\sqrt{6}$
NH ₃ ad ²	$S_{15} = (R_{15} - R_{16})/\sqrt{2}$
NH ₃ r ¹	$S_{16} = (2R_{17} - R_{18} - R_{19})/\sqrt{6}$
NH ₃ r ²	$S_{17} = (R_{18} - R_{19})/\sqrt{2}$
CN t	$S_{18} = R_{20}$

Table 3.10: (continued)

^aAbbreviations: s = stretch, t = torsion, ss = symmetric stretch, as = antisymmetric stretch, sd = symmetric deformation, ad = antisymmetric deformation, r = rock, ob = out of plane bend.

Table 3.11: Optimized Internal Coordinates for Methylamine in Acid and Base

Internal Coordinate	One water, base	Three water, acid
Bond Stretches		
N ² -C ¹	1.4626	1.4945
H ³ -N ²	0.9975	1.0222
H ⁴ -N ²	0.9978	1.0222
H ⁵ -C ¹	1.0859	1.0766
H ⁶ -C ¹	1.0794	1.0766
H ⁷ -C ¹	1.0801	1.0766
H ⁸ -N ²		1.0222
Angle bends		
H ³ -N ² -C ¹	114.66	110.20
H ⁴ -N ² -C ¹	114.32	110.20
H ⁵ -C ¹ -N ²	113.69	109.21
H ⁶ -C ¹ -N ²	109.09	109.21
H ⁷ -C ¹ -N ²	109.19	109.21
H ⁸ -N ² -C ¹		110.20
Torsions		
H ⁴ -N ² -C ¹ -H ³	130.25	-60.00
H ⁵ -C ¹ -N ² -H ³	-66.37	59.90
H ⁶ -C ¹ -N ² -H ⁴	-57.66	120.00
H ⁷ -C ¹ -N ² -N ³	54.72	-120.00
H ⁸ -N ² -C ¹ -H ⁶		-60.00

Internal and symmetry coordinate definitions for acetate are listed in Tables 3.12 and 3.13, respectively. Optimized internal coordinates are given in Table 3.14. Raman spectra of acetate are shown in Figures 3.15 and 3.16. Spectra are from Williams and Lowrey [1991].

Table 3.12: Redundant Internal Coordinates for Acetate

$R_1 = \Delta\gamma(\text{C}^2\text{-C}^1)^a$	$R_{10} = \Delta\theta(\text{H}^5\text{-C}^1\text{-C}^2)$
$R_2 = \Delta\gamma(\text{O}^3\text{-C}^2)$	$R_{11} = \Delta\theta(\text{H}^7\text{-C}^1\text{-C}^2)$
$R_3 = \Delta\gamma(\text{O}^4\text{-C}^2)$	$R_{12} = \Delta\theta(\text{H}^6\text{-C}^1\text{-C}^2)$
$R_4 = \Delta\gamma(\text{H}^5\text{-C}^1)$	$R_{13} = \Delta\theta(\text{O}^4\text{-C}^2\text{-O}^3)$
$R_5 = \Delta\gamma(\text{H}^6\text{-C}^1)$	$R_{14} = \Delta\theta(\text{O}^4\text{-C}^2\text{-C}^1)$
$R_6 = \Delta\gamma(\text{H}^7\text{-C}^1)$	$R_{15} = \Delta\theta(\text{O}^3\text{-C}^2\text{-C}^1)$
$R_7 = \Delta\theta(\text{H}^6\text{-C}^1\text{-H}^7)$	$R_{16} = \Delta\omega(\text{C}^1\text{-O}^4\text{-O}^3\text{-C}^2)$
$R_8 = \Delta\theta(\text{H}^6\text{-C}^1\text{-H}^5)$	$R_{17} = \Delta\tau(\text{C}^2\text{-C}^1)$
$R_9 = \Delta\theta(\text{H}^7\text{-C}^1\text{-H}^5)$	

^aSymbols: γ = stretch, θ = bend, ω = out of plane bend, τ = torsion.

Table 3.13: Symmetry Coordinate Definitions for Acetate.

CC s ^a	$S_1 = R_1$
CO ss	$S_2 = (R_2 + R_3)/\sqrt{2}$
CO as	$S_3 = (R_2 - R_3)/\sqrt{2}$
CH ₃ ss	$S_4 = (R_4 + R_5 + R_6)/\sqrt{3}$
CH ₃ as ¹	$S_5 = (2R_4 - R_5 - R_6)/\sqrt{6}$
CH ₃ as ²	$S_6 = (R_5 - R_6)/\sqrt{2}$
CH ₃ sd	$S_7 = (R_7 + R_8 + R_9 - R_{10} - R_{11} - R_{12})/\sqrt{6}$
CH ₃ ad ¹	$S_8 = (2R_7 - R_8 - R_9)/\sqrt{6}$
CH ₃ ad ²	$S_9 = (R_8 - R_9)/\sqrt{2}$
CH ₃ r ¹	$S_{10} = (2R_{10} - R_{11} - R_{12})/\sqrt{6}$
CH ₃ r ²	$S_{11} = (R_{11} - R_{12})/\sqrt{2}$
CO sd	$S_{12} = (2R_{13} - R_{14} - R_{15})/\sqrt{6}$
CO r	$S_{13} = (R_{14} - R_{15})/\sqrt{2}$
CO ob	$S_{14} = R_{16}$
CC t	$S_{15} = R_{17}$

^aAbbreviations: s = stretch, t = torsion, ss = symmetric stretch, as = antisymmetric stretch, sd = symmetric defor-

Table 3.13: (continued)

mation, ad = antisymmetric deformation, r = rock, ob = out of plane bend.

Table 3.14: Optimized Internal Coordinates for Acetate One Water Supermolecule in Base

Internal Coordinate	One Water, Base
Bond Stretches	
C ² -C ¹	1.5287
O ³ -C ²	1.2574
O ⁴ -C ²	1.2608
H ⁵ -C ¹	1.0798
H ⁶ -C ¹	1.0843
H ⁷ -C ¹	1.0841
Angle bends	
O ³ -C ² -C ¹	117.02
O ⁴ -C ² -C ¹	115.83
H ⁵ -C ¹ -C ²	110.92
H ⁶ -C ¹ -C ²	109.41
H ⁷ -C ¹ -C ²	109.47
Torsions	
O ⁴ -C ² -C ¹ -O ³	179.93
H ⁵ -C ¹ -C ² -O ⁴	180.67
H ⁶ -C ¹ -C ² -O ⁴	59.37
H ⁷ -C ¹ -C ² -O ⁴	-57.89

Internal and symmetry coordinates for glycine and glycinate are listed in Tables 3.15 and 3.16, respectively. Optimized internal coordinates for glycine and glycinate in various states of hydration are listed in Table 3.17. Raman spectra of glycine are shown in Figures 3.18 and 3.19 for H₂O and D₂O, respectively. Spectra are from Williams *et al* [1993]. Only four spectra are shown. Experimental frequencies for the other four isotopic species originally used for determination of the PED for glycine are listed in Williams *et al* [1993]. Raman spectra for glycinate are shown in Figures 3.20, 3.21, and 3.22. Not all isotopic species whose Raman spectra are shown were used in determination of the scale factors in this study. The spectra are included to demonstrate that the PED from which the PED for this study were patterned after included eight isotopic species.

Table 3.15: Redundant Internal Coordinates for Glycine in Base and Acid

Base ^a	
$R_1 = \Delta\gamma(\text{O}^4\text{-C}^3)$	$R_{13} = \Delta\theta(\text{H}^9\text{-C}^2\text{-C}^3)$
$R_2 = \Delta\gamma(\text{O}^5\text{-C}^3)$	$R_{14} = \Delta\theta(\text{H}^9\text{-C}^2\text{-N}^1)$
$R_3 = \Delta\gamma(\text{H}^8\text{-C}^2)$	$R_{15} = \Delta\theta(\text{O}^5\text{-C}^3\text{-O}^4)$
$R_4 = \Delta\gamma(\text{H}^9\text{-C}^2)$	$R_{16} = \Delta\theta(\text{O}^5\text{-C}^3\text{-C}^2)$
$R_5 = \Delta\gamma(\text{C}^3\text{-C}^2)$	$R_{17} = \Delta\theta(\text{O}^4\text{-C}^3\text{-C}^2)$
$R_6 = \Delta\gamma(\text{C}^2\text{-N}^1)$	$R_{18} = \Delta\omega(\text{C}^2\text{-O}^5\text{-O}^4\text{-C}^3)$
$R_7 = \Delta\gamma(\text{H}^6\text{-N}^1)$	$R_{19} = \Delta\theta(\text{H}^7\text{-N}^1\text{-H}^6)$
$R_8 = \Delta\gamma(\text{H}^7\text{-N}^1)$	$R_{20} = \Delta\theta(\text{H}^7\text{-N}^1\text{-C}^2)$
$R_9 = \Delta\theta(\text{H}^9\text{-C}^2\text{-H}^8)$	$R_{21} = \Delta\theta(\text{H}^6\text{-N}^1\text{-HC}^2)$
$R_{10} = \Delta\theta(\text{C}^3\text{-C}^2\text{-N}^1)$	$R_{22} = \Delta\omega(\text{C}^2\text{-H}^7\text{-H}^6\text{-N}^1)$
$R_{11} = \Delta\theta(\text{H}^8\text{-C}^2\text{-C}^3)$	$R_{23} = \Delta\tau(\text{C}^2\text{-N}^1)$
$R_{12} = \Delta\theta(\text{H}^8\text{-C}^2\text{-N}^1)$	$R_{24} = \Delta\tau(\text{C}^3\text{-C}^2)$
Acid	
$R_1 = \Delta\gamma(\text{H}^9\text{-C}^2)$	$R_{16} = \Delta\theta(\text{H}^{10}\text{-C}^2\text{-C}^3)$
$R_2 = \Delta\gamma(\text{H}^{10}\text{-C}^2)$	$R_{17} = \Delta\theta(\text{H}^{10}\text{-C}^2\text{-N}^1)$
$R_3 = \Delta\gamma(\text{C}^3\text{-C}^2)$	$R_{18} = \Delta\theta(\text{H}^8\text{-N}^1\text{-H}^6)$
$R_4 = \Delta\gamma(\text{O}^4\text{-C}^3)$	$R_{19} = \Delta\theta(\text{H}^7\text{-N}^1\text{-H}^6)$
$R_5 = \Delta\gamma(\text{O}^5\text{-C}^3)$	$R_{20} = \Delta\theta(\text{H}^8\text{-N}^1\text{-H}^7)$
$R_6 = \Delta\gamma(\text{H}^{11}\text{-O}^5)$	$R_{21} = \Delta\theta(\text{H}^7\text{-N}^1\text{-C}^2)$
$R_7 = \Delta\gamma(\text{C}^2\text{-N}^1)$	$R_{22} = \Delta\theta(\text{H}^8\text{-N}^1\text{-C}^2)$
$R_8 = \Delta\gamma(\text{H}^7\text{-N}^1)$	$R_{23} = \Delta\theta(\text{H}^6\text{-N}^1\text{-C}^2)$
$R_9 = \Delta\gamma(\text{H}^6\text{-N}^1)$	$R_{24} = \Delta\theta(\text{O}^5\text{-C}^3\text{-C}^2)$
$R_{10} = \Delta\gamma(\text{H}^8\text{-N}^1)$	$R_{25} = \Delta\theta(\text{O}^5\text{-C}^3\text{-O}^4)$
$R_{11} = \Delta\theta(\text{H}^{11}\text{-O}^5\text{-C}^3)$	$R_{26} = \Delta\theta(\text{O}^4\text{-C}^3\text{-C}^2)$
$R_{12} = \Delta\theta(\text{H}^{10}\text{-C}^2\text{-H}^9)$	$R_{27} = \Delta\omega(\text{O}^4\text{-O}^5\text{-C}^2\text{-C}^3)$
$R_{13} = \Delta\theta(\text{C}^3\text{-C}^2\text{-N}^1)$	$R_{28} = \Delta\tau(\text{C}^2\text{-N}^1)$
$R_{14} = \Delta\theta(\text{H}^9\text{-C}^2\text{-C}^3)$	$R_{29} = \Delta\tau(\text{C}^3\text{-C}^2)$
$R_{15} = \Delta\theta(\text{H}^9\text{-C}^2\text{-N}^1)$	$R_{30} = \Delta\tau(\text{O}^5\text{-C}^3)$

^aSymbols: γ = stretch, θ = bend, ω = out of plane bend, τ = torsion.

Table 3.16: Symmetry Coordinate Definitions for Glycine in Base and Acid

Base	
COO ss ^a	$S_1 = (R_1 + R_2)/\sqrt{2}$
COO as	$S_2 = (R_1 - R_2)/\sqrt{2}$
CH s ¹	$S_3 = R_3$
CH s ²	$S_4 = R_4$
CC s	$S_5 = R_5$
CN s	$S_6 = R_6$
NH ₂ ss	$S_7 = (R_7 + R_8)/\sqrt{2}$
NH ₂ as	$S_8 = (R_7 - R_8)/\sqrt{2}$
CH ₂ scissor	$S_9 = (5R_9 + R_{10})/\sqrt{26}$
NCC scissor	$S_{10} = R_{10}$
CH ₂ r	$S_{11} = (R_{11} - R_{12} + R_{13} - R_{14})/2$
CH ₂ wag	$S_{12} = (R_{11} - R_{12} - R_{13} + R_{14})/2$
CH ₂ twist	$S_{13} = (R_{11} + R_{12} - R_{13} - R_{14})/2$
CCOO sd	$S_{14} = (2R_{15} - R_{16} - R_{17})/\sqrt{6}$
CCOO r	$S_{15} = (R_{16} - R_{17})/\sqrt{2}$
CCOO wag	$S_{16} = R_{18}$
CNH ₂ scissor	$S_{17} = (2R_{19} - R_{20} - R_{21})/\sqrt{6}$
CNH ₂ twist	$S_{18} = (R_{20} - R_{21})/\sqrt{2}$
CNH ₂ wag	$S_{19} = R_{22}$
CN t	$S_{20} = R_{23}$
CC t	$S_{21} = R_{24}$
Acid	
CH s ¹	$S_1 = R_1$
CH s ²	$S_2 = R_2$
CC ^{ter} s	$S_3 = R_3$
CO s	$S_4 = R_4$
CO ^H s	$S_5 = R_5$
OH s	$S_6 = R_6$
CN _n s	$S_7 = R_7$
NH ₃ ss	$S_8 = (R_8 + R_9 + R_{10})/\sqrt{3}$
NH ₃ as ¹	$S_9 = (2R_8 - R_9 - R_{10})/\sqrt{6}$
NH ₃ as ²	$S_{10} = (R_9 - R_{10})/\sqrt{2}$
OH b	$S_{11} = R_{11}$
CH ₂ scissor	$S_{12} = (5R_{12} + R_{13})/\sqrt{26}$
NCC scissor	$S_{13} = R_{13}$

Table 3.16: (continued)

CH ₂ r	$S_{14} = (R_{14} - R_{15} + R_{16} - R_{17})/2$
CH ₂ wag	$S_{15} = (R_{14} - R_{15} - R_{16} + R_{17})/2$
CH ₂ twist	$S_{16} = (R_{14} + R_{15} - R_{16} - R_{17})/2$
NH ₃ sd	$S_{17} = (R_{18} + R_{19} + R_{20} - R_{21} - R_{22} - R_{23})/\sqrt{6}$
NH ₃ ad ¹	$S_{18} = (2R_{18} - R_{19} - R_{20})/\sqrt{6}$
NH ₃ ad ²	$S_{19} = (R_{19} - R_{20})/\sqrt{2}$
NH ₃ r ¹	$S_{20} = (2R_{21} - R_{22} - R_{23})/\sqrt{6}$
NH ₃ r ²	$S_{21} = (R_{22} - R_{23})/\sqrt{2}$
COO sd	$S_{22} = (2R_{24} - R_{25} - R_{26})/\sqrt{6}$
COO r	$S_{23} = (R_{25} - R_{26})/\sqrt{2}$
COO wag	$S_{24} = R_{27}$
CN ⁿ t	$S_{25} = R_{28}$
CC t	$S_{26} = R_{29}$
CO ^H t	$S_{27} = R_{30}$

Abbreviations: s = stretch, t = torsion, ss = symmetric stretch, as = antisymmetric stretch, sd = symmetric deformation, ad =antisymmetric deformation, r = rock, b = bend, ob = out of plane bend.

Table 3.17: Optimized Internal Coordinates for Glycinate and Glycine.

Internal Coordinate	Base			Acid
	One Water	Two Water	Four Water	One Water
Bond Stretches				
C ² -N ¹	1.4594	1.4523	1.4454	1.5136
C ³ -C ²	1.5335	1.5315	1.5270	1.5114
O ⁴ -C ³	1.2587	1.2684	1.2692	1.2152
O ⁵ -C ³	1.2580	1.2512	1.2549	1.2926
H ⁶ -N ¹	1.0001	0.9984	0.9970	1.0243
H ⁷ -N ¹	1.0003	0.9989	0.9976	1.0080
H ⁸ -C ²	1.0815	1.0820	1.0825	1.0772
H ⁹ -C ²	1.0844	1.0841	1.0833	1.0772
H ¹⁰ -N ¹				1.0079
H ¹¹ -O ⁵				1.0015
Angle bends				
C ³ -C ² -N ¹	115.06	116.94	116.96	106.83
O ⁴ -C ³ -C ²	116.88	118.01	118.78	119.85
O ⁵ -C ³ -C ²	115.53	115.72	116.38	112.14
H ⁶ -N ¹ -C ²	111.42	112.41	114.34	106.46
H ⁷ -N ¹ -C ²	109.63	113.28	114.26	112.38
H ⁸ -C ² -N ¹	109.83	109.62	109.76	109.85
H ⁹ -C ² -N ¹	109.29	109.10	109.48	109.85
H ¹⁰ -N ¹ -C ²				112.38
H ¹¹ -O ⁵ -C ³				118.74
Torsions				
O ⁴ -C ³ -C ² -N ¹	11.29	8.92	363.73	-0.00
O ⁵ -C ³ -C ² -N ¹	189.67	187.93	183.22	179.99
H ⁶ -N ¹ -C ² -C ³	75.52	63.66	66.31	0.02
H ⁷ -N ¹ -C ² -C ³	-43.78	-60.31	298.25	-118.86
H ⁸ -C ² -N ¹ -C ³	237.30	237.50	237.55	-119.97
H ⁹ -C ² -N ¹ -C ³	120.88	121.73	121.72	119.97
H ¹⁰ -N ¹ -C ² -C ³				118.91
H ¹¹ -O ⁵ -C ³ -C ²				180.01

Scale factors determined from force constants calculated based on the optimized geometries of methylamine one water supermolecule in base, methylamine three water supermolecule in acid, acetate one water supermolecule, glycinate one, two, and four water supermolecules, and glycine one water supermolecule, all water-excluded, are listed in Table 3.18. The scale factors for methylamine in base were based on experimental spectra of four isotopic species, for methylamine in acid two isotopic species were used. Acetate scale factors were optimized based on experimental spectra of two isotopic species. Glycine one water in base scale factors were optimized to experimental spectra of six isotopic species while the two and four water supermolecules were both optimized to four isotopic species. The glycine in acid scale factors were optimized to experimental frequencies for eight isotopic species.

Table 3.18: Scale factors for methylamine, acetate and glycine

Coordinate	Methylamine		Acetate	Glycine			
	1w base	3w acid	1w base	1w base	2w base	4w base	1w acid
COO ss ^a			87.20	85.00	83.78	80.23	
COO as			77.60	78.00	79.35	82.25	
CH s ¹				81.01	80.00	83.00	81.54
CH s ²				81.00	80.22	83.00	81.64
CC s			100.78	103.90	101.20	106.66	99.93
CN s	84.76	91.25		82.77	84.74	81.74	97.00
NH ₂ ss	81.81			67.72	67.00	67.00	
NH ₂ as	79.23			75.00	70.00	70.00	
NH ₃ ss		77.53					81.00
NH ₃ as ¹		92.00					81.00
NH ₃ as ²		92.00					81.00
CH ₂ sis				76.30	77.31	77.25	77.86
NCC sis				89.59	75.77	83.02	85.55
CH ₂ r				80.50	79.53	78.47	79.76
CH ₂ wag				82.50	79.18	77.52	83.99
CH ₂ twist				71.03	70.47	69.08	71.39
CCOO sd			78.94	75.21	83.36	77.46	76.12
CCOO r			87.60	90.79	84.00	72.42	87.24
CCOO wag			82.00	92.99	95.06	93.62	91.67
NH ₂ sis	75.46			73.50	72.99	72.67	
NH ₂ twist	86.26			80.00	83.53	84.11	
NH ₂ wag	121.89			85.98	89.53	103.42	
NH ₃ sd		68.40					76.05
NH ₃ ad ¹		68.26					75.21
NH ₃ ad ²		68.26					75.21
NH ₃ r ¹		81.89					84.56
NH ₃ r ²		67.37					80.01
CN t	120.00	80.00		100.00	90.00	90.00	80.00
CC t			200.00	200.00	90.00	90.00	100.00
CH ₃ ss	80.77	84.11	86.75				
CH ₃ as ¹	84.69	82.71	86.50				
CH ₃ as ²	82.60	82.71	85.80				
CH ₃ sd	78.73	77.52	77.31				

Table 3.18: (continued)

Coordinate	Methylamine		Acetate	Glycine			
	1w base	3w acid	1w base	1w base	2w base	4w base	1w acid
CH ₃ ad ¹	78.57	77.37	78.86				
CH ₃ ad ²	77.39	77.37	76.78				
CH ₃ r ¹	81.85	81.07	79.02				
CH ₃ r ²	78.64	82.84	76.80				
C=O s							83.20
CO ^H s						80.22	
OH s							83.43
OH b							88.95
CO ^H t							95.00

^aAbbreviations: s = stretch, t = torsion, ss = symmetric stretch, as = antisymmetric stretch, sd = symmetric deformation, sis = scissor, ad = antisymmetric deformation, r = rock, b = in plane bend.

The PED calculated from normal mode analyses using the scaled force constants for methylamine one water basic structure is given in Table 3.19, for the methylamine three water acidic structure in Table 3.20. Acetate PED for the one water supermolecule structure is given in Table 3.21.

The PED for the various hydration states of glycinate are listed in Tables 3.22, 3.23, and 3.24, and the PED for glycine in acid in Table 3.25.

Table 3.19: Scaled 4-31G Frequencies and Potential Energy Distribution for Water-Excluded Methylamine One-water Supermolecule in Base.

frequency (cm^{-1})			CH ₃ NH ₂ (mean deviation = 12 cm^{-1})
obs.	calc.	dev.	
			Potential Energy Distribution
—	476	—	CN t(99)
955	951	-4	CNH ₂ ob(54), CN s(23), NCH ₃ r ² (18)
—	968	—	NCH ₃ r ¹ (41), CNH ₂ r(38), NCH ₃ r ² (8), CNH ₂ ob(7)
1034	1037	3	CN s(72), CNH ₂ ob(13), NCH ₃ r ² (10)
1172	1180	8	NCH ₃ r ² (49), CNH ₂ ob(25), NCH ₃ r ¹ (17)
1323	1340	17	CNH ₂ r(56), NCH ₃ r ¹ (27), NCH ₃ r ² (8), NCH ₃ ad ¹ (7)
1428	1443	15	NCH ₃ sd(86), NCH ₃ ad ² (12)
1465	1471	6	NCH ₃ ad ² (75), NCH ₃ sd(15)
1479	1493	14	NCH ₃ ad ¹ (82), NCH ₃ r ¹ (9)
1602	1608	6	CNH ₂ sissor(100)
2822	2854	32	CH ₃ ss(91), CH ₃ as ¹ (9)
2964	2977	13	CH ₃ as ¹ (78), CH ₃ as ² (15), CH ₃ ss(8)
2980	2990	10	CH ₃ as ² (85), CH ₃ as ¹ (13)
—	3384	—	NH ₂ ss(100)
—	3422	22	NH ₂ as(100)

frequency (cm^{-1})			CH ₃ ND ₂ (mean deviation = 12 cm^{-1})
obs.	calc.	dev.	
			Potential Energy Distribution
—	393	—	CN t(99)
760	764	4	CNH ₂ ob(93)
—	789	—	CNH ₂ r(75), NCH ₃ r ¹ (17)
995	981	-14	CN s(88), CNH ₂ sissor(12)
1144	1146	2	NCH ₃ r ² (59), NCH ₃ r ¹ (13), CNH ₂ sissor(12)
1210	1205	-5	CNH ₂ sissor(76), NCH ₃ r ² (13), CN s(8)
1222	1225	3	NCH ₃ r ¹ (59), CNH ₂ r(23), NCH ₃ r ² (10)
1427	1443	16	NCH ₃ sd(88), NCH ₃ ad ² (11)
1464	1471	7	NCH ₃ ad ² (78), NCH ₃ sd(13)
1476	1491	15	NCH ₃ ad ¹ (86), NCH ₃ r ¹ (8)
—	2444	—	NH ₂ ss(100)
—	2528	—	NH ₂ as(100)
2821	2854	33	CH ₃ ss(91), CH ₃ as ¹ (9)

Table 3.19: (continued)

frequency (cm^{-1})			Potential Energy Distribution
obs.	calc.	dev.	
2961	2977	16	CH_3 as ¹ (78), CH_3 as ² (14), CH_3 ss(8)
2975	2991	16	CH_3 as ² (86), CH_3 as ¹ (13)

frequency (cm^{-1})			¹³ CD ₃ NH ₂ (mean deviation = 14 cm^{-1})
obs.	calc.	dev.	
—	432	—	CN t(98)
804	783	−21	NCH ₃ r ¹ (44), NCH ₃ r ² (35), CNH ₂ r(16)
826	824	−2	NCH ₃ r ² (44), NCH ₃ r ¹ (34), CNH ₂ ob(19)
949	947	−2	CN s(82), NCH ₃ sd(13)
1045	1038	−7	CNH ₂ ob(45), NCH ₃ sd(33), NCH ₃ r ² (11), NCH ₃ ad ² (8)
1065	1058	−7	NCH ₃ ad ² (82), NCH ₃ ad ¹ (8), CNH ₂ ob(8)
1065	1072	7	NCH ₃ ad ¹ (89), NCH ₃ ad ² (9)
1113	1135	22	NCH ₃ sd(51), CNH ₂ ob(26), CN s(20)
1256	1258	2	CNH ₂ r(83), NCH ₃ r ¹ (12)
—	1607	7	CNH ₂ sissor(100)
2078	2045	−33	CH_3 ss(96)
2207	2189	−18	CH_3 as ¹ (88), CH_3 as ² (8)
2222	2202	−20	CH_3 as ² (91), CH_3 as ¹ (8)
—	3384	—	NH ₂ ss(100)
—	3422	—	NH ₂ as(100)

frequency (cm^{-1})			¹³ CD ₃ ND ₂ (mean deviation = 17 cm^{-1})
obs.	calc.	dev.	
—	339	—	CN t(99)
704	692	−12	CNH ₂ r(45), NCH ₃ r ¹ (30), NCH ₃ r ² (21)
726	716	−10	CNH ₂ ob(67), NCH ₃ r ² (16), NCH ₃ r ¹ (15)
896	914	18	CN s(63), NCH ₃ r ² (12), CNH ₂ sissor(8)
930	936	6	NCH ₃ r ² (38), CNH ₂ ob(24), CN s(15), NCH ₃ r ¹ (12), NCH ₃ sd(10)
1031	1048	17	CNH ₂ r(42), NCH ₃ r ¹ (33), NCH ₃ ad ² (12), NCH ₃ r ² (11)
1064	1056	−8	NCH ₃ ad ² (73), NCH ₃ ad ¹ (16)

Table 3.19: (continued)

frequency (cm^{-1})			Potential Energy Distribution
obs.	calc.	dev.	
1097	1074	-23	NCH ₃ ad ¹ (81), NCH ₃ ad ² (13)
1139	1106	-33	NCH ₃ sd(82), CN s(11)
1198	1196	-2	CNH ₂ sissor(90), CN s(11)
2078	2045	-33	CH ₃ ss(96)
2204	2189	-15	CH ₃ as ¹ (88), CH ₃ as ² (8)
2209	2202	-7	CH ₃ as ² (91), CH ₃ as ¹ (8)
—	2444	—	NH ₂ ss(100)
—	2528	—	NH ₂ as(100)

Table 3.20: Scaled 4-31G Frequencies and Potential Energy Distribution for Water-Excluded Methylamine Three-water Supermolecule in Acid.

frequency (cm^{-1})			CH ₃ NH ₃ (mean deviation = 11 cm^{-1})
obs.	calc.	dev.	Potential Energy Distribution
—	472	—	CN t(100)
959	981	22	CNH ₃ r ² (56), NCH ₃ r ² (39)
995	993	-2	CN s(104)
—	1020	—	NCH ₃ r ¹ (58), CNH ₃ r ¹ (35)
1266	1246	-20	NCH ₃ r ² (50), CNH ₃ r ² (37), NCH ₃ ad ^{1,2} (10)
—	1296	—	CNH ₃ r ¹ (52), NCH ₃ r ¹ (30), NCH ₃ ad ^{1,2} (9), CNH ₃ ad ^{1,2} (8)
1426	1427	1	NCH ₃ sd(99)
1468	1468	0	NCH ₃ ad ^{1,2} (86), NCH ₃ r ¹ (11)
1468	1469	1	NCH ₃ ad ^{1,2} (87), NCH ₃ r ² (11)
1505	1506	1	CNH ₃ sd(99)
1594	1591	-3	CNH ₃ ad ^{1,2} (91)
1594	1605	11	CNH ₃ ad ^{1,2} (85), CNH ₃ r ¹ (12)
2960	2958	-2	NH ₃ ss(76), CH ₃ ss(24)
2977	2982	5	CH ₃ ss(76), NH ₃ ss(24)
3039	3040	1	CH ₃ as ^{1,2} (97)
3039	3040	1	CH ₃ as ^{1,2} (97)
3113	3297	—	NH ₃ as ¹ (54), NH ₃ as ¹ (46)
—	3298	—	NH ₃ as ¹ (54), NH ₃ as ¹ (46)

frequency (cm^{-1})			CH ₃ ND ₃ (mean deviation = 4 cm^{-1})
obs.	calc.	dev.	Potential Energy Distribution
—	405	—	CN t(100)
774	781	7	CNH ₃ r ² (85), NCH ₃ r ² (12)
845	843	-2	CNH ₃ r ¹ (76), NCH ₃ r ¹ (19)
947	950	3	CN s(90), CNH ₃ sd(12)
1149	1144	-5	CNH ₃ ad ^{1,2} (89), CNH ₃ ad ^{1,2} (7)
1149	1147	-2	CNH ₃ ad ^{1,2} (82), CNH ₃ sd(7)
1149	1148	-1	CNH ₃ sd(81), CN s(11), CNH ₃ ad ^{1,2} (7)
1194	1186	-8	NCH ₃ r ² (77), CNH ₃ r ² (11), NCH ₃ ad ^{1,2} (10)
1194	1194	0	NCH ₃ r ¹ (69), CNH ₃ r ¹ (21), NCH ₃ ad ^{1,2} (9)
1429	1428	-1	NCH ₃ sd(103)

Table 3.20: (continued)

frequency (cm^{-1})			Potential Energy Distribution
obs.	calc.	dev.	
1467	1467	0	NCH_3 $\text{ad}^{1,2}(90)$, NCH_3 $\text{r}^1(9)$
1467	1469	2	NCH_3 $\text{ad}^{1,2}(90)$, NCH_3 $\text{r}^2(10)$
—	2125	—	NH_3 $\text{ss}(99)$
—	2436	—	NH_3 $\text{as}^1(89)$, NH_3 $\text{as}^1(10)$
—	2436	—	NH_3 $\text{as}^1(89)$, NH_3 $\text{as}^1(10)$
2980	2977	-3	CH_3 $\text{ss}(100)$
3042	3041	-1	CH_3 $\text{as}^{1,2}(95)$
3042	3041	-1	CH_3 $\text{as}^{1,2}(95)$

Table 3.21: Scaled 4-31G Frequencies and Potential Energy Distributions for One-Water Acetic Acid Supermolecule Water-Excluded in Base.

frequency (cm^{-1})			CH_3CO_2^- (mean deviation = 5 cm^{-1})
obs.	calc.	dev.	Potential Energy Distribution
—	220	—	CC t(98)
470	470	0	CO r(86), CH3 r ¹ (11)
620	619	-1	CO o(72), CH3 r ² (25)
650	646	-4	CO sd(77), CC s(20)
920	929	9	CC s(58), CO ss(29), CO sd(10)
1015	1019	4	CH3 r ¹ (78), CO as(11), CO r(7)
1055	1041	-14	CH3 r ² (70), CO o(26)
1345	1346	1	CH3 sd(91), CO ss(8)
1410	1409	-1	CO ss(59), CC s(21), CO sd(11)
1438	1443	5	CH3 ad ² (94)
1438	1445	7	CH3 ad ¹ (88)
1560	1564	4	CO as(80), CH3 r ¹ (8), CO r(7)
2961	2962	1	CH3 ss(96)
2997	2996	-1	CH3 as ² (100)
3048	3048	0	CH3 as ¹ (97)

frequency (cm^{-1})			$^{13}\text{CD}_3^{13}\text{CO}_2^-$ (mean deviation = 7 cm^{-1})
obs.	calc.	dev.	Potential Energy Distribution
—	162	—	CC t(98)
415	415	0	CO r(75), CH3 r ¹ (23)
520	519	-1	CO o(50), CH3 r ² (48)
610	610	0	CO sd(66), CC s(28)
820	815	-5	CH3 r ¹ (72), CO r(18), CO as(9)
850	862	12	CC s(34), CH3 sd(22), CO sd(22), CO ss(20)
875	890	15	CH3 r ² (50), CO o(49)
1045	1041	-4	CH3 ad ² (98)
1050	1044	-6	CH3 ad ¹ (92)
1070	1064	-6	CH3 sd(66), CC s(19), CO ss(8), CH3 ad ¹ (7)
1380	1371	-9	CO ss(70), CC s(18), CO sd(11)
1510	1506	-4	CO as(89)
—	2123	—	CH3 ss(99)

Table 3.21: (continued)

frequency (cm^{-1})			Potential Energy Distribution
obs.	calc.	dev.	
—	2201	—	CH3 as ² (100)
—	2242	—	CH3 as ¹ (99)

Table 3.22: Scaled 4-31G Frequencies and Potential Energy Distribution for One-Water Glycine Supramolecule Water-Excluded in Base.

frequency (cm ⁻¹)			NH ₂ CH ₂ CO ₂ ⁻¹ (mean deviation = 10 cm ⁻¹)
obs.	calc.	dev.	
			Potential Energy Distribution
—	163	—	CN t(65), CC t(33)
—	224	—	CC t(67), CN t(31)
330	333	3	NCC sis(54), CCOO r(39)
511	516	5	CCOO r(34), CCOO sd(16), NCC sis(13), CC s(11), CN s(10)
578	582	4	CCOO wag(45), CH ₂ twist(33), CCOO sd(11)
674	674	0	CCOO sd(51), NCC sis(13), CCOO r(12)
901	875	-26	NH ₂ wag(26), CC s(25), CN s(17), COO ss(14), CCOO sd(9)
—	908	—	CH ₂ twist(34), CCOO wag(31), NH ₂ twist(17), NH ₂ wag(11)
968	982	14	NH ₂ wag(29), CC s(27), COO ss(16), CN s(14)
1108	1105	-3	CN s(50), NH ₂ wag(26), NCC sis(8)
1171	1151	-20	CH ₂ wag(39), NH ₂ twist(32), CH ₂ twist(9), CCOO wag(8)
1314	1317	3	CH ₂ r(80), COO ss(7)
1341	1353	12	CH ₂ wag(43), NH ₂ twist(42)
1403	1409	6	COO ss(50), CC s(24), CH ₂ sis(10), CCOO sd(9)
1430	1431	1	CH ₂ sis(88)
1566	1569	3	COO as(86), CCOO r(7)
1603	1608	5	NH ₂ sissor(100)
—	2873	—	CH s ² (87), CH s ¹ (13)
—	2920	—	CH s ¹ (87), CH s ² (13)
—	3052	—	NH ₂ ss(100)
—	3288	—	NH ₂ as(100)

frequency (cm ⁻¹)			ND ₂ CH ₂ CO ₂ ⁻¹ (mean deviation = 15 cm ⁻¹)
obs.	calc.	dev.	
			Potential Energy Distribution
—	122	—	CN t(84), CC t(14)
—	208	—	CC t(84), CN t(12)
311	310	-1	NCC sis(58), CCOO r(31), NH ₂ wag(8)
501	500	-1	CCOO r(44), CCOO sd(11), CN s(9), NCC sis(9), CC s(8)

Table 3.22: (continued)

frequency (cm^{-1})			Potential Energy Distribution
obs.	calc.	dev.	
592	576	-16	CCOO wag(42), CH ₂ twist(36), CCOO sd(9)
647	644	-3	CCOO sd(50), NH ₂ wag(17), CC s(10), CCOO r(9)
761	767	6	NH ₂ wag(51), NH ₂ twist(16), CCOO wag(7)
847	796	-51	NH ₂ twist(38), CCOO wag(16), CCOO sd(10), CN s(8), NH ₂ wag(7)
926	948	22	CC s(43), COO ss(23), NCC sis(10), NH ₂ wag(8)
1057	1043	-14	CN s(48), CH ₂ twist(13), CCOO wag(11)
1057	1054	-3	CH ₂ twist(31), NH ₂ twist(22), CN s(18), CCOO wag(14)
1192	1186	-6	NH ₂ sissor(90), CN s(9)
1275	1278	3	CH ₂ wag(85), NH ₂ twist(9)
1323	1321	-2	CH ₂ r(82), COO ss(10)
1413	1409	-4	COO ss(51), CC s(24), CH ₂ sis(10), CCOO sd(9)
1432	1431	-1	CH ₂ sis(88)
1577	1569	-8	COO as(86), CCOO r(7)
—	2204	—	NH ₂ ss(100)
—	2423	—	NH ₂ as(100)
—	2873	—	CH s ² (86), CH s ¹ (14)
—	2921	—	CH s ¹ (86), CH s ² (14)

frequency (cm ⁻¹)			NH ₂ CH ₂ ¹³ CO ₂ ⁻¹ (mean deviation = 10 cm ⁻¹)
obs.	calc.	dev.	
Potential Energy Distribution			
—	163	—	CN t(65), CC t(33)
—	224	—	CC t(67), CN t(31)
330	333	3	NCC sis(54), CCOO r(40)
511	514	3	CCOO r(34), CCOO sd(15), NCC sis(14), CC s(11), CN s(10)
576	575	-1	CCOO wag(48), CH ₂ twist(30), CCOO sd(11)
680	671	-9	CCOO sd(53), NCC sis(13), CCOO r(12)
896	871	-25	CC s(26), NH ₂ wag(24), CN s(16), COO ss(13), CCOO sd(9)
—	898	—	CH ₂ twist(37), CCOO wag(30), NH ₂ twist(15), NH ₂ wag(11)
968	980	12	NH ₂ wag(31), CC s(27), COO ss(15), CN s(15)

Table 3.22: (continued)

frequency (cm^{-1})			Potential Energy Distribution
obs.	calc.	dev.	
1109	1104	-5	CN s(48), NH ₂ wag(25), NCC sis(8)
1171	1147	-24	CH ₂ wag(39), NH ₂ twist(31), CN s(8), CH ₂ twist(8)
1313	1314	1	CH ₂ r(75), COO ss(13)
1335	1351	16	CH ₂ wag(42), NH ₂ twist(39), COO ss(9)
1383	1382	-1	COO ss(45), CC s(22), CH ₂ r(11), CCOO sd(7)
1431	1430	-1	CH ₂ sis(95)
1530	1526	-4	COO as(85), CCOO r(7)
1603	1608	5	NH ₂ sissor(101)
—	2873	—	CH s ² (87), CH s ¹ (13)
—	2920	—	CH s ¹ (87), CH s ² (13)
—	3052	—	NH ₂ ss(100)
—	3288	—	NH ₂ as(100)

frequency (cm^{-1})			NH ₂ ¹³ CH ₂ CO ₂ ⁻¹ (mean deviation = 9 cm^{-1})
obs.	calc.	dev.	
—	162	—	CN t(64), CC t(34)
—	222	—	CC t(66), CN t(32)
330	333	3	NCC sis(55), CCOO r(39)
511	514	3	CCOO r(34), CCOO sd(16), NCC sis(13), CC s(12), CN s(9)
584	580	-4	CCOO wag(44), CH ₂ twist(33), CCOO sd(12)
665	667	2	CCOO sd(48), NCC sis(14), CCOO r(13)
896	869	-27	CC s(25), NH ₂ wag(22), CN s(18), COO ss(15), CCOO sd(10)
900	904	4	CH ₂ twist(35), CCOO wag(33), NH ₂ twist(15), NH ₂ wag(10)
968	972	4	NH ₂ wag(29), CC s(26), CN s(18), COO ss(16)
1087	1089	2	CN s(50), NH ₂ wag(31), NCC sis(9)
1168	1145	-23	CH ₂ wag(40), NH ₂ twist(35), CH ₂ twist(9), CCOO wag(8)
1311	1309	-2	CH ₂ r(85)
1341	1350	9	CH ₂ wag(45), NH ₂ twist(42)
1401	1403	2	COO ss(54), CC s(22), CH ₂ sis(10), CCOO sd(10)
1426	1427	1	CH ₂ sis(87)

Table 3.22: (continued)

frequency (cm^{-1})			Potential Energy Distribution
obs.	calc.	dev.	
1570	1569	-1	COO as(86), CCOO r(7)
1601	1608	7	NH ₂ sissor(100)
—	2866	—	CH s ² (89), CH s ¹ (11)
—	2910	—	CH s ¹ (89), CH s ² (11)
—	3052	—	NH ₂ ss(100)
—	3288	—	NH ₂ as(100)

frequency (cm^{-1})			NH ₂ CD ₂ CO ₂ ⁻¹ (mean deviation = 17 cm^{-1})
obs.	calc.	dev.	
—	160	—	CN t(52), CC t(46)
—	207	—	CC t(55), CN t(45)
—	331	—	NCC sis(54), CCOO r(40)
490	479	-11	CH ₂ twist(43), CCOO wag(26), CCOO r(12)
509	525	16	CCOO sd(22), CCOO r(17), CC s(15), CH ₂ twist(13), CCOO wag(10), CN s(7), NCC sis(7)
667	654	-13	CCOO sd(46), CCOO r(17), NCC sis(14), CC s(7)
831	791	-40	CH ₂ wag(44), CH ₂ twist(22), CCOO wag(18), NH ₂ twist(13)
877	863	-14	CC s(32), COO ss(21), CCOO sd(16), NH ₂ wag(9), CH ₂ r(8)
877	881	4	CH ₂ r(35), CN s(33), NH ₂ wag(29)
932	957	25	CCOO wag(43), CH ₂ wag(41), CH ₂ twist(12)
1015	1005	-10	CH ₂ sis(55), NH ₂ wag(31), CH ₂ r(8)
1066	1091	25	CH ₂ sis(32), NH ₂ wag(20), CH ₂ r(19), CC s(11), NCC sis(8), COO ss(7)
1146	1148	2	CN s(45), CH ₂ r(22), CH ₂ sis(7)
1267	1256	-11	NH ₂ twist(82), CH ₂ twist(7)
1408	1406	-2	COO ss(62), CC s(25), CCOO sd(11)
1558	1564	6	COO as(89), CCOO r(7)
—	1607	—	NH ₂ sissor(101)
—	2095	—	CH s ² (69), CH s ¹ (29)
—	2164	—	CH s ¹ (69), CH s ² (30)
—	3052	—	NH ₂ ss(100)

Table 3.22: (continued)

frequency (cm^{-1})			Potential Energy Distribution
obs.	calc.	dev.	
—	3287	—	NH ₂ as(100)
<hr/>			
frequency (cm^{-1})			Potential Energy Distribution
obs.	calc.	dev.	
—	122	—	CN t(82), CC t(16)
—	190	—	CC t(85), CN t(15)
310	308	-2	NCC sis(58), CCOO r(32), NH ₂ wag(7)
501	467	-34	CH ₂ twist(41), CCOO wag(21), CCOO r(18)
501	513	12	CCOO r(23), CH ₂ twist(17), CCOO sd(15), CC s(11), CCOO wag(11)
640	629	-11	CCOO sd(48), CCOO r(13), NH ₂ wag(13), CC s(12)
714	718	4	NH ₂ twist(33), CH ₂ wag(31), CCOO wag(19), NH ₂ wag(11)
738	773	35	NH ₂ wag(52), CN s(17), CCOO sd(8), NCC sis(7)
876	867	-9	CH ₂ r(29), CC s(27), COO ss(19), CCOO sd(14)
960	944	-16	CN s(33), CH ₂ sis(24), CH ₂ r(18), NH ₂ wag(8), NCC sis(7)
960	956	-4	CCOO wag(47), CH ₂ wag(33), CH ₂ twist(16)
1002	1029	27	NH ₂ twist(47), CH ₂ wag(24), CH ₂ twist(15), CH ₂ sis(8)
1065	1079	14	CH ₂ sis(57), NCC sis(9), CC s(7), NH ₂ twist(7)
1151	1119	-32	CH ₂ r(30), NH ₂ sissor(25), CN s(19), COO ss(7), CC s(7)
1216	1200	-16	NH ₂ sissor(73), CN s(16)
1409	1407	-2	COO ss(62), CC s(25), CCOO sd(11)
1574	1563	-11	COO as(89), CCOO r(7)
—	2095	—	CH s ² (70), CH s ¹ (29)
—	2163	—	CH s ¹ (69), CH s ² (29)
—	2205	—	NH ₂ ss(99)
—	2423	—	NH ₂ as(100)

Table 3.23: Scaled 4-31G Frequencies and Potential Energy Distribution for Two-Water Glycine Supramolecule Water-Excluded in Base.

frequency (cm^{-1})			$\text{NH}_2\text{CH}_2\text{CO}_2^-$ (mean deviation = 9 cm^{-1})
obs.	calc.	dev.	
			Potential Energy Distribution
—	170	—	CC t(101)
—	289	—	CN t(58), NCC sis(25), CCOO r(12)
330	339	9	CN t(40), NCC sis(32), CCOO r(28)
511	517	6	CCOO r(38), NCC sis(18), CC s(12), CN s(10), CCOO sd(10)
578	594	16	CCOO wag(47), CH_2 twist(39)
674	679	5	CCOO sd(57), NCC sis(12), CC s(11), CCOO r(9)
901	885	-16	NH_2 wag(37), CC s(17), CN s(15), COO ss(14), CCOO sd(14)
—	906	—	CH_2 twist(38), CCOO wag(34), NH_2 twist(18)
968	960	-8	NH_2 wag(40), CC s(26), COO ss(17)
1108	1116	8	CN s(68), NH_2 wag(17)
1171	1162	-9	CH_2 wag(48), NH_2 twist(30), CCOO wag(11), CH_2 twist(10)
1314	1321	7	CH_2 r(89)
1341	1353	12	NH_2 twist(49), CH_2 wag(44)
1403	1408	5	COO ss(50), CC s(23), CH_2 sis(10), CCOO sd(10)
1430	1435	5	CH_2 sis(88)
1566	1572	6	COO as(83)
1603	1609	6	NH_2 sissor(100)
—	2863	—	CH s ² (73), CH s ¹ (27)
—	2900	—	CH s ¹ (73), CH s ² (27)
—	3054	—	NH_2 ss(100)
—	3199	—	NH_2 as(100)

frequency (cm^{-1})			$\text{ND}_2\text{CH}_2\text{CO}_2^-$ (mean deviation = 13 cm^{-1})
obs.	calc.	dev.	
			Potential Energy Distribution
—	159	—	CC t(95)
—	224	—	CN t(86)
311	307	-4	NCC sis(56), CCOO r(32), CN t(8)
501	500	-1	CCOO r(46), NCC sis(13), CC s(9), CN s(9), CCOO sd(7)

Table 3.23: (continued)

frequency (cm^{-1})			Potential Energy Distribution
obs.	calc.	dev.	
592	584	-8	CH ₂ twist(42), CCOO wag(41)
647	650	3	CCOO sd(47), NH ₂ wag(26), CC s(15)
761	763	2	NH ₂ wag(56), CCOO sd(19), NCC sis(7)
847	797	-50	NH ₂ twist(51), CCOO wag(27), CH ₂ twist(8), CH ₂ wag(7)
926	928	2	CC s(41), COO ss(28), CCOO sd(10), NCC sis(8)
1057	1056	-1	CN s(64), NH ₂ sissor(15)
1057	1064	7	CH ₂ twist(42), NH ₂ twist(28), CCOO wag(24)
1192	1194	2	NH ₂ sissor(84), CN s(13)
1275	1271	-4	CH ₂ wag(87), NH ₂ twist(9)
1323	1325	2	CH ₂ r(87)
1413	1409	-4	COO ss(49), CC s(23), CH ₂ sis(11), CCOO sd(10)
1432	1435	3	CH ₂ sis(88)
1577	1571	-6	COO as(83)
—	2207	—	NH ₂ ss(99)
—	2360	—	NH ₂ as(99)
—	2864	—	CH s ² (73), CH s ¹ (27)
—	2900	—	CH s ¹ (73), CH s ² (27)

frequency (cm^{-1})			NH ₂ CD ₂ CO ₂ ⁻¹ (mean deviation = 17 cm^{-1})
obs.	calc.	dev.	
—	155	—	CC t(103)
—	286	—	CN t(59), NCC sis(25), CCOO r(12)
—	337	—	CN t(40), NCC sis(32), CCOO r(28)
490	486	-4	CH ₂ twist(40), CCOO wag(22), CCOO r(16), NCC sis(7)
509	527	18	CCOO r(19), CH ₂ twist(18), CC s(14), CCOO wag(12), NCC sis(11), CCOO sd(11), CN s(7)
667	657	-10	CCOO sd(49), CC s(14), NCC sis(12), CCOO r(12)
831	792	-39	CH ₂ wag(47), CH ₂ twist(22), CCOO wag(18), NH ₂ twist(12)
877	876	-1	CC s(26), COO ss(24), CCOO sd(24), NH ₂ wag(8)
877	885	8	NH ₂ wag(40), CH ₂ r(30), CN s(27)
932	960	28	CCOO wag(46), CH ₂ wag(41), CH ₂ twist(12)
1015	994	-21	CH ₂ sis(40), NH ₂ wag(31), CH ₂ r(18), CN s(7)

Table 3.23: (continued)

frequency (cm^{-1})			Potential Energy Distribution
obs.	calc.	dev.	
1066	1076	10	CH ₂ sis(51), CH ₂ r(16), NH ₂ wag(12), CC s(9)
1146	1161	15	CN s(50), CH ₂ r(22), COO ss(7)
1267	1265	-2	NH ₂ twist(86), CH ₂ twist(7)
1408	1409	1	COO ss(58), CC s(25), CCOO sd(12)
1558	1566	8	COO as($\delta\tau$)
1601	1608	7	NH ₂ sissor(101)
—	2086	—	CH s ² (60), CH s ¹ (39)
—	2150	—	CH s ¹ (60), CH s ² (39)
—	3054	—	NH ₂ ss(100)
—	3198	—	NH ₂ as(100)

frequency (cm^{-1})			ND ₂ CD ₂ CO ₂ ⁻¹ (mean deviation = 16 cm^{-1})
obs.	calc.	dev.	
—	148	—	CC t(101)
—	218	—	CN t(91)
310	305	-5	NCC sis(56), CCOO r(32), CN t(8)
501	473	-28	CH ₂ twist(38), CCOO r(22), CCOO wag(18)
501	513	12	CH ₂ twist(23), CCOO r(23), CCOO wag(12), CC s(10), NCC sis(9), CCOO sd(7)
640	636	-4	CCOO sd(46), CC s(19), NH ₂ wag(18), CCOO r(8)
714	722	8	CH ₂ wag(34), NH ₂ twist(33), CCOO wag(20), CH ₂ twist(7)
738	755	17	NH ₂ wag(60), CCOO sd(10), CN s(9), NCC sis(7)
876	878	2	CC s(26), COO ss(24), CCOO sd(22), CH ₂ r(21)
960	943	-17	CN s(36), CH ₂ r(28), CH ₂ sis(18)
960	960	0	CCOO wag(46), CH ₂ wag(41), CH ₂ twist(12)
1002	1040	38	NH ₂ twist(58), CH ₂ wag(19), CH ₂ twist(19)
1065	1065	0	CH ₂ sis(70), CH ₂ r(10), CC s(7)
1151	1121	-30	NH ₂ sissor(30), CH ₂ r(26), CN s(21), CH ₂ sis(7)
1216	1209	-7	NH ₂ sissor(67), CN s(22)
1409	1410	1	COO ss(57), CC s(25), CCOO sd(12)
1574	1566	-8	COO as(87)
—	2086	—	CH s ² (60), CH s ¹ (39)
—	2150	—	CH s ¹ (60), CH s ² (39)

Table 3.23: (continued)

frequency (cm^{-1})			Potential Energy Distribution
obs.	calc.	dev.	
—	2207	—	NH ₂ ss(99)
—	2360	—	NH ₂ as(100)

Table 3.24: Scaled 4-31G Frequencies and Potential Energy Distribution for Four-Water Glycine Supramolecule Water-Excluded in Base.

frequency (cm ⁻¹)			NH ₂ CH ₂ CO ₂ ⁻¹ (mean deviation = 8 cm ⁻¹)
obs.	calc.	dev.	
			Potential Energy Distribution
—	210	—	CC t(99)
330	325	-5	CCOO r(53), NCC sis(42)
—	348	—	CN t(99)
511	521	10	CCOO r(29), NCC sis(25), CCOO sd(16), CC s(14), CN s(12)
578	592	14	CCOO wag(50), CH ₂ twist(43)
674	677	3	CCOO sd(61), NCC sis(18), CC s(7), CCOO r(7)
901	886	-15	NH ₂ wag(37), CC s(18), CN s(16), COO ss(15), CCOO sd(9)
—	905	—	CH ₂ twist(39), CCOO wag(37), NH ₂ twist(17)
968	962	-6	NH ₂ wag(39), CC s(27), COO ss(21)
1108	1118	10	CN s(65), NH ₂ wag(21)
1171	1167	-4	CH ₂ wag(48), NH ₂ twist(31), CCOO wag(11), CH ₂ twist(9)
1314	1321	7	CH ₂ r(88), COO ss(7)
1341	1349	8	NH ₂ twist(50), CH ₂ wag(43)
1403	1407	4	COO ss(42), CC s(26), CH ₂ sis(17), CCOO sd(8)
1430	1436	6	CH ₂ sis(81), COO ss(9)
1566	1572	6	COO as(85)
1603	1609	6	NH ₂ sissor(98)
—	2921	—	CH s ² (62), CH s ¹ (38)
—	2956	—	CH s ¹ (62), CH s ² (38)
—	3070	—	NH ₂ ss(100)
—	3220	—	NH ₂ as(100)

frequency (cm ⁻¹)			ND ₂ CH ₂ CO ₂ ⁻¹ (mean deviation = 13 cm ⁻¹)
obs.	calc.	dev.	
			Potential Energy Distribution
—	198	—	CC t(94)
—	256	—	CN t(97)
311	311	0	CCOO r(48), NCC sis(47)
501	504	3	CCOO r(36), NCC sis(22), CC s(11), CN s(11), CCOO sd(11)

Table 3.24: (continued)

frequency (cm ⁻¹)			Potential Energy Distribution
obs.	calc.	dev.	
592	581	-11	CH ₂ twist(45), CCOO wag(43)
647	652	5	CCOO sd(52), NH ₂ wag(23), CC s(11), NCC sis(7)
761	756	-5	NH ₂ wag(62), CCOO sd(17), CN s(8), NCC sis(7)
847	800	-47	NH ₂ twist(52), CCOO wag(30), CH ₂ twist(8), CH ₂ wag(7)
926	931	5	CC s(42), COO ss(32), NCC sis(9), CCOO sd(7)
1057	1055	-2	CN s(61), NH ₂ sissor(13)
1057	1063	6	CH ₂ twist(39), NH ₂ twist(30), CCOO wag(22)
1192	1194	2	NH ₂ sissor(84), CN s(13)
1275	1268	-7	CH ₂ wag(87), NH ₂ twist(9)
1323	1324	1	CH ₂ r(86), COO ss(9)
1413	1408	-5	COO ss(40), CC s(26), CH ₂ sis(18), CCOO sd(8)
1432	1436	4	CH ₂ sis(81), COO ss(10)
1577	1571	-6	COO as(85)
—	2218	—	NH ₂ ss(99)
—	2378	—	NH ₂ as(99)
—	2921	—	CH s ² (62), CH s ¹ (38)
—	2956	—	CH s ¹ (62), CH s ² (38)

frequency (cm ⁻¹)			NH ₂ CD ₂ CO ₂ ⁻¹ (mean deviation = 16 cm ⁻¹)
obs.	calc.	dev.	
—	192	—	CC t(102)
—	323	—	CCOO r(53), NCC sis(42)
—	344	—	CN t(99)
490	499	9	CH ₂ twist(56), CCOO wag(32)
509	515	6	CCOO r(25), NCC sis(21), CCOO sd(17), CC s(15), CN s(9)
667	658	-9	CCOO sd(53), NCC sis(19), CC s(9), CCOO r(9)
831	792	-39	CH ₂ wag(47), CH ₂ twist(22), CCOO wag(19), NH ₂ twist(11)
877	873	-4	CC s(28), COO ss(26), CCOO sd(18), CH ₂ r(10)
877	888	11	NH ₂ wag(40), CN s(30), CH ₂ r(28)
932	962	30	CCOO wag(46), CH ₂ wag(42), CH ₂ twist(12)
1015	995	-20	CH ₂ sis(44), NH ₂ wag(32), CH ₂ r(16)

Table 3.24: (continued)

frequency (cm^{-1})			Potential Energy Distribution
obs.	calc.	dev.	
1066	1077	11	CH_2 sis(46), CH_2 r(20), NH_2 wag(12), CC s(9), COO ss(7)
1146	1160	14	CN s(49), CH_2 r(19), COO ss(8), NH_2 wag(7)
1267	1265	-2	NH_2 twist(87)
1408	1410	2	COO ss(54), CC s(31), CCOO sd(10)
1558	1566	8	COO as(89)
1601	1608	7	NH_2 sissor(100)
—	2128	—	CH s^2 (55), CH s^1 (44)
—	2192	—	CH s^1 (55), CH s^2 (44)
—	3070	—	NH_2 ss(100)
—	3219	—	NH_2 as(100)

frequency (cm^{-1})			ND ₂ CD ₂ CO ₂ ⁻¹ (mean deviation = 13 cm^{-1})
obs.	calc.	dev.	
—	184	—	CC t(101)
—	251	—	CN t(101)
310	309	-1	CCOO r(48), NCC sis(47)
501	486	-15	CH_2 twist(54), CCOO wag(26)
501	499	-2	CCOO r(30), NCC sis(17), CCOO sd(12), CC s(11), CN s(8), CH_2 twist(8)
640	638	-2	CCOO sd(51), NH_2 wag(16), CC s(13), NCC sis(9), CCOO r(7)
714	726	12	CH_2 wag(34), NH_2 twist(32), CCOO wag(20), CH_2 twist(7)
738	751	13	NH_2 wag(63), CN s(10), CCOO sd(9)
876	875	-1	CC s(27), COO ss(25), CH_2 r(25), CCOO sd(16)
960	943	-17	CN s(34), CH_2 r(25), CH_2 sis(21), NH_2 wag(7)
960	962	2	CCOO wag(46), CH_2 wag(42), CH_2 twist(12)
1002	1037	35	NH_2 twist(60), CH_2 twist(18), CH_2 wag(17)
1065	1066	1	CH_2 sis(66), CH_2 r(11), CC s(7)
1151	1118	-33	NH_2 sissor(27), CH_2 r(26), CN s(23), CH_2 sis(8), COO ss(7)
1216	1207	-9	NH_2 sissor(70), CN s(20)
1409	1411	2	COO ss(54), CC s(31), CCOO sd(10)
1574	1566	-8	COO as(89)
—	2128	—	CH s^2 (55), CH s^1 (44)

Table 3.24: (continued)

frequency (cm^{-1})			Potential Energy Distribution
obs.	calc.	dev.	
—	2191	—	CH s^1 (55), CH s^2 (44)
—	2219	—	NH ₂ ss(99)
—	2378	—	NH ₂ as(100)

Table 3.25: Scaled 4-31G Frequencies and Potential Energy Distribution for One-water Glycine Supramolecule Water-Excluded in Acid.

frequency (cm^{-1})			+NH ₃ CH ₂ COOH (mean deviation = 16 cm^{-1})
obs.	calc.	dev.	Potential Energy Distribution
—	80	—	CN ⁿ t(60), CC ^c t(46)
—	190	—	CC ^c t(56), CN ⁿ t(43)
301	328	27	NCC sis(47), CCOO sd(40), CCOO r(13)
504	507	3	CCOO sd(50), NCC sis(23), CC ^{ter} s(10), CN ⁿ s(10)
568	565	-3	CCOO wag(66), CH ₂ twist(36)
657	679	22	CCOO r(68), CO ^H s(13), NCC sis(12)
873	886	13	CC ^{ter} s(42), CN ⁿ s(19), CNH ₃ r ² (9), C=O s(8), CO ^H s(7), CCOO sd(7)
917	912	-5	CH ₂ twist(46), CCOO wag(28), CNH ₃ r ¹ (16)
—	957	—	CO ^H t(99)
1044	996	-48	CN ⁿ s(73), CC ^{ter} s(16)
1125	1121	-4	CNH ₃ r ² (47), CH ₂ wag(15), CNH ₃ r ¹ (12), CH ₂ twist(11), CCOO wag(7)
1135	1141	6	CNH ₃ r ¹ (46), CNH ₃ r ² (20), CH ₂ r(9)
1263	1258	-5	CO ^H s(33), OH b(28), CH ₂ r(23)
1320	1313	-7	CH ₂ wag(73), CNH ₃ r ¹ (15)
1378	1390	12	CH ₂ r(54), OH b(25)
1435	1434	-1	CH ₂ sis(95)
1512	1507	-5	CNH ₃ sd(29), OH b(28), CO ^H s(19), CC ^{ter} s(7)
1512	1522	10	CNH ₃ sd(65), OH b(12), CO ^H s(8)
1607	1605	-2	CNH ₃ ad ^{1,2} (68), CNH ₃ ad ^{1,2} (18)
1607	1620	13	CNH ₃ ad ^{1,2} (77), CNH ₃ ad ^{1,2} (21)
1740	1732	-8	C=O s(76), CO ^H s(11)
—	2824	—	OH s(100)
2973	2965	-8	CH s ¹ (51), CH s ² (48)
3012	3026	14	CH s ² (51), CH s ¹ (48)
—	3073	—	NH ₃ ss(51), NH ₃ as ^{1,2} (36), NH ₃ as ^{1,2} (12)
—	3290	—	NH ₃ ss(49), NH ₃ as ^{1,2} (38), NH ₃ as ^{1,2} (13)
—	3341	—	NH ₃ as ^{1,2} (75), NH ₃ as ^{1,2} (25)
frequency (cm^{-1})			+ND ₃ CH ₂ COOD (mean deviation = 17 cm^{-1})

Table 3.25: (continued)

frequency (cm ⁻¹)			Potential Energy Distribution
obs.	calc.	dev.	
obs.	calc.	dev.	Potential Energy Distribution
—	65	—	CN ⁿ t(82), CC ^c t(23)
—	161	—	CC ^c t(79), CN ⁿ t(22)
287	304	17	NCC sis(50), CCOO sd(35), CCOO r(11)
485	479	-6	CCOO sd(54), NCC sis(19), CN ⁿ s(10), CC ^{ter} s(7)
561	554	-7	CCOO wag(65), CH ₂ twist(38)
618	647	29	CCOO r(67), CO ^H s(11), NCC sis(8)
—	704	—	CO ^H t(96)
780	775	-5	CNH ₃ r ² (50), CC ^{ter} s(16), CN ⁿ s(7)
815	785	-30	CNH ₃ r ¹ (57), CC ^{ter} s(10), CCOO wag(9), CH ₂ twist(7)
951	958	7	CN ⁿ s(69), CNH ₃ sd(9), NCC sis(8)
1008	976	-32	CNH ₃ r ² (28), CC ^{ter} s(26), OH b(15), CNH ₃ r ¹ (9), NCC sis(8)
1043	1023	-20	CH ₂ twist(54), CCOO wag(23), CNH ₃ r ¹ (18)
1073	1067	-6	OH b(62), CO ^H s(18), C=O s(11)
1163	1136	-27	CNH ₃ ad ^{1,2} (48), CNH ₃ sd(30), CNH ₃ ad ^{1,2} (15)
1163	1168	5	CNH ₃ ad ^{1,2} (73), CNH ₃ ad ^{1,2} (24)
1163	1175	12	CNH ₃ sd(59), CNH ₃ ad ^{1,2} (25), CNH ₃ ad ^{1,2} (9)
1278	1286	8	CH ₂ wag(88)
1340	1320	-20	CH ₂ r(66), CO ^H s(21)
1429	1433	4	CH ₂ sis(92)
1439	1456	17	CO ^H s(27), CH ₂ r(27), CC ^{ter} s(22), CCOO r(11)
1733	1725	-8	C=O s(78), CO ^H s(13)
—	2066	—	OH s(98)
—	2226	—	NH ₃ ss(70), NH ₃ as ^{1,2} (22), NH ₃ as ^{1,2} (7)
—	2399	—	NH ₃ as ^{1,2} (52), NH ₃ ss(30), NH ₃ as ^{1,2} (18)
—	2464	—	NH ₃ as ^{1,2} (75), NH ₃ as ^{1,2} (25)
2975	2965	-10	CH s ¹ (51), CH s ² (48)
3015	3026	11	CH s ² (51), CH s ¹ (49)

frequency (cm ⁻¹)			+NH ₃ CD ₂ COOH (mean deviation = 23 cm ⁻¹)
obs.	calc.	dev.	
Potential Energy Distribution			

Table 3.25: (continued)

frequency (cm^{-1})			Potential Energy Distribution
obs.	calc.	dev.	
—	75	—	CN ⁿ t(53), CC ^c t(52)
—	186	—	CC ^c t(51), CN ⁿ t(49)
301	325	24	NCC sis(46), CCOO sd(41), CCOO r(12)
480	484	4	CH ₂ twist(51), CCOO wag(46), CH ₂ wag(7)
520	499	-21	CCOO sd(47), NCC sis(24), CC ^{ter} s(11), CN ⁿ s(8)
644	666	22	CCOO r(64), NCC sis(13), CO ^H s(11)
804	802	-2	CH ₂ twist(37), CH ₂ wag(28), CCOO wag(22), CNH ₃ r ¹ (9)
842	852	10	CC ^{ter} s(40), CH ₂ r(12), C=O s(9), CO ^H s(9), CCOO sd(8)
918	912	-6	CN ⁿ s(59), CH ₂ r(33)
926	935	9	CH ₂ wag(37), CO ^H t(37), CCOO wag(24)
—	970	—	CO ^H t(63), CH ₂ wag(20), CCOO wag(8), CH ₂ twist(7)
1044	1039	-5	CH ₂ sis(37), CNH ₃ r ² (19), CN ⁿ s(12), CH ₂ r(11), CC ^{ter} s(10)
1112	1062	-50	CH ₂ sis(54), CH ₂ r(20), CN ⁿ s(13)
1201	1163	-38	CNH ₃ r ² (38), CNH ₃ r ¹ (36), CH ₂ wag(7)
1210	1186	-24	CNH ₃ r ¹ (37), CO ^H s(16), CNH ₃ r ² (13), CH ₂ r(8), NCC sis(7)
1317	1321	4	OH b(42), CC ^{ter} s(16), CO ^H s(14), CH ₂ r(8), CNH ₃ r ² (8)
1443	1504	61	OH b(40), CO ^H s(25), CNH ₃ sd(12), CC ^{ter} s(9), CCOO r(8)
1518	1519	1	CNH ₃ sd(82)
1608	1604	-4	CNH ₃ ad ^{1,2} (69), CNH ₃ ad ^{1,2} (18)
1608	1620	12	CNH ₃ ad ^{1,2} (76), CNH ₃ ad ^{1,2} (21)
1741	1728	-13	C=O s(77), CO ^H s(11)
2166	2160	-6	CH s ¹ (50), CH s ² (48)
2232	2250	18	CH s ² (50), CH s ¹ (49)
—	2824	—	OH s(100)
—	3073	—	NH ₃ ss(51), NH ₃ as ^{1,2} (37), NH ₃ as ^{1,2} (12)
—	3290	—	NH ₃ ss(49), NH ₃ as ^{1,2} (38), NH ₃ as ^{1,2} (13)
—	3341	—	NH ₃ as ^{1,2} (75), NH ₃ as ^{1,2} (25)

frequency (cm^{-1})			+ND ₃ CD ₂ COOD (mean deviation = 19 cm^{-1})
obs.	calc.	dev.	Potential Energy Distribution

Table 3.25: (continued)

frequency (cm ⁻¹)			Potential Energy Distribution
obs.	calc.	dev.	
—	62	—	CN ⁿ t(76), CC ^c t(29)
—	156	—	CC ^c t(74), CN ⁿ t(27)
270	301	31	NCC sis(50), CCOO sd(36), CCOO r(11)
480	472	-8	CCOO sd(52), NCC sis(19), CN ⁿ s(9), CC ^{ter} s(8)
480	474	-6	CH ₂ twist(54), CCOO wag(45)
613	639	26	CCOO r(66), CO ^H s(10), NCC sis(8)
—	698	—	CO ^H t(79), CNH ₃ r ¹ (8)
728	727	-1	CNH ₃ r ¹ (24), CO ^H t(23), CH ₂ wag(22), CNH ₃ r ² (12), CH ₂ twist(11), CCOO wag(10)
772	774	2	CC ^{ter} s(27), CNH ₃ r ² (24), CN ⁿ s(14), CNH ₃ r ¹ (10), OH b(8)
845	857	12	CH ₂ r(42), CC ^{ter} s(16), CN ⁿ s(14), CNH ₃ r ² (9)
932	932	0	CN ⁿ s(44), CNH ₃ r ² (23), CH ₂ sis(11), NCC sis(10)
962	942	-20	CCOO wag(38), CH ₂ twist(24), CH ₂ wag(22), CNH ₃ r ¹ (11)
1018	986	-32	CH ₂ wag(49), CNH ₃ r ¹ (30), CH ₂ twist(11), CNH ₃ r ² (7)
1059	1055	-4	CH ₂ sis(58), OH b(21), CO ^H s(7)
1079	1068	-11	OH b(52), CH ₂ sis(20), CO ^H s(7)
1130	1123	-7	CH ₂ r(37), CNH ₃ sd(13), CC ^{ter} s(11), CO ^H s(9), CNH ₃ ad ^{1,2} (8)
1170	1140	-30	CNH ₃ ad ^{1,2} (39), CNH ₃ sd(21), CNH ₃ ad ^{1,2} (13)
1170	1173	3	CNH ₃ ad ^{1,2} (75), CNH ₃ ad ^{1,2} (24)
1170	1175	5	CNH ₃ sd(57), CNH ₃ ad ^{1,2} (26), CNH ₃ ad ^{1,2} (9)
1390	1431	41	CO ^H s(43), CC ^{ter} s(27), CCOO r(15)
1733	1721	-12	C=O s(80), CO ^H s(13)
—	2065	—	OH s(98)
—	2160	—	CH s ¹ (50), CH s ² (48)
—	2226	—	NH ₃ ss(70), NH ₃ as ^{1,2} (22), NH ₃ as ^{1,2} (7)
—	2249	—	CH s ² (50), CH s ¹ (49)
—	2399	—	NH ₃ as ^{1,2} (53), NH ₃ ss(30), NH ₃ as ^{1,2} (18)
—	2464	—	NH ₃ as ^{1,2} (75), NH ₃ as ^{1,2} (25)
frequency (cm ⁻¹)			Potential Energy Distribution
obs.	calc.	dev.	
—	80	—	CN ⁿ t(60), CC ^c t(46)

+NH₃CH₂¹³COOH (mean deviation = 17 cm⁻¹)

Table 3.25: (continued)

frequency (cm ⁻¹)			Potential Energy Distribution
obs.	calc.	dev.	
—	190	—	CC ^c t(56), CN ⁿ t(43)
301	327	26	NCC sis(46), CCOO sd(41), CCOO r(13)
502	506	4	CCOO sd(50), NCC sis(24), CN ⁿ s(10), CC ^{ter} s(9)
559	556	-3	CCOO wag(69), CH ₂ twist(33)
656	677	21	CCOO r(69), CO ^H s(12), NCC sis(12)
869	883	14	CC ^{ter} s(44), CN ⁿ s(18), CNH ₃ r ² (9), C=O s(8), CO ^H s(7), CCOO sd(7)
910	903	-7	CH ₂ twist(50), CCOO wag(27), CNH ₃ r ¹ (15)
—	957	—	CO ^H t(100)
1044	996	-48	CN ⁿ s(73), CC ^{ter} s(16)
1119	1118	-1	CNH ₃ r ² (43), CH ₂ wag(17), CNH ₃ r ¹ (17), CH ₂ twist(11)
1139	1140	1	CNH ₃ r ¹ (43), CNH ₃ r ² (25), CH ₂ r(9)
1246	1245	-1	CO ^H s(39), OH b(23), CH ₂ r(21)
1320	1312	-8	CH ₂ wag(72), CNH ₃ r ¹ (16)
1370	1389	19	CH ₂ r(55), OH b(22), CC ^{ter} s(7)
1437	1434	-3	CH ₂ sis(94)
1500	1487	-13	OH b(44), CO ^H s(23), CC ^{ter} s(9), CCOO r(8), CH ₂ r(7)
1520	1518	-2	CNH ₃ sd(90)
1614	1604	-10	CNH ₃ ad ^{1,2} (68), CNH ₃ ad ^{1,2} (18)
1614	1620	6	CNH ₃ ad ^{1,2} (76), CNH ₃ ad ^{1,2} (21)
1701	1690	-11	C=O s(75), CO ^H s(10)
—	2824	—	OH s(100)
—	2965	—	CH s ¹ (51), CH s ² (48)
—	3026	—	CH s ² (51), CH s ¹ (48)
—	3073	—	NH ₃ ss(51), NH ₃ as ^{1,2} (36), NH ₃ as ^{1,2} (12)
—	3290	—	NH ₃ ss(49), NH ₃ as ^{1,2} (38), NH ₃ as ^{1,2} (13)
—	3341	—	NH ₃ as ^{1,2} (75), NH ₃ as ^{1,2} (25)

frequency (cm ⁻¹)			Potential Energy Distribution
obs.	calc.	dev.	
—	65	—	CN ⁿ t(82), CC ^c t(23)
—	161	—	CC ^c t(79), CN ⁿ t(22)
287	303	16	NCC sis(50), CCOO sd(36), CCOO r(11)

Table 3.25: (continued)

frequency (cm^{-1})			Potential Energy Distribution
obs.	calc.	dev.	
483	477	-6	CCOO sd(54), NCC sis(19), CN^n s(10), CC^{ter} s(7)
555	546	-9	CCOO wag(68), CH_2 twist(35)
614	645	31	CCOO r(68), CO^H s(10), NCC sis(8)
—	704	—	CO^H t(96)
776	772	-4	CNH_3 r^2 (49), CC^{ter} s(15)
808	782	-26	CNH_3 r^1 (54), CC^{ter} s(13), CH_2 twist(7), CCOO wag(7)
949	958	9	CN^n s(69), CNH_3 sd(9), NCC sis(8)
1007	975	-32	CNH_3 r^2 (29), CC^{ter} s(26), OH b(14), NCC sis(8), CNH_3 r^1 (8)
1025	1014	-11	CH_2 twist(54), CCOO wag(21), CNH_3 r^1 (20)
1066	1067	1	OH b(63), CO^H s(18), C=O s(11)
1120	1136	16	CNH_3 $\text{ad}^{1,2}$ (48), CNH_3 sd(30), CNH_3 $\text{ad}^{1,2}$ (15)
1168	1168	0	CNH_3 $\text{ad}^{1,2}$ (73), CNH_3 $\text{ad}^{1,2}$ (24)
1168	1175	7	CNH_3 sd(59), CNH_3 $\text{ad}^{1,2}$ (25), CNH_3 $\text{ad}^{1,2}$ (9)
1271	1284	13	CH_2 wag(88)
1321	1306	-15	CH_2 r(53), CO^H s(29), CCOO r(7)
1406	1425	19	CH_2 sis(30), CH_2 r(22), CC^{ter} s(18), CO^H s(16)
1438	1439	1	CH_2 sis(68), CH_2 r(18), CO^H s(7)
1688	1680	-8	C=O s(79), CO^H s(12)
—	2065	—	OH s(98)
—	2226	—	NH_3 ss(70), NH_3 $\text{as}^{1,2}$ (22), NH_3 $\text{as}^{1,2}$ (7)
—	2399	—	NH_3 $\text{as}^{1,2}$ (52), NH_3 ss(30), NH_3 $\text{as}^{1,2}$ (18)
—	2464	—	NH_3 $\text{as}^{1,2}$ (75), NH_3 $\text{as}^{1,2}$ (25)
—	2965	—	CH s^1 (51), CH s^2 (48)
—	3026	—	CH s^2 (51), CH s^1 (49)

frequency (cm^{-1})			Potential Energy Distribution
obs.	calc.	dev.	
—	80	—	CN^n t(60), CC^c t(46)
—	190	—	CC^c t(56), CN^n t(44)
310	327	17	NCC sis(47), CCOO sd(40), CCOO r(13)
501	505	4	CCOO sd(50), NCC sis(23), CC^{ter} s(10), CN^n s(9)
566	564	-2	CCOO wag(65), CH_2 twist(36)

Table 3.25: (continued)

frequency (cm^{-1})			Potential Energy Distribution
obs.	calc.	dev.	
648	674	26	CCOO r(67), NCC sis(13), CO ^H s(12)
864	875	11	CC ^{ter} s(41), CN ⁿ s(22), C=O s(8), CO ^H s(8), CCOO sd(8), CNH ₃ r ² (7)
915	907	-8	CH ₂ twist(47), CCOO wag(29), CNH ₃ r ¹ (15)
—	957	—	CO ^H t(99)
1027	976	-51	CN ⁿ s(70), CC ^{ter} s(18), CO ^H s(7)
1113	1116	3	CNH ₃ r ² (48), CH ₂ wag(14), CNH ₃ r ¹ (14), CH ₂ twist(11), CCOO wag(7)
1133	1137	4	CNH ₃ r ¹ (47), CNH ₃ r ² (22), CH ₂ r(8)
1263	1257	-6	CO ^H s(33), OH b(27), CH ₂ r(25)
1316	1312	-4	CH ₂ wag(74), CNH ₃ r ¹ (15)
1360	1379	19	CH ₂ r(54), OH b(22)
1431	1431	0	CH ₂ sis(94)
—	1505	5	OH b(33), CO ^H s(22), CNH ₃ sd(21), CC ^{ter} s(7), CCOO r(7)
1510	1521	11	CNH ₃ sd(73), OH b(9)
1608	1604	-4	CNH ₃ ad ^{1,2} (68), CNH ₃ ad ^{1,2} (18)
1608	1620	12	CNH ₃ ad ^{1,2} (77), CNH ₃ ad ^{1,2} (21)
1741	1732	-9	C=O s(76), CO ^H s(11)
—	2824	—	OH s(100)
—	2959	—	CH s ¹ (52), CH s ² (48)
—	3014	—	CH s ² (52), CH s ¹ (48)
—	3073	—	NH ₃ ss(51), NH ₃ as ^{1,2} (36), NH ₃ as ^{1,2} (12)
—	3290	—	NH ₃ ss(49), NH ₃ as ^{1,2} (38), NH ₃ as ^{1,2} (13)
—	3341	—	NH ₃ as ^{1,2} (75), NH ₃ as ^{1,2} (25)

frequency (cm^{-1})			Potential Energy Distribution
obs.	calc.	dev.	
—	65	—	CN ⁿ t(82), CC ^c t(24)
—	161	—	CC ^c t(78), CN ⁿ t(22)
290	303	13	NCC sis(51), CCOO sd(35), CCOO r(11)
483	478	-5	CCOO sd(55), NCC sis(19), CN ⁿ s(10), CC ^{ter} s(8)
558	554	-4	CCOO wag(64), CH ₂ twist(38)
608	643	35	CCOO r(67), CO ^H s(10), NCC sis(8)

Table 3.25: (continued)

frequency (cm ⁻¹)			Potential Energy Distribution
obs.	calc.	dev.	
—	704	—	CO ^H t(96)
775	773	-2	CNH ₃ r ² (46), CC ^{ter} s(20), CN ⁿ s(9)
805	784	-21	CNH ₃ r ¹ (58), CCOO wag(10), CC ^{ter} s(8), CH ₂ twist(8)
941	938	-3	CN ⁿ s(69), NCC sis(8), CNH ₃ sd(7)
989	964	-25	CNH ₃ r ² (30), CC ^{ter} s(27), OH b(12), CNH ₃ r ¹ (9), NCC sis(7)
1032	1012	-20	CH ₂ twist(53), CCOO wag(23), CNH ₃ r ¹ (19)
1066	1065	-1	OH b(65), CO ^H s(18), C=O s(10)
1166	1136	-30	CNH ₃ ad ^{1,2} (47), CNH ₃ sd(31), CNH ₃ ad ^{1,2} (15)
1166	1168	2	CNH ₃ ad ^{1,2} (73), CNH ₃ ad ^{1,2} (24)
—	1174	—	CNH ₃ sd(59), CNH ₃ ad ^{1,2} (26), CNH ₃ ad ^{1,2} (9)
1277	1285	8	CH ₂ wag(88)
1336	1315	-21	CH ₂ r(70), CO ^H s(18)
1411	1428	17	CH ₂ sis(83)
1435	1449	14	CO ^H s(26), CH ₂ r(23), CC ^{ter} s(18), CH ₂ sis(15), CCOO r(10)
1732	1725	-7	C=O s(78), CO ^H s(13)
—	2066	—	OH s(98)
—	2226	—	NH ₃ ss(70), NH ₃ as ^{1,2} (22), NH ₃ as ^{1,2} (7)
—	2399	—	NH ₃ as ^{1,2} (52), NH ₃ ss(30), NH ₃ as ^{1,2} (18)
—	2464	—	NH ₃ as ^{1,2} (75), NH ₃ as ^{1,2} (25)
—	2959	—	CH s ¹ (52), CH s ² (48)
—	3014	—	CH s ² (52), CH s ¹ (48)

The optimized geometries for NMA one-water supermolecule structures are shown in Figure 3.23 and for the two-water and three-water supermolecules in Figure 3.24.

Internal coordinate definitions used for all of the NMA structures are provided in Table 3.26 and the symmetry coordinates in Table 3.27. Optimized internal coordinates for NMA in various states of hydration are listed in Table 3.28. Force constants calculated from the optimized geometries were scaled to frequencies from aqueous NMA. Results for each of the differently hydrated structures are listed in Table 3.29.

Figure 3.23: NMA one water supermolecules, with the water hydrogen bonded to the carbonyl oxygen (top), and with the water hydrogen bonded to the amide hydrogen (bottom).

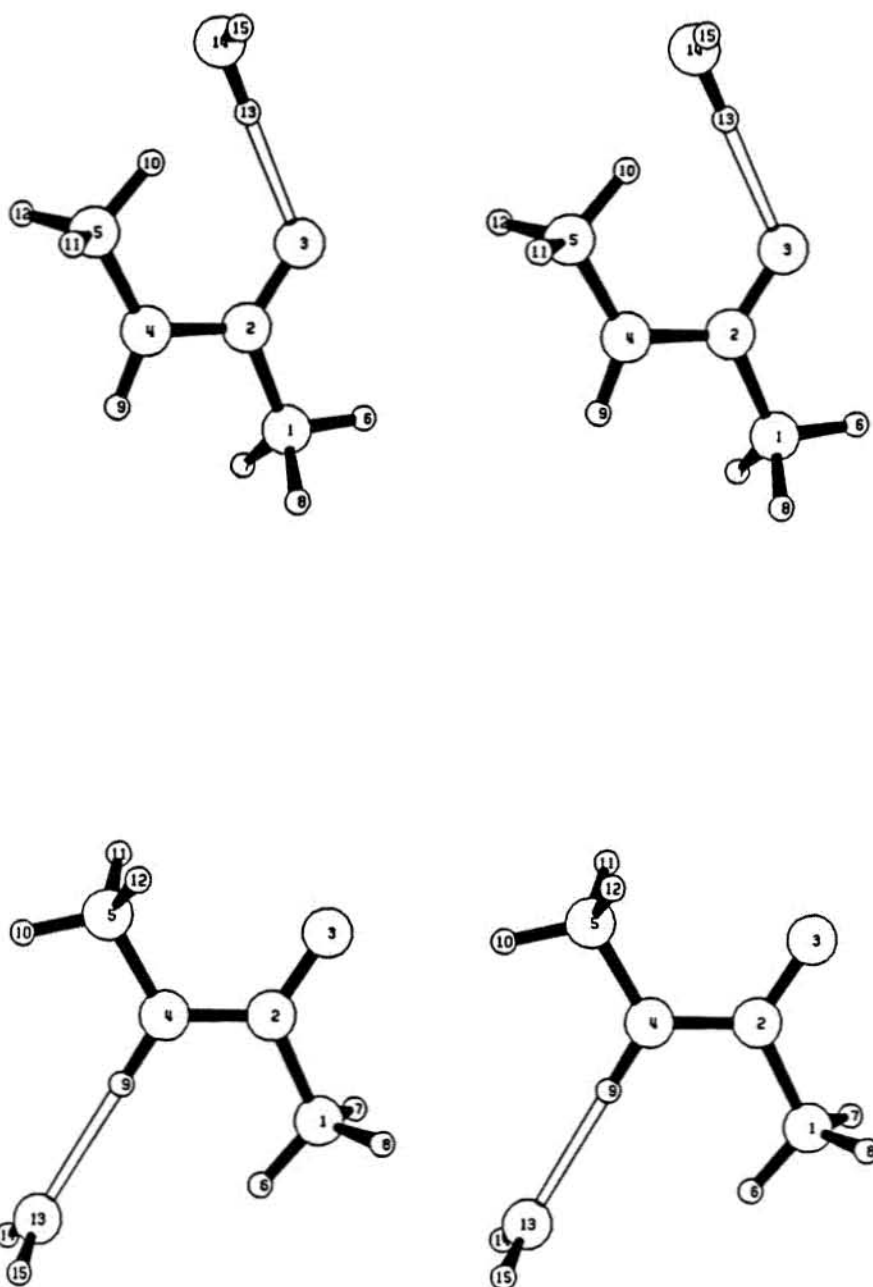


Figure 3.24: NMA two water supermolecule, one water hydrogen bonded to the amide hydrogen, the other to the carbonyl oxygen (top), NMA two water supermolecule, both waters hydrogen bonded with the carbonyl oxygen (middle), and the NMA three water supermolecule (bottom).

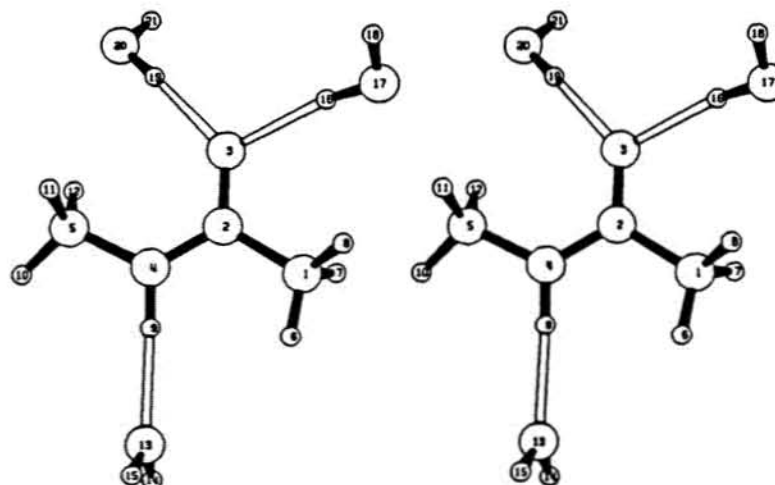
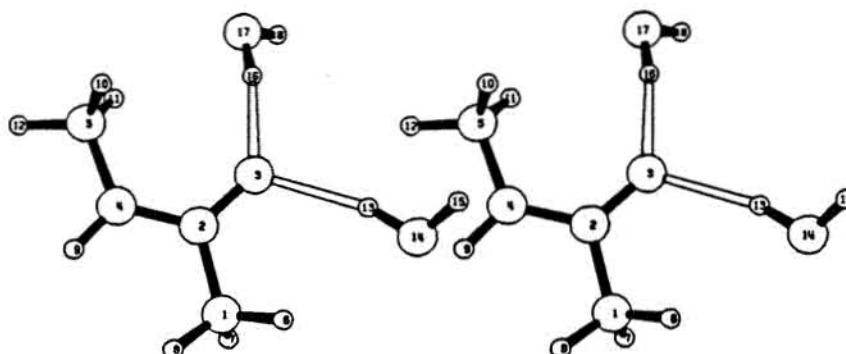
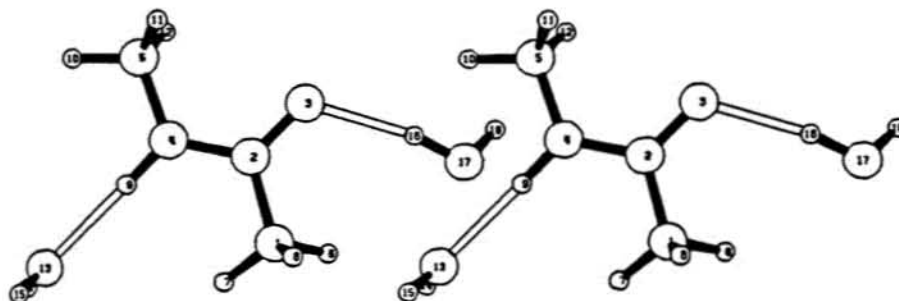


Figure 3.25: Raman spectra of *N*-Methylacetamide. Dotted line, top, 50% v/v in H₂O; solid line, bottom, 50% v/v in D₂O.

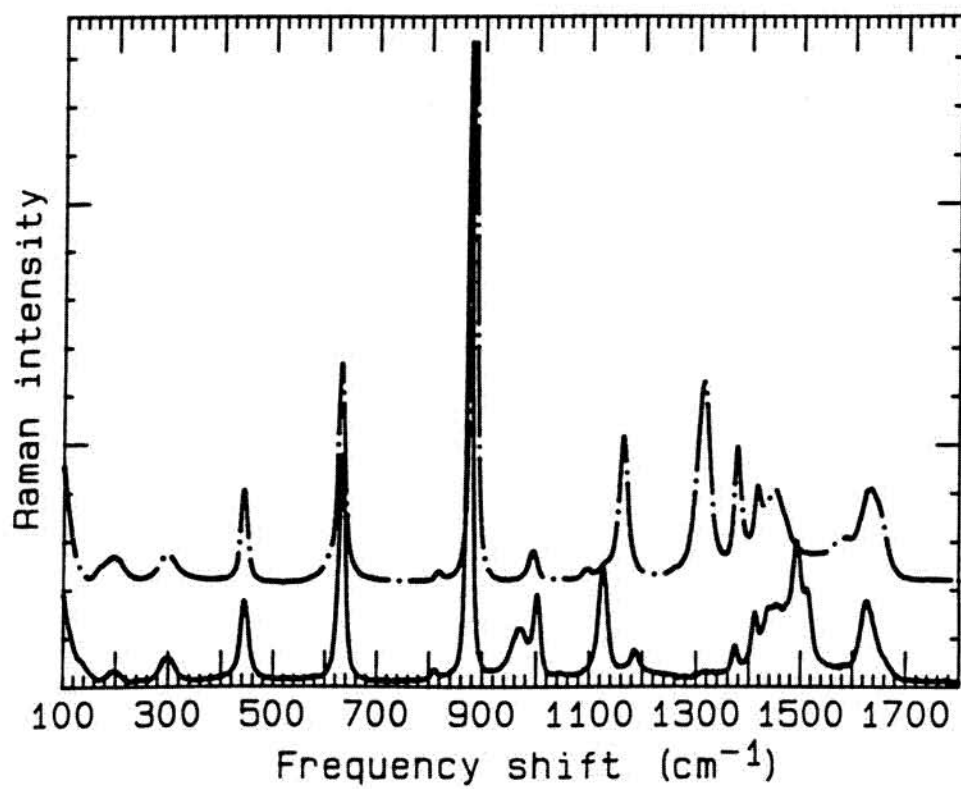


Table 3.26: Redundant Internal Coordinates for *trans* N-Methylacetamide

$R_1 = \Delta\gamma(\text{O}^3\text{-C}^2)^a$	$R_{18} = \Delta\theta(\text{H}^{12}\text{-C}^5\text{-H}^{11})$
$R_2 = \Delta\gamma(\text{N}^4\text{-C}^2)$	$R_{19} = \Delta\theta(\text{H}^{11}\text{-C}^5\text{-H}^{10})$
$R_3 = \Delta\gamma(\text{C}^2\text{-C}^1)$	$R_{20} = \Delta\theta(\text{H}^{12}\text{-C}^5\text{-H}^{10})$
$R_4 = \Delta\gamma(\text{C}^5\text{-N}^4)$	$R_{21} = \Delta\theta(\text{H}^{10}\text{-C}^5\text{-N}^4)$
$R_5 = \Delta\gamma(\text{H}^9\text{-N}^4)$	$R_{22} = \Delta\theta(\text{H}^{12}\text{-C}^5\text{-N}^4)$
$R_6 = \Delta\gamma(\text{H}^6\text{-C}^1)$	$R_{23} = \Delta\theta(\text{H}^{11}\text{-C}^5\text{-N}^4)$
$R_7 = \Delta\gamma(\text{H}^7\text{-C}^1)$	$R_{24} = \Delta\theta(\text{C}^5\text{-N}^4\text{-C}^2)$
$R_8 = \Delta\gamma(\text{H}^8\text{-C}^1)$	$R_{25} = \Delta\theta(\text{H}^9\text{-N}^4\text{-C}^2)$
$R_9 = \Delta\gamma(\text{H}^{10}\text{-C}^5)$	$R_{26} = \Delta\theta(\text{H}^9\text{-N}^4\text{-C}^5)$
$R_{10} = \Delta\gamma(\text{H}^{11}\text{-C}^5)$	$R_{27} = \Delta\omega(\text{H}^9\text{-C}^5\text{-C}^2\text{-N}^4)$
$R_{11} = \Delta\gamma(\text{H}^{12}\text{-C}^5)$	$R_{28} = \Delta\theta(\text{N}^4\text{-C}^2\text{-C}^1)$
$R_{12} = \Delta\theta(\text{H}^8\text{-C}^1\text{-H}^7)$	$R_{29} = \Delta\theta(\text{N}^4\text{-C}^2\text{-O}^3)$
$R_{13} = \Delta\theta(\text{H}^7\text{-C}^1\text{-H}^6)$	$R_{30} = \Delta\theta(\text{O}^3\text{-C}^2\text{-C}^1)$
$R_{14} = \Delta\theta(\text{H}^8\text{-C}^1\text{-H}^6)$	$R_{31} = \Delta\omega(\text{O}^3\text{-N}^4\text{-C}^1\text{-C}^2)$
$R_{15} = \Delta\theta(\text{H}^6\text{-C}^1\text{-C}^2)$	$R_{32} = \Delta\tau(\text{C}^2\text{-C}^1)$
$R_{16} = \Delta\theta(\text{H}^8\text{-C}^1\text{-C}^2)$	$R_{33} = \Delta\tau(\text{N}^4\text{-C}^2)$
$R_{17} = \Delta\theta(\text{H}^7\text{-C}^1\text{-C}^2)$	$R_{34} = \Delta\tau(\text{C}^5\text{-N}^4)$

^aSymbols: γ = stretch, θ = bend, ω = out of plane bend, τ = torsion.

Table 3.27: Symmetry Coordinate Definitions for *trans* N-Methylacetamide

CO s ^a	$S_1 = R_1$
CN s	$S_2 = R_2$
CC s	$S_3 = R_3$
NC s	$S_4 = R_4$
NH s	$S_5 = R_5$
CCH ₃ ss	$S_6 = (R_6 + R_7 + R_8)/\sqrt{3}$
CCH ₃ as ¹	$S_7 = (2R_6 - R_7 - R_8)/\sqrt{6}$
CCH ₃ as ²	$S_8 = (R_7 - R_8)/\sqrt{2}$
NCH ₃ ss	$S_9 = (R_9 + R_{10} + R_{11})/\sqrt{3}$
NCH ₃ as ¹	$S_{10} = (2R_9 - R_{10} - R_{11})/\sqrt{6}$
NCH ₃ as ²	$S_{11} = (R_{10} - R_{11})/\sqrt{2}$
CCH ₃ sd	$S_{12} = (R_{12} + R_{13} + R_{14} - R_{15} - R_{16} - R_{17})/\sqrt{6}$
CCH ₃ ad ¹	$S_{13} = (2R_{12} - R_{13} - R_{14})/\sqrt{6}$
CCH ₃ ad ²	$S_{14} = (R_{13} - R_{14})/\sqrt{2}$
CCH ₃ r ¹	$S_{15} = (2R_{15} - R_{16} - R_{17})/\sqrt{6}$
CCH ₃ r ²	$S_{16} = (R_{16} - R_{17})/\sqrt{2}$
NCH ₃ sd	$S_{17} = (R_{18} + R_{19} + R_{20} - R_{21} - R_{22} - R_{23})/\sqrt{6}$
NCH ₃ ad ¹	$S_{18} = (2R_{18} - R_{19} - R_{20})/\sqrt{6}$
NCH ₃ ad ²	$S_{19} = (R_{19} - R_{20})/\sqrt{2}$
NCH ₃ r ¹	$S_{20} = (2R_{21} - R_{22} - R_{23})/\sqrt{6}$
NCH ₃ r ²	$S_{21} = (R_{22} - R_{23})/\sqrt{2}$
CNHC sd	$S_{22} = (2R_{24} - R_{25} - R_{26})/\sqrt{6}$
NH ib	$S_{23} = (R_{25} - R_{26})/\sqrt{2}$
NH ob	$S_{24} = R_{27}$
CO sd	$S_{25} = (2R_{28} - R_{29} - R_{30})/\sqrt{6}$
CO r	$S_{26} = (R_{29} - R_{30})/\sqrt{2}$
CO ob	$S_{27} = R_{31}$
CC t	$S_{28} = R_{32}$
C ² N t	$S_{29} = R_{33}$
NC t	$S_{30} = R_{34}$

^aAbbreviations: ss = symmetric stretch, as = antisymmetric stretch, s = stretch, r = rock, sd = symmetric deformation, ob = out of plane bend, ib = in plane bend, ad = antisymmetric deformation, t = torsion.

Table 3.28: Optimized Internal Coordinates for *trans* *N*-Methylacetamide

Internal Coordinate	No H ₂ O ^a	1 H ₂ O HN ^a	1 H ₂ O OC ^a	2 H ₂ O HN,OC	2 H ₂ O OC ^a	3 H ₂ O ^a
Bond Stretches						
C ² -C ¹	1.5049	1.5061	1.5027	1.5029	1.5011	1.5013
O ³ -C ²	1.2237	1.2289	1.2331	1.2385	1.2424	1.2478
N ⁴ -C ²	1.3502	1.3415	1.3415	1.3330	1.3318	1.3240
C ⁵ -N ⁴	1.4519	1.4489	1.4536	1.4507	1.4597	1.4562
H ⁶ -C ¹	1.0770	1.0793	1.0776	1.0792	1.0786	1.0784
H ⁷ -C ¹	1.0832	1.0816	1.0840	1.0790	1.0834	1.0813
H ⁸ -C ¹	1.0832	1.0816	1.0814	1.0834	1.0800	1.0813
H ⁹ -N ⁴	0.9899	0.9964	0.9900	0.9979	0.9904	0.9990
H ¹⁰ -C ⁵	1.0792	1.0796	1.0796	1.0791	1.0808	1.0787
H ¹¹ -C ⁵	1.0803	1.0811	1.0801	1.0806	1.0767	1.0795
H ¹² -C ⁵	1.0803	1.0811	1.0788	1.0807	1.0785	1.0795
Angle bends						
O ³ -C ² -C ¹	122.26	121.13	122.00	121.04	120.64	120.07
N ⁴ -C ² -O ³	121.85	122.48	121.06	121.81	121.82	122.31
C ⁵ -N ⁴ -C ²	121.49	120.98	121.82	121.41	123.17	122.51
H ⁶ -C ¹ -C ²	108.91	112.84	109.30	109.18	109.21	112.44
H ⁷ -C ¹ -C ²	110.76	108.87	109.26	112.39	108.79	108.90
H ⁸ -C ¹ -C ²	110.76	108.87	111.88	108.76	112.59	108.90
H ⁹ -N ⁴ -C ²	119.64	120.38	119.43	120.06	118.73	119.51
H ¹⁰ -C ⁵ -N ⁴	108.78	108.56	110.69	108.41	110.92	108.07
H ¹¹ -C ⁵ -N ⁴	110.91	111.15	110.89	111.06	110.84	111.19
H ¹² -C ⁵ -N ⁴	110.91	111.15	108.68	111.08	108.34	111.19
Torsions						
N ⁴ -C ² -O ³ -C ¹	180.00	180.00	181.42	178.83	181.25	180.65
C ⁵ -N ⁴ -C ² -C ¹	180.00	180.00	181.73	178.59	180.41	180.18
H ⁶ -C ¹ -C ² -N ⁴	180.00	0.00	201.49	140.13	216.29	-11.63
H ⁷ -C ¹ -C ² -N ⁴	60.00	121.66	83.45	17.22	99.36	109.38
H ⁸ -C ¹ -C ² -N ²	-60.00	-121.66	-36.53	-103.32	-21.17	-134.33
H ⁹ -N ⁴ -C ² -C ¹	0.00	0.00	1.02	-1.76	1.88	1.22
H ¹⁰ -C ⁵ -N ⁴ -C ²			301.25	180.29	287.62	173.13
H ¹¹ -C ⁵ -N ⁴ -C ²			61.39	-59.78	47.96	-67.22
H ¹² -C ⁵ -N ⁴ -C ²			181.38	60.37	167.97	53.01

^aFrom Williams, 1992

Table 3.29: Scale factors for *trans* N-Methylacetamide in different hydration states

Coordinate	Water-excluded					Super
	1w-H	1w-O	2w-H,O	2w-O,O	3w	2w-H,O
CO s	0.7129	0.7727	0.8104	0.8309	0.8564	0.7965
CN s	0.9800	0.9345	0.8909	0.8920	0.8670	0.9073
CC s	0.8262	0.9325	0.8400	0.9336	0.8660	0.8337
NC s	0.8125	0.8657	0.8680	0.8958	0.8699	0.8486
NH s	0.6750	0.7968	0.6850	0.6450	0.6900	0.6900
CCH ₃ ss	0.8363	0.8468	0.8434	0.8447	0.8380	0.8430
CCH ₃ as ¹	0.8359	0.8056	0.8131	0.8138	0.8176	0.8228
CCH ₃ as ²	0.8340	0.8520	0.8424	0.8443	0.8410	0.8353
NCH ₃ ss	0.8451	0.8380	0.8376	0.8316	0.8311	0.8379
NCH ₃ as ¹	0.8455	0.8430	0.8381	0.8393	0.8352	0.8414
NCH ₃ as ²	0.8361	0.8200	0.8375	0.8059	0.8200	0.8344
CCH ₃ sd	0.7572	0.7513	0.7509	0.7469	0.7458	0.7511
CCH ₃ ad ¹	0.7574	0.7870	0.7750	0.7830	0.7664	0.7735
CCH ₃ ad ²	0.7683	0.7410	0.7590	0.7472	0.7650	0.7526
CCH ₃ r ¹	0.8071	0.7300	0.7360	0.7326	0.7334	0.7456
CCH ₃ r ²	0.7331	0.7520	0.7320	0.7369	0.7361	0.7599
NCH ₃ sd	0.7627	0.7624	0.7631	0.7563	0.7552	0.7607
NCH ₃ ad ¹	0.7598	0.7770	0.7588	0.7634	0.7608	0.7644
NCH ₃ ad ²	0.7760	0.7610	0.7747	0.7599	0.7673	0.7729
NCH ₃ r ¹	0.7498	0.8120	0.7760	0.8230	0.7730	0.7620
NCH ₃ r ²	0.7720	0.7160	0.7780	0.7189	0.7851	0.7743
CNHC sd	1.0066	0.8650	0.7700	0.8276	0.7340	0.8780
NH ib	0.7316	0.7889	0.7120	0.7726	0.7067	0.7199
NH ob	0.7000	1.5060	0.7300	1.3000	0.7058	0.5803
CO sd	0.9535	0.8720	0.7725	0.7582	0.7666	0.8630
CO r	0.8533	0.7643	0.8710	0.7549	0.8028	0.8754
CO ob	0.7500	0.7500	0.7500	0.7280	0.7131	0.6520
CC t	0.5000	0.5800	0.5000	0.5000	0.4500	1.0000
C ² N t	0.8000	0.8400	0.7250	0.7200	0.6000	0.8400
NC t	1.8000	1.5000	0.7000	0.8048	0.4500	2.9090

PED and predicted frequencies for the NMA two-water supermolecule (water included), one water hydrogen bonded to the amide hydrogen, the other to the carbonyl oxygen, are listed in Table 3.30. PED and predicted frequencies for the water-excluded one-water supermolecule with the water hydrogen bonded to the amide hydrogen are given in Table 3.31, and with the water hydrogen bonded to the carbonyl oxygen are in Table 3.32. The water-excluded results for the two-water supermolecule with one water hydrogen bonded to the amide hydrogen, the other to the carbonyl oxygen are given in Table 3.33 and for both waters hydrogen bonded to the carbonyl oxygen in Table 3.34. The PED and predicted frequencies for the water-excluded three-water supermolecule are listed in Table 3.35.

Table 3.30: Scaled 4-31G Frequencies and Potential Energy Distributions for *trans* N-methylacetamide Two-water Supermolecule.

frequency (cm ⁻¹)			<i>trans</i> CH ₃ CONHCH ₃ (mean deviation = 6 cm ⁻¹)
obs.	calc.	dev.	
Potential Energy Distribution			
—	3	—	Hb*b(85), OHO*b(11)
—	25	—	CO t*(66), Hb*b(28), OHO*b(7)
—	60	—	Hb*b(102), OHO*b(23), C ² N t(12), COH*b(10)
—	65	—	COH*b(38), Hb*b(32), OHO*b(14), NO*t(11), CO t*(8), CC t(7), C ² N t(7)
—	81	—	Hb*b(51), OO*t(43), CC t(38), OHO*b(10)
—	113	—	NO*t(139), OO*t(33)
150	128	-22	CC t(44), Hb*b(35), OO*t(34)
160	137	-23	Hb*s(82), Hb*s(12)
160	157	-3	Hb*s(45), NC t(31), Hb*s(10), CNHC sd(7)
171	163	-8	NC t(63), Hb*s(24)
195	192	-3	C ² N t(45), NH ob(35), CO ob(7)
240	226	-14	HOH53(130), NH ob(21), C ² N t(8)
—	249	—	HOH*w(97)
297	296	-1	CNHC sd(48), CO sd(28), Hb*s(15)
370	395	25	OHO*b(40), COH*b(36), CO t*(19), HOH37(11)
443	442	-1	CO sd(43), CO r(24), CNHC sd(9)
—	570	—	CO ob(71), CCH ₃ r ² (9)
630	638	8	CC s(37), CO r(35), CNHC sd(9)
660	675	15	OHO*b(91), CO t*(9)
840	811	-29	HOH53(66), NH ob(24), C ² N t(19)
883	881	-2	NCH ₃ r ¹ (21), CN s(19), CC s(17), CO s(9), CO r(9), NC s(7), CNHC sd(7)
994	994	0	CCH ₃ r ¹ (32), CCH ₃ r ² (23), NC s(17), CC s(15), CO s(7)
1044	1045	1	CCH ₃ r ² (45), CCH ₃ r ¹ (29), CO ob(16)
1095	1096	1	NC s(52), CCH ₃ r ¹ (14), CC s(9), CCH ₃ r ² (7)
1129	1132	3	NCH ₃ r ² (90), NCH ₃ ad ² (7)
1164	1171	7	NCH ₃ r ¹ (60), CNHC sd(11), CO s(8), NC s(7), NCH ₃ ad ¹ (7)
1312	1330	18	NH ib(36), CN s(18), CCH ₃ sd(10), CO s(8), CC s(8)
1378	1376	-2	CCH ₃ sd(79), CCH ₃ ad ² (13)
1416	1416	0	NCH ₃ sd(87)
1428	1433	5	CCH ₃ ad ² (54), CCH ₃ ad ¹ (24), CCH ₃ sd(8)
1440	1439	-1	CCH ₃ ad ¹ (67), CCH ₃ ad ² (21)

Table 3.30: (continued)

frequency (cm^{-1})			Potential Energy Distribution
obs.	calc.	dev.	
1449	1453	4	NCH ₃ ad ² (93), NCH ₃ r ² (7)
1467	1467	0	NCH ₃ ad ¹ (86), NCH ₃ r ¹ (8)
1577	1569	-8	NH ib(45), CN s(31)
1629	1625	-4	HOH54(94)
1630	1634	4	CO s(53), CN s(13), HOH37(7)
1630	1647	17	HOH37(80)
2925	2935	10	NCH ₃ ss(99)
2942	2943	1	CCH ₃ ss(85), CCH ₃ as ¹ (8), CCH ₃ as ² (7)
2973	2986	13	NCH ₃ as ² (100)
2992	2992	0	CCH ₃ as ¹ (46), CCH ₃ as ² (40), CCH ₃ ss(15)
3009	3014	5	CCH ₃ as ² (53), CCH ₃ as ¹ (46)
3020	3019	-1	NCH ₃ as ¹ (98)
3120	3134	14	NH s(99)
3434	3409	-25	OH*s(93), OH*s(7)
3559	3559	0	OH*s(50), OH*s(50)
3646	3646	0	OH*s(92), OH*s(8)
3687	3688	1	OH*s(50), OH*s(50)

frequency (cm^{-1})			<i>trans</i> CH ₃ CONDCH ₃ (mean deviation = 7 cm^{-1})
obs.	calc.	dev.	
—	3	—	Hb*b(85), OHO*b(11)
—	24	—	CO t*(66), Hb*b(32)
—	56	—	Hb*b(124), OHO*b(16), C ² N t(11)
—	61	—	OO*t(42), COH*b(27), CC t(15), Hb*b(11)
—	67	—	Hb*b(55), OHO*b(33), OO*t(29), COH*b(15), Hb*b(13)
—	82	—	NO*t(141), OO*t(21)
—	116	—	CC t(73), OO*t(21), Hb*b(10)
—	130	—	Hb*s(83), Hb*s(14)
160	152	-8	Hb*s(61), Hb*s(12), NC t(9), CNHC sd(8)
149	160	11	NC t(84), HOH53(17)
—	172	—	HOH53(94), C ² N t(42)
—	191	—	HOH*w(96)
195	194	-1	NH ob(56), HOH53(30), C ² N t(17)

Table 3.30: (continued)

frequency (cm ⁻¹)			Potential Energy Distribution
obs.	calc.	dev.	
295	283	-12	OHO*b(27), COH*b(20), CNHC sd(19), CO t*(13), CO sd(9), HOH37(7)
—	298	—	CNHC sd(29), COH*b(21), CO sd(20), OHO*b(11), Hb*s(8), CO t*(7)
444	438	-6	CO sd(44), CO r(26), CNHC sd(9)
480	486	6	OHO*b(90), CO t*(8)
—	568	—	CO ob(64), C ² N t(11), HOH53(8), CCH ₃ r ² (7)
—	596	—	HOH53(56), NH ob(33), C ² N t(11)
630	636	6	CC s(36), CO r(36), CNHC sd(9)
875	869	-6	NCH ₃ r ¹ (19), CN s(18), CC s(17), NC s(11), CO s(8), CO r(8)
968	967	-1	NH ib(61), CN s(9), CCH ₃ r ¹ (9), CCH ₃ r ² (8)
1002	995	-7	NC s(27), CCH ₃ r ¹ (24), CC s(17), CCH ₃ r ² (16), CO s(9)
1044	1044	0	CCH ₃ r ² (45), CCH ₃ r ¹ (30), CO ob(16)
—	1128	—	NCH ₃ r ² (91), NCH ₃ ad ² (7)
1126	1130	4	NC s(37), CCH ₃ r ¹ (12), NH ib(10), NCH ₃ r ¹ (8), CC s(7)
1185	1180	-5	NCH ₃ r ¹ (57), NH ib(10), CNHC sd(8)
—	1195	—	HOH54(99)
—	1204	—	HOH37(87)
1374	1374	0	CCH ₃ sd(91), CCH ₃ ad ² (8)
1412	1408	-4	NCH ₃ sd(82)
1436	1428	-8	CCH ₃ ad ² (67), CCH ₃ ad ¹ (10), NCH ₃ sd(10)
1436	1439	3	CCH ₃ ad ¹ (78), CCH ₃ ad ² (13)
1460	1453	-7	NCH ₃ ad ² (93), NCH ₃ r ² (7)
1460	1466	6	NCH ₃ ad ¹ (88), NCH ₃ r ¹ (8)
1503	1507	4	CN s(37), CO s(15), CC s(13), NH ib(10), CO r(8), NC s(7)
1628	1628	0	CO s(59), CN s(22)
—	2307	—	NH s(97)
2480	2461	-19	OH*s(85), OH*s(16)
2560	2556	-4	OH*s(50), OH*s(50)
2670	2668	-2	OH*s(85), OH*s(16)
2710	2711	1	OH*s(50), OH*s(50)
2943	2935	-8	NCH ₃ ss(99)
2943	2943	0	CCH ₃ ss(85), CCH ₃ as ¹ (8), CCH ₃ as ² (7)

Table 3.30: (continued)

frequency (cm^{-1})			Potential Energy Distribution
obs.	calc.	dev.	
2992	2986	-6	NCH ₃ as ² (100)
2992	2992	0	CCH ₃ as ¹ (46), CCH ₃ as ² (40), CCH ₃ ss(15)
3020	3014	-6	CCH ₃ as ² (53), CCH ₃ as ¹ (46)
3020	3019	-1	NCH ₃ as ¹ (98)

Table 3.31: Scaled 4-31G Frequencies and Potential Energy Distribution for Water-Excluded *trans* N-Methylacetamide One-water on the Amide Hydrogen Supermolecule.

frequency (cm ⁻¹)			<i>trans</i> CH ₃ CONHCH ₃ (mean deviation = 7 cm ⁻¹)
obs.	calc.	dev.	
			Potential Energy Distribution
—	53	—	CC t(94)
171	157	-14	NC t(69), C ² N t(31)
195	204	9	NH ob(52), C ² N t(20), NC t(14)
297	297	0	CNHC sd(58), CO sd(29), CO r(10)
443	445	2	CO sd(44), CO r(33), CCH ₃ r ¹ (7)
—	599	—	CO ob(70), CCH ₃ r ² (19)
630	632	2	CC s(40), CO r(30), CNHC sd(11), NC s(9)
748	746	-2	NH ob(47), C ² N t(38), NC t(13)
883	881	-2	NCH ₃ r ¹ (24), CN s(16), CC s(16), CO s(12), CO r(9), CNHC sd(8)
994	1000	6	CCH ₃ r ¹ (42), NC s(29), CC s(19)
1044	1044	0	CCH ₃ r ² (73), CO ob(21)
1095	1092	-3	NC s(41), CCH ₃ r ¹ (32)
1129	1129	0	NCH ₃ r ² (91), NCH ₃ ad ² (7)
1164	1170	6	NCH ₃ r ¹ (57), CNHC sd(12), CO s(11)
1312	1326	14	NH ib(35), CN s(17), CCH ₃ sd(12), CO s(9), CC s(7)
1378	1376	-2	CCH ₃ sd(77), CCH ₃ ad ¹ (14)
1416	1418	2	NCH ₃ sd(88)
1428	1434	6	CCH ₃ ad ¹ (74), CCH ₃ sd(9)
1440	1438	-2	CCH ₃ ad ² (94)
1449	1455	6	NCH ₃ ad ² (93), NCH ₃ r ² (7)
1467	1464	-3	NCH ₃ ad ¹ (84), NCH ₃ r ¹ (7)
1577	1570	-7	NH ib(51), CN s(25)
1629	1631	2	CO s(49), CN s(27), CCH ₃ r ¹ (8), CO sd(7)
2925	2934	9	CCH ₃ ss(99)
2942	2942	0	NCH ₃ ss(99)
2973	2983	10	NCH ₃ as ² (100)
2992	2992	0	CCH ₃ as ² (100)
3009	3014	5	CCH ₃ as ¹ (99)
3020	3020	0	NCH ₃ as ¹ (98)
3120	3121	1	NH s(99)

Table 3.31: (continued)

frequency (cm^{-1})			<i>trans</i> CH ₃ CONDCH ₃ (mean deviation = 5 cm^{-1})
obs.	calc.	dev.	Potential Energy Distribution
—	53	—	CC t(94)
149	156	7	NC t(66), C ² N t(34)
195	203	8	NH ob(49), C ² N t(21), NC t(16)
295	295	0	CNHC sd(58), CO sd(30), CO r(9)
444	443	-1	CO sd(44), CO r(33), CCH ₃ r ¹ (7)
—	548	—	C ² N t(41), NH ob(33), NC t(14), CO ob(10)
—	607	—	CO ob(60), CCH ₃ r ² (19), NH ob(19)
630	629	-1	CC s(39), CO r(31), CNHC sd(11), NC s(8)
875	869	-6	NCH ₃ r ¹ (22), CC s(16), CN s(15), CO s(10), NC s(10), CO r(8), CNHC sd(7)
968	966	-2	NH ib(63), NC s(14), CN s(8)
1002	999	-3	CCH ₃ r ¹ (43), NC s(26), CC s(19)
1044	1044	0	CCH ₃ r ² (73), CO ob(21)
—	1126	—	NCH ₃ r ² (91), NCH ₃ ad ² (7)
1126	1127	1	NC s(30), CCH ₃ r ¹ (23), CO s(10), NH ib(10), NCH ₃ r ¹ (7)
1185	1181	-4	NCH ₃ r ¹ (56), CNHC sd(10), NH ib(10), CO r(7)
1374	1373	-1	CCH ₃ sd(91), CCH ₃ ad ¹ (8)
1412	1410	-2	NCH ₃ sd(78), CCH ₃ ad ¹ (8)
1436	1430	-6	CCH ₃ ad ¹ (73), NCH ₃ sd(14)
1436	1438	2	CCH ₃ ad ² (94)
1460	1454	-6	NCH ₃ ad ² (93), NCH ₃ r ² (7)
1460	1463	3	NCH ₃ ad ¹ (87), NCH ₃ r ¹ (7)
1503	1501	-2	CN s(31), CO s(21), CC s(14), NH ib(10), CO r(7)
1628	1624	-4	CO s(47), CN s(30), CCH ₃ r ¹ (8)
—	2300	—	NH s(97)
2943	2934	-9	CCH ₃ ss(99)
2943	2943	0	NCH ₃ ss(99)
2992	2982	-10	NCH ₃ as ² (100)
2992	2992	0	CCH ₃ as ² (100)
3020	3014	-6	CCH ₃ as ¹ (99)
3020	3020	0	NCH ₃ as ¹ (98)

Table 3.32: Scaled 4-31G Frequencies and Potential Energy Distribution for Water-Excluded *trans* *N*-methylacetamide One-water on the Amide Carbonyl Oxygen Supermolecule.

frequency (cm^{-1})			NMA (mean deviation = 10 cm^{-1})
obs.	calc.	dev.	
			Potential Energy Distribution
—	75	—	CC t(81), NC t(19)
171	155	−16	NC t(85), CC t(17)
195	209	14	C ² N t(75), NH ob(13), CO ob(9)
297	301	4	CNHC sd(56), CO sd(37)
443	438	−5	CO sd(38), CO r(32), CNHC sd(12)
—	589	—	CO ob(63), C ² N t(16), CCH ₃ r ² (12)
630	635	5	CO r(41), CC s(26), CNHC sd(11)
748	737	−11	NH ob(84), C ² N t(10)
883	878	−5	CN s(21), CC s(18), NCH ₃ r ² (17), NC s(11), CO s(8)
994	982	−12	CCH ₃ r ¹ (49), CC s(15), NC s(11), CO s(8), CCH ₃ r ² (8)
1044	1051	7	CCH ₃ r ² (62), CO ob(20), CCH ₃ r ¹ (8)
1095	1095	0	NC s(42), CCH ₃ r ¹ (14), NCH ₃ r ² (14), CC s(13)
1129	1127	−2	NCH ₃ r ² (46), NCH ₃ r ¹ (26), NC s(12)
1164	1178	14	NCH ₃ r ¹ (57), NCH ₃ r ² (9), NC s(7), CNHC sd(7)
1312	1327	15	NH ib(37), CN s(20), CCH ₃ sd(12), CC s(10), CO s(7)
1378	1377	−1	CCH ₃ sd(80), CCH ₃ ad ² (9)
1416	1418	2	NCH ₃ sd(85)
1428	1427	−1	CCH ₃ ad ² (78), CCH ₃ ad ¹ (7)
1440	1444	4	CCH ₃ ad ¹ (82)
1449	1447	−2	NCH ₃ ad ² (60), NCH ₃ ad ¹ (29)
1467	1470	3	NCH ₃ ad ¹ (61), NCH ₃ ad ² (27)
1577	1570	−7	CN s(40), NH ib(38)
1636	1638	2	CO s(62), NH ib(9), CN s(7), CO sd(7)
2925	2934	9	CCH ₃ ss(70), CCH ₃ as ¹ (29)
2942	2941	−1	NCH ₃ ss(98)
2973	2982	9	NCH ₃ as ² (95)
2992	2992	0	CCH ₃ as ¹ (68), CCH ₃ ss(30)
3009	3015	6	CCH ₃ as ² (97)
3020	3021	1	NCH ₃ as ¹ (97)
—	3477	—	NH s(100)

Table 3.32: (continued)

frequency (cm^{-1})			NMA in D_2O (mean deviation = 9 cm^{-1})
obs.	calc.	dev.	
			Potential Energy Distribution
—	75	—	CC t(82), NC t(19)
149	152	3	NC t(83), CC t(16)
195	203	8	C^2N t(78), NH ob(9), CO ob(8)
295	299	4	CNHC sd(56), CO sd(37)
444	435	-9	CO sd(37), CO r(32), CNHC sd(13)
—	521	—	NH ob(44), CO ob(33), C^2N t(22)
—	626	—	CO r(38), CC s(23), CNHC sd(10), NH ob(10)
630	649	19	NH ob(37), CO ob(34), CCH_3 r ² (11), CO r(7)
875	867	-8	CN s(18), CC s(18), NC s(17), NCH_3 r ² (15), CO s(7)
968	958	-10	NH ib(55), CCH_3 r ¹ (20), CN s(11)
1002	986	-16	CCH_3 r ¹ (31), NC s(22), CC s(18), CO s(13)
1044	1049	5	CCH_3 r ² (63), CO ob(20), CCH_3 r ¹ (9)
—	1122	—	NCH_3 r ² (56), NCH_3 r ¹ (18), NC s(8)
1126	1145	19	NC s(32), NCH_3 r ¹ (15), CCH_3 r ¹ (13), NH ib(13), CC s(12)
1185	1187	2	NCH_3 r ¹ (50), NCH_3 r ² (13), NH ib(8)
1374	1373	-1	CCH_3 sd(93)
1412	1410	-2	NCH_3 sd(76), CCH_3 ad ² (7)
1436	1425	-11	CCH_3 ad ² (76), NCH_3 sd(11)
1436	1443	7	CCH_3 ad ¹ (83)
1460	1447	-13	NCH_3 ad ² (62), NCH_3 ad ¹ (29)
1460	1470	10	NCH_3 ad ¹ (61), NCH_3 ad ² (27)
1503	1512	9	CN s(43), CC s(14), NH ib(10), CO s(7), NC s(7)
1628	1627	-1	CO s(64), CN s(14)
—	2551	—	NH s(98)
2943	2934	-9	CCH_3 ss(70), CCH_3 as ¹ (29)
2943	2941	-2	NCH_3 ss(98)
2992	2982	-10	NCH_3 as ² (95)
2992	2992	0	CCH_3 as ¹ (68), CCH_3 ss(30)
3020	3015	-5	CCH_3 as ² (97)
3020	3021	1	NCH_3 as ¹ (97)

Table 3.33: Scaled 4-31G Frequencies and Potential Energy Distribution for Water-Excluded *trans* *N*-methylacetamide Two-Water, One Water on the Amide Hydrogen, One Water on the Carbonyl Oxygen, Supermolecule.

frequency (cm ⁻¹)			<i>trans</i> CH ₃ CONHCH ₃ (mean deviation = 7 cm ⁻¹)
obs.	calc.	dev.	
			Potential Energy Distribution
—	79	—	CC t(67), NC t(33)
171	163	-8	NC t(56), CC t(27), C ² N t(18)
195	201	6	NH ob(44), C ² N t(37), CO ob(7)
297	297	0	CNHC sd(58), CO sd(38)
443	435	-8	CO sd(41), CO r(25), CNHC sd(17)
—	596	—	CO ob(64), CCH ₃ r ² (11), C ² N t(8), CCH ₃ r ¹ (7)
630	638	8	CO r(41), CC s(33), CNHC sd(7)
748	748	0	NH ob(56), C ² N t(36)
883	875	-8	CN s(21), CC s(20), NCH ₃ r ¹ (17), CO r(10), CO s(9), NC s(8)
994	989	-5	CCH ₃ r ² (32), CCH ₃ r ¹ (30), CC s(13), NC s(11)
1044	1046	2	CCH ₃ r ² (38), CCH ₃ r ¹ (32), CO ob(21)
1095	1099	4	NC s(59), CC s(11), CCH ₃ r ¹ (11)
1129	1129	0	NCH ₃ r ² (92), NCH ₃ ad ² (7)
1164	1172	8	NCH ₃ r ¹ (63), CNHC sd(9), NCH ₃ ad ¹ (8), NC s(7)
1312	1325	13	NH ib(39), CN s(19), CCH ₃ sd(9), CO s(8), CC s(8)
1378	1376	-2	CCH ₃ sd(82), CCH ₃ ad ² (10)
1416	1418	2	NCH ₃ sd(87)
1428	1435	7	CCH ₃ ad ² (61), CCH ₃ ad ¹ (19), CCH ₃ sd(7)
1440	1439	-1	CCH ₃ ad ¹ (71), CCH ₃ ad ² (19)
1449	1454	5	NCH ₃ ad ² (93), NCH ₃ r ² (7)
1467	1463	-4	NCH ₃ ad ¹ (84), NCH ₃ r ¹ (8)
1577	1559	-18	NH ib(44), CN s(33)
1629	1633	4	CO s(64), CN s(14)
2925	2934	9	NCH ₃ ss(99)
2942	2943	1	CCH ₃ ss(80), CCH ₃ as ¹ (14)
2973	2982	9	CCH ₃ as ¹ (76), CCH ₃ ss(19)
2992	2992	0	NCH ₃ as ² (100)
3009	3014	5	NCH ₃ as ¹ (98)
3020	3020	0	CCH ₃ as ² (88), CCH ₃ as ¹ (10)
3120	3123	3	NH s(99)

Table 3.33: (continued)

frequency (cm ⁻¹)			<i>trans</i> CH ₃ CONDCH ₃ (mean deviation = 8 cm ⁻¹)
obs.	calc.	dev.	
Potential Energy Distribution			
—	79	—	CC t(67), NC t(33)
149	163	14	NC t(55), CC t(26), C ² N t(19)
195	199	4	NH ob(40), C ² N t(39), CC t(7)
295	295	0	CNHC sd(57), CO sd(38)
444	433	-11	CO sd(41), CO r(25), CNHC sd(17)
—	540	—	C ² N t(40), NH ob(33), CO ob(18)
—	612	—	CO ob(40), NH ob(23), CCH ₃ r ² (10), CO r(9), CC s(7)
630	637	7	CO r(36), CC s(27), CO ob(13)
875	864	-11	CN s(20), CC s(20), NCH ₃ r ¹ (16), NC s(11), CO s(8), CO r(8)
968	959	-9	NH ib(58), CCH ₃ r ¹ (12), CCH ₃ r ² (12), CN s(9)
1002	995	-7	NC s(26), CCH ₃ r ¹ (18), CCH ₃ r ² (18), CC s(15), CO s(9), NH ib(9)
1044	1045	1	CCH ₃ r ² (39), CCH ₃ r ¹ (33), CO ob(21)
—	1128	—	NCH ₃ r ² (91), NCH ₃ ad ² (7)
1126	1130	4	NC s(42), CCH ₃ r ¹ (11), NH ib(10), CC s(9), NCH ₃ r ¹ (7)
1185	1182	-3	NCH ₃ r ¹ (61), NH ib(9), NCH ₃ ad ¹ (7), CNHC sd(7), CO r(7)
1374	1374	0	CCH ₃ sd(92), CCH ₃ ad ² (7)
1412	1410	-2	NCH ₃ sd(78)
1436	1431	-5	CCH ₃ ad ² (69), NCH ₃ sd(12), CCH ₃ ad ¹ (7)
1436	1439	3	CCH ₃ ad ¹ (81), CCH ₃ ad ² (10)
1460	1454	-6	NCH ₃ ad ² (93), NCH ₃ r ² (7)
1460	1463	3	NCH ₃ ad ¹ (86), NCH ₃ r ¹ (8)
1503	1501	-2	CN s(38), CO s(13), CC s(13), NH ib(9), CO r(8), NC s(7)
1628	1626	-2	CO s(63), CN s(19)
2300	2298	-2	NH s(97)
2943	2934	-9	NCH ₃ ss(99)
2943	2943	0	CCH ₃ ss(80), CCH ₃ as ¹ (14)
2992	2982	-10	CCH ₃ as ¹ (76), CCH ₃ ss(19)
2992	2992	0	NCH ₃ as ² (100)
3020	3015	-5	NCH ₃ as ¹ (98)
3020	3020	0	CCH ₃ as ² (88), CCH ₃ as ¹ (10)

Table 3.34: Scaled 4-31G Frequencies and Potential Energy Distribution for Water-Excluded *trans* *N*-methylacetamide Two-Water, Both on the Amide Carbonyl Oxygen, Supermolecule.

frequency (cm ⁻¹)			<i>trans</i> CH ₃ CONHCH ₃ (mean deviation = 8 cm ⁻¹)
obs.	calc.	dev.	
			Potential Energy Distribution
—	92	−8	CC t(66), NC t(33)
171	155	−16	NC t(63), CC t(31)
195	212	17	C ² N t(70), NH ob(13), CO ob(9)
297	299	2	CNHC sd(50), CO sd(41)
443	443	0	CO sd(36), CO r(31), CNHC sd(16)
—	585	—	CO ob(63), C ² N t(14), CCH ₃ r ² (9)
630	629	−1	CO r(44), CC s(23), CNHC sd(10)
748	746	−2	NH ob(82), C ² N t(12)
883	876	−7	CN s(21), CC s(18), NCH ₃ r ² (18), NC s(13), CO s(8)
994	994	0	CCH ₃ r ¹ (35), CCH ₃ r ² (26), CC s(15), CO s(8), NC s(8)
1044	1048	4	CCH ₃ r ² (44), CCH ₃ r ¹ (25), CO ob(19)
1095	1096	1	NC s(52), CC s(15), CCH ₃ r ¹ (13)
1129	1130	1	NCH ₃ r ² (50), NCH ₃ r ¹ (24)
1164	1172	8	NCH ₃ r ¹ (61), NCH ₃ r ² (12), NCH ₃ ad ¹ (8)
1312	1325	13	NH ib(39), CN s(19), CC s(10), CCH ₃ sd(10), CO s(7)
1378	1375	−3	CCH ₃ sd(77), CCH ₃ ad ² (16)
1416	1418	2	NCH ₃ sd(88)
1428	1434	6	CCH ₃ ad ² (67), CCH ₃ sd(11), CCH ₃ ad ¹ (7)
1440	1439	−1	CCH ₃ ad ¹ (83), CCH ₃ ad ² (7)
1452	1451	−1	NCH ₃ ad ² (51), NCH ₃ ad ¹ (36)
1462	1465	3	NCH ₃ ad ¹ (53), NCH ₃ ad ² (36)
1577	1569	−8	CN s(40), NH ib(37)
1636	1637	1	CO s(65), CN s(8), NH ib(8)
2925	2934	9	NCH ₃ ss(93)
2942	2942	0	CCH ₃ ss(82), CCH ₃ as ¹ (16)
2973	2983	10	NCH ₃ as ² (89), NCH ₃ as ¹ (10)
2992	2992	0	CCH ₃ as ¹ (74), CCH ₃ ss(18), CCH ₃ as ² (8)
3009	3015	6	CCH ₃ as ² (89), CCH ₃ as ¹ (11)
3020	3022	2	NCH ₃ as ¹ (86), NCH ₃ as ² (8)
3120	3125	5	NH s(99)

Table 3.34: (continued)

frequency (cm^{-1})			<i>trans</i> CH ₃ CONDCH ₃ (mean deviation = 9 cm^{-1})
obs.	calc.	dev.	Potential Energy Distribution
—	92	—	CC t(66), NC t(33)
149	152	3	NC t(60), CC t(30), C ² N t(7)
195	207	12	C ² N t(71), NH ob(9), CO ob(7)
295	297	2	CNHC sd(49), CO sd(41)
444	440	-4	CO sd(35), CO r(30), CNHC sd(17)
—	528	—	NH ob(37), CO ob(37), C ² N t(23)
—	616	—	CO r(39), CC s(20), NH ob(12), CNHC sd(9)
630	646	16	NH ob(39), CO ob(30), CO r(10), CCH ₃ r ¹ (7)
875	864	-11	CN s(19), CC s(18), NC s(18), NCH ₃ r ² (16)
968	960	-8	NH ib(59), CCH ₃ r ¹ (11), CN s(10), CCH ₃ r ² (9)
1002	997	-5	CCH ₃ r ¹ (25), CC s(19), CCH ₃ r ² (18), NC s(17), CO s(12)
1044	1046	2	CCH ₃ r ² (44), CCH ₃ r ¹ (27), CO ob(20)
1100	1118	18	NCH ₃ r ² (33), NC s(28), NCH ₃ r ¹ (9)
1126	1152	26	NCH ₃ r ¹ (35), NC s(14), CC s(11), NCH ₃ r ² (10), NH ib(10)
1185	1177	-8	NCH ₃ r ¹ (41), NCH ₃ r ² (25), NH ib(8)
1374	1373	-1	CCH ₃ sd(88), CCH ₃ ad ² (10)
1412	1409	-3	NCH ₃ sd(77), CN s(7)
1436	1428	-8	CCH ₃ ad ² (69), NCH ₃ sd(13), CCH ₃ sd(8)
1436	1439	3	CCH ₃ ad ¹ (84)
1460	1451	-9	NCH ₃ ad ² (53), NCH ₃ ad ¹ (35)
1460	1465	5	NCH ₃ ad ¹ (54), NCH ₃ ad ² (36)
1503	1516	13	CN s(41), CC s(14), NH ib(9), CO s(8), NC s(7)
1628	1627	-1	CO s(66), CN s(15)
2300	2296	-4	NH s(98)
2943	2934	-9	NCH ₃ ss(93)
2943	2942	-1	CCH ₃ ss(82), CCH ₃ as ¹ (16)
2992	2983	-9	NCH ₃ as ² (89), NCH ₃ as ¹ (10)
2992	2992	0	CCH ₃ as ¹ (74), CCH ₃ ss(18), CCH ₃ as ² (8)
3020	3015	-5	CCH ₃ as ² (90), CCH ₃ as ¹ (11)
3020	3022	2	NCH ₃ as ¹ (86), NCH ₃ as ² (8)

Table 3.35: Scaled 4-31G Frequencies and Potential Energy Distribution for Water-Excluded *trans* *N*-methylacetamide Three-water Supermolecule.

frequency (cm ⁻¹)			<i>trans</i> CH ₃ CONHCH ₃ (mean deviation = 4 cm ⁻¹)
obs.	calc.	dev.	
Potential Energy Distribution			
—	89	—	CC t(51), NC t(49)
171	171	0	CC t(46), NC t(45), C ² N t(7)
195	197	2	C ² N t(50), NH ob(38), CO ob(7)
297	298	1	CNHC sd(59), CO sd(35)
443	445	2	CO sd(43), CO r(26), CNHC sd(14)
—	584	—	CO ob(66), CCH ₃ r ² (14), C ² N t(10)
630	629	-1	CO r(46), CC s(28), CNHC sd(7)
748	745	-3	NH ob(61), C ² N t(32)
883	877	-6	CN s(21), CC s(20), NCH ₃ r ¹ (15), NC s(10), CO s(9), CNHC sd(7), CO r(7)
994	997	3	CCH ₃ r ¹ (58), CC s(15), NC s(11), CO s(7)
1044	1045	1	CCH ₃ r ² (69), CO ob(19)
1095	1092	-3	NC s(58), CCH ₃ r ¹ (14), CC s(12)
1129	1128	-1	NCH ₃ r ² (88), NCH ₃ ad ² (9)
1164	1169	5	NCH ₃ r ¹ (67), CNHC sd(8), NCH ₃ ad ¹ (7)
1312	1328	16	NH ib(39), CN s(18), CCH ₃ sd(11), CO s(9), CC s(8)
1378	1376	-2	CCH ₃ sd(79), CCH ₃ ad ¹ (11)
1416	1418	2	NCH ₃ sd(87)
1428	1431	3	CCH ₃ ad ² (67), CCH ₃ ad ¹ (22)
1440	1442	2	CCH ₃ ad ¹ (55), CCH ₃ ad ² (23), CCH ₃ sd(8)
1452	1455	3	NCH ₃ ad ² (89), NCH ₃ r ² (9)
1462	1463	1	NCH ₃ ad ¹ (85), NCH ₃ r ¹ (7)
1577	1565	-12	NH ib(42), CN s(33), CC s(7)
1636	1634	-2	CO s(63), CN s(16)
2925	2933	8	NCH ₃ ss(99)
2942	2942	0	CCH ₃ ss(98)
2973	2982	9	NCH ₃ as ² (97)
2992	2992	0	CCH ₃ as ¹ (94)
3009	3015	6	CCH ₃ as ² (96)
3020	3020	0	NCH ₃ as ¹ (97)
3120	3119	-1	NH s(99)

Table 3.35: (continued)

frequency (cm^{-1})			<i>trans</i> CH ₃ CONDCH ₃ (mean deviation = 10 cm^{-1})
obs.	calc.	dev.	
			Potential Energy Distribution
—	89	—	CC t(51), NC t(49)
149	171	22	CC t(46), NC t(45), C ² N t(7)
195	194	−1	C ² N t(54), NH ob(34), CO ob(7)
295	296	1	CNHC sd(58), CO sd(35)
444	443	−1	CO sd(42), CO r(25), CNHC sd(15)
—	531	—	C ² N t(37), NH ob(31), CO ob(25)
—	609	—	CO ob(31), NH ob(26), CO r(14), CC s(9), CCH ₃ r ² (9)
630	629	−1	CO r(36), CC s(20), CO ob(16), NH ob(8)
875	865	−10	CN s(20), CC s(20), NC s(14), NCH ₃ r ¹ (13), CO s(8)
968	963	−5	NH ib(62), CCH ₃ r ¹ (19), CN s(8)
1002	1000	−2	CCH ₃ r ¹ (40), NC s(23), CC s(19), CO s(10)
1044	1044	0	CCH ₃ r ² (70), CO ob(19), CCH ₃ ad ² (7)
—	1121	—	NC s(28), NCH ₃ r ² (28), CCH ₃ r ¹ (11), NH ib(9), CC s(7)
1126	1130	4	NCH ₃ r ² (59), NC s(11), NCH ₃ r ¹ (8)
1185	1180	−5	NCH ₃ r ¹ (61), NH ib(9)
1374	1373	−1	CCH ₃ sd(92)
1412	1409	−3	NCH ₃ sd(82)
1436	1430	−6	CCH ₃ ad ² (47), CCH ₃ ad ¹ (37), NCH ₃ sd(9)
1436	1437	1	CCH ₃ ad ² (43), CCH ₃ ad ¹ (39)
1460	1455	−5	NCH ₃ ad ² (90), NCH ₃ r ² (9)
1460	1463	3	NCH ₃ ad ¹ (86), NCH ₃ r ¹ (7)
1503	1509	6	CN s(36), CO s(15), CC s(14), NH ib(9), CO r(7)
1628	1628	0	CO s(61), CN s(22)
—	2295	—	NH s(97)
2943	2933	−10	NCH ₃ ss(99)
2943	2942	−1	CCH ₃ ss(98)
2992	2982	−10	NCH ₃ as ² (97)
2992	2993	1	CCH ₃ as ¹ (94)
3020	3015	−5	CCH ₃ as ² (96)
3020	3020	0	NCH ₃ as ¹ (98)

3.4 Alanine—Development of C^α Coordinates

Figure 3.26 shows the structures of the one water alaninate supermolecules (bottom, CO₂ bridged; middle, NH—CO bridged) and the one water alanine (pH=1) supermolecule (top) optimized using the 4-31G basis set. Raman spectra of alaninate, NH₂CHCH₃CO₂[−], alaninate deuterated at the methyl carbon, NH₂CHCD₃CO₂[−] (alaninate-*d*3), and alaninate deuterated at both the α- and methyl-carbons, NH₂CD₃CO₂[−] (alaninate-*d*4), in both H₂O and D₂O are shown in Figures 3.27 and 3.28. Raman spectra of alanine at pH=1, ⁺NH₃CHCH₃CO₂H, and alanine at pH=1, deuterated at the methyl carbon, ⁺NH₃CHCD₃CO₂H, in H₂O and D₂O and alanine at pH=1, deuterated at both the α- and methyl-carbons, ⁺NH₃CD₃CO₂H, in H₂O are shown in Figures 3.29 and 3.30. The CH(D) stretch regions (not shown) were measured and analyzed for alaninate and alaninate-*d*4 in H₂O and D₂O, ¹⁵N substituted alaninate in H₂O, and, at pH=1, for alanine, alanine-*d*3, alanine-*d*4, and ¹⁵N substituted alanine in H₂O, and alanine in D₂O. All frequencies observed in the FT-IR spectra (not shown, taken by Victor Kalashinsky) were also observed in the Raman spectra. Difference spectra between alaninate or alanine at pH=1 and the respective ¹³C methyl (top) and ¹⁵N substituted (bottom) alanine, showing contributions to the spectra from CC^{me} and CN^{ter} stretching, respectively, are shown in Figures 3.31 and 3.32.

Internal coordinate definitions for alaninate and alanine at pH=1 are given in Table 3.36. The symmetry coordinate definitions are given in Tables 3.37 and 3.38. Our symmetry coordinate definitions are those recommended by Pulay *et al*, [1979] using the optional symmetrized combinations of the CH₃ and CO₂[−] stretches [Fogarasi and Pulay, 1985].

The optimized geometries for isolated alaninate, the one water alaninate supermolecule and the one water alanine at pH=1 supermolecule for each of the basis sets are given in Tables 3.39, 3.40, and 3.41, respectively.

Figure 3.26: Optimized structures of the Alaninate one water supermolecules (bottom CO₂ bridged, middle NH-CO bridged) and Alanine at pH=1 one water supermolecule (top). Covalent bonds are solid, hydrogen bonds are outlined.

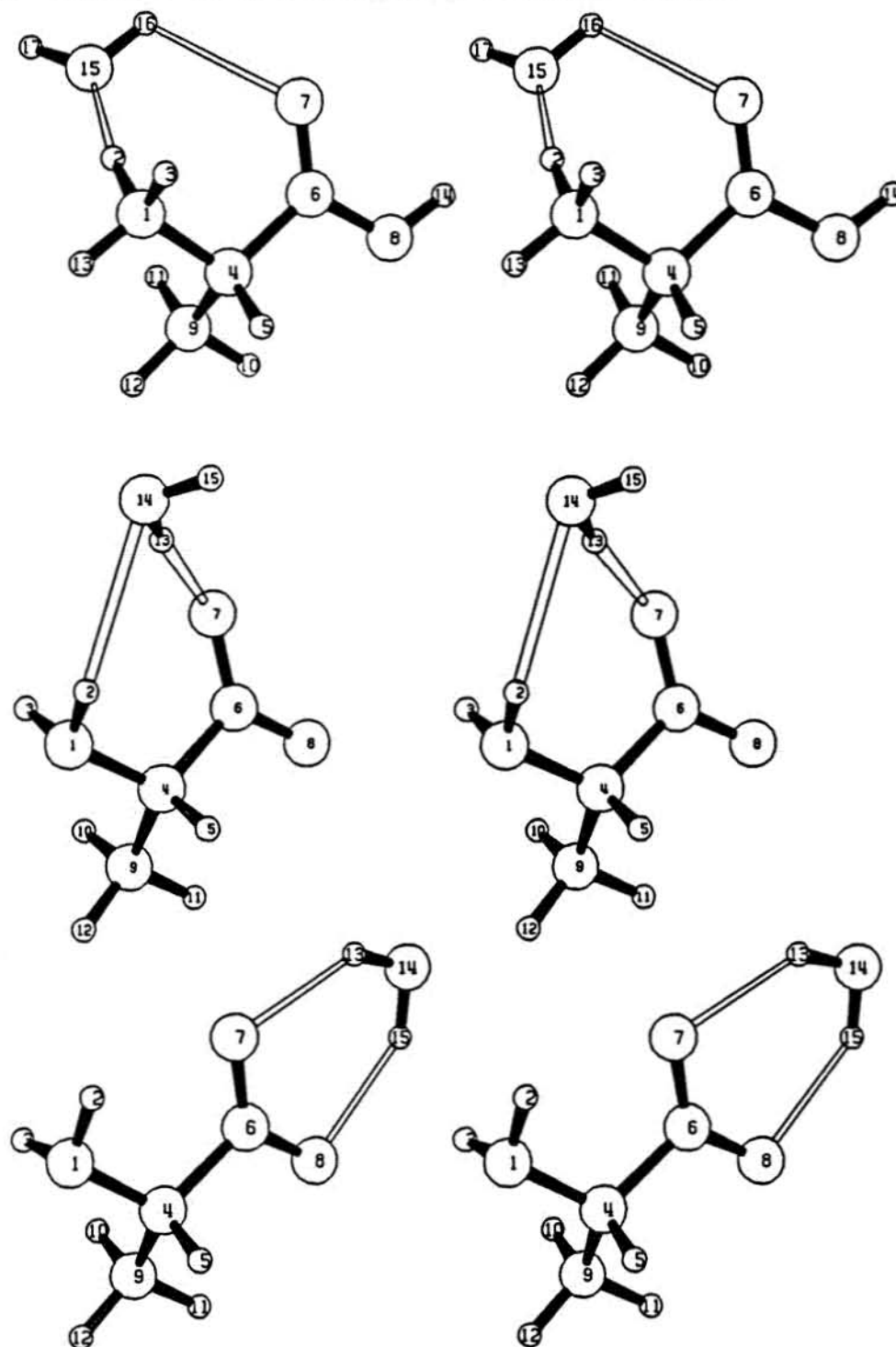


Figure 3.27: Raman spectra of alaninate in H_2O pH 13 (bottom), alanine(3,3,3- d_3) pH 13 (middle), and alanine(2,3,3,3- d_4) pH 13 (top).

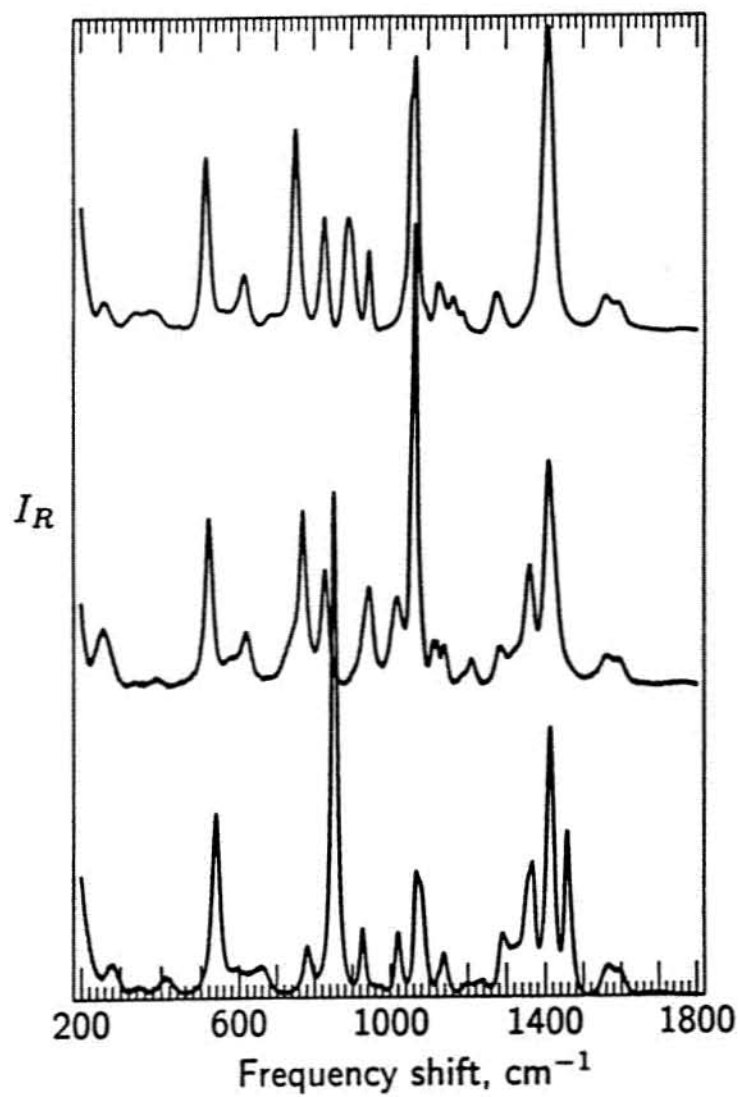


Figure 3.27: Raman spectra of alaninate in H_2O pH 13 (bottom), alanine(3,3,3- d_3) pH 13 (middle), and alanine(2,3,3,3- d_4) pH 13 (top).

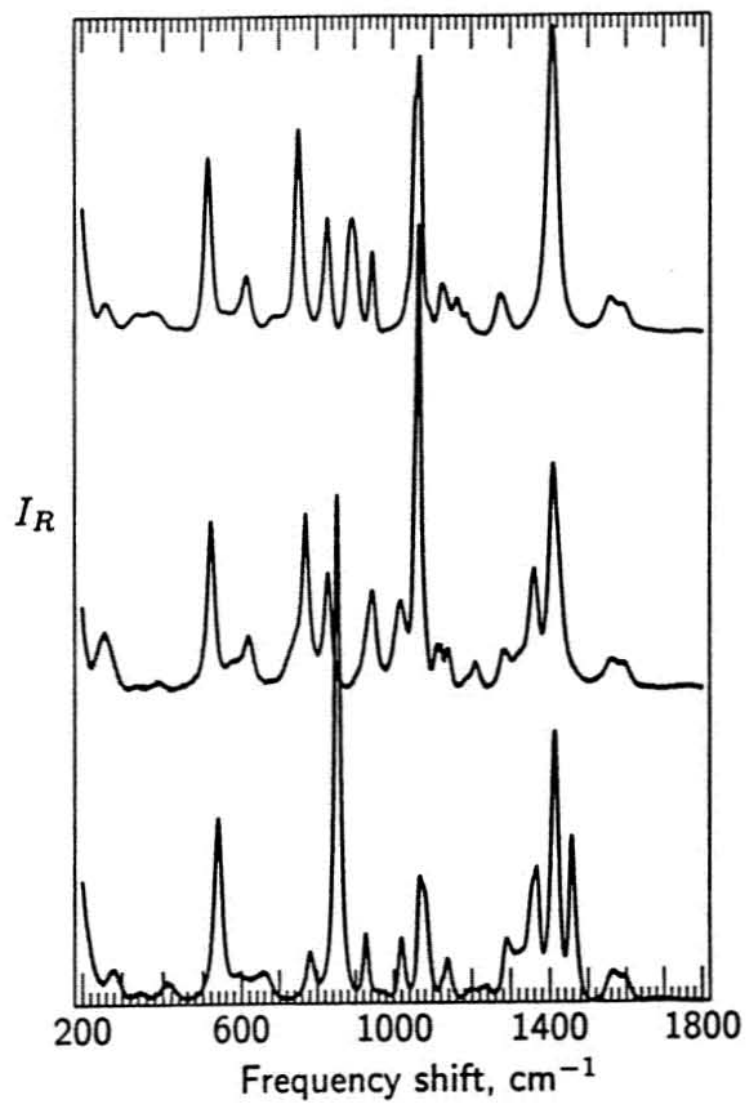


Figure 3.28: Raman spectra of alaninate in D₂O pD 13 (bottom), alanine(3,3,3-*d*₃) in D₂O pD 13 (middle), and alanine(2,3,3,3-*d*₄) in D₂O pD 13 (top).

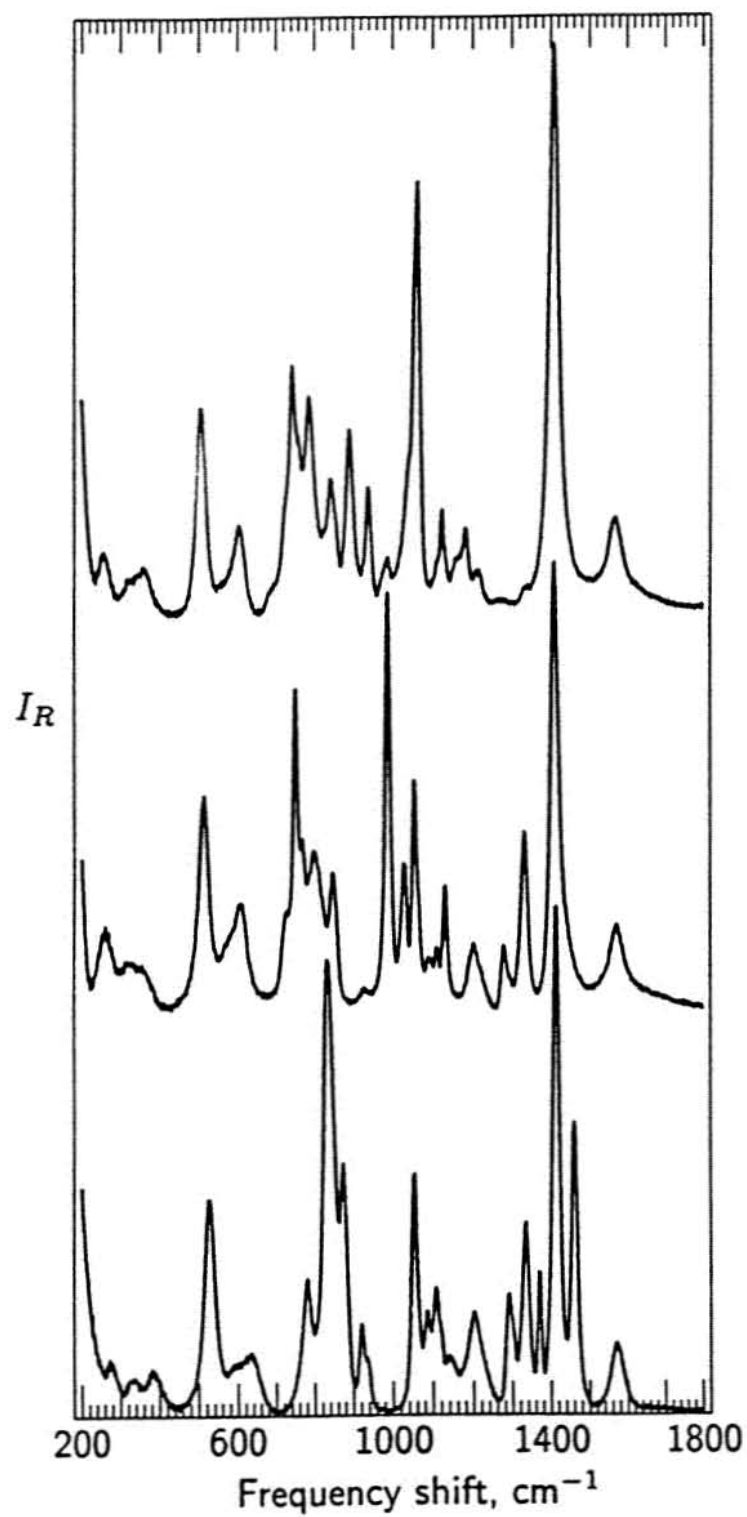


Figure 3.29: Raman spectra of alanine at pH=1 in H₂O (bottom), alanine(3,3,3-*d*₃) pH 1 (middle), and alanine(2,3,3,3-*d*₄) pH 1 (top).

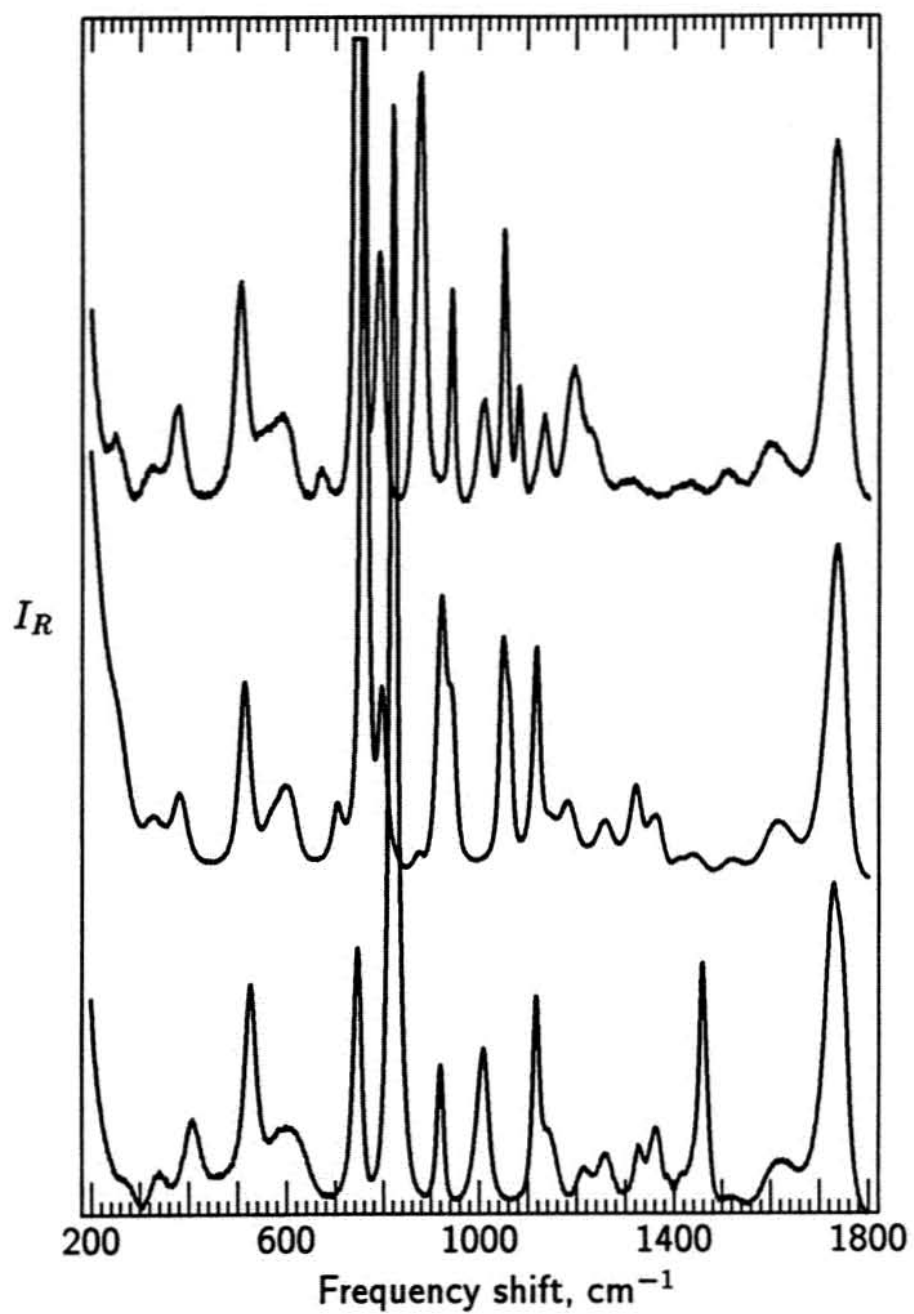


Figure 3.30: Raman spectra of alanine at pD1 in D₂O (bottom), alanine(3,3,3-*d*₃) pD 1 (top).

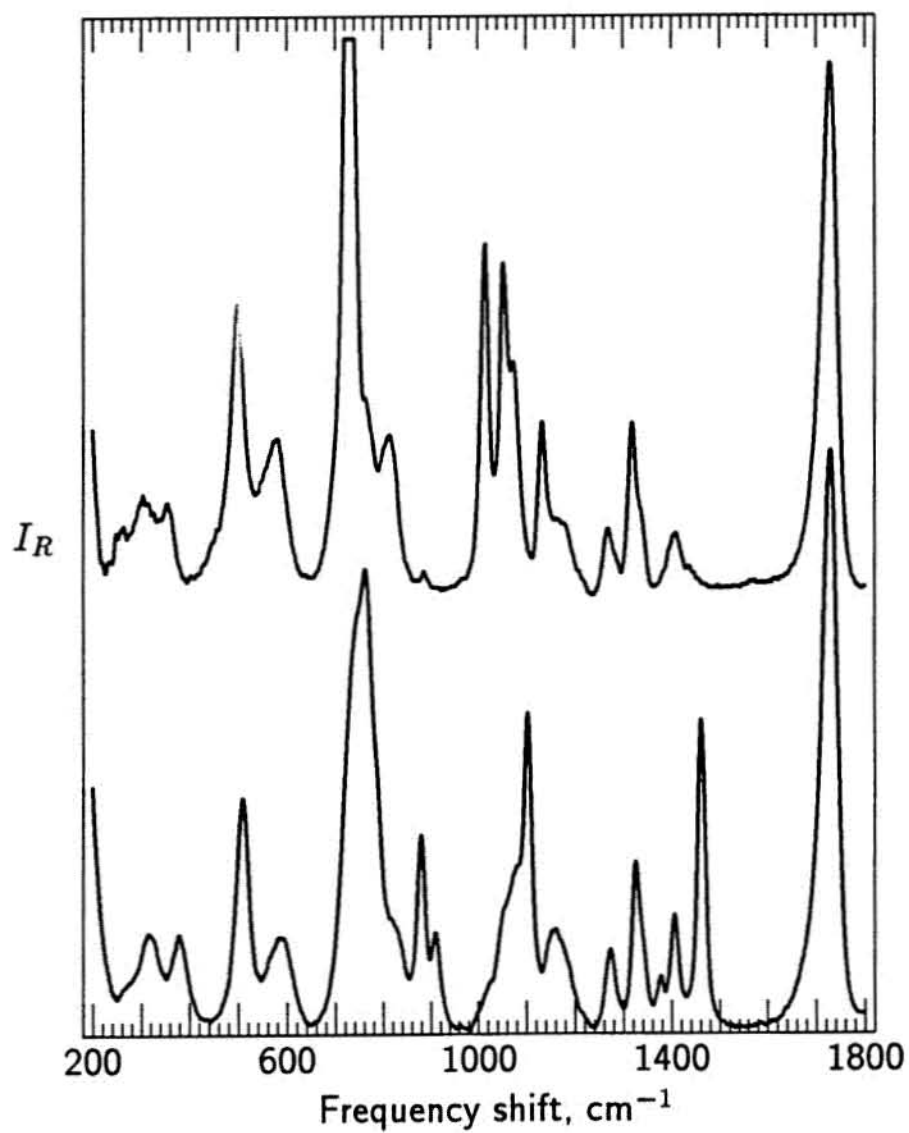


Figure 3.31: Difference spectra of alaninate and alaninate($3\text{-}^{13}\text{C}$) (top) and alaninate and alaninate(^{15}N) (bottom).

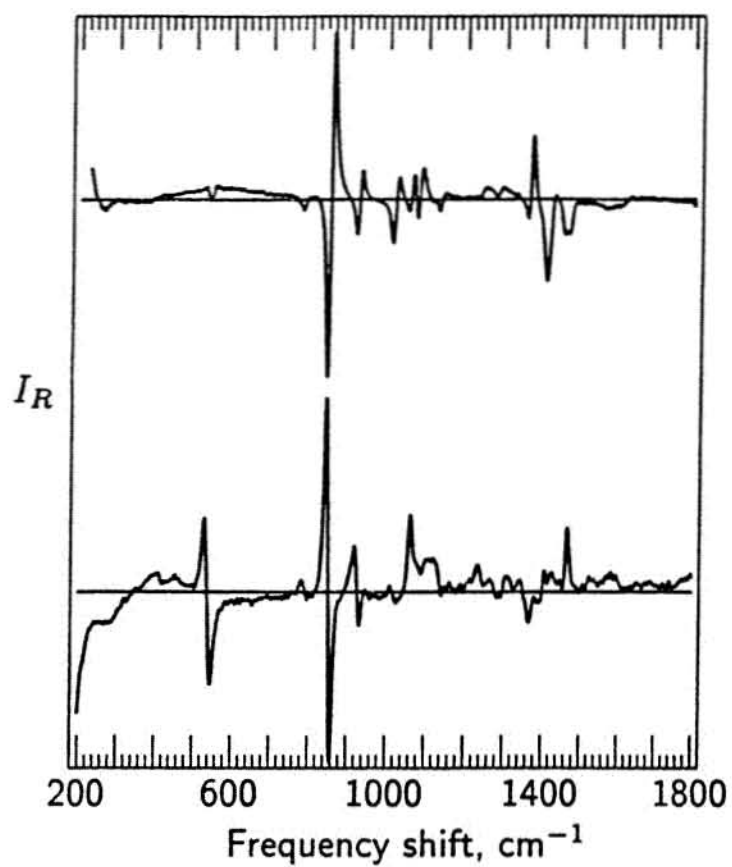


Figure 3.32: Difference spectra of alanine and alanine($3\text{-}^{13}\text{C}$) (top) and alanine and alanine(^{15}N) (bottom), all at pH=1.

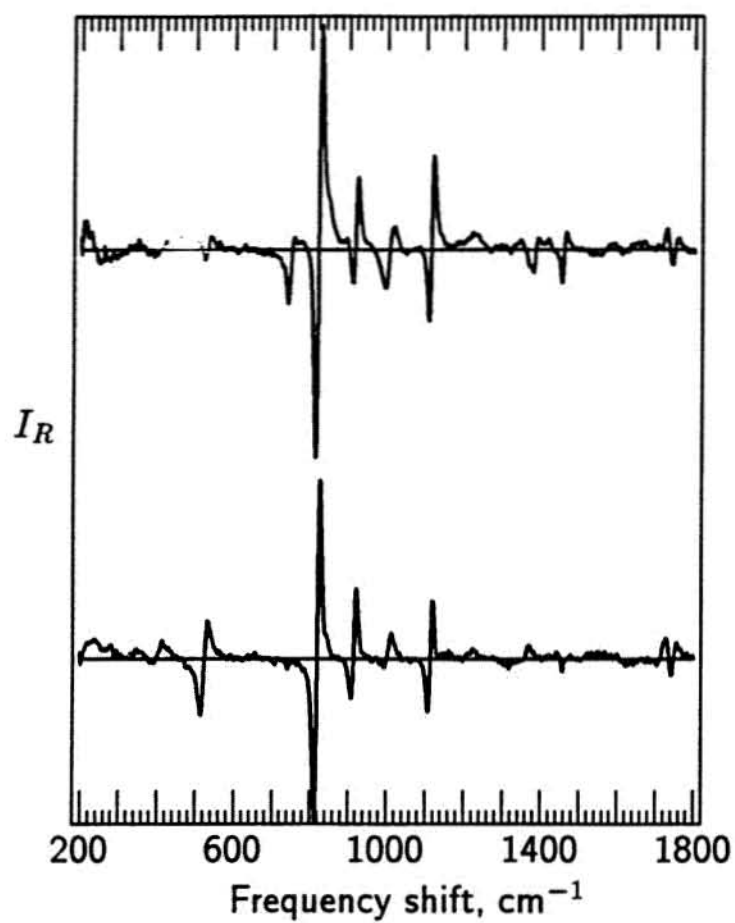


Table 3.36: Redundant Internal Coordinates for Alanine in Base and Acid.

Base	
$R_1 = \Delta\gamma(\text{O}^7\text{-C}^6)$	$R_{18} = \Delta\omega(\text{C}^4\text{-O}^8\text{-O}^7\text{-C}^6)$
$R_2 = \Delta\gamma(\text{O}^8\text{-C}^6)$	$R_{19} = \Delta\theta(\text{H}^3\text{-N}^1\text{-H}^2)$
$R_3 = \Delta\gamma(\text{H}^5\text{-C}^4)$	$R_{20} = \Delta\theta(\text{C}^4\text{-N}^1\text{-H}^3)$
$R_4 = \Delta\gamma(\text{C}^9\text{-C}^4)$	$R_{21} = \Delta\theta(\text{C}^4\text{-N}^1\text{-H}^2)$
$R_5 = \Delta\gamma(\text{C}^6\text{-C}^4)$	$R_{22} = \Delta\theta(\text{C}^4\text{-H}^3\text{-H}^2\text{-N}^1)$
$R_6 = \Delta\gamma(\text{C}^4\text{-N}^1)$	$R_{23} = \Delta\theta(\text{H}^{12}\text{-C}^9\text{-H}^{11})$
$R_7 = \Delta\gamma(\text{H}^2\text{-N}^1)$	$R_{24} = \Delta\theta(\text{H}^{11}\text{-C}^9\text{-H}^{10})$
$R_8 = \Delta\gamma(\text{H}^3\text{-N}^1)$	$R_{25} = \Delta\theta(\text{H}^{12}\text{-C}^9\text{-H}^{10})$
$R_9 = \Delta\theta(\text{H}^5\text{-C}^4\text{-N}^1)$	$R_{26} = \Delta\theta(\text{H}^{10}\text{-C}^9\text{-C}^4)$
$R_{10} = \Delta\theta(\text{C}^9\text{-C}^4\text{-H}^5)$	$R_{27} = \Delta\theta(\text{H}^{12}\text{-C}^9\text{-C}^4)$
$R_{11} = \Delta\theta(\text{C}^6\text{-C}^4\text{-H}^5)$	$R_{28} = \Delta\theta(\text{H}^{11}\text{-C}^9\text{-C}^4)$
$R_{12} = \Delta\theta(\text{C}^9\text{-C}^4\text{-N}^1)$	$R_{29} = \Delta\gamma(\text{H}^{10}\text{-C}^9)$
$R_{13} = \Delta\theta(\text{C}^9\text{-C}^4\text{-C}^6)$	$R_{30} = \Delta\gamma(\text{H}^{11}\text{-C}^9)$
$R_{14} = \Delta\theta(\text{C}^6\text{-C}^4\text{-N}^1)$	$R_{31} = \Delta\gamma(\text{H}^{12}\text{-C}^9)$
$R_{15} = \Delta\theta(\text{O}^8\text{-C}^6\text{-O}^7)$	$R_{32} = \Delta\tau(\text{C}^4\text{-N}^1)$
$R_{16} = \Delta\theta(\text{O}^8\text{-C}^6\text{-C}^4)$	$R_{33} = \Delta\tau(\text{C}^6\text{-C}^4)$
$R_{17} = \Delta\theta(\text{O}^7\text{-C}^4\text{-C}^6)$	$R_{34} = \Delta\tau(\text{C}^9\text{-C}^4)$

Acid	
$R_1 = \Delta\gamma(\text{O}^4\text{-C}^3)$	$R_{21} = \Delta\theta(\text{H}^{14}\text{-C}^8\text{-H}^{12})$
$R_2 = \Delta\gamma(\text{O}^5\text{-C}^3)$	$R_{22} = \Delta\theta(\text{H}^{12}\text{-C}^8\text{-C}^2)$
$R_3 = \Delta\gamma(\text{H}^{10}\text{-O}^5)$	$R_{23} = \Delta\theta(\text{H}^{14}\text{-C}^8\text{-C}^2)$
$R_4 = \Delta\gamma(\text{H}^9\text{-C}^2)$	$R_{24} = \Delta\theta(\text{H}^{13}\text{-C}^8\text{-C}^2)$
$R_5 = \Delta\gamma(\text{C}^8\text{-C}^2)$	$R_{25} = \Delta\theta(\text{H}^{11}\text{-N}^1\text{-H}^7)$
$R_6 = \Delta\gamma(\text{C}^3\text{-C}^2)$	$R_{26} = \Delta\theta(\text{H}^7\text{-N}^1\text{-H}^6)$
$R_7 = \Delta\gamma(\text{C}^2\text{-N}^1)$	$R_{27} = \Delta\theta(\text{H}^{11}\text{-N}^1\text{-H}^6)$
$R_8 = \Delta\theta(\text{H}^{10}\text{-O}^5\text{-C}^3)$	$R_{28} = \Delta\theta(\text{H}^6\text{-N}^1\text{-C}^2)$
$R_9 = \Delta\theta(\text{H}^9\text{-C}^2\text{-N}^1)$	$R_{29} = \Delta\theta(\text{H}^{11}\text{-N}^1\text{-C}^2)$
$R_{10} = \Delta\theta(\text{H}^9\text{-C}^2\text{-C}^8)$	$R_{30} = \Delta\theta(\text{H}^7\text{-N}^1\text{-C}^2)$
$R_{11} = \Delta\theta(\text{H}^9\text{-C}^2\text{-C}^3)$	$R_{31} = \Delta\theta(\text{H}^{12}\text{-C}^8)$
$R_{12} = \Delta\theta(\text{C}^8\text{-C}^2\text{-N}^1)$	$R_{32} = \Delta\gamma(\text{H}^{13}\text{-C}^8)$
$R_{13} = \Delta\theta(\text{C}^8\text{-C}^2\text{-C}^3)$	$R_{33} = \Delta\gamma(\text{H}^{14}\text{-C}^8)$
$R_{14} = \Delta\theta(\text{C}^3\text{-C}^2\text{-N}^1)$	$R_{34} = \Delta\gamma(\text{H}^6\text{-N}^1)$
$R_{15} = \Delta\theta(\text{O}^5\text{-C}^3\text{-O}^4)$	$R_{35} = \Delta\gamma(\text{H}^7\text{-N}^1)$

Table 3.36: (continued)

$R_{16} = \Delta\theta(\text{O}^5\text{-C}^3\text{-C}^2)$	$R_{36} = \Delta\gamma(\text{H}^{11}\text{-N}^1)$
$R_{17} = \Delta\theta(\text{O}^4\text{-C}^3\text{-C}^2)$	$R_{37} = \Delta\tau(\text{C}^2\text{-N}^1)$
$R_{18} = \Delta\omega(\text{C}^2\text{-O}^5\text{-O}^4\text{-C}^3)$	$R_{38} = \Delta\tau(\text{C}^3\text{-C}^2)$
$R_{19} = \Delta\theta(\text{H}^{14}\text{-C}^8\text{-H}^{13})$	$R_{39} = \Delta\tau(\text{C}^8\text{-C}^2)$
$R_{20} = \Delta\theta(\text{H}^{13}\text{-C}^8\text{-H}^{12})$	$R_{40} = \Delta\tau(\text{O}^5\text{-C}^3)$

Symbols: γ = stretch, θ = bend, ω = out of plane bend,
 τ = torsion.

Table 3.37: Symmetry Coordinate Definitions for Alanine in Base

COO ss ^a	$S_1 = (R_1 + R_2)/\sqrt{2}$
COO as	$S_2 = (R_1 - R_2)/\sqrt{2}$
CH s	$S_3 = R_3$
CC ^{me} s	$S_4 = R_4$
CC ^{ter} s	$S_5 = R_5$
CN ^{ter} s	$S_6 = R_6$
NH ₂ ss	$S_7 = (R_7 + R_8)/\sqrt{2}$
NH ₂ as	$S_8 = (R_7 - R_8)/\sqrt{2}$
C ^α H r ¹	$S_9 = (2R_9 - R_{10} - R_{11})/\sqrt{6}$
C ^α H r ²	$S_{10} = (R_{10} - R_{11})/\sqrt{2}$
C ^α H d ¹	$S_{11} = (4R_{12} + R_{13} + R_{14})/\sqrt{18}$
C ^α H d ²	$S_{12} = (R_{12} + 4R_{13} + R_{14})/\sqrt{18}$
C ^α H d ³	$S_{13} = (R_{12} + R_{13} + 4R_{14})/\sqrt{18}$
CCOO sd	$S_{14} = (2R_{15} - R_{16} - R_{17})/\sqrt{6}$
CCOO r	$S_{15} = (R_{16} - R_{17})/\sqrt{2}$
CCOO w ^b	$S_{16} = R_{18}$
NH ₂ sis	$S_{17} = (2R_{19} - R_{20} - R_{21})/\sqrt{6}$
NH ₂ tw	$S_{18} = (R_{20} - R_{21})/\sqrt{2}$
NH ₂ w	$S_{19} = R_{22}$
CH ₃ sd	$S_{20} = (R_{23} + R_{24} + R_{25} - R_{26} - R_{27} - R_{28})/\sqrt{6}$
CH ₃ ad ¹	$S_{21} = (2R_{23} - R_{24} - R_{25})/\sqrt{6}$
CH ₃ ad ²	$S_{22} = (R_{24} - R_{25})/\sqrt{2}$
CH ₃ r ¹	$S_{23} = (2R_{26} - R_{27} - R_{28})/\sqrt{6}$
CH ₃ r ²	$S_{24} = (R_{27} - R_{28})/\sqrt{2}$
CH ₃ ss	$S_{25} = (R_{29} + R_{30} + R_{31})/\sqrt{3}$
CH ₃ as ¹	$S_{26} = (2R_{29} - R_{30} - R_{31})/\sqrt{6}$
CH ₃ as ²	$S_{27} = (R_{30} - R_{31})/\sqrt{2}$
CN t	$S_{28} = R_{32}$
CC ^{ter} t	$S_{29} = R_{33}$
CC ^{me} t	$S_{30} = R_{34}$

^aAbbreviations: ss = symmetric stretch, as = antisymmetric stretch, s = stretch, r = rock, d = deformation, sd = symmetric deformation, w = wag, sis = scissor, tw = twist, ad = antisymmetric deformation, t = torsion.

^bThe CCOO wag was previously referred to as the CO out of plane bend [Williams and Lowrey, 1991].

Table 3.38: Symmetry Coordinate Definitions for Alanine in Acid.

C=O s ^a	$S_1 = R_1$
C-OH s	$S_2 = R_2$
OH s	$S_3 = R_3$
CH s	$S_4 = R_4$
CC ^{me} s	$S_5 = R_5$
CC ^{ter} s	$S_6 = R_6$
CN ^{ter} s	$S_7 = R_7$
COH b	$S_8 = R_8$
C ^α H r ¹	$S_9 = (2R_9 - R_{10} - R_{11})/\sqrt{6}$
C ^α H r ²	$S_{10} = (R_{10} - R_{11})/\sqrt{2}$
C ^α H d ¹	$S_{11} = (4R_{12} + R_{13} + R_{14})/\sqrt{18}$
C ^α H d ²	$S_{12} = (R_{12} + 4R_{13} + R_{14})/\sqrt{18}$
C ^α H d ³	$S_{13} = (R_{12} + R_{13} + 4R_{14})/\sqrt{18}$
CCOO sd	$S_{14} = (2R_{15} - R_{16} - R_{17})/\sqrt{6}$
CCOO r	$S_{15} = (R_{16} - R_{17})/\sqrt{2}$
CCOO w ^b	$S_{16} = R_{18}$
CH ₃ sd	$S_{17} = (R_{19} + R_{20} + R_{21} - R_{22} - R_{23} - R_{24})/\sqrt{6}$
CH ₃ ad ¹	$S_{18} = (2R_{19} - R_{20} - R_{21})/\sqrt{6}$
CH ₃ ad ²	$S_{19} = (R_{20} - R_{21})/\sqrt{2}$
CH ₃ r ¹	$S_{20} = (2R_{22} - R_{23} - R_{24})/\sqrt{6}$
CH ₃ r ²	$S_{21} = (R_{23} - R_{24})/\sqrt{2}$
NH ₃ sd	$S_{22} = (R_{25} + R_{26} + R_{27} - R_{28} - R_{29} - R_{30})/\sqrt{6}$
NH ₃ ad ¹	$S_{23} = (2R_{26} - R_{26} - R_{27})/\sqrt{6}$
NH ₃ ad ²	$S_{24} = (R_{26} - R_{27})/\sqrt{2}$
NH ₃ r ¹	$S_{25} = (2R_{28} - R_{29} - R_{30})/\sqrt{6}$
NH ₃ r ²	$S_{26} = (R_{29} - R_{30})/\sqrt{2}$
CH ₃ ss	$S_{27} = (R_{31} + R_{32} + R_{33})/\sqrt{3}$
CH ₃ as ¹	$S_{28} = (2R_{31} - R_{32} - R_{33})/\sqrt{6}$
CH ₃ as ²	$S_{29} = (R_{32} - R_{33})/\sqrt{2}$
NH ₃ ss	$S_{30} = (R_{34} + R_{35} + R_{36})/\sqrt{3}$
NH ₃ as ¹	$S_{31} = (2R_{34} - R_{35} - R_{36})/\sqrt{6}$
NH ₃ as ²	$S_{32} = (R_{35} - R_{36})/\sqrt{2}$
CN t	$S_{33} = R_{37}$
CC ^{ter} t	$S_{34} = R_{38}$
CC ^{me} t	$S_{35} = R_{39}$
C-OH t	$S_{36} = R_{40}$

^aAbbreviations: ss = symmetric stretch, as = antisymmetric stretch, s = stretch, r = rock, d = deformation, sd = symmetric deformation, w = wag, ad = antisymmetric deformation, t = torsion, b = in

Table 3.38: (continued)

plane bend.

^bThe CCOO wag was previously referred to as the CO out of plane bend [Williams and Lowrey, 1991].

Table 3.39: Optimized Internal Coordinates for Isolated Structures of Alaninate Using Several different Basis Sets.

Internal Coordinate	4-31G	4-31G*	6-31G**	6-31+G**	Acetate	Methyl- amine
					6-31G**	
Bond Stretches						
H ² -N ¹	1.0015	1.0048	1.0015	1.0042		0.9937
H ³ -N ¹	1.0020	1.0063	1.0020	1.0050		0.9937
C ⁴ -N ¹	1.4675	1.4647	1.4675	1.4647		1.4506
H ⁵ -C ⁴	1.0870	1.0901	1.0870	1.0916		
C ⁶ -C ⁴	1.5522	1.5608	1.5522	1.5607	1.5011	
O ⁷ -C ⁶	1.2566	1.2339	1.2566	1.2364	1.1872	
O ⁸ -C ⁶	1.2546	1.2310	1.2546	1.2338	1.3310	
C ⁹ -C ⁴	1.5235	1.5227	1.5235	1.5246		
H ¹⁰ -C ⁹	1.0871	1.0892	1.0871	1.0902	1.0795	1.0892
H ¹¹ -C ⁹	1.0783	1.0799	1.0783	1.0811	1.0840	1.0813
H ¹² -C ⁹	1.0856	1.0880	1.0856	1.0889	1.0840	1.0813
Angle bends						
H ³ -N ¹ -H ²	107.96	102.56	107.96	102.88		113.21
C ⁴ -N ¹ -H ²	108.28	104.37	108.28	104.54		116.36
H ⁵ -C ⁴ -N ¹	107.59	107.00	107.59	107.13		
C ⁶ -C ⁴ -N ¹	112.89	113.85	112.89	113.90		
O ⁷ -C ⁶ -C ⁴	115.92	115.35	115.92	115.48	125.71	
O ⁸ -C ⁶ -C ⁴	128.49	129.51	128.49	129.28	122.37	
C ⁹ -C ⁴ -C ⁶	111.60	112.05	111.60	112.07		
H ¹⁰ -C ⁹ -C ⁴	110.41	110.61	110.41	110.61	109.55	114.52
H ¹¹ -C ⁹ -C ⁴	109.54	109.90	109.54	109.82	109.58	109.46
H ¹² -C ⁹ -C ⁴	110.96	111.19	110.96	111.16	109.58	109.46
Torsions						
C ⁴ -N ¹ -H ² -H ³	120.28	111.33	120.28	111.80		68.74
H ⁵ -C ⁴ -N ¹ -H ²	-277.01	-278.14	-277.01	-277.59		
C ⁶ -C ⁴ -N ¹ -H ²	-33.34	-34.52	-33.34	-33.76		
O ⁷ -C ⁶ -C ⁴ -N ¹	13.24	12.45	13.24	12.97		
O ⁸ -C ⁶ -O ⁷ -C ⁴	-177.18	-177.65	-177.18	-177.54	180.00	
C ⁹ -C ⁴ -C ⁶ -O ⁸	-43.86	-43.41	-43.86	-42.87		
H ¹⁰ -C ⁹ -C ⁴ -C ⁶	-65.00	-64.57	-65.00	-64.90		

Table 3.39: (continued)

Internal Coordinate	4-31G	4-31G*	6-31G**	6-31+G**	Acetate	Methyl- amine
					6-31G**	
H ¹¹ -C ⁹ -C ⁴ -C ⁶	53.44	54.06	53.44	53.67		
H ¹² -C ⁹ -C ⁴ -C ⁶	-184.94	-184.23	-184.94	-184.60		
H ⁵ -C ¹ -C ² -O ⁴					180.00	
H ⁶ -C ¹ -C ² -O ⁴					58.97	
H ⁷ -C ¹ -C ² -O ⁴					-58.97	
H ⁴ -C ¹ -N ² -H ⁴						-68.71
H ⁶ -C ¹ -N ² -H ⁵						52.55
H ⁷ -C ¹ -N ² -H ³						-52.53

Table 3.40: Optimized Internal Coordinates for One-water Supermolecule Structures of Alaninate Using Several different Basis Sets and Structures

Internal Coordinate	CO ₂				NH-OC
	4-31G	4-31G*	6-31G**	6-31+G**	4-31G
Bond Stretches					
H ² -N ¹	1.0003	1.0039	1.0031	1.0021	0.9998
H ³ -N ¹	1.0015	1.0056	1.0045	1.0033	1.0007
C ⁴ -N ¹	1.4634	1.4611	1.4613	1.4608	1.4604
H ⁵ -C ⁴	1.0860	1.0887	1.0903	1.0857	1.0855
C ⁶ -C ⁴	1.5422	1.5521	1.5528	1.5478	1.5469
O ⁷ -C ⁶	1.2586	1.2358	1.2381	1.2410	1.2664
O ⁸ -C ⁶	1.2587	1.2347	1.2375	1.2394	1.2473
C ⁹ -C ⁴	1.5244	1.5236	1.5253	1.5295	1.5271
H ¹⁰ -C ⁹	1.0866	1.0886	1.0896	1.0880	1.0867
H ¹¹ -C ⁹	1.0783	1.0800	1.0811	1.0845	1.0789
H ¹² -C ⁹	1.0842	1.0867	1.0877	1.0868	1.0837
Angle bends					
H ³ -N ¹ -H ²	107.89	102.64	102.94	104.36	107.85
C ⁴ -N ¹ -H ²	109.64	105.74	105.81	108.67	112.45
H ⁵ -C ⁴ -N ¹	107.60	107.20	107.30	108.15	107.48
C ⁶ -C ⁴ -N ¹	113.33	114.23	114.28	114.19	114.98
O ⁷ -C ⁶ -C ⁴	116.80	116.09	116.24	116.60	117.12
O ⁸ -C ⁶ -C ⁴	127.13	128.56	128.31	127.75	127.13
C ⁹ -C ⁴ -C ⁶	111.36	111.58	111.65	109.27	110.30
H ¹⁰ -C ⁹ -C ⁴	110.42	110.60	110.59	110.32	110.24
H ¹¹ -C ⁹ -C ⁴	109.81	110.09	110.02	110.50	109.97
H ¹² -C ⁹ -C ⁴	110.56	110.82	110.83	110.30	110.35
Torsions					
C ⁴ -N ¹ -H ² -H ³	121.12	112.00	112.46	113.81	122.91
H ⁵ -C ⁴ -N ¹ -H ²	-284.45	-284.27	-283.36	-308.29	-300.25
C ⁶ -C ⁴ -N ¹ -H ²	-41.03	-41.03	-39.84	-67.74	-58.01
O ⁷ -C ⁶ -C ⁴ -N ¹	11.04	8.26	9.27	-23.27	3.85
O ⁸ -C ⁶ -O ⁷ -C ⁴	-177.44	-178.12	-177.91	-181.74	-178.86
C ⁹ -C ⁴ -C ⁶ -O ⁸	-46.12	-47.67	-46.64	-78.78	-52.43
H ¹⁰ -C ⁹ -C ⁴ -C ⁶	-65.00	-64.70	-65.01	-64.28	-66.31

Table 3.40: (continued)

Internal	CO ₂				NH-OC
Coordinate	4-31G	4-31G*	6-31G**	6-31+G**	4-31G, H,O
H ¹¹ -C ⁹ -C ⁴ -C ⁶	53.76	54.24	53.86	55.36	52.73
H ¹² -C ⁹ -C ⁴ -C ⁶	-184.70	-184.17	-184.52	-183.56	-185.56

Table 3.41: Optimized Internal Coordinates for Supermolecule Structures of Alanine in Acid Using Several different Basis Sets

Internal Coordinate	4-31G	4-31G*	6-31G**	6-31+G**
Bond Stretches				
C ² -N ¹	1.5076	1.4982	1.4975	1.4976
C ³ -C ²	1.5063	1.5185	1.5195	1.5198
O ⁴ -C ³	1.2073	1.1850	1.1876	1.1883
O ⁵ -C ³	1.3214	1.3042	1.3048	1.3052
H ⁶ -N ¹	1.0462	1.0295	1.0284	1.0259
H ⁷ -N ¹	1.0087	1.0103	1.0091	1.0094
C ⁸ -C ²	1.5296	1.5256	1.5270	1.5272
H ⁹ -C ²	1.0797	1.0813	1.0831	1.0832
H ¹⁰ -O ⁵	0.9578	0.9566	0.9514	0.9518
H ¹¹ -N ¹	1.0072	1.0093	1.0076	1.0078
H ¹² -C ⁸	1.0814	1.0830	1.0840	1.0841
H ¹³ -C ⁸	1.0811	1.0824	1.0834	1.0838
H ¹⁴ -C ⁸	1.0788	1.0800	1.0809	1.0811
Angle bends				
C ³ -C ² -N ¹	106.78	105.84	105.92	106.09
O ⁴ -C ³ -C ²	123.50	122.28	122.22	122.20
O ⁵ -C ³ -O ⁴	125.40	126.28	126.12	126.05
H ⁶ -N ¹ -C ²	110.25	110.40	110.43	111.17
H ⁷ -N ¹ -C ²	111.51	111.28	111.06	111.28
C ⁸ -C ² -C ³	112.33	113.54	113.64	113.70
H ⁹ -C ² -C ³	108.79	108.65	108.40	108.38
H ¹⁰ -O ⁵ -C ³	116.91	110.84	111.01	111.33
H ¹¹ -N ¹ -C ²	110.72	111.31	111.22	111.05
H ¹² -C ⁸ -C ³	144.06	143.67	143.60	143.49
H ¹³ -C ⁸ -C ³	92.33	91.91	92.01	92.03
H ¹⁴ -C ⁸ -C ³	90.91	91.60	91.62	91.88
Torsions				
O ⁴ -C ³ -C ² -N ¹	-6.25	-1.11	-0.60	-1.27
O ⁵ -C ³ -O ⁴ -C ²	179.81	180.62	180.73	180.69
H ⁶ -N ¹ -C ² -C ³	58.85	63.33	64.12	63.64
H ⁷ -N ¹ -C ² -C ³	-59.22	-54.60	-53.55	-54.32

Table 3.41: (continued)

Internal Coordinate	4-31G	4-31G*	6-31G**	6-31+G**
C ⁸ -C ² -C ³ -O ⁴	114.49	120.05	120.88	120.41
H ⁹ -C ² -C ³ -O ⁴	-122.72	-116.20	-115.65	-116.24
H ¹⁰ -O ⁵ -C ³ -O ⁴	0.18	0.23	0.32	0.39
H ¹¹ -C ² -C ² -C ³	-180.20	-175.58	-174.60	-175.22
H ¹² -C ⁸ -C ³ -O ⁴	-93.67	-84.99	-84.22	-83.89
H ¹³ -C ⁸ -C ³ -O ⁴	34.20	41.84	42.67	42.81
H ¹⁴ -C ⁸ -C ³ -O ⁴	-216.91	-209.19	-208.39	-208.34

In the scaling of alanine, the assignment of the CCOO wag coordinate was uncertain. In acetate and glycinate, this coordinate vibrates at about 600 cm⁻¹. If the scale factor for these molecules is transferred to alanine, the CCOO wag is predicted to contribute to a vibration at 785 cm⁻¹. There are peaks near 600 cm⁻¹ in the alanine spectrum to which the CCOO wag could contribute. Since chemical groups generally vibrate in the same frequency range we were not certain if this prediction (785 cm⁻¹) was accurate. To check the placement of the CCOO wag in alanine calculations using the 6-31G** basis set were performed on methylamine and acetate and scaled. The scale factors from these calculations are listed in Table 3.42 and the PED distributions predicted for methylamine in Table 3.43 and for acetate in Table 3.44. The PED predicted at this level for acetate are based on previous results [Williams and Lowrey, 1991] and can be compared to the results at the 4-31G level for the one water water-excluded supermolecule calculations in Table 3.21. The predicted PED for methylamine are based on previous results of Lowrey and Williams [1992a] and can be compared to the results using the 4-31G basis set in Table 3.19.

The scale factors from acetate and methylamine were transferred directly to alanine for a normal mode analysis. The optimized alanine geometry and force constants used for this calculation were determined using the 6-31G** basis set; the internal coordinates are listed in Table 3.39. The predicted frequencies and PED

assignments from this calculation are given in Table 3.45. The CCOO wag is unambiguously assigned to the 785 cm^{-1} vibration even though not all frequencies are completely optimized.

Table 3.42: Scale factors for Methylamine and Acetate using the 6-31G** basis set

Coordinate	Methylamine	Acetate
CN s ^a	81.03	
CH ₃ ss	80.10	81.17
CH ₃ as ¹	85.79	88.87
CH ₃ as ²	83.60	87.45
NH ₂ ss	80.60	
NH ₂ as	78.00	
CH ₃ sd	80.01	85.80
CH ₃ ad ¹	80.47	81.17
CH ₃ ad ²	80.63	79.02
CH ₃ r ¹	83.00	87.47
CH ₃ r ²	76.28	87.89
CNH ₂ scissor	78.59	
CNH ₂ r	79.88	
CNH ₂ ob	115.40	
CN t	100.00	
CO ss		80.85
CO as		63.83
CC s		99.61
CO sd		86.00
CO r		105.03
CO wag		81.27
CC t		200.00

^aAbbreviations: s = stretch, t = torsion, ss = symmetric stretch, as = antisymmetric stretch, sd = symmetric deformation, ad = antisymmetric deformation, r = rock, ob = out of plane bend.

Table 3.43: Scaled 6-31G** Frequencies and Potential Energy Distribution for Isolated Methylamine in Base.

frequency (cm^{-1})			NH ₂ CH ₃ (mean deviation = 5 cm^{-1})
obs.	calc.	dev.	
			Potential Energy Distribution
—	336	—	CN t(100)
—	933	—	NCH ₃ r ² (37), CNH ₂ r(28), CNH ₂ ob(18), NCH ₃ r ¹ (12)
955	948	-7	CNH ₂ ob(41), NCH ₃ r ¹ (32), CNH ₂ r(15), CN s(8)
1034	1034	0	CN s(87), NCH ₃ r ² (7)
1172	1181	9	NCH ₃ r ² (41), CNH ₂ ob(39), NCH ₃ r ¹ (12)
1323	1315	-8	CNH ₂ r(55), NCH ₃ r ¹ (31), NCH ₃ ad ¹ (7)
1428	1427	-1	NCH ₃ sd(90), NCH ₃ ad ² (7)
1465	1462	-3	NCH ₃ ad ² (70), NCH ₃ ad ¹ (15), NCH ₃ sd(9)
1479	1480	1	NCH ₃ ad ¹ (73), NCH ₃ ad ² (17), NCH ₃ r ¹ (8)
1602	1600	-2	CNH ₂ sissor(99)
2822	2821	-1	CH ₃ ss(92), CH ₃ as ¹ (8)
2964	2965	1	CH ₃ as ¹ (92), CH ₃ ss(8)
2980	2978	-2	CH ₃ as ² (100)
—	3363	—	NH ₂ ss(100)
—	3384	—	NH ₂ as(100)

Table 3.44: Scaled 6-31G** Frequencies and Potential Energy Distribution for Isolated Acetate.

frequency (cm^{-1})			CH_3CO_2^- (mean deviation = 3 cm^{-1})
obs.	calc.	dev.	Potential Energy Distribution
—	23	—	CC t(97)
470	470	0	CO r(81), CH3 r ¹ (15)
620	620	0	CO o(67), CH3 r ² (30)
650	650	0	CO sd(62), CC s(35)
920	919	-1	CC s(50), CO ss(23), CO sd(23)
1015	1015	0	CH3 r ¹ (73), CO as(15), CO r(9)
1055	1054	-1	CH3 r ² (64), CO o(31)
1345	1339	-6	CH3 sd(66), CO ss(29)
1410	1419	9	CO ss(38), CH3 sd(24), CH3 ad ¹ (18), CC s(11), CO sd(8)
1438	1438	0	CH3 ad ² (94)
1438	1438	0	CH3 ad ¹ (74), CO ss(8)
1560	1560	0	CO as(76), CH3 r ¹ (10), CO r(9)
2961	2961	0	CH3 ss(98)
2997	2997	0	CH3 as ² (100)
3048	3048	0	CH3 as ¹ (99)

Table 3.45: Frequencies and Potential Energy Distribution for Alanine in base, 6-31G** basis set, scale factors from methylamine and acetate transferred without change: Placement of CCOO wag coordinate.

frequency (cm ⁻¹)			Alanine (mean deviation = 26 cm ⁻¹)
obs.	calc.	dev.	
			Potential Energy Distribution
—	84	—	CC t(95)
—	214	—	CN t(92), CC ^{me} t(7)
—	248	—	CC ^{me} t(73), C ^α H d ² (12)
279	291	12	C ^α H d ² (46), CCOO r(17), C ^α H d ³ (13), CC ^{me} t(11)
343	346	3	C ^α H d ³ (52), CCOO r(12), C ^α H d ² (9)
415	414	-1	C ^α H d ¹ (75), CCOO wag (7)
539	541	2	CCOO r(41), CC ^{term} s(13), CN ^{term} s(13), CCOO sd(10), C ^α H d ³ (8), COO as(7)
654	612	-42	CCOO sd(26), CC ^{term} s(22), CCOO r(13), CCOO wag (13), CC ^{me} s(12), C ^α H d ³ (7)
785	783	-2	CCOO wag (45), CCOO sd(21), CCH ₃ r ¹ (8)
853	848	-5	CCOO sd(21), CC ^{me} s(18), CN ^{term} s(15), CCH ₃ r ¹ (15), COO ss(8), CC ^{term} s(8)
927	936	9	CCH ₃ r ² (33), CN ^{term} s(23), CC ^{term} s(20), COO ss(9)
—	1010	—	CNH ₂ twist(35), CCH ₃ r ¹ (23), C ^α H r ¹ (12), CC ^{me} s(11)
1020	1033	13	CC ^{me} s(21), C ^α H r ² (15), CCH ₃ r ² (13), CN ^{term} s(11), CNH ₂ wag(7)
1072	1139	67	CN ^{term} s(18), C ^α H r ¹ (18), CCH ₃ r ² (16), CC ^{me} s(14), C ^α H d ² (7)
1140	1216	76	C ^α H r ² (37), CNH ₂ wag(37), CCH ₃ r ¹ (8)
1230	1254	24	CNH ₂ twist(22), CCH ₃ r ¹ (17), C ^α H r ¹ (14), C ^α H d ¹ (10), CCH ₃ r ² (10), CN ^{term} s(8)
1286	1325	39	CNH ₂ wag(42), COO ss(14), C ^α H r ² (14), C ^α H r ¹ (11)
1353	1352	-1	C ^α H r ¹ (37), CNH ₂ twist(29), CCH ₃ sd(14)
1368	1411	43	CCH ₃ sd(56), CC ^{me} s(10), CCH ₃ ad ¹ (9)
1414	1427	13	COO ss(37), CCH ₃ ad ² (27), CCH ₃ sd(13), CC ^{term} s(10), CCOO sd(8)
1459	1458	-1	CCH ₃ ad ² (58), COO ss(9), CCH ₃ r ² (9), CCH ₃ ad ¹ (8)
1459	1466	7	CCH ₃ ad ¹ (74), CCH ₃ r ¹ (7)
1564	1540	-24	COO as(82), CCOO r(9)
1591	1610	19	CNH ₂ sissor(99)

Table 3.45: (continued)

frequency (cm^{-1})			Potential Energy Distribution
obs.	calc.	dev.	
—	2803	—	C^αH s(100)
—	2956	—	CH_3 ss(86), CH_3 as ² (10)
—	3003	—	CH_3 as ¹ (67), CH_3 as ² (33)
—	3088	—	CH_3 as ² (57), CH_3 as ¹ (28), CH_3 ss(14)
—	3304	—	NH_2 ss(54), NH_2 as(46)
—	3337	—	NH_2 as(54), NH_2 ss(46)

After conformation of the assignment for the CCOO wag coordinate, assignment of other peaks in the range from 600 to 900 cm^{-1} was difficult. Five experimental frequencies were observed but only four were predicted for this region. Assignments for the CC^{me} s and CN^{ter} s coordinates were based on the ^{13}C and ^{15}N difference spectra in Figure 3.31 top and bottom, respectively. With these constraints, a predicted frequency at about 620 cm^{-1} fell between two observed peaks at 590 and 654 cm^{-1} . Altering scale factors for the symmetry coordinates contributing to the normal mode could not adjust the predicted frequency to agree with either of the observed peaks. A Fermi-resonance analysis [Krimm and Dwivedi, 1982] suggests that the two observed peaks may be due to a resonance between a combination of peaks at 279 and 343 cm^{-1} and a fundamental peak at 623 cm^{-1} in the normal isotopic alanine. This calculated unperturbed fundamental agrees well with the predicted normal mode and provides an explanation for the difference between the number of experimentally observed and calculated vibrations in this frequency range.

Scale factors determined for isolated structures of alanine using the 4-31G, 4-31G*, 6-31G**, and 6-31+G** basis sets are listed in Table 3.46. Predicted PED and frequencies using these scale factors are provided in Tables 3.47, 3.48, 3.49, and 3.50 for the 4-31G, 4-31G*, 6-31G**, and 6-31+G** basis sets, respectively.

Table 3.46: Scale factors for isolated alaninate structures using several basis sets.

Coordinate	4-31G	4-31G*	6-31G**	6-31+G**
COO ss	87.70	80.85	76.80	79.51
COO as	74.16	63.83	66.90	67.39
C α H s	83.60	80.07	84.73	80.00
CC ^{me} s	95.00	84.00	94.83	91.34
CC ^{ter} s	104.00	99.61	102.90	99.19
CN ^{ter} s	80.50	72.00	76.20	72.95
NH ₂ ss	77.00	68.00	77.00	67.00
NH ₂ as	70.00	60.01	70.00	60.00
C α H r ¹	82.35	77.00	82.40	79.75
C α H r ²	72.51	78.00	76.70	77.12
C α H d ¹	86.19	87.00	88.24	87.20
C α H d ²	76.52	87.00	81.90	84.47
C α H d ³	93.60	87.00	95.22	87.45
CCOO sd	100.91	86.00	90.00	96.50
CCOO r	95.05	105.03	97.20	107.27
CCOO wag	93.09	81.27	86.13	79.94
NH ₂ scissor	71.96	71.50	75.66	76.53
NH ₂ twist	74.84	79.00	74.60	79.51
NH ₂ wag	80.33	95.00	69.50	81.00
CCH ₃ sd	77.27	85.80	79.44	81.84
CCH ₃ ad ¹	78.62	81.17	80.70	80.81
CCH ₃ ad ²	76.32	79.02	80.50	78.31
CH ₃ r ¹	80.14	87.47	90.21	84.79
CH ₃ r ²	79.10	87.89	83.96	93.97
CH ₃ ss	85.90	88.17	85.65	88.17
CH ₃ as ¹	85.17	88.87	87.34	88.87
CH ₃ as ²	84.33	87.45	84.60	87.45
CN t	94.00	94.00	94.00	94.00
CC t	100.00	100.00	100.00	100.00
CC ^{me} t	70.00	100.08	70.00	102.83

^aAbbreviations: s = stretch, t = torsion, ss = symmetric stretch, as = antisymmetric stretch, sd = symmetric deformation, ad = antisymmetric deformation, r = rock, d = deformation.

Table 3.47: Scaled 4-31G Frequencies and Potential Energy Distribution for Isolated Alaninate.

frequency (cm ⁻¹)			NH ₂ CHCH ₃ COO ⁻ (mean deviation = 7 cm ⁻¹)
obs.	calc.	dev.	
			Potential Energy Distribution
—	63	—	CC t(98)
—	163	—	CN t(95)
—	210	—	CC ^{me} t(89)
279	280	1	C ^α H d ² (62), CCOO r(16)
343	348	5	C ^α H d ³ (52), CCOO r(17), C ^α H d ² (8), CCOO wag(7)
415	415	0	C ^α H d ¹ (77), CCOO wag(7)
539	543	4	CCOO r(36), CN ^{ter} s(15), CC ^{ter} s(13), CCOO sd(12), C ^α H d ³ (9)
622	612	-10	CCOO sd(29), CC ^{ter} s(18), CCOO r(14), CCOO wag(13), CC ^{me} s(10), C ^α H d ³ (8)
785	775	-10	CCOO wag(44), CCOO sd(22)
853	835	-18	CN ^{ter} s(19), CCOO sd(18), CC ^{ter} s(11), CH ₃ r ¹ (11), CC ^{me} s(10), NH ₂ wag(9), COO ss(8), CCOO wag(7)
927	918	-9	CH ₃ r ² (30), CN ^{ter} s(26), CC ^{ter} s(17), NH ₂ wag(14), COO ss(7)
—	960	—	NH ₂ wag(50), CH ₃ r ¹ (18), CC ^{me} s(14)
1020	1013	-7	NH ₂ twist(40), CC ^{me} s(24), CH ₃ r ¹ (12)
1080	1078	-2	C ^α H r ² (27), CH ₃ r ² (15), CCOO wag(12), NH ₂ wag(12), CH ₃ r ¹ (9)
1140	1159	19	CN ^{ter} s(31), CC ^{me} s(19), CH ₃ r ² (18), C ^α H r ¹ (7)
1238	1245	7	CH ₃ r ¹ (27), NH ₂ twist(26), C ^α H r ² (19), C ^α H d ¹ (9)
1286	1286	0	C ^α H r ² (31), C ^α H r ¹ (27), COO ss(8), CH ₃ r ² (7)
1353	1357	4	C ^α H r ¹ (41), CCH ₃ sd(33), NH ₂ twist(12)
1368	1373	5	CCH ₃ sd(55), C ^α H r ¹ (14), CC ^{me} s(11), NH ₂ twist(11)
1414	1416	2	COO ss(57), CC ^{ter} s(16), CCOO sd(10), CCH ₃ ad ² (7)
1459	1459	0	CCH ₃ ad ² (55), CCH ₃ ad ¹ (33)
1459	1466	7	CCH ₃ ad ¹ (57), CCH ₃ ad ² (31)
1564	1563	-1	COO as(85), CCOO r(7)
1591	1588	-3	NH ₂ sissor(99)
2885	2885	0	C ^α H s(98)
2940	2941	1	CH ₃ ss(94)
2980	2976	-4	CH ₃ as ¹ (51), CH ₃ as ² (47)
2993	2998	5	CH ₃ as ¹ (48), CH ₃ as ² (48)

Table 3.47: (continued)

frequency (cm^{-1})			Potential Energy Distribution
obs.	calc.	dev.	
—	3156	—	NH ₂ as(98)
—	3235	—	NH ₂ ss(98)

frequency (cm^{-1})			Potential Energy Distribution
obs.	calc.	dev.	
—	62	—	CC t(98)
—	118	—	CN t(99)
—	208	—	CC ^{me} t(93)
275	276	1	C ^{α} H d ² (54), CCOO r(19), C ^{α} H d ³ (14)
331	325	-6	C ^{α} H d ³ (45), C ^{α} H d ² (15), C ^{α} H d ¹ (8), CCOO r(8), CCOO wag(7), NH ₂ wag(7)
384	392	8	C ^{α} H d ¹ (73), NH ₂ twist(7)
527	528	1	CCOO r(46), CN ^{ter} s(14), CC ^{ter} s(8), CCOO sd(8), COO as(7)
621	604	-17	CCOO sd(34), CC ^{ter} s(24), CCOO r(10), CCOO wag(10), CC ^{me} s(8)
—	738	—	NH ₂ wag(49), CCOO wag(36)
780	788	8	CCOO sd(29), CN ^{ter} s(18), NH ₂ wag(16), CCOO wag(10), COO ss(7)
836	828	-8	NH ₂ twist(64), CC ^{me} s(16)
870	862	-8	CH ₃ r ¹ (28), CC ^{ter} s(10), CCOO sd(9), CC ^{me} s(8), NH ₂ wag(8), C ^{α} H d ³ (7), CCOO wag(7)
922	918	-4	CH ₃ r ² (30), CN ^{ter} s(27), CC ^{ter} s(21), COO ss(9)
1053	1066	13	C ^{α} H r ² (28), CH ₃ r ¹ (15), CCOO wag(12), CH ₃ r ² (10), C ^{α} H d ³ (7)
1108	1132	24	NH ₂ sissor(36), CH ₃ r ² (21), CC ^{me} s(12), CN ^{ter} s(12)
1143	1175	32	NH ₂ sissor(39), CC ^{me} s(21), CH ₃ r ¹ (14), CN ^{ter} s(8)
1201	1189	-12	NH ₂ sissor(23), CH ₃ r ¹ (16), CN ^{ter} s(11), C ^{α} H d ¹ (11), CH ₃ r ² (11), NH ₂ twist(9)
1290	1280	-10	C ^{α} H r ² (50), C ^{α} H r ¹ (10), COO ss(7)
1334	1335	1	C ^{α} H r ¹ (75)
1370	1368	-2	CCH ₃ sd(85)

Table 3.47: (continued)

frequency (cm ⁻¹)			Potential Energy Distribution
obs.	calc.	dev.	
1414	1415	1	COO ss(58), CC ^{ter} s(15), CCOO sd(10), CCH ₃ sd(7), CCH ₃ ad ² (7)
1462	1459	-3	CCH ₃ ad ² (51), CCH ₃ ad ¹ (38)
1462	1467	5	CCH ₃ ad ¹ (53), CCH ₃ ad ² (35)
1571	1563	-8	COO as(86), CCOO r(8)
—	2323	—	NH ₂ as(72), NH ₂ ss(27)
—	2339	—	NH ₂ ss(72), NH ₂ as(27)
2887	2885	-2	C ^α H s(98)
2942	2941	-1	CH ₃ ss(94)
2980	2976	-4	CH ₃ as ¹ (51), CH ₃ as ² (47)
2990	2998	8	CH ₃ as ¹ (48), CH ₃ as ² (48)

frequency (cm ⁻¹)			NH ₂ CD ₂ CD ₃ COO ⁻ (mean deviation = 12 cm ⁻¹)
obs.	calc.	dev.	
—	61	—	CC t(98)
—	146	—	CC ^{me} t(81), CN t(16)
—	167	—	CN t(82), CC ^{me} t(15)
257	253	-4	C ^α H d ² (68), CCOO r(10)
335	340	5	C ^α H d ³ (57), CCOO r(23)
382	378	-4	C ^α H d ¹ (73), CH ₃ r ¹ (8)
514	527	13	CCOO r(29), CC ^{ter} s(21), CCOO sd(17), CN ^{ter} s(11), C ^α H d ³ (7)
593	579	-14	CCOO r(21), CCOO sd(17), CC ^{ter} s(15), CCOO wag(13), CC ^{me} s(10), C ^α H r ² (9), C ^α H d ³ (8)
688	669	-19	CH ₃ r ¹ (37), C ^α H r ² (23), CCOO wag(19)
752	755	3	CH ₃ r ² (36), CN ^{ter} s(24), CC ^{me} s(9), CCOO sd(8)
827	810	-17	CCOO sd(36), CH ₃ r ² (24), COO ss(11), CC ^{ter} s(8)
884	869	-15	C ^α H r ¹ (32), NH ₂ wag(26), CN ^{ter} s(22), NH ₂ twist(7)
897	890	-7	C ^α H r ² (32), CCOO wag(14), CC ^{ter} s(10), CC ^{me} s(9), CH ₃ r ¹ (9), CCH ₃ sd(8)
947	954	7	C ^α H r ¹ (34), CH ₃ r ¹ (22), NH ₂ wag(15), CCOO wag(9)
—	967	—	NH ₂ wag(28), CCH ₃ sd(16), CCOO wag(15), C ^α H r ² (14), CC ^{me} s(9), NH ₂ twist(8)

Table 3.47: (continued)

frequency (cm^{-1})			Potential Energy Distribution
obs.	calc.	dev.	
1055	1051	-4	CCH ₃ ad ² (75), CCH ₃ ad ¹ (21)
1055	1058	3	CCH ₃ ad ¹ (67), CCH ₃ ad ² (24)
—	1079	—	CCH ₃ sd(37), NH ₂ wag(14), CCH ₃ ad ¹ (9), C ^{α} H r ² (8), C ^{α} H d ³ (8)
1126	1112	-14	C ^{α} H r ¹ (16), CCH ₃ sd(16), NH ₂ twist(15), CC ^{ter} s(12), CC ^{me} s(10), CH ₃ r ² (7)
1158	1172	14	CN ^{ter} s(32), NH ₂ twist(16), CC ^{me} s(9), CH ₃ r ² (8)
1276	1302	26	NH ₂ twist(46), CC ^{me} s(24)
1408	1414	6	COO ss(66), CC ^{ter} s(18), CCOO sd(12)
1555	1560	5	COO as(87), CCOO r(7)
1582	1587	5	NH ₂ sissor(101)
2076	2113	37	CH ₃ ss(92), C ^{α} H s(7)
2125	2125	0	C ^{α} H s(90), CH ₃ ss(7)
2235	2204	-31	CH ₃ as ¹ (53), CH ₃ as ² (46)
2246	2219	-27	CH ₃ as ² (53), CH ₃ as ¹ (46)
—	3156	—	NH ₂ as(98)
—	3235	—	NH ₂ ss(98)

frequency (cm^{-1})			ND ₂ CDCD ₃ COO ⁻ (mean deviation = 11 cm^{-1})
obs.	calc.	dev.	
—	60	—	CC t(98)
—	117	—	CN t(96)
—	151	—	CC ^{me} t(93)
257	252	-5	C ^{α} H d ² (66), CCOO r(11)
327	315	-12	C ^{α} H d ³ (55), CCOO r(15), NH ₂ wag(8), C ^{α} H d ¹ (7)
363	358	-5	C ^{α} H d ¹ (68), CH ₃ r ¹ (7)
506	515	9	CCOO r(40), CC ^{ter} s(14), CCOO sd(11), CN ^{ter} s(10)
590	574	-16	CCOO sd(23), CC ^{ter} s(21), CCOO r(16), CCOO wag(10), CC ^{me} s(9), C ^{α} H r ² (8)
683	665	-18	CH ₃ r ¹ (33), C ^{α} H r ² (25), CCOO wag(22)
729	731	2	NH ₂ wag(22), CH ₃ r ² (22), NH ₂ twist(15), CH ₃ r ¹ (14), C ^{α} H r ¹ (9)
756	759	3	NH ₂ wag(43), CN ^{ter} s(26), CH ₃ r ² (21)

Table 3.47: (continued)

frequency (cm ⁻¹)			Potential Energy Distribution
obs.	calc.	dev.	
790	779	-11	NH ₂ twist(28), CC ^{me} s(25), CCOO sd(18), CCH ₃ sd(9)
845	835	-10	CCOO sd(26), CC ^{ter} s(16), NH ₂ twist(14), COO ss(13), CH ₃ r ² (11)
893	899	6	C ^α H r ² (40), CCOO wag(18), CH ₃ r ¹ (11)
940	941	1	C ^α H r ¹ (46), CCOO wag(16), CN ^{ter} s(8)
1036	1025	-11	CH ₃ r ¹ (20), NH ₂ twist(17), C ^α H r ¹ (9), C ^α H d ² (9), CCH ₃ sd(9), C ^α H d ¹ (8)
1055	1049	-6	CCH ₃ ad ² (49), CCH ₃ ad ¹ (37), CCH ₃ sd(8)
1055	1055	0	CCH ₃ ad ² (49), CCH ₃ ad ¹ (30), CCH ₃ sd(12)
—	1072	—	CCH ₃ sd(45), CCH ₃ ad ¹ (31), C ^α H r ² (7)
1123	1121	-2	NH ₂ sissor(35), CN ^{ter} s(11), C ^α H r ¹ (11), CH ₃ r ² (11), CC ^{ter} s(9), C ^α H d ¹ (7)
1182	1187	5	NH ₂ sissor(64), CN ^{ter} s(17)
1215	1239	24	CC ^{me} s(48), NH ₂ twist(9)
1409	1413	4	COO ss(68), CC ^{ter} s(18), CCOO sd(12)
1567	1560	-7	COO as(88), CCOO r(7)
2076	2112	36	CH ₃ ss(91), C ^α H s(8)
2125	2124	-1	C ^α H s(90), CH ₃ ss(8)
2235	2204	-31	CH ₃ as ¹ (53), CH ₃ as ² (46)
2246	2219	-27	CH ₃ as ² (53), CH ₃ as ¹ (46)
—	2323	—	NH ₂ as(73), NH ₂ ss(27)
—	2339	—	NH ₂ ss(73), NH ₂ as(27)

frequency (cm ⁻¹)			NH ₂ CHCD ₃ COO ⁻ (mean deviation = 10 cm ⁻¹)
obs.	calc.	dev.	
			Potential Energy Distribution
—	61	—	CC t(98)
—	146	—	CC ^{me} t(82), CN t(15)
—	168	—	CN t(83), CC ^{me} t(15)
255	254	-1	C ^α H d ² (67), CCOO r(11)
340	343	3	C ^α H d ³ (56), CCOO r(22)
390	381	-9	C ^α H d ¹ (71), CH ₃ r ¹ (8)
521	533	12	CCOO r(35), CC ^{ter} s(17), CCOO sd(14), CN ^{ter} s(11), C ^α H d ³ (8)

Table 3.47: (continued)

frequency (cm^{-1})			Potential Energy Distribution
obs.	calc.	dev.	
607	596	-11	CCOO sd(24), CC ^{ter} s(18), CCOO r(15), CC ^{me} s(13), CCOO wag(10), C ^{α} H d ³ (9)
741	710	-31	CCOO wag(41), CH ₃ r ¹ (38), CH ₃ r ² (10)
771	764	-7	CN ^{ter} s(31), CH ₃ r ² (30), CH ₃ r ¹ (15), CC ^{me} s(8), CCOO sd(8)
828	811	-17	CCOO sd(38), CH ₃ r ² (24), COO ss(12), CC ^{ter} s(8)
910	906	-4	NH ₂ wag(52), CH ₃ r ¹ (16), CCOO wag(11)
947	945	-2	CCH ₃ sd(31), CC ^{me} s(20), NH ₂ twist(13), CC ^{ter} s(11), NH ₂ wag(8)
1020	1031	11	NH ₂ wag(18), CC ^{ter} s(16), CCOO wag(13), C ^{α} H d ² (11), C ^{α} H r ² (8), CH ₃ r ² (8), COO ss(7), C ^{α} H d ³ (7)
1058	1050	-8	CCH ₃ ad ² (69), CCH ₃ ad ¹ (28)
1058	1058	0	CCH ₃ ad ¹ (67), CCH ₃ ad ² (26)
—	1072	—	CCH ₃ sd(41), CN ^{ter} s(19), NH ₂ twist(12), NH ₂ wag(8)
1141	1159	18	CC ^{me} s(26), CN ^{ter} s(24), CCH ₃ sd(16), C ^{α} H r ² (12)
1189	1197	8	C ^{α} H r ² (32), NH ₂ twist(30), CH ₃ r ¹ (10)
1283	1278	-5	C ^{α} H r ¹ (31), C ^{α} H r ² (31), CC ^{me} s(9), NH ₂ twist(7)
1360	1361	1	C ^{α} H r ¹ (54), NH ₂ twist(25), CC ^{me} s(8)
1413	1414	1	COO ss(65), CC ^{ter} s(18), CCOO sd(12)
1563	1562	-1	COO as(86), CCOO r(7)
1587	1588	1	NH ₂ sissor(100)
2076	2113	37	CH ₃ ss(99)
2125	2203	78	CH ₃ as ¹ (56), CH ₃ as ² (43)
2235	2219	-16	CH ₃ as ² (56), CH ₃ as ¹ (43)
—	2886	—	C ^{α} H s(100)
—	3156	—	NH ₂ as(98)
—	3235	—	NH ₂ ss(98)

frequency (cm^{-1})			ND ₂ CHCD ₃ COO ⁻ (mean deviation = 12 cm^{-1})
obs.	calc.	dev.	
—	61	—	CC t(98)
—	117	—	CN t(96)
—	151	—	CC ^{me} t(93)

Table 3.47: (continued)

frequency (cm ⁻¹)			Potential Energy Distribution
obs.	calc.	dev.	
258	253	-5	C ^α H d ² (65), CCOO r(12)
320	317	-3	C ^α H d ³ (54), CCOO r(14), C ^α H d ¹ (9), NH ₂ wag(8)
348	361	13	C ^α H d ¹ (66), CH ₃ r ¹ (8)
512	521	9	CCOO r(46), CC ^{ter} s(11), CN ^{ter} s(11), CCOO sd(9)
595	589	-6	CCOO sd(29), CC ^{ter} s(25), CCOO r(12), CC ^{me} s(11), CCOO wag(7)
—	706	—	CCOO wag(46), CH ₃ r ¹ (29), CH ₃ r ² (10), C ^α H r ² (7)
723	746	23	CH ₃ r ¹ (31), NH ₂ wag(19), CH ₃ r ² (18), NH ₂ twist(12), CN ^{ter} s(7)
751	760	9	NH ₂ wag(50), CN ^{ter} s(21), CH ₃ r ² (20)
799	785	-14	NH ₂ twist(29), CCOO sd(24), CC ^{me} s(21), CCH ₃ sd(8)
852	841	-11	NH ₂ twist(23), CCOO sd(19), CC ^{ter} s(15), COO ss(11), CH ₃ r ² (10), CCOO wag(7)
988	1011	23	CCOO wag(19), CC ^{ter} s(18), C ^α H d ² (13), CH ₃ r ¹ (12), C ^α H d ³ (10), COO ss(7)
1028	1022	-6	CCH ₃ sd(64), NH ₂ twist(9), CN ^{ter} s(8)
1056	1050	-6	CCH ₃ ad ² (69), CCH ₃ ad ¹ (29)
1056	1058	2	CCH ₃ ad ¹ (68), CCH ₃ ad ² (29)
1109	1098	-11	CN ^{ter} s(27), NH ₂ sissor(17), C ^α H d ¹ (13), CH ₃ r ² (10), NH ₂ twist(9), CH ₃ r ¹ (7)
1131	1162	31	CC ^{me} s(33), C ^α H r ² (26), CCH ₃ sd(20)
—	1177	—	NH ₂ sissor(75), CN ^{ter} s(16)
1281	1268	-13	C ^α H r ² (51), CC ^{me} s(13), C ^α H r ¹ (8)
1332	1329	-3	C ^α H r ¹ (81)
1412	1414	2	COO ss(67), CC ^{ter} s(18), CCOO sd(12)
1576	1561	-15	COO as(87), CCOO r(8)
2076	2113	37	CH ₃ ss(99)
2125	2203	78	CH ₃ as ¹ (56), CH ₃ as ² (43)
2235	2219	-16	CH ₃ as ² (56), CH ₃ as ¹ (43)
2246	2323	77	NH ₂ as(72), NH ₂ ss(27)
—	2339	—	NH ₂ ss(72), NH ₂ as(27)
—	2887	—	C ^α H s(100)

Table 3.47: (continued)

frequency (cm ⁻¹)			Potential Energy Distribution
obs.	calc.	dev.	
frequency (cm ⁻¹)			NH ₂ CH ¹³ CH ₃ COO ⁻ (mean deviation = 8 cm ⁻¹)
obs.	calc.	dev.	
Potential Energy Distribution			
—	63	—	CC t(98)
—	163	—	CN t(95)
—	210	—	CC ^{me} t(89)
273	277	4	C ^α H d ² (63), CCOO r(16)
344	348	4	C ^α H d ³ (52), CCOO r(18), C ^α H d ² (7), CCOO wag(7)
409	412	3	C ^α H d ¹ (77), CCOO wag(7)
538	543	5	CCOO r(36), CN ^{ter} s(15), CC ^{ter} s(13), CCOO sd(12), C ^α H d ³ (9)
624	609	-15	CCOO sd(28), CC ^{ter} s(18), CCOO r(14), CCOO wag(14), CC ^{me} s(11), C ^α H d ³ (8)
779	774	-5	CCOO wag(44), CCOO sd(23)
849	833	-16	CN ^{ter} s(18), CCOO sd(17), CH ₃ r ¹ (12), CC ^{me} s(11), CC ^{ter} s(10), NH ₂ wag(9), COO ss(8), CCOO wag(8)
922	915	-7	CH ₃ r ² (32), CN ^{ter} s(25), CC ^{ter} s(17), NH ₂ wag(13), COO ss(7)
—	955	—	NH ₂ wag(52), CH ₃ r ¹ (18), CC ^{me} s(15)
1015	1009	-6	NH ₂ twist(39), CC ^{me} s(24), CH ₃ r ¹ (13)
1073	1076	3	C ^α H r ² (26), CH ₃ r ² (15), NH ₂ wag(13), CCOO wag(12), CH ₃ r ¹ (10), C ^α H d ² (7), C ^α H d ³ (7)
1134	1155	21	CN ^{ter} s(32), CC ^{me} s(18), CH ₃ r ² (16), C ^α H r ¹ (7)
1231	1240	9	NH ₂ twist(26), CH ₃ r ¹ (26), C ^α H r ² (19), C ^α H d ¹ (8)
1288	1284	-4	C ^α H r ² (32), C ^α H r ¹ (27), COO ss(8)
1355	1354	-1	CCH ₃ sd(67), C ^α H r ¹ (19)
1360	1365	5	C ^α H r ¹ (36), CCH ₃ sd(24), NH ₂ twist(19), CC ^{me} s(10)
1412	1415	3	COO ss(58), CC ^{ter} s(16), CCOO sd(10), CCH ₃ ad ² (7)
1458	1457	-1	CCH ₃ ad ² (51), CCH ₃ ad ¹ (36)
1458	1464	6	CCH ₃ ad ¹ (54), CCH ₃ ad ² (33)
1562	1563	1	COO as(85), CCOO r(7)
1596	1588	-8	NH ₂ sissor(99)
2885	2884	-1	C ^α H s(98)
2940	2938	-2	CH ₃ ss(93), CH ₃ as ² (7)

Table 3.47: (continued)

frequency (cm ⁻¹)			Potential Energy Distribution
obs.	calc.	dev.	
2980	2966	-14	CH ₃ as ¹ (51), CH ₃ as ² (46)
2993	2988	-5	CH ₃ as ¹ (48), CH ₃ as ² (47)
—	3156	—	NH ₂ as(98)
—	3235	—	NH ₂ ss(98)

frequency (cm ⁻¹)			Potential Energy Distribution
obs.	calc.	dev.	
—	63	—	CC t(98)
—	162	—	CN t(95)
—	210	—	CC ^{me} t(90)
279	279	0	C ^α H d ² (61), CCOO r(17), C ^α H d ³ (7)
343	345	2	C ^α H d ³ (51), CCOO r(16), C ^α H d ² (8), CCOO wag(7)
421	412	-9	C ^α H d ¹ (76), CCOO wag(7)
535	537	2	CCOO r(36), CN ^{ter} s(16), CC ^{ter} s(13), CCOO sd(12), C ^α H d ³ (8)
632	612	-20	CCOO sd(29), CC ^{ter} s(18), CCOO r(14), CCOO wag(13), CC ^{me} s(10), C ^α H d ³ (8)
793	774	-19	CCOO wag(43), CCOO sd(23)
851	831	-20	CN ^{ter} s(20), CCOO sd(16), NH ₂ wag(12), CH ₃ r ¹ (11), CC ^{me} s(9), CC ^{ter} s(9), CCOO wag(8), COO ss(7)
924	912	-12	CH ₃ r ² (28), CN ^{ter} s(23), CC ^{ter} s(19), NH ₂ wag(15), COO ss(8)
—	957	—	NH ₂ wag(49), CH ₃ r ¹ (18), CC ^{me} s(14)
1019	1012	-7	NH ₂ twist(41), CC ^{me} s(23), CH ₃ r ¹ (13)
1072	1077	5	C ^α H r ² (27), CH ₃ r ² (15), NH ₂ wag(12), CCOO wag(11), CH ₃ r ¹ (10)
1134	1156	22	CN ^{ter} s(29), CC ^{me} s(20), CH ₃ r ² (19), C ^α H r ¹ (7)
1234	1243	9	NH ₂ twist(27), CH ₃ r ¹ (27), C ^α H r ² (19), C ^α H d ¹ (9)
1291	1285	-6	C ^α H r ² (32), C ^α H r ¹ (26), COO ss(8), CH ₃ r ² (7)
1360	1356	-4	C ^α H r ¹ (44), CCH ₃ sd(28), NH ₂ twist(13)
1370	1373	3	CCH ₃ sd(60), C ^α H r ¹ (12), CC ^{me} s(10), NH ₂ twist(9)
1414	1416	2	COO ss(57), CC ^{ter} s(16), CCOO sd(10), CCH ₃ ad ² (7)
1460	1459	-1	CCH ₃ ad ² (55), CCH ₃ ad ¹ (33)

Table 3.47: (continued)

frequency (cm^{-1})			Potential Energy Distribution
obs.	calc.	dev.	
1460	1466	6	CCH ₃ ad ¹ (57), CCH ₃ ad ² (31)
1567	1563	-4	COO as(85), CCOO r(7)
1593	1585	-8	NH ₂ sissor(99)
2885	2885	0	C ^{α} H s(98)
2940	2941	1	CH ₃ ss(94)
2980	2976	-4	CH ₃ as ¹ (51), CH ₃ as ² (47)
2993	2998	5	CH ₃ as ¹ (48), CH ₃ as ² (48)
—	3148	—	NH ₂ as(98)
—	3231	—	NH ₂ ss(98)

Table 3.48: Scaled 4-31G* Frequencies and Potential Energy Distribution for Isolated Alaninate.

frequency (cm ⁻¹)			NH ₂ CHCH ₃ COO ⁻ (mean deviation = 10 cm ⁻¹)
obs.	calc.	dev.	
			Potential Energy Distribution
—	57	—	CC t(97)
—	199	—	CN t(56), CC ^{me} t(41)
—	215	—	CC ^{me} t(50), CN t(42)
279	281	2	C ^α H d ² (61), CCOO r(15)
343	349	6	C ^α H d ³ (53), CCOO r(18)
415	414	-1	C ^α H d ¹ (76)
539	538	-1	CCOO r(37), CN ^{ter} s(14), CC ^{ter} s(13), CCOO sd(12), C ^α H d ³ (8)
622	612	-10	CCOO sd(30), CC ^{ter} s(18), CCOO r(14), CCOO wag(11), CC ^{me} s(10), C ^α H d ³ (9)
785	780	-5	CCOO wag(44), CCOO sd(22)
853	842	-11	CN ^{ter} s(17), CCOO sd(16), CH ₃ r ¹ (15), CC ^{me} s(13), CC ^{ter} s(10), CCOO wag(9), COO ss(7)
927	931	4	CH ₃ r ² (35), CN ^{ter} s(26), CC ^{ter} s(20), COO ss(9)
—	955	—	NH ₂ wag(66), CH ₃ r ¹ (13), CC ^{me} s(9)
1020	1005	-15	NH ₂ twist(42), CC ^{me} s(18), CH ₃ r ¹ (14), C ^α H r ¹ (8)
1080	1078	-2	C ^α H r ² (28), NH ₂ wag(17), CCOO wag(13), CH ₃ r ² (11), C ^α H d ³ (8)
1140	1149	9	CN ^{ter} s(25), CC ^{me} s(19), CH ₃ r ² (17), C ^α H r ¹ (11)
1238	1245	7	NH ₂ twist(29), CH ₃ r ¹ (23), C ^α H d ¹ (11), C ^α H r ² (10), CH ₃ r ² (7)
1286	1284	-2	C ^α H r ² (35), COO ss(19), C ^α H r ¹ (15)
1353	1341	-12	CCH ₃ sd(50), C ^α H r ¹ (35), NH ₂ twist(9)
1368	1385	17	CCH ₃ sd(34), C ^α H r ¹ (20), CC ^{me} s(16), NH ₂ twist(15)
1414	1413	-1	COO ss(50), CC ^{ter} s(16), CCH ₃ ad ² (13), CCOO sd(10)
1459	1459	0	CCH ₃ ad ² (59), CCH ₃ ad ¹ (25), CH ₃ r ² (7)
1459	1464	5	CCH ₃ ad ¹ (63), CCH ₃ ad ² (19)
1564	1566	2	COO as(85), CCOO r(8)
1591	1587	-4	NH ₂ sissor(100)
2885	2885	0	C ^α H s(98)
2940	2913	-27	CH ₃ ss(83), CH ₃ as ² (15)
2980	2964	-16	CH ₃ as ¹ (56), CH ₃ as ² (40)
2993	3045	52	CH ₃ as ² (45), CH ₃ as ¹ (40), CH ₃ ss(15)

Table 3.48: (continued)

frequency (cm ⁻¹)			Potential Energy Distribution
obs.	calc.	dev.	
—	3121	—	NH ₂ as(96)
—	3224	—	NH ₂ ss(96)

frequency (cm ⁻¹)			Potential Energy Distribution
obs.	calc.	dev.	
—	56	—	CC t(97)
—	149	—	CN t(96)
—	209	—	CC ^{me} t(90)
275	277	2	C ^α H d ² (54), CCOO r(18), C ^α H d ³ (12)
331	327	-4	C ^α H d ³ (47), C ^α H d ² (13), CCOO r(9), NH ₂ wag(8)
384	392	8	C ^α H d ¹ (73), NH ₂ twist(7)
527	521	-6	CCOO r(48), CN ^{ter} s(13), COO as(7), CC ^{ter} s(7), CCOO sd(7)
621	602	-19	CCOO sd(36), CC ^{ter} s(25), CCOO r(9), CC ^{me} s(8), CCOO wag(8), NH ₂ wag(7)
—	746	—	CCOO wag(39), NH ₂ wag(39)
780	803	23	NH ₂ twist(31), CCOO sd(19), CN ^{ter} s(15), CC ^{me} s(14), NH ₂ wag(9)
836	817	-19	NH ₂ twist(35), NH ₂ wag(21), CCOO sd(9), CCOO wag(9), C ^α H d ³ (7)
870	856	-14	CH ₃ r ¹ (34), CC ^{me} s(8), CCOO wag(8), CN ^{ter} s(7), C ^α H d ³ (7), NH ₂ twist(7)
922	925	3	CH ₃ r ² (32), CN ^{ter} s(25), CC ^{ter} s(22), COO ss(10)
1053	1060	7	C ^α H r ² (27), CCOO wag(14), CH ₃ r ¹ (11), CC ^{me} s(8), C ^α H d ³ (8)
1108	1126	18	NH ₂ sissor(35), CH ₃ r ² (22), CC ^{me} s(12), CN ^{ter} s(9)
1143	1169	26	NH ₂ sissor(41), CC ^{me} s(17), CH ₃ r ¹ (15)
1201	1188	-13	NH ₂ sissor(21), CH ₃ r ¹ (15), CN ^{ter} s(11), CH ₃ r ² (11), C ^α H d ¹ (10), NH ₂ twist(8)
1290	1282	-8	C ^α H r ² (42), COO ss(19), C ^α H r ¹ (8)
1334	1326	-8	C ^α H r ¹ (60), CCH ₃ sd(20)
1370	1371	1	CCH ₃ sd(62), CC ^{me} s(15)
1414	1413	-1	COO ss(49), CC ^{ter} s(16), CCH ₃ ad ² (14), CCOO sd(9)

Table 3.48: (continued)

frequency (cm^{-1})			Potential Energy Distribution
obs.	calc.	dev.	
1462	1459	-3	CCH ₃ ad ² (47), CCH ₃ ad ¹ (37)
1462	1466	4	CCH ₃ ad ¹ (51), CCH ₃ ad ² (29)
1571	1566	-5	COO as(86), CCOO r(8)
—	2293	—	NH ₂ as(88), NH ₂ ss(12)
—	2337	—	NH ₂ ss(89), NH ₂ as(12)
2887	2885	-2	C ^{α} H s(98)
2942	2913	-29	CH ₃ ss(83), CH ₃ as ² (15)
2980	2964	-16	CH ₃ as ¹ (56), CH ₃ as ² (40)
2990	3045	55	CH ₃ as ² (45), CH ₃ as ¹ (40), CH ₃ ss(15)

frequency (cm^{-1})			Potential Energy Distribution
obs.	calc.	dev.	
—	56	—	CC t(97)
—	150	—	CC ^{me} t(94)
—	206	—	CN t(96)
257	253	-4	C ^{α} H d ² (68), CCOO r(9)
335	341	6	C ^{α} H d ³ (59), CCOO r(24)
382	377	-5	C ^{α} H d ¹ (73), CH ₃ r ¹ (8)
514	521	7	CCOO r(30), CC ^{ter} s(21), CCOO sd(17), CN ^{ter} s(10)
593	577	-16	CCOO r(22), CCOO sd(17), CC ^{ter} s(15), CC ^{me} s(11), CCOO wag(11), C ^{α} H r ² (9), C ^{α} H d ³ (9)
688	666	-22	CH ₃ r ¹ (39), C ^{α} H r ² (26), CCOO wag(16)
752	753	1	CH ₃ r ² (32), CN ^{ter} s(20), CC ^{me} s(11), CCOO sd(11), CCOO wag(7)
827	813	-14	CCOO sd(33), CH ₃ r ² (29), COO ss(9), CC ^{ter} s(7)
884	858	-26	C ^{α} H r ¹ (44), CN ^{ter} s(23), NH ₂ wag(11), NH ₂ twist(9)
897	889	-8	C ^{α} H r ² (26), CCOO wag(12), CH ₃ r ¹ (11), CC ^{ter} s(10), CC ^{me} s(8), CCH ₃ sd(8)
947	952	5	C ^{α} H r ¹ (20), CCOO wag(20), CH ₃ r ¹ (20), NH ₂ wag(12), C ^{α} H d ² (8)
—	967	—	NH ₂ wag(40), C ^{α} H r ² (19), CCOO wag(12), CCH ₃ sd(11)
1055	1046	-9	CCH ₃ ad ² (97)
1055	1053	-2	CCH ₃ ad ¹ (87)

Table 3.48: (continued)

frequency (cm^{-1})			Potential Energy Distribution
obs.	calc.	dev.	
—	1072	—	CCH ₃ sd(42), NH ₂ wag(13), CCH ₃ ad ¹ (10), C ^{α} H d ³ (8)
1126	1147	21	NH ₂ twist(22), CC ^{ter} s(11), C ^{α} H r ¹ (11), NH ₂ wag(11), COO ss(8), CC ^{me} s(7)
1158	1179	21	CN ^{ter} s(30), NH ₂ twist(15), CH ₃ r ² (10), CC ^{me} s(7), C ^{α} H d ¹ (7)
1276	1305	29	NH ₂ twist(38), CC ^{me} s(28)
1408	1410	2	COO ss(62), CC ^{ter} s(19), CCOO sd(12)
1555	1563	8	COO as(86), CCOO r(8)
1582	1586	4	NH ₂ sissor(101)
2076	2100	24	CH ₃ ss(92)
2125	2125	0	C ^{α} H s(96)
2235	2196	-39	CH ₃ as ¹ (54), CH ₃ as ² (45)
2246	2251	5	CH ₃ as ² (50), CH ₃ as ¹ (44)
—	3121	—	NH ₂ as(96)
—	3224	—	NH ₂ ss(96)

frequency (cm^{-1})			ND ₂ CD ₂ CD ₃ COO ⁻ (mean deviation = 13 cm^{-1})
obs.	calc.	dev.	
—	55	—	CC t(97)
—	144	—	CN t(56), CC ^{me} t(41)
—	155	—	CC ^{me} t(54), CN t(41)
257	252	-5	C ^{α} H d ² (67), CCOO r(10)
327	317	-10	C ^{α} H d ³ (57), CCOO r(15), NH ₂ wag(9)
363	358	-5	C ^{α} H d ¹ (69), CH ₃ r ¹ (8)
506	508	2	CCOO r(42), CC ^{ter} s(13), CN ^{ter} s(10), CCOO sd(10)
590	571	-19	CCOO sd(24), CC ^{ter} s(23), CCOO r(16), CC ^{me} s(9), CCOO wag(9), C ^{α} H r ² (8)
690	663	-27	CH ₃ r ¹ (37), C ^{α} H r ² (27), CCOO wag(19)
729	720	-9	CH ₃ r ² (22), NH ₂ wag(20), NH ₂ twist(12), C ^{α} H r ¹ (10), CH ₃ r ¹ (9), CCOO wag(8)
756	763	7	NH ₂ twist(36), CC ^{me} s(22), CCH ₃ sd(10), CCOO sd(9), NH ₂ wag(7)
790	784	-6	NH ₂ wag(40), CN ^{ter} s(28), CH ₃ r ² (21)

Table 3.48: (continued)

frequency (cm^{-1})			Potential Energy Distribution
obs.	calc.	dev.	
845	833	-12	CCOO sd(33), CC^{ter} s(16), COO ss(14), CH_3 r ² (12), NH_2 wag(7)
893	897	4	C^αH r ² (31), CH_3 r ¹ (15), C^αH r ¹ (12), CCOO wag(12), CN^{ter} s(8)
940	934	-6	C^αH r ¹ (36), CCOO wag(26), C^αH r ² (9)
1036	1030	-6	CCH ₃ sd(26), NH_2 twist(21), C^αH d ¹ (9), CH_3 r ¹ (9), CCH ₃ ad ¹ (8), C^αH r ¹ (7), C^αH d ² (7)
1055	1045	-10	CCH ₃ ad ² (86)
1055	1051	-4	CCH ₃ ad ¹ (34), CH_3 r ¹ (14), CCH ₃ sd(12), CCH ₃ ad ² (12)
—	1062	—	CCH ₃ ad ¹ (51), CCH ₃ sd(27), C^αH r ² (7)
1123	1127	4	NH_2 sissor(55), C^αH r ¹ (8), CH_3 r ² (8), CC^{ter} s(7)
1182	1200	18	NH_2 sissor(45), CN^{ter} s(20), COO ss(9), CH_3 r ² (7)
1215	1256	41	CC^{me} s(47), CCH ₃ sd(8), CN^{ter} s(7), NH_2 twist(7)
1409	1410	1	COO ss(63), CC^{ter} s(20), CCOO sd(12)
1567	1564	-3	COO as(87), CCOO r(8)
2076	2100	24	CH_3 ss(92)
2125	2125	0	C^αH s(96)
2235	2196	-39	CH_3 as ¹ (54), CH_3 as ² (45)
2246	2251	5	CH_3 as ² (50), CH_3 as ¹ (44)
—	2293	—	NH_2 as(88), NH_2 ss(11)
—	2337	—	NH_2 ss(89), NH_2 as(11)

frequency (cm^{-1})			$\text{NH}_2\text{CHCD}_3\text{COO}^-$ (mean deviation = 10 cm^{-1})
obs.	calc.	dev.	
—	56	—	CC t(97)
—	150	—	CC^{me} t(94)
—	206	—	CN t(97)
255	254	-1	C^αH d ² (67), CCOO r(10)
340	344	4	C^αH d ³ (58), CCOO r(23)
390	380	-10	C^αH d ¹ (71), CH_3 r ¹ (9)
521	528	7	CCOO r(36), CC^{ter} s(17), CCOO sd(14), CN^{ter} s(11), C^αH d ³ (7)

Table 3.48: (continued)

frequency (cm^{-1})			Potential Energy Distribution
obs.	calc.	dev.	
607	594	-13	CCOO sd(24), CC ^{ter} s(18), CCOO r(15), CC ^{me} s(14), C ^{α} H d ³ (9), CCOO wag(8)
741	714	-27	CH ₃ r ¹ (44), CCOO wag(38), C ^{α} H r ² (8)
771	760	-11	CN ^{ter} s(28), CH ₃ r ² (28), CCOO sd(11), CC ^{me} s(10), CH ₃ r ¹ (10)
828	813	-15	CCOO sd(33), CH ₃ r ² (30), COO ss(10), CC ^{ter} s(8)
910	916	6	NH ₂ wag(39), CCOO wag(15), CH ₃ r ¹ (15), CN ^{ter} s(7), C ^{α} H d ² (7), NH ₂ twist(7)
947	934	-13	CCH ₃ sd(29), NH ₂ wag(16), CC ^{me} s(14), CC ^{ter} s(14), NH ₂ twist(9), COO ss(7)
1020	1043	23	CCH ₃ ad ² (36), NH ₂ wag(13), CCOO wag(9), CC ^{ter} s(7), C ^{α} H d ² (7), CCH ₃ ad ¹ (7)
1058	1045	-13	CCH ₃ ad ² (51), CCH ₃ ad ¹ (17), NH ₂ wag(10)
1058	1054	-4	CCH ₃ ad ¹ (65), NH ₂ wag(9), CCH ₃ sd(9)
—	1059	—	CCH ₃ sd(23), CN ^{ter} s(21), NH ₂ twist(11), CCH ₃ ad ² (10), C ^{α} H r ¹ (7), CCH ₃ ad ¹ (7)
1141	1159	18	CC ^{me} s(29), CCH ₃ sd(20), C ^{α} H r ² (17), CN ^{ter} s(15)
1189	1195	6	NH ₂ twist(36), C ^{α} H r ² (19), CH ₃ r ¹ (10), CN ^{ter} s(9), C ^{α} H d ¹ (9), C ^{α} H r ¹ (7)
1283	1279	-4	C ^{α} H r ² (32), C ^{α} H r ¹ (26), COO ss(15), CC ^{me} s(7)
1360	1367	7	C ^{α} H r ¹ (47), NH ₂ twist(25), CC ^{me} s(11)
1413	1414	1	COO ss(58), CC ^{ter} s(20), CCOO sd(11)
1563	1564	1	COO as(86), CCOO r(8)
1587	1586	-1	NH ₂ sissor(101)
2076	2100	24	CH ₃ ss(93)
2125	2195	70	CH ₃ as ¹ (55), CH ₃ as ² (44)
2235	2251	16	CH ₃ as ² (51), CH ₃ as ¹ (43)
—	2886	—	C ^{α} H s(100)
—	3121	—	NH ₂ as(96)
—	3224	—	NH ₂ ss(96)

frequency (cm^{-1})			ND ₂ CHCD ₃ COO ⁻ (mean deviation = 10 cm^{-1})
obs.	calc.	dev.	
			Potential Energy Distribution

Table 3.48: (continued)

frequency (cm ⁻¹)			Potential Energy Distribution
obs.	calc.	dev.	
—	55	—	CC t(96)
—	144	—	CN t(56), CC ^{me} t(42)
—	155	—	CC ^{me} t(54), CN t(41)
258	253	-5	C ^α H d ² (66), CCOO r(11)
320	319	-1	C ^α H d ³ (56), CCOO r(15), NH ₂ wag(9)
348	361	13	C ^α H d ¹ (68), CH ₃ r ¹ (8)
512	514	2	CCOO r(47), CN ^{ter} s(11), CC ^{ter} s(10), CCOO sd(8)
595	586	-9	CCOO sd(30), CC ^{ter} s(26), CC ^{me} s(11), CCOO r(10)
700	711	11	CCOO wag(42), CH ₃ r ¹ (35), C ^α H r ² (7), CH ₃ r ² (7)
723	733	10	CH ₃ r ¹ (25), NH ₂ wag(19), CH ₃ r ² (16), CN ^{ter} s(10), CC ^{me} s(7), NH ₂ twist(7)
751	770	19	NH ₂ twist(35), CH ₃ r ² (19), CC ^{me} s(14), NH ₂ wag(12), CCOO sd(9), CCH ₃ sd(7)
799	789	-10	NH ₂ wag(38), CN ^{ter} s(24), CCOO sd(8), CH ₃ r ² (8), NH ₂ twist(7)
852	841	-11	CCOO sd(26), CC ^{ter} s(15), NH ₂ twist(15), CH ₃ r ² (13), COO ss(12), CCOO wag(8)
988	1002	14	CCH ₃ sd(56), CN ^{ter} s(10)
1028	1021	-7	CCOO wag(22), C ^α H d ² (13), CC ^{ter} s(12), CH ₃ r ¹ (11), C ^α H d ³ (8)
1056	1046	-10	CCH ₃ ad ² (92)
1056	1053	-3	CCH ₃ ad ¹ (88)
1109	1097	-12	CN ^{ter} s(23), NH ₂ sissor(21), C ^α H d ¹ (13), CH ₃ r ² (10), NH ₂ twist(9), CH ₃ r ¹ (7)
1131	1159	28	CC ^{me} s(29), C ^α H r ² (28), CCH ₃ sd(20), NH ₂ sissor(7)
—	1176	—	NH ₂ sissor(68), CN ^{ter} s(16), C ^α H r ¹ (7)
1281	1277	-4	C ^α H r ² (40), C ^α H r ¹ (16), COO ss(15), CC ^{me} s(9)
1332	1332	0	C ^α H r ¹ (63), CC ^{me} s(12), C ^α H r ² (7)
1412	1415	3	COO ss(58), CC ^{ter} s(20), CCOO sd(11)
1576	1564	-12	COO as(87), CCOO r(8)
2076	2100	24	CH ₃ ss(93)
2125	2195	70	CH ₃ as ¹ (55), CH ₃ as ² (44)
2235	2251	16	CH ₃ as ² (51), CH ₃ as ¹ (43)
2246	2293	47	NH ₂ as(88), NH ₂ ss(12)

Table 3.48: (continued)

frequency (cm ⁻¹)			Potential Energy Distribution
obs.	calc.	dev.	
—	2337	—	NH ₂ ss(89), NH ₂ as(12)
—	2887	—	C ^α H s(100)

frequency (cm ⁻¹)			NH ₂ CH ¹³ CH ₃ COO ⁻ (mean deviation = 8 cm ⁻¹)
obs.	calc.	dev.	
—	57	—	CC t(97)
—	199	—	CN t(56), CC ^{me} t(41)
—	215	—	CC ^{me} t(49), CN t(42)
273	278	5	C ^α H d ² (61), CCOO r(14)
344	349	5	C ^α H d ³ (54), CCOO r(18)
409	411	2	C ^α H d ¹ (76)
538	538	0	CCOO r(37), CN ^{ter} s(14), CC ^{ter} s(13), CCOO sd(12), C ^α H d ³ (8)
624	609	-15	CCOO sd(29), CC ^{ter} s(19), CCOO r(14), CCOO wag(12), CC ^{me} s(11), C ^α H d ³ (9)
779	779	0	CCOO wag(42), CCOO sd(23)
849	838	-11	CN ^{ter} s(16), CCOO sd(16), CH ₃ r ¹ (16), CC ^{me} s(14), CCOO wag(10), CC ^{ter} s(8), COO ss(7)
922	928	6	CH ₃ r ² (36), CN ^{ter} s(24), CC ^{ter} s(20), COO ss(9)
—	952	—	NH ₂ wag(66), CH ₃ r ¹ (12), CC ^{me} s(9)
1015	1001	-14	NH ₂ twist(41), CC ^{me} s(18), CH ₃ r ¹ (15), C ^α H r ¹ (7)
1073	1076	3	C ^α H r ² (27), NH ₂ wag(18), CCOO wag(13), CH ₃ r ² (10), C ^α H d ³ (8)
1134	1145	11	CN ^{ter} s(27), CC ^{me} s(19), CH ₃ r ² (16), C ^α H r ¹ (11)
1231	1239	8	NH ₂ twist(29), CH ₃ r ¹ (22), C ^α H r ² (11), C ^α H d ¹ (11)
1288	1282	-6	C ^α H r ² (35), COO ss(18), C ^α H r ¹ (15)
1355	1335	-20	CCH ₃ sd(63), C ^α H r ¹ (27)
1360	1377	17	C ^α H r ¹ (28), CCH ₃ sd(23), NH ₂ twist(18), CC ^{me} s(14), C ^α H r ² (7)
1412	1412	0	COO ss(50), CC ^{ter} s(16), CCH ₃ ad ² (14), CCOO sd(10)
1458	1458	0	CCH ₃ ad ² (52), CCH ₃ ad ¹ (32)
1458	1463	5	CCH ₃ ad ¹ (56), CCH ₃ ad ² (24)
1562	1566	4	COO as(85), CCOO r(8)

Table 3.48: (continued)

frequency (cm^{-1})			Potential Energy Distribution
obs.	calc.	dev.	
1596	1587	-9	NH ₂ sissor(100)
2885	2884	-1	C α H s(98)
2940	2909	-31	CH ₃ ss(81), CH ₃ as ² (17)
2980	2954	-26	CH ₃ as ¹ (57), CH ₃ as ² (39)
2993	3035	42	CH ₃ as ² (44), CH ₃ as ¹ (40), CH ₃ ss(16)
—	3121	—	NH ₂ as(96)
—	3224	—	NH ₂ ss(96)

frequency (cm^{-1})			¹⁵ NH ₂ CHCH ₃ COO ⁻ (mean deviation = 12 cm^{-1})
obs.	calc.	dev.	
—	57	—	CC t(97)
—	199	—	CN t(56), CC ^{me} t(41)
—	215	—	CC ^{me} t(50), CN t(41)
279	281	2	C α H d ² (60), CCOO r(15), C α H d ³ (7)
343	345	2	C α H d ³ (53), CCOO r(17), C α H d ² (7)
421	412	-9	C α H d ¹ (76), CCOO wag(7)
535	533	-2	CCOO r(37), CN ^{ter} s(15), CC ^{ter} s(14), CCOO sd(12), C α H d ³ (7)
632	612	-20	CCOO sd(29), CC ^{ter} s(18), CCOO r(14), CCOO wag(11), CC ^{me} s(10), C α H d ³ (9)
793	779	-14	CCOO wag(43), CCOO sd(23)
851	838	-13	CN ^{ter} s(18), CCOO sd(15), CH ₃ r ¹ (15), CC ^{me} s(12), CCOO wag(10), CC ^{ter} s(8)
924	927	3	CH ₃ r ² (35), CN ^{ter} s(26), CC ^{ter} s(21), COO ss(9)
—	950	—	NH ₂ wag(65), CH ₃ r ¹ (15), CC ^{me} s(11)
1019	1004	-15	NH ₂ twist(42), CC ^{me} s(17), CH ₃ r ¹ (14), C α H r ¹ (8)
1072	1077	5	C α H r ² (28), NH ₂ wag(16), CCOO wag(13), CH ₃ r ² (10), C α H d ³ (8)
1134	1146	12	CN ^{ter} s(24), CC ^{me} s(19), CH ₃ r ² (18), C α H r ¹ (11)
1234	1243	9	NH ₂ twist(29), CH ₃ r ¹ (23), C α H d ¹ (11), C α H r ² (10)
1291	1283	-8	C α H r ² (36), COO ss(18), C α H r ¹ (15)
1360	1339	-21	CCH ₃ sd(48), C α H r ¹ (37), NH ₂ twist(9)
1370	1384	14	CCH ₃ sd(35), C α H r ¹ (19), CC ^{me} s(16), NH ₂ twist(14)

Table 3.48: (continued)

frequency (cm ⁻¹)			Potential Energy Distribution
obs.	calc.	dev.	
1414	1413	-1	COO ss(50), CC ^{ter} s(16), CCH ₃ ad ² (13), CCOO sd(10)
1460	1459	-1	CCH ₃ ad ² (59), CCH ₃ ad ¹ (24), CH ₃ r ² (7)
1460	1464	4	CCH ₃ ad ¹ (64), CCH ₃ ad ² (19)
1567	1566	-1	COO as(85), CCOO r(8)
1593	1584	-9	NH ₂ sissor(100)
2885	2885	0	C ^α H s(98)
2940	2913	-27	CH ₃ ss(83), CH ₃ as ² (15)
2980	2964	-16	CH ₃ as ¹ (56), CH ₃ as ² (40)
2993	3045	52	CH ₃ as ² (45), CH ₃ as ¹ (40), CH ₃ ss(15)
—	3113	—	NH ₂ as(96)
—	3219	—	NH ₂ ss(97)

Table 3.49: Scaled 6-31G** Frequencies and Potential Energy Distribution for Isolated Alaninate.

frequency (cm ⁻¹)			NH ₂ CHCH ₃ COO ⁻ (mean deviation = 9 cm ⁻¹)
obs.	calc.	dev.	
			Potential Energy Distribution
—	60	—	CC t(98)
—	201	—	CN t(50), CC ^{me} t(48)
—	218	—	CN t(48), CC ^{me} t(44)
279	280	1	C ^α H d ² (60), CCOO r(17)
343	348	5	C ^α H d ³ (51), CCOO r(18), C ^α H d ² (8)
415	414	-1	C ^α H d ¹ (76)
539	535	-4	CCOO r(41), CN ^{ter} s(14), CC ^{ter} s(11), C ^α H d ³ (11), CCOO sd(7)
622	621	-1	CCOO sd(28), CC ^{ter} s(25), CCOO wag(12), CC ^{me} s(11), CCOO r(9), C ^α H d ³ (7)
785	793	8	CCOO wag(44), CCOO sd(20)
853	852	-1	CN ^{ter} s(21), CCOO sd(19), CC ^{me} s(13), CH ₃ r ¹ (12), COO ss(9), CCOO wag(7)
927	925	-2	CH ₃ r ² (38), CN ^{ter} s(24), CC ^{ter} s(17), COO ss(11), CCOO sd(7)
—	952	—	NH ₂ wag(67), CH ₃ r ¹ (13), CC ^{me} s(10)
1020	1008	-12	NH ₂ twist(44), CC ^{me} s(16), CH ₃ r ¹ (13), C ^α H r ¹ (8)
1080	1075	-5	C ^α H r ² (29), CCOO wag(14), NH ₂ wag(14), CH ₃ r ² (9), C ^α H d ³ (8), CH ₃ r ¹ (7)
1140	1145	5	CN ^{ter} s(27), CC ^{me} s(20), CH ₃ r ² (18), C ^α H r ¹ (8)
1238	1245	7	NH ₂ twist(30), CH ₃ r ¹ (25), C ^α H d ¹ (12)
1286	1280	-6	C ^α H r ² (38), COO ss(18), C ^α H r ¹ (14)
1353	1341	-12	CCH ₃ sd(51), C ^α H r ¹ (36), NH ₂ twist(7)
1368	1387	19	CCH ₃ sd(32), C ^α H r ¹ (22), CC ^{me} s(16), NH ₂ twist(14)
1414	1414	0	COO ss(46), CC ^{ter} s(18), CCOO sd(12), CCH ₃ ad ² (10)
1459	1460	1	CCH ₃ ad ¹ (60), CCH ₃ ad ² (28)
1459	1466	7	CCH ₃ ad ² (55), CCH ₃ ad ¹ (26)
1564	1567	3	COO as(86), CCOO r(7)
1591	1588	-3	NH ₂ sissor(100)
2885	2884	-1	C ^α H s(98)
2940	2914	-26	CH ₃ ss(85), CH ₃ as ² (13)
2980	2969	-11	CH ₃ as ¹ (56), CH ₃ as ² (42)
2993	3046	53	CH ₃ as ² (46), CH ₃ as ¹ (41), CH ₃ ss(14)

Table 3.49: (continued)

frequency (cm ⁻¹)			Potential Energy Distribution
obs.	calc.	dev.	
—	3144	—	NH ₂ as(98)
—	3246	—	NH ₂ ss(98)

frequency (cm ⁻¹)			Potential Energy Distribution
obs.	calc.	dev.	
—	59	—	CC t(97)
—	151	—	CN t(97)
—	210	—	CC ^{me} t(91)
275	276	1	C ^α H d ² (53), CCOO r(19), C ^α H d ³ (13)
331	326	-5	C ^α H d ³ (45), C ^α H d ² (15), CCOO r(9), NH ₂ wag(8), C ^α H d ¹ (7)
384	392	8	C ^α H d ¹ (73), NH ₂ twist(7)
527	516	-11	CCOO r(50), CN ^{ter} s(13), COO as(7), NH ₂ wag(7)
621	613	-8	CCOO sd(32), CC ^{ter} s(31), CCOO wag(9), CC ^{me} s(8)
—	746	—	NH ₂ wag(49), CCOO wag(33)
780	807	27	NH ₂ twist(55), CC ^{me} s(16), CCOO sd(10), CN ^{ter} s(9)
836	820	-16	NH ₂ wag(22), CCOO sd(19), NH ₂ twist(14), CCOO wag(13), CN ^{ter} s(8), C ^α H d ³ (8)
870	864	-6	CH ₃ r ¹ (30), CN ^{ter} s(11), CCOO wag(10), CC ^{me} s(9), C ^α H d ³ (7)
922	920	-2	CH ₃ r ² (31), CC ^{ter} s(21), CN ^{ter} s(21), COO ss(14), CCOO sd(10)
1053	1061	8	C ^α H r ² (28), CCOO wag(14), CH ₃ r ¹ (10), CC ^{me} s(9), C ^α H d ³ (8), CH ₃ r ² (7)
1108	1120	12	NH ₂ sissor(32), CH ₃ r ² (24), CN ^{ter} s(12), CC ^{me} s(10)
1143	1174	31	NH ₂ sissor(52), CC ^{me} s(13), CN ^{ter} s(10), CH ₃ r ¹ (8)
1201	1188	-13	CH ₃ r ¹ (24), C ^α H d ¹ (13), NH ₂ sissor(13), NH ₂ twist(10), CC ^{me} s(8), CH ₃ r ² (8)
1290	1279	-11	C ^α H r ² (42), COO ss(18), C ^α H r ¹ (10)
1334	1330	-4	C ^α H r ¹ (59), CCH ₃ sd(24)
1370	1372	2	CCH ₃ sd(57), CC ^{me} s(16), C ^α H r ¹ (8)
1414	1414	0	COO ss(46), CC ^{ter} s(18), CCOO sd(12), CCH ₃ ad ² (11)
1462	1460	-2	CCH ₃ ad ¹ (61), CCH ₃ ad ² (26)

Table 3.49: (continued)

frequency (cm^{-1})			Potential Energy Distribution
obs.	calc.	dev.	
1462	1468	6	CCH ₃ ad ² (55), CCH ₃ ad ¹ (24), CH ₃ r ² (7)
1571	1567	-4	COO as(87), CCOO r(7)
—	2311	—	NH ₂ as(92), NH ₂ ss(8)
—	2351	—	NH ₂ ss(92), NH ₂ as(8)
2887	2885	-2	C ^α H s(98)
2942	2914	-28	CH ₃ ss(85), CH ₃ as ² (13)
2980	2969	-11	CH ₃ as ¹ (56), CH ₃ as ² (42)
2990	3046	56	CH ₃ as ² (46), CH ₃ as ¹ (41), CH ₃ ss(14)

frequency (cm^{-1})			NH ₂ CD ₂ CD ₃ COO ⁻ (mean deviation = 11 cm^{-1})
obs.	calc.	dev.	
—	58	—	CC t(97)
—	150	—	CC ^{me} t(95)
—	210	—	CN t(97)
257	252	-5	C ^α H d ² (67), CCOO r(10)
335	340	5	C ^α H d ³ (57), CCOO r(24)
382	377	-5	C ^α H d ¹ (72), CH ₃ r ¹ (8)
514	521	7	CCOO r(36), CC ^{ter} s(17), CN ^{ter} s(10), C ^α H d ³ (10), CCOO sd(10)
593	581	-12	CC ^{ter} s(22), CCOO sd(18), CCOO r(14), CCOO wag(12), CC ^{me} s(10), C ^α H r ² (10)
688	673	-15	CH ₃ r ¹ (36), C ^α H r ² (27), CCOO wag(15)
752	751	-1	CH ₃ r ² (43), CN ^{ter} s(21), CC ^{me} s(8)
827	825	-2	CCOO sd(39), CH ₃ r ² (18), COO ss(11), CC ^{me} s(8), CCOO wag(7)
884	859	-25	C ^α H r ¹ (43), CN ^{ter} s(23), NH ₂ wag(15), NH ₂ twist(8)
897	895	-2	C ^α H r ² (23), CCOO wag(11), CH ₃ r ¹ (11), CC ^{ter} s(10), CCOO sd(9), COO ss(8), CCH ₃ sd(8), CC ^{me} s(7)
947	956	9	NH ₂ wag(29), C ^α H r ¹ (21), CH ₃ r ¹ (21), CCOO wag(9)
—	966	—	CCOO wag(23), NH ₂ wag(23), C ^α H r ² (18), CCH ₃ sd(16), NH ₂ twist(7)
1055	1050	-5	CCH ₃ ad ¹ (65), CCH ₃ ad ² (29)
1055	1052	-3	CCH ₃ ad ² (69), CCH ₃ ad ¹ (26)

Table 3.49: (continued)

frequency (cm ⁻¹)			Potential Energy Distribution
obs.	calc.	dev.	
—	1071	—	CCH ₃ sd(40), NH ₂ wag(12), C ^α H d ³ (9), CCH ₃ ad ¹ (8), CH ₃ r ¹ (7)
1126	1141	15	NH ₂ twist(20), C ^α H r ¹ (14), CC ^{ter} s(11), COO ss(10), NH ₂ wag(9)
1158	1171	13	CN ^{ter} s(27), NH ₂ twist(19), CH ₃ r ² (9), CC ^{me} s(8), C ^α H d ¹ (8)
1276	1305	29	NH ₂ twist(35), CC ^{me} s(30)
1408	1411	3	COO ss(56), CC ^{ter} s(21), CCOO sd(15)
1555	1565	10	COO as(88), CCOO r(7)
1582	1586	4	NH ₂ sissor(101)
2076	2100	24	CH ₃ ss(92)
2125	2125	0	C ^α H s(96)
2235	2200	-35	CH ₃ as ¹ (54), CH ₃ as ² (45)
2246	2253	7	CH ₃ as ² (51), CH ₃ as ¹ (44)
—	3144	—	NH ₂ as(98)
—	3246	—	NH ₂ ss(98)

frequency (cm ⁻¹)			ND ₂ CD ₂ CD ₃ COO ⁻ (mean deviation = 12 cm ⁻¹)
obs.	calc.	dev.	
—	57	—	CC t(97)
—	145	—	CN t(50), CC ^{me} t(48)
—	157	—	CN t(48), CC ^{me} t(48)
257	251	-6	C ^α H d ² (66), CCOO r(11)
327	316	-11	C ^α H d ³ (55), CCOO r(16), NH ₂ wag(8)
363	358	-5	C ^α H d ¹ (69), CH ₃ r ¹ (7)
506	505	-1	CCOO r(47), CC ^{ter} s(10), CN ^{ter} s(10), NH ₂ wag(7)
590	577	-13	CC ^{ter} s(29), CCOO sd(23), CCOO r(10), CCOO wag(10), CC ^{me} s(9), C ^α H r ² (9)
690	669	-21	CH ₃ r ¹ (33), C ^α H r ² (28), CCOO wag(18)
729	718	-11	CH ₃ r ² (26), NH ₂ wag(18), NH ₂ twist(15), CH ₃ r ¹ (11), C ^α H r ¹ (10)
756	765	9	NH ₂ twist(29), NH ₂ wag(26), CC ^{me} s(17), CCH ₃ sd(8), CH ₃ r ² (8)

Table 3.49: (continued)

frequency (cm^{-1})			Potential Energy Distribution
obs.	calc.	dev.	
790	776	-14	CN ^{ter} s(32), NH ₂ wag(23), CH ₃ r ² (16), NH ₂ twist(8)
845	846	1	CCOO sd(39), COO ss(17), CC ^{ter} s(11), CH ₃ r ² (9)
893	901	8	C ^α H r ² (28), CH ₃ r ¹ (15), C ^α H r ¹ (11), CCOO wag(11), CN ^{ter} s(9)
940	937	-3	C ^α H r ¹ (35), CCOO wag(26), C ^α H r ² (10), NH ₂ twist(7)
1036	1029	-7	CCH ₃ sd(30), NH ₂ twist(18), CCH ₃ ad ¹ (12), C ^α H d ¹ (9), C ^α H r ¹ (7), C ^α H d ² (7), CH ₃ r ¹ (7)
1055	1049	-6	CCH ₃ ad ² (41), CCH ₃ ad ¹ (30), CH ₃ r ¹ (10)
1055	1053	-2	CCH ₃ ad ² (56), CCH ₃ ad ¹ (15), CH ₃ r ¹ (9)
—	1060	—	CCH ₃ ad ¹ (41), CCH ₃ sd(30), C ^α H r ² (8)
1123	1121	-2	NH ₂ sissor(49), C ^α H r ¹ (10), CH ₃ r ² (8), COO ss(7), CC ^{ter} s(7), CN ^{ter} s(7)
1182	1197	15	NH ₂ sissor(51), CN ^{ter} s(18), COO ss(9)
1215	1260	45	CC ^{me} s(49), CCH ₃ sd(9), NH ₂ twist(7)
1409	1410	1	COO ss(57), CC ^{ter} s(21), CCOO sd(15)
1567	1565	-2	COO as(88), CCOO r(7)
2076	2100	24	CH ₃ ss(92)
2125	2125	0	C ^α H s(96)
2235	2200	-35	CH ₃ as ¹ (54), CH ₃ as ² (45)
2246	2253	7	CH ₃ as ² (51), CH ₃ as ¹ (44)
—	2311	—	NH ₂ as(92), NH ₂ ss(8)
—	2351	—	NH ₂ ss(92), NH ₂ as(8)

frequency (cm^{-1})			NH ₂ CHCD ₃ COO ⁻ (mean deviation = 8 cm^{-1})
obs.	calc.	dev.	
—	58	—	CC t(97)
—	150	—	CC ^{me} t(95)
—	210	—	CN t(97)
255	253	-2	C ^α H d ² (66), CCOO r(11)
340	342	2	C ^α H d ³ (56), CCOO r(24)
390	381	-9	C ^α H d ¹ (70), CH ₃ r ¹ (8)
521	525	4	CCOO r(41), CC ^{ter} s(14), CN ^{ter} s(11), C ^α H d ³ (11), CCOO sd(8)

Table 3.49: (continued)

frequency (cm^{-1})			Potential Energy Distribution
obs.	calc.	dev.	
607	601	-6	CC^{ter} s(25), CCOO sd(23), CC^{me} s(14), CCOO r(10), CCOO wag(8), $\text{C}^{\alpha}\text{H}$ d ³ (7)
741	723	-18	CCOO wag(38), CH_3 r ¹ (37), CH_3 r ² (12), $\text{C}^{\alpha}\text{H}$ r ² (7)
771	760	-11	CH_3 r ² (35), CN^{ter} s(28), CH_3 r ¹ (15), CC^{me} s(7)
828	826	-2	CCOO sd(42), CH_3 r ² (17), COO ss(12), CC^{me} s(7)
910	916	6	NH_2 wag(50), CCOO wag(12), CH_3 r ¹ (12), CN^{ter} s(7)
947	935	-12	CCH_3 sd(31), CC^{me} s(13), CC^{ter} s(12), NH_2 twist(12), COO ss(8), NH_2 wag(8)
1020	1041	21	CCH_3 ad ¹ (22), NH_2 wag(21), CCOO wag(14), $\text{C}^{\alpha}\text{H}$ r ² (10), CC^{ter} s(8), $\text{C}^{\alpha}\text{H}$ d ³ (8), $\text{C}^{\alpha}\text{H}$ d ² (7)
1058	1048	-10	CCH_3 ad ² (61), CN^{ter} s(11), CCH_3 sd(9)
1058	1052	-6	CCH_3 ad ¹ (57), CCH_3 sd(11), NH_2 wag(9)
—	1058	—	CCH_3 ad ² (37), CN^{ter} s(13), CCH_3 sd(12), CCH_3 ad ¹ (12)
1141	1159	18	CC^{me} s(29), CCH_3 sd(20), CN^{ter} s(17), $\text{C}^{\alpha}\text{H}$ r ² (14)
1189	1191	2	NH_2 twist(34), $\text{C}^{\alpha}\text{H}$ r ² (23), CH_3 r ¹ (12), $\text{C}^{\alpha}\text{H}$ d ¹ (8), $\text{C}^{\alpha}\text{H}$ r ¹ (7)
1283	1278	-5	$\text{C}^{\alpha}\text{H}$ r ² (31), $\text{C}^{\alpha}\text{H}$ r ¹ (26), COO ss(15), CC^{me} s(8)
1360	1369	9	$\text{C}^{\alpha}\text{H}$ r ¹ (50), NH_2 twist(23), CC^{me} s(12)
1413	1415	2	COO ss(52), CC^{ter} s(22), CCOO sd(14)
1563	1566	3	COO as(87), CCOO r(7)
1587	1587	0	NH_2 sissor(101)
2076	2100	24	CH_3 ss(94)
2125	2199	74	CH_3 as ¹ (55), CH_3 as ² (44)
2235	2253	18	CH_3 as ² (51), CH_3 as ¹ (43)
—	2886	—	$\text{C}^{\alpha}\text{H}$ s(100)
—	3144	—	NH_2 as(98)
—	3246	—	NH_2 ss(98)

frequency (cm^{-1})			Potential Energy Distribution
obs.	calc.	dev.	
—	58	—	CC t(97)
—	145	—	CN t(50), CC^{me} t(49)
—	157	—	CN t(49), CC^{me} t(47)

Table 3.49: (continued)

frequency (cm ⁻¹)			Potential Energy Distribution
obs.	calc.	dev.	
258	252	-6	C ^α H d ² (64), CCOO r(12)
320	318	-2	C ^α H d ³ (54), CCOO r(15), NH ₂ wag(9), C ^α H d ¹ (7)
348	361	13	C ^α H d ¹ (67), CH ₃ r ¹ (7)
512	509	-3	CCOO r(50), CN ^{ter} s(10), CC ^{ter} s(8), NH ₂ wag(7)
595	595	0	CC ^{ter} s(32), CCOO sd(27), CC ^{me} s(11), CCOO r(7)
—	717	—	CCOO wag(42), CH ₃ r ² (18), CH ₃ r ¹ (16), NH ₂ wag(10)
723	735	12	CH ₃ r ¹ (42), CH ₃ r ² (13), NH ₂ twist(12), NH ₂ wag(10), CN ^{ter} s(7)
751	768	17	NH ₂ wag(38), CH ₃ r ² (20), NH ₂ twist(17), CC ^{me} s(8)
799	787	-12	NH ₂ twist(27), CN ^{ter} s(20), NH ₂ wag(14), CC ^{me} s(12), CCOO sd(11), CCH ₃ sd(7)
852	851	-1	CCOO sd(34), COO ss(16), CC ^{ter} s(11), NH ₂ twist(11), CH ₃ r ² (10), CCOO wag(8)
988	999	11	CCH ₃ sd(56), CN ^{ter} s(11)
1028	1023	-5	CCOO wag(22), C ^α H d ² (13), CC ^{ter} s(12), CH ₃ r ¹ (10), C ^α H d ³ (7)
1056	1049	-7	CCH ₃ ad ¹ (55), CCH ₃ ad ² (39)
1056	1053	-3	CCH ₃ ad ² (58), CCH ₃ ad ¹ (36)
1109	1091	-18	CN ^{ter} s(24), NH ₂ sissor(18), C ^α H d ¹ (13), NH ₂ twist(9), CH ₃ r ¹ (9), CH ₃ r ² (9)
1131	1162	31	C ^α H r ² (29), CC ^{me} s(27), CCH ₃ sd(18), NH ₂ sissor(12)
—	1176	—	NH ₂ sissor(66), CN ^{ter} s(15), C ^α H r ¹ (7)
1281	1276	-5	C ^α H r ² (38), COO ss(16), C ^α H r ¹ (16), CC ^{me} s(10)
1332	1337	5	C ^α H r ¹ (64), CC ^{me} s(12), C ^α H r ² (7)
1412	1416	4	COO ss(52), CC ^{ter} s(22), CCOO sd(14)
1576	1565	-11	COO as(87), CCOO r(7)
2076	2100	24	CH ₃ ss(94)
2125	2199	74	CH ₃ as ¹ (55), CH ₃ as ² (44)
2235	2253	18	CH ₃ as ² (51), CH ₃ as ¹ (43)
2246	2311	65	NH ₂ as(92), NH ₂ ss(8)
—	2351	—	NH ₂ ss(92), NH ₂ as(8)
—	2886	—	C ^α H s(100)

Table 3.49: (continued)

frequency (cm^{-1})			Potential Energy Distribution
obs.	calc.	dev.	
frequency (cm^{-1})			$\text{NH}_2\text{CH}^{13}\text{CH}_3\text{COO}^-$ (mean deviation = 7 cm^{-1})
obs.	calc.	dev.	Potential Energy Distribution
—	60	—	CC t(98)
—	201	—	CN t(50), CC^{me} t(48)
—	218	—	CN t(49), CC^{me} t(44)
273	276	3	C^αH d ² (61), CCOO r(16)
344	348	4	C^αH d ³ (52), CCOO r(19), C^αH d ² (7)
409	411	2	C^αH d ¹ (76)
538	535	-3	CCOO r(41), CN^{ter} s(14), CC^{ter} s(11), C^αH d ³ (11), CCOO sd(7)
624	617	-7	CCOO sd(27), CC^{ter} s(25), CCOO wag(13), CC^{me} s(12), CCOO r(9), C^αH d ³ (7)
779	793	14	CCOO wag(43), CCOO sd(21)
849	849	0	CN^{ter} s(21), CCOO sd(19), CC^{me} s(14), CH_3 r ¹ (13), COO ss(8), CCOO wag(8)
922	922	0	CH_3 r ² (39), CN^{ter} s(22), CC^{ter} s(17), COO ss(11), CCOO sd(8)
—	949	—	NH_2 wag(67), CH_3 r ¹ (13), CC^{me} s(11)
1015	1004	-11	NH_2 twist(43), CC^{me} s(16), CH_3 r ¹ (14), C^αH r ¹ (8)
1073	1074	1	C^αH r ² (28), NH_2 wag(15), CCOO wag(14), CH_3 r ² (9), C^αH d ³ (8), CH_3 r ¹ (7)
1134	1140	6	CN^{ter} s(29), CC^{me} s(20), CH_3 r ² (17), C^αH r ¹ (8)
1231	1239	8	NH_2 twist(30), CH_3 r ¹ (24), C^αH d ¹ (11), C^αH r ² (8)
1288	1279	-9	C^αH r ² (38), COO ss(18), C^αH r ¹ (14)
1355	1335	-20	CCH ₃ sd(64), C^αH r ¹ (28)
1360	1379	19	C^αH r ¹ (31), CCH ₃ sd(22), NH_2 twist(17), CC^{me} s(14)
1412	1413	1	COO ss(46), CC^{ter} s(18), CCOO sd(12), CCH ₃ ad ² (11)
1458	1458	0	CCH ₃ ad ¹ (61), CCH ₃ ad ² (26), CH_3 r ¹ (7)
1458	1465	7	CCH ₃ ad ² (54), CCH ₃ ad ¹ (24), CH_3 r ² (7)
1562	1567	5	COO as(87), CCOO r(7)
1596	1588	-8	NH_2 sissor(100)
2885	2884	-1	C^αH s(98)
2940	2909	-31	CH_3 ss(83), CH_3 as ² (15)

Table 3.49: (continued)

frequency (cm ⁻¹)			Potential Energy Distribution
obs.	calc.	dev.	
2980	2959	-21	CH ₃ as ¹ (56), CH ₃ as ² (40)
2993	3036	43	CH ₃ as ² (45), CH ₃ as ¹ (40), CH ₃ ss(15)
—	3144	—	NH ₂ as(98)
—	3246	—	NH ₂ ss(98)

frequency (cm ⁻¹)			Potential Energy Distribution
obs.	calc.	dev.	
—	60	—	CC t(98)
—	201	—	CN t(50), CC ^{me} t(47)
—	218	—	CN t(48), CC ^{me} t(44)
279	279	0	C ^α H d ² (59), CCOO r(17), C ^α H d ³ (7)
343	345	2	C ^α H d ³ (51), CCOO r(17), C ^α H d ² (8)
421	412	-9	C ^α H d ¹ (76), CCOO wag(7)
535	530	-5	CCOO r(41), CN ^{ter} s(16), CC ^{ter} s(11), C ^α H d ³ (10), CCOO sd(7)
632	620	-12	CCOO sd(27), CC ^{ter} s(25), CCOO wag(12), CC ^{me} s(11), CCOO r(10), C ^α H d ³ (7)
793	793	0	CCOO wag(43), CCOO sd(21)
851	847	-4	CN ^{ter} s(23), CCOO sd(18), CC ^{me} s(12), CH ₃ r ¹ (12), CCOO wag(8), COO ss(7)
924	921	-3	CH ₃ r ² (36), CN ^{ter} s(22), CC ^{ter} s(18), COO ss(12), CCOO sd(8)
—	947	—	NH ₂ wag(65), CH ₃ r ¹ (14), CC ^{me} s(11)
1019	1006	-13	NH ₂ twist(45), CC ^{me} s(15), CH ₃ r ¹ (13), C ^α H r ¹ (8)
1072	1074	2	C ^α H r ² (29), CCOO wag(14), NH ₂ wag(14), CH ₃ r ² (9), C ^α H d ³ (8), CH ₃ r ¹ (7)
1134	1142	8	CN ^{ter} s(26), CC ^{me} s(20), CH ₃ r ² (19), C ^α H r ¹ (8)
1234	1244	10	NH ₂ twist(30), CH ₃ r ¹ (25), C ^α H d ¹ (11)
1291	1280	-11	C ^α H r ² (38), COO ss(18), C ^α H r ¹ (14)
1360	1340	-20	CCH ₃ sd(49), C ^α H r ¹ (38), NH ₂ twist(7)
1370	1386	16	CCH ₃ sd(34), C ^α H r ¹ (21), CC ^{me} s(16), NH ₂ twist(13)
1414	1414	0	COO ss(46), CC ^{ter} s(18), CCOO sd(12), CCH ₃ ad ² (10)
1460	1460	0	CCH ₃ ad ¹ (60), CCH ₃ ad ² (28)

Table 3.49: (continued)

frequency (cm^{-1})			Potential Energy Distribution
obs.	calc.	dev.	
1460	1466	6	CCH ₃ ad ² (55), CCH ₃ ad ¹ (26)
1567	1567	0	COO as(86), CCOO r(7)
1593	1585	-8	NH ₂ sissor(100)
2885	2884	-1	C ^{α} H s(98)
2940	2914	-26	CH ₃ ss(85), CH ₃ as ² (13)
2980	2969	-11	CH ₃ as ¹ (56), CH ₃ as ² (42)
2993	3046	53	CH ₃ as ² (46), CH ₃ as ¹ (41), CH ₃ ss(14)
—	3136	—	NH ₂ as(98)
—	3241	—	NH ₂ ss(98)

Table 3.50: Scaled 6-31+G** Frequencies and Potential Energy Distribution for Isolated Alaninate.

frequency (cm ⁻¹)			NH ₂ CHCH ₃ COO ⁻ (mean deviation = 7 cm ⁻¹)
obs.	calc.	dev.	
			Potential Energy Distribution
—	64	—	CC t(98)
—	161	—	CN t(95)
—	209	—	CC ^{me} t(90)
279	281	2	C ^α H d ² (63), CCOO r(14)
343	348	5	C ^α H d ³ (52), CCOO r(22), C ^α H d ² (8)
415	414	-1	C ^α H d ¹ (79)
539	538	-1	CCOO r(32), CN ^{ter} s(16), CC ^{ter} s(15), CCOO sd(15), C ^α H d ³ (8)
622	620	-2	CCOO sd(29), CCOO r(16), CC ^{ter} s(15), C ^α H d ³ (12), CCOO wag(11), CC ^{me} s(8)
785	783	-2	CCOO wag(46), CCOO sd(21)
853	835	-18	CN ^{ter} s(18), CCOO sd(16), CC ^{ter} s(13), NH ₂ wag(10), CH ₃ r ¹ (10), CCOO wag(9), COO ss(8), CC ^{me} s(7)
927	916	-11	CH ₃ r ² (31), CN ^{ter} s(25), CC ^{ter} s(16), NH ₂ wag(16), COO ss(7)
—	959	—	NH ₂ wag(51), CH ₃ r ¹ (16), CC ^{me} s(13)
1020	1020	0	NH ₂ twist(44), CC ^{me} s(17), CH ₃ r ¹ (14), C ^α H r ¹ (7)
1080	1072	-8	C ^α H r ² (29), CH ₃ r ² (14), CCOO wag(11), NH ₂ wag(9), CH ₃ r ¹ (8)
1140	1159	19	CN ^{ter} s(28), CC ^{me} s(21), CH ₃ r ² (20)
1238	1247	9	CH ₃ r ¹ (30), NH ₂ twist(25), C ^α H r ² (14), C ^α H d ¹ (9)
1286	1288	2	C ^α H r ² (36), C ^α H r ¹ (20), COO ss(8), CC ^{me} s(7)
1353	1354	1	C ^α H r ¹ (48), CCH ₃ sd(31), NH ₂ twist(11)
1368	1373	5	CCH ₃ sd(55), CC ^{me} s(13), C ^α H r ¹ (13), NH ₂ twist(10)
1414	1415	1	COO ss(59), CC ^{ter} s(16), CCOO sd(10), CCH ₃ sd(7)
1459	1457	-2	CCH ₃ ad ² (49), CCH ₃ ad ¹ (41)
1459	1470	11	CCH ₃ ad ¹ (49), CCH ₃ ad ² (38)
1564	1567	3	COO as(80), NH ₂ sissor(8), CCOO r(7)
1591	1583	-8	NH ₂ sissor(92)
2885	2885	0	C ^α H s(98)
2940	2942	2	CH ₃ ss(94)
2980	2975	-5	CH ₃ as ¹ (50), CH ₃ as ² (47)
2993	2998	5	CH ₃ as ¹ (48), CH ₃ as ² (48)

Table 3.50: (continued)

frequency (cm^{-1})			Potential Energy Distribution
obs.	calc.	dev.	
—	3150	—	NH ₂ as(99)
—	3242	—	NH ₂ ss(99)

frequency (cm^{-1})			Potential Energy Distribution
obs.	calc.	dev.	
—	63	—	CC t(98)
—	117	—	CN t(99)
—	208	—	CC ^{me} t(93)
275	277	2	C ^{α} H d ² (56), CCOO r(17), C ^{α} H d ³ (12)
331	325	-6	C ^{α} H d ³ (46), C ^{α} H d ² (15), CCOO r(11), NH ₂ wag(8)
384	392	8	C ^{α} H d ¹ (76), NH ₂ twist(7)
527	522	-5	CCOO r(43), CN ^{ter} s(15), CC ^{ter} s(9), CCOO sd(9)
621	607	-14	CCOO sd(35), CC ^{ter} s(22), CCOO r(11), NH ₂ wag(9), CCOO wag(7)
—	747	—	NH ₂ wag(49), CCOO wag(33)
780	791	11	CCOO sd(30), CN ^{ter} s(16), CCOO wag(16), NH ₂ wag(11), COO ss(7)
836	821	-15	NH ₂ twist(64), CC ^{me} s(15)
870	863	-7	CH ₃ r ¹ (26), CC ^{ter} s(11), C ^{α} H d ³ (8), CCOO sd(8), CCOO wag(8), NH ₂ twist(8), NH ₂ wag(7)
922	918	-4	CH ₃ r ² (31), CN ^{ter} s(30), CC ^{ter} s(20), COO ss(8)
1053	1062	9	C ^{α} H r ² (29), CH ₃ r ¹ (15), CCOO wag(12), CH ₃ r ² (9), CC ^{me} s(7)
1108	1135	27	NH ₂ sissor(44), CH ₃ r ² (21), CN ^{ter} s(9), CC ^{me} s(8)
1143	1169	26	NH ₂ sissor(51), CN ^{ter} s(18), CC ^{me} s(10), CH ₃ r ² (7)
1201	1195	-6	CH ₃ r ¹ (31), CC ^{me} s(19), C ^{α} H d ¹ (13), NH ₂ twist(11)
1290	1285	-5	C ^{α} H r ² (49), CC ^{me} s(8), COO ss(7), CH ₃ r ¹ (7)
1334	1335	1	C ^{α} H r ¹ (79)
1370	1367	-3	CCH ₃ sd(83), CC ^{me} s(8)
1414	1415	1	COO ss(59), CC ^{ter} s(16), CCOO sd(10), CCH ₃ sd(7)
1462	1457	-5	CCH ₃ ad ² (47), CCH ₃ ad ¹ (43)
1462	1471	9	CCH ₃ ad ¹ (47), CCH ₃ ad ² (40)
1571	1567	-4	COO as(87), CCOO r(7)

Table 3.50: (continued)

frequency (cm ⁻¹)			Potential Energy Distribution
obs.	calc.	dev.	
—	2315	—	NH ₂ as(93), NH ₂ ss(7)
—	2346	—	NH ₂ ss(93), NH ₂ as(7)
2887	2885	-2	C ^α H s(98)
2942	2942	0	CH ₃ ss(94)
2980	2975	-5	CH ₃ as ¹ (50), CH ₃ as ² (47)
2990	2998	8	CH ₃ as ¹ (48), CH ₃ as ² (48)

frequency (cm ⁻¹)			Potential Energy Distribution
obs.	calc.	dev.	
—	62	—	CC t(98)
—	146	—	CC ^{me} t(80), CN t(17)
—	165	—	CN t(81), CC ^{me} t(16)
257	254	-3	C ^α H d ² (69), CCOO r(8)
335	339	4	C ^α H d ³ (57), CCOO r(28)
382	379	-3	C ^α H d ¹ (76), CH ₃ r ¹ (7)
514	522	8	CCOO r(26), CC ^{ter} s(22), CCOO sd(20), CN ^{ter} s(12), C ^α H d ³ (7)
593	588	-5	CCOO r(23), CCOO sd(18), CC ^{ter} s(13), C ^α H d ³ (11), CCOO wag(11), C ^α H r ² (9), CC ^{me} s(8)
688	674	-14	CH ₃ r ¹ (34), C ^α H r ² (27), CCOO wag(19), CH ₃ r ² (7)
752	756	4	CH ₃ r ² (38), CN ^{ter} s(25), CC ^{me} s(8)
827	810	-17	CCOO sd(38), CH ₃ r ² (20), COO ss(12), CC ^{ter} s(10)
884	870	-14	C ^α H r ¹ (32), NH ₂ wag(25), CN ^{ter} s(23), NH ₂ twist(7)
897	893	-4	C ^α H r ² (31), CCOO wag(13), CH ₃ r ¹ (12), CCH ₃ sd(11), CC ^{me} s(10), CC ^{ter} s(8)
947	950	3	NH ₂ wag(41), C ^α H r ¹ (25), CH ₃ r ¹ (13), C ^α H r ² (7)
—	967	—	CCOO wag(26), CCH ₃ sd(18), CH ₃ r ¹ (10), C ^α H d ² (9), CC ^{me} s(7), C ^α H r ¹ (7)
1055	1051	-4	CCH ₃ ad ² (64), CCH ₃ ad ¹ (34)
1055	1058	3	CCH ₃ ad ¹ (54), CCH ₃ ad ² (32)
—	1076	—	CCH ₃ sd(38), NH ₂ wag(12), CCH ₃ ad ¹ (10), C ^α H r ² (9), C ^α H d ³ (8), CH ₃ r ¹ (7)

Table 3.50: (continued)

frequency (cm ⁻¹)			Potential Energy Distribution
obs.	calc.	dev.	
1126	1124	-2	C ^α H r ¹ (19), NH ₂ twist(17), CC ^{ter} s(13), CCH ₃ sd(10), CC ^{me} s(8), CH ₃ r ² (7)
1158	1166	8	CN ^{ter} s(26), NH ₂ twist(23), CC ^{me} s(10), C ^α H d ¹ (7), CH ₃ r ² (7)
1276	1301	25	NH ₂ twist(38), CC ^{me} s(32)
1408	1413	5	COO ss(67), CC ^{ter} s(18), CCOO sd(11)
1555	1565	10	COO as(85), CCOO r(7)
1582	1581	-1	NH ₂ sissor(97)
2076	2114	38	CH ₃ ss(89), C ^α H s(9)
2125	2125	0	C ^α H s(88), CH ₃ ss(9)
2235	2203	-32	CH ₃ as ¹ (52), CH ₃ as ² (47)
2246	2220	-26	CH ₃ as ² (52), CH ₃ as ¹ (46)
—	3150	—	NH ₂ as(99)
—	3242	—	NH ₂ ss(99)

frequency (cm ⁻¹)			ND ₂ CD ₂ CD ₃ COO ⁻ (mean deviation = 12 cm ⁻¹)
obs.	calc.	dev.	
—	61	—	CC t(98)
—	116	—	CN t(96)
—	150	—	CC ^{me} t(93)
257	252	-5	C ^α H d ² (68), CCOO r(9)
327	315	-12	C ^α H d ³ (56), CCOO r(19), NH ₂ wag(9)
363	359	-4	C ^α H d ¹ (73)
506	510	4	CCOO r(38), CC ^{ter} s(15), CCOO sd(13), CN ^{ter} s(11)
590	579	-11	CCOO sd(25), CC ^{ter} s(20), CCOO r(18), CCOO wag(8), CC ^{me} s(7), C ^α H r ² (7)
690	669	-21	CH ₃ r ¹ (30), C ^α H r ² (29), CCOO wag(22)
729	733	4	CH ₃ r ² (26), NH ₂ twist(21), CH ₃ r ¹ (14), NH ₂ wag(13), C ^α H r ¹ (10)
756	757	1	NH ₂ wag(52), CN ^{ter} s(20), CH ₃ r ² (18)
790	780	-10	NH ₂ twist(26), CC ^{me} s(24), CCOO sd(19), CN ^{ter} s(11), CCH ₃ sd(10)

Table 3.50: (continued)

frequency (cm ⁻¹)			Potential Energy Distribution
obs.	calc.	dev.	
845	832	-13	CCOO sd(25), CC ^{ter} s(15), CH ₃ r ² (13), COO ss(12), NH ₂ twist(12)
893	896	3	C ^α H r ² (35), CCOO wag(19), CH ₃ r ¹ (11), CN ^{ter} s(7)
940	947	7	C ^α H r ¹ (45), CCOO wag(18), CN ^{ter} s(8)
1036	1025	-11	NH ₂ twist(19), CH ₃ r ¹ (19), CCH ₃ sd(12), C ^α H d ¹ (9), C ^α H d ² (9), C ^α H r ¹ (8)
1055	1050	-5	CCH ₃ ad ¹ (46), CCH ₃ ad ² (44)
1055	1055	0	CCH ₃ ad ² (43), CCH ₃ sd(20), CCH ₃ ad ¹ (14)
—	1069	—	CCH ₃ ad ¹ (37), CCH ₃ sd(34), CCH ₃ ad ² (10), C ^α H r ² (7)
1123	1118	-5	NH ₂ sissor(39), C ^α H r ¹ (11), CN ^{ter} s(10), CH ₃ r ² (10), CC ^{ter} s(8), C ^α H d ¹ (7)
1182	1178	-4	NH ₂ sissor(59), CN ^{ter} s(17)
1215	1252	37	CC ^{me} s(53), NH ₂ twist(7)
1409	1412	3	COO ss(68), CC ^{ter} s(18), CCOO sd(12)
1567	1565	-2	COO as(88), CCOO r(7)
2076	2114	38	CH ₃ ss(88), C ^α H s(10)
2125	2125	0	C ^α H s(87), CH ₃ ss(10)
2235	2203	-32	CH ₃ as ¹ (52), CH ₃ as ² (47)
2246	2219	-27	CH ₃ as ² (52), CH ₃ as ¹ (46)
—	2315	—	NH ₂ as(93), NH ₂ ss(7)
—	2346	—	NH ₂ ss(93), NH ₂ as(7)

frequency (cm ⁻¹)			NH ₂ CHCD ₃ COO ⁻ (mean deviation = 8 cm ⁻¹)
obs.	calc.	dev.	
			Potential Energy Distribution
—	62	—	CC t(98)
—	146	—	CC ^{me} t(80), CN t(17)
—	166	—	CN t(81), CC ^{me} t(16)
255	255	0	C ^α H d ² (68), CCOO r(9)
340	342	2	C ^α H d ³ (56), CCOO r(27)
390	382	-8	C ^α H d ¹ (75), CH ₃ r ¹ (7)
521	528	7	CCOO r(31), CC ^{ter} s(19), CCOO sd(17), CN ^{ter} s(13), C ^α H d ³ (7)

Table 3.50: (continued)

frequency (cm^{-1})			Potential Energy Distribution
obs.	calc.	dev.	
607	604	-3	CCOO sd(23), CCOO r(18), CC^{ter} s(16), $\text{C}^{\alpha}\text{H}$ d ³ (12), CC^{me} s(11), CCOO wag(7)
741	719	-22	CCOO wag(41), CH_3 r ¹ (33), CH_3 r ² (15), $\text{C}^{\alpha}\text{H}$ r ² (7)
771	766	-5	CN^{ter} s(31), CH_3 r ² (28), CH_3 r ¹ (18), CC^{me} s(7), CCOO sd(7)
828	810	-18	CCOO sd(37), CH_3 r ² (20), COO ss(12), CC^{ter} s(10)
910	906	-4	NH_2 wag(55), CH_3 r ¹ (14), CCOO wag(10)
947	948	1	CCH ₃ sd(34), CC^{me} s(17), NH_2 twist(15), CC^{ter} s(7)
1020	1028	8	NH_2 wag(22), CC^{ter} s(15), CCOO wag(14), $\text{C}^{\alpha}\text{H}$ r ² (10), $\text{C}^{\alpha}\text{H}$ d ³ (9), $\text{C}^{\alpha}\text{H}$ d ² (8), COO ss(7)
1058	1049	-9	CCH ₃ ad ² (65), CCH ₃ ad ¹ (27)
1058	1058	0	CCH ₃ ad ¹ (64), CCH ₃ ad ² (16), CCH ₃ sd(8)
—	1069	—	CCH ₃ sd(24), CN^{ter} s(20), CCH ₃ ad ² (18), NH_2 twist(10)
1141	1159	18	CC^{me} s(26), CN^{ter} s(20), CCH ₃ sd(17), $\text{C}^{\alpha}\text{H}$ r ² (11), NH_2 twist(9)
1189	1192	3	$\text{C}^{\alpha}\text{H}$ r ² (33), NH_2 twist(27), CH_3 r ¹ (11), $\text{C}^{\alpha}\text{H}$ r ¹ (7)
1283	1283	0	$\text{C}^{\alpha}\text{H}$ r ² (31), $\text{C}^{\alpha}\text{H}$ r ¹ (25), CC^{me} s(14)
1360	1359	-1	$\text{C}^{\alpha}\text{H}$ r ¹ (58), NH_2 twist(22), CC^{me} s(10)
1413	1413	0	COO ss(67), CC^{ter} s(18), CCOO sd(11)
1563	1566	3	COO as(82), CCOO r(7)
1587	1582	-5	NH_2 sissor(94)
2076	2115	39	CH_3 ss(98)
2125	2202	77	CH_3 as ¹ (56), CH_3 as ² (44)
2235	2219	-16	CH_3 as ² (55), CH_3 as ¹ (44)
—	2886	—	$\text{C}^{\alpha}\text{H}$ s(100)
—	3150	—	NH_2 as(99)
—	3242	—	NH_2 ss(99)

frequency (cm^{-1})			ND ₂ CHCD ₃ COO ⁻ (mean deviation = 12 cm^{-1})
obs.	calc.	dev.	
—	61	—	CC t(98)
—	116	—	CN t(96)
—	150	—	CC^{me} t(94)

Table 3.50: (continued)

frequency (cm ⁻¹)			Potential Energy Distribution
obs.	calc.	dev.	
258	253	-5	C ^α H d ² (66), CCOO r(10)
320	318	-2	C ^α H d ³ (56), CCOO r(18), NH ₂ wag(10)
348	361	13	C ^α H d ¹ (71)
512	515	3	CCOO r(43), CC ^{ter} s(12), CN ^{ter} s(12), CCOO sd(11)
595	593	-2	CCOO sd(30), CC ^{ter} s(23), CCOO r(14), CC ^{me} s(9), NH ₂ wag(8)
—	716	—	CCOO wag(45), CH ₃ r ¹ (24), CH ₃ r ² (16), C ^α H r ² (7)
723	749	26	CH ₃ r ¹ (34), NH ₂ twist(18), CH ₃ r ² (18), NH ₂ wag(12), CN ^{ter} s(8)
751	759	8	NH ₂ wag(56), CN ^{ter} s(16), CH ₃ r ² (16), C ^α H d ³ (7)
799	785	-14	NH ₂ twist(27), CCOO sd(26), CC ^{me} s(19), CN ^{ter} s(9), CCH ₃ sd(9)
852	839	-13	NH ₂ twist(23), CCOO sd(18), CC ^{ter} s(14), CH ₃ r ² (12), CCOO wag(10), COO ss(9)
988	1006	18	CC ^{ter} s(17), CCH ₃ sd(17), CCOO wag(14), C ^α H d ³ (11), C ^α H r ² (10), COO ss(7)
1028	1019	-9	CCH ₃ sd(48), CH ₃ r ¹ (10), C ^α H d ² (9), NH ₂ twist(9)
1056	1050	-6	CCH ₃ ad ² (55), CCH ₃ ad ¹ (43)
1056	1060	4	CCH ₃ ad ¹ (53), CCH ₃ ad ² (42)
1109	1097	-12	CN ^{ter} s(29), NH ₂ sissor(14), C ^α H d ¹ (13), CH ₃ r ² (11), NH ₂ twist(8), CH ₃ r ¹ (7)
1131	1163	32	NH ₂ sissor(78), CN ^{ter} s(9)
—	1170	—	CC ^{me} s(32), C ^α H r ² (28), CCH ₃ sd(18)
1281	1276	-5	C ^α H r ² (43), CC ^{me} s(22)
1332	1330	-2	C ^α H r ¹ (83)
1412	1413	1	COO ss(67), CC ^{ter} s(18), CCOO sd(11)
1576	1566	-10	COO as(87), CCOO r(7)
2076	2115	39	CH ₃ ss(98)
2125	2202	77	CH ₃ as ¹ (56), CH ₃ as ² (44)
2235	2219	-16	CH ₃ as ² (55), CH ₃ as ¹ (44)
2246	2315	69	NH ₂ as(93), NH ₂ ss(7)
—	2346	—	NH ₂ ss(93), NH ₂ as(7)
—	2887	—	C ^α H s(100)

Table 3.50: (continued)

frequency (cm ⁻¹)			Potential Energy Distribution
obs.	calc.	dev.	
frequency (cm ⁻¹)			Potential Energy Distribution
obs.	calc.	dev.	
—	64	—	CC t(98)
—	161	—	CN t(95)
—	209	—	CC ^{me} t(90)
273	278	5	C ^α H d ² (64), CCOO r(13)
344	347	3	C ^α H d ³ (52), CCOO r(23), C ^α H d ² (7)
409	411	2	C ^α H d ¹ (79)
538	538	0	CCOO r(31), CN ^{ter} s(16), CC ^{ter} s(15), CCOO sd(15), C ^α H d ³ (8)
624	617	-7	CCOO sd(29), CCOO r(16), CC ^{ter} s(15), C ^α H d ³ (12), CCOO wag(11), CC ^{me} s(9)
779	782	3	CCOO wag(45), CCOO sd(22)
849	833	-16	CN ^{ter} s(18), CCOO sd(16), CC ^{ter} s(12), CH ₃ r ¹ (11), CCOO wag(10), NH ₂ wag(9), COO ss(8), CC ^{me} s(8)
922	912	-10	CH ₃ r ² (33), CN ^{ter} s(25), CC ^{ter} s(15), NH ₂ wag(14)
—	955	—	NH ₂ wag(53), CH ₃ r ¹ (15), CC ^{me} s(14)
1015	1017	2	NH ₂ twist(43), CC ^{me} s(18), CH ₃ r ¹ (15)
1073	1070	-3	C ^α H r ² (28), CH ₃ r ² (13), CCOO wag(11), NH ₂ wag(10), CH ₃ r ¹ (8)
1134	1154	20	CN ^{ter} s(29), CC ^{me} s(20), CH ₃ r ² (19)
1231	1240	9	CH ₃ r ¹ (29), NH ₂ twist(26), C ^α H r ² (15), C ^α H d ¹ (9)
1288	1287	-1	C ^α H r ² (36), C ^α H r ¹ (20), COO ss(8), CC ^{me} s(7)
1355	1350	-5	CCH ₃ sd(60), C ^α H r ¹ (27)
1360	1364	4	C ^α H r ¹ (34), CCH ₃ sd(29), NH ₂ twist(16), CC ^{me} s(12)
1412	1415	3	COO ss(60), CC ^{ter} s(16), CCOO sd(10)
1458	1455	-3	CCH ₃ ad ² (48), CCH ₃ ad ¹ (41)
1458	1468	10	CCH ₃ ad ¹ (48), CCH ₃ ad ² (39)
1562	1567	5	COO as(80), NH ₂ sissor(8), CCOO r(7)
1596	1583	-13	NH ₂ sissor(92)
2885	2885	0	C ^α H s(98)
2940	2939	-1	CH ₃ ss(92), CH ₃ as ² (7)
2980	2965	-15	CH ₃ as ¹ (50), CH ₃ as ² (46)

Table 3.50: (continued)

frequency (cm ⁻¹)			Potential Energy Distribution
obs.	calc.	dev.	
2993	2988	-5	CH ₃ as ¹ (48), CH ₃ as ² (47)
—	3150	—	NH ₂ as(99)
—	3242	—	NH ₂ ss(99)

frequency (cm ⁻¹)			Potential Energy Distribution
obs.	calc.	dev.	
—	64	—	CC t(98)
—	161	—	CN t(95)
—	209	—	CC ^{me} t(90)
279	280	1	C ^α H d ² (63), CCOO r(14)
343	344	1	C ^α H d ³ (52), CCOO r(21), C ^α H d ² (8)
421	412	-9	C ^α H d ¹ (78)
535	533	-2	CCOO r(32), CN ^{ter} s(18), CC ^{ter} s(15), CCOO sd(14), C ^α H d ³ (8)
632	620	-12	CCOO sd(29), CCOO r(16), CC ^{ter} s(15), C ^α H d ³ (12), CCOO wag(11), CC ^{me} s(8)
793	782	-11	CCOO wag(45), CCOO sd(22)
851	831	-20	CN ^{ter} s(20), CCOO sd(15), NH ₂ wag(12), CCOO wag(11), CC ^{ter} s(10), CH ₃ r ¹ (10), COO ss(7)
924	910	-14	CH ₃ r ² (30), CN ^{ter} s(22), CC ^{ter} s(18), NH ₂ wag(16), COO ss(8)
—	956	—	NH ₂ wag(50), CH ₃ r ¹ (15), CC ^{me} s(13)
1019	1019	0	NH ₂ twist(44), CC ^{me} s(16), CH ₃ r ¹ (14), C ^α H r ¹ (7)
1072	1071	-1	C ^α H r ² (29), CH ₃ r ² (13), CCOO wag(11), NH ₂ wag(9), CH ₃ r ¹ (8)
1134	1156	22	CN ^{ter} s(26), CC ^{me} s(21), CH ₃ r ² (21)
1234	1245	11	CH ₃ r ¹ (30), NH ₂ twist(26), C ^α H r ² (14), C ^α H d ¹ (9)
1291	1287	-4	C ^α H r ² (36), C ^α H r ¹ (19), COO ss(8), CC ^{me} s(7)
1360	1352	-8	C ^α H r ¹ (51), CCH ₃ sd(27), NH ₂ twist(11)
1370	1372	2	CCH ₃ sd(59), CC ^{me} s(13), C ^α H r ¹ (11), NH ₂ twist(8)
1414	1415	1	COO ss(59), CC ^{ter} s(16), CCOO sd(10), CCH ₃ sd(7)
1460	1457	-3	CCH ₃ ad ² (49), CCH ₃ ad ¹ (41)
1460	1470	10	CCH ₃ ad ¹ (49), CCH ₃ ad ² (38)

Table 3.50: (continued)

frequency (cm^{-1})			Potential Energy Distribution
obs.	calc.	dev.	
1567	1566	-1	COO as(78), NH ₂ sissor(11)
1593	1581	-12	NH ₂ sissor(89), COO as(9)
2885	2885	0	C ^{α} H s(98)
2940	2942	2	CH ₃ ss(94)
2980	2975	-5	CH ₃ as ¹ (50), CH ₃ as ² (47)
2993	2998	5	CH ₃ as ¹ (48), CH ₃ as ² (48)
—	3142	—	NH ₂ as(99)
—	3237	—	NH ₂ ss(99)

Tables 3.52, 3.53, 3.54, 3.55, 3.56, and 3.57 list the observed and calculated frequencies and potential energy distributions (PED) for the alaninate one water supermolecule, the water-excluded one water alaninate (CO₂ bridged) using the 4-31G, 4-31G*, 6-31G**, 6-31+G** basis sets and for alaninate NH-CO bridged using the 4-31G basis set, respectively. Scale factors determined using the SQMFF method for each of the basis sets and the two geometries are listed in table 3.51.

Table 3.51: Scale factors for alanine in base one-water supermolecule and water-excluded structures using different basis sets.

Coordinate	super- molecule	NH-OC bridge	CO ₂ bridge	4-31G*	6-31G**	6-31+G**
COO ss	85.59	88.14	86.78	76.50	76.91	77.57
COO as	78.38	75.21	78.97	68.47	69.46	73.70
C ^α H s	82.91	82.47	82.89	83.04	83.86	80.84
CC ^{me} s	95.30	95.10	95.00	93.20	90.00	96.60
CC ^{ter} s	100.80	102.00	101.00	101.50	98.40	98.00
CN ^{ter} s	79.84	83.20	84.00	76.50	76.80	75.80
NH ₂ ss	77.00	77.00	77.00	77.00	77.00	77.00
NH ₂ as	70.00	70.00	70.00	70.00	70.00	70.00
C ^α H r ¹	81.07	78.70	80.62	78.50	81.50	79.90
C ^α H r ²	73.65	74.50	74.69	79.00	80.05	80.30
C ^α H d ¹	87.56	83.96	85.35	88.40	87.85	99.73
C ^α H d ²	75.85	64.83	59.10	60.80	60.57	95.95
C ^α H d ³	84.59	90.01	78.87	77.38	78.13	85.10
CCOO sd	82.59	83.60	77.47	73.30	86.00	73.80
CCOO r	96.47	91.18	93.51	100.93	103.00	97.30
CCOO wag	88.31	95.00	95.78	82.00	81.27	78.60
NH ₂ sissor	71.92	71.82	71.86	72.94	75.78	76.31
NH ₂ twist	77.28	78.10	77.60	75.40	78.74	80.90
NH ₂ wag	84.81	87.50	83.40	68.00	72.09	76.70
CCH ₃ sd	77.20	76.70	76.69	77.63	80.04	79.75
CCH ₃ ad ¹	77.56	77.80	78.14	78.70	81.02	82.05
CCH ₃ ad ²	77.32	76.89	76.65	78.10	79.60	80.60
CH ₃ r ¹	80.74	84.20	81.40	85.00	86.60	83.80
CH ₃ r ²	78.70	76.00	79.10	82.90	84.48	84.10
CH ₃ ss	85.90	84.90	84.89	84.30	85.18	85.18
CH ₃ as ¹	85.17	86.24	86.17	86.82	87.63	87.26
CH ₃ as ²	84.39	83.23	83.23	82.74	84.10	84.33
CN t	94.00	100.00	94.00	94.00	94.00	94.00
CC t	100.00	100.00	100.00	100.00	100.00	100.00
CC ^{me} t	70.00	60.00	60.00	60.00	60.00	60.00

Table 3.52: Scaled 4-31G Frequencies and Potential Energy Distribution for Alaninate One-water Supramolecule.

frequency (cm ⁻¹)			NH ₂ CHCH ₃ CO ₂ ⁻ ·H ₂ O (mean deviation = 10 cm ⁻¹)
obs.	calc.	dev.	
Potential Energy Distribution			
—	39	—	CO* t(98)
—	49	—	CC t(89)
—	76	—	COH* b(39), OHO* b(38), Hb1* s(16)
—	168	—	CN t(92)
—	185	—	Hb1* s(91), COH* b(16)
—	212	—	CC ^{me} t(91)
279	269	-10	C ^α H d ² (42), OHO* b(29), CCOO r(16), C ^α H d ³ (14)
—	321	—	COH* b(31), C ^α H d ² (24), OHO* b(19), C ^α H d ³ (7)
343	351	8	C ^α H d ³ (38), OHO* b(26), COH* b(14), CCOO r(11)
—	407	—	COHO* t(167)
415	415	0	C ^α H d ¹ (77)
539	539	0	CCOO r(39), CN ^{ter} s(13), CCOO sd(12), C ^α H d ³ (11), CC ^{ter} s(10)
622	615	-7	CCOO sd(34), CC ^{ter} s(19), CCOO wag(12), CCOO r(11), CC ^{me} s(9), C ^α H d ³ (8)
785	764	-21	CCOO wag(36), OHOH* t(28), CCOO sd(16)
—	813	—	OHOH* t(113), CO* t(10), CCOO sd(7), CCOO wag(7)
853	837	-16	CN ^{ter} s(16), CCOO sd(13), CH ₃ r ¹ (12), CC ^{ter} s(11), CCOO wag(11), OHOH* t(10), COO ss(8), CC ^{me} s(8), NH ₂ wag(8)
927	916	-11	CH ₃ r ² (31), CN ^{ter} s(26), CC ^{ter} s(15), NH ₂ wag(15), COO ss(8)
—	956	—	NH ₂ wag(50), CH ₃ r ¹ (17), CC ^{me} s(15)
1020	1012	-8	NH ₂ twist(39), CC ^{me} s(20), CH ₃ r ¹ (17), C ^α H r ¹ (7)
1080	1080	0	C ^α H r ² (22), CH ₃ r ² (20), NH ₂ wag(12), CCOO wag(10), CH ₃ r ¹ (8)
1140	1157	17	CN ^{ter} s(31), CC ^{me} s(21), CH ₃ r ² (15), C ^α H r ¹ (7)
1238	1247	9	NH ₂ twist(27), CH ₃ r ¹ (25), C ^α H r ² (15), C ^α H d ¹ (9)
1286	1284	-2	C ^α H r ² (42), C ^α H r ¹ (21), COO ss(9)
1353	1359	6	C ^α H r ¹ (41), CCH ₃ sd(33), NH ₂ twist(14)
1368	1374	6	CCH ₃ sd(54), C ^α H r ¹ (15), NH ₂ twist(12), CC ^{me} s(10)
1414	1412	-2	COO ss(52), CC ^{ter} s(20), CCOO sd(10), CCH ₃ sd(7)
1459	1459	0	CCH ₃ ad ¹ (80), CCH ₃ ad ² (10)
1459	1465	6	CCH ₃ ad ² (78), CCH ₃ ad ¹ (10)

Table 3.52: (continued)

frequency (cm^{-1})			Potential Energy Distribution
obs.	calc.	dev.	
1564	1564	0	COO as(87)
1591	1589	-2	NH ₂ sissor(100)
1648	1671	23	HOH* b(99)
2885	2886	1	C α H s(98)
2940	2931	-9	CH ₃ ss(80), CH ₃ as ¹ (15)
2980	2968	-12	CH ₃ as ¹ (61), CH ₃ as ² (34)
2993	3040	47	CH ₃ as ² (61), CH ₃ as ¹ (23), CH ₃ ss(16)
—	3167	—	NH ₂ as(97)
—	3250	—	NH ₂ ss(96)
—	3510	—	HO2* s(70), HO1* s(29)
—	3561	—	HO1* s(70), HO2* s(30)

frequency (cm^{-1})			ND ₂ CHCH ₃ CO ₂ ⁻ ·D ₂ O (mean deviation = 12 cm^{-1})
obs.	calc.	dev.	
—	39	—	CO* t(96)
—	47	—	CC t(83), CO* t(8), CN t(7)
—	72	—	OHO* b(42), COH* b(35), Hb1* s(17)
—	124	—	CN t(90), CC t(9)
—	177	—	Hb1* s(90), COH* b(18)
—	211	—	CC ^{me} t(93)
—	221	—	OHO* b(65), COH* b(23), C α H d ² (8), C α H d ³ (8), CCOO r(7)
269	285	16	C α H d ² (40), COH* b(21), COHO* t(18), C α H d ³ (8), CCOO r(8)
—	293	—	COHO* t(151)
331	323	-8	C α H d ³ (41), C α H d ² (17), CCOO wag(7), NH ₂ wag(7)
384	391	7	C α H d ¹ (75), NH ₂ twist(8)
527	524	-3	CCOO r(48), CN ^{ter} s(12), COO as(7), C α H d ³ (7), CCOO sd(7)
—	583	—	OHOH* t(130), CO* t(7)
621	612	-9	CCOO sd(35), CC ^{ter} s(21), OHOH* t(19), CCOO r(7), CCOO wag(7)
—	745	—	NH ₂ wag(46), CCOO wag(36)

Table 3.52: (continued)

frequency (cm^{-1})			Potential Energy Distribution
obs.	calc.	dev.	
780	787	7	CCOO sd(27), NH_2 wag(19), CN^{ter} s(16), CCOO wag(12), COO ss(8)
836	824	-12	NH_2 twist(57), CC^{me} s(20)
870	862	-8	CH_3 r^1 (29), NH_2 twist(13), CC^{ter} s(10), CCOO sd(7)
922	916	-6	CH_3 r^2 (31), CN^{ter} s(27), CC^{ter} s(20), COO ss(10)
1053	1066	13	C^αH r^2 (23), CH_3 r^1 (16), CH_3 r^2 (12), CCOO wag(11)
1108	1129	21	NH_2 sissor(31), CH_3 r^2 (22), CC^{me} s(13), CN^{ter} s(13)
1143	1175	32	NH_2 sissor(40), CC^{me} s(20), CH_3 r^1 (14), CN^{ter} s(7)
1201	1190	-11	NH_2 sissor(25), CH_3 r^1 (15), CN^{ter} s(11), C^αH d^1 (10), CH_3 r^2 (10), NH_2 twist(9)
—	1223	—	HOH^* b(97)
1290	1282	-8	C^αH r^2 (55), C^αH r^1 (8), COO ss(7)
1334	1332	-2	C^αH r^1 (77)
1370	1370	0	CCH_3 sd(86)
1414	1416	2	COO ss(52), CC^{ter} s(19), CCOO sd(11), CCH_3 ad^2 (7)
1462	1459	-3	CCH_3 ad^1 (78), CCH_3 ad^2 (12)
1462	1467	5	CCH_3 ad^2 (74), CCH_3 ad^1 (12)
1571	1563	-8	COO as(87)
—	2329	—	NH_2 as(68), NH_2 ss(32)
—	2352	—	NH_2 ss(68), NH_2 as(32)
—	2526	—	$\text{HO}2^*$ s(59), $\text{HO}1^*$ s(41)
—	2609	—	$\text{HO}1^*$ s(58), $\text{HO}2^*$ s(41)
2887	2886	-1	C^αH s(98)
2942	2931	-11	CH_3 ss(80), CH_3 as^1 (15)
2980	2968	-12	CH_3 as^1 (61), CH_3 as^2 (34)
2990	3040	50	CH_3 as^2 (61), CH_3 as^1 (23), CH_3 ss(16)

frequency (cm^{-1})			Potential Energy Distribution
obs.	calc.	dev.	
—	38	—	CO^* t(94)
—	48	—	CC t(86), CO^* t(8)
—	75	—	COH^* b(39), OHO^* b(38), $\text{Hb}1^*$ s(15)
—	150	—	CC^{me} t(87), CN t(10)

Table 3.52: (continued)

frequency (cm ⁻¹)			Potential Energy Distribution
obs.	calc.	dev.	
—	170	—	CN t(85), CC ^{me} t(9)
—	183	—	Hb1* s(95), COH* b(15)
257	250	-7	C ^α H d ² (55), OHO* b(25), CCOO r(10)
—	311	—	COH* b(24), OHO* b(20), C ^α H d ³ (19), C ^α H d ² (12), CCOO r(7)
335	347	12	C ^α H d ³ (34), OHO* b(32), COH* b(21), CCOO r(11)
382	378	-4	C ^α H d ¹ (73), CH ₃ r ¹ (8)
—	407	—	COHO* t(169)
514	526	12	CCOO r(35), CC ^{ter} s(16), CCOO sd(16), CN ^{ter} s(10), C ^α H d ³ (9)
593	583	-10	CCOO sd(23), CC ^{ter} s(17), CCOO r(16), CCOO wag(12), CC ^{me} s(9), C ^α H r ² (8), C ^α H d ³ (8)
688	668	-20	CH ₃ r ¹ (37), C ^α H r ² (22), CCOO wag(20)
752	753	1	CH ₃ r ² (34), CN ^{ter} s(22), CC ^{me} s(10), CCOO sd(7)
—	800	—	OHOH* t(84), CH ₃ r ² (16), CCOO sd(12)
827	813	-14	OHOH* t(60), CCOO sd(23), COO ss(10), CH ₃ r ² (9), CC ^{ter} s(7)
884	866	-18	C ^α H r ¹ (34), CN ^{ter} s(24), NH ₂ wag(21), NH ₂ twist(8)
897	893	-4	C ^α H r ² (30), CC ^{me} s(12), CCOO wag(11), CCH ₃ sd(10), CH ₃ r ¹ (10), CC ^{ter} s(9)
947	951	4	C ^α H r ¹ (31), NH ₂ wag(23), CH ₃ r ¹ (22)
—	965	—	NH ₂ wag(24), CCOO wag(21), CCH ₃ sd(14), C ^α H r ² (13), CC ^{me} s(8), C ^α H d ² (7)
1055	1052	-3	CCH ₃ ad ¹ (71), CCH ₃ ad ² (18)
1055	1057	2	CCH ₃ ad ² (80), CCH ₃ ad ¹ (17)
—	1073	—	CCH ₃ sd(42), NH ₂ wag(13), C ^α H r ² (10), CCH ₃ ad ¹ (10), C ^α H d ³ (7)
1126	1120	-6	C ^α H r ¹ (17), CCH ₃ sd(14), CC ^{ter} s(12), NH ₂ twist(11), CC ^{me} s(10), COO ss(8), CN ^{ter} s(7), CH ₃ r ² (7)
1158	1174	16	CN ^{ter} s(30), NH ₂ twist(18), CC ^{me} s(11)
1276	1301	25	NH ₂ twist(47), CC ^{me} s(24)
1408	1409	1	COO ss(60), CC ^{ter} s(22), CCOO sd(12)
1555	1561	6	COO as(88)
1582	1588	6	NH ₂ sissor(100)

Table 3.52: (continued)

frequency (cm^{-1})			Potential Energy Distribution
obs.	calc.	dev.	
1648	1671	23	HOH* b(99)
2076	2112	36	CH ₃ ss(93)
2125	2125	0	C α H s(96)
2235	2196	-39	CH ₃ as ¹ (73), CH ₃ as ² (25)
2246	2246	0	CH ₃ as ² (73), CH ₃ as ¹ (22)
—	3166	—	NH ₂ as(97)
—	3250	—	NH ₂ ss(96)
—	3510	—	HO2* s(70), HO1* s(29)
—	3561	—	HO1* s(70), HO2* s(30)

frequency (cm^{-1})			Potential Energy Distribution
obs.	calc.	dev.	
	38	—	CO* t(92)
	46	—	CC t(81), CO* t(11)
	71	—	OHO* b(42), COH* b(35), Hb1* s(15)
	123	—	CN t(88), CC t(8)
	152	—	CC ^{me} t(93)
	175	—	Hb1* s(95), COH* b(19)
	217	—	OHO* b(70), C α H d ² (14), COH* b(14), C α H d ³ (9), CCOO r(8)
	267	10	C α H d ² (49), COH* b(29)
	292	—	COHO* t(167)
	313	-14	C α H d ³ (51), CCOO r(12), NH ₂ wag(8)
	358	-5	C α H d ¹ (70), CH ₃ r ¹ (7)
	513	7	CCOO r(44), CCOO sd(11), CC ^{ter} s(10), CN ^{ter} s(9), C α H d ³ (7)
	571	-19	OHOH* t(51), CCOO sd(16), CC ^{ter} s(13), CCOO r(9), CCOO wag(8)
	593	-7	OHOH* t(95), CCOO sd(12), CC ^{ter} s(9), CO* t(8)
	668	-15	CH ₃ r ¹ (34), C α H r ² (25), CCOO wag(23)
	732	3	CH ₃ r ² (27), NH ₂ twist(16), NH ₂ wag(14), CH ₃ r ¹ (12), C α H r ¹ (10), CCOO wag(7)
	758	2	NH ₂ wag(54), CN ^{ter} s(20), CH ₃ r ² (18)

Table 3.52: (continued)

frequency (cm^{-1})			Potential Energy Distribution
obs.	calc.	dev.	
	778	-12	NH ₂ twist(27), CC ^{me} s(25), CCOO sd(18), CN ^{ter} s(10), CCH ₃ sd(9)
	828	-17	CCOO sd(23), COO ss(14), CC ^{ter} s(14), CH ₃ r ² (13), NH ₂ twist(11)
	900	7	C ^{α} H r ² (38), CCOO wag(14), CH ₃ r ¹ (11), C ^{α} H r ¹ (8)
	942	2	C ^{α} H r ¹ (40), CCOO wag(20)
	1029	-7	CH ₃ r ¹ (20), NH ₂ twist(19), C ^{α} H r ¹ (8), C ^{α} H d ² (8), C ^{α} H d ¹ (7), C ^{α} H d ³ (7)
	1049	-6	CCH ₃ ad ¹ (64), CCH ₃ sd(20), CCH ₃ ad ² (7)
	1056	1	CCH ₃ ad ² (91)
	1068	—	CCH ₃ sd(48), CCH ₃ ad ¹ (31), C ^{α} H r ² (7)
	1118	-5	NH ₂ sissor(33), CN ^{ter} s(12), C ^{α} H r ¹ (11), CH ₃ r ² (10), CC ^{ter} s(8), C ^{α} H d ¹ (8)
	1188	6	NH ₂ sissor(65), CN ^{ter} s(17)
	1224	—	HOH* b(97)
	1237	22	CC ^{me} s(49), NH ₂ twist(9)
	1413	4	COO ss(61), CC ^{ter} s(22), CCOO sd(13)
	1561	-6	COO as(89)
	2111	35	CH ₃ ss(93)
	2125	0	C ^{α} H s(96)
	2196	-39	CH ₃ as ¹ (73), CH ₃ as ² (25)
	2246	0	CH ₃ as ² (73), CH ₃ as ¹ (22)
	2329	—	NH ₂ as(68), NH ₂ ss(32)
	2352	—	NH ₂ ss(68), NH ₂ as(32)
	2526	—	HO2* s(59), HO1* s(41)
	2609	—	HO1* s(58), HO2* s(41)

frequency (cm^{-1})			NH ₂ CHCD ₃ CO ₂ ⁻ ·H ₂ O (mean deviation = 10 cm^{-1})
obs.	calc.	dev.	
			Potential Energy Distribution
—	39	—	CO* t(94)
—	48	—	CC t(86), CO* t(8)
—	75	—	COH* b(39), OHO* b(38), Hb1* s(15)
—	150	—	CC ^{me} t(87), CN t(9)

Table 3.52: (continued)

frequency (cm ⁻¹)			Potential Energy Distribution
obs.	calc.	dev.	
—	170	—	CN t(85), CC ^{me} t(9)
—	184	—	Hb1* s(95), COH* b(15)
255	251	-4	C ^α H d ² (53), OHO* b(26), CCOO r(11), C ^α H d ³ (7)
—	312	—	COH* b(27), OHO* b(21), C ^α H d ³ (17), C ^α H d ² (12)
340	348	8	C ^α H d ³ (35), OHO* b(31), COH* b(19), CCOO r(11)
390	381	-9	C ^α H d ¹ (72), CH ₃ r ¹ (8)
—	407	—	COHO* t(169)
521	530	9	CCOO r(39), CC ^{ter} s(13), CCOO sd(13), CN ^{ter} s(10), C ^α H d ³ (10)
607	599	-8	CCOO sd(29), CC ^{ter} s(19), CC ^{me} s(12), CCOO r(12), C ^α H d ³ (8), CCOO wag(8)
741	705	-36	CCOO wag(39), CH ₃ r ¹ (36), CH ₃ r ² (9)
771	763	-8	CH ₃ r ² (30), CN ^{ter} s(29), CH ₃ r ¹ (15), CC ^{me} s(8), CCOO sd(7)
—	802	—	OHOH* t(69), CCOO sd(19), CH ₃ r ² (17)
828	815	-13	OHOH* t(76), CCOO sd(17), CH ₃ r ² (8), COO ss(7), CO* t(7)
910	906	-4	NH ₂ wag(49), CH ₃ r ¹ (14), CCOO wag(12), CN ^{ter} s(7)
947	942	-5	CCH ₃ sd(29), CC ^{me} s(20), NH ₂ twist(14), NH ₂ wag(9), CC ^{ter} s(7)
1020	1027	7	NH ₂ wag(21), CC ^{ter} s(16), CCOO wag(11), COO ss(10), C ^α H d ² (9), CH ₃ r ² (9), C ^α H d ³ (7)
1058	1051	-7	CCH ₃ ad ¹ (76), CCH ₃ ad ² (20)
1058	1057	-1	CCH ₃ ad ² (75), CCH ₃ ad ¹ (19)
—	1070	—	CCH ₃ sd(40), CN ^{ter} s(21), NH ₂ twist(10), NH ₂ wag(7)
1141	1162	21	CC ^{me} s(28), CN ^{ter} s(22), CCH ₃ sd(17), C ^α H r ² (14)
1189	1200	11	NH ₂ twist(32), C ^α H r ² (26), C ^α H r ¹ (9), CH ₃ r ¹ (9), CN ^{ter} s(7), C ^α H d ¹ (7)
1283	1277	-6	C ^α H r ² (39), C ^α H r ¹ (25), CC ^{me} s(9), COO ss(7)
1360	1364	4	C ^α H r ¹ (54), NH ₂ twist(27), CC ^{me} s(8)
1413	1410	-3	COO ss(59), CC ^{ter} s(22), CCOO sd(11)
1563	1563	0	COO as(88)
1587	1588	1	NH ₂ sissor(100)
1648	1671	23	HOH* b(99)

Table 3.52: (continued)

frequency (cm^{-1})			Potential Energy Distribution
obs.	calc.	dev.	
2076	2112	36	CH ₃ ss(94)
2125	2195	70	CH ₃ as ¹ (75), CH ₃ as ² (24)
2235	2246	11	CH ₃ as ² (73), CH ₃ as ¹ (22)
—	2888	—	C ^{α} H s(100)
—	3167	—	NH ₂ as(97)
—	3250	—	NH ₂ ss(96)
—	3510	—	HO2* s(70), HO1* s(29)
—	3561	—	HO1* s(70), HO2* s(30)

frequency (cm^{-1})			Potential Energy Distribution
obs.	calc.	dev.	
—	38	—	CO* t(92)
—	46	—	CC t(81), CO* t(11)
—	71	—	OHO* b(42), COH* b(35), Hb1* s(15)
—	123	—	CN t(88), CC t(8)
—	152	—	CC ^{me} t(93)
—	175	—	Hb1* s(95), COH* b(19)
—	217	—	OHO* b(71), COH* b(15), C ^{α} H d ² (13), C ^{α} H d ³ (9), CCOO r(8)
258	268	10	C ^{α} H d ² (48), COH* b(30)
—	292	—	COHO* t(167)
320	315	-5	C ^{α} H d ³ (50), CCOO r(12), NH ₂ wag(8)
348	360	12	C ^{α} H d ¹ (69), CH ₃ r ¹ (7)
512	517	5	CCOO r(48), CN ^{ter} s(10), CCOO sd(9), CC ^{ter} s(8), COO as(7), C ^{α} H d ³ (7)
—	580	—	OHOH* t(105), CCOO sd(9), CC ^{ter} s(7)
595	598	3	OHOH* t(43), CCOO sd(25), CC ^{ter} s(18)
—	710	—	CCOO wag(44), CH ₃ r ¹ (33), CH ₃ r ² (8)
723	746	23	CH ₃ r ¹ (26), CH ₃ r ² (26), CN ^{ter} s(12), NH ₂ twist(11), NH ₂ wag(9)
751	759	8	NH ₂ wag(63), CN ^{ter} s(13), CH ₃ r ² (13)
799	785	-14	NH ₂ twist(28), CCOO sd(25), CC ^{me} s(19), CN ^{ter} s(7), CCH ₃ sd(7)

Table 3.52: (continued)

frequency (cm^{-1})			Potential Energy Distribution
obs.	calc.	dev.	
852	836	-16	NH ₂ twist(23), CCOO sd(16), CC ^{ter} s(13), COO ss(11), CH ₃ r ² (11), CCOO wag(9)
988	1006	18	CC ^{ter} s(19), CCOO wag(16), COO ss(11), C ^{α} H d ² (10), C ^{α} H d ³ (10), CH ₃ r ¹ (9)
1028	1023	-5	CCH ₃ sd(59), CN ^{ter} s(9), NH ₂ twist(9)
1056	1051	-5	CCH ₃ ad ¹ (80), CCH ₃ ad ² (17)
1056	1057	1	CCH ₃ ad ² (81), CCH ₃ ad ¹ (17)
1109	1098	-11	CN ^{ter} s(27), NH ₂ sissor(16), C ^{α} H d ¹ (14), NH ₂ twist(11), CH ₃ r ² (9), CH ₃ r ¹ (7)
1131	1164	33	CC ^{me} s(36), C ^{α} H r ² (25), CCH ₃ sd(21)
—	1178	—	NH ₂ sissor(78), CN ^{ter} s(16)
—	1223	—	HOH* b(97)
1281	1272	-9	C ^{α} H r ² (55), CC ^{me} s(13)
1332	1327	-5	C ^{α} H r ¹ (81)
1412	1414	2	COO ss(59), CC ^{ter} s(22), CCOO sd(12)
1576	1562	-14	COO as(88)
—	2112	—	CH ₃ ss(94)
—	2195	—	CH ₃ as ¹ (75), CH ₃ as ² (24)
—	2246	—	CH ₃ as ² (73), CH ₃ as ¹ (22)
—	2329	—	NH ₂ as(68), NH ₂ ss(32)
—	2352	—	NH ₂ ss(68), NH ₂ as(32)
—	2526	—	HO2* s(59), HO1* s(41)
—	2609	—	HO1* s(58), HO2* s(41)
—	2888	—	C ^{α} H s(100)

frequency (cm ⁻¹)			NH ₂ CH ¹³ CH ₃ CO ₂ ⁻ ·H ₂ O (mean deviation = 8 cm ⁻¹)
obs.	calc.	dev.	
Potential Energy Distribution			
—	39	—	CO* t(97)
—	49	—	CC t(88)
—	76	—	COH* b(39), OHO* b(38), Hb1* s(16)
—	168	—	CN t(92)
—	185	—	Hb1* s(91), COH* b(16)
—	212	—	CC ^{me} t(90)

Table 3.52: (continued)

frequency (cm ⁻¹)			Potential Energy Distribution
obs.	calc.	dev.	
273	267	-6	C ^α H d ² (44), OHO* b(29), CCOO r(16), C ^α H d ³ (13)
—	320	—	COH* b(31), C ^α H d ² (23), OHO* b(19), C ^α H d ³ (8)
344	351	7	C ^α H d ³ (38), OHO* b(27), COH* b(14), CCOO r(11)
—	407	—	COHO* t(164)
409	412	3	C ^α H d ¹ (75)
538	539	1	CCOO r(40), CN ^{ter} s(13), C ^α H d ³ (11), CCOO sd(11), CC ^{ter} s(10)
624	612	-12	CCOO sd(33), CC ^{ter} s(19), CCOO wag(13), CCOO r(11), CC ^{me} s(10), C ^α H d ³ (8)
779	763	-16	CCOO wag(35), OHOH* t(27), CCOO sd(17)
—	813	—	OHOH* t(111), CO* t(10), CCOO sd(8)
849	835	-14	CN ^{ter} s(15), OHOH* t(13), CCOO sd(12), CCOO wag(12), CH ₃ r ¹ (12), CC ^{ter} s(9), COO ss(8), CC ^{me} s(8), NH ₂ wag(7)
922	913	-9	CH ₃ r ² (33), CN ^{ter} s(26), CC ^{ter} s(15), NH ₂ wag(14), COO ss(8)
—	952	—	NH ₂ wag(52), CC ^{me} s(16), CH ₃ r ¹ (16)
1015	1007	-8	NH ₂ twist(38), CC ^{me} s(20), CH ₃ r ¹ (18), C ^α H r ¹ (7)
1073	1076	3	C ^α H r ² (21), CH ₃ r ² (20), NH ₂ wag(12), CCOO wag(10), CH ₃ r ¹ (9)
1134	1152	18	CN ^{ter} s(32), CC ^{me} s(20), CH ₃ r ² (14), C ^α H r ¹ (7)
1231	1241	10	NH ₂ twist(27), CH ₃ r ¹ (23), C ^α H r ² (15), C ^α H d ¹ (9)
1288	1282	-6	C ^α H r ² (42), C ^α H r ¹ (21), COO ss(9)
1355	1356	1	CCH ₃ sd(70), C ^α H r ¹ (17)
1360	1367	7	C ^α H r ¹ (38), NH ₂ twist(22), CCH ₃ sd(20), CC ^{me} s(9)
1412	1412	0	COO ss(52), CC ^{ter} s(20), CCOO sd(10)
1458	1457	-1	CCH ₃ ad ¹ (81), CCH ₃ ad ² (9), CH ₃ r ¹ (7)
1458	1464	6	CCH ₃ ad ² (77), CCH ₃ ad ¹ (9), CH ₃ r ² (7)
1562	1564	2	COO as(87)
1596	1589	-7	NH ₂ sissor(100)
1648	1671	23	HOH* b(99)
2885	2886	1	C ^α H s(97)
2940	2927	-13	CH ₃ ss(77), CH ₃ as ¹ (18)
2980	2958	-22	CH ₃ as ¹ (58), CH ₃ as ² (36)
2993	3031	38	CH ₃ as ² (59), CH ₃ as ¹ (23), CH ₃ ss(18)

Table 3.52: (continued)

frequency (cm ⁻¹)			Potential Energy Distribution
obs.	calc.	dev.	
—	3167	—	NH ₂ as(97)
—	3250	—	NH ₂ ss(96)
—	3510	—	HO2* s(70), HO1* s(29)
—	3561	—	HO1* s(70), HO2* s(30)

frequency (cm ⁻¹)			Potential Energy Distribution
obs.	calc.	dev.	
—	39	—	CO* t(98)
—	49	—	CC t(89)
—	76	—	COH* b(39), OHO* b(37), Hb1* s(17)
—	167	—	CN t(92)
—	185	—	Hb1* s(90), COH* b(16)
—	212	—	CC ^{me} t(91)
279	268	-11	C ^α H d ² (41), OHO* b(29), CCOO r(17), C ^α H d ³ (15)
—	321	—	COH* b(29), C ^α H d ² (25), OHO* b(16), C ^α H d ³ (8)
343	349	6	C ^α H d ³ (36), OHO* b(30), COH* b(15), CCOO r(10)
—	407	—	COHO* t(165)
421	412	-9	C ^α H d ¹ (75), CCOO wag(7)
535	534	-1	CCOO r(39), CN ^{ter} s(15), CCOO sd(11), CC ^{ter} s(10), C ^α H d ³ (10)
632	615	-17	CCOO sd(33), CC ^{ter} s(18), CCOO wag(12), CCOO r(11), CC ^{me} s(9), C ^α H d ³ (8)
793	763	-30	CCOO wag(35), OHOH* t(27), CCOO sd(17)
—	812	—	OHOH* t(108), CO* t(10), CCOO sd(9)
851	834	-17	CN ^{ter} s(17), OHOH* t(16), CCOO wag(13), CCOO sd(11), CH ₃ r ¹ (11), NH ₂ wag(9), CC ^{ter} s(8), CC ^{me} s(7)
924	911	-13	CH ₃ r ² (29), CN ^{ter} s(23), CC ^{ter} s(17), NH ₂ wag(16), COO ss(9)
—	953	—	NH ₂ wag(49), CC ^{me} s(16), CH ₃ r ¹ (16)
1019	1010	-9	NH ₂ twist(39), CC ^{me} s(19), CH ₃ r ¹ (17), C ^α H r ¹ (7)
1072	1078	6	C ^α H r ² (22), CH ₃ r ² (19), NH ₂ wag(11), CCOO wag(10), CH ₃ r ¹ (8)
1134	1153	19	CN ^{ter} s(30), CC ^{me} s(21), CH ₃ r ² (16), C ^α H r ¹ (7)

Table 3.52: (continued)

frequency (cm^{-1})			Potential Energy Distribution
obs.	calc.	dev.	
1234	1245	11	NH ₂ twist(28), CH ₃ r ¹ (25), C ^{α} H r ² (15), C ^{α} H d ¹ (9)
1291	1283	-8	C ^{α} H r ² (42), C ^{α} H r ¹ (21), COO ss(9)
1360	1358	-2	C ^{α} H r ¹ (45), CCH ₃ sd(27), NH ₂ twist(15)
1370	1373	3	CCH ₃ sd(60), C ^{α} H r ¹ (11), CC ^{<i>me</i>} s(10), NH ₂ twist(10)
1414	1412	-2	COO ss(52), CC ^{<i>ter</i>} s(20), CCOO sd(10), CCH ₃ sd(7)
1460	1459	-1	CCH ₃ ad ¹ (80), CCH ₃ ad ² (10)
1460	1465	5	CCH ₃ ad ² (78), CCH ₃ ad ¹ (10)
1567	1564	-3	COO as(87)
1593	1585	-8	NH ₂ sissor(100)
1648	1671	23	HOH* b(99)
2885	2886	1	C ^{α} H s(98)
2940	2931	-9	CH ₃ ss(80), CH ₃ as ¹ (15)
2980	2968	-12	CH ₃ as ¹ (61), CH ₃ as ² (34)
2993	3040	47	CH ₃ as ² (61), CH ₃ as ¹ (23), CH ₃ ss(16)
—	3158	—	NH ₂ as(97)
—	3246	—	NH ₂ ss(97)
—	3510	—	HO2* s(70), HO1* s(29)
—	3561	—	HO1* s(70), HO2* s(30)

Table 3.53: Scaled 4-31G Frequencies and Potential Energy Distribution for Water-Excluded Alaninate One-water Supermolecule.

frequency (cm^{-1})			$\text{NH}_2\text{CHCH}_3\text{CO}_2^-$ (mean deviation = 9 cm^{-1})
obs.	calc.	dev.	
			Potential Energy Distribution
—	100	—	CC t(95)
—	169	—	CN t(84), CC^{me} t(13)
—	212	—	CC^{me} t(81), CN t(12)
279	282	3	C^αH d ² (79)
343	347	4	C^αH d ³ (64), CCOO r(22)
415	414	-1	C^αH d ¹ (80)
539	532	-7	CCOO r(45), C^αH d ³ (12), CN^{ter} s(11), CCOO sd(10), CC^{ter} s(9)
622	613	-9	CCOO sd(43), CC^{ter} s(19), CCOO r(9), CCOO wag(9), CC^{me} s(8), C^αH d ³ (8)
785	781	-4	CCOO wag(49), CCOO sd(19)
853	839	-14	CC^{ter} s(15), CN^{ter} s(14), CCOO sd(13), CCOO wag(12), CH_3 r ¹ (12), COO ss(9), CC^{me} s(9), NH_2 wag(8)
927	925	-2	CH_3 r ² (30), CN^{ter} s(26), NH_2 wag(22), CC^{ter} s(13)
—	955	—	NH_2 wag(47), CC^{me} s(16), CH_3 r ¹ (16)
1020	1013	-7	NH_2 twist(38), CC^{me} s(21), CH_3 r ¹ (18), C^αH r ¹ (7)
1080	1078	-2	CH_3 r ² (23), C^αH r ² (18), CCOO wag(10), NH_2 wag(10), CH_3 r ¹ (10), CC^{ter} s(7)
1140	1163	23	CN^{ter} s(35), CC^{me} s(21), CH_3 r ² (12), C^αH r ¹ (7)
1238	1249	11	NH_2 twist(28), CH_3 r ¹ (23), C^αH r ² (12), C^αH d ¹ (10)
1286	1288	2	C^αH r ² (46), C^αH r ¹ (23), COO ss(8)
1353	1357	4	C^αH r ¹ (37), CCH ₃ sd(36), NH_2 twist(14)
1368	1372	4	CCH ₃ sd(54), C^αH r ¹ (15), NH_2 twist(12), CC^{me} s(10)
1414	1415	1	COO ss(54), CC^{ter} s(20), CCOO sd(9), CCH ₃ ad ² (7)
1459	1459	0	CCH ₃ ad ² (75), CCH ₃ ad ¹ (12)
1459	1466	7	CCH ₃ ad ¹ (79), CCH ₃ ad ² (11)
1564	1567	3	COO as(88), CCOO r(7)
1591	1588	-3	NH_2 sissor(100)
2885	2886	1	C^αH s(99)
2940	2917	-23	CH_3 ss(86), CH_3 as ² (9)
2980	2970	-10	CH_3 as ² (50), CH_3 as ¹ (49)
2993	3033	40	CH_3 as ¹ (46), CH_3 as ² (41), CH_3 ss(14)
—	3167	—	NH_2 as(97)

Table 3.53: (continued)

frequency (cm ⁻¹)			Potential Energy Distribution
obs.	calc.	dev.	
—	3250	—	NH ₂ ss(96)

frequency (cm ⁻¹)			ND ₂ CHCH ₃ CO ₂ ⁻ (mean deviation = 11 cm ⁻¹)
obs.	calc.	dev.	
Potential Energy Distribution			
—	96	—	CC t(82), CN t(15)
—	127	—	CN t(82), CC t(15)
—	208	—	CC ^{me} t(91)
275	280	5	C ^α H d ² (76), CC ^{me} t(7)
331	323	-8	C ^α H d ³ (61), CCOO r(14), NH ₂ wag(8)
384	391	7	C ^α H d ¹ (77), NH ₂ twist(7)
527	517	-10	CCOO r(54), CN ^{ter} s(10), COO as(7), C ^α H d ³ (7)
621	605	-16	CCOO sd(46), CC ^{ter} s(23)
—	749	—	NH ₂ wag(56), CCOO wag(32)
780	787	7	CCOO sd(25), CCOO wag(19), CN ^{ter} s(14), NH ₂ wag(13), COO ss(8)
836	826	-10	NH ₂ twist(58), CC ^{me} s(18), CCOO wag(8)
870	863	-7	CH ₃ r ¹ (29), NH ₂ twist(13), CC ^{ter} s(12), CCOO wag(7)
922	925	3	CH ₃ r ² (32), CN ^{ter} s(27), CC ^{ter} s(19), COO ss(9)
1053	1067	14	C ^α H r ² (19), CH ₃ r ¹ (18), CH ₃ r ² (15), CCOO wag(12)
1108	1130	22	NH ₂ sissor(36), CH ₃ r ² (18), CC ^{me} s(15), CN ^{ter} s(14)
1143	1174	31	NH ₂ sissor(29), CC ^{me} s(23), CH ₃ r ¹ (19), NH ₂ twist(8), C ^α H d ¹ (7)
1201	1194	-7	NH ₂ sissor(32), CN ^{ter} s(18), CH ₃ r ² (11), CH ₃ r ¹ (9), C ^α H d ¹ (8), NH ₂ twist(7)
1290	1288	-2	C ^α H r ² (57), C ^α H r ¹ (11), COO ss(7)
1334	1329	-5	C ^α H r ¹ (73)
1370	1367	-3	CCH ₃ sd(88)
1414	1415	1	COO ss(55), CC ^{ter} s(20), CCOO sd(9), CCH ₃ ad ² (7)
1462	1459	-3	CCH ₃ ad ² (70), CCH ₃ ad ¹ (18)
1462	1467	5	CCH ₃ ad ¹ (73), CCH ₃ ad ² (16)
1571	1567	-4	COO as(88), CCOO r(8)
—	2329	—	NH ₂ as(68), NH ₂ ss(31)
—	2353	—	NH ₂ ss(68), NH ₂ as(31)

Table 3.53: (continued)

frequency (cm^{-1})			Potential Energy Distribution
obs.	calc.	dev.	
2887	2886	-1	C^αH s(99)
2942	2917	-25	CH_3 ss(86), CH_3 as ² (9)
2980	2970	-10	CH_3 as ² (50), CH_3 as ¹ (49)
2990	3033	43	CH_3 as ¹ (46), CH_3 as ² (41), CH_3 ss(14)

frequency (cm^{-1})			Potential Energy Distribution
obs.	calc.	dev.	
—	97	—	CC t(95)
—	144	—	CC^{me} t(84), CN t(14)
—	179	—	CN t(83), CC^{me} t(14)
257	253	-4	C^αH d ² (82)
335	343	8	C^αH d ³ (66), CCOO r(25)
382	377	-5	C^αH d ¹ (75), CH_3 r ¹ (8)
514	520	6	CCOO r(43), CC^{ter} s(13), CCOO sd(13), C^αH d ³ (11), CN^{ter} s(8)
593	583	-10	CCOO sd(32), CC^{ter} s(19), CCOO r(13), CCOO wag(9), CC^{me} s(8), C^αH d ³ (7)
688	677	-11	CH_3 r ¹ (37), C^αH r ² (27), CCOO wag(22)
752	758	6	CH_3 r ² (35), CN^{ter} s(19), CC^{me} s(11), CCOO sd(8)
827	802	-25	CCOO sd(31), CH_3 r ² (28), COO ss(12), CC^{ter} s(11)
884	868	-16	C^αH r ¹ (33), CN^{ter} s(22), NH_2 wag(21), NH_2 twist(8)
897	897	0	C^αH r ² (25), CC^{me} s(13), CCH_3 sd(12), CC^{ter} s(10), CCOO wag(10), CH_3 r ¹ (10)
947	952	5	C^αH r ¹ (33), NH_2 wag(24), CH_3 r ¹ (21)
—	965	—	CCOO wag(27), NH_2 wag(24), C^αH r ² (14), CCH_3 sd(11)
1055	1050	-5	CCH_3 ad ² (85), CCH_3 ad ¹ (8)
1055	1057	2	CCH_3 ad ¹ (71), CCH_3 ad ² (13), CCH_3 sd(8)
—	1070	—	CCH_3 sd(37), CCH_3 ad ¹ (18), C^αH r ² (12), NH_2 wag(11)
1126	1119	-7	CCH_3 sd(16), C^αH r ¹ (15), NH_2 twist(14), CC^{me} s(12), CC^{ter} s(11), COO ss(7)
1158	1181	23	CN^{ter} s(36), NH_2 twist(16), CC^{me} s(10)
1276	1300	24	NH_2 twist(48), CC^{me} s(24)
1408	1413	5	COO ss(62), CC^{ter} s(23), CCOO sd(11)

Table 3.53: (continued)

frequency (cm^{-1})			Potential Energy Distribution
obs.	calc.	dev.	
1555	1565	10	COO as(89), CCOO r(7)
1582	1587	5	NH ₂ sissor(100)
2076	2100	24	CH ₃ ss(94)
2125	2125	0	C ^{α} H s(97)
2235	2199	-36	CH ₃ as ² (50), CH ₃ as ¹ (49)
2246	2241	-5	CH ₃ as ¹ (48), CH ₃ as ² (47)
—	3167	—	NH ₂ as(97)
—	3250	—	NH ₂ ss(96)

frequency (cm^{-1})			ND ₂ CD ₂ CD ₃ CO ₂ ⁻ (mean deviation = 11 cm^{-1})
obs.	calc.	dev.	
—	94	—	CC t(86), CN t(12)
—	123	—	CN t(74), CC ^{me} t(14), CC t(10)
—	153	—	CC ^{me} t(83), CN t(13)
257	252	-5	C ^{α} H d ² (82)
327	317	-10	C ^{α} H d ³ (65), CCOO r(17), NH ₂ wag(8)
363	357	-6	C ^{α} H d ¹ (71), CH ₃ r ¹ (7)
506	507	1	CCOO r(52), CC ^{ter} s(8), CCOO sd(8), CN ^{ter} s(7), C ^{α} H d ³ (7)
590	578	-12	CCOO sd(37), CC ^{ter} s(24), CCOO r(10), CC ^{me} s(7), CCOO wag(7)
690	674	-16	CH ₃ r ¹ (35), C ^{α} H r ² (29), CCOO wag(24)
729	733	4	NH ₂ wag(23), CH ₃ r ² (21), NH ₂ twist(14), CH ₃ r ¹ (12), C ^{α} H r ¹ (11), CCOO wag(8)
756	759	3	NH ₂ wag(49), CH ₃ r ² (26), CN ^{ter} s(15)
790	777	-13	CC ^{me} s(24), NH ₂ twist(23), CCOO sd(20), CN ^{ter} s(12), CCH ₃ sd(9)
845	825	-20	CCOO sd(19), CH ₃ r ² (15), CC ^{ter} s(14), NH ₂ twist(14), COO ss(11)
893	907	14	C ^{α} H r ² (32), C ^{α} H r ¹ (13), CH ₃ r ¹ (13), CCOO wag(12), CN ^{ter} s(8)
940	947	7	C ^{α} H r ¹ (34), CCOO wag(27)
1036	1020	-16	NH ₂ twist(20), CH ₃ r ¹ (19), C ^{α} H r ¹ (11), C ^{α} H d ¹ (7)

Table 3.53: (continued)

frequency (cm^{-1})			Potential Energy Distribution
obs.	calc.	dev.	
1055	1049	-6	CCH ₃ ad ² (40), CCH ₃ ad ¹ (33), CCH ₃ sd(19)
1055	1053	-2	CCH ₃ ad ² (57), CCH ₃ ad ¹ (19), CCH ₃ sd(13)
—	1068	—	CCH ₃ ad ¹ (46), CCH ₃ sd(38)
1123	1120	-3	NH ₂ sissor(38), CN ^{ter} s(13), C ^{α} H r ¹ (9), CH ₃ r ² (9), C ^{α} H d ¹ (8)
1182	1193	11	NH ₂ sissor(60), CN ^{ter} s(20)
1215	1235	20	CC ^{me} s(49), CN ^{ter} s(9), NH ₂ twist(9)
1409	1413	4	COO ss(64), CC ^{ter} s(23), CCOO sd(11)
1567	1565	-2	COO as(90), CCOO r(8)
2076	2100	24	CH ₃ ss(94)
2125	2124	-1	C ^{α} H s(97)
2235	2199	-36	CH ₃ as ² (50), CH ₃ as ¹ (49)
2246	2241	-5	CH ₃ as ¹ (48), CH ₃ as ² (47)
—	2329	—	NH ₂ as(69), NH ₂ ss(31)
—	2353	—	NH ₂ ss(69), NH ₂ as(31)

frequency (cm^{-1})			NH ₂ CHCD ₃ CO ₂ ⁻ (mean deviation = 10 cm^{-1})
obs.	calc.	dev.	
			Potential Energy Distribution
—	98	—	CC t(95)
—	144	—	CC ^{me} t(84), CN t(14)
—	179	—	CN t(83), CC ^{me} t(14)
255	254	-1	C ^{α} H d ² (81)
340	345	5	C ^{α} H d ³ (65), CCOO r(24)
390	380	-10	C ^{α} H d ¹ (74), CH ₃ r ¹ (8)
521	524	3	CCOO r(46), CC ^{ter} s(11), C ^{α} H d ³ (11), CCOO sd(11), CN ^{ter} s(8)
607	596	-11	CCOO sd(36), CC ^{ter} s(20), CC ^{me} s(10), CCOO r(10), C ^{α} H d ³ (8)
741	724	-17	CCOO wag(41), CH ₃ r ¹ (39), CH ₃ r ² (9), C ^{α} H r ² (7)
771	767	-4	CH ₃ r ² (28), CN ^{ter} s(27), CH ₃ r ¹ (14), CC ^{me} s(10), CCOO sd(9)
828	802	-26	CCOO sd(30), CH ₃ r ² (29), COO ss(12), CC ^{ter} s(10)
910	907	-3	NH ₂ wag(51), CH ₃ r ¹ (14), CCOO wag(13)

Table 3.53: (continued)

frequency (cm ⁻¹)			Potential Energy Distribution
obs.	calc.	dev.	
947	940	-7	CCH ₃ sd(30), CC ^{me} s(20), NH ₂ twist(13), NH ₂ wag(10)
1020	1022	2	NH ₂ wag(22), CC ^{ter} s(19), CCOO wag(12), COO ss(10), C ^α H d ³ (7), CH ₃ r ² (7)
1058	1051	-7	CCH ₃ ad ² (85), CCH ₃ ad ¹ (12)
1058	1057	-1	CCH ₃ ad ¹ (83), CCH ₃ ad ² (11)
—	1074	—	CCH ₃ sd(42), CN ^{ter} s(21), NH ₂ twist(13)
1141	1167	26	CC ^{me} s(28), CN ^{ter} s(25), C ^α H r ² (14), CCH ₃ sd(14)
1189	1204	15	NH ₂ twist(33), C ^α H r ² (22), CN ^{ter} s(9), C ^α H r ¹ (9), CH ₃ r ¹ (9), C ^α H d ¹ (7)
1283	1282	-1	C ^α H r ² (44), C ^α H r ¹ (26), CC ^{me} s(7)
1360	1361	1	C ^α H r ¹ (52), NH ₂ twist(28), CC ^{me} s(8)
1413	1414	1	COO ss(61), CC ^{ter} s(23), CCOO sd(10)
1563	1566	3	COO as(89), CCOO r(8)
1587	1587	0	NH ₂ sissor(101)
2076	2100	24	CH ₃ ss(95)
2125	2198	73	CH ₃ as ¹ (50), CH ₃ as ² (50)
2235	2241	6	CH ₃ as ¹ (48), CH ₃ as ² (48)
—	2887	—	C ^α H s(100)
—	3167	—	NH ₂ as(97)
—	3250	—	NH ₂ ss(96)

frequency (cm ⁻¹)			ND ₂ CHCD ₃ CO ₂ ⁻ (mean deviation = 11 cm ⁻¹)
obs.	calc.	dev.	
—	94	—	CC t(85), CN t(12)
—	124	—	CN t(74), CC ^{me} t(14), CC t(11)
—	153	—	CC ^{me} t(83), CN t(13)
258	253	-5	C ^α H d ² (81)
320	319	-1	C ^α H d ³ (64), CCOO r(17), NH ₂ wag(8)
348	360	12	C ^α H d ¹ (70), CH ₃ r ¹ (7)
512	511	-1	CCOO r(55), CN ^{ter} s(8), COO as(7), CC ^{ter} s(7), C ^α H d ³ (7), CCOO sd(7)
595	590	-5	CCOO sd(41), CC ^{ter} s(25), CC ^{me} s(8), CCOO r(7)
—	722	—	CCOO wag(43), CH ₃ r ¹ (37), CH ₃ r ² (8), C ^α H r ² (7)

Table 3.53: (continued)

frequency (cm ⁻¹)			Potential Energy Distribution
obs.	calc.	dev.	
723	747	24	NH ₂ wag(32), CH ₃ r ¹ (24), CH ₃ r ² (14), NH ₂ twist(8)
751	760	9	NH ₂ wag(42), CH ₃ r ² (29), CN ^{ter} s(17)
799	782	-17	CCOO sd(26), NH ₂ twist(23), CC ^{me} s(18), COO ss(7), CN ^{ter} s(7), CCH ₃ sd(7)
852	836	-16	NH ₂ twist(27), CCOO wag(13), CC ^{ter} s(12), CCOO sd(12), CH ₃ r ² (11), COO ss(8)
988	1001	13	CC ^{ter} s(22), CCOO wag(19), COO ss(11), CH ₃ r ¹ (11), C ^α H d ³ (9), C ^α H d ² (8)
1028	1020	-8	CCH ₃ sd(63), NH ₂ twist(10), CN ^{ter} s(9)
1056	1051	-5	CCH ₃ ad ² (86), CCH ₃ ad ¹ (12)
1056	1057	1	CCH ₃ ad ¹ (84), CCH ₃ ad ² (12)
1109	1104	-5	CN ^{ter} s(27), NH ₂ sissor(22), C ^α H d ¹ (12), NH ₂ twist(9), CH ₃ r ² (8), CH ₃ r ¹ (7)
1131	1164	33	CC ^{me} s(37), C ^α H r ² (22), CCH ₃ sd(21)
—	1183	—	NH ₂ sissor(71), CN ^{ter} s(21)
1281	1278	-3	C ^α H r ² (59), CC ^{me} s(11), C ^α H r ¹ (7)
1332	1323	-9	C ^α H r ¹ (80)
1412	1414	2	COO ss(62), CC ^{ter} s(23), CCOO sd(10)
1576	1566	-10	COO as(89), CCOO r(8)
2076	2100	24	CH ₃ ss(95)
2125	2198	73	CH ₃ as ¹ (50), CH ₃ as ² (50)
2235	2241	6	CH ₃ as ¹ (48), CH ₃ as ² (48)
2246	2329	83	NH ₂ as(68), NH ₂ ss(31)
—	2353	—	NH ₂ ss(68), NH ₂ as(31)
—	2888	—	C ^α H s(100)

frequency (cm ⁻¹)			NH ₂ CH ¹³ CH ₃ CO ₂ ⁻ (mean deviation = 8 cm ⁻¹)
obs.	calc.	dev.	
—	100	—	CC t(95)
—	169	—	CN t(84), CC ^{me} t(13)
—	212	—	CC ^{me} t(80), CN t(12)
273	278	5	C ^α H d ² (79), CC ^{me} t(7)
344	347	3	C ^α H d ³ (64), CCOO r(22)

Table 3.53: (continued)

frequency (cm ⁻¹)			Potential Energy Distribution
obs.	calc.	dev.	
409	411	2	C ^α H d ¹ (80)
538	532	-6	CCOO r(45), C ^α H d ³ (12), CN ^{ter} s(11), CCOO sd(10), CC ^{ter} s(9)
624	611	-13	CCOO sd(42), CC ^{ter} s(19), CCOO r(9), CCOO wag(9), CC ^{me} s(8), C ^α H d ³ (8)
779	780	1	CCOO wag(48), CCOO sd(20)
849	836	-13	CC ^{ter} s(14), CN ^{ter} s(13), CCOO sd(13), CCOO wag(13), CH ₃ r ¹ (13), COO ss(9), CC ^{me} s(9), NH ₂ wag(7)
922	923	1	CH ₃ r ² (33), CN ^{ter} s(26), NH ₂ wag(19), CC ^{ter} s(13)
—	951	—	NH ₂ wag(50), CC ^{me} s(17), CH ₃ r ¹ (15)
1015	1009	-6	NH ₂ twist(37), CC ^{me} s(21), CH ₃ r ¹ (19), C ^α H r ¹ (7)
1073	1075	2	CH ₃ r ² (22), C ^α H r ² (17), NH ₂ wag(11), CH ₃ r ¹ (11), CCOO wag(10), CC ^{ter} s(7)
1134	1158	24	CN ^{ter} s(36), CC ^{me} s(20), CH ₃ r ² (11), C ^α H r ¹ (8)
1231	1244	13	NH ₂ twist(28), CH ₃ r ¹ (22), C ^α H r ² (13), C ^α H d ¹ (9)
1288	1287	-1	C ^α H r ² (47), C ^α H r ¹ (23), COO ss(7)
1355	1353	-2	CCH ₃ sd(74), C ^α H r ¹ (15)
1360	1364	4	C ^α H r ¹ (38), NH ₂ twist(23), CCH ₃ sd(19), CC ^{me} s(9)
1412	1415	3	COO ss(55), CC ^{ter} s(20), CCOO sd(9), CCH ₃ ad ² (8)
1458	1457	-1	CCH ₃ ad ² (72), CCH ₃ ad ¹ (13), CH ₃ r ² (7)
1458	1464	6	CCH ₃ ad ¹ (77), CCH ₃ ad ² (12)
1562	1567	5	COO as(88), CCOO r(7)
1596	1588	-8	NH ₂ sissor(100)
2885	2886	1	C ^α H s(98)
2940	2913	-27	CH ₃ ss(84), CH ₃ as ² (11)
2980	2959	-21	CH ₃ as ² (50), CH ₃ as ¹ (49)
2993	3023	30	CH ₃ as ¹ (45), CH ₃ as ² (40), CH ₃ ss(15)
—	3167	—	NH ₂ as(97)
—	3250	—	NH ₂ ss(96)

frequency (cm ⁻¹)			Potential Energy Distribution
obs.	calc.	dev.	
—	100	—	CC t(95)

¹⁵NH₂CHCH₃CO₂⁻ (mean deviation = 10 cm⁻¹)

Table 3.53: (continued)

frequency (cm ⁻¹)			Potential Energy Distribution
obs.	calc.	dev.	
—	169	—	CN t(84), CC ^{me} t(13)
—	212	—	CC ^{me} t(81), CN t(12)
279	281	2	C ^α H d ² (79)
343	344	1	C ^α H d ³ (64), CCOO r(21)
417	411	-6	C ^α H d ¹ (80)
535	528	-7	CCOO r(46), CN ^{ter} s(12), C ^α H d ³ (11), CCOO sd(10), CC ^{ter} s(9)
632	613	-19	CCOO sd(42), CC ^{ter} s(18), CCOO r(10), CCOO wag(9), CC ^{me} s(8), C ^α H d ³ (8)
793	780	-13	CCOO wag(48), CCOO sd(20)
851	835	-16	CN ^{ter} s(15), CCOO wag(14), CC ^{ter} s(13), CCOO sd(12), CH ₃ r ¹ (12), NH ₂ wag(10), COO ss(8), CC ^{me} s(8)
924	919	-5	CH ₃ r ² (28), NH ₂ wag(24), CN ^{ter} s(23), CC ^{ter} s(14), COO ss(7)
—	953	—	NH ₂ wag(45), CC ^{me} s(16), CH ₃ r ¹ (15), CH ₃ r ² (7)
1019	1012	-7	NH ₂ twist(39), CC ^{me} s(20), CH ₃ r ¹ (18), C ^α H r ¹ (7)
1072	1077	5	CH ₃ r ² (22), C ^α H r ² (18), CCOO wag(10), NH ₂ wag(10), CH ₃ r ¹ (10), CC ^{ter} s(7)
1134	1158	24	CN ^{ter} s(33), CC ^{me} s(21), CH ₃ r ² (14), C ^α H r ¹ (7)
1234	1247	13	NH ₂ twist(29), CH ₃ r ¹ (23), C ^α H r ² (12), C ^α H d ¹ (10)
1291	1288	-3	C ^α H r ² (47), C ^α H r ¹ (23), COO ss(8)
1360	1355	-5	C ^α H r ¹ (41), CCH ₃ sd(30), NH ₂ twist(15)
1370	1371	1	CCH ₃ sd(60), C ^α H r ¹ (12), CC ^{me} s(10), NH ₂ twist(10)
1414	1415	1	COO ss(55), CC ^{ter} s(20), CCOO sd(9), CCH ₃ ad ² (7)
1460	1459	-1	CCH ₃ ad ² (75), CCH ₃ ad ¹ (12)
1460	1466	6	CCH ₃ ad ¹ (79), CCH ₃ ad ² (11)
1567	1567	0	COO as(88), CCOO r(8)
1593	1585	-8	NH ₂ sissor(100)
2885	2886	1	C ^α H s(99)
2940	2917	-23	CH ₃ ss(86), CH ₃ as ² (9)
2980	2970	-10	CH ₃ as ² (50), CH ₃ as ¹ (49)
2993	3033	40	CH ₃ as ¹ (46), CH ₃ as ² (41), CH ₃ ss(14)
—	3158	—	NH ₂ as(97)
—	3246	—	NH ₂ ss(97)

Table 3.54: Scaled 4-31G* Frequencies and Potential Energy Distribution for Water-Excluded Alaninate One-water Supermolecule.

frequency (cm ⁻¹)			NH ₂ CHCH ₃ CO ₂ ⁻ (mean deviation = 10 cm ⁻¹)
obs.	calc.	dev.	
			Potential Energy Distribution
—	90	—	CC t(94)
—	189	—	CN t(53), CC ^{me} t(41)
—	217	—	CC ^{me} t(47), CN t(42)
279	282	3	C ^α H d ² (76), CC ^{me} t(11)
343	346	3	C ^α H d ³ (70), CCOO r(20)
415	414	-1	C ^α H d ¹ (80)
539	534	-5	CCOO r(45), CN ^{ter} s(13), CCOO sd(12), CC ^{ter} s(11), C ^α H d ³ (7)
622	615	-7	CCOO sd(40), CC ^{ter} s(17), CCOO r(13), CCOO wag(9), CC ^{me} s(8), C ^α H d ³ (7)
785	768	-17	CCOO wag(54), CCOO sd(15)
853	838	-15	CN ^{ter} s(18), CCOO sd(16), CC ^{me} s(13), CC ^{ter} s(13), CH ₃ r ¹ (12), COO ss(9), CCOO wag(8)
927	930	3	CH ₃ r ² (38), CN ^{ter} s(26), CC ^{ter} s(18), COO ss(9)
—	952	—	NH ₂ wag(69), CH ₃ r ¹ (12), CC ^{me} s(10)
1020	1004	-16	NH ₂ twist(37), CH ₃ r ¹ (20), CC ^{me} s(14), C ^α H r ¹ (10)
1080	1074	-6	C ^α H r ² (20), CH ₃ r ² (16), NH ₂ wag(15), CCOO wag(9), CC ^{ter} s(7), CH ₃ r ¹ (7)
1140	1138	-2	CN ^{ter} s(28), CC ^{me} s(23), CH ₃ r ² (14), C ^α H r ¹ (9)
1238	1247	9	NH ₂ twist(28), CH ₃ r ¹ (18), C ^α H d ¹ (12), C ^α H r ¹ (11), CH ₃ r ² (8)
1286	1289	3	C ^α H r ² (49), COO ss(16), C ^α H r ¹ (13)
1353	1342	-11	CCH ₃ sd(45), C ^α H r ¹ (34), NH ₂ twist(14)
1368	1388	20	CCH ₃ sd(42), CC ^{me} s(15), C ^α H r ¹ (15), NH ₂ twist(13)
1414	1414	0	COO ss(46), CC ^{ter} s(21), CCH ₃ ad ² (11), CCOO sd(9)
1459	1460	1	CCH ₃ ad ¹ (62), CCH ₃ ad ² (26)
1459	1465	6	CCH ₃ ad ² (56), CCH ₃ ad ¹ (25)
1564	1566	2	COO as(85), CCOO r(9)
1591	1589	-2	NH ₂ sissor(98)
2885	2886	1	C ^α H s(99)
2940	2916	-24	CH ₃ ss(84), CH ₃ as ² (13)
2980	2971	-9	CH ₃ as ² (57), CH ₃ as ¹ (39)
2993	3040	47	CH ₃ as ¹ (58), CH ₃ as ² (30), CH ₃ ss(12)

Table 3.54: (continued)

frequency (cm ⁻¹)			Potential Energy Distribution
obs.	calc.	dev.	
—	3133	—	NH ₂ as(97)
—	3236	—	NH ₂ ss(97)

frequency (cm ⁻¹)			ND ₂ CHCH ₃ CO ₂ ⁻ (mean deviation = 13 cm ⁻¹)
obs.	calc.	dev.	Potential Energy Distribution
—	87	—	CC t(88), CN t(10)
—	147	—	CN t(85), CC t(10)
—	207	—	CC ^{me} t(85), C ^α H d ² (8)
275	280	5	C ^α H d ² (75), CC ^{me} t(11)
331	322	-9	C ^α H d ³ (67), CCOO r(13), NH ₂ wag(8)
384	392	8	C ^α H d ¹ (78), NH ₂ twist(7)
527	518	-9	CCOO r(54), CN ^{ter} s(12), COO as(7), CCOO sd(7)
621	605	-16	CCOO sd(45), CC ^{ter} s(23), CCOO r(8), NH ₂ wag(7)
—	744	—	CCOO wag(46), NH ₂ wag(33)
780	797	17	NH ₂ wag(37), CCOO sd(20), CN ^{ter} s(12), COO ss(7), CCOO wag(7)
836	809	-27	NH ₂ twist(54), CC ^{me} s(19), CCOO wag(7)
870	855	-15	CH ₃ r ¹ (30), NH ₂ twist(18), CN ^{ter} s(7)
922	922	0	CH ₃ r ² (34), CN ^{ter} s(25), CC ^{ter} s(22), COO ss(11)
1053	1055	2	C ^α H r ² (21), CH ₃ r ¹ (17), CCOO wag(10), CC ^{me} s(9), CH ₃ r ² (9)
1108	1116	8	NH ₂ sissor(25), CH ₃ r ² (22), CC ^{me} s(16), CN ^{ter} s(14), C ^α H r ¹ (7)
1143	1167	24	NH ₂ sissor(48), CC ^{me} s(15), CH ₃ r ¹ (13)
1201	1188	-13	NH ₂ sissor(24), CH ₃ r ¹ (13), CN ^{ter} s(10), C ^α H d ¹ (10), CH ₃ r ² (10), NH ₂ twist(9)
1290	1288	-2	C ^α H r ² (39), C ^α H r ¹ (22), COO ss(19)
1334	1322	-12	C ^α H r ¹ (50), CCH ₃ sd(18), C ^α H r ² (14)
1370	1376	6	CCH ₃ sd(68), CC ^{me} s(14)
1414	1415	1	COO ss(45), CC ^{ter} s(21), CCH ₃ ad ² (12), CCOO sd(8)
1462	1460	-2	CCH ₃ ad ¹ (63), CCH ₃ ad ² (25)
1462	1468	6	CCH ₃ ad ² (55), CCH ₃ ad ¹ (24), CH ₃ r ² (7)
1571	1566	-5	COO as(87), CCOO r(9)

Table 3.54: (continued)

frequency (cm^{-1})			Potential Energy Distribution
obs.	calc.	dev.	
—	2302	—	NH ₂ as(89), NH ₂ ss(10)
—	2346	—	NH ₂ ss(90), NH ₂ as(10)
2887	2886	−1	C ^α H s(99)
2942	2916	−26	CH ₃ ss(84), CH ₃ as ² (13)
2980	2971	−9	CH ₃ as ² (57), CH ₃ as ¹ (39)
2990	3040	50	CH ₃ as ¹ (58), CH ₃ as ² (30), CH ₃ ss(12)

frequency (cm^{-1})			Potential Energy Distribution
obs.	calc.	dev.	
—	88	—	CC t(95)
—	146	—	CC ^{me} t(92)
—	203	—	CN t(92)
257	251	−6	C ^α H d ² (81)
335	342	7	C ^α H d ³ (72), CCOO r(22)
382	377	−5	C ^α H d ¹ (76), CH ₃ r ¹ (7)
514	520	6	CCOO r(40), CC ^{ter} s(16), CCOO sd(16), CN ^{ter} s(9)
593	585	−8	CCOO sd(27), CCOO r(19), CC ^{ter} s(17), CC ^{me} s(9), CCOO wag(8), C ^α H d ³ (7)
688	668	−20	CH ₃ r ¹ (36), C ^α H r ² (26), CCOO wag(24)
752	748	−4	CH ₃ r ² (30), CN ^{ter} s(18), CC ^{me} s(13), CCOO sd(9), C ^α H r ¹ (7)
827	803	−24	CH ₃ r ² (33), CCOO sd(29), COO ss(10), CC ^{ter} s(8)
884	849	−35	C ^α H r ¹ (45), CN ^{ter} s(24), NH ₂ twist(9), NH ₂ wag(8)
897	892	−5	C ^α H r ² (25), CC ^{ter} s(12), CC ^{me} s(10), CCOO wag(10), CCH ₃ sd(10), CH ₃ r ¹ (8), COO ss(7)
947	941	−6	CCOO wag(24), CH ₃ r ¹ (22), C ^α H r ¹ (18), CCH ₃ sd(9), C ^α H d ² (7)
—	965	—	NH ₂ wag(58), C ^α H r ² (19), CCOO wag(7)
1055	1049	−6	CCH ₃ ad ² (74), CCH ₃ ad ¹ (20)
1055	1052	−3	CCH ₃ ad ¹ (64), CCH ₃ ad ² (24)
—	1066	—	CCH ₃ sd(42), CCH ₃ ad ¹ (14), NH ₂ wag(11), C ^α H r ² (9)
1126	1148	22	C ^α H r ¹ (16), COO ss(14), CC ^{ter} s(12), NH ₂ twist(12), CN ^{ter} s(9), C ^α H r ² (8), CH ₃ r ² (8)

Table 3.54: (continued)

frequency (cm^{-1})			Potential Energy Distribution
obs.	calc.	dev.	
1158	1176	18	NH ₂ twist(25), CN ^{ter} s(24), CC ^{me} s(14), CCH ₃ sd(8)
1276	1304	28	NH ₂ twist(42), CC ^{me} s(27)
1408	1410	2	COO ss(57), CC ^{ter} s(24), CCOO sd(11)
1555	1563	8	COO as(85), CCOO r(8)
1582	1588	6	NH ₂ sissor(97)
2076	2101	25	CH ₃ ss(93)
2125	2125	0	C ^{α} H s(96)
2235	2201	-34	CH ₃ as ² (63), CH ₃ as ¹ (36)
2246	2249	3	CH ₃ as ¹ (62), CH ₃ as ² (33)
—	3132	—	NH ₂ as(97)
—	3236	—	NH ₂ ss(97)

frequency (cm^{-1})			ND ₂ CD ₂ CO ₂ ⁻ (mean deviation = 13 cm^{-1})
obs.	calc.	dev.	
—	85	—	CC t(89), CN t(9)
—	138	—	CC ^{me} t(47), CN t(46)
—	158	—	CC ^{me} t(49), CN t(44)
257	250	-7	C ^{α} H d ² (81)
327	317	-10	C ^{α} H d ³ (71), CCOO r(15), NH ₂ wag(8)
363	358	-5	C ^{α} H d ¹ (73), CH ₃ r ¹ (7)
506	508	2	CCOO r(50), CC ^{ter} s(10), CCOO sd(10), CN ^{ter} s(9)
590	579	-11	CCOO sd(34), CC ^{ter} s(23), CCOO r(13), CC ^{me} s(8)
690	666	-24	CH ₃ r ¹ (35), C ^{α} H r ² (27), CCOO wag(25)
729	719	-10	CH ₃ r ² (22), NH ₂ wag(17), NH ₂ twist(12), C ^{α} H r ¹ (11), CH ₃ r ¹ (11), CCOO wag(8), CC ^{me} s(7)
756	759	3	NH ₂ twist(31), CC ^{me} s(18), NH ₂ wag(17), CH ₃ r ² (10), CCH ₃ sd(8), CCOO sd(7)
790	777	-13	NH ₂ wag(34), CN ^{ter} s(29), CH ₃ r ² (15)
845	820	-25	CCOO sd(27), CH ₃ r ² (15), CC ^{ter} s(14), COO ss(12), NH ₂ wag(9)
893	899	6	C ^{α} H r ² (29), C ^{α} H r ¹ (12), CH ₃ r ¹ (12), CN ^{ter} s(9), CCOO wag(8), CCH ₃ sd(8)
940	927	-13	C ^{α} H r ¹ (30), CCOO wag(29), C ^{α} H r ² (9)

Table 3.54: (continued)

frequency (cm^{-1})			Potential Energy Distribution
obs.	calc.	dev.	
1036	1025	-11	NH ₂ twist(27), CH ₃ r ¹ (14), CCH ₃ sd(11), C ^{α} H d ¹ (10), C ^{α} H r ¹ (8)
1055	1045	-10	CCH ₃ ad ¹ (31), CCH ₃ sd(24), CCH ₃ ad ² (18), CH ₃ r ¹ (8)
1055	1051	-4	CCH ₃ ad ² (79)
—	1060	—	CCH ₃ ad ¹ (59), CCH ₃ sd(25)
1123	1121	-2	NH ₂ sissor(48), C ^{α} H r ¹ (9), CN ^{ter} s(8), CH ₃ r ² (8), COO ss(7), CC ^{ter} s(7)
1182	1197	15	NH ₂ sissor(51), CN ^{ter} s(21), COO ss(9)
1215	1252	37	CC ^{me} s(49), CCH ₃ sd(10), C ^{α} H r ² (7), NH ₂ twist(7)
1409	1410	1	COO ss(58), CC ^{ter} s(25), CCOO sd(11)
1567	1564	-3	COO as(88), CCOO r(9)
2076	2101	25	CH ₃ ss(93)
2125	2125	0	C ^{α} H s(96)
2235	2201	-34	CH ₃ as ² (63), CH ₃ as ¹ (36)
2246	2249	3	CH ₃ as ¹ (62), CH ₃ as ² (33)
—	2302	—	NH ₂ as(89), NH ₂ ss(10)
—	2346	—	NH ₂ ss(90), NH ₂ as(10)

frequency (cm^{-1})			NH ₂ CHCD ₃ CO ₂ ⁻ (mean deviation = 11 cm^{-1})
obs.	calc.	dev.	
—	88	—	CC t(94)
—	146	—	CC ^{me} t(92)
—	203	—	CN t(92)
255	253	-2	C ^{α} H d ² (80)
340	344	4	C ^{α} H d ³ (71), CCOO r(21)
390	380	-10	C ^{α} H d ¹ (75), CH ₃ r ¹ (7)
521	526	5	CCOO r(45), CCOO sd(14), CC ^{ter} s(13), CN ^{ter} s(10)
607	598	-9	CCOO sd(33), CC ^{ter} s(18), CCOO r(14), CC ^{me} s(11), C ^{α} H d ³ (7)
741	713	-28	CCOO wag(45), CH ₃ r ¹ (37), CH ₃ r ² (8), C ^{α} H r ² (7)
771	757	-14	CN ^{ter} s(27), CH ₃ r ² (25), CH ₃ r ¹ (14), CC ^{me} s(12), CCOO sd(10)
828	803	-25	CH ₃ r ² (33), CCOO sd(28), COO ss(10), CC ^{ter} s(8)

Table 3.54: (continued)

frequency (cm^{-1})			Potential Energy Distribution
obs.	calc.	dev.	
910	908	-2	NH ₂ wag(28), CH ₃ r ¹ (18), CCOO wag(17), NH ₂ twist(8), CN ^{ter} s(7)
947	932	-15	CCH ₃ sd(27), NH ₂ wag(24), CC ^{me} s(14), CC ^{ter} s(11), NH ₂ twist(7)
1020	1030	10	NH ₂ wag(35), CC ^{ter} s(12), CCOO wag(9), COO ss(8), C ^{α} H d ³ (8), C ^{α} H r ² (7)
1058	1047	-11	CCH ₃ ad ² (66), CN ^{ter} s(9), CCH ₃ ad ¹ (8), CCH ₃ sd(7)
1058	1052	-6	CCH ₃ ad ¹ (79), CCH ₃ sd(8)
—	1057	—	CCH ₃ ad ² (30), CN ^{ter} s(18), CCH ₃ sd(14), NH ₂ twist(7)
1141	1163	22	CC ^{me} s(33), CCH ₃ sd(22), CN ^{ter} s(15), C ^{α} H r ² (12)
1189	1201	12	NH ₂ twist(34), C ^{α} H r ² (15), C ^{α} H r ¹ (14), C ^{α} H d ¹ (9), CH ₃ r ¹ (9), CN ^{ter} s(7)
1283	1284	1	C ^{α} H r ² (43), C ^{α} H r ¹ (23), COO ss(15)
1360	1366	6	C ^{α} H r ¹ (43), NH ₂ twist(28), CC ^{me} s(11), C ^{α} H r ² (7)
1413	1415	2	COO ss(51), CC ^{ter} s(25), CCOO sd(10)
1563	1564	1	COO as(85), CCOO r(9)
1587	1588	1	NH ₂ sissor(98)
2076	2101	25	CH ₃ ss(94)
2125	2201	76	CH ₃ as ² (62), CH ₃ as ¹ (37)
2235	2249	14	CH ₃ as ¹ (62), CH ₃ as ² (34)
—	2887	—	C ^{α} H s(100)
—	3133	—	NH ₂ as(97)
—	3236	—	NH ₂ ss(97)

frequency (cm^{-1})			ND ₂ CHCD ₃ CO ₂ ⁻ (mean deviation = 12 cm^{-1})
obs.	calc.	dev.	
—	85	—	CC t(88), CN t(9)
—	139	—	CC ^{me} t(48), CN t(45)
—	158	—	CC ^{me} t(48), CN t(45)
258	252	-6	C ^{α} H d ² (80)
320	319	-1	C ^{α} H d ³ (70), CCOO r(14), NH ₂ wag(8)
348	361	13	C ^{α} H d ¹ (72), CH ₃ r ¹ (7)
512	513	1	CCOO r(54), CN ^{ter} s(10), CC ^{ter} s(8), CCOO sd(8)

Table 3.54: (continued)

frequency (cm^{-1})			Potential Energy Distribution
obs.	calc.	dev.	
595	590	-5	CCOO sd(39), CC ^{ter} s(24), CC ^{me} s(9), CCOO r(9)
—	711	—	CCOO wag(47), CH ₃ r ¹ (31), CH ₃ r ² (8)
723	733	10	CH ₃ r ¹ (28), NH ₂ wag(19), CH ₃ r ² (14), CC ^{me} s(10), CN ^{ter} s(10)
751	765	14	CH ₃ r ² (28), NH ₂ wag(25), NH ₂ twist(24), CC ^{me} s(8)
799	786	-13	NH ₂ wag(29), CN ^{ter} s(18), NH ₂ twist(15), CCOO sd(13), CC ^{me} s(7)
852	830	-22	CCOO sd(18), NH ₂ twist(18), CH ₃ r ² (15), CCOO wag(13), CC ^{ter} s(12), COO ss(10)
988	996	8	CCH ₃ sd(33), CC ^{ter} s(14), C ^{α} H d ³ (9), COO ss(8), CN ^{ter} s(7), C ^{α} H r ² (7), CCOO wag(7)
1028	1005	-23	CCH ₃ sd(25), CH ₃ r ¹ (12), CCOO wag(11), NH ₂ twist(10), C ^{α} H d ² (8), CC ^{ter} s(7), CN ^{ter} s(7)
1056	1049	-7	CCH ₃ ad ² (62), CCH ₃ ad ¹ (35)
1056	1053	-3	CCH ₃ ad ¹ (59), CCH ₃ ad ² (36)
1109	1094	-15	CN ^{ter} s(23), NH ₂ sissor(19), C ^{α} H d ¹ (13), NH ₂ twist(11), CH ₃ r ² (9), CH ₃ r ¹ (7)
1131	1167	36	CC ^{me} s(37), CCH ₃ sd(23), C ^{α} H r ² (22)
—	1175	—	NH ₂ sissor(77), CN ^{ter} s(14)
1281	1284	3	C ^{α} H r ² (40), C ^{α} H r ¹ (26), COO ss(18)
1332	1326	-6	C ^{α} H r ¹ (52), C ^{α} H r ² (16), CC ^{me} s(15)
1412	1416	4	COO ss(51), CC ^{ter} s(25), CCOO sd(10)
1576	1565	-11	COO as(88), CCOO r(9)
2076	2101	25	CH ₃ ss(94)
2125	2201	76	CH ₃ as ² (62), CH ₃ as ¹ (37)
2235	2249	14	CH ₃ as ¹ (62), CH ₃ as ² (34)
2246	2302	56	NH ₂ as(89), NH ₂ ss(10)
—	2346	—	NH ₂ ss(90), NH ₂ as(10)
—	2887	—	C ^{α} H s(100)

frequency (cm^{-1})			Potential Energy Distribution
obs.	calc.	dev.	
—	90	—	CC t(94)

Table 3.54: (continued)

frequency (cm ⁻¹)			Potential Energy Distribution
obs.	calc.	dev.	
—	189	—	CN t(53), CC ^{me} t(41)
—	217	—	CC ^{me} t(46), CN t(42)
273	278	5	C ^α H d ² (75), CC ^{me} t(12)
344	346	2	C ^α H d ³ (70), CCOO r(20)
409	411	2	C ^α H d ¹ (80)
538	534	-4	CCOO r(45), CN ^{ter} s(13), CCOO sd(12), CC ^{ter} s(11), C ^α H d ³ (7)
624	612	-12	CCOO sd(39), CC ^{ter} s(18), CCOO r(13), CC ^{me} s(9), CCOO wag(9), C ^α H d ³ (7)
779	767	-12	CCOO wag(53), CCOO sd(16)
849	834	-15	CN ^{ter} s(18), CCOO sd(16), CC ^{me} s(14), CH ₃ r ¹ (13), CC ^{ter} s(12), COO ss(9), CCOO wag(8)
922	925	3	CH ₃ r ² (39), CN ^{ter} s(24), CC ^{ter} s(19), COO ss(9)
—	949	—	NH ₂ wag(69), CH ₃ r ¹ (11), CC ^{me} s(10)
1015	1001	-14	NH ₂ twist(36), CH ₃ r ¹ (21), CC ^{me} s(14), C ^α H r ¹ (10)
1073	1071	-2	C ^α H r ² (20), NH ₂ wag(16), CH ₃ r ² (16), CCOO wag(9), CC ^{ter} s(7), CH ₃ r ¹ (7)
1134	1134	0	CN ^{ter} s(29), CC ^{me} s(23), CH ₃ r ² (13), C ^α H r ¹ (10)
1231	1242	11	NH ₂ twist(28), CH ₃ r ¹ (18), C ^α H r ¹ (11), C ^α H d ¹ (11), CH ₃ r ² (8)
1288	1288	0	C ^α H r ² (48), COO ss(16), C ^α H r ¹ (14)
1355	1338	-17	CCH ₃ sd(58), C ^α H r ¹ (27), NH ₂ twist(10)
1360	1379	19	CCH ₃ sd(31), C ^α H r ¹ (22), NH ₂ twist(17), CC ^{me} s(13), C ^α H r ² (7)
1412	1413	1	COO ss(46), CC ^{ter} s(21), CCH ₃ ad ² (12), CCOO sd(9)
1458	1459	1	CCH ₃ ad ¹ (64), CCH ₃ ad ² (23)
1458	1464	6	CCH ₃ ad ² (56), CCH ₃ ad ¹ (22), CH ₃ r ² (7)
1562	1566	4	COO as(85), CCOO r(9)
1596	1589	-7	NH ₂ sissor(98)
2885	2885	0	C ^α H s(99)
2940	2911	-29	CH ₃ ss(82), CH ₃ as ² (16)
2980	2960	-20	CH ₃ as ² (55), CH ₃ as ¹ (40)
2993	3030	37	CH ₃ as ¹ (57), CH ₃ as ² (30), CH ₃ ss(14)
—	3133	—	NH ₂ as(97)

Table 3.54: (continued)

frequency (cm ⁻¹)			Potential Energy Distribution
obs.	calc.	dev.	
—	3236	—	NH ₂ ss(97)

frequency (cm ⁻¹)			¹⁵ NH ₂ CHCH ₃ CO ₂ ⁻ (mean deviation = 12 cm ⁻¹)
obs.	calc.	dev.	
Potential Energy Distribution			
—	90	—	CC t(95)
—	188	—	CN t(54), CC ^{me} t(41)
—	217	—	CC ^{me} t(48), CN t(41)
279	282	3	C ^α H d ² (76), CC ^{me} t(11)
343	342	-1	C ^α H d ³ (70), CCOO r(19)
421	411	-10	C ^α H d ¹ (80)
535	529	-6	CCOO r(45), CN ^{ter} s(14), CCOO sd(12), CC ^{ter} s(11)
632	615	-17	CCOO sd(39), CC ^{ter} s(17), CCOO r(13), CCOO wag(9), CC ^{me} s(8), C ^α H d ³ (8)
793	767	-26	CCOO wag(54), CCOO sd(16)
851	834	-17	CN ^{ter} s(20), CCOO sd(15), CC ^{me} s(13), CH ₃ r ¹ (12), CC ^{ter} s(11), COO ss(8), CCOO wag(8)
924	925	1	CH ₃ r ² (38), CN ^{ter} s(26), CC ^{ter} s(19), COO ss(9)
—	947	—	NH ₂ wag(68), CH ₃ r ¹ (13), CC ^{me} s(12)
1019	1003	-16	NH ₂ twist(37), CH ₃ r ¹ (21), CC ^{me} s(13), C ^α H r ¹ (10)
1072	1073	1	C ^α H r ² (20), CH ₃ r ² (16), NH ₂ wag(14), CCOO wag(9), CC ^{ter} s(7), CH ₃ r ¹ (7)
1134	1135	1	CN ^{ter} s(26), CC ^{me} s(24), CH ₃ r ² (15), C ^α H r ¹ (9)
1234	1245	11	NH ₂ twist(28), CH ₃ r ¹ (18), C ^α H d ¹ (12), C ^α H r ¹ (10), CH ₃ r ² (8)
1291	1288	-3	C ^α H r ² (48), COO ss(16), C ^α H r ¹ (14)
1360	1341	-19	CCH ₃ sd(43), C ^α H r ¹ (35), NH ₂ twist(14)
1370	1387	17	CCH ₃ sd(44), CC ^{me} s(15), C ^α H r ¹ (14), NH ₂ twist(12)
1414	1414	0	COO ss(46), CC ^{ter} s(21), CCH ₃ ad ² (11), CCOO sd(9)
1460	1460	0	CCH ₃ ad ¹ (62), CCH ₃ ad ² (26)
1460	1465	5	CCH ₃ ad ² (56), CCH ₃ ad ¹ (25)
1567	1566	-1	COO as(84), CCOO r(9)
1593	1586	-7	NH ₂ sissor(97)
2885	2886	1	C ^α H s(99)

Table 3.54: (continued)

frequency (cm ⁻¹)			Potential Energy Distribution
obs.	calc.	dev.	
2940	2916	-24	CH ₃ ss(84), CH ₃ as ² (13)
2980	2971	-9	CH ₃ as ² (57), CH ₃ as ¹ (39)
2993	3040	47	CH ₃ as ¹ (58), CH ₃ as ² (30), CH ₃ ss(12)
—	3125	—	NH ₂ as(97)
—	3231	—	NH ₂ ss(97)

Table 3.55: Scaled 6-31G** Frequencies and Potential Energy distribution for Water-Excluded Alaninate One-water Supramolecule.

frequency (cm ⁻¹)			NH ₂ CHC ₃ CO ₂ ⁻ (mean deviation = 9 cm ⁻¹)
obs.	calc.	dev.	
			Potential Energy Distribution
—	90	—	CC t(95)
—	189	—	CN t(55), CC ^{me} t(41)
—	217	—	CC ^{me} t(48), CN t(41)
279	280	1	C ^α H d ² (77), CC ^{me} t(10)
343	346	3	C ^α H d ³ (70), CCOO r(19)
415	413	-2	C ^α H d ¹ (80)
539	539	0	CCOO r(49), CN ^{ter} s(13), CC ^{ter} s(10), C ^α H d ³ (8), COO as(7), CCOO sd(7)
622	625	3	CCOO sd(30), CC ^{ter} s(25), CCOO wag(12), CC ^{me} s(11), CCOO r(10)
785	770	-15	CCOO wag(55), CCOO sd(15), CH ₃ r ¹ (7)
853	846	-7	CCOO sd(24), CN ^{ter} s(20), CC ^{me} s(16), COO ss(11), CH ₃ r ¹ (10), CC ^{ter} s(7)
927	930	3	CH ₃ r ² (34), CN ^{ter} s(23), CC ^{ter} s(19), COO ss(12)
—	953	—	NH ₂ wag(68), CC ^{me} s(10), CH ₃ r ¹ (10)
1020	1007	-13	NH ₂ twist(36), CH ₃ r ¹ (23), CC ^{me} s(15), C ^α H r ¹ (9)
1080	1069	-11	C ^α H r ² (21), NH ₂ wag(17), CH ₃ r ² (16), CCOO wag(8), CH ₃ r ¹ (7)
1140	1135	-5	CN ^{ter} s(30), CC ^{me} s(20), CH ₃ r ² (16), C ^α H r ¹ (9)
1238	1250	12	NH ₂ twist(30), CH ₃ r ¹ (19), C ^α H d ¹ (11), C ^α H r ¹ (10), CH ₃ r ² (7)
1286	1289	3	C ^α H r ² (50), COO ss(14), C ^α H r ¹ (13)
1353	1349	-4	CCH ₃ sd(51), C ^α H r ¹ (32), NH ₂ twist(11)
1368	1389	21	CCH ₃ sd(36), C ^α H r ¹ (21), NH ₂ twist(16), CC ^{me} s(13)
1414	1422	8	COO ss(44), CC ^{ter} s(18), CCH ₃ ad ² (17), CCOO sd(11)
1459	1458	-1	CCH ₃ ad ² (56), CCH ₃ ad ¹ (25)
1459	1465	6	CCH ₃ ad ¹ (63), CCH ₃ ad ² (19)
1564	1568	4	COO as(85), CCOO r(9)
1591	1589	-2	NH ₂ sissor(98)
2885	2887	2	C ^α H s(99)
2940	2915	-25	CH ₃ ss(88), CH ₃ as ² (9)
2980	2979	-1	CH ₃ as ² (55), CH ₃ as ¹ (43)
2993	3045	52	CH ₃ as ¹ (53), CH ₃ as ² (36), CH ₃ ss(11)

Table 3.55: (continued)

frequency (cm ⁻¹)			Potential Energy Distribution
obs.	calc.	dev.	
—	3155	—	NH ₂ as(97)
—	3259	—	NH ₂ ss(98)

frequency (cm ⁻¹)			ND ₂ CHCH ₃ CO ₂ ⁻ (mean deviation = 12 cm ⁻¹)
obs.	calc.	dev.	Potential Energy Distribution
—	86	—	CC t(90), CN t(8)
—	146	—	CN t(87), CC t(8)
—	207	—	CC ^{me} t(85), C ^α H d ² (7)
275	278	3	C ^α H d ² (75), CC ^{me} t(10)
331	322	-9	C ^α H d ³ (67), CCOO r(13), NH ₂ wag(8)
384	392	8	C ^α H d ¹ (78), NH ₂ twist(7)
527	523	-4	CCOO r(56), CN ^{ter} s(12), COO as(7)
621	618	-3	CCOO sd(34), CC ^{ter} s(31), CCOO wag(9), CC ^{me} s(8)
—	740	—	CCOO wag(44), NH ₂ wag(36)
780	807	27	NH ₂ wag(40), CCOO wag(16), C ^α H d ³ (11), CCOO sd(10), NH ₂ twist(7)
836	813	-23	NH ₂ twist(44), CC ^{me} s(19), CCOO sd(14), CN ^{ter} s(13)
870	859	-11	CH ₃ r ¹ (27), NH ₂ twist(20), CN ^{ter} s(10), CCOO sd(9)
922	923	1	CH ₃ r ² (31), CN ^{ter} s(22), CC ^{ter} s(21), COO ss(14), CCOO sd(8)
1053	1050	-3	C ^α H r ² (21), CH ₃ r ¹ (16), CCOO wag(10), CH ₃ r ² (10), CC ^{me} s(9)
1108	1112	4	NH ₂ sissor(23), CH ₃ r ² (21), CC ^{me} s(18), CN ^{ter} s(14)
1143	1164	21	NH ₂ sissor(44), CH ₃ r ¹ (16), CC ^{me} s(14), C ^α H d ¹ (7), NH ₂ twist(7)
1201	1189	-12	NH ₂ sissor(29), CN ^{ter} s(13), CH ₃ r ¹ (11), CH ₃ r ² (10), C ^α H d ¹ (9), NH ₂ twist(8)
1290	1289	-1	C ^α H r ² (47), COO ss(16), C ^α H r ¹ (14)
1334	1329	-5	C ^α H r ¹ (60), CCH ₃ sd(16), C ^α H r ² (9)
1370	1375	5	CCH ₃ sd(70), CC ^{me} s(11)
1414	1422	8	COO ss(43), CCH ₃ ad ² (19), CC ^{ter} s(17), CCOO sd(11)
1462	1459	-3	CCH ₃ ad ² (45), CCH ₃ ad ¹ (38)
1462	1467	5	CCH ₃ ad ¹ (49), CCH ₃ ad ² (28)

Table 3.55: (continued)

frequency (cm ⁻¹)			Potential Energy Distribution
obs.	calc.	dev.	
1571	1568	-3	COO as(87), CCOO r(9)
—	2320	—	NH ₂ as(91), NH ₂ ss(9)
—	2361	—	NH ₂ ss(91), NH ₂ as(9)
2887	2887	0	C ^α H s(99)
2942	2915	-27	CH ₃ ss(88), CH ₃ as ² (9)
2980	2979	-1	CH ₃ as ² (55), CH ₃ as ¹ (43)
2990	3045	55	CH ₃ as ¹ (53), CH ₃ as ² (36), CH ₃ ss(11)

frequency (cm ⁻¹)			NH ₂ CD ₂ CO ₂ ⁻ (mean deviation = 12 cm ⁻¹)
obs.	calc.	dev.	
—	87	—	CC t(95)
—	146	—	CC ^{me} t(93)
—	203	—	CN t(92)
257	249	-8	C ^α H d ² (81)
335	342	7	C ^α H d ³ (72), CCOO r(21)
382	376	-6	C ^α H d ¹ (76), CH ₃ r ¹ (7)
514	526	12	CCOO r(44), CC ^{ter} s(15), CCOO sd(10), CN ^{ter} s(9), C ^α H d ³ (7)
593	590	-3	CC ^{ter} s(23), CCOO sd(21), CCOO r(15), CC ^{me} s(11), CCOO wag(11), C ^α H r ² (7)
688	666	-22	CH ₃ r ¹ (37), C ^α H r ² (24), CCOO wag(22)
752	751	-1	CH ₃ r ² (38), CN ^{ter} s(18), CC ^{me} s(11), CCOO sd(7)
827	819	-8	CCOO sd(34), CH ₃ r ² (25), COO ss(10), CCOO wag(8), CC ^{me} s(7)
884	855	-29	C ^α H r ¹ (43), CN ^{ter} s(22), NH ₂ twist(9), NH ₂ wag(9)
897	892	-5	C ^α H r ² (25), CC ^{ter} s(12), CCOO sd(11), COO ss(10), CCOO wag(9), CC ^{me} s(8), CH ₃ r ¹ (8), CCH ₃ sd(7)
947	939	-8	CCOO wag(24), CH ₃ r ¹ (21), C ^α H r ¹ (19), CCH ₃ sd(9), C ^α H d ² (7)
—	967	—	NH ₂ wag(58), C ^α H r ² (18)
1055	1046	-9	CCH ₃ ad ² (92)
1055	1052	-3	CCH ₃ ad ¹ (77), CCH ₃ sd(7)
1100	1066	-34	CCH ₃ sd(42), CCH ₃ ad ¹ (16), NH ₂ wag(12), C ^α H r ² (9)

Table 3.55: (continued)

frequency (cm ⁻¹)			Potential Energy Distribution
obs.	calc.	dev.	
1126	1145	19	C ^α H r ¹ (15), COO ss(12), CC ^{ter} s(12), NH ₂ twist(11), C ^α H r ² (8), CN ^{ter} s(7), NH ₂ wag(7), CH ₃ r ² (7)
1158	1175	17	CN ^{ter} s(27), NH ₂ twist(20), CC ^{me} s(14), CCH ₃ sd(8)
1276	1303	27	NH ₂ twist(48), CC ^{me} s(22)
1408	1420	12	COO ss(56), CC ^{ter} s(22), CCOO sd(14)
1555	1566	11	COO as(85), CCOO r(9)
1582	1587	5	NH ₂ sissor(97)
2076	2100	24	CH ₃ ss(94)
2125	2126	1	C ^α H s(97)
2235	2208	-27	CH ₃ as ² (57), CH ₃ as ¹ (42)
2246	2253	7	CH ₃ as ¹ (56), CH ₃ as ² (40)
—	3155	—	NH ₂ as(98)
—	3259	—	NH ₂ ss(98)

frequency (cm ⁻¹)			ND ₂ CDCD ₃ CO ₂ ⁻ (mean deviation = 11 cm ⁻¹)
obs.	calc.	dev.	
—	84	—	CC t(91), CN t(7)
—	138	—	CN t(48), CC ^{me} t(46)
—	157	—	CC ^{me} t(50), CN t(44)
257	248	-9	C ^α H d ² (81)
327	317	-10	C ^α H d ³ (71), CCOO r(15), NH ₂ wag(8)
363	358	-5	C ^α H d ¹ (73), CH ₃ r ¹ (7)
506	513	7	CCOO r(53), CC ^{ter} s(10), CN ^{ter} s(9)
590	586	-4	CC ^{ter} s(29), CCOO sd(25), CCOO r(11), CC ^{me} s(10), CCOO wag(9)
690	664	-26	CH ₃ r ¹ (35), C ^α H r ² (25), CCOO wag(24)
729	721	-8	CH ₃ r ² (23), NH ₂ wag(19), NH ₂ twist(10), CH ₃ r ¹ (10), C ^α H r ¹ (9), CC ^{me} s(7), CCOO wag(7)
756	764	8	NH ₂ twist(31), NH ₂ wag(23), CC ^{me} s(17), CH ₃ r ² (11)
790	779	-11	CN ^{ter} s(29), NH ₂ wag(27), CH ₃ r ² (16), NH ₂ twist(7)
845	838	-7	CCOO sd(35), COO ss(15), CH ₃ r ² (12), CC ^{ter} s(8), NH ₂ wag(8), CCOO wag(7)

Table 3.55: (continued)

frequency (cm^{-1})			Potential Energy Distribution
obs.	calc.	dev.	
893	899	6	C^αH r^2 (31), CH_3 r^1 (11), CCOO wag(10), CN^{ter} s(8), C^αH r^1 (8)
940	926	-14	C^αH r^1 (33), CCOO wag(24), CH_3 r^1 (7)
1036	1026	-10	NH_2 twist(27), CH_3 r^1 (16), C^αH d^1 (9), C^αH r^1 (8)
1055	1044	-11	CCH_3 ad^2 (48), CCH_3 ad^1 (23), CCH_3 sd (17)
1055	1049	-6	CCH_3 ad^2 (48), CCH_3 sd (17), CCH_3 ad^1 (12), CH_3 r^1 (7)
—	1061	—	CCH_3 ad^1 (59), CCH_3 sd (26)
1123	1118	-5	NH_2 sissor(48), C^αH r^1 (10), CN^{ter} s(8), CH_3 r^2 (8), COO ss(7)
1182	1199	17	NH_2 sissor(52), CN^{ter} s(21), COO ss(8)
1215	1241	26	CC^{me} s(46), CCH_3 sd (10), C^αH r^2 (8), NH_2 twist(8)
1409	1421	12	COO ss(57), CC^{ter} s(23), CCOO sd (15)
1567	1566	-1	COO as(88), CCOO r (9)
2076	2100	24	CH_3 ss(94)
2125	2126	1	C^αH s(97)
2235	2208	-27	CH_3 as^2 (57), CH_3 as^1 (42)
2246	2253	7	CH_3 as^1 (56), CH_3 as^2 (40)
—	2320	—	NH_2 as(91), NH_2 ss(9)
—	2361	—	NH_2 ss(92), NH_2 as(9)

frequency (cm ⁻¹)			NH ₂ CHCD ₃ CO ₂ ⁻ (mean deviation = 10 cm ⁻¹)
obs.	calc.	dev.	
Potential Energy Distribution			
—	87	—	CC t(95)
—	146	—	CC ^{me} t(93)
—	203	3	CN t(93)
255	251	-4	C ^α H d ² (80)
340	344	4	C ^α H d ³ (71), CCOO r(20)
390	379	-11	C ^α H d ¹ (74), CH ₃ r ¹ (7)
521	531	10	CCOO r(48), CC ^{ter} s(12), CN ^{ter} s(10), CCOO sd(8), C ^α H d ³ (7)
607	605	-2	CC ^{ter} s(26), CCOO sd(25), CC ^{me} s(14), CCOO r(11), CCOO wag(7)
741	709	-32	CCOO wag(45), CH ₃ r ¹ (37), CH ₃ r ² (8)

Table 3.55: (continued)

frequency (cm^{-1})			Potential Energy Distribution
obs.	calc.	dev.	
771	761	-10	CH_3 r ² (34), CN^{ter} s(26), CH_3 r ¹ (13), CC^{me} s(10)
828	821	-7	CCOO sd(38), CH_3 r ² (23), COO ss(12)
910	908	-2	NH_2 wag(22), CH_3 r ¹ (21), CCOO wag(17), NH_2 twist(9)
947	932	-15	NH_2 wag(26), CCH_3 sd(23), CC^{me} s(14), CC^{ter} s(12), COO ss(8)
1020	1027	7	NH_2 wag(36), CC^{ter} s(12), CCOO wag(9), COO ss(8), C^αH r ² (7), C^αH d ³ (7)
1058	1044	-14	CCH_3 ad ² (82), CCH_3 ad ¹ (7)
1058	1053	-5	CCH_3 ad ¹ (81), CCH_3 sd(7)
—	1058	—	CN^{ter} s(24), CCH_3 sd(22), CCH_3 ad ² (12), NH_2 twist(9)
1141	1155	14	CC^{me} s(32), CCH_3 sd(24), CN^{ter} s(16), C^αH r ² (12)
1189	1205	16	NH_2 twist(37), C^αH r ² (16), C^αH r ¹ (12), CH_3 r ¹ (9), C^αH d ¹ (8), CN^{ter} s(7)
1283	1284	1	C^αH r ² (45), C^αH r ¹ (21), COO ss(13)
1360	1372	12	C^αH r ¹ (48), NH_2 twist(29), CC^{me} s(9)
1413	1424	11	COO ss(52), CC^{ter} s(22), CCOO sd(14)
1563	1567	4	COO as(85), CCOO r(9)
1587	1588	1	NH_2 sissor(98)
2076	2100	24	CH_3 ss(95)
2125	2207	82	CH_3 as ² (56), CH_3 as ¹ (43)
2235	2253	18	CH_3 as ¹ (55), CH_3 as ² (41)
—	2888	—	C^αH s(100)
—	3155	—	NH_2 as(97)
—	3259	—	NH_2 ss(98)

frequency (cm^{-1})			ND ₂ CHCD ₃ CO ₂ ⁻ (mean deviation = 11 cm^{-1})
obs.	calc.	dev.	
			Potential Energy Distribution
—	85	—	CC t(90), CN t(7)
—	138	—	CN t(48), CC^{me} t(47)
—	157	—	CC^{me} t(50), CN t(44)
258	250	-8	C^αH d ² (80)
320	319	-1	C^αH d ³ (70), CCOO r(14), NH_2 wag(8)
348	360	12	C^αH d ¹ (72), CH_3 r ¹ (7)

Table 3.55: (continued)

frequency (cm^{-1})			Potential Energy Distribution
obs.	calc.	dev.	
512	517	5	CCOO r(56), CN ^{ter} s(10), COO as(7), CC ^{ter} s(7)
595	600	5	CC ^{ter} s(31), CCOO sd(29), CC ^{me} s(12), CCOO r(7)
—	706	—	CCOO wag(48), CH ₃ r ¹ (29), CH ₃ r ² (9)
723	734	11	CH ₃ r ¹ (28), NH ₂ wag(20), CH ₃ r ² (16), CN ^{ter} s(9), CC ^{me} s(8)
751	769	18	NH ₂ wag(35), CH ₃ r ² (27), NH ₂ twist(18)
799	793	-6	NH ₂ twist(27), CN ^{ter} s(17), NH ₂ wag(15), CC ^{me} s(12), CCOO sd(11)
852	843	-9	CCOO sd(31), COO ss(14), CH ₃ r ² (12), CCOO wag(10), NH ₂ twist(10), CC ^{ter} s(9)
988	993	5	CC ^{ter} s(19), CCOO wag(13), COO ss(12), CCH ₃ sd(12), C ^α H d ³ (10), C ^α H r ² (7)
1028	1004	-24	CCH ₃ sd(44), CN ^{ter} s(12), NH ₂ twist(11), CH ₃ r ¹ (8)
1056	1046	-10	CCH ₃ ad ² (87), CCH ₃ ad ¹ (11)
1056	1053	-3	CCH ₃ ad ¹ (84), CCH ₃ ad ² (11)
1109	1094	-15	CN ^{ter} s(23), NH ₂ sissor(20), C ^α H d ¹ (13), NH ₂ twist(11), CH ₃ r ² (9), CH ₃ r ¹ (7)
1131	1158	27	CC ^{me} s(36), CCH ₃ sd(26), C ^α H r ² (20)
—	1176	—	NH ₂ sissor(75), CN ^{ter} s(15)
1281	1284	3	C ^α H r ² (49), C ^α H r ¹ (15), COO ss(14)
1332	1331	-1	C ^α H r ¹ (65), CC ^{me} s(10), C ^α H r ² (10)
1412	1426	14	COO ss(52), CC ^{ter} s(23), CCOO sd(14)
1576	1567	-9	COO as(88), CCOO r(9)
2076	2100	24	CH ₃ ss(95)
2125	2207	82	CH ₃ as ² (56), CH ₃ as ¹ (43)
2235	2253	18	CH ₃ as ¹ (55), CH ₃ as ² (41)
2246	2320	74	NH ₂ as(91), NH ₂ ss(9)
—	2361	—	NH ₂ ss(91), NH ₂ as(9)
—	2888	—	C ^α H s(100)

frequency (cm^{-1})			Potential Energy Distribution
obs.	calc.	dev.	
—	89	—	CC t(95)

Table 3.55: (continued)

frequency (cm ⁻¹)			Potential Energy Distribution
obs.	calc.	dev.	
—	189	—	CN t(54), CC ^{me} t(41)
—	217	—	CC ^{me} t(47), CN t(42)
273	276	3	C ^α H d ² (76), CC ^{me} t(11)
344	346	2	C ^α H d ³ (70), CCOO r(19)
409	410	1	C ^α H d ¹ (80)
538	539	1	CCOO r(49), CN ^{ter} s(13), CC ^{ter} s(10), C ^α H d ³ (8), COO as(7), CCOO sd(7)
624	622	-2	CCOO sd(30), CC ^{ter} s(25), CC ^{me} s(12), CCOO wag(12), CCOO r(9)
779	770	-9	CCOO wag(54), CCOO sd(15), CH ₃ r ¹ (7)
849	842	-7	CCOO sd(24), CN ^{ter} s(20), CC ^{me} s(18), CH ₃ r ¹ (11), COO ss(10)
922	926	4	CH ₃ r ² (35), CN ^{ter} s(20), CC ^{ter} s(19), COO ss(12), CCOO sd(7)
—	950	—	NH ₂ wag(68), CC ^{me} s(10), CH ₃ r ¹ (9)
1015	1003	-12	NH ₂ twist(35), CH ₃ r ¹ (24), CC ^{me} s(15), C ^α H r ¹ (9)
1073	1066	-7	C ^α H r ² (20), NH ₂ wag(18), CH ₃ r ² (16), CCOO wag(9), CH ₃ r ¹ (7)
1134	1130	-4	CN ^{ter} s(31), CC ^{me} s(20), CH ₃ r ² (15), C ^α H r ¹ (9)
1231	1245	14	NH ₂ twist(31), CH ₃ r ¹ (18), C ^α H d ¹ (11), C ^α H r ¹ (10), CH ₃ r ² (7)
1288	1287	-1	C ^α H r ² (49), COO ss(14), C ^α H r ¹ (14)
1355	1343	-12	CCH ₃ sd(65), C ^α H r ¹ (23), NH ₂ twist(7)
1360	1381	21	C ^α H r ¹ (29), CCH ₃ sd(24), NH ₂ twist(21), CC ^{me} s(11), C ^α H r ² (7)
1412	1421	9	COO ss(44), CCH ₃ ad ² (18), CC ^{ter} s(17), CCOO sd(11)
1458	1457	-1	CCH ₃ ad ² (51), CCH ₃ ad ¹ (30)
1458	1464	6	CCH ₃ ad ¹ (57), CCH ₃ ad ² (21)
1562	1568	6	COO as(85), CCOO r(9)
1596	1588	-8	NH ₂ sissor(98)
2885	2887	2	C ^α H s(99)
2940	2911	-29	CH ₃ ss(86), CH ₃ as ² (11)
2980	2969	-11	CH ₃ as ² (54), CH ₃ as ¹ (44)
2993	3035	42	CH ₃ as ¹ (52), CH ₃ as ² (35), CH ₃ ss(12)

Table 3.55: (continued)

frequency (cm ⁻¹)			Potential Energy Distribution
obs.	calc.	dev.	
—	3155	—	NH ₂ as(97)
—	3259	—	NH ₂ ss(98)

frequency (cm ⁻¹)			¹⁵ NH ₂ CHC ₃ CO ₂ ⁻ (mean deviation = 12 cm ⁻¹)
obs.	calc.	dev.	Potential Energy Distribution
—	89	—	CC t(95)
—	188	—	CN t(55), CC ^{me} t(41)
—	217	—	CC ^{me} t(48), CN t(41)
279	279	0	C ^α H d ² (76), CC ^{me} t(10)
334	342	8	C ^α H d ³ (70), CCOO r(18)
417	411	-6	C ^α H d ¹ (80)
535	534	-1	CCOO r(49), CN ^{ter} s(14), CC ^{ter} s(10), COO as(7), C ^α H d ³ (7), CCOO sd(7)
632	625	-7	CCOO sd(30), CC ^{ter} s(25), CCOO wag(12), CC ^{me} s(11), CCOO r(10)
793	770	-23	CCOO wag(54), CCOO sd(15), CH ₃ r ¹ (7)
851	841	-10	CCOO sd(24), CN ^{ter} s(22), CC ^{me} s(16), COO ss(10), CH ₃ r ¹ (10)
924	927	3	CH ₃ r ² (35), CN ^{ter} s(23), CC ^{ter} s(20), COO ss(12), CCOO sd(7)
—	947	—	NH ₂ wag(69), CC ^{me} s(12), CH ₃ r ¹ (11)
1019	1006	-13	NH ₂ twist(36), CH ₃ r ¹ (23), CC ^{me} s(14), C ^α H r ¹ (9)
1072	1068	-4	C ^α H r ² (20), NH ₂ wag(17), CH ₃ r ² (16), CCOO wag(8), CH ₃ r ¹ (7)
1134	1132	-2	CN ^{ter} s(28), CC ^{me} s(21), CH ₃ r ² (17), C ^α H r ¹ (9)
1234	1248	14	NH ₂ twist(31), CH ₃ r ¹ (19), C ^α H d ¹ (11), C ^α H r ¹ (9), CH ₃ r ² (7)
1291	1288	-3	C ^α H r ² (49), COO ss(14), C ^α H r ¹ (14)
1360	1348	-12	CCH ₃ sd(49), C ^α H r ¹ (34), NH ₂ twist(12)
1370	1388	18	CCH ₃ sd(38), C ^α H r ¹ (19), NH ₂ twist(15), CC ^{me} s(13)
1414	1422	8	COO ss(44), CC ^{ter} s(18), CCH ₃ ad ² (17), CCOO sd(11)
1460	1458	-2	CCH ₃ ad ² (57), CCH ₃ ad ¹ (25)
1460	1465	5	CCH ₃ ad ¹ (63), CCH ₃ ad ² (18)

Table 3.55: (continued)

frequency (cm^{-1})			Potential Energy Distribution
obs.	calc.	dev.	
1567	1568	1	COO as(84), CCOO r(9)
1593	1585	-8	NH ₂ sissor(97)
2885	2887	2	C ^{α} H s(99)
2940	2915	-25	CH ₃ ss(88), CH ₃ as ² (9)
2980	2979	-1	CH ₃ as ² (55), CH ₃ as ¹ (43)
2993	3045	52	CH ₃ as ¹ (53), CH ₃ as ² (36), CH ₃ ss(11)
—	3147	—	NH ₂ as(98)
—	3254	—	NH ₂ ss(98)

Table 3.56: Scaled 6-31+G** Frequencies and Potential Energy Distribution for Water-Excluded Alaninate One-water Supermolecule.

frequency (cm ⁻¹)			NH ₂ CHCH ₃ CO ₂ ⁻ (mean deviation = 12 cm ⁻¹)
obs.	calc.	dev.	
			Potential Energy Distribution
—	94	—	CC t(99)
—	210	—	CC ^{me} t(78), CN t(19)
—	227	—	CN t(76), CC ^{me} t(18)
279	284	5	C ^α H d ² (58), CCOO wag(16), C ^α H d ³ (13)
343	340	-3	C ^α H d ³ (45), CCOO r(31), C ^α H d ² (10)
415	410	-5	C ^α H d ¹ (66), CCOO r(8)
539	539	0	CCOO r(25), CCOO sd(19), CC ^{ter} s(13), CN ^{ter} s(13), C ^α H d ¹ (13)
622	657	35	CCOO sd(42), C ^α H d ³ (16), CCOO r(16)
785	779	-6	CCOO wag(65), C ^α H d ² (11), CC ^{me} s(7), CH ₃ r ¹ (7)
853	832	-21	CN ^{ter} s(19), CCOO sd(18), CC ^{ter} s(17), CC ^{me} s(14), COO ss(11), CH ₃ r ¹ (11)
927	924	-3	CH ₃ r ² (29), CN ^{ter} s(22), CC ^{ter} s(20), COO ss(10)
—	943	—	NH ₂ wag(68), CC ^{me} s(12), CN ^{ter} s(8)
1020	1004	-16	NH ₂ twist(33), CH ₃ r ¹ (28), C ^α H r ¹ (11)
1080	1084	4	C ^α H r ² (25), CH ₃ r ² (20), NH ₂ wag(11), CC ^{me} s(9)
1140	1132	-8	CC ^{me} s(26), CN ^{ter} s(23), CH ₃ r ² (14), C ^α H r ¹ (7), C ^α H d ² (7)
1238	1250	12	NH ₂ twist(21), C ^α H r ¹ (17), C ^α H d ¹ (14), CH ₃ r ² (10), COO ss(9), CH ₃ r ¹ (9)
1286	1282	-4	C ^α H r ² (51), CH ₃ r ¹ (14), COO ss(11), NH ₂ twist(7)
1353	1350	-3	CCH ₃ sd(61), C ^α H r ¹ (24), NH ₂ twist(11)
1368	1382	14	CCH ₃ sd(25), C ^α H r ¹ (23), NH ₂ twist(17), CC ^{me} s(13), C ^α H r ² (7)
1414	1414	0	COO ss(41), CC ^{ter} s(19), CCH ₃ ad ² (14), C ^α H r ¹ (7), CCOO sd(7)
1459	1458	-1	CCH ₃ ad ² (58), CCH ₃ ad ¹ (26)
1459	1463	4	CCH ₃ ad ¹ (65), CCH ₃ ad ² (21)
1564	1566	2	COO as(86), CCOO r(8)
1591	1588	-3	NH ₂ sissor(99)
2885	2883	-2	C ^α H s(99)
2940	2922	-18	CH ₃ ss(95)
2980	2979	-1	CH ₃ as ² (86), CH ₃ as ¹ (12)
2993	3019	26	CH ₃ as ¹ (87), CH ₃ as ² (10)

Table 3.56: (continued)

frequency (cm^{-1})			Potential Energy Distribution
obs.	calc.	dev.	
—	3175	—	NH ₂ as(100)
—	3268	—	NH ₂ ss(100)

frequency (cm^{-1})			Potential Energy Distribution
obs.	calc.	dev.	
—	92	—	CC t(98)
—	163	—	CN t(96)
—	214	—	CC ^{me} t(94)
275	278	3	C ^α H d ² (48), C ^α H d ³ (23), CCOO wag(14)
331	322	−9	C ^α H d ³ (39), C ^α H d ² (21), CCOO r(21)
384	387	3	C ^α H d ¹ (68), CCOO r(11)
527	524	−3	CCOO r(35), CN ^{ter} s(14), CCOO sd(12), C ^α H d ¹ (11), CC ^{ter} s(9)
621	627	6	CCOO sd(43), NH ₂ wag(16), CC ^{ter} s(13), CCOO r(10)
—	770	—	NH ₂ wag(35), CCOO wag(33), NH ₂ twist(9)
780	784	4	CCOO wag(34), NH ₂ wag(31), CC ^{me} s(13)
836	802	−34	NH ₂ twist(25), CN ^{ter} s(20), CCOO sd(20), CC ^{me} s(13), CC ^{ter} s(9), COO ss(8)
870	866	−4	CH ₃ r ¹ (36), NH ₂ twist(31)
922	917	−5	CH ₃ r ² (29), CN ^{ter} s(25), CC ^{ter} s(23), COO ss(11)
1053	1061	8	C ^α H r ² (24), CC ^{me} s(17), CN ^{ter} s(8), CH ₃ r ² (8), CH ₃ r ¹ (7)
1108	1112	4	CH ₃ r ² (27), NH ₂ sissor(17), CC ^{me} s(14), CN ^{ter} s(11), C ^α H r ¹ (7), C ^α H d ² (7)
1143	1165	22	NH ₂ sissor(62), CC ^{me} s(10)
1201	1193	−8	CH ₃ r ¹ (21), NH ₂ sissor(15), C ^α H d ¹ (14), NH ₂ twist(12), CC ^{me} s(7), CN ^{ter} s(7), CH ₃ r ² (7)
1290	1276	−14	C ^α H r ² (45), COO ss(20), C ^α H r ¹ (8)
1334	1329	−5	C ^α H r ¹ (59), CCH ₃ sd(17), C ^α H r ² (9)
1370	1370	0	CCH ₃ sd(70), CC ^{me} s(12)
1414	1414	0	COO ss(43), CC ^{ter} s(21), CCH ₃ ad ² (16), CCOO sd(8)
1462	1458	−4	CCH ₃ ad ² (43), CCH ₃ ad ¹ (42)
1462	1464	2	CCH ₃ ad ¹ (49), CCH ₃ ad ² (34)
1571	1566	−5	COO as(86), CCOO r(8)

Table 3.56: (continued)

frequency (cm ⁻¹)			Potential Energy Distribution
obs.	calc.	dev.	
—	2337	—	NH ₂ as(100)
—	2365	—	NH ₂ ss(100)
2887	2883	-4	C ^α H s(99)
2942	2922	-20	CH ₃ ss(95)
2980	2979	-1	CH ₃ as ² (86), CH ₃ as ¹ (12)
2990	3019	29	CH ₃ as ¹ (87), CH ₃ as ² (10)

frequency (cm ⁻¹)			Potential Energy Distribution
obs.	calc.	dev.	
—	91	—	CC t(98)
—	153	—	CC ^{me} t(98)
—	223	—	CN t(94)
257	258	1	C ^α H d ² (65), CCOO wag(15), C ^α H d ³ (7)
335	332	-3	C ^α H d ³ (51), CCOO r(34)
382	380	-2	C ^α H d ¹ (66), CH ₃ r ² (7)
514	512	-2	CCOO r(27), CCOO sd(21), CC ^{ter} s(18), CN ^{ter} s(9)
593	615	22	CCOO sd(24), CH ₃ r ¹ (24), CCOO r(16), C ^α H d ³ (11), CC ^{ter} s(9)
688	688	0	CCOO wag(29), C ^α H r ² (23), CH ₃ r ¹ (16), CCOO sd(8)
752	746	-6	CH ₃ r ² (27), CC ^{me} s(21), CN ^{ter} s(13), CCOO wag(10), CCH ₃ sd(8)
827	812	-15	CH ₃ r ² (26), CCOO sd(23), CC ^{ter} s(14), COO ss(11)
884	845	-39	C ^α H r ¹ (49), CN ^{ter} s(20), NH ₂ twist(9), C ^α H r ² (7)
897	870	-27	C ^α H r ² (26), CN ^{ter} s(15), CC ^{ter} s(9), CCOO wag(9), CC ^{me} s(7), NH ₂ wag(7)
947	945	-2	CCOO wag(22), NH ₂ wag(18), CCH ₃ sd(13), C ^α H d ² (12), CH ₃ r ¹ (9)
—	961	—	NH ₂ wag(47), CH ₃ r ¹ (17), C ^α H r ¹ (14), C ^α H r ² (11)
1055	1048	-7	CCH ₃ ad ² (87), CCH ₃ ad ¹ (11)
1055	1053	-2	CCH ₃ ad ¹ (53), CCH ₃ sd(20), CCH ₃ ad ² (9)
—	1060	—	CCH ₃ ad ¹ (35), CCH ₃ sd(33), C ^α H r ² (7), NH ₂ wag(7)
1126	1157	31	CN ^{ter} s(28), COO ss(15), C ^α H r ¹ (14), CH ₃ r ² (13), CC ^{ter} s(9), C ^α H d ¹ (8)

Table 3.56: (continued)

frequency (cm^{-1})			Potential Energy Distribution
obs.	calc.	dev.	
1158	1193	35	CC^{me} s(26), NH_2 twist(23), CCH_3 sd(10), C^αH d ³ (8), NH_2 wag(7)
1276	1293	17	NH_2 twist(53), CC^{me} s(21), C^αH r ¹ (7)
1408	1406	-2	COO ss(58), CC^{ter} s(25), CCOO sd(10)
1555	1561	6	COO as(88), CCOO r(8)
1582	1587	5	NH_2 sissor(100)
2076	2101	25	CH_3 ss(97)
2125	2129	4	C^αH s(96)
2235	2208	-27	CH_3 as ² (88), CH_3 as ¹ (11)
2246	2236	-10	CH_3 as ¹ (88), CH_3 as ² (11)
—	3174	—	NH_2 as(100)
—	3268	—	NH_2 ss(100)

frequency (cm^{-1})			Potential Energy Distribution
obs.	calc.	dev.	
—	89	—	CC t(98)
—	152	—	CC^{me} t(87), CN t(12)
—	164	—	CN t(85), CC^{me} t(11)
257	255	-2	C^αH d ² (62), CCOO wag(15), C^αH d ³ (10)
327	313	-14	C^αH d ³ (53), CCOO r(24), C^αH d ² (8)
363	359	-4	C^αH d ¹ (68)
506	501	-5	CCOO r(35), CCOO sd(15), CC^{ter} s(14), CN^{ter} s(9)
590	600	10	CCOO sd(32), CC^{ter} s(15), CCOO r(14), CH_3 r ¹ (12), NH_2 wag(8)
683	674	-9	CH_3 r ¹ (30), CCOO wag(23), C^αH r ² (22)
729	735	6	CH_3 r ² (34), CCOO wag(15), NH_2 twist(13), C^αH r ¹ (10), CC^{me} s(9), CH_3 r ¹ (8)
756	753	-3	NH_2 twist(25), NH_2 wag(24), CC^{me} s(22), CCH_3 sd(8)
790	780	-10	NH_2 wag(44), CN^{ter} s(22)
845	819	-26	CCOO sd(24), CH_3 r ² (18), CC^{ter} s(17), COO ss(13)
893	875	-18	C^αH r ² (41), CCOO wag(14), CN^{ter} s(8)
940	926	-14	C^αH r ¹ (38), CCOO wag(16), CH_3 r ¹ (12), C^αH d ² (7), NH_2 twist(7)

Table 3.56: (continued)

frequency (cm^{-1})			Potential Energy Distribution
obs.	calc.	dev.	
1036	1041	5	CCH ₃ sd(57), CCH ₃ ad ¹ (9), C ^{α} H r ² (8)
1055	1048	-7	CCH ₃ ad ² (90)
1055	1057	2	CCH ₃ ad ¹ (85)
—	1072	—	NH ₂ twist(26), CH ₃ r ¹ (21), C ^{α} H d ¹ (10), C ^{α} H d ³ (10), CN ^{ter} s(9)
1123	1118	-5	NH ₂ sissor(48), C ^{α} H r ¹ (11), COO ss(9), CC ^{ter} s(8), CH ₃ r ² (8)
1182	1201	19	NH ₂ sissor(50), CN ^{ter} s(20), COO ss(10)
1215	1233	18	CC ^{me} s(51), CCH ₃ sd(11), C ^{α} H r ² (7)
1409	1408	-1	COO ss(57), CC ^{ter} s(26), CCOO sd(10)
1567	1561	-6	COO as(89), CCOO r(8)
2076	2101	25	CH ₃ ss(97)
2125	2128	3	C ^{α} H s(96)
2235	2208	-27	CH ₃ as ² (88), CH ₃ as ¹ (11)
2246	2236	-10	CH ₃ as ¹ (88), CH ₃ as ² (11)
—	2337	—	NH ₂ as(100)
—	2365	—	NH ₂ ss(100)

frequency (cm^{-1})			NH ₂ CHCD ₃ CO ₂ ⁻ (mean deviation = 10 cm^{-1})
obs.	calc.	dev.	
			Potential Energy Distribution
—	91	—	CC t(98)
—	153	—	CC ^{me} t(98)
—	223	—	CN t(94)
255	259	4	C ^{α} H d ² (64), CCOO wag(15), C ^{α} H d ³ (7)
340	334	-6	C ^{α} H d ³ (50), CCOO r(33)
390	382	-8	C ^{α} H d ¹ (66)
521	521	0	CCOO r(29), CCOO sd(20), CC ^{ter} s(17), CN ^{ter} s(10)
607	620	13	CCOO sd(26), CH ₃ r ¹ (23), CCOO r(16), C ^{α} H d ³ (12), CC ^{ter} s(9)
741	724	-17	CCOO wag(45), CH ₃ r ¹ (17), CH ₃ r ² (12), CCOO sd(9)
771	755	-16	CN ^{ter} s(22), CC ^{me} s(18), CH ₃ r ² (18), CH ₃ r ¹ (17), CCOO sd(9), CCH ₃ sd(8)

Table 3.56: (continued)

frequency (cm^{-1})			Potential Energy Distribution
obs.	calc.	dev.	
828	814	-14	CH_3 r^2 (28), CCOO sd (19), CC^{ter} s (12), COO ss (9), CCOO wag (9)
910	911	1	NH_2 wag (45), CN^{ter} s (13), CC^{ter} s (10)
947	933	-14	CCH_3 sd (20), NH_2 $twist$ (16), CCOO wag (14), CH_3 r^1 (14), C^αH d^2 (10), CC^{me} s (9)
1020	1025	5	NH_2 wag (38), CCH_3 sd (25), C^αH r^2 (7), C^αH d^3 (7)
1058	1048	-10	CCH_3 ad^2 (72), CCH_3 ad^1 (14)
1058	1053	-5	CCH_3 ad^2 (20), CN^{ter} s (19), CCH_3 ad^1 (9), CH_3 r^2 (9), CC^{ter} s (8), C^αH r^1 (8), CCH_3 sd (8)
—	1055	—	CCH_3 ad^1 (72)
1141	1158	17	CC^{me} s (34), CCH_3 sd (22), C^αH r^2 (15), CN^{ter} s (13)
1189	1216	27	NH_2 $twist$ (35), C^αH r^1 (22), C^αH d^1 (10), CH_3 r^1 (8), CN^{ter} s (7)
1283	1269	-14	C^αH r^2 (52), COO ss (14), CC^{me} s (9), C^αH r^1 (7)
1360	1372	12	C^αH r^1 (44), NH_2 $twist$ (29), CC^{me} s (8)
1413	1414	1	COO ss (49), CC^{ter} s (24), CCOO sd (9), C^αH r^1 (8)
1563	1566	3	COO as (86), CCOO r (8)
1587	1587	0	NH_2 $sisso$ (100)
2076	2102	26	CH_3 ss (98)
2125	2208	83	CH_3 as^2 (87), CH_3 as^1 (12)
2235	2236	1	CH_3 as^1 (87), CH_3 as^2 (12)
—	2884	—	C^αH s (100)
—	3175	—	NH_2 as (100)
—	3268	—	NH_2 ss (100)

frequency (cm^{-1})			ND ₂ CHCD ₃ CO ₂ ⁻ (mean deviation = 11 cm^{-1})
obs.	calc.	dev.	
—	90	—	CC t (98)
—	152	—	CC^{me} t (87), CN t (11)
—	164	—	CN t (85), CC^{me} t (11)
258	256	-2	C^αH d^2 (61), CCOO wag (15), C^αH d^3 (11)
320	314	-6	C^αH d^3 (52), CCOO r (24), C^αH d^2 (9)
348	360	12	C^αH d^1 (68)

Table 3.56: (continued)

frequency (cm ⁻¹)			Potential Energy Distribution
obs.	calc.	dev.	
512	510	-2	CCOO r(38), CCOO sd(14), CC ^{ter} s(12), CN ^{ter} s(11)
595	604	9	CCOO sd(33), CC ^{ter} s(14), CCOO r(13), CH ₃ r ¹ (12), NH ₂ wag(8)
—	709	—	CH ₃ r ¹ (36), CCOO wag(30), NH ₂ wag(15)
723	743	20	CH ₃ r ² (27), CC ^{me} s(20), CN ^{ter} s(14), CCOO wag(13), CH ₃ r ¹ (9), CCH ₃ sd(7)
751	762	11	NH ₂ wag(34), NH ₂ twist(29), CC ^{me} s(10), CH ₃ r ² (8)
799	794	-5	NH ₂ wag(26), CCOO sd(23), NH ₂ twist(12), CN ^{ter} s(10), COO ss(9), CC ^{ter} s(9)
852	836	-16	CCOO wag(22), NH ₂ twist(17), CH ₃ r ² (16), CN ^{ter} s(12), CC ^{ter} s(8), C ^α H d ² (8), CCOO sd(7)
988	986	-2	CCH ₃ sd(49), CC ^{ter} s(9), CN ^{ter} s(8)
1028	1029	1	CC ^{ter} s(14), C ^α H d ² (14), CCOO wag(11), CH ₃ r ² (9), COO ss(8), CCH ₃ sd(8), CH ₃ r ¹ (7), α NH ₂ twist(5)
1056	1048	-8	CCH ₃ ad ² (84), CCH ₃ ad ¹ (14)
1056	1054	-2	CCH ₃ ad ¹ (81), CCH ₃ ad ² (15)
1109	1098	-11	CN ^{ter} s(20), NH ₂ twist(16), C ^α H d ¹ (14), NH ₂ sissor(14), CH ₃ r ¹ (9)
1131	1164	33	CC ^{me} s(38), CCH ₃ sd(21), C ^α H r ² (14)
—	1173	—	NH ₂ sissor(72), CN ^{ter} s(11), C ^α H r ² (9)
1281	1270	-11	C ^α H r ² (45), COO ss(17), C ^α H r ¹ (11), CC ^{me} s(7)
1332	1332	0	C ^α H r ¹ (63), C ^α H r ² (11), CC ^{me} s(9)
1412	1415	3	COO ss(51), CC ^{ter} s(25), CCOO sd(9)
1576	1566	-10	COO as(87), CCOO r(8)
2076	2102	26	CH ₃ ss(98)
2125	2208	83	CH ₃ as ² (87), CH ₃ as ¹ (12)
2235	2236	1	CH ₃ as ¹ (87), CH ₃ as ² (12)
2246	2337	91	NH ₂ as(100)
—	2365	—	NH ₂ ss(100)
—	2884	—	C ^α H s(100)

Table 3.56: (continued)

frequency (cm ⁻¹)			Potential Energy Distribution
obs.	calc.	dev.	
frequency (cm ⁻¹)			Potential Energy Distribution
obs.	calc.	dev.	
—	93	—	CC t(99)
—	210	—	CC ^{me} t(78), CN t(19)
—	227	—	CN t(76), CC ^{me} t(18)
273	280	7	C ^α H d ² (59), CCOO wag(16), C ^α H d ³ (12)
344	339	-5	C ^α H d ³ (46), CCOO r(32), C ^α H d ² (9)
409	407	-2	C ^α H d ¹ (67), CCOO r(8)
538	539	1	CCOO r(25), CCOO sd(19), CC ^{ter} s(13), CN ^{ter} s(13), C ^α H d ¹ (13)
624	657	33	CCOO sd(41), C ^α H d ³ (16), CCOO r(16)
779	777	-2	CCOO wag(64), C ^α H d ² (10), CC ^{me} s(8), CH ₃ r ¹ (7)
849	829	-20	CN ^{ter} s(19), CCOO sd(18), CC ^{me} s(15), CC ^{ter} s(15), CH ₃ r ¹ (13), COO ss(11)
922	920	-2	CH ₃ r ² (29), CC ^{ter} s(21), CN ^{ter} s(19), COO ss(10)
—	940	—	NH ₂ wag(67), CC ^{me} s(11), CN ^{ter} s(10)
1015	1001	-14	NH ₂ twist(32), CH ₃ r ¹ (29), C ^α H r ¹ (10)
1073	1081	8	C ^α H r ² (24), CH ₃ r ² (20), NH ₂ wag(12), CC ^{me} s(8)
1134	1127	-7	CC ^{me} s(25), CN ^{ter} s(25), CH ₃ r ² (13), C ^α H r ¹ (7), C ^α H d ² (7), NH ₂ wag(7)
1231	1246	15	NH ₂ twist(23), C ^α H r ¹ (18), C ^α H d ¹ (13), CH ₃ r ¹ (10), CH ₃ r ² (9), COO ss(8)
1288	1278	-10	C ^α H r ² (53), COO ss(12), CH ₃ r ¹ (12)
1355	1343	-12	CCH ₃ sd(76), C ^α H r ¹ (14)
1360	1377	17	C ^α H r ¹ (34), NH ₂ twist(22), CCH ₃ sd(12), CC ^{me} s(10), C ^α H r ² (8)
1412	1412	0	COO ss(42), CC ^{ter} s(19), CCH ₃ ad ² (15), CCOO sd(8)
1458	1456	-2	CCH ₃ ad ² (54), CCH ₃ ad ¹ (29)
1458	1462	4	CCH ₃ ad ¹ (61), CCH ₃ ad ² (24)
1562	1566	4	COO as(86), CCOO r(8)
1596	1588	-8	NH ₂ sissor(99)
2885	2883	-2	C ^α H s(99)
2940	2919	-21	CH ₃ ss(94)

Table 3.56: (continued)

frequency (cm ⁻¹)			Potential Energy Distribution
obs.	calc.	dev.	
2980	2968	-12	CH ₃ as ² (85), CH ₃ as ¹ (12)
2993	3008	15	CH ₃ as ¹ (86), CH ₃ as ² (10)
—	3175	—	NH ₂ as(100)
—	3268	—	NH ₂ ss(100)

frequency (cm ⁻¹)			¹⁵ NH ₂ CHCH ₃ CO ₂ ⁻ (mean deviation = 11 cm ⁻¹)
obs.	calc.	dev.	
—	93	—	CC t(99)
—	210	—	CC ^{me} t(77), CN t(20)
—	227	—	CN t(75), CC ^{me} t(19)
279	283	4	C ^α H d ² (57), CCOO wag(16), C ^α H d ³ (14)
343	337	-6	C ^α H d ³ (45), CCOO r(30), C ^α H d ² (12)
417	407	-10	C ^α H d ¹ (67), CCOO r(9)
535	534	-1	CCOO r(26), CCOO sd(18), CN ^{ter} s(15), CC ^{ter} s(13), C ^α H d ¹ (13)
632	657	25	CCOO sd(42), C ^α H d ³ (16), CCOO r(16)
793	779	-14	CCOO wag(65), C ^α H d ² (11), CH ₃ r ¹ (8)
851	828	-23	CN ^{ter} s(22), CCOO sd(18), CC ^{ter} s(15), CC ^{me} s(14), CH ₃ r ¹ (11), COO ss(10)
924	921	-3	CH ₃ r ² (31), CN ^{ter} s(25), CC ^{ter} s(22), COO ss(10)
—	936	—	NH ₂ wag(70), CC ^{me} s(15)
1019	1003	-16	NH ₂ twist(33), CH ₃ r ¹ (29), C ^α H r ¹ (11)
1072	1083	11	C ^α H r ² (24), CH ₃ r ² (19), NH ₂ wag(10), CC ^{me} s(9)
1134	1129	-5	CC ^{me} s(26), CN ^{ter} s(22), CH ₃ r ² (15), C ^α H r ¹ (7), C ^α H d ² (7)
1234	1248	14	NH ₂ twist(22), C ^α H r ¹ (17), C ^α H d ¹ (14), CH ₃ r ² (10), CH ₃ r ¹ (9), COO ss(8)
1291	1281	-10	C ^α H r ² (51), CH ₃ r ¹ (14), COO ss(11), NH ₂ twist(7)
1360	1349	-11	CCH ₃ sd(58), C ^α H r ¹ (27), NH ₂ twist(12)
1370	1381	11	CCH ₃ sd(28), C ^α H r ¹ (22), NH ₂ twist(15), CC ^{me} s(13), C ^α H r ² (7)
1414	1413	-1	COO ss(42), CC ^{ter} s(19), CCH ₃ ad ² (14), CCOO sd(8)
1460	1458	-2	CCH ₃ ad ² (58), CCH ₃ ad ¹ (25)
1460	1463	3	CCH ₃ ad ¹ (66), CCH ₃ ad ² (21)

Table 3.56: (continued)

frequency (cm^{-1})			Potential Energy Distribution
obs.	calc.	dev.	
1567	1566	-1	COO as(86), CCOO r(8)
1593	1585	-8	NH ₂ sissor(99)
2885	2883	-2	C ^{α} H s(99)
2940	2922	-18	CH ₃ ss(95)
2980	2979	-1	CH ₃ as ² (86), CH ₃ as ¹ (12)
2993	3019	26	CH ₃ as ¹ (87), CH ₃ as ² (10)
—	3166	—	NH ₂ as(100)
—	3263	—	NH ₂ ss(100)

Table 3.57: Scaled 4-31G Frequencies and Potential Energy Distribution for Water-Excluded Alaninate One-water Supramolecule, bridging one carboxyl oxygen and an amine hydrogen.

frequency (cm^{-1})			$\text{H}_2\text{NCHCH}_3\text{CO}_2^-$ (mean deviation = 7 cm^{-1})
obs.	calc.	dev.	
			Potential Energy Distribution
—	121	—	CC t(100)
—	201	—	CC ^{me} t(91)
—	265	—	CN t(68), C ^{α} H d ³ (14), CCOO r(9)
279	281	2	C ^{α} H d ² (71), CCOO r(7), CCOO wag(7)
343	345	2	C ^{α} H d ³ (37), CCOO r(31), CN t(18)
415	412	-3	C ^{α} H d ¹ (77)
539	540	1	CCOO r(31), CC ^{ter} s(15), CN ^{ter} s(14), C ^{α} H d ³ (14), CCOO sd(11)
622	632	10	CCOO sd(36), CC ^{ter} s(15), C ^{α} H d ³ (14), CCOO r(10), CC ^{me} s(8), CCOO wag(8)
785	785	0	CCOO wag(53), CCOO sd(15)
853	849	-4	CCOO sd(21), CC ^{ter} s(15), CN ^{ter} s(13), CC ^{me} s(11), CH ₃ r ¹ (11), COO ss(10), CCOO wag(7)
927	921	-6	CH ₃ r ² (34), CN ^{ter} s(29), NH ₂ wag(19), CC ^{ter} s(11)
—	957	—	NH ₂ wag(52), CC ^{me} s(20), CH ₃ r ¹ (11)
1020	1011	-9	NH ₂ twist(38), CH ₃ r ¹ (24), CC ^{me} s(12), C ^{α} H r ¹ (11)
1080	1080	0	CH ₃ r ² (26), C ^{α} H r ² (21), CCOO wag(9), CC ^{ter} s(8), NH ₂ wag(7)
1140	1161	21	CN ^{ter} s(34), CC ^{me} s(22), NH ₂ wag(10), CH ₃ r ² (8), C ^{α} H r ¹ (7)
1238	1247	9	NH ₂ twist(28), C ^{α} H r ¹ (15), CH ₃ r ¹ (14), C ^{α} H d ¹ (12), CH ₃ r ² (8)
1286	1281	-5	C ^{α} H r ² (57), CH ₃ r ¹ (14)
1353	1355	2	C ^{α} H r ¹ (44), CCH ₃ sd(28), NH ₂ twist(18)
1368	1365	-3	CCH ₃ sd(63), C ^{α} H r ¹ (13), NH ₂ twist(9), CC ^{me} s(8)
1414	1414	0	COO ss(57), CC ^{ter} s(18), CCOO sd(9)
1459	1459	0	CCH ₃ ad ² (76), CCH ₃ ad ¹ (13)
1459	1465	6	CCH ₃ ad ¹ (77), CCH ₃ ad ² (13)
1564	1566	2	COO as(81)
1591	1592	1	NH ₂ sissor(99)
2885	2885	0	C ^{α} H s(99)
2940	2918	-22	CH ₃ ss(87)

Table 3.57: (continued)

frequency (cm ⁻¹)			Potential Energy Distribution
obs.	calc.	dev.	
2980	2972	-8	CH ₃ as ² (57), CH ₃ as ¹ (43)
2993	3027	34	CH ₃ as ¹ (50), CH ₃ as ² (37), CH ₃ ss(13)
—	3178	—	NH ₂ as(98)
—	3259	—	NH ₂ ss(98)

frequency (cm ⁻¹)			D ₂ NCHCH ₃ CO ₂ ⁻ (mean deviation = 11 cm ⁻¹)
obs.	calc.	dev.	
Potential Energy Distribution			
—	118	—	CC t(98)
—	192	—	CN t(60), CC ^{me} t(33)
—	207	—	CC ^{me} t(60), CN t(28)
275	278	3	C ^α H d ² (67), CCOO r(15)
331	319	-12	C ^α H d ³ (45), CCOO r(23), C ^α H d ² (8), CN t(7)
384	386	2	C ^α H d ¹ (79), NH ₂ twist(7)
527	522	-5	CCOO r(41), CN ^{ter} s(13), C ^α H d ³ (12), CC ^{ter} s(9)
621	616	-5	CCOO sd(40), CC ^{ter} s(21), NH ₂ wag(10), CCOO r(7)
—	759	—	NH ₂ wag(45), CCOO wag(36), CC ^{me} s(7)
780	796	16	NH ₂ wag(27), CCOO wag(23), CCOO sd(16), CN ^{ter} s(7)
836	813	-23	NH ₂ twist(47), CC ^{me} s(18), CCOO sd(13), CN ^{ter} s(9)
870	876	6	CH ₃ r ¹ (30), NH ₂ twist(21), CC ^{ter} s(10)
922	920	-2	CH ₃ r ² (35), CN ^{ter} s(24), CC ^{ter} s(18), COO ss(8)
1053	1071	18	C ^α H r ² (23), CH ₃ r ² (18), CH ₃ r ¹ (11), CCOO wag(10), CC ^{me} s(8), CC ^{ter} s(7)
1108	1124	16	NH ₂ sissor(28), CN ^{ter} s(18), CH ₃ r ² (17), CC ^{me} s(14)
1143	1171	28	NH ₂ sissor(30), CC ^{me} s(23), CH ₃ r ¹ (18), C ^α H d ¹ (7), NH ₂ twist(7)
1201	1196	-5	NH ₂ sissor(37), CN ^{ter} s(14), CH ₃ r ¹ (12), C ^α H d ¹ (8), NH ₂ twist(8), CH ₃ r ² (7)
1290	1279	-11	C ^α H r ² (55), C ^α H r ¹ (12), CH ₃ r ¹ (8)
1334	1325	-49	C ^α H r ¹ (70), C ^α H r ² (7)
1370	1363	-7	CCH ₃ sd(90)
1414	1415	1	COO ss(56), CC ^{ter} s(18), CCOO sd(9)
1462	1459	-3	CCH ₃ ad ² (69), CCH ₃ ad ¹ (19)
1462	1465	3	CCH ₃ ad ¹ (71), CCH ₃ ad ² (19)

Table 3.57: (continued)

frequency (cm ⁻¹)			Potential Energy Distribution
obs.	calc.	dev.	
1571	1566	-5	COO as(83)
—	2339	—	NH ₂ as(73), NH ₂ ss(27)
—	2359	—	NH ₂ ss(73), NH ₂ as(27)
2887	2886	-1	C ^α H s(99)
2942	2918	-24	CH ₃ ss(87)
2980	2972	-8	CH ₃ as ² (57), CH ₃ as ¹ (43)
2990	3027	37	CH ₃ as ¹ (50), CH ₃ as ² (37), CH ₃ ss(13)

frequency (cm ⁻¹)			H ₂ NCDCD ₃ CO ₂ ⁻ (mean deviation = 11 cm ⁻¹)
obs.	calc.	dev.	
—	117	—	CC t(100)
—	145	—	CC ^{me} t(97)
—	251	—	C ^α H d ² (73), CCOO r(9)
257	264	7	CN t(70), C ^α H d ³ (10)
335	336	1	C ^α H d ³ (36), CCOO r(32), CN t(14), C ^α H d ¹ (8)
382	383	1	C ^α H d ¹ (65), CN t(9)
514	524	10	CCOO r(27), CC ^{ter} s(21), CCOO sd(15), C ^α H d ³ (13), CN ^{ter} s(10)
593	599	6	CCOO sd(24), C ^α H d ³ (16), CCOO r(16), CC ^{ter} s(14), CC ^{me} s(9), CCOO wag(7)
688	676	-12	CH ₃ r ¹ (34), C ^α H r ² (29), CCOO wag(23), CH ₃ r ² (8)
752	756	4	CH ₃ r ² (41), CN ^{ter} s(15), CC ^{me} s(12), C ^α H r ¹ (7), CH ₃ r ¹ (7)
827	808	-19	CCOO sd(37), CH ₃ r ² (18), COO ss(11), CC ^{ter} s(8), CC ^{me} s(7), CCOO wag(7)
884	859	-25	C ^α H r ¹ (44), CN ^{ter} s(24), NH ₂ twist(10), NH ₂ wag(10)
897	896	-1	C ^α H r ² (26), CC ^{me} s(10), CCOO wag(10), CH ₃ r ¹ (10), CC ^{ter} s(9), CCH ₃ sd(9), NH ₂ wag(7)
947	957	10	CCOO wag(28), NH ₂ wag(23), C ^α H r ² (11), CCH ₃ sd(10), C ^α H d ² (7)
—	962	—	NH ₂ wag(34), CH ₃ r ¹ (24), C ^α H r ¹ (23)
1055	1051	-4	CCH ₃ ad ² (59), CCH ₃ ad ¹ (32)
1055	1056	1	CCH ₃ ad ¹ (49), CCH ₃ ad ² (40)
—	1072	—	CCH ₃ sd(47), CCH ₃ ad ¹ (18), C ^α H r ² (9), NH ₂ wag(9)

Table 3.57: (continued)

frequency (cm^{-1})			Potential Energy Distribution
obs.	calc.	dev.	
1126	1132	6	CC^{ter} s(15), $\text{C}^{\alpha}\text{H}$ r ¹ (14), CN^{ter} s(12), CC^{me} s(10), COO ss(9), CH_3 r ² (9), $\text{C}^{\alpha}\text{H}$ r ² (8), CCH_3 sd(8)
1158	1188	30	CN^{ter} s(30), NH_2 twist(23), CC^{me} s(10), $\text{C}^{\alpha}\text{H}$ d ³ (7), NH_2 wag(7)
1276	1283	7	NH_2 twist(49), CC^{me} s(24), $\text{C}^{\alpha}\text{H}$ r ¹ (7)
1408	1413	5	COO ss(63), CC^{ter} s(19), CCOO sd(10)
1555	1563	8	COO as(83)
1582	1591	9	NH_2 sissor(98)
2076	2100	24	CH_3 ss(95)
2125	2125	0	$\text{C}^{\alpha}\text{H}$ s(97)
2235	2201	-34	CH_3 as ² (54), CH_3 as ¹ (45)
2246	2237	-9	CH_3 as ¹ (52), CH_3 as ² (44)
—	3178	—	NH_2 as(98)
—	3259	—	NH_2 ss(98)

frequency (cm^{-1})			$\text{D}_2\text{NCD}_2\text{CD}_3\text{CO}_2^-$ (mean deviation = 10 cm^{-1})
obs.	calc.	dev.	
—	115	—	CC t(98)
—	145	—	CC^{me} t(96)
—	196	—	CN t(87)
257	251	-6	$\text{C}^{\alpha}\text{H}$ d ² (77), CCOO r(7)
327	311	-16	$\text{C}^{\alpha}\text{H}$ d ³ (50), CCOO r(30)
363	356	-7	$\text{C}^{\alpha}\text{H}$ d ¹ (73)
506	510	4	CCOO r(37), CC^{ter} s(14), $\text{C}^{\alpha}\text{H}$ d ³ (11), CN^{ter} s(10), CCOO sd(9)
590	587	-3	CCOO sd(31), CC^{ter} s(20), CCOO r(12), CC^{me} s(8), $\text{C}^{\alpha}\text{H}$ d ³ (7)
690	675	-15	CH_3 r ¹ (33), $\text{C}^{\alpha}\text{H}$ r ² (30), CCOO wag(24), CH_3 r ² (7)
729	733	4	CH_3 r ² (32), NH_2 twist(20), $\text{C}^{\alpha}\text{H}$ r ¹ (14), CH_3 r ¹ (12)
756	757	1	NH_2 wag(63), CH_3 r ² (10), CC^{me} s(8)
790	778	-12	CN^{ter} s(25), NH_2 twist(23), CC^{me} s(19), CCOO sd(10), CCH_3 sd(7)

Table 3.57: (continued)

frequency (cm ⁻¹)			Potential Energy Distribution
obs.	calc.	dev.	
845	825	-20	CCOO sd(31), CH ₃ r ² (14), COO ss(12), CC ^{ter} s(12), NH ₂ wag(8)
893	904	11	C ^α H r ² (35), CCOO wag(15), CH ₃ r ¹ (13)
940	940	0	C ^α H r ¹ (39), CCOO wag(22), CH ₃ r ¹ (8)
1036	1043	7	CCH ₃ sd(33), CCH ₃ ad ¹ (23), NH ₂ twist(19), C ^α H r ¹ (7)
1055	1050	-5	CCH ₃ ad ² (57), CCH ₃ ad ¹ (15), CH ₃ r ¹ (7)
1055	1058	3	CCH ₃ ad ² (41), CCH ₃ ad ¹ (11), CH ₃ r ¹ (11)
—	1066	—	CCH ₃ ad ¹ (50), CCH ₃ sd(31), C ^α H r ² (8)
1123	1114	-9	NH ₂ sissor(34), CN ^{ter} s(13), C ^α H r ¹ (10), CC ^{ter} s(9), CH ₃ r ² (9), C ^α H d ¹ (7)
1182	1196	14	NH ₂ sissor(64), CN ^{ter} s(16)
1215	1224	9	CC ^{me} s(47), CN ^{ter} s(13)
1409	1414	5	COO ss(63), CC ^{ter} s(20), CCOO sd(10)
1567	1563	-4	COO as(85)
2076	2100	24	CH ₃ ss(95)
2125	2125	0	C ^α H s(97)
2235	2201	-34	CH ₃ as ² (54), CH ₃ as ¹ (45)
2246	2237	-9	CH ₃ as ¹ (52), CH ₃ as ² (44)
—	2339	—	NH ₂ as(73), NH ₂ ss(26)
—	2359	—	NH ₂ ss(73), NH ₂ as(26)

frequency (cm ⁻¹)			H ₂ NCHCD ₃ CO ₂ ⁻ (mean deviation = 10 cm ⁻¹)
obs.	calc.	dev.	
—	118	—	CC t(100)
—	145	—	CC ^{me} t(97)
—	252	—	C ^α H d ² (70), CCOO r(10)
255	265	10	CN t(70), C ^α H d ³ (8), C ^α H d ² (7)
340	338	-2	C ^α H d ³ (37), CCOO r(32), CN t(14)
390	385	-5	C ^α H d ¹ (66), CN t(8)
521	530	9	CCOO r(30), CC ^{ter} s(18), C ^α H d ³ (13), CCOO sd(13), CN ^{ter} s(11)
607	611	4	CCOO sd(28), CC ^{ter} s(15), C ^α H d ³ (15), CCOO r(12), CC ^{me} s(10)

Table 3.57: (continued)

frequency (cm^{-1})			Potential Energy Distribution
obs.	calc.	dev.	
741	723	-18	CCOO wag(43), CH ₃ r ¹ (31), CH ₃ r ² (15), C ^{α} H r ² (7)
771	768	-3	CH ₃ r ² (33), CN ^{ter} s(23), CH ₃ r ¹ (20), CC ^{me} s(9)
828	808	-20	CCOO sd(38), CH ₃ r ² (17), COO ss(12), CC ^{ter} s(8), CC ^{me} s(7), CCOO wag(7)
910	918	8	NH ₂ wag(44), CH ₃ r ¹ (13), CCOO wag(12), CN ^{ter} s(10), NH ₂ twist(7)
947	938	-9	CCH ₃ sd(25), CC ^{me} s(18), NH ₂ wag(14), NH ₂ twist(12), CCOO wag(8), CH ₃ r ¹ (7)
1020	1025	5	NH ₂ wag(20), CC ^{ter} s(18), COO ss(10), CCOO wag(9), CCH ₃ sd(8), CH ₃ r ² (8), C ^{α} H r ² (7), C ^{α} H d ³ (7)
1058	1051	-7	CCH ₃ ad ² (64), CCH ₃ ad ¹ (33)
1058	1057	-1	CCH ₃ ad ¹ (62), CCH ₃ ad ² (33)
—	1072	—	CCH ₃ sd(39), CN ^{ter} s(19), NH ₂ twist(11)
1141	1165	24	CC ^{me} s(29), CN ^{ter} s(19), C ^{α} H r ² (19), CCH ₃ sd(14)
1189	1206	17	NH ₂ twist(36), CN ^{ter} s(14), C ^{α} H r ¹ (13), C ^{α} H d ¹ (9), CH ₃ r ¹ (9)
1283	1265	-18	C ^{α} H r ² (56), C ^{α} H r ¹ (13), CC ^{me} s(9)
1360	1357	-3	C ^{α} H r ¹ (56), NH ₂ twist(29), CC ^{me} s(7)
1413	1413	0	COO ss(62), CC ^{ter} s(20), CCOO sd(10)
1563	1565	2	COO as(82)
1587	1591	4	NH ₂ sissor(99)
2076	2100	24	CH ₃ ss(95)
2125	2200	75	CH ₃ as ² (53), CH ₃ as ¹ (47)
2235	2237	2	CH ₃ as ¹ (51), CH ₃ as ² (45)
—	2887	—	C ^{α} H s(100)
—	3178	—	NH ₂ as(98)
—	3259	—	NH ₂ ss(98)

frequency (cm^{-1})			D ₂ NCHCD ₃ CO ₂ ⁻ (mean deviation = 12 cm^{-1})
obs.	calc.	dev.	
—	115	—	CC t(98)
—	145	—	CC ^{me} t(96)
—	197	—	CN t(87)

Table 3.57: (continued)

frequency (cm ⁻¹)			Potential Energy Distribution
obs.	calc.	dev.	
258	252	-6	C ^α H d ² (77), CCOO r(7)
320	313	-7	C ^α H d ³ (50), CCOO r(29)
348	358	10	C ^α H d ¹ (73)
512	515	3	CCOO r(40), CC ^{ter} s(12), C ^α H d ³ (12), CN ^{ter} s(11), CCOO sd(8)
595	598	3	CCOO sd(34), CC ^{ter} s(22), CCOO r(9), CC ^{me} s(8), C ^α H d ³ (7), NH ₂ wag(7)
—	723	—	CCOO wag(42), CH ₃ r ¹ (30), CH ₃ r ² (15), C ^α H r ² (7)
723	751	28	CH ₃ r ² (32), CH ₃ r ¹ (28), CN ^{ter} s(14), NH ₂ twist(14)
751	758	7	NH ₂ wag(63), CC ^{me} s(12)
799	794	-5	NH ₂ twist(28), CCOO sd(23), CN ^{ter} s(14), CC ^{me} s(11), NH ₂ wag(9)
852	833	-19	NH ₂ twist(19), CCOO sd(18), CCOO wag(16), CH ₃ r ² (13), CC ^{ter} s(10), COO ss(9)
988	1006	18	CCH ₃ sd(31), CC ^{ter} s(17), COO ss(10), C ^α H d ³ (9), C ^α H r ² (8)
1028	1024	-4	CCH ₃ sd(33), CCOO wag(10), CH ₃ r ¹ (10), NH ₂ twist(9), CN ^{ter} s(8), C ^α H d ² (7)
1056	1051	-5	CCH ₃ ad ² (62), CCH ₃ ad ¹ (36)
1056	1057	1	CCH ₃ ad ¹ (60), CCH ₃ ad ² (36)
1109	1103	-6	CN ^{ter} s(25), NH ₂ sissor(20), C ^α H d ¹ (12), NH ₂ twist(12), CH ₃ r ¹ (9)
1131	1158	27	CC ^{me} s(41), CCH ₃ sd(22), C ^α H r ² (18)
—	1185	—	NH ₂ sissor(73), CN ^{ter} s(19)
1281	1265	-16	C ^α H r ² (61), CC ^{me} s(10)
1332	1317	-15	C ^α H r ¹ (79)
1412	1414	2	COO ss(62), CC ^{ter} s(20), CCOO sd(10)
1576	1565	-11	COO as(84)
2076	2100	24	CH ₃ ss(95)
2125	2200	75	CH ₃ as ² (53), CH ₃ as ¹ (47)
2235	2237	2	CH ₃ as ¹ (51), CH ₃ as ² (45)
2246	2339	93	NH ₂ as(73), NH ₂ ss(27)
—	2359	—	NH ₂ ss(73), NH ₂ as(27)
—	2887	—	C ^α H s(100)

Table 3.57: (continued)

frequency (cm ⁻¹)			Potential Energy Distribution
obs.	calc.	dev.	

frequency (cm ⁻¹)			H ₂ NCH(¹³ CH ₃)CO ₂ ⁻ (mean deviation = 6 cm ⁻¹)
obs.	calc.	dev.	
			Potential Energy Distribution
—	120	—	CC t(100)
—	201	—	CC ^{me} t(91)
—	264	—	CN t(66), C ^α H d ³ (14), CCOO r(9)
273	277	4	C ^α H d ² (70), CN t(8), CCOO wag(7)
344	344	0	C ^α H d ³ (37), CCOO r(31), CN t(17)
409	410	1	C ^α H d ¹ (77)
538	540	2	CCOO r(31), CC ^{ter} s(15), CN ^{ter} s(14), C ^α H d ³ (14), CCOO sd(11)
624	629	5	CCOO sd(35), CC ^{ter} s(15), C ^α H d ³ (14), CCOO r(10), CC ^{me} s(9), CCOO wag(8)
779	784	5	CCOO wag(52), CCOO sd(16)
849	846	-3	CCOO sd(20), CC ^{ter} s(13), CN ^{ter} s(13), CC ^{me} s(12), CH ₃ r ¹ (12), COO ss(10), CCOO wag(9)
922	918	-4	CH ₃ r ² (37), CN ^{ter} s(28), NH ₂ wag(15), CC ^{ter} s(11)
—	953	—	NH ₂ wag(55), CC ^{me} s(20), CH ₃ r ¹ (9)
1015	1008	-7	NH ₂ twist(37), CH ₃ r ¹ (25), CC ^{me} s(12), C ^α H r ¹ (11)
1073	1076	3	CH ₃ r ² (25), C ^α H r ² (20), CCOO wag(9), CC ^{ter} s(8), NH ₂ wag(8)
1134	1157	23	CN ^{ter} s(35), CC ^{me} s(21), NH ₂ wag(10), C ^α H r ¹ (7), CH ₃ r ² (7)
1231	1242	11	NH ₂ twist(29), C ^α H r ¹ (15), CH ₃ r ¹ (15), C ^α H d ¹ (12), CH ₃ r ² (8)
1288	1278	-10	C ^α H r ² (58), CH ₃ r ¹ (11)
1355	1351	-4	CCH ₃ sd(82), C ^α H r ¹ (9)
1360	1358	-2	C ^α H r ¹ (48), NH ₂ twist(24), CCH ₃ sd(11), CC ^{me} s(8)
1412	1414	2	COO ss(57), CC ^{ter} s(18), CCOO sd(9)
1458	1457	-1	CCH ₃ ad ² (75), CCH ₃ ad ¹ (12)
1458	1463	5	CCH ₃ ad ¹ (76), CCH ₃ ad ² (12), CH ₃ r ¹ (7)
1562	1566	4	COO as(81)
1596	1592	-4	NH ₂ sissor(99)

Table 3.57: (continued)

frequency (cm ⁻¹)			Potential Energy Distribution
obs.	calc.	dev.	
2885	2885	0	C ^α H s(98)
2940	2914	-26	CH ₃ ss(86), CH ₃ as ¹ (7), CH ₃ as ² (7)
2980	2962	-18	CH ₃ as ² (57), CH ₃ as ¹ (42)
2993	3017	24	CH ₃ as ¹ (49), CH ₃ as ² (36), CH ₃ ss(14)
—	3178	—	NH ₂ as(98)
—	3259	—	NH ₂ ss(98)

frequency (cm ⁻¹)			H ₂ (¹⁵ N)CHCH ₃ CO ₂ ⁻ (mean deviation = 8 cm ⁻¹)
obs.	calc.	dev.	
—	120	—	CC t(100)
—	201	—	CC ^{me} t(91)
—	264	—	CN t(66), C ^α H d ³ (15), CCOO r(9)
279	281	2	C ^α H d ² (71), CCOO r(7), CCOO wag(7), CN t(7)
343	343	0	C ^α H d ³ (37), CCOO r(29), CN t(19)
417	409	-8	C ^α H d ¹ (78)
535	534	-1	CCOO r(32), CN ^{ter} s(15), CC ^{ter} s(14), C ^α H d ³ (14), CCOO sd(11)
632	631	-1	CCOO sd(36), CC ^{ter} s(15), C ^α H d ³ (14), CCOO r(11), CC ^{me} s(8), CCOO wag(8)
793	785	-8	CCOO wag(53), CCOO sd(15)
851	846	-5	CCOO sd(20), CN ^{ter} s(16), CC ^{ter} s(13), CC ^{me} s(11), CH ₃ r ¹ (11), COO ss(9), CCOO wag(8)
924	915	-9	CH ₃ r ² (32), CN ^{ter} s(26), NH ₂ wag(21), CC ^{ter} s(12)
—	954	—	NH ₂ wag(49), CC ^{me} s(20), CH ₃ r ¹ (10), CH ₃ r ² (7)
1019	1010	-9	NH ₂ twist(38), CH ₃ r ¹ (24), CC ^{me} s(11), C ^α H r ¹ (11)
1072	1079	7	CH ₃ r ² (25), C ^α H r ² (21), CCOO wag(9), CC ^{ter} s(8), NH ₂ wag(7)
1134	1157	23	CN ^{ter} s(33), CC ^{me} s(23), NH ₂ wag(10), CH ₃ r ² (9), C ^α H r ¹ (7)
1234	1245	11	NH ₂ twist(29), CH ₃ r ¹ (15), C ^α H r ¹ (14), C ^α H d ¹ (12), CH ₃ r ² (8)
1291	1280	-11	C ^α H r ² (57), CH ₃ r ¹ (13)
1360	1353	-7	C ^α H r ¹ (49), NH ₂ twist(20), CCH ₃ sd(20)

Table 3.57: (continued)

frequency (cm ⁻¹)			Potential Energy Distribution
obs.	calc.	dev.	
1370	1364	-6	CCH ₃ sd(71), C ^α H r ¹ (9), CC ^{me} s(8)
1414	1414	0	COO ss(57), CC ^{ter} s(18), CCOO sd(9)
1460	1459	-1	CCH ₃ ad ² (76), CCH ₃ ad ¹ (13)
1460	1465	5	CCH ₃ ad ¹ (77), CCH ₃ ad ² (13)
1567	1566	-1	COO as(81)
1593	1588	-5	NH ₂ sissor(98)
2885	2885	0	C ^α H s(99)
2940	2918	-22	CH ₃ ss(87)
2980	2972	-8	CH ₃ as ² (57), CH ₃ as ¹ (43)
2993	3027	34	CH ₃ as ¹ (50), CH ₃ as ² (37), CH ₃ ss(13)
—	3169	—	NH ₂ as(98)
—	3255	—	NH ₂ ss(98)

Tables 3.59, 3.60, 3.61, and 3.62 list the observed and calculated frequencies and potential energy distributions (PED) for the water-excluded one-water alanine at pH=1 (CO₂ bridged) using the 4-31G, 4-31G*, 6-31G**, 6-31+G** basis sets. The water-excluded one-water alanine at pH=1 supermolecule scale factors determined from the SQMFF procedure using the 4-31G, 4-31G*, 6-31G** and 6-31+G** basis sets are listed in Table 3.58.

Table 3.58: Scale factors for alanine in acid, one-water water-excluded geometries using several basis sets.

Coordinate	4-31G	4-31G*	6-31G**	6-31+G**
C=O s	77.60	68.00	68.80	69.55
C-OH s	94.00	84.20	87.70	88.20
OH s	80.00	80.00	80.00	80.00
C $^{\alpha}$ H s	81.59	81.15	82.15	82.25
CC ^{me} s	93.00	88.00	88.40	90.00
CC ^{ter} s	99.50	98.00	95.50	97.80
CN ^{+ter} s	88.00	86.50	88.00	85.00
COH b	111.00	97.70	99.00	101.00
C $^{\alpha}$ H r ¹	79.30	79.30	80.60	81.40
C $^{\alpha}$ H r ²	77.00	76.75	79.30	79.10
C $^{\alpha}$ H d ¹	101.00	102.50	102.00	104.60
C $^{\alpha}$ H d ²	101.00	104.50	103.50	108.05
C $^{\alpha}$ H d ³	92.50	95.50	94.20	98.50
CCOO sd	81.00	89.60	89.00	89.80
CCOO r	94.00	98.80	102.00	101.50
CCOO wag	95.70	97.10	97.80	95.90
CH ₃ sd	77.30	79.00	80.85	80.80
CH ₃ ad ¹	77.50	79.15	80.78	81.75
CH ₃ ad ²	78.50	79.40	81.72	82.40
CH ₃ r ¹	80.50	84.50	85.30	84.70
CH ₃ r ²	78.50	80.20	79.70	81.30
NH ₃ sd	72.20	78.50	80.80	80.90
NH ₃ ad ¹	75.50	77.30	80.20	80.50
NH ₃ ad ²	75.50	78.50	80.80	81.30
NH ₃ r ¹	78.06	90.80	92.50	89.60
NH ₃ r ²	67.50	71.80	71.90	76.20
CH ₃ ss	81.26	80.24	81.25	81.43
CH ₃ as ^{1,2}	83.43	82.73	83.52	83.70
CH ₃ as ^{1,2}	83.43	82.73	83.52	83.70
NH ₃ ss,as	85.90	85.90	85.90	85.90
NH ₃ ss,as	85.90	85.90	85.90	85.90
NH ₃ ss,as	85.90	85.90	85.90	85.90
CN t	40.00	40.00	50.00	40.00
CC t	70.00	70.00	70.00	70.00

Table 3.58: (continued)

Coordinate	4-31G	4-31G*	6-31G**	6-31+G**
CC ^{me} t	80.00	80.00	80.00	80.00
C-OH t	200.00	200.00	200.00	200.00

Table 3.59: Scaled 4-31G Frequencies and Potential Energy Distribution for Water-Excluded Alanine One-water Supermolecule in Acid.

frequency (cm^{-1})			+NH ₃ CHCH ₃ COOH (mean deviation = 10 cm^{-1})
obs.	calc.	dev.	Potential Energy Distribution
—	88	—	CC t(98)
—	234	—	CN t(66), C $^{\alpha}$ H d ² (9), C $^{\alpha}$ H d ³ (9), CCOO r(9)
—	248	—	CC ^{me} t(88)
275	281	6	C $^{\alpha}$ H d ² (37), CN t(28), CCOO r(16), CCOO wag(7)
335	337	2	C $^{\alpha}$ H d ³ (29), C $^{\alpha}$ H d ² (23), CCOO r(22), CCOO wag(9), CC ^{me} t(8)
409	411	2	C $^{\alpha}$ H d ¹ (66)
526	508	-18	CCOO sd(36), C $^{\alpha}$ H d ¹ (15), CN ^{+ter} s(13), CCOO r(12), CC ^{ter} s(8), C $^{\alpha}$ H d ³ (7)
603	630	27	CCOO sd(31), C $^{\alpha}$ H d ³ (22), CCOO r(19), C-OH s(8)
746	744	-2	CCOO wag(38), CC ^{me} s(17), CCOO sd(9), CC ^{ter} s(8), C $^{\alpha}$ H d ² (7)
823	816	-7	CN ^{+ter} s(20), CCOO wag(16), CC ^{ter} s(12), CH ₃ r ² (11), CH ₃ r ¹ (7)
920	920	0	CN ^{+ter} s(27), CC ^{ter} s(26), CH ₃ r ¹ (12), CH ₃ r ² (9), C-OH s(8)
—	951	—	NH ₃ r ² (50), CC ^{me} s(23), CH ₃ r ¹ (11)
—	976	—	C-OH t(89)
1008	1013	5	NH ₃ r ¹ (28), CH ₃ r ² (23), C $^{\alpha}$ H r ¹ (10), CN ^{+ter} s(8)
1117	1120	3	CC ^{me} s(26), CH ₃ r ¹ (16), CN ^{+ter} s(14), NH ₃ r ² (11), NH ₃ r ¹ (10)
1146	1146	0	CH ₃ r ¹ (23), C $^{\alpha}$ H r ² (22), NH ₃ r ² (8), C $^{\alpha}$ H r ¹ (7), C $^{\alpha}$ H d ² (7), CCOO wag(7), NH ₃ r ¹ (7)
1214	1220	6	CH ₃ r ² (26), NH ₃ r ¹ (14), C-OH s(10), C $^{\alpha}$ H d ¹ (10), CC ^{me} s(7), C $^{\alpha}$ H r ¹ (7), NH ₃ r ² (7)
1261	1255	-6	COH b(26), C-OH s(24), C $^{\alpha}$ H r ² (12), C=O s(7), CH ₃ r ² (7), NH ₃ r ¹ (7)
1328	1321	-7	C $^{\alpha}$ H r ² (39), C $^{\alpha}$ H r ¹ (20), CC ^{me} s(8), NH ₃ r ² (7)
1364	1368	4	C $^{\alpha}$ H r ¹ (50), COH b(17), NH ₃ r ¹ (8)
1393	1401	8	CH ₃ sd(97)
1460	1460	0	CH ₃ ad ¹ (83), CH ₃ r ¹ (7)
1460	1464	4	CH ₃ ad ² (89), CH ₃ r ² (8)
1523	1524	1	C-OH s(30), COH b(22), CC ^{ter} s(13), CCOO sd(8)

Table 3.59: (continued)

frequency (cm^{-1})			Potential Energy Distribution
obs.	calc.	dev.	
1523	1526	3	NH ₃ sd(89)
1635	1615	-20	NH ₃ ad ¹ (82), NH ₃ r ¹ (12)
1635	1633	-2	NH ₃ ad ² (93)
1735	1739	4	C=O s(69), COH b(10)
—	2791	—	NH ₃ ss,as(60), NH ₃ ss,as(39)
2895	2896	1	CH ₃ ss(98)
2956	2961	5	C ^{α} H s(97)
2998	3006	8	CH ₃ as ^{1,2} (83), CH ₃ as ^{1,2} (15)
3007	3031	24	CH ₃ as ^{1,2} (83), CH ₃ as ^{1,2} (15)
—	3381	—	NH ₃ ss,as(59), NH ₃ ss,as(39)
—	3447	—	NH ₃ ss,as(98)
—	3517	—	OH s(100)

frequency (cm^{-1})			+ND ₃ CHCH ₃ COOD (mean deviation = 13 cm^{-1})
obs.	calc.	dev.	Potential Energy Distribution
—	85	—	CC t(97)
—	175	—	CN t(90)
—	246	—	CC ^{me} t(83), C ^{α} H d ³ (7), CCOO r(7)
276	261	-15	C ^{α} H d ² (35), CCOO r(24), C ^{α} H d ³ (18), CCOO wag(8), CN t(7)
319	320	1	C ^{α} H d ² (32), C ^{α} H d ³ (26), CCOO r(12), CCOO wag(10), CC ^{me} t(9)
380	381	1	C ^{α} H d ¹ (64), CCOO r(9), NH ₃ r ² (7)
508	479	-29	CCOO sd(38), CN ^{+ter} s(13), C ^{α} H d ¹ (13), CCOO r(10), C ^{α} H d ³ (7)
588	591	3	CCOO sd(27), CCOO r(22), C ^{α} H d ³ (14), C-OH s(7), CN ^{+ter} s(7), NH ₃ r ² (7)
—	669	—	C-OH t(50), CCOO wag(16), CC ^{me} s(7), C ^{α} H d ² (7)
730	725	-5	CC ^{ter} s(19), NH ₃ r ² (16), CN ^{+ter} s(14), NH ₃ r ¹ (14), C-OH t(11), COH b(7)
764	766	2	NH ₃ r ² (52), CC ^{me} s(20), NH ₃ r ¹ (13)
825	818	-7	CCOO wag(40), C-OH t(34), NH ₃ r ¹ (8)
881	877	-4	NH ₃ r ¹ (34), CH ₃ r ² (28), CN ^{+ter} s(10)

Table 3.59: (continued)

frequency (cm^{-1})			Potential Energy Distribution
obs.	calc.	dev.	
919	902	-17	CH_3 r ¹ (27), CC^{ter} s(23), $\text{CN}^{+\text{ter}}$ s(23)
1060	1051	-9	COH b(36), CC^{me} s(20), C-OH s(9), $\text{CN}^{+\text{ter}}$ s(8), C^αH r ² (7)
1104	1094	-10	COH b(26), CC^{me} s(14), C=O s(12), C-OH s(8), C^αH r ² (8)
1114	1134	20	CH_3 r ¹ (40), NH_3 sd(12), C^αH d ² (11), C^αH r ² (8), CCOO wag(8)
1149	1155	6	NH_3 ad ¹ (87), NH_3 sd(8)
1157	1164	7	NH_3 sd(61), $\text{CN}^{+\text{ter}}$ s(11)
1174	1175	1	NH_3 ad ² (31), CH_3 r ² (20), CC^{me} s(13), C^αH d ¹ (8), NH_3 sd(8), NH_3 r ¹ (8)
1183	1192	9	NH_3 ad ² (62), CH_3 r ² (19)
1274	1300	26	C^αH r ² (59), C-OH s(11), CH_3 r ¹ (7)
1324	1319	-5	C^αH r ¹ (77), C-OH s(8)
1408	1400	-8	CH_3 sd(94)
1437	1444	7	CH_3 ad ¹ (59), C-OH s(16), CC^{ter} s(9)
1463	1465	2	CH_3 ad ² (89), CH_3 r ² (8)
1463	1485	22	CH_3 ad ¹ (32), C-OH s(19), CC^{ter} s(16), CH_3 r ¹ (9)
1727	1721	-6	C=O s(78)
—	2044	—	NH_3 ss,as(50), NH_3 ss,as(47)
—	2452	—	NH_3 ss,as(52), NH_3 ss,as(47)
—	2540	—	NH_3 ss,as(99)
—	2562	—	OH s(100)
2898	2896	-2	CH_3 ss(98)
2956	2960	4	C^αH s(97)
3002	3006	4	CH_3 as ^{1,2} (83), CH_3 as ^{1,2} (15)
3011	3031	20	CH_3 as ^{1,2} (83), CH_3 as ^{1,2} (15)

frequency (cm^{-1})			Potential Energy Distribution
obs.	calc.	dev.	
—	85	—	CC t(97)
—	180	—	CC^{me} t(94)
—	230	—	CN t(52), C^αH d ² (17), CCOO r(12), C^αH d ³ (11)
246	263	17	C^αH d ² (39), CN t(39), CCOO wag(7)
331	322	-9	C^αH d ³ (36), CCOO r(33), C^αH d ² (12)

Table 3.59: (continued)

frequency (cm ⁻¹)			Potential Energy Distribution
obs.	calc.	dev.	
378	383	5	C ^α H d ¹ (70), CH ₃ r ² (9)
506	487	-19	CCOO sd(39), CCOO r(13), CC ^{ter} s(11), CN ^{+ter} s(10), C ^α H d ³ (9)
594	612	18	CCOO sd(25), C ^α H d ³ (23), CCOO r(22), C-OH s(7)
674	674	0	CCOO wag(34), C ^α H r ² (24), CH ₃ r ¹ (24), CH ₃ r ² (10)
748	727	-21	CN ^{+ter} s(24), CC ^{me} s(22), CH ₃ r ² (15), CCOO sd(12), CC ^{ter} s(7)
794	790	-4	CH ₃ r ¹ (36), CC ^{ter} s(16), CH ₃ r ² (16)
879	865	-14	C ^α H r ¹ (42), CN ^{+ter} s(29), NH ₃ r ¹ (12)
879	872	-7	C ^α H r ² (26), CC ^{me} s(18), CC ^{ter} s(11), NH ₃ r ² (11), CH ₃ r ² (8)
944	956	12	C-OH t(36), NH ₃ r ² (24), C ^α H r ² (9), C ^α H r ¹ (7)
—	975	—	NH ₃ r ² (23), C ^α H r ² (16), CH ₃ r ² (16), CH ₃ r ¹ (13)
1010	992	-18	C-OH t(51), CCOO wag(21), C ^α H d ² (7)
1053	1051	-2	CH ₃ ad ¹ (78), CH ₃ ad ² (18)
1053	1053	0	CH ₃ ad ² (78), CH ₃ ad ¹ (19)
1083	1075	-8	CH ₃ sd(63), CN ^{+ter} s(9), C ^α H r ¹ (9)
1134	1116	-18	CN ^{+ter} s(20), CH ₃ sd(17), CC ^{me} s(12), C-OH s(10), CH ₃ r ² (8), NH ₃ r ¹ (7)
1199	1205	6	NH ₃ r ¹ (46), C-OH s(13), C ^α H r ¹ (7)
1231	1230	-1	CC ^{me} s(28), NH ₃ r ² (18), NH ₃ r ¹ (12), C ^α H d ¹ (7)
1304	1297	-7	COH b(45), CC ^{ter} s(17), C-OH s(9)
1508	1512	4	C-OH s(37), COH b(31), CC ^{ter} s(13), CCOO sd(11)
1530	1525	-5	NH ₃ sd(95)
1606	1613	7	NH ₃ ad ¹ (84), NH ₃ r ¹ (11)
1638	1632	-6	NH ₃ ad ² (94)
1735	1737	2	C=O s(69), COH b(10)
2080	2082	2	CH ₃ ss(99)
2188	2185	-3	C ^α H s(97)
2253	2229	-24	CH ₃ as ^{1,2} (85), CH ₃ as ^{1,2} (14)
2253	2247	-6	CH ₃ as ^{1,2} (85), CH ₃ as ^{1,2} (14)
—	2791	—	NH ₃ ss,as(60), NH ₃ ss,as(39)
—	3381	—	NH ₃ ss,as(59), NH ₃ ss,as(39)
—	3447	—	NH ₃ ss,as(98)
—	3517	—	OH s(100)

Table 3.59: (continued)

frequency (cm ⁻¹)			Potential Energy Distribution
obs.	calc.	dev.	

frequency (cm ⁻¹)			+NH ₃ CHCD ₃ COOH (mean deviation = 14 cm ⁻¹)
obs.	calc.	dev.	Potential Energy Distribution
—	85	—	CC t(96)
—	180	—	CC ^{me} t(94)
—	231	—	CN t(52), C ^α H d ² (16), CCOO r(12), C ^α H d ³ (11)
243	264	21	C ^α H d ² (39), CN t(39)
332	325	-7	C ^α H d ³ (36), CCOO r(32), C ^α H d ² (13)
380	385	5	C ^α H d ¹ (69), CH ₃ r ² (9)
514	493	-21	CCOO sd(38), CCOO r(15), CN ^{+ter} s(11), CC ^{ter} s(10), C ^α H d ³ (9)
598	616	18	CCOO sd(27), C ^α H d ³ (22), CCOO r(20), C-OH s(7)
710	707	-3	CCOO wag(48), CH ₃ r ¹ (28), CC ^{me} s(7)
760	734	-26	CN ^{+ter} s(27), CH ₃ r ² (23), CC ^{me} s(15), CCOO sd(12), CC ^{ter} s(8)
799	793	-6	CH ₃ r ¹ (32), CH ₃ r ² (21), CC ^{ter} s(13), CN ^{+ter} s(10)
921	918	-3	NH ₃ r ² (43), CC ^{me} s(21), CC ^{ter} s(16), CH ₃ sd(10)
939	940	1	NH ₃ r ¹ (22), CH ₃ r ² (14), CN ^{+ter} s(12), C-OH t(11), C ^α H d ² (8), CCOO wag(7), CH ₃ r ¹ (7)
—	981	—	C-OH t(84), CCOO wag(7)
1050	1041	-9	CH ₃ sd(27), CN ^{+ter} s(19), CH ₃ ad ² (18), CH ₃ r ¹ (8)
1050	1051	1	CH ₃ ad ¹ (91)
1064	1054	-10	CH ₃ ad ² (72), CH ₃ sd(12)
1118	1100	-18	CH ₃ sd(32), NH ₃ r ² (12), CN ^{+ter} s(9), CC ^{me} s(7)
1141	1139	-2	C ^α H r ² (19), CC ^{me} s(17), NH ₃ r ¹ (16), NH ₃ r ² (13), CH ₃ sd(10)
1186	1171	-15	NH ₃ r ¹ (31), C ^α H r ¹ (13), CH ₃ r ² (11), C ^α H d ¹ (9), CC ^{me} s(8), C ^α H r ² (8)
1260	1251	-9	C-OH s(31), COH b(30), C ^α H r ² (12), C=O s(9)
1322	1311	-11	C ^α H r ² (43), C ^α H r ¹ (14), CC ^{me} s(9), NH ₃ r ² (8), COH b(7)
1364	1367	3	C ^α H r ¹ (56), COH b(17), NH ₃ r ¹ (9)
1522	1518	-4	C-OH s(34), COH b(27), CC ^{ter} s(14), CCOO sd(10)
1522	1526	4	NH ₃ sd(93)

Table 3.59: (continued)

frequency (cm ⁻¹)			Potential Energy Distribution
obs.	calc.	dev.	
1623	1615	-8	NH ₃ ad ¹ (82), NH ₃ r ¹ (12)
1623	1633	10	NH ₃ ad ² (93)
1735	1738	3	C=O s(69), COH b(10)
2081	2082	1	CH ₃ ss(99)
2246	2229	-17	CH ₃ as ^{1,2} (86), CH ₃ as ^{1,2} (14)
2262	2247	-15	CH ₃ as ^{1,2} (85), CH ₃ as ^{1,2} (14)
—	2791	—	NH ₃ ss,as(60), NH ₃ ss,as(39)
2974	2962	-12	C ^α H s(100)
—	3381	—	NH ₃ ss,as(59), NH ₃ ss,as(39)
—	3447	—	NH ₃ ss,as(98)
—	3517	—	OH s(100)

frequency (cm ⁻¹)			ND ₃ CHCD ₃ COOD (mean deviation = 15 cm ⁻¹)
obs.	calc.	dev.	
—	83	—	CC t(96)
—	172	—	CN t(73), CC ^{me} t(21)
—	181	—	CC ^{me} t(73), CN t(17)
256	245	-11	C ^α H d ² (46), CCOO r(20), C ^α H d ³ (12), CCOO wag(9)
309	305	-4	C ^α H d ³ (38), CCOO r(22), C ^α H d ² (19), CCOO wag(7)
356	357	1	C ^α H d ¹ (68), CH ₃ r ² (8)
498	467	-31	CCOO sd(40), CCOO r(13), CN ^{+ter} s(11), C ^α H d ³ (9), CC ^{ter} s(8)
577	583	6	CCOO sd(26), CCOO r(24), C ^α H d ³ (15), NH ₃ r ² (8)
—	651	—	C-OH t(44), CCOO wag(24), CH ₃ r ¹ (9), CC ^{me} s(7)
731	697	-34	CN ^{+ter} s(23), CH ₃ r ² (17), CC ^{ter} s(15), COH b(8)
731	741	10	NH ₃ r ² (46), CH ₃ r ¹ (17), CC ^{me} s(13), NH ₃ r ¹ (8), CH ₃ r ² (7)
768	769	1	C-OH t(33), CH ₃ r ¹ (31), NH ₃ r ¹ (10), CCOO wag(8)
—	778	—	CH ₃ r ² (30), NH ₃ r ² (16), NH ₃ r ¹ (15), CC ^{ter} s(12)
816	829	13	NH ₃ r ¹ (28), CCOO wag(22), C-OH t(18)
1015	1016	1	CH ₃ sd(35), CN ^{+ter} s(14), CC ^{me} s(11), COH b(7)
1054	1047	-7	COH b(16), CH ₃ ad ¹ (15), C ^α H d ² (14), CCOO wag(10), CH ₃ sd(9), CH ₃ r ¹ (9)
1054	1050	-4	CH ₃ ad ² (51), CH ₃ ad ¹ (41)

Table 3.59: (continued)

frequency (cm^{-1})			Potential Energy Distribution
obs.	calc.	dev.	
1054	1054	0	CH_3 ad ¹ (40), CH_3 ad ² (38), COH b(8)
1078	1074	-4	CN^{+ter} s(18), CH_3 r ² (16), CH_3 sd(13), C^αH d ¹ (12)
1078	1085	7	COH b(33), C-OH s(15), C=O s(14)
1133	1137	4	CC^{me} s(36), CH_3 sd(29), C^αH r ² (12)
1153	1157	4	NH_3 ad ¹ (82), NH_3 sd(10)
1178	1164	-14	NH_3 sd(76), NH_3 ad ¹ (8), CN^{+ter} s(7)
1178	1185	7	NH_3 ad ² (95)
1270	1287	17	C^αH r ² (65), CC^{me} s(8), C-OH s(7)
1322	1317	-5	C^αH r ¹ (79), C-OH s(10)
1408	1462	54	C-OH s(38), CC^{ter} s(26), C^αH r ¹ (10), CCOO sd(10)
1726	1721	-5	C=O s(78)
—	2044	—	NH_3 ss,as(50), NH_3 ss,as(47)
—	2082	—	CH_3 ss(99)
—	2229	—	CH_3 as ^{1,2} (86), CH_3 as ^{1,2} (14)
—	2247	—	CH_3 as ^{1,2} (85), CH_3 as ^{1,2} (14)
—	2452	—	NH_3 ss,as(52), NH_3 ss,as(47)
—	2540	—	NH_3 ss,as(99)
—	2562	—	OH s(100)
2974	2962	-12	C^αH s(100)

frequency (cm^{-1})			Potential Energy Distribution
obs.	calc.	dev.	
—	88	—	CC t(98)
—	233	—	CN t(65), C^αH d ³ (10), C^αH d ² (9), CCOO r(9)
—	248	—	CC^{me} t(88)
266	280	14	C^αH d ² (36), CN t(29), CCOO r(16), C^αH d ³ (7), CCOO wag(7)
326	335	9	C^αH d ³ (29), C^αH d ² (24), CCOO r(21), CCOO wag(9), CC^{me} t(8)
405	408	3	C^αH d ¹ (66)
522	503	-19	CCOO sd(34), CN^{+ter} s(15), C^αH d ¹ (15), CCOO r(13), CC^{ter} s(8), C^αH d ³ (7)
608	628	20	CCOO sd(33), C^αH d ³ (21), CCOO r(19), C-OH s(8)

Table 3.59: (continued)

frequency (cm ⁻¹)			Potential Energy Distribution
obs.	calc.	dev.	
746	743	-3	CCOO wag(37), CC ^{me} s(17), CCOO sd(9), CC ^{ter} s(8), CN ^{+ter} s(7), C ^α H d ² (7)
821	814	-7	CN ^{+ter} s(20), CCOO wag(17), CC ^{ter} s(11), CH ₃ r ² (11)
916	916	0	CC ^{ter} s(27), CN ^{+ter} s(26), CH ₃ r ¹ (12), C-OH s(8), CH ₃ r ² (8), NH ₃ r ² (7)
916	948	32	NH ₃ r ² (51), CC ^{me} s(23), CH ₃ r ¹ (11)
1006	976	-30	C-OH t(89)
1006	1012	6	NH ₃ r ¹ (29), CH ₃ r ² (23), C ^α H r ¹ (10), CN ^{+ter} s(7)
1114	1117	3	CC ^{me} s(26), CH ₃ r ¹ (14), CN ^{+ter} s(13), NH ₃ r ¹ (12), NH ₃ r ² (11)
1140	1145	5	CH ₃ r ¹ (25), C ^α H r ² (21), C ^α H d ² (7), CCOO wag(7), NH ₃ r ¹ (7), NH ₃ r ² (7)
1213	1218	5	CH ₃ r ² (27), NH ₃ r ¹ (14), C ^α H d ¹ (11), C-OH s(9), CC ^{me} s(8), NH ₃ r ² (7)
1260	1254	-6	COH b(27), C-OH s(25), C ^α H r ² (12), C=O s(7), NH ₃ r ¹ (7)
1326	1319	-7	C ^α H r ² (39), C ^α H r ¹ (22), CC ^{me} s(8)
1361	1366	5	C ^α H r ¹ (49), COH b(17), NH ₃ r ¹ (7)
1391	1401	10	CH ₃ sd(96)
1459	1459	0	CH ₃ ad ¹ (83), CH ₃ r ¹ (7)
1459	1464	5	CH ₃ ad ² (89), CH ₃ r ² (8)
1520	1520	0	NH ₃ sd(92)
1520	1524	4	C-OH s(31), COH b(23), CC ^{ter} s(14), CCOO sd(9)
1613	1614	1	NH ₃ ad ¹ (81), NH ₃ r ¹ (12)
1613	1631	18	NH ₃ ad ² (92)
1733	1739	6	C=O s(69), COH b(10)
—	2785	—	NH ₃ ss,as(61), NH ₃ ss,as(39)
2956	2896	-60	CH ₃ ss(98)
2998	2961	-37	C ^α H s(97)
3007	3006	-1	CH ₃ as ^{1,2} (83), CH ₃ as ^{1,2} (15)
—	3031	—	CH ₃ as ^{1,2} (83), CH ₃ as ^{1,2} (15)
—	3375	—	NH ₃ ss,as(60), NH ₃ ss,as(38)
—	3437	—	NH ₃ ss,as(98)
—	3517	—	OH s(100)

Table 3.59: (continued)

frequency (cm ⁻¹)			Potential Energy Distribution
obs.	calc.	dev.	
frequency (cm ⁻¹)			Potential Energy Distribution
obs.	calc.	dev.	
—	88	—	CC t(98)
—	233	—	CN t(64), C ^α H d ² (10), C ^α H d ³ (9), CCOO r(9)
—	248	—	CC ^{me} t(88)
273	278	5	C ^α H d ² (38), CN t(30), CCOO r(14), CCOO wag(7)
338	336	-2	C ^α H d ³ (30), CCOO r(24), C ^α H d ² (22), CCOO wag(8), CC ^{me} t(8)
404	408	4	C ^α H d ¹ (67)
524	507	-17	CCOO sd(36), CN ^{+ter} s(14), C ^α H d ¹ (14), CCOO r(12), CC ^{ter} s(8), C ^α H d ³ (7)
607	629	22	CCOO sd(30), C ^α H d ³ (22), CCOO r(19), C-OH s(8)
746	739	-7	CCOO wag(36), CC ^{me} s(19), CCOO sd(10), CC ^{ter} s(8), CN ^{+ter} s(7), C ^α H d ² (7)
820	815	-5	CN ^{+ter} s(19), CCOO wag(17), CC ^{ter} s(11), CH ₃ r ² (11), CH ₃ r ¹ (7)
914	916	2	CC ^{ter} s(27), CN ^{+ter} s(25), CH ₃ r ¹ (12), CH ₃ r ² (9), C-OH s(8), NH ₃ r ² (7)
—	946	—	NH ₃ r ² (48), CC ^{me} s(23), CH ₃ r ¹ (12)
1004	976	-28	C-OH t(88)
1004	1010	6	NH ₃ r ¹ (28), CH ₃ r ² (23), CN ^{+ter} s(9), C ^α H r ¹ (9)
1112	1114	2	CC ^{me} s(24), CH ₃ r ¹ (18), CN ^{+ter} s(15), NH ₃ r ² (10), NH ₃ r ¹ (9)
1142	1143	1	C ^α H r ² (22), CH ₃ r ¹ (20), NH ₃ r ² (10), NH ₃ r ¹ (8), C ^α H r ¹ (7)
1211	1215	4	CH ₃ r ² (27), NH ₃ r ¹ (16), C ^α H d ¹ (11), C-OH s(8), C ^α H r ¹ (7), NH ₃ r ² (7)
1259	1254	-5	COH b(27), C-OH s(26), C ^α H r ² (12), C=O s(7)
1326	1318	-8	C ^α H r ² (40), C ^α H r ¹ (18), CC ^{me} s(7), NH ₃ r ² (7)
1368	1367	-1	C ^α H r ¹ (51), COH b(16), NH ₃ r ¹ (8)
1368	1393	25	CH ₃ sd(97)
1458	1458	0	CH ₃ ad ¹ (82), CH ₃ r ¹ (8)
1458	1463	5	CH ₃ ad ² (88), CH ₃ r ² (9)
1525	1524	-1	C-OH s(30), COH b(22), CC ^{ter} s(13), CCOO sd(8)

Table 3.59: (continued)

frequency (cm^{-1})			Potential Energy Distribution
obs.	calc.	dev.	
1525	1526	1	NH ₃ sd(88)
1610	1615	5	NH ₃ ad ¹ (82), NH ₃ r ¹ (12)
1620	1633	13	NH ₃ ad ² (93)
1732	1739	7	C=O s(69), COH b(10)
—	2791	—	NH ₃ ss,as(60), NH ₃ ss,as(39)
—	2893	—	CH ₃ ss(98)
—	2960	—	C ^{α} H s(95)
—	2996	—	CH ₃ as ^{1,2} (82), CH ₃ as ^{1,2} (14)
—	3020	—	CH ₃ as ^{1,2} (83), CH ₃ as ^{1,2} (15)
—	3381	—	NH ₃ ss,as(59), NH ₃ ss,as(39)
—	3447	—	NH ₃ ss,as(98)
—	3517	—	OH s(100)

Table 3.60: Scaled 4-31G* Frequencies and Potential Energy Distribution for Water-Excluded Alanine One-water Supermolecule in Acid.

frequency (cm ⁻¹)			NH ₃ ⁺ CHCH ₃ CO ₂ H (mean deviation = 9 cm ⁻¹)
obs.	calc.	dev.	
			Potential Energy Distribution
—	79	—	CC t(98)
—	215	—	CN t(92)
—	242	—	CC ^{me} t(89)
275	274	-1	C ^α H d ² (42), CCOO r(26), C ^α H d ³ (14)
335	339	4	C ^α H d ³ (36), C ^α H d ² (20), CCOO r(20), CCOO wag(8), CC ^{me} t(7)
409	409	0	C ^α H d ¹ (72)
526	514	-12	CCOO sd(27), CCOO r(18), CN ^{+ter} s(15), C ^α H d ³ (11), C ^α H d ¹ (10), CC ^{ter} s(9)
603	630	27	CCOO sd(30), CCOO r(17), C ^α H d ³ (16), CC ^{ter} s(8), C-OH s(7), CC ^{me} s(7), CCOO wag(7)
746	745	-1	CCOO wag(30), CCOO sd(15), CC ^{me} s(14), CN ^{+ter} s(7)
823	820	-3	CN ^{+ter} s(16), CCOO wag(16), CH ₃ r ² (13), CC ^{ter} s(10), CH ₃ r ¹ (7)
920	916	-4	CC ^{ter} s(25), CN ^{+ter} s(22), CH ₃ r ² (10), CC ^{me} s(9), CH ₃ r ¹ (9), C-OH s(8), NH ₃ r ² (8)
—	948	—	NH ₃ r ² (46), CC ^{me} s(20), CH ₃ r ¹ (15), CN ^{+ter} s(7)
—	977	—	C-OH t(75)
1008	1006	-2	NH ₃ r ¹ (24), CH ₃ r ² (18), C-OH t(14), C ^α H r ¹ (11), CN ^{+ter} s(10)
1117	1122	5	CC ^{me} s(20), NH ₃ r ² (17), C ^α H r ² (16), CN ^{+ter} s(11), NH ₃ r ¹ (11)
1146	1142	-4	CH ₃ r ¹ (33), C ^α H r ² (13), CCOO wag(11), C ^α H d ² (10)
1214	1221	7	CH ₃ r ² (20), C-OH s(15), C ^α H r ¹ (11), NH ₃ r ¹ (10), COH b(9), C ^α H d ¹ (9)
1261	1258	-3	COH b(21), C-OH s(16), NH ₃ r ¹ (13), C ^α H r ² (12), CH ₃ r ² (10), C=O s(9)
1328	1329	1	C ^α H r ² (34), COH b(13), C ^α H r ¹ (10), CC ^{me} s(7), NH ₃ r ² (7)
1364	1365	1	C ^α H r ¹ (50), COH b(18), NH ₃ r ¹ (10)
1393	1401	8	CH ₃ sd(90)
1460	1457	-3	CH ₃ ad ¹ (73)
1460	1461	1	CH ₃ ad ² (82), CH ₃ r ² (9)

Table 3.60: (continued)

frequency (cm^{-1})			Potential Energy Distribution
obs.	calc.	dev.	
1523	1512	-11	C-OH s(22), NH ₃ sd(15), CC ^{ter} s(14), COH b(10), CCOO sd(8), CH ₃ ad ¹ (8)
1523	1531	8	NH ₃ sd(78)
1635	1617	-18	NH ₃ ad ¹ (74), NH ₃ r ¹ (17)
1635	1630	-5	NH ₃ ad ² (91)
1735	1742	7	C=O s(68), COH b(10)
2895	2895	0	CH ₃ ss(98)
2956	2961	5	C ^{α} H s(97)
2998	3005	7	CH ₃ as ^{1,2} (85), CH ₃ as ^{1,2} (12)
3007	3030	23	CH ₃ as ^{1,2} (86), CH ₃ as ^{1,2} (12)
—	3105	—	NH ₃ ss,as(53), NH ₃ ss,as(46)
—	3404	—	NH ₃ ss,as(53), NH ₃ ss,as(46)
—	3464	—	NH ₃ ss,as(99)
—	3573	—	OH s(100)

frequency (cm^{-1})			ND ₃ ⁺ CHCH ₃ CO ₂ D (mean deviation = 12 cm^{-1})
obs.	calc.	dev.	
—	76	—	CC t(96)
—	156	—	CN t(94)
—	241	—	CC ^{me} t(88)
276	262	-14	C ^{α} H d ² (34), CCOO r(30), C ^{α} H d ³ (23)
319	320	1	C ^{α} H d ³ (32), C ^{α} H d ² (27), CCOO r(10), CCOO wag(9), CC ^{me} t(9)
380	379	-1	C ^{α} H d ¹ (68), CCOO r(7)
508	485	-23	CCOO sd(29), CCOO r(17), CN ^{+ter} s(15), C ^{α} H d ³ (10), C ^{α} H d ¹ (8), CC ^{ter} s(7)
588	589	1	CCOO sd(28), CCOO r(21), C ^{α} H d ³ (9), NH ₃ r ² (8)
—	658	—	C-OH t(48), CCOO wag(13), CCOO sd(7)
730	722	-8	CC ^{ter} s(19), NH ₃ r ² (18), CN ^{+ter} s(13), COH b(11), C-OH t(11), NH ₃ r ¹ (9)
764	770	6	NH ₃ r ² (48), CC ^{me} s(23), NH ₃ r ¹ (13)
825	834	9	CCOO wag(36), C-OH t(30), NH ₃ r ¹ (13)
881	876	-5	CH ₃ r ² (34), NH ₃ r ¹ (28), CN ^{+ter} s(9), CC ^{me} s(7)

Table 3.60: (continued)

frequency (cm^{-1})			Potential Energy Distribution
obs.	calc.	dev.	
919	895	-24	CH_3 r ¹ (30), CN^{+ter} s(19), CC^{ter} s(18)
1060	1047	-13	COH b(27), CC^{me} s(20), C^αH r ² (10), C-OH s(9), CN^{+ter} s(8)
1104	1094	-10	COH b(31), C=O s(14), C-OH s(9), CC^{me} s(8), C^αH r ² (7)
1114	1130	16	CH_3 r ¹ (38), NH_3 sd(13), C^αH r ² (10), C^αH d ² (10), CCOO wag(9)
1149	1144	-5	NH_3 ad ¹ (83)
1157	1177	20	NH_3 ad ² (83)
1174	1187	13	NH_3 sd(27), CH_3 r ² (16), CC^{me} s(11), NH_3 ad ² (9), NH_3 r ¹ (9)
1183	1191	8	NH_3 sd(41), CN^{+ter} s(17), CH_3 r ² (14), C^αH d ¹ (7)
1274	1288	14	C^αH r ² (41), C-OH s(19)
1324	1325	1	C^αH r ¹ (66), C^αH r ² (11)
1408	1402	-6	CH_3 sd(91)
1437	1445	8	CH_3 ad ¹ (61), C-OH s(13), CC^{ter} s(9)
1463	1461	-2	CH_3 ad ² (87), CH_3 r ² (9)
1463	1496	33	CH_3 ad ¹ (28), C-OH s(17), CC^{ter} s(17), CH_3 r ¹ (11), C^αH r ¹ (7)
1727	1723	-4	C=O s(77), C-OH s(7)
—	2262	—	NH_3 ss,as(63), NH_3 ss,as(36)
—	2481	—	NH_3 ss,as(62), NH_3 ss,as(37)
—	2556	—	NH_3 ss,as(99)
—	2602	—	OH s(100)
2898	2895	-3	CH_3 ss(98)
2956	2962	6	C^αH s(97)
3002	3005	3	CH_3 as ^{1,2} (86), CH_3 as ^{1,2} (12)
3011	3030	19	CH_3 as ^{1,2} (86), CH_3 as ^{1,2} (12)

frequency (cm^{-1})			Potential Energy Distribution
obs.	calc.	dev.	
—	76	—	CC t(97)
—	175	—	CC^{me} t(94)
—	214	—	CN t(91)
246	253	7	C^αH d ² (55), CCOO r(15), CCOO wag(8)

Table 3.60: (continued)

frequency (cm ⁻¹)			Potential Energy Distribution
obs.	calc.	dev.	
331	325	-6	C ^α H d ³ (44), CCOO r(31), C ^α H d ² (10)
378	378	0	C ^α H d ¹ (72), CH ₃ r ² (10)
506	494	-12	CCOO sd(29), CCOO r(18), CC ^{ter} s(13), C ^α H d ³ (13), CN ^{+ter} s(10)
594	608	14	CCOO sd(21), CCOO r(20), C ^α H d ³ (16), CC ^{me} s(10), CC ^{ter} s(10)
674	665	-9	C ^α H r ² (27), CCOO wag(26), CH ₃ r ¹ (22), CH ₃ r ² (15)
748	728	-20	CC ^{me} s(20), CN ^{+ter} s(20), CCOO sd(17), CH ₃ r ² (13)
794	789	-5	CH ₃ r ¹ (37), CC ^{ter} s(14), CH ₃ r ² (14), CCOO sd(8)
879	854	-25	C ^α H r ¹ (48), CN ^{+ter} s(21), NH ₃ r ¹ (13)
879	860	-19	C ^α H r ² (23), CC ^{me} s(14), CC ^{ter} s(10), NH ₃ r ² (10), CN ^{+ter} s(8)
944	949	5	C-OH t(43), NH ₃ r ² (18), C ^α H r ² (7)
—	971	—	NH ₃ r ² (28), C ^α H r ² (17), CH ₃ r ² (14), CH ₃ r ¹ (12)
1010	1011	1	C-OH t(41), CCOO wag(30), C ^α H d ² (8)
1053	1047	-6	CH ₃ ad ² (83), CH ₃ ad ¹ (13)
1053	1051	-2	CH ₃ ad ¹ (84), CH ₃ ad ² (13)
1083	1074	-9	CH ₃ sd(64), CN ^{+ter} s(8), C ^α H r ¹ (8), NH ₃ r ² (7)
1134	1135	1	CN ^{+ter} s(22), C-OH s(16), CH ₃ sd(11), CC ^{me} s(8), CH ₃ r ² (7)
1199	1221	22	NH ₃ r ¹ (35), C-OH s(13), C=O s(8), C ^α H d ³ (8), NH ₃ ad ¹ (7)
1231	1255	24	CC ^{me} s(27), NH ₃ r ¹ (20), NH ₃ r ² (10)
1304	1299	-5	COH b(52), CC ^{ter} s(13)
1508	1491	-17	C-OH s(35), COH b(21), CC ^{ter} s(17), CCOO sd(14)
1530	1528	-2	NH ₃ sd(92)
1606	1612	6	NH ₃ ad ¹ (79), NH ₃ r ¹ (16)
1638	1630	-8	NH ₃ ad ² (93)
1735	1741	6	C=O s(68), COH b(10)
2080	2081	1	CH ₃ ss(99)
2188	2188	0	C ^α H s(97)
2253	2230	-23	CH ₃ as ^{1,2} (88), CH ₃ as ^{1,2} (11)
2253	2249	-4	CH ₃ as ^{1,2} (88), CH ₃ as ^{1,2} (11)
—	3104	—	NH ₃ ss,as(53), NH ₃ ss,as(46)
—	3404	—	NH ₃ ss,as(53), NH ₃ ss,as(45)

Table 3.60: (continued)

frequency (cm ⁻¹)			Potential Energy Distribution
obs.	calc.	dev.	
—	3464	—	NH ₃ ss,as(99)
—	3573	—	OH s(100)

frequency (cm ⁻¹)			Potential Energy Distribution
obs.	calc.	dev.	
—	77	—	CC t(97)
—	175	—	CC ^{me} t(94)
—	215	—	CN t(91)
243	254	11	C ^α H d ² (54), CCOO r(15), CCOO wag(8)
332	329	-3	C ^α H d ³ (44), CCOO r(30), C ^α H d ² (11)
380	381	1	C ^α H d ¹ (72), CH ₃ r ² (10)
514	501	-13	CCOO sd(29), CCOO r(21), CN ^{+ter} s(12), C ^α H d ³ (12), CC ^{ter} s(11)
598	614	16	CCOO sd(25), CCOO r(18), C ^α H d ³ (16), CC ^{me} s(11), CC ^{ter} s(10)
710	706	-4	CCOO wag(42), CH ₃ r ¹ (27), CH ₃ r ² (9)
760	736	-24	CN ^{+ter} s(25), CH ₃ r ² (24), CCOO sd(16), CC ^{me} s(15)
799	790	-9	CH ₃ r ¹ (34), CH ₃ r ² (18), CC ^{ter} s(12), CN ^{+ter} s(7), CCOO sd(7)
921	908	-13	NH ₃ r ² (39), CC ^{me} s(19), CC ^{ter} s(17), CH ₃ sd(11)
939	937	-2	NH ₃ r ¹ (20), C-OH t(20), CN ^{+ter} s(11), CH ₃ r ² (11), C ^α H d ² (8)
—	987	—	C-OH t(71), CCOO wag(10)
1050	1038	-12	CH ₃ ad ² (29), CH ₃ sd(24), CN ^{+ter} s(14), NH ₃ r ² (8)
1050	1049	-1	CH ₃ ad ¹ (73), CH ₃ ad ² (15)
1064	1052	-12	CH ₃ ad ² (51), CH ₃ ad ¹ (23), CH ₃ sd(13)
1118	1103	-15	NH ₃ r ² (20), CH ₃ sd(14), C ^α H r ² (9), CCOO wag(8), CH ₃ r ¹ (8)
1141	1138	-3	C ^α H r ² (25), CH ₃ sd(25), CC ^{me} s(22)
1186	1181	-5	NH ₃ r ¹ (31), C ^α H r ¹ (18), CH ₃ r ² (11), C ^α H d ¹ (9)
1260	1253	-7	COH b(28), C-OH s(24), C=O s(12), C ^α H r ² (9)
1322	1323	1	C ^α H r ² (38), COH b(15), CC ^{me} s(12), NH ₃ r ² (9)
1364	1366	2	C ^α H r ¹ (54), COH b(17), NH ₃ r ¹ (11)

Table 3.60: (continued)

frequency (cm^{-1})			Potential Energy Distribution
obs.	calc.	dev.	
1522	1501	-21	C-OH s(30), CC ^{ter} s(17), COH b(17), CCOO sd(12), NH ₃ sd(7)
1522	1529	7	NH ₃ sd(86)
1623	1616	-7	NH ₃ ad ¹ (74), NH ₃ r ¹ (17)
1623	1630	7	NH ₃ ad ² (91)
1735	1742	7	C=O s(68), COH b(10)
2081	2081	0	CH ₃ ss(99)
2246	2230	-16	CH ₃ as ^{1,2} (88), CH ₃ as ^{1,2} (11)
2262	2249	-13	CH ₃ as ^{1,2} (88), CH ₃ as ^{1,2} (11)
2974	2963	-11	C ^{α} H s(100)
—	3105	—	NH ₃ ss,as(53), NH ₃ ss,as(46)
—	3404	—	NH ₃ ss,as(53), NH ₃ ss,as(46)
—	3464	—	NH ₃ ss,as(99)
—	3573	—	OH s(100)

frequency (cm^{-1})			ND ₃ ⁺ CHCD ₃ CO ₂ D (mean deviation = 16 cm^{-1})
obs.	calc.	dev.	
—	74	—	CC t(96)
—	155	—	CN t(94)
—	175	—	CC ^{me} t(93)
256	245	-11	C ^{α} H d ² (50), CCOO r(20), C ^{α} H d ³ (11), CCOO wag(8)
309	306	-3	C ^{α} H d ³ (45), CCOO r(20), C ^{α} H d ² (14)
356	353	-3	C ^{α} H d ¹ (68), CH ₃ r ² (9)
498	475	-23	CCOO sd(30), CCOO r(20), CN ^{+ter} s(13), C ^{α} H d ³ (11), CC ^{ter} s(8)
577	581	4	CCOO sd(26), CCOO r(21), C ^{α} H d ³ (9), CC ^{ter} s(8), NH ₃ r ² (8)
—	640	—	C-OH t(44), CCOO wag(19), CH ₃ r ¹ (8)
731	693	-38	CN ^{+ter} s(21), CH ₃ r ² (18), CC ^{ter} s(13), COH b(11), CCOO sd(8), CC ^{me} s(7)
731	739	8	NH ₃ r ² (41), CH ₃ r ¹ (20), CC ^{me} s(13), CH ₃ r ² (8), NH ₃ r ¹ (8)
768	770	2	CH ₃ r ² (23), NH ₃ r ² (20), CC ^{ter} s(15), CC ^{me} s(8), CN ^{+ter} s(7)
—	775	—	CH ₃ r ¹ (28), C-OH t(28), NH ₃ r ¹ (18), CCOO wag(7)

Table 3.60: (continued)

frequency (cm ⁻¹)			Potential Energy Distribution
obs.	calc.	dev.	
816	837	21	NH ₃ r ¹ (28), CCOO wag(24), C-OH t(21), CN ^{+ter} s(7)
1015	1004	-11	CH ₃ sd(38), CN ^{+ter} s(11), CC ^{me} s(10)
1054	1046	-8	CH ₃ ad ² (37), CH ₃ ad ¹ (34)
1054	1047	-7	CH ₃ ad ² (54), CH ₃ ad ¹ (25)
1054	1055	1	CH ₃ ad ¹ (36), COH b(19), CH ₃ r ¹ (13), CCOO wag(7)
1054	1074	20	CH ₃ r ² (15), CH ₃ sd(12), C-OH s(11), C ^α H d ¹ (11), CN ^{+ter} s(10), NH ₃ r ¹ (8)
1078	1093	15	COH b(25), C=O s(12), C-OH s(10)
1133	1138	5	CH ₃ sd(30), CC ^{me} s(24), C ^α H r ² (16), NH ₃ ad ¹ (14)
1153	1155	2	NH ₃ ad ¹ (69), NH ₃ r ¹ (13)
1178	1179	1	NH ₃ ad ² (95)
1178	1188	10	NH ₃ sd(74), CN ^{+ter} s(19)
1270	1283	13	C ^α H r ² (45), C-OH s(16), CC ^{me} s(8)
1322	1323	1	C ^α H r ¹ (66), C ^α H r ² (8), CC ^{me} s(7)
1408	1470	62	C-OH s(31), CC ^{ter} s(27), C ^α H r ¹ (11), CCOO sd(11)
1726	1723	-3	C=O s(77), C-OH s(7)
—	2081	—	CH ₃ ss(99)
—	2230	—	CH ₃ as ^{1,2} (88), CH ₃ as ^{1,2} (11)
—	2249	—	CH ₃ as ^{1,2} (88), CH ₃ as ^{1,2} (11)
—	2262	—	NH ₃ ss,as(62), NH ₃ ss,as(36)
—	2481	—	NH ₃ ss,as(62), NH ₃ ss,as(37)
—	2556	—	NH ₃ ss,as(99)
—	2602	—	OH s(100)
2974	2963	—	C ^α H s(100)

frequency (cm ⁻¹)			¹⁵ NH ₃ ⁺ CHCH ₃ CO ₂ H (mean deviation = 11 cm ⁻¹)
obs.	calc.	dev.	
—	79	—	CC t(98)
—	215	—	CN t(92)
—	242	—	CC ^{me} t(89)
266	273	7	C ^α H d ² (41), CCOO r(26), C ^α H d ³ (15)
326	337	11	C ^α H d ³ (36), C ^α H d ² (21), CCOO r(18), CCOO wag(8), CC ^{me} t(7)

Table 3.60: (continued)

frequency (cm ⁻¹)			Potential Energy Distribution
obs.	calc.	dev.	
405	407	2	C ^α H d ¹ (72)
522	509	-13	CCOO sd(26), CCOO r(19), CN ^{+ter} s(17), C ^α H d ³ (11), CC ^{ter} s(9), C ^α H d ¹ (9)
608	629	21	CCOO sd(32), CCOO r(17), C ^α H d ³ (16), CC ^{ter} s(8), C-OH s(7), CC ^{me} s(7), CCOO wag(7)
746	744	-2	CCOO wag(29), CCOO sd(16), CC ^{me} s(15), CN ^{+ter} s(7)
821	818	-3	CN ^{+ter} s(17), CCOO wag(16), CH ₃ r ² (14), CC ^{ter} s(9)
916	912	-4	CC ^{ter} s(26), CN ^{+ter} s(22), CH ₃ r ¹ (10), C-OH s(9), CH ₃ r ² (9), CC ^{me} s(8), NH ₃ r ² (8)
916	945	29	NH ₃ r ² (47), CC ^{me} s(20), CH ₃ r ¹ (15), CN ^{+ter} s(7)
1006	977	-29	C-OH t(73)
1006	1004	-2	NH ₃ r ¹ (24), CH ₃ r ² (18), C-OH t(16), C ^α H r ¹ (11), CN ^{+ter} s(9)
1114	1119	5	CC ^{me} s(21), C ^α H r ² (16), NH ₃ r ² (16), NH ₃ r ¹ (12), CN ^{+ter} s(10)
1140	1141	1	CH ₃ r ¹ (34), C ^α H r ² (13), CCOO wag(11), C ^α H d ² (10)
1213	1220	7	CH ₃ r ² (21), C-OH s(14), NH ₃ r ¹ (11), C ^α H r ¹ (10), C ^α H d ¹ (10), COH b(8)
1260	1256	-4	COH b(21), C-OH s(17), C ^α H r ² (12), NH ₃ r ¹ (12), C=O s(9), CH ₃ r ² (9)
1326	1327	1	C ^α H r ² (35), COH b(12), C ^α H r ¹ (12), CC ^{me} s(8), NH ₃ r ² (7)
1361	1362	1	C ^α H r ¹ (49), COH b(20), NH ₃ r ¹ (9)
1391	1401	10	CH ₃ sd(91)
1459	1457	-2	CH ₃ ad ¹ (73)
1459	1461	2	CH ₃ ad ² (82), CH ₃ r ² (9)
1520	1510	-10	NH ₃ sd(30), C-OH s(19), CC ^{ter} s(11), COH b(9), CCOO sd(7), CH ₃ ad ¹ (7)
1520	1525	5	NH ₃ sd(64)
1613	1616	3	NH ₃ ad ¹ (72), NH ₃ r ¹ (17)
1613	1628	15	NH ₃ ad ² (90)
1733	1742	9	C=O s(68), COH b(10)
2895	2895	0	CH ₃ ss(98)
2956	2961	5	C ^α H s(97)
2998	3005	7	CH ₃ as ^{1,2} (85), CH ₃ as ^{1,2} (12)

Table 3.60: (continued)

frequency (cm ⁻¹)			Potential Energy Distribution
obs.	calc.	dev.	
3007	3030	23	CH ₃ as ^{1,2} (86), CH ₃ as ^{1,2} (12)
—	3098	—	NH ₃ ss,as(55), NH ₃ ss,as(45)
—	3397	—	NH ₃ ss,as(54), NH ₃ ss,as(44)
—	3454	—	NH ₃ ss,as(99)
—	3573	—	OH s(100)

frequency (cm ⁻¹)			Potential Energy Distribution
obs.	calc.	dev.	
—	79	—	CC t(98)
—	215	—	CN t(92)
—	241	—	CC ^{me} t(88)
273	271	-2	C ^α H d ² (43), CCOO r(25), C ^α H d ³ (13)
338	339	1	C ^α H d ³ (37), CCOO r(21), C ^α H d ² (19), CCOO wag(8), CC ^{me} t(7)
404	406	2	C ^α H d ¹ (72)
524	514	-10	CCOO sd(27), CCOO r(18), CN ^{+ter} s(15), C ^α H d ³ (11), CC ^{ter} s(9), C ^α H d ¹ (9)
607	628	21	CCOO sd(29), CCOO r(18), C ^α H d ³ (16), CC ^{me} s(8), CC ^{ter} s(8), CCOO wag(8), C-OH s(7)
746	741	-5	CCOO wag(28), CCOO sd(17), CC ^{me} s(16), CN ^{+ter} s(7)
820	818	-2	CCOO wag(17), CN ^{+ter} s(16), CH ₃ r ² (14), CC ^{ter} s(9), CH ₃ r ¹ (7)
914	912	-2	CC ^{ter} s(26), CN ^{+ter} s(20), CH ₃ r ¹ (10), CH ₃ r ² (10), CC ^{me} s(9), C-OH s(8), NH ₃ r ² (8)
—	944	—	NH ₃ r ² (45), CC ^{me} s(20), CH ₃ r ¹ (16), CN ^{+ter} s(8), CH ₃ r ² (7)
1004	977	-27	C-OH t(73)
1004	1004	0	NH ₃ r ¹ (23), CH ₃ r ² (18), C-OH t(16), C ^α H r ¹ (11), CN ^{+ter} s(10)
1112	1119	7	CC ^{me} s(21), NH ₃ r ² (16), CN ^{+ter} s(13), C ^α H r ² (13), NH ₃ r ¹ (10), CH ₃ r ¹ (7)
1142	1138	-4	CH ₃ r ¹ (29), C ^α H r ² (16), CCOO wag(11), C ^α H d ² (9), C ^α H r ¹ (7)

Table 3.60: (continued)

frequency (cm ⁻¹)			Potential Energy Distribution
obs.	calc.	dev.	
1211	1217	6	CH ₃ r ² (21), C-OH s(13), NH ₃ r ¹ (13), C ^α H r ¹ (12), C ^α H d ¹ (10), COH b(7)
1259	1257	-2	COH b(22), C-OH s(18), C ^α H r ² (12), NH ₃ r ¹ (11), C=O s(9), CH ₃ r ² (7)
1326	1327	1	C ^α H r ² (35), COH b(14), C ^α H r ¹ (9), CC ^{me} s(8), NH ₃ r ² (7)
1368	1364	-4	C ^α H r ¹ (51), COH b(17), NH ₃ r ¹ (10)
1368	1391	23	CH ₃ sd(92)
1458	1455	-3	CH ₃ ad ¹ (73), CH ₃ r ¹ (7)
1458	1460	2	CH ₃ ad ² (83), CH ₃ r ² (10)
1525	1512	-13	C-OH s(22), NH ₃ sd(15), CC ^{ter} s(14), COH b(11), CCOO sd(8), CH ₃ ad ¹ (8)
1525	1531	6	NH ₃ sd(78)
1610	1617	7	NH ₃ ad ¹ (74), NH ₃ r ¹ (17)
1620	1630	10	NH ₃ ad ² (91)
1732	1742	10	C=O s(68), COH b(10)
—	2891	—	CH ₃ ss(98)
—	2961	—	C ^α H s(95)
—	2994	—	CH ₃ as ^{1,2} (84), CH ₃ as ^{1,2} (12)
—	3019	—	CH ₃ as ^{1,2} (86), CH ₃ as ^{1,2} (13)
—	3105	—	NH ₃ ss,as(53), NH ₃ ss,as(46)
—	3404	—	NH ₃ ss,as(53), NH ₃ ss,as(46)
—	3464	—	NH ₃ ss,as(99)
—	3573	—	OH s(100)

Table 3.61: Scaled 6-31G** Frequencies and Potential Energy Distribution for Water-Excluded Alanine One-water Supramolecule in Acid.

frequency (cm ⁻¹)			NH ₃ ⁺ CHCH ₃ CO ₂ H (mean deviation = 9 cm ⁻¹)
obs.	calc.	dev.	
			Potential Energy Distribution
—	77	—	CC t(98)
—	233	—	CN t(72), CC ^{me} t(12), C ^α H d ² (7)
—	239	—	CC ^{me} t(77), CN t(14)
275	276	1	C ^α H d ² (43), CCOO r(22), C ^α H d ³ (12), CN t(11)
335	339	4	C ^α H d ³ (40), CCOO r(20), C ^α H d ² (18), CCOO wag(8), CC ^{me} t(7)
409	409	0	C ^α H d ¹ (72)
526	514	-12	CCOO sd(28), CCOO r(18), CN ^{+ter} s(14), C ^α H d ³ (10), CC ^{ter} s(9), C ^α H d ¹ (9)
603	628	25	CCOO sd(28), CCOO r(19), C ^α H d ³ (16), CC ^{ter} s(8), CC ^{me} s(7), CCOO wag(7)
746	744	-2	CCOO wag(30), CCOO sd(16), CC ^{me} s(14), CN ^{+ter} s(7)
823	818	-5	CCOO wag(16), CN ^{+ter} s(15), CH ₃ r ² (13), CC ^{ter} s(11), CH ₃ r ¹ (7)
920	914	-6	CC ^{ter} s(24), CN ^{+ter} s(20), CC ^{me} s(11), CH ₃ r ² (11), NH ₃ r ² (9), CH ₃ r ¹ (8), C-OH s(7)
—	944	44	NH ₃ r ² (46), CC ^{me} s(17), CH ₃ r ¹ (16), CH ₃ r ² (8), CN ^{+ter} s(7)
—	970	—	C-OH t(79)
1008	1003	-5	NH ₃ r ¹ (26), CH ₃ r ² (18), CN ^{+ter} s(12), C ^α H r ¹ (11), C-OH t(10)
1117	1123	6	CC ^{me} s(21), NH ₃ r ² (18), C ^α H r ² (17), CN ^{+ter} s(11), NH ₃ r ¹ (10)
1146	1141	-5	CH ₃ r ¹ (35), C ^α H d ² (11), CCOO wag(11), C ^α H r ² (10), CN ^{+ter} s(7)
1214	1222	8	CH ₃ r ² (23), NH ₃ r ¹ (16), C ^α H d ¹ (11), C-OH s(10), C ^α H r ¹ (10)
1261	1265	4	COH b(28), C-OH s(20), C=O s(12), C ^α H r ² (11), NH ₃ r ¹ (9)
1328	1330	2	C ^α H r ² (38), COH b(14), C ^α H r ¹ (8), CC ^{me} s(7)
1364	1365	1	C ^α H r ¹ (53), COH b(16), NH ₃ r ¹ (10)
1393	1403	10	CH ₃ sd(90)
1460	1455	-5	CH ₃ ad ¹ (78), CH ₃ r ¹ (7)
1460	1463	3	CH ₃ ad ² (86), CH ₃ r ² (8)

Table 3.61: (continued)

frequency (cm^{-1})			Potential Energy Distribution
obs.	calc.	dev.	
1523	1515	-8	C-OH s(23), NH ₃ sd(22), CC ^{ter} s(13), COH b(10), CCOO sd(8)
1523	1531	8	NH ₃ sd(70)
1635	1618	-17	NH ₃ ad ¹ (74), NH ₃ r ¹ (17)
1635	1629	-6	NH ₃ ad ² (92)
1735	1742	7	C=O s(68), COH b(9)
2895	2895	0	CH ₃ ss(98)
2956	2962	6	C ^{α} H s(97)
2998	3006	8	CH ₃ as ^{1,2} (85), CH ₃ as ^{1,2} (13)
3007	3032	25	CH ₃ as ^{1,2} (85), CH ₃ as ^{1,2} (13)
—	3103	—	NH ₃ ss,as(53), NH ₃ ss,as(46)
—	3415	—	NH ₃ ss,as(53), NH ₃ ss,as(45)
—	3481	—	NH ₃ ss,as(98)
—	3656	—	OH s(100)

frequency (cm^{-1})			ND ₃ ⁺ CHCH ₃ CO ₂ D (mean deviation = 13 cm^{-1})
obs.	calc.	dev.	
—	74	—	CC t(97)
—	170	—	CN t(94)
—	237	—	CC ^{me} t(88)
276	263	-13	C ^{α} H d ² (36), CCOO r(28), C ^{α} H d ³ (23)
319	319	0	C ^{α} H d ³ (35), C ^{α} H d ² (25), CCOO r(10), CCOO wag(8), CC ^{me} t(8)
380	379	-1	C ^{α} H d ¹ (68), CCOO r(7)
508	485	-23	CCOO sd(30), CCOO r(17), CN ^{+ter} s(15), C ^{α} H d ³ (9), C ^{α} H d ¹ (8), CC ^{ter} s(7)
588	589	1	CCOO sd(25), CCOO r(23), NH ₃ r ² (9), C ^{α} H d ³ (8), CC ^{ter} s(7)
—	656	—	C-OH t(49), CCOO wag(12), CCOO sd(8)
730	719	-11	CC ^{ter} s(20), NH ₃ r ² (19), CN ^{+ter} s(12), COH b(11), C-OH t(10), NH ₃ r ¹ (8)
764	766	2	NH ₃ r ² (46), CC ^{me} s(23), NH ₃ r ¹ (13)
825	829	4	CCOO wag(36), C-OH t(28), NH ₃ r ¹ (15)

Table 3.61: (continued)

frequency (cm^{-1})			Potential Energy Distribution
obs.	calc.	dev.	
881	873	-8	CH_3 r^2 (36), NH_3 r^1 (28), CN^{+ter} s(8), CC^{me} s(7)
919	893	-26	CH_3 r^1 (29), CN^{+ter} s(20), CC^{ter} s(18)
1060	1049	-11	COH b(25), CC^{me} s(21), C^αH r^2 (9), CN^{+ter} s(8), C-OH s(7)
1104	1096	-8	COH b(33), C=O s(14), C-OH s(8), CC^{me} s(7)
1114	1128	14	CH_3 r^1 (38), NH_3 sd(13), C^αH r^2 (10), C^αH d^2 (10), CCOO wag(9)
1149	1144	-5	NH_3 ad ¹ (80), CH_3 r^2 (7)
1157	1175	18	NH_3 ad ² (72)
1174	1184	10	NH_3 ad ² (24), CH_3 r^2 (23), NH_3 r^1 (11), CC^{me} s(9), C^αH d^1 (8), NH_3 ad ¹ (8)
1183	1194	11	NH_3 sd(62), CN^{+ter} s(22)
1274	1296	22	C^αH r^2 (43), C-OH s(18)
1324	1329	5	C^αH r^1 (66), C^αH r^2 (11)
1408	1404	-4	CH_3 sd(91)
1437	1446	9	CH_3 ad ¹ (68), C-OH s(12)
1463	1463	0	CH_3 ad ² (88), CH_3 r^2 (9)
1463	1499	36	CH_3 ad ¹ (22), C-OH s(21), CC^{ter} s(18), CH_3 r^1 (10), C^αH r^1 (7), CCOO sd(7)
1727	1724	-3	C=O s(76), C-OH s(8)
—	2261	—	NH_3 ss,as(62), NH_3 ss,as(36)
—	2489	—	NH_3 ss,as(61), NH_3 ss,as(37)
—	2568	—	NH_3 ss,as(99)
—	2662	—	OH s(100)
2898	2895	-3	CH_3 ss(98)
2956	2962	6	C^αH s(98)
3002	3006	4	CH_3 as ^{1,2} (85), CH_3 as ^{1,2} (13)
3011	3032	21	CH_3 as ^{1,2} (85), CH_3 as ^{1,2} (13)

frequency (cm ⁻¹)			NH ₃ ⁺ CDClD ₃ CO ₂ H (mean deviation = 11 cm ⁻¹)
obs.	calc.	dev.	
Potential Energy Distribution			
—	74	—	CC t(97)
—	172	—	CC ^{me} t(94)
—	232	—	CN t(76), C ^α H d ² (10)

Table 3.61: (continued)

frequency (cm ⁻¹)			Potential Energy Distribution
obs.	calc.	dev.	
246	255	9	C ^α H d ² (49), CN t(21), CCOO r(10)
331	326	-5	C ^α H d ³ (47), CCOO r(30), C ^α H d ² (9)
378	377	-1	C ^α H d ¹ (72), CH ₃ r ² (11)
506	494	-12	CCOO sd(30), CCOO r(18), CC ^{ter} s(14), C ^α H d ³ (11), CN ^{+ter} s(10)
594	606	12	CCOO r(22), CCOO sd(20), C ^α H d ³ (16), CC ^{me} s(11), CC ^{ter} s(10)
674	664	-10	C ^α H r ² (26), CCOO wag(26), CH ₃ r ¹ (22), CH ₃ r ² (16)
748	727	-21	CC ^{me} s(20), CN ^{+ter} s(20), CCOO sd(18), CH ₃ r ² (13)
794	785	-9	CH ₃ r ¹ (37), CH ₃ r ² (15), CC ^{ter} s(14), CCOO sd(9)
879	855	-24	C ^α H r ¹ (36), CN ^{+ter} s(13), NH ₃ r ¹ (10), CC ^{me} s(8), C ^α H r ² (8), CH ₃ r ² (7)
879	861	-18	CN ^{+ter} s(16), C ^α H r ² (16), C ^α H r ¹ (13), CC ^{me} s(10), NH ₃ r ² (9), CC ^{ter} s(8)
944	945	1	C-OH t(49), NH ₃ r ² (16)
—	967	—	NH ₃ r ² (30), C ^α H r ² (19), CH ₃ r ² (14), CH ₃ r ¹ (11)
1010	1006	-4	C-OH t(37), CCOO wag(32), C ^α H d ² (8)
1053	1048	-5	CH ₃ ad ¹ (73), CH ₃ ad ² (24)
1053	1051	-2	CH ₃ ad ² (73), CH ₃ ad ¹ (24)
1083	1074	-9	CH ₃ sd(66), CN ^{+ter} s(8), C ^α H r ¹ (7), NH ₃ r ² (7)
1134	1141	7	CN ^{+ter} s(24), C-OH s(14), CH ₃ sd(10), CC ^{me} s(8), CH ₃ r ² (7), NH ₃ r ¹ (7)
1199	1223	24	NH ₃ r ¹ (37), C-OH s(11), C=O s(7), C ^α H d ³ (7), NH ₃ ad ¹ (7)
1231	1256	25	CC ^{me} s(28), NH ₃ r ¹ (18), NH ₃ r ² (11)
1304	1299	-5	COH b(56), CC ^{ter} s(11), C=O s(8)
1508	1496	-12	C-OH s(37), COH b(20), CC ^{ter} s(17), CCOO sd(14)
1530	1528	-2	NH ₃ sd(90)
1606	1614	8	NH ₃ ad ¹ (79), NH ₃ r ¹ (16)
1638	1628	-10	NH ₃ ad ² (93)
1735	1741	6	C=O s(68), COH b(9)
2080	2082	2	CH ₃ ss(98)
2188	2188	0	C ^α H s(97)
2253	2231	-22	CH ₃ as ^{1,2} (87), CH ₃ as ^{1,2} (12)
2253	2249	-4	CH ₃ as ^{1,2} (87), CH ₃ as ^{1,2} (12)

Table 3.61: (continued)

frequency (cm ⁻¹)			Potential Energy Distribution
obs.	calc.	dev.	
—	3103	—	NH ₃ ss,as(53), NH ₃ ss,as(46)
—	3415	—	NH ₃ ss,as(53), NH ₃ ss,as(45)
—	3481	—	NH ₃ ss,as(98)
—	3656	—	OH s(100)

frequency (cm ⁻¹)			NH ₃ ⁺ CHCD ₃ CO ₂ H (mean deviation = 11 cm ⁻¹)
obs.	calc.	dev.	
—	75	—	CC t(97)
—	173	—	CC ^{me} t(94)
—	232	—	CN t(76), C ^α H d ² (9)
243	256	13	C ^α H d ² (48), CN t(20), CCOO r(11)
332	329	-3	C ^α H d ³ (47), CCOO r(29), C ^α H d ² (9)
380	380	0	C ^α H d ¹ (72), CH ₃ r ² (11)
514	501	-13	CCOO sd(30), CCOO r(21), CC ^{ter} s(12), CN ^{+ter} s(11), C ^α H d ³ (11)
598	612	14	CCOO sd(23), CCOO r(19), C ^α H d ³ (15), CC ^{me} s(11), CC ^{ter} s(10)
710	704	-6	CCOO wag(42), CH ₃ r ¹ (26), CH ₃ r ² (11)
760	735	-25	CN ^{+ter} s(25), CH ₃ r ² (23), CCOO sd(17), CC ^{me} s(15)
799	787	-12	CH ₃ r ¹ (34), CH ₃ r ² (18), CC ^{ter} s(12), CCOO sd(8), CN ^{+ter} s(7)
921	904	-17	NH ₃ r ² (40), CC ^{me} s(18), CC ^{ter} s(17), CH ₃ sd(11)
939	934	-5	C-OH t(24), NH ₃ r ¹ (19), CH ₃ r ² (11), CN ^{+ter} s(10), C ^α H d ² (8), CH ₃ r ¹ (7)
—	981	—	C-OH t(68), CCOO wag(11)
1050	1040	-10	CH ₃ ad ² (27), CH ₃ sd(26), CN ^{+ter} s(15), NH ₃ r ² (8)
1050	1048	-2	CH ₃ ad ¹ (91)
1064	1053	-11	CH ₃ ad ² (66), CH ₃ sd(16)
1118	1101	-17	NH ₃ r ² (20), C ^α H r ² (10), CH ₃ sd(10), CCOO wag(9), CH ₃ r ¹ (9), CC ^{ter} s(7)
1141	1142	1	CH ₃ sd(27), CC ^{me} s(25), C ^α H r ² (21), CN ^{+ter} s(7)
1186	1182	-4	NH ₃ r ¹ (33), C ^α H r ¹ (17), CH ₃ r ² (11), C ^α H d ¹ (9)
1260	1263	3	COH b(31), C-OH s(24), C=O s(14), C ^α H r ² (9)

Table 3.61: (continued)

frequency (cm ⁻¹)			Potential Energy Distribution
obs.	calc.	dev.	
1322	1325	3	C ^α H r ² (42), COH b(16), CC ^{me} s(11), NH ₃ r ² (8)
1364	1366	2	C ^α H r ¹ (56), COH b(15), NH ₃ r ¹ (11)
1522	1505	-17	C-OH s(32), CC ^{ter} s(16), COH b(15), CCOO sd(11), NH ₃ sd(11)
1522	1529	7	NH ₃ sd(82)
1623	1617	-6	NH ₃ ad ¹ (75), NH ₃ r ¹ (17)
1623	1628	5	NH ₃ ad ² (92)
1735	1742	7	C=O s(68), COH b(9)
2081	2082	1	CH ₃ ss(98)
2246	2231	-15	CH ₃ as ^{1,2} (88), CH ₃ as ^{1,2} (12)
2262	2250	-12	CH ₃ as ^{1,2} (87), CH ₃ as ^{1,2} (11)
2974	2963	-11	C ^α H s(100)
—	3103	—	NH ₃ ss,as(53), NH ₃ ss,as(46)
—	3415	—	NH ₃ ss,as(53), NH ₃ ss,as(45)
—	3481	—	NH ₃ ss,as(98)
—	3656	—	OH s(100)

frequency (cm ⁻¹)			ND ₃ ⁺ CHCD ₃ CO ₂ D (mean deviation = 17 cm ⁻¹)
obs.	calc.	dev.	
—	73	—	CC t(96)
—	168	—	CN t(73), CC ^{me} t(21)
—	173	—	CC ^{me} t(73), CN t(21)
256	245	-11	C ^α H d ² (52), CCOO r(18), C ^α H d ³ (10), CCOO wag(8)
309	306	-3	C ^α H d ³ (48), CCOO r(19), C ^α H d ² (12)
356	352	-4	C ^α H d ¹ (68), CH ₃ r ² (9)
498	475	-23	CCOO sd(31), CCOO r(20), CN ^{+ter} s(12), C ^α H d ³ (10), CC ^{ter} s(9)
577	580	3	CCOO sd(24), CCOO r(23), C ^α H d ³ (9), CC ^{ter} s(8), NH ₃ r ² (8)
—	638	—	C-OH t(45), CCOO wag(19), CH ₃ r ¹ (7)
731	691	-40	CN ^{+ter} s(20), CH ₃ r ² (18), CC ^{ter} s(13), COH b(12), CCOO sd(9), CC ^{me} s(7)
731	736	5	NH ₃ r ² (40), CH ₃ r ¹ (20), CC ^{me} s(13), NH ₃ r ¹ (8), CH ₃ r ² (7)

Table 3.61: (continued)

frequency (cm^{-1})			Potential Energy Distribution
obs.	calc.	dev.	
768	765	-3	CH_3 r^2 (28), NH_3 r^2 (19), CC^{ter} s(13), NH_3 r^1 (9)
—	771	—	CH_3 r^1 (32), C-OH t(28), NH_3 r^1 (12), CCOO wag(8), $\text{CN}^{\text{+ter}}$ s(7)
816	833	17	NH_3 r^1 (30), CCOO wag(24), C-OH t(19), $\text{CN}^{\text{+ter}}$ s(7)
1015	1005	-10	CH_3 sd(39), CC^{me} s(10), $\text{CN}^{\text{+ter}}$ s(10), NH_3 r^2 (7)
1054	1044	-10	CH_3 ad ¹ (46), C^αH d ² (10), COH b(9), CCOO wag(9)
1054	1049	-5	CH_3 ad ² (91)
1054	1053	-1	CH_3 ad ¹ (49), COH b(14), CH_3 r^1 (12)
1054	1075	21	CH_3 r^2 (16), C^αH d ¹ (13), $\text{CN}^{\text{+ter}}$ s(11), NH_3 r^1 (11), CH_3 sd(10), C-OH s(8), NH_3 sd(8)
1078	1094	16	COH b(31), C=O s(14), C-OH s(12)
1133	1140	7	CH_3 sd(30), CC^{me} s(25), C^αH r^2 (15), NH_3 ad ¹ (14)
1153	1156	3	NH_3 ad ¹ (69), NH_3 r^1 (12)
1178	1178	0	NH_3 ad ² (96)
1178	1191	13	NH_3 sd(72), $\text{CN}^{\text{+ter}}$ s(20)
1270	1291	21	C^αH r^2 (48), C-OH s(15), CC^{me} s(7)
1322	1328	6	C^αH r^1 (67), C^αH r^2 (9), CC^{me} s(7)
1408	1477	69	C-OH s(34), CC^{ter} s(26), CCOO sd(12), C^αH r^1 (10)
1726	1724	-2	C=O s(76), C-OH s(8)
—	2082	—	CH_3 ss(99)
—	2231	—	CH_3 as ^{1,2} (88), CH_3 as ^{1,2} (12)
—	2249	—	CH_3 as ^{1,2} (87), CH_3 as ^{1,2} (11)
—	2261	—	NH_3 ss,as(62), NH_3 ss,as(36)
—	2489	—	NH_3 ss,as(61), NH_3 ss,as(37)
—	2568	—	NH_3 ss,as(99)
—	2662	—	OH s(100)
2974	2963	-11	C^αH s(100)

frequency (cm ⁻¹)			¹⁵ NH ₃ ⁺ CHCH ₃ CO ₂ H (mean deviation = 12 cm ⁻¹)
obs.	calc.	dev.	
Potential Energy Distribution			
—	77	—	CC t(98)
—	232	—	CN t(72), CC ^{me} t(12), C ^α H d ² (7)
—	239	—	CC ^{me} t(77), CN t(14)

Table 3.61: (continued)

frequency (cm ⁻¹)			Potential Energy Distribution
obs.	calc.	dev.	
266	275	9	C ^α H d ² (42), CCOO r(22), C ^α H d ³ (13), CN t(11)
326	337	11	C ^α H d ³ (39), C ^α H d ² (19), CCOO r(19), CCOO wag(8), CC ^{me} t(7)
405	406	1	C ^α H d ¹ (72)
522	509	-13	CCOO sd(27), CCOO r(19), CN ^{+ter} s(16), C ^α H d ³ (10), CC ^{ter} s(9), C ^α H d ¹ (9)
608	627	19	CCOO sd(30), CCOO r(19), C ^α H d ³ (16), CC ^{ter} s(8), CC ^{me} s(7), CCOO wag(7)
746	743	-3	CCOO wag(29), CCOO sd(17), CC ^{me} s(14), CN ^{+ter} s(7)
821	816	-5	CCOO wag(17), CN ^{+ter} s(16), CH ₃ r ² (14), CC ^{ter} s(10)
916	911	-5	CC ^{ter} s(25), CN ^{+ter} s(20), CC ^{me} s(10), CH ₃ r ² (10), NH ₃ r ² (10), CH ₃ r ¹ (8), C-OH s(7)
916	941	25	NH ₃ r ² (47), CC ^{me} s(17), CH ₃ r ¹ (16), CN ^{+ter} s(7), CH ₃ r ² (7)
1006	970	-36	C-OH t(78)
1006	1001	-5	NH ₃ r ¹ (26), CH ₃ r ² (19), CN ^{+ter} s(11), C ^α H r ¹ (11), C-OH t(11)
1114	1120	6	CC ^{me} s(22), C ^α H r ² (17), NH ₃ r ² (17), CN ^{+ter} s(11), NH ₃ r ¹ (11)
1140	1141	1	CH ₃ r ¹ (35), C ^α H r ² (11), C ^α H d ² (11), CCOO wag(11)
1213	1220	7	CH ₃ r ² (24), NH ₃ r ¹ (17), C ^α H d ¹ (11), C-OH s(9), C ^α H r ¹ (9)
1260	1264	4	COH b(28), C-OH s(21), C=O s(12), C ^α H r ² (11), NH ₃ r ¹ (8)
1326	1329	3	C ^α H r ² (38), COH b(13), C ^α H r ¹ (9), CC ^{me} s(7)
1361	1362	1	C ^α H r ¹ (52), COH b(18), NH ₃ r ¹ (9)
1391	1403	12	CH ₃ sd(90)
1459	1455	-4	CH ₃ ad ¹ (78), CH ₃ r ¹ (7)
1459	1463	4	CH ₃ ad ² (86), CH ₃ r ² (8)
1520	1512	-8	NH ₃ sd(44), C-OH s(17), CC ^{ter} s(9), COH b(7)
1520	1526	6	NH ₃ sd(49), C-OH s(11), CC ^{ter} s(9)
1613	1617	4	NH ₃ ad ¹ (73), NH ₃ r ¹ (17)
1613	1627	14	NH ₃ ad ² (90)
1733	1742	9	C=O s(68), COH b(9)
2895	2895	0	CH ₃ ss(98)
2956	2962	6	C ^α H s(97)
2998	3006	8	CH ₃ as ^{1,2} (85), CH ₃ as ^{1,2} (13)

Table 3.61: (continued)

frequency (cm ⁻¹)			Potential Energy Distribution
obs.	calc.	dev.	
3007	3032	25	CH ₃ as ^{1,2} (85), CH ₃ as ^{1,2} (13)
—	3097	—	NH ₃ ss,as(54), NH ₃ ss,as(45)
—	3409	—	NH ₃ ss,as(54), NH ₃ ss,as(44)
—	3471	—	NH ₃ ss,as(98)
—	3656	—	OH s(100)

frequency (cm ⁻¹)			Potential Energy Distribution
obs.	calc.	dev.	
—	77	—	CC t(98)
—	232	—	CN t(71), CC ^{me} t(13), C ^α H d ² (8)
—	239	—	CC ^{me} t(76), CN t(15)
273	273	0	C ^α H d ² (43), CCOO r(21), C ^α H d ³ (11), CN t(11)
338	338	0	C ^α H d ³ (40), CCOO r(21), C ^α H d ² (17), CCOO wag(7), CC ^{me} t(7)
404	406	2	C ^α H d ¹ (72)
524	514	-10	CCOO sd(29), CCOO r(18), CN ^{+ter} s(14), C ^α H d ³ (10), CC ^{ter} s(9), C ^α H d ¹ (9)
607	626	19	CCOO sd(27), CCOO r(19), C ^α H d ³ (16), CC ^{me} s(8), CC ^{ter} s(8), CCOO wag(8)
746	740	-6	CCOO wag(28), CCOO sd(18), CC ^{me} s(15), CN ^{+ter} s(7)
820	816	-4	CCOO wag(17), CN ^{+ter} s(15), CH ₃ r ² (14), CC ^{ter} s(10), CH ₃ r ¹ (7)
914	910	-4	CC ^{ter} s(25), CN ^{+ter} s(18), CC ^{me} s(11), CH ₃ r ² (11), NH ₃ r ² (10), CH ₃ r ¹ (8), C-OH s(7)
—	939	—	NH ₃ r ² (44), CC ^{me} s(17), CH ₃ r ¹ (16), CH ₃ r ² (9), CN ^{+ter} s(8)
1004	970	-34	C-OH t(78)
1004	1001	-3	NH ₃ r ¹ (25), CH ₃ r ² (18), CN ^{+ter} s(12), C ^α H r ¹ (11), C-OH t(11)
1112	1120	8	CC ^{me} s(22), NH ₃ r ² (18), C ^α H r ² (15), CN ^{+ter} s(13), NH ₃ r ¹ (9)
1142	1137	-5	CH ₃ r ¹ (32), C ^α H r ² (13), CCOO wag(11), C ^α H d ² (10), C ^α H r ¹ (7)

Table 3.61: (continued)

frequency (cm ⁻¹)			Potential Energy Distribution
obs.	calc.	dev.	
1211	1217	6	CH ₃ r ² (23), NH ₃ r ¹ (18), C ^α H r ¹ (11), C ^α H d ¹ (11), C-OH s(9)
1259	1264	5	COH b(28), C-OH s(21), C=O s(12), C ^α H r ² (11), NH ₃ r ¹ (8)
1326	1329	3	C ^α H r ² (38), COH b(15), CC ^{me} s(7), C ^α H r ¹ (7)
1368	1365	-3	C ^α H r ¹ (53), COH b(15), NH ₃ r ¹ (10)
1368	1393	25	CH ₃ sd(92)
1458	1454	-4	CH ₃ ad ¹ (77), CH ₃ r ¹ (7)
1458	1461	3	CH ₃ ad ² (86), CH ₃ r ² (9)
1525	1515	-10	C-OH s(23), NH ₃ sd(23), CC ^{ter} s(13), COH b(10), CCOO sd(8)
1525	1531	6	NH ₃ sd(70)
1610	1618	8	NH ₃ ad ¹ (74), NH ₃ r ¹ (17)
1620	1629	9	NH ₃ ad ² (92)
1732	1742	10	C=O s(68), COH b(9)
—	2891	—	CH ₃ ss(98)
—	2961	—	C ^α H s(96)
—	2995	—	CH ₃ as ^{1,2} (84), CH ₃ as ^{1,2} (13)
—	3020	—	CH ₃ as ^{1,2} (85), CH ₃ as ^{1,2} (13)
—	3103	—	NH ₃ ss,as(53), NH ₃ ss,as(46)
—	3415	—	NH ₃ ss,as(53), NH ₃ ss,as(45)
—	3481	—	NH ₃ ss,as(98)
—	3656	—	OH s(100)

Table 3.62: Scaled 6-31+G** Frequencies and Potential Energy Distribution for Water-Excluded Alanine One-water Supermolecule in Acid.

frequency (cm ⁻¹)			NH ₃ ⁺ CHCH ₃ CO ₂ H (mean deviation = 10 cm ⁻¹)
obs.	calc.	dev.	
			Potential Energy Distribution
—	71	—	CC t(97)
—	200	—	CN t(94)
—	231	—	CC ^{me} t(90)
275	274	-1	C ^α H d ² (42), CCOO r(26), C ^α H d ³ (15)
335	339	4	C ^α H d ³ (37), C ^α H d ² (20), CCOO r(20), CCOO wag(8)
409	410	1	C ^α H d ¹ (72)
526	514	-12	CCOO sd(28), CCOO r(18), CN ^{+ter} s(16), C ^α H d ³ (10), CC ^{ter} s(9), C ^α H d ¹ (9)
603	630	27	CCOO sd(29), CCOO r(18), C ^α H d ³ (16), CCOO wag(8), C-OH s(7), CC ^{me} s(7), CC ^{ter} s(7)
746	743	-3	CCOO wag(30), CCOO sd(16), CC ^{me} s(13), CN ^{+ter} s(7)
823	817	-6	CN ^{+ter} s(17), CCOO wag(15), CH ₃ r ² (13), CC ^{ter} s(10)
920	915	-5	CC ^{ter} s(25), CN ^{+ter} s(24), CH ₃ r ¹ (13), CH ₃ r ² (12), C-OH s(8)
—	953	—	NH ₃ r ² (39), CC ^{me} s(20), CH ₃ r ¹ (14), C-OH t(11)
—	960	—	C-OH t(70), NH ₃ r ² (10)
1008	995	-13	NH ₃ r ¹ (30), CH ₃ r ² (19), C ^α H r ¹ (11), CN ^{+ter} s(10), C-OH t(8)
1117	1125	8	CC ^{me} s(18), C ^α H r ² (16), NH ₃ r ² (16), CN ^{+ter} s(12), NH ₃ r ¹ (12)
1146	1141	-5	CH ₃ r ¹ (32), C ^α H r ² (14), C ^α H d ² (11), CCOO wag(11), C ^α H r ¹ (7)
1214	1222	8	CH ₃ r ² (27), NH ₃ r ¹ (15), C ^α H d ¹ (12), C-OH s(7), C ^α H r ¹ (7)
1261	1264	3	COH b(28), C-OH s(23), C=O s(12), C ^α H r ² (10), NH ₃ r ¹ (7)
1328	1333	5	C ^α H r ² (35), COH b(14), C ^α H r ¹ (10), CC ^{me} s(8), NH ₃ r ² (8)
1364	1368	4	C ^α H r ¹ (53), COH b(18), NH ₃ r ¹ (8)
1393	1401	8	CH ₃ sd(90)
1460	1457	-3	CH ₃ ad ¹ (79)
1460	1465	5	CH ₃ ad ² (87), CH ₃ r ² (9)
1523	1515	-8	C-OH s(23), NH ₃ sd(21), CC ^{ter} s(13), COH b(9), CCOO sd(7), CH ₃ ad ¹ (7)
1523	1533	10	NH ₃ sd(72)
1635	1618	-17	NH ₃ ad ¹ (78), NH ₃ r ¹ (15)

Table 3.62: (continued)

frequency (cm^{-1})			Potential Energy Distribution
obs.	calc.	dev.	
1635	1631	-4	NH ₃ ad ² (92)
1735	1737	2	C=O s(67), COH b(10)
2895	2895	0	CH ₃ ss(98)
2956	2961	5	C ^{α} H s(97)
2998	3004	6	CH ₃ as ^{1,2} (82), CH ₃ as ^{1,2} (15)
3007	3032	25	CH ₃ as ^{1,2} (82), CH ₃ as ^{1,2} (16)
—	3145	—	NH ₃ ss,as(52), NH ₃ ss,as(48)
—	3413	—	NH ₃ ss,as(51), NH ₃ ss,as(47)
—	3477	—	NH ₃ ss,as(98)
—	3648	—	OH s(100)

frequency (cm^{-1})			ND ₃ ⁺ CHCH ₃ CO ₂ D (mean deviation = 13 cm^{-1})
obs.	calc.	dev.	
—	68	—	CC t(95)
—	145	—	CN t(94)
—	230	—	CC ^{me} t(90)
276	262	-14	C ^{α} H d ² (34), CCOO r(30), C ^{α} H d ³ (24)
319	320	1	C ^{α} H d ³ (32), C ^{α} H d ² (27), CCOO r(10), CCOO wag(9), CC ^{me} t(7)
380	379	-1	C ^{α} H d ¹ (68), CCOO r(7), CCOO wag(7)
508	484	-24	CCOO sd(29), CCOO r(17), CN ^{+ter} s(16), C ^{α} H d ³ (9), C ^{α} H d ¹ (8), CC ^{ter} s(7)
588	590	2	CCOO sd(26), CCOO r(21), C ^{α} H d ³ (9), NH ₃ r ² (7)
—	653	—	C-OH t(52), CCOO wag(11), CCOO sd(8)
730	719	-11	CC ^{ter} s(19), CN ^{+ter} s(15), NH ₃ r ¹ (13), COH b(11), NH ₃ r ² (10), C-OH t(10)
764	774	10	NH ₃ r ² (53), CC ^{me} s(19), NH ₃ r ¹ (13)
825	820	-5	CCOO wag(37), C-OH t(29), NH ₃ r ¹ (15)
881	869	-12	CH ₃ r ² (34), NH ₃ r ¹ (24), CN ^{+ter} s(10), CC ^{me} s(7)
919	891	-28	CH ₃ r ¹ (31), CN ^{+ter} s(19), CC ^{ter} s(18)
1060	1050	-10	COH b(26), CC ^{me} s(20), C ^{α} H r ² (10), C-OH s(7), CN ^{+ter} s(7)
1104	1097	-7	COH b(34), C=O s(14), C-OH s(7), CC ^{me} s(7)

Table 3.62: (continued)

frequency (cm^{-1})			Potential Energy Distribution
obs.	calc.	dev.	
1114	1128	14	CH_3 r^1 (37), NH_3 sd (11), C^αH r^2 (10), C^αH d^2 (10), CCOO wag (9)
1149	1148	-1	NH_3 ad^1 (84)
1157	1177	20	NH_3 ad^2 (84)
1174	1186	12	CH_3 r^2 (29), CC^{me} s (12), NH_3 ad^2 (12), C^αH d^1 (11), NH_3 r^1 (11), NH_3 ad^1 (7)
1183	1194	11	NH_3 sd (67), CN^{+ter} s (19)
1274	1295	21	C^αH r^2 (42), C-OH s (19)
1324	1333	9	C^αH r^1 (68), C^αH r^2 (9)
1408	1402	-6	CH_3 sd (91)
1437	1448	11	CH_3 ad^1 (68), C-OH s (12), CC^{ter} s (7)
1463	1466	3	CH_3 ad^2 (87), CH_3 r^2 (9)
1463	1501	38	CH_3 ad^1 (22), C-OH s (20), CC^{ter} s (19), CH_3 r^1 (10), C^αH r^1 (8), CCOO sd (7)
1727	1718	-9	C=O s (76), C-OH s (7)
—	2289	—	NH_3 ss,as (66), NH_3 ss,as (33)
—	2489	—	NH_3 ss,as (65), NH_3 ss,as (33)
—	2566	—	NH_3 ss,as (98)
—	2657	—	OH s (100)
2898	2895	-3	CH_3 ss (98)
2956	2961	5	C^αH s (97)
3002	3004	2	CH_3 $as^{1,2}$ (82), CH_3 $as^{1,2}$ (15)
3011	3032	21	CH_3 $as^{1,2}$ (82), CH_3 $as^{1,2}$ (16)

frequency (cm^{-1})			Potential Energy Distribution
obs.	calc.	dev.	
—	68	—	CC t (97)
—	167	—	CC^{me} t (94)
—	199	—	CN t (94)
246	253	7	C^αH d^2 (55), CCOO r (15), CCOO wag (8)
331	325	-6	C^αH d^3 (45), CCOO r (30), C^αH d^2 (10)
378	378	0	C^αH d^1 (72), CH_3 r^2 (11)

Table 3.62: (continued)

frequency (cm ⁻¹)			Potential Energy Distribution
obs.	calc.	dev.	
506	494	-12	CCOO sd(30), CCOO r(18), CC ^{ter} s(13), CN ^{+ter} s(11), C ^α H d ³ (11)
594	608	14	CCOO r(21), CCOO sd(20), C ^α H d ³ (17), CC ^{me} s(10), CC ^{ter} s(9)
674	663	-11	C ^α H r ² (26), CCOO wag(26), CH ₃ r ¹ (23), CH ₃ r ² (15)
748	727	-21	CN ^{+ter} s(22), CC ^{me} s(19), CCOO sd(17), CH ₃ r ² (14)
794	786	-8	CH ₃ r ¹ (36), CC ^{ter} s(14), CH ₃ r ² (13), CCOO sd(10)
879	852	-27	C ^α H r ¹ (46), CN ^{+ter} s(23), NH ₃ r ¹ (16)
879	862	-17	C ^α H r ² (26), CC ^{me} s(14), CC ^{ter} s(10), NH ₃ r ² (8), C-OH t(8)
944	941	-3	C-OH t(58), NH ₃ r ² (9), CC ^{me} s(7)
—	975	—	NH ₃ r ² (36), C ^α H r ² (21), CH ₃ r ² (11), CH ₃ r ¹ (9)
1010	1001	-9	CCOO wag(32), C-OH t(29), C ^α H d ² (10), C ^α H r ¹ (7)
1053	1051	-2	CH ₃ ad ¹ (61), CH ₃ ad ² (36)
1053	1052	-1	CH ₃ ad ² (60), CH ₃ ad ¹ (36)
1083	1075	-8	CH ₃ sd(63), CN ^{+ter} s(8), C ^α H r ¹ (8), NH ₃ r ² (8)
1134	1136	2	CN ^{+ter} s(21), C-OH s(12), CH ₃ sd(11), NH ₃ r ¹ (11), CC ^{me} s(8), CH ₃ r ² (8), C ^α H d ¹ (7)
1199	1214	15	NH ₃ r ¹ (43), C-OH s(11), C ^α H r ¹ (9), NH ₃ ad ¹ (7)
1231	1260	29	CC ^{me} s(29), NH ₃ r ² (15), NH ₃ r ¹ (7)
1304	1304	0	COH b(55), CC ^{ter} s(11)
1508	1494	-14	C-OH s(37), COH b(18), CC ^{ter} s(17), CCOO sd(13)
1530	1530	0	NH ₃ sd(90)
1606	1614	8	NH ₃ ad ¹ (81), NH ₃ r ¹ (14)
1638	1630	-8	NH ₃ ad ² (93)
1735	1737	2	C=O s(67), COH b(10)
2080	2082	2	CH ₃ ss(98)
2188	2187	-1	C ^α H s(97)
2253	2230	-23	CH ₃ as ^{1,2} (84), CH ₃ as ^{1,2} (15)
2253	2249	-4	CH ₃ as ^{1,2} (84), CH ₃ as ^{1,2} (15)
—	3144	—	NH ₃ ss,as(52), NH ₃ ss,as(48)
—	3413	—	NH ₃ ss,as(51), NH ₃ ss,as(47)
—	3477	—	NH ₃ ss,as(98)
—	3648	—	OH s(100)

Table 3.62: (continued)

frequency (cm ⁻¹)			Potential Energy Distribution
obs.	calc.	dev.	

frequency (cm ⁻¹)			NH ₃ ⁺ CHCD ₃ CO ₂ H (mean deviation = 11 cm ⁻¹)
obs.	calc.	dev.	
—	69	—	CC t(97)
—	167	—	CC ^{me} t(94)
—	199	—	CN t(94)
243	253	10	C ^α H d ² (54), CCOO r(16), CCOO wag(8), C ^α H d ³ (7)
332	328	-4	C ^α H d ³ (45), CCOO r(29), C ^α H d ² (11)
380	380	0	C ^α H d ¹ (71), CH ₃ r ² (11)
514	501	-13	CCOO sd(30), CCOO r(20), CN ^{+ter} s(12), CC ^{ter} s(11), C ^α H d ³ (11)
598	615	17	CCOO sd(24), CCOO r(19), C ^α H d ³ (16), CC ^{me} s(11), CC ^{ter} s(9)
710	702	-8	CCOO wag(42), CH ₃ r ¹ (28), CH ₃ r ² (10)
760	734	-26	CN ^{+ter} s(27), CH ₃ r ² (24), CCOO sd(16), CC ^{me} s(14)
799	787	-12	CH ₃ r ¹ (33), CH ₃ r ² (17), CC ^{ter} s(13), CCOO sd(8)
921	915	-6	NH ₃ r ² (36), CC ^{me} s(18), CC ^{ter} s(18), CH ₃ sd(12)
939	926	-13	C-OH t(26), NH ₃ r ¹ (21), CH ₃ r ² (11), CN ^{+ter} s(10), C ^α H d ² (7)
—	970	—	C-OH t(65), CCOO wag(11), CN ^{+ter} s(7)
1050	1040	-10	CH ₃ sd(27), CH ₃ ad ² (20), CN ^{+ter} s(16), NH ₃ r ² (8), CH ₃ r ¹ (7)
1050	1051	1	CH ₃ ad ¹ (90)
1064	1054	-10	CH ₃ ad ² (70), CH ₃ sd(12), CH ₃ ad ¹ (7)
1118	1107	-11	NH ₃ r ² (21), CH ₃ sd(16), C ^α H r ² (9), CCOO wag(8), CH ₃ r ¹ (7)
1141	1141	0	C ^α H r ² (22), CH ₃ sd(20), CC ^{me} s(19), NH ₃ r ¹ (10), CN ^{+ter} s(7)
1186	1175	-11	NH ₃ r ¹ (29), C ^α H r ¹ (12), CH ₃ r ² (12), C ^α H d ¹ (10), C ^α H r ² (9)
1260	1263	3	COH b(31), C-OH s(26), C=O s(14), C ^α H r ² (7)
1322	1328	6	C ^α H r ² (38), COH b(15), CC ^{me} s(12), NH ₃ r ² (9)
1364	1369	5	C ^α H r ¹ (57), COH b(18), NH ₃ r ¹ (9)
1522	1505	-17	C-OH s(31), CC ^{ter} s(16), COH b(14), CCOO sd(11), NH ₃ sd(10)

Table 3.62: (continued)

frequency (cm^{-1})			Potential Energy Distribution
obs.	calc.	dev.	
1522	1531	9	NH ₃ sd(83)
1623	1617	-6	NH ₃ ad ¹ (78), NH ₃ r ¹ (15)
1623	1630	7	NH ₃ ad ² (93)
1735	1737	2	C=O s(67), COH b(10)
2081	2082	1	CH ₃ ss(98)
2246	2230	-16	CH ₃ as ^{1,2} (85), CH ₃ as ^{1,2} (15)
2262	2250	-12	CH ₃ as ^{1,2} (84), CH ₃ as ^{1,2} (14)
2974	2962	-12	C ^{α} H s(100)
—	3145	—	NH ₃ ss,as(52), NH ₃ ss,as(48)
—	3413	—	NH ₃ ss,as(51), NH ₃ ss,as(47)
—	3477	—	NH ₃ ss,as(98)
—	3648	—	OH s(100)

frequency (cm^{-1})			ND ₃ ⁺ CHCD ₃ CO ₂ D (mean deviation = 17 cm^{-1})
obs.	calc.	dev.	
—	66	—	CC t(95)
—	144	—	CN t(94)
—	167	—	CC ^{me} t(94)
256	245	-11	C ^{α} H d ² (50), CCOO r(20), C ^{α} H d ³ (11), CCOO wag(8)
309	306	-3	C ^{α} H d ³ (45), CCOO r(20), C ^{α} H d ² (14)
356	353	-3	C ^{α} H d ¹ (68), CH ₃ r ² (9)
498	474	-24	CCOO sd(31), CCOO r(20), CN ^{+ter} s(13), C ^{α} H d ³ (10), CC ^{ter} s(9)
577	582	5	CCOO sd(24), CCOO r(22), C ^{α} H d ³ (9), CC ^{me} s(7), CC ^{ter} s(7), NH ₃ r ² (7)
—	635	—	C-OH t(46), CCOO wag(18), CH ₃ r ¹ (8)
731	691	-40	CN ^{+ter} s(22), CH ₃ r ² (18), CC ^{ter} s(12), COH b(11), CC ^{me} s(9), CCOO sd(8)
731	739	8	NH ₃ r ² (27), CH ₃ r ¹ (19), CH ₃ r ² (17), NH ₃ r ¹ (15), CC ^{me} s(8)
768	763	-5	CH ₃ r ¹ (30), C-OH t(25), NH ₃ r ¹ (17), CCOO wag(8), CH ₃ r ² (7)
—	772	—	NH ₃ r ² (33), CC ^{me} s(13), CC ^{ter} s(13), CH ₃ r ² (13)
816	823	7	NH ₃ r ¹ (27), CCOO wag(24), C-OH t(19), CN ^{+ter} s(7)

Table 3.62: (continued)

frequency (cm ⁻¹)			Potential Energy Distribution
obs.	calc.	dev.	
1015	1006	-9	CH ₃ sd(39), CN ^{+ter} s(11), CC ^{me} s(9)
1054	1047	-7	CH ₃ ad ¹ (44), C ^α H d ² (11), COH b(10), CCOO wag(9)
1054	1050	-4	CH ₃ ad ² (87)
1054	1055	1	CH ₃ ad ¹ (48), COH b(15), CH ₃ r ¹ (11)
1078	1073	-5	CH ₃ r ² (19), C ^α H d ¹ (14), CH ₃ sd(12), CN ^{+ter} s(10), NH ₃ r ¹ (10), NH ₃ sd(8)
1078	1096	18	COH b(31), C=O s(15), C-OH s(13)
1133	1142	9	CH ₃ sd(27), CC ^{me} s(24), C ^α H r ² (16), NH ₃ ad ¹ (16)
1153	1157	4	NH ₃ ad ¹ (69), NH ₃ r ¹ (10)
1178	1179	1	NH ₃ ad ² (94)
1178	1192	14	NH ₃ sd(74), CN ^{+ter} s(18)
1270	1291	21	C ^α H r ² (45), C-OH s(16), CC ^{me} s(9)
1322	1331	9	C ^α H r ¹ (67), C ^α H r ² (8), CC ^{me} s(7)
1408	1479	71	C-OH s(33), CC ^{ter} s(26), C ^α H r ¹ (12), CCOO sd(11)
1726	1718	-8	C=O s(76), C-OH s(7)
—	2082	—	CH ₃ ss(98)
—	2230	—	CH ₃ as ^{1,2} (85), CH ₃ as ^{1,2} (15)
—	2249	—	CH ₃ as ^{1,2} (84), CH ₃ as ^{1,2} (14)
—	2289	—	NH ₃ ss,as(66), NH ₃ ss,as(33)
—	2489	—	NH ₃ ss,as(65), NH ₃ ss,as(33)
—	2566	—	NH ₃ ss,as(98)
—	2657	—	OH s(100)
2974	2962	-12	C ^α H s(100)

frequency (cm ⁻¹)			Potential Energy Distribution
obs.	calc.	dev.	
—	70	—	CC t(97)
—	200	—	CN t(94)
—	231	—	CC ^{me} t(90)
266	273	7	C ^α H d ² (41), CCOO r(26), C ^α H d ³ (16)
326	337	11	C ^α H d ³ (36), C ^α H d ² (21), CCOO r(18), CCOO wag(8)
405	407	2	C ^α H d ¹ (72)

Table 3.62: (continued)

frequency (cm ⁻¹)			Potential Energy Distribution
obs.	calc.	dev.	
522	509	-13	CCOO sd(27), CCOO r(19), CN ^{+ter} s(17), C ^α H d ³ (10), CC ^{ter} s(9), C ^α H d ¹ (9)
608	630	22	CCOO sd(30), CCOO r(18), C ^α H d ³ (16), CCOO wag(8), C-OH s(7), CC ^{me} s(7), CC ^{ter} s(7)
746	742	-4	CCOO wag(30), CCOO sd(16), CC ^{me} s(14), CN ^{+ter} s(8)
821	814	-7	CN ^{+ter} s(18), CCOO wag(15), CH ₃ r ² (14), CC ^{ter} s(9)
916	912	-4	CC ^{ter} s(26), CN ^{+ter} s(24), CH ₃ r ¹ (14), CH ₃ r ² (11), C-OH s(8)
916	951	35	NH ₃ r ² (45), CC ^{me} s(22), CH ₃ r ¹ (13)
1006	960	-46	C-OH t(76)
1006	993	-13	NH ₃ r ¹ (30), CH ₃ r ² (19), C ^α H r ¹ (11), CN ^{+ter} s(9), C-OH t(8)
1114	1121	7	CC ^{me} s(19), C ^α H r ² (16), NH ₃ r ² (16), CN ^{+ter} s(12), NH ₃ r ¹ (12), C ^α H d ³ (7)
1140	1140	0	CH ₃ r ¹ (32), C ^α H r ² (14), C ^α H d ² (11), CCOO wag(11), C ^α H r ¹ (7)
1213	1220	7	CH ₃ r ² (28), NH ₃ r ¹ (15), C ^α H d ¹ (12)
1260	1263	3	COH b(28), C-OH s(24), C=O s(12), C ^α H r ² (10)
1326	1331	5	C ^α H r ² (35), COH b(13), C ^α H r ¹ (11), CC ^{me} s(8), NH ₃ r ² (7)
1361	1365	4	C ^α H r ¹ (53), COH b(20), NH ₃ r ¹ (7)
1391	1401	10	CH ₃ sd(90)
1459	1457	-2	CH ₃ ad ¹ (79)
1459	1465	6	CH ₃ ad ² (87), CH ₃ r ² (9)
1520	1513	-7	NH ₃ sd(40), C-OH s(18), CC ^{ter} s(9), COH b(7)
1520	1527	7	NH ₃ sd(53), C-OH s(10), CC ^{ter} s(8)
1613	1617	4	NH ₃ ad ¹ (77), NH ₃ r ¹ (15)
1613	1629	16	NH ₃ ad ² (92)
1733	1737	4	C=O s(67), COH b(10)
2895	2895	0	CH ₃ ss(98)
2956	2961	5	C ^α H s(97)
2998	3004	6	CH ₃ as ^{1,2} (82), CH ₃ as ^{1,2} (15)
3007	3032	25	CH ₃ as ^{1,2} (82), CH ₃ as ^{1,2} (16)
—	3138	—	NH ₃ ss,as(53), NH ₃ ss,as(47)
—	3407	—	NH ₃ ss,as(52), NH ₃ ss,as(45)

Table 3.62: (continued)

frequency (cm ⁻¹)			Potential Energy Distribution
obs.	calc.	dev.	
—	3467	—	NH ₃ ss,as(98)
—	3648	—	OH s(100)

frequency (cm ⁻¹)			Potential Energy Distribution
obs.	calc.	dev.	
—	70	—	CC t(97)
—	200	—	CN t(94)
—	231	—	CC ^{me} t(90)
273	271	-2	C ^α H d ² (44), CCOO r(25), C ^α H d ³ (14)
338	338	0	C ^α H d ³ (38), CCOO r(21), C ^α H d ² (19), CCOO wag(8)
404	406	2	C ^α H d ¹ (72)
524	513	-11	CCOO sd(28), CCOO r(18), CN ^{+ter} s(16), C ^α H d ³ (10), CC ^{ter} s(9), C ^α H d ¹ (9)
607	628	21	CCOO sd(28), CCOO r(18), C ^α H d ³ (17), CC ^{me} s(8), CCOO wag(8), CC ^{ter} s(7)
746	740	-6	CCOO wag(29), CCOO sd(17), CC ^{me} s(14), CN ^{+ter} s(8)
820	815	-5	CN ^{+ter} s(17), CCOO wag(16), CH ₃ r ² (14), CC ^{ter} s(9), CH ₃ r ¹ (7)
914	912	-2	CC ^{ter} s(26), CN ^{+ter} s(22), CH ₃ r ¹ (14), CH ₃ r ² (12), C-OH s(8)
—	949	—	NH ₃ r ² (43), CC ^{me} s(22), CH ₃ r ¹ (14)
1004	960	-44	C-OH t(76)
1004	992	-12	NH ₃ r ¹ (29), CH ₃ r ² (19), CN ^{+ter} s(10), C ^α H r ¹ (10), C-OH t(9)
1112	1121	9	CC ^{me} s(20), CN ^{+ter} s(15), NH ₃ r ² (15), C ^α H r ² (12), NH ₃ r ¹ (10), CH ₃ r ¹ (9)
1142	1137	-5	CH ₃ r ¹ (27), C ^α H r ² (18), CCOO wag(11), C ^α H d ² (9), C ^α H r ¹ (7)
1211	1217	6	CH ₃ r ² (27), NH ₃ r ¹ (17), C ^α H d ¹ (12), C ^α H r ¹ (7)
1259	1264	5	COH b(29), C-OH s(24), C=O s(13), C ^α H r ² (10)
1326	1331	5	C ^α H r ² (35), COH b(14), C ^α H r ¹ (9), CC ^{me} s(8), NH ₃ r ² (8)
1368	1367	-1	C ^α H r ¹ (54), COH b(18), NH ₃ r ¹ (8)
1368	1391	23	CH ₃ sd(92)

Table 3.62: (continued)

frequency (cm ⁻¹)			Potential Energy Distribution
obs.	calc.	dev.	
1458	1456	-2	CH ₃ ad ¹ (78)
1458	1464	6	CH ₃ ad ² (87), CH ₃ r ² (9)
1525	1515	-10	C-OH s(23), NH ₃ sd(21), CC ^{ter} s(13), COH b(9), CCOO sd(7), CH ₃ ad ¹ (7)
1525	1533	8	NH ₃ sd(72)
1610	1618	8	NH ₃ ad ¹ (78), NH ₃ r ¹ (15)
1620	1631	11	NH ₃ ad ² (92)
1732	1737	5	C=O s(67), COH b(10)
—	2891	—	CH ₃ ss(98)
—	2961	—	C ^α H s(95)
—	2994	—	CH ₃ as ^{1,2} (81), CH ₃ as ^{1,2} (15)
—	3021	—	CH ₃ as ^{1,2} (82), CH ₃ as ^{1,2} (16)
—	3145	—	NH ₃ ss,as(52), NH ₃ ss,as(48)
—	3413	—	NH ₃ ss,as(51), NH ₃ ss,as(47)
—	3477	—	NH ₃ ss,as(98)
—	3648	—	OH s(100)

Our normal mode assignments and optimizations of scale factors were performed simultaneously on the observed frequencies of eight isotopic species of alaninate or seven isotopic species of alanine at pH=1. NH stretches and torsional modes were not observed. The PED results for the two supermolecular structures of alaninate are very similar (Table 3.53 has the results of the CO₂ bridged supermolecule, and Table 3.57 has the results from the CO-NH bridged supermolecule). At each frequency the largest contributing coordinate remained the same. The percent contribution for that coordinate varied by less than 10% between the two structures except at 343, 1286, 1353, and 1368 cm⁻¹. In the CO-HN structure, the C^α deformation 3 (*d*³) contributes less at 343 cm⁻¹, redistributing to both lower and higher frequencies. The C^α rock^{1,2} (*r*^{1,2}) and the CH₃ symmetric deformation (*sd*) coordinates each increase their percent contributions at 1353, 1286, and 1368 cm⁻¹, respectively, resulting in

reduced mixing of these coordinates with other modes.

In alaninate, the amount of mixing of the CH_3 sd and C^αH r^1 coordinates, at 1368 and 1353 cm^{-1} , varies depending on the choice of basis set. Using the 4-31G basis set, the CH_3 sd contributes most at 1368 cm^{-1} and the C^αH r^1 contributes most at 1353 cm^{-1} , both making small contributions to the other frequency (Table 3.53). Using the 4-31G*, 6-31G**, and 6-31+G** basis sets, the CH_3 sd dominates both frequencies and both coordinates make greater contributions at 1353 cm^{-1} than at 1368 cm^{-1} (Tables 3.54, 3.55 and 3.56, respectively). The mixing calculated for these coordinates using the isolated geometry scaled to aqueous frequencies also depended upon the basis set used (Tables 3.47, 3.48, 3.49, and 3.50). The 4-31G and 6-31+G** basis sets calculate mixing similar to the water-excluded 4-31G calculations while the isolated structure 4-31G* and 6-31G** basis set calculations predict mixing similar to the water-excluded 4-31G*, 6-31G**, and 6-31+G** calculations. One set of calculations was performed using the water-included supermolecule model and the 4-31G basis. The predicted mixing of the CH_3 sd and C^αH r^1 coordinates using this model was similar to the water-excluded 4-31G*, 6-31G**, and 6-31+G** calculations (Table 3.52). There is no mixing of these coordinates predicted in the corresponding alanine at pH=1 modes at 1393 and 1364 cm^{-1} .

3.5 Alanyl-alanine-Peptide Coordinates and Defined Hydrogen Bonds

Internal coordinate definitions used are given in Tables 3.63, 3.64, and 3.65 for basic, zwitterionic, and acidic structures of alanyl-alanine, respectively. Symmetry coordinate definitions are given in Tables 3.66, 3.67, and 3.68 for the basic, zwitterionic, and acidic conformations, respectively. Optimized internal coordinates for the isolated, one water on the amide hydrogen, one water on the carboxyl oxygen, two-water, and three-water supermolecule structures for alanyl-alanine in ba-

sis solution are listed in Table 3.69. The optimized isolated and two water supermolecule structures for alanyl-alanine in neutral and in acidic solutions are listed in Table 3.70. Figure 3.33 shows the optimized structures for the three- and one-water supermolecules in basic solution, Figure 3.34 shows the isolated and two-water supermolecules in basic solution, Figure 3.37 shows the optimized isolated and two-water supermolecule zwitterion structures while Figure 3.40 shows the isolated and two-water supermolecule acid structures.

Raman spectra for aqueous alanyl-alanine at pH=13, pH=7, and pH=1 are shown in Figures 3.35, 3.38, and 3.41, respectively. IR spectra, shown in Figures 3.36, 3.39, and 3.42, were used to help identify frequencies in the amide II region.

Table 3.71 lists the scale factors for the isolated and two-water water-excluded structures of the basic, neutral, and acidic conformations of alanyl-alanine. Observed and calculated frequencies and potential energy distributions (PED) for the isolated and the two-water water-excluded supermolecule structures of alanyl-alanine in base are listed in tables 3.72 and 3.73. The assignments are based on four isotopic species. Observed and predicted frequencies for the isolated and two-water water-excluded supermolecule structures of alanyl-alanine in acid are listed in Tables 3.76 and 3.77. The assignments are based on four isotopic species. For the zwitterion isolated and two-water water-excluded structures, eight isotopic species were used. The frequencies for three of these isotopic species were from Oboodi *et al* [1984] (with one alpha hydrogen deuterated in D₂O, with both alpha hydrogens deuterated in H₂O, and with both alpha hydrogens deuterated in D₂O). Observed and predicted frequencies for zwitterionic isolated and two-water water-excluded structures are listed in Tables 3.74 and 3.75.

Table 3.63: Redundant Internal Coordinates for Dialanine in Base.

$R_1 = \Delta\gamma(\text{C}^6\text{--O}^8)^a$	$R_{35} = \Delta\tau(\text{C}^{10}\text{--N}^7)$
$R_2 = \Delta\gamma(\text{C}^6\text{--N}^7)$	$R_{36} = \Delta\gamma(\text{O}^{13}\text{--C}^{12})$
$R_3 = \Delta\gamma(\text{C}^4\text{--C}^6)$	$R_{37} = \Delta\gamma(\text{O}^{14}\text{--C}^{12})$
$R_4 = \Delta\gamma(\text{N}^7\text{--C}^{10})$	$R_{38} = \Delta\gamma(\text{C}^4\text{--N}^1)$
$R_5 = \Delta\gamma(\text{N}^7\text{--H}^9)$	$R_{39} = \Delta\gamma(\text{H}^2\text{--N}^1)$
$R_6 = \Delta\gamma(\text{C}^4\text{--H}^5)$	$R_{40} = \Delta\gamma(\text{H}^3\text{--N}^1)$
$R_7 = \Delta\gamma(\text{C}^{10}\text{--H}^{11})$	$R_{41} = \Delta\theta(\text{H}^3\text{--N}^1\text{--H}^2)$
$R_8 = \Delta\gamma(\text{C}^{10}\text{--C}^{12})$	$R_{42} = \Delta\theta(\text{C}^4\text{--N}^1\text{--H}^3)$
$R_9 = \Delta\theta(\text{C}^{10}\text{--N}^7\text{--C}^6)$	$R_{43} = \Delta\theta(\text{C}^4\text{--N}^1\text{--H}^2)$
$R_{10} = \Delta\theta(\text{H}^9\text{--N}^7\text{--C}^6)$	$R_{44} = \Delta\omega(\text{C}^4\text{--H}^2\text{--H}^3\text{--N}^1)$
$R_{11} = \Delta\theta(\text{C}^{10}\text{--N}^7\text{--H}^9)$	$R_{45} = \Delta\tau(\text{C}^4\text{--N}^1)$
$R_{12} = \Delta\omega(\text{H}^9\text{--C}^6\text{--C}^{10}\text{--N}^7)$	$R_{46} = \Delta\tau(\text{C}^{12}\text{--C}^{10})$
$R_{13} = \Delta\theta(\text{H}^5\text{--C}^4\text{--N}^1)$	$R_{47} = \Delta\gamma(\text{C}^{15}\text{--C}^4)$
$R_{14} = \Delta\theta(\text{H}^5\text{--C}^4\text{--C}^{15})$	$R_{48} = \Delta\gamma(\text{H}^{16}\text{--C}^{15})$
$R_{15} = \Delta\theta(\text{H}^5\text{--C}^4\text{--C}^6)$	$R_{49} = \Delta\gamma(\text{H}^{17}\text{--C}^{15})$
$R_{16} = \Delta\theta(\text{C}^{15}\text{--C}^4\text{--N}^1)$	$R_{50} = \Delta\gamma(\text{H}^{18}\text{--C}^{15})$
$R_{17} = \Delta\theta(\text{C}^{15}\text{--C}^4\text{--C}^6)$	$R_{51} = \Delta\theta(\text{H}^{18}\text{--C}^{15}\text{--H}^{17})$
$R_{18} = \Delta\theta(\text{C}^6\text{--C}^4\text{--N}^1)$	$R_{52} = \Delta\theta(\text{H}^{17}\text{--C}^{15}\text{--H}^{16})$
$R_{19} = \Delta\theta(\text{H}^{11}\text{--C}^{10}\text{--N}^7)$	$R_{53} = \Delta\theta(\text{H}^{18}\text{--C}^{15}\text{--H}^{16})$
$R_{20} = \Delta\theta(\text{H}^{11}\text{--C}^{10}\text{--C}^{19})$	$R_{54} = \Delta\theta(\text{H}^{16}\text{--C}^{15}\text{--C}^4)$
$R_{21} = \Delta\theta(\text{H}^{11}\text{--C}^{10}\text{--C}^{12})$	$R_{55} = \Delta\theta(\text{H}^{18}\text{--C}^{15}\text{--C}^4)$
$R_{22} = \Delta\theta(\text{C}^{19}\text{--C}^{10}\text{--N}^7)$	$R_{56} = \Delta\theta(\text{H}^{17}\text{--C}^{15}\text{--C}^4)$
$R_{23} = \Delta\theta(\text{C}^{19}\text{--C}^{10}\text{--C}^{12})$	$R_{57} = \Delta\tau(\text{C}^{15}\text{--C}^4)$
$R_{24} = \Delta\theta(\text{C}^{12}\text{--C}^{10}\text{--N}^7)$	$R_{58} = \Delta\gamma(\text{C}^{19}\text{--C}^{10})$
$R_{25} = \Delta\theta(\text{N}^7\text{--C}^6\text{--C}^4)$	$R_{59} = \Delta\gamma(\text{H}^{20}\text{--C}^{19})$
$R_{26} = \Delta\theta(\text{N}^7\text{--C}^6\text{--O}^8)$	$R_{60} = \Delta\gamma(\text{H}^{21}\text{--C}^{19})$
$R_{27} = \Delta\theta(\text{O}^8\text{--C}^6\text{--C}^4)$	$R_{61} = \Delta\gamma(\text{H}^{22}\text{--C}^{19})$
$R_{28} = \Delta\omega(\text{O}^8\text{--N}^7\text{--C}^4\text{--C}^6)$	$R_{62} = \Delta\theta(\text{H}^{22}\text{--C}^{19}\text{--H}^{21})$
$R_{29} = \Delta\theta(\text{O}^{14}\text{--C}^{12}\text{--O}^{13})$	$R_{63} = \Delta\theta(\text{H}^{21}\text{--C}^{19}\text{--C}^{20})$
$R_{30} = \Delta\theta(\text{O}^{14}\text{--C}^{12}\text{--C}^{10})$	$R_{64} = \Delta\theta(\text{H}^{22}\text{--C}^{19}\text{--C}^{20})$
$R_{31} = \Delta\theta(\text{O}^{13}\text{--C}^{12}\text{--C}^{10})$	$R_{65} = \Delta\theta(\text{H}^{20}\text{--C}^{19}\text{--C}^{10})$
$R_{32} = \Delta\omega(\text{C}^{10}\text{--O}^{14}\text{--O}^{13}\text{--C}^{12})$	$R_{66} = \Delta\theta(\text{H}^{22}\text{--C}^{19}\text{--C}^{10})$
$R_{33} = \Delta\tau(\text{C}^6\text{--C}^4)$	$R_{67} = \Delta\theta(\text{H}^{21}\text{--C}^{19}\text{--C}^{10})$
$R_{34} = \Delta\tau(\text{N}^7\text{--C}^6)$	$R_{68} = \Delta\tau(\text{C}^{19}\text{--C}^{10})$

^aSymbols: γ = stretch, θ = bend, ω = out of plane bend, τ = torsion.

Table 3.64: Redundant Internal Coordinates for Dialanine Zwitterion.

$R_1 = \Delta\gamma(\text{C}^6\text{--O}^8)^a$	$R_{37} = \Delta\gamma(\text{O}^{14}\text{--C}^{12})$
$R_2 = \Delta\gamma(\text{C}^6\text{--N}^7)$	$R_{38} = \Delta\gamma(\text{C}^4\text{--N}^1)$
$R_3 = \Delta\gamma(\text{C}^4\text{--C}^6)$	$R_{39} = \Delta\gamma(\text{H}^2\text{--N}^1)$
$R_4 = \Delta\gamma(\text{N}^7\text{--C}^{10})$	$R_{40} = \Delta\gamma(\text{H}^3\text{--N}^1)$
$R_5 = \Delta\gamma(\text{N}^7\text{--H}^9)$	$R_{41} = \Delta\gamma(\text{H}^{23}\text{--N}^1)$
$R_6 = \Delta\gamma(\text{C}^4\text{--H}^5)$	$R_{42} = \Delta\theta(\text{H}^{23}\text{--N}^1\text{--H}^3)$
$R_7 = \Delta\gamma(\text{C}^{10}\text{--H}^{11})$	$R_{43} = \Delta\theta(\text{H}^3\text{--N}^1\text{--H}^2)$
$R_8 = \Delta\gamma(\text{C}^{10}\text{--C}^{12})$	$R_{44} = \Delta\theta(\text{H}^{23}\text{--N}^1\text{--H}^2)$
$R_9 = \Delta\theta(\text{C}^{10}\text{--N}^7\text{--C}^6)$	$R_{45} = \Delta\theta(\text{C}^4\text{--N}^1\text{--H}^2)$
$R_{10} = \Delta\theta(\text{H}^9\text{--N}^7\text{--C}^6)$	$R_{46} = \Delta\theta(\text{C}^4\text{--N}^1\text{--H}^{23})$
$R_{11} = \Delta\theta(\text{C}^{10}\text{--N}^7\text{--H}^9)$	$R_{47} = \Delta\theta(\text{C}^4\text{--N}^1\text{--H}^3)$
$R_{12} = \Delta\omega(\text{H}^9\text{--C}^6\text{--C}^{10}\text{--N}^7)$	$R_{48} = \Delta\tau(\text{C}^4\text{--N}^1)$
$R_{13} = \Delta\theta(\text{H}^5\text{--C}^4\text{--N}^1)$	$R_{49} = \Delta\tau(\text{C}^{12}\text{--C}^{10})$
$R_{14} = \Delta\theta(\text{H}^5\text{--C}^4\text{--C}^{15})$	$R_{50} = \Delta\gamma(\text{C}^{15}\text{--C}^4)$
$R_{15} = \Delta\theta(\text{H}^5\text{--C}^4\text{--C}^6)$	$R_{51} = \Delta\gamma(\text{H}^{16}\text{--C}^{15})$
$R_{16} = \Delta\theta(\text{C}^{15}\text{--C}^4\text{--N}^1)$	$R_{52} = \Delta\gamma(\text{H}^{17}\text{--C}^{15})$
$R_{17} = \Delta\theta(\text{C}^{15}\text{--C}^4\text{--C}^6)$	$R_{53} = \Delta\gamma(\text{H}^{18}\text{--C}^{15})$
$R_{18} = \Delta\theta(\text{C}^6\text{--C}^4\text{--N}^1)$	$R_{54} = \Delta\theta(\text{H}^{18}\text{--C}^{15}\text{--H}^{17})$
$R_{19} = \Delta\theta(\text{H}^{11}\text{--C}^{10}\text{--N}^7)$	$R_{55} = \Delta\theta(\text{H}^{17}\text{--C}^{15}\text{--H}^{16})$
$R_{20} = \Delta\theta(\text{H}^{11}\text{--C}^{10}\text{--C}^{19})$	$R_{56} = \Delta\theta(\text{H}^{18}\text{--C}^{15}\text{--H}^{16})$
$R_{21} = \Delta\theta(\text{H}^{11}\text{--C}^{10}\text{--C}^{12})$	$R_{57} = \Delta\theta(\text{H}^{16}\text{--C}^{15}\text{--C}^4)$
$R_{22} = \Delta\theta(\text{C}^{19}\text{--C}^{10}\text{--N}^7)$	$R_{58} = \Delta\theta(\text{H}^{18}\text{--C}^{15}\text{--C}^4)$
$R_{23} = \Delta\theta(\text{C}^{19}\text{--C}^{10}\text{--C}^{12})$	$R_{59} = \Delta\theta(\text{H}^{17}\text{--C}^{15}\text{--C}^4)$
$R_{24} = \Delta\theta(\text{C}^{12}\text{--C}^{10}\text{--N}^7)$	$R_{60} = \Delta\tau(\text{C}^{15}\text{--C}^4)$
$R_{25} = \Delta\theta(\text{N}^7\text{--C}^6\text{--C}^4)$	$R_{61} = \Delta\gamma(\text{C}^{19}\text{--C}^{10})$
$R_{26} = \Delta\theta(\text{N}^7\text{--C}^6\text{--O}^8)$	$R_{62} = \Delta\gamma(\text{H}^{20}\text{--C}^{19})$
$R_{27} = \Delta\theta(\text{O}^8\text{--C}^6\text{--C}^4)$	$R_{63} = \Delta\gamma(\text{H}^{21}\text{--C}^{19})$
$R_{28} = \Delta\omega(\text{O}^8\text{--N}^7\text{--C}^4\text{--C}^6)$	$R_{64} = \Delta\gamma(\text{H}^{22}\text{--C}^{19})$
$R_{29} = \Delta\theta(\text{O}^{14}\text{--C}^{12}\text{--O}^{13})$	$R_{65} = \Delta\theta(\text{H}^{22}\text{--C}^{19}\text{--H}^{21})$
$R_{30} = \Delta\theta(\text{O}^{14}\text{--C}^{12}\text{--C}^{10})$	$R_{66} = \Delta\theta(\text{H}^{21}\text{--C}^{19}\text{--H}^{20})$
$R_{31} = \Delta\theta(\text{O}^{13}\text{--C}^{12}\text{--C}^{10})$	$R_{67} = \Delta\theta(\text{H}^{22}\text{--C}^{19}\text{--H}^{20})$
$R_{32} = \Delta\omega(\text{C}^{10}\text{--O}^{14}\text{--O}^{13}\text{--C}^{12})$	$R_{68} = \Delta\theta(\text{H}^{20}\text{--C}^{19}\text{--C}^{10})$
$R_{33} = \Delta\tau(\text{C}^6\text{--C}^4)$	$R_{69} = \Delta\theta(\text{H}^{22}\text{--C}^{19}\text{--C}^{10})$
$R_{34} = \Delta\tau(\text{N}^7\text{--C}^6)$	$R_{70} = \Delta\theta(\text{H}^{21}\text{--C}^{19}\text{--C}^{10})$
$R_{35} = \Delta\tau(\text{C}^{10}\text{--N}^7)$	$R_{71} = \Delta\tau(\text{C}^{19}\text{--C}^{10})$
$R_{36} = \Delta\gamma(\text{O}^{13}\text{--C}^{12})$	

^aSymbols: γ = stretch, θ = bend, ω = out of plane bend, τ = torsion.

Table 3.65: Redundant Internal Coordinates for Dialanine in Acid.

$R_1 = \Delta\gamma(C^6-O^8)^a$	$R_{38} = \Delta\gamma(H^{15}-O^{14})$
$R_2 = \Delta\gamma(C^6-N^7)$	$R_{39} = \Delta\gamma(C^4-N^1)$
$R_3 = \Delta\gamma(C^4-C^6)$	$R_{40} = \Delta\gamma(H^2-N^1)$
$R_4 = \Delta\gamma(N^7-C^{10})$	$R_{41} = \Delta\gamma(H^3-N^1)$
$R_5 = \Delta\gamma(N^7-H^9)$	$R_{42} = \Delta\gamma(H^{24}-N^1)$
$R_6 = \Delta\gamma(C^4-H^5)$	$R_{43} = \Delta\theta(H^{15}-O^{14}-C^{12})$
$R_7 = \Delta\gamma(C^{10}-H^{11})$	$R_{44} = \Delta\theta(H^{24}-N^1-H^3)$
$R_8 = \Delta\gamma(C^{10}-C^{12})$	$R_{45} = \Delta\theta(H^3-N^1-H^2)$
$R_9 = \Delta\theta(C^{10}-N^7-C^6)$	$R_{46} = \Delta\theta(H^{24}-N^1-H^2)$
$R_{10} = \Delta\theta(H^9-N^7-C^6)$	$R_{47} = \Delta\theta(C^4-N^1-H^2)$
$R_{11} = \Delta\theta(C^{10}-N^7-H^9)$	$R_{48} = \Delta\theta(C^4-N^1-H^{24})$
$R_{12} = \Delta\omega(H^9-C^6-C^{10}-N^7)$	$R_{49} = \Delta\theta(C^4-N^1-H^3)$
$R_{13} = \Delta\theta(H^5-C^4-N^1)$	$R_{50} = \Delta\tau(C^4-N^1)$
$R_{14} = \Delta\theta(H^5-C^4-C^{16})$	$R_{51} = \Delta\tau(C^{12}-C^{10})$
$R_{15} = \Delta\theta(H^5-C^4-C^6)$	$R_{52} = \Delta\tau(O^{14}-C^{12})$
$R_{16} = \Delta\theta(C^{16}-C^4-N^1)$	$R_{53} = \Delta\gamma(C^{16}-C^4)$
$R_{17} = \Delta\theta(C^{16}-C^4-C^6)$	$R_{54} = \Delta\gamma(H^{17}-C^{16})$
$R_{18} = \Delta\theta(C^6-C^4-N^1)$	$R_{55} = \Delta\gamma(H^{18}-C^{16})$
$R_{19} = \Delta\theta(H^{11}-C^{10}-N^7)$	$R_{56} = \Delta\gamma(H^{19}-C^{16})$
$R_{20} = \Delta\theta(H^{11}-C^{10}-C^{20})$	$R_{57} = \Delta\theta(H^{19}-C^{16}-H^{18})$
$R_{21} = \Delta\theta(H^{11}-C^{10}-C^{12})$	$R_{58} = \Delta\theta(H^{18}-C^{16}-H^{17})$
$R_{22} = \Delta\theta(C^{20}-C^{10}-N^7)$	$R_{59} = \Delta\theta(H^{19}-C^{16}-H^{17})$
$R_{23} = \Delta\theta(C^{20}-C^{10}-C^{12})$	$R_{60} = \Delta\theta(H^{17}-C^{16}-C^4)$
$R_{24} = \Delta\theta(C^{12}-C^{10}-N^7)$	$R_{61} = \Delta\theta(H^{19}-C^{16}-C^4)$
$R_{25} = \Delta\theta(N^7-C^6-C^4)$	$R_{62} = \Delta\theta(H^{18}-C^{16}-C^4)$
$R_{26} = \Delta\theta(N^7-C^6-O^8)$	$R_{63} = \Delta\tau(C^{16}-C^4)$
$R_{27} = \Delta\theta(O^8-C^6-C^4)$	$R_{64} = \Delta\gamma(C^{20}-C^{10})$
$R_{28} = \Delta\omega(O^8-N^7-C^4-C^6)$	$R_{65} = \Delta\gamma(H^{21}-C^{20})$
$R_{29} = \Delta\theta(O^{14}-C^{12}-C^{10})$	$R_{66} = \Delta\gamma(H^{22}-C^{20})$
$R_{30} = \Delta\theta(O^{14}-C^{12}-O^{13})$	$R_{67} = \Delta\gamma(H^{23}-C^{20})$
$R_{31} = \Delta\theta(O^{13}-C^{12}-C^{10})$	$R_{68} = \Delta\theta(H^{23}-C^{20}-H^{22})$
$R_{32} = \Delta\omega(O^{13}-C^{10}-O^{14}-C^{12})$	$R_{69} = \Delta\theta(H^{22}-C^{20}-H^{21})$
$R_{33} = \Delta\tau(C^6-C^4)$	$R_{70} = \Delta\theta(H^{23}-C^{20}-H^{21})$
$R_{34} = \Delta\tau(N^7-C^6)$	$R_{71} = \Delta\theta(H^{21}-C^{20}-C^{10})$
$R_{35} = \Delta\tau(C^{10}-N^7)$	$R_{72} = \Delta\theta(H^{23}-C^{20}-C^{10})$
$R_{36} = \Delta\gamma(O^{13}-C^{12})$	$R_{73} = \Delta\theta(H^{22}-C^{20}-C^{10})$
$R_{37} = \Delta\gamma(O^{14}-C^{12})$	$R_{74} = \Delta\tau(C^{20}-C^{10})$

Table 3.65: (continued)

^aSymbols: γ = stretch, θ = bend, ω = out of plane bend, τ = torsion.

Table 3.66: Symmetry Coordinate Definitions for Dialanine in Base.

CO ^a s ^a	$S_1 = R_1$
CN ^a s	$S_2 = R_2$
CC ^ψ s	$S_3 = R_3$
NC ^φ s	$S_4 = R_4$
NH ^a s	$S_5 = R_5$
C ^{α1} H s	$S_6 = R_6$
C ^{α2} H s	$S_7 = R_7$
CC ^c s	$S_8 = R_8$
CNHC sd	$S_9 = (2R_9 - R_{10} - R_{11})/\sqrt{6}$
NH ^a ib	$S_{10} = R_{10} - R_{11}/\sqrt{2}$
NH ^a ob	$S_{11} = R_{12}$
C ^{α1} H r ¹	$S_{12} = (2R_{13} - R_{14} - R_{14})/\sqrt{6}$
C ^{α1} H r ²	$S_{13} = (R_{14} - R_{15})/\sqrt{2}$
C ^{α1} H d ¹	$S_{14} = (4R_{16} + R_{17} + R_{18})/\sqrt{18}$
C ^{α1} H d ²	$S_{15} = (R_{16} + 4R_{17} + R_{18})/\sqrt{18}$
C ^{α1} H d ³	$S_{16} = (R_{16} + R_{17} + 4R_{18})/\sqrt{18}$
C ^{α2} H r ¹	$S_{17} = (2R_{19} - R_{20} - R_{21})/\sqrt{6}$
C ^{α2} H r ²	$S_{18} = (R_{20} - R_{21})/\sqrt{2}$
C ^{α2} H d ¹	$S_{19} = (4R_{22} + R_{23} + R_{24})/\sqrt{18}$
C ^{α2} H d ²	$S_{20} = (R_{22} + 4R_{23} + R_{24})/\sqrt{18}$
C ^{α2} H d ³	$S_{21} = (R_{22} + R_{23} + 4R_{24})/\sqrt{18}$
CO ^a sd	$S_{22} = (2R_{25} - R_{26} - R_{27})/\sqrt{6}$
CO ^a r	$S_{23} = (R_{26} - R_{27})/\sqrt{2}$
CO ^a ob	$S_{24} = R_{28}$
CC ^c sd	$S_{25} = (2R_{29} - R_{30} - R_{31})/\sqrt{6}$
CC ^c r	$S_{26} = (R_{30} - R_{31})/\sqrt{2}$
CC ^c ob ^b	$S_{27} = R_{32}$
CC ^ψ t	$S_{28} = R_{33}$
C ^ω N t	$S_{29} = R_{34}$
NC ^φ t	$S_{30} = R_{35}$
CO ^c ss	$S_{31} = (R_{36} + R_{37})/\sqrt{2}$
CO ^c as	$S_{32} = (R_{36} - R_{37})/\sqrt{2}$
CN ⁿ s	$S_{33} = R_{38}$
NH ₂ ss	$S_{34} = (R_{39} + R_{40})/\sqrt{2}$
NH ₂ as	$S_{35} = (R_{39} - R_{40})/\sqrt{2}$
NH ₂ sis	$S_{36} = (2R_{41} - R_{42} - R_{43})/\sqrt{6}$
NH ₂ r	$S_{37} = (R_{42} - R_{43})/\sqrt{2}$
NH ₂ w	$S_{38} = R_{44}$
CN ⁿ t	$S_{39} = R_{45}$

Table 3.66: (continued)

CC ^c t	$S_{40} = R_{46}$
CC ^{me} s	$S_{41} = R_{47}$
CH ₃ ss	$S_{42} = (R_{48} + R_{49} + R_{50})/\sqrt{3}$
CH ₃ as ¹	$S_{43} = (2R_{48} - R_{49} - R_{50})/\sqrt{6}$
CH ₃ as ²	$S_{44} = (R_{49} - R_{50})/\sqrt{2}$
CH ₃ sd	$S_{45} = (R_{51} + R_{52} + R_{53} - R_{54} - R_{55} - R_{56})/\sqrt{6}$
CH ₃ ad ¹	$S_{46} = (2R_{51} - R_{52} - R_{53})/\sqrt{6}$
CH ₃ ad ²	$S_{47} = (R_{52} - R_{53})/\sqrt{2}$
CH ₃ r ¹	$S_{48} = (2R_{54} - R_{55} - R_{56})/\sqrt{6}$
CH ₃ r ²	$S_{49} = (R_{55} - R_{56})/\sqrt{2}$
CC ^{me} t	$S_{50} = R_{57}$
CC ^{me} s	$S_{51} = R_{58}$
CH ₃ ss	$S_{52} = (R_{59} + R_{60} + R_{61})/\sqrt{3}$
CH ₃ as ¹	$S_{53} = (2R_{59} - R_{60} - R_{61})/\sqrt{6}$
CH ₃ as ²	$S_{54} = (R_{60} - R_{61})/\sqrt{2}$
CH ₃ sd	$S_{55} = (R_{62} + R_{63} + R_{64} - R_{65} - R_{66} - R_{67})/\sqrt{6}$
CH ₃ ad ¹	$S_{56} = (2R_{62} - R_{63} - R_{64})/\sqrt{6}$
CH ₃ ad ²	$S_{57} = (R_{63} - R_{64})/\sqrt{2}$
CH ₃ r ¹	$S_{58} = (2R_{65} - R_{66} - R_{67})/\sqrt{6}$
CH ₃ r ²	$S_{59} = (R_{66} - R_{67})/\sqrt{2}$
CC ^{me} t	$S_{60} = R_{68}$

^aAbbreviations: s = stretch, t = torsion, ss = symmetric stretch, as = antisymmetric stretch, d = deformation, sd = symmetric deformation, ad = antisymmetric deformation, r = rock, ob = out of plane bend, ib = in plane bend, sis = scissor, w = wag.

^bThe CC^c ob was referred to as the CCOO w in alaninate and glycinate.

Table 3.67: Symmetry Coordinate Definitions for Dialanine Zwitterion.

CO ^a s ^a	$S_1 = R_1$
CN ^a s	$S_2 = R_2$
CC ^ψ s	$S_3 = R_3$
NC ^φ s	$S_4 = R_4$
NH ^a s	$S_5 = R_5$
C ^{α1} H s	$S_6 = R_6$
C ^{α2} H s	$S_7 = R_7$
CC ^c s	$S_8 = R_8$
CNHC sd	$S_9 = (2R_9 - R_{10} - R_{11})/\sqrt{6}$
NH ^a ib	$S_{10} = R_{10} - R_{11}/\sqrt{2}$
NH ^a ob	$S_{11} = R_{12}$
C ^{α1} H r ¹	$S_{12} = (2R_{13} - R_{14} - R_{14})/\sqrt{6}$
C ^{α1} H r ²	$S_{13} = (R_{14} - R_{15})/\sqrt{2}$
C ^{α1} H d ¹	$S_{14} = (4R_{16} + R_{17} + R_{18})/\sqrt{18}$
C ^{α1} H d ²	$S_{15} = (R_{16} + 4R_{17} + R_{18})/\sqrt{18}$
C ^{α1} H d ³	$S_{16} = (R_{16} + R_{17} + 4R_{18})/\sqrt{18}$
C ^{α2} H r ¹	$S_{17} = (2R_{19} - R_{20} - R_{21})/\sqrt{6}$
C ^{α2} H r ²	$S_{18} = (R_{20} - R_{21})/\sqrt{2}$
C ^{α2} H d ¹	$S_{19} = (4R_{22} + R_{23} + R_{24})/\sqrt{18}$
C ^{α2} H d ²	$S_{20} = (R_{22} + 4R_{23} + R_{24})/\sqrt{18}$
C ^{α2} H d ³	$S_{21} = (R_{22} + R_{23} + 4R_{24})/\sqrt{18}$
CO ^a sd	$S_{22} = (2R_{25} - R_{26} - R_{27})/\sqrt{6}$
CO ^a r	$S_{23} = (R_{26} - R_{27})/\sqrt{2}$
CO ^a ob	$S_{24} = R_{28}$
CC ^c sd	$S_{25} = (2R_{29} - R_{30} - R_{31})/\sqrt{6}$
CC ^c r	$S_{26} = (R_{30} - R_{31})/\sqrt{2}$
CC ^c ob	$S_{27} = R_{32}$
CC ^ψ t	$S_{28} = R_{33}$
C ^ω N t	$S_{29} = R_{34}$
NC ^φ t	$S_{30} = R_{35}$
CO ^c ss	$S_{31} = (R_{36} + R_{37})/\sqrt{2}$
CO ^c as	$S_{32} = (R_{36} - R_{37})/\sqrt{2}$
CN ⁿ s	$S_{33} = R_{38}$
NH ₃ ss	$S_{34} = (R_{39} + R_{40} + R_{41})/\sqrt{3}$
NH ₃ as ¹	$S_{35} = (2R_{39} - R_{40} - R_{41})/\sqrt{6}$
NH ₃ as ²	$S_{36} = (R_{40} - R_{41})/\sqrt{2}$
NH ₃ sd	$S_{37} = (R_{42} + R_{43} + R_{44} - R_{45} - R_{46} - R_{47})/\sqrt{6}$

NH ₃ ad ¹	$S_{38} = (2R_{42} - R_{43} - R_{44})/\sqrt{6}$
NH ₃ ad ²	$S_{39} = (R_{43} - R_{44})/\sqrt{2}$
NH ₃ r ¹	$S_{40} = (2R_{45} - R_{46} - R_{47})/\sqrt{6}$
NH ₃ r ²	$S_{41} = (R_{46} - R_{47})/\sqrt{2}$
CN ⁿ t	$S_{42} = R_{48}$
CC ^c t	$S_{43} = R_{49}$
CC ^{me} s	$S_{44} = R_{50}$
CH ₃ ss	$S_{45} = (R_{51} + R_{52} + R_{53})/\sqrt{3}$
CH ₃ as ¹	$S_{46} = (2R_{51} - R_{52} - R_{53})/\sqrt{6}$
CH ₃ as ²	$S_{47} = (R_{52} - R_{53})/\sqrt{2}$
CH ₃ sd	$S_{48} = (R_{54} + R_{55} + R_{56} - R_{57} - R_{58} - R_{59})/\sqrt{6}$
CH ₃ ad ¹	$S_{49} = (2R_{54} - R_{55} - R_{56})/\sqrt{6}$
CH ₃ ad ²	$S_{50} = (R_{55} - R_{56})/\sqrt{2}$
CH ₃ r ¹	$S_{51} = (2R_{57} - R_{58} - R_{59})/\sqrt{6}$
CH ₃ r ²	$S_{52} = (R_{58} - R_{59})/\sqrt{2}$
CC ^{me} t	$S_{53} = R_{60}$
CC ^{me} s	$S_{54} = R_{61}$
CH ₃ ss	$S_{55} = (R_{62} + R_{63} + R_{64})/\sqrt{3}$
CH ₃ as ¹	$S_{56} = (2R_{62} - R_{63} - R_{64})/\sqrt{6}$
CH ₃ as ²	$S_{57} = (R_{63} - R_{64})/\sqrt{2}$
CH ₃ sd	$S_{58} = (R_{65} + R_{66} + R_{67} - R_{68} - R_{69} - R_{70})/\sqrt{6}$
CH ₃ ad ¹	$S_{59} = (2R_{65} - R_{66} - R_{67})/\sqrt{6}$
CH ₃ ad ²	$S_{60} = (R_{66} - R_{67})/\sqrt{2}$
CH ₃ r ¹	$S_{61} = (2R_{68} - R_{69} - R_{70})/\sqrt{6}$
CH ₃ r ²	$S_{62} = (R_{69} - R_{70})/\sqrt{2}$
CC ^{me} t	$S_{63} = R_{71}$

Abbreviations: s = stretch, b = bend, t = torsion, ss = symmetric stretch, as = antisymmetric stretch, d = deformation, sd = symmetric deformation, ad = antisymmetric deformation, r = rock, ib = in plane bend, ob = out of plane bend, sis = scissor, w = wag.

^bThe CCOO w was referred to as the CO ob previously.

Table 3.68: Symmetry Coordinate Definitions for Dialanine in Acid.

$\text{CO}^a \text{ s}^a$	$S_1 = R_1$
$\text{CN}^a \text{ s}$	$S_2 = R_2$
$\text{CC}^\psi \text{ s}$	$S_3 = R_3$
$\text{NC}^\phi \text{ s}$	$S_4 = R_4$
$\text{NH}^a \text{ s}$	$S_5 = R_5$
$\text{C}^{\alpha 1} \text{H s}$	$S_6 = R_6$
$\text{C}^{\alpha 2} \text{H s}$	$S_7 = R_7$
$\text{CC}^c \text{ s}$	$S_8 = R_8$
CNHC sd	$S_9 = (2R_9 - R_{10} - R_{11})/\sqrt{6}$
$\text{NH}^a \text{ ib}$	$S_{10} = R_{10} - R_{11}/\sqrt{2}$
$\text{NH}^a \text{ ob}$	$S_{11} = R_{12}$
$\text{C}^{\alpha 1} \text{H r}^1$	$S_{12} = (2R_{13} - R_{14} - R_{14})/\sqrt{6}$
$\text{C}^{\alpha 1} \text{H r}^2$	$S_{13} = (R_{14} - R_{15})/\sqrt{2}$
$\text{C}^{\alpha 1} \text{H d}^1$	$S_{14} = (4R_{16} + R_{17} + R_{18})/\sqrt{18}$
$\text{C}^{\alpha 1} \text{H d}^2$	$S_{15} = (R_{16} + 4R_{17} + R_{18})/\sqrt{18}$
$\text{C}^{\alpha 1} \text{H d}^3$	$S_{16} = (R_{16} + R_{17} + 4R_{18})/\sqrt{18}$
$\text{C}^{\alpha 2} \text{H r}^1$	$S_{17} = (2R_{19} - R_{20} - R_{21})/\sqrt{6}$
$\text{C}^{\alpha 2} \text{H r}^2$	$S_{18} = (R_{20} - R_{21})/\sqrt{2}$
$\text{C}^{\alpha 2} \text{H d}^1$	$S_{19} = (4R_{22} + R_{23} + R_{24})/\sqrt{18}$
$\text{C}^{\alpha 2} \text{H d}^2$	$S_{20} = (R_{22} + 4R_{23} + R_{24})/\sqrt{18}$
$\text{C}^{\alpha 2} \text{H d}^3$	$S_{21} = (R_{22} + R_{23} + 4R_{24})/\sqrt{18}$
$\text{CO}^a \text{ sd}$	$S_{22} = (2R_{25} - R_{26} - R_{27})/\sqrt{6}$
$\text{CO}^a \text{ r}$	$S_{23} = (R_{26} - R_{27})/\sqrt{2}$
$\text{CO}^a \text{ ob}$	$S_{24} = R_{28}$
$\text{CC}^c \text{ sd}$	$S_{25} = (2R_{29} - R_{30} - R_{31})/\sqrt{6}$
$\text{CC}^c \text{ r}$	$S_{26} = (R_{30} - R_{31})/\sqrt{2}$
$\text{CC}^c \text{ ob}$	$S_{27} = R_{32}$
$\text{CC}^\psi \text{ t}$	$S_{28} = R_{33}$
$\text{C}^\omega \text{N t}$	$S_{29} = R_{34}$
$\text{NC}^\phi \text{ t}$	$S_{30} = R_{35}$
$\text{CO}^c \text{ s}$	$S_{31} = R_{36}$
$\text{CO}^H \text{ s}$	$S_{32} = R_{37}$
OH s	$S_{33} = R_{38}$
$\text{CN}^n \text{ s}$	$S_{34} = R_{39}$
$\text{NH}_3 \text{ ss}$	$S_{35} = (R_{40} + R_{41} + R_{42})/\sqrt{3}$
$\text{NH}_3 \text{ as}^1$	$S_{36} = (2R_{40} - R_{41} - R_{42})/\sqrt{6}$
$\text{NH}_3 \text{ as}^2$	$S_{37} = (R_{41} - R_{42})/\sqrt{2}$

Table 3.68: (continued)

OH b	$S_{38} = R_{43}$
NH ₃ sd	$S_{39} = (R_{44} + R_{45} + R_{46} - R_{47} - R_{48} - R_{49})/\sqrt{6}$
NH ₃ ad ¹	$S_{40} = (2R_{44} - R_{45} - R_{46})/\sqrt{6}$
NH ₃ ad ²	$S_{41} = (R_{45} - R_{46})/\sqrt{2}$
NH ₃ r ¹	$S_{42} = (2R_{47} - R_{48} - R_{49})/\sqrt{6}$
NH ₃ r ²	$S_{43} = (R_{48} - R_{49})/\sqrt{2}$
CN ⁿ t	$S_{44} = R_{50}$
CC ^c t	$S_{45} = R_{51}$
CO ^H t	$S_{46} = R_{52}$
CC ^{me} s	$S_{47} = R_{53}$
CH ₃ ss	$S_{48} = (R_{54} + R_{55} + R_{56})/\sqrt{3}$
CH ₃ as ¹	$S_{49} = (2R_{54} - R_{55} - R_{56})/\sqrt{6}$
CH ₃ as ²	$S_{50} = (R_{55} - R_{56})/\sqrt{2}$
CH ₃ sd	$S_{51} = (R_{57} + R_{58} + R_{59} - R_{60} - R_{61} - R_{62})/\sqrt{6}$
CH ₃ ad ¹	$S_{52} = (2R_{57} - R_{58} - R_{59})/\sqrt{6}$
CH ₃ ad ²	$S_{53} = (R_{58} - R_{59})/\sqrt{2}$
CH ₃ r ¹	$S_{54} = (2R_{60} - R_{61} - R_{62})/\sqrt{6}$
CH ₃ r ²	$S_{55} = (R_{61} - R_{62})/\sqrt{2}$
CC ^{me} t	$S_{56} = R_{63}$
CC ^{me} s	$S_{57} = R_{64}$
CH ₃ ss	$S_{58} = (R_{65} + R_{66} + R_{67})/\sqrt{3}$
CH ₃ as ¹	$S_{59} = (2R_{65} - R_{66} - R_{67})/\sqrt{6}$
CH ₃ as ²	$S_{60} = (R_{66} - R_{67})/\sqrt{2}$
CH ₃ sd	$S_{61} = (R_{68} + R_{69} + R_{70} - R_{71} - R_{72} - R_{73})/\sqrt{6}$
CH ₃ ad ¹	$S_{62} = (2R_{68} - R_{69} - R_{70})/\sqrt{6}$
CH ₃ ad ²	$S_{63} = (R_{69} - R_{70})/\sqrt{2}$
CH ₃ r ¹	$S_{64} = (2R_{71} - R_{72} - R_{73})/\sqrt{6}$
CH ₃ r ²	$S_{65} = (R_{72} - R_{73})/\sqrt{2}$
CC ^{me} t	$S_{66} = R_{74}$

^aAbbreviations: s = stretch, b = bend, t = torsion, ss = symmetric stretch, as = antisymmetric stretch, d = deformation, sd = symmetric deformation, ad = antisymmetric deformation, r = rock, ib = in plane bend, ob = out of plane bend, sis = scissor, w = wag.

Table 3.69: Optimized internal coordinates calculated for dialanine isolated and supermolecule structures in base.

Internal Coordinate ^a	isolated	1w-O	1w-H	2w	3w
Bond stretches:					
H ² -N ^{1b}	0.9964	0.9977	0.9964	0.9979	0.9977
H ³ -N ¹	0.9940	0.9952	0.9941	0.9952	0.9947
C ⁴ -N ¹	1.4495	1.4528	1.4523	1.4552	1.4532
H ⁵ -C ⁴	1.0831	1.0811	1.0828	1.0794	1.0792
C ⁶ -C ⁴	1.5274	1.5204	1.5264	1.5190	1.5167
N ⁷ -C ⁶	1.3212	1.3131	1.3273	1.3179	1.3125
O ⁸ -C ⁶	1.2385	1.2480	1.2372	1.2469	1.2544
H ⁹ -N ⁷	1.0012	1.0021	0.9956	0.9957	0.9969
C ¹⁰ -N ⁷	1.4537	1.4556	1.4543	1.4552	1.4571
H ¹¹ -C ¹⁰	1.0826	1.0819	1.0818	1.0811	1.0806
C ¹² -C ¹⁰	1.5529	1.5533	1.5447	1.5461	1.5466
O ¹³ -C ¹²	1.2605	1.2604	1.2685	1.2671	1.2663
O ¹⁴ -C ¹²	1.2463	1.2453	1.2398	1.2398	1.2392
C ¹⁵ -C ⁴	1.5386	1.5377	1.5380	1.5367	1.5369
H ¹⁶ -C ¹⁵	1.0832	1.0820	1.0840	1.0822	1.0821
H ¹⁷ -C ¹⁵	1.0822	1.0837	1.0803	1.0834	1.0833
H ¹⁸ -C ¹⁵	1.0852	1.0844	1.0855	1.0840	1.0837
C ¹⁹ -C ¹⁰	1.5277	1.5276	1.5300	1.5301	1.5306
H ²⁰ -C ¹⁹	1.0843	1.0841	1.0842	1.0841	1.0836
H ²¹ -C ¹⁹	1.0802	1.0800	1.0801	1.0799	1.0800
H ²² -C ¹⁹	1.0818	1.0816	1.0813	1.0812	1.0814
H ²³ -N ¹					
H ²⁴ -O ¹⁴					
Angle bends:					
H ³ -N ¹ -H ²	114.68	113.40	114.32	113.36	113.56
C ⁴ -N ¹ -H ²	112.97	115.19	112.99	115.07	115.64
H ⁵ -C ⁴ -N ¹	109.79	107.99	109.81	108.37	108.54
C ⁶ -C ⁴ -N ¹	108.31	108.65	108.15	108.27	107.78
N ⁷ -C ⁶ -C ⁴	115.26	116.53	115.71	116.45	117.20
O ⁸ -C ⁶ -N ⁷	124.91	123.87	123.99	123.43	123.36
H ⁹ -N ⁷ -C ⁶	122.56	122.69	120.60	119.76	119.52
C ¹⁰ -N ⁷ -C ⁶	126.59	126.82	124.76	125.46	125.47

Table 3.69: (continued)

Internal Coordinate	isolated	1w-O	1w-H	2w	3w
H ¹¹ -C ¹⁰ -N ⁷	109.48	109.40	108.94	108.85	108.68
C ¹² -C ¹⁰ -N ⁷	107.21	106.98	109.42	109.32	109.44
O ¹³ -C ¹² -C ¹⁰	115.78	115.64	116.66	116.76	116.71
O ¹⁴ -C ¹² -O ¹³	129.15	129.34	127.84	128.00	128.24
C ¹⁵ -C ⁴ -C ⁶	108.69	108.74	109.32	108.83	109.08
H ¹⁶ -C ¹⁵ -C ⁴	109.82	109.84	110.15	110.13	110.41
H ¹⁷ -C ¹⁵ -C ⁴	111.43	111.40	111.21	111.22	111.24
H ¹⁸ -C ¹⁵ -C ⁴	110.08	109.92	109.49	109.72	109.54
C ¹⁹ -C ¹⁰ -N ⁷	112.43	112.44	111.89	111.90	111.85
H ²⁰ -C ¹⁹ -C ¹⁰	109.97	110.00	110.03	110.07	110.04
H ²¹ -C ¹⁹ -C ¹⁰	109.06	108.90	109.33	109.21	109.15
H ²² -C ¹⁹ -C ¹⁰	110.67	110.81	110.30	110.39	111.06
H ²³ -N ¹ -H ²					
H ²⁴ -O ¹⁴ -C ¹²					
Torsions:					
C ⁴ -N ¹ -H ² -H ³	135.83	134.94	134.64	134.4	135.94
H ⁵ -C ⁴ -N ¹ -H ²	-220.16	-190.40	-222.66	-185.23	-187.22
C ⁶ -C ⁴ -N ¹ -H ²	21.76	51.96	19.58	56.98	55.27
N ⁷ -C ⁶ -C ⁴ -N ¹	155.83	133.52	158.43	129.97	129.75
O ⁸ -C ⁶ -O ⁷ -C ⁴	182.78	183.13	181.88	182.61	182.41
H ⁹ -N ⁷ -C ⁶ -C ⁴	0.38	0.22	1.96	-0.68	0.23
C ¹⁰ -N ⁷ -C ⁶ -C ⁴	173.34	174.79	174.87	174.76	174.80
H ¹¹ -C ¹⁰ -N ⁷ -C ⁶	-49.28	-50.58	-45.44	-45.85	-41.76
C ¹² -C ¹⁰ -N ⁷ -C ⁶	-166.14	-167.52	-162.81	-163.28	-159.12
O ¹³ -C ¹² -C ¹⁰ -N ⁷	-4.28	-4.74	-5.32	-7.04	-8.46
O ¹⁴ -C ¹² -O ¹³ -C ¹⁰	-180.73	-180.89	-181.28	-181.52	-181.78
C ¹⁵ -C ⁴ -C ⁶ -N ⁷	-81.15	-102.25	-78.06	-105.97	-105.93
H ¹⁶ -C ¹⁵ -C ⁴ -C ⁶	-59.28	-60.67	-56.03	-60.43	-60.62
H ¹⁷ -C ¹⁵ -C ⁴ -C ⁶	61.28	59.89	65.97	60.41	60.54
H ¹⁸ -C ¹⁵ -C ⁴ -C ⁶	-178.66	-180.03	-174.99	-179.94	-179.96
C ¹⁹ -C ¹⁰ -N ⁷ -C ⁶	72.15	71.05	74.82	74.56	78.96
H ²⁰ -C ¹⁹ -C ¹⁰ -N ⁷	57.92	57.43	59.30	59.11	58.88
H ²¹ -C ²⁰ -C ¹⁰ -N ⁷	-183.18	-183.74	-181.48	-181.69	-182.03

Table 3.69: (continued)

Internal Coordinate	isolated	1w-O	1w-H	2w	3w
H ²² -C ²⁰ -C ¹⁰ -N ⁷	-62.31	-62.93	-60.79	-61.02	-61.20

^aSuperscripted numbers refer to the atom numbering shown in Figures 3.33 and 3.34.

^bOptimized values taken from the Z-matrices, Bond lengths in Å, angles in degrees. Water coordinates are not included in the table.

Table 3.70: Optimized internal coordinates calculated for dialanine isolated and supermolecule structures in neutral and acid solutions.

Internal Coordinate	Neutral		Acid	
	isolated	2w	isolated	2w
Bond stretches:				
H ² -N ¹ <i>b</i>	1.0458	1.0391	1.0268	1.0449
H ³ -N ¹	1.0045	1.0049	1.0070	1.0062
C ⁴ -N ¹	1.5250	1.5204	1.5229	1.5110
H ⁵ -C ⁴	1.0779	1.0771	1.0784	1.0788
C ⁶ -C ⁴	1.5419	1.5267	1.5309	1.5228
N ⁷ -C ⁶	1.2880	1.2996	1.3160	1.3207
O ⁸ -C ⁶	1.2509	1.2474	1.2325	1.2350
H ⁹ -N ⁷	1.0205	1.0003	0.9979	1.0054
C ¹⁰ -N ⁷	1.4667	1.4634	1.4631	1.4543
H ¹¹ -C ¹⁰	1.0812	1.0806	1.0803	1.0789
C ¹² -C ¹⁰	1.5620	1.5521	1.5051	1.5051
O ¹³ -C ¹²	1.2681	1.2701	1.2090	1.2114
O ¹⁴ -C ¹²	1.2328	1.2312	1.3268	1.3296
C ¹⁵ -C ⁴	1.5243	1.5262	1.5288	1.5290
H ¹⁶ -C ¹⁵	1.0826	1.0809	1.0820	1.0808
H ¹⁷ -C ¹⁵	1.0803	1.0784	1.0801	1.0783
H ¹⁸ -C ¹⁵	1.0824	1.0838	1.0817	1.0824
C ¹⁹ -C ¹⁰	1.5230	1.5263	1.5336	1.5361
H ²⁰ -C ¹⁹	1.0832	1.0833	1.0817	1.0819
H ²¹ -C ¹⁹	1.0794	1.0793	1.0793	1.0794
H ²² -C ¹⁹	1.0823	1.0822	1.0792	1.0799
H ²³ -N ¹	1.0047	1.0067	1.0083	1.0076
H ²⁴ -O ¹⁴			0.9566	0.9564
Angle bends:				
H ³ -N ¹ -H ²	110.74	109.49	110.42	109.28
C ⁴ -N ¹ -H ²	101.69	110.08	105.47	110.18
H ⁵ -C ⁴ -N ¹	107.87	107.96	107.75	107.70
C ⁶ -C ⁴ -N ¹	103.40	106.73	104.15	106.67
N ⁷ -C ⁶ -C ⁴	115.38	114.89	117.02	115.71
O ⁸ -C ⁶ -N ⁷	128.86	126.51	125.46	124.87

Table 3.70: (continued)

Internal Coordinate ^a	Neutral		Acid	
	isolated	2w	isolated	2w
H ⁹ -N ⁷ -C ⁶	124.50	120.22	121.86	119.43
C ¹⁰ -N ⁷ -C ⁶	129.26	126.99	123.15	122.11
H ¹¹ -C ¹⁰ -N ⁷	109.30	108.70	109.11	108.50
C ¹² -C ¹⁰ -N ⁷	103.96	107.19	105.72	108.61
O ¹³ -C ¹² -C ¹⁰	114.04	115.56	123.70	125.67
O ¹⁴ -C ¹² -O ¹³	130.42	129.13	124.28	122.96
C ¹⁵ -C ⁴ -C ⁶	112.65	111.96	111.99	112.19
H ¹⁶ -C ¹⁵ -C ⁴	110.92	110.94	111.03	110.81
H ¹⁷ -C ¹⁵ -C ⁴	109.54	108.35	109.92	109.29
H ¹⁸ -C ¹⁵ -C ⁴	111.27	110.60	110.97	110.55
C ¹⁹ -C ¹⁰ -N ⁷	112.91	112.19	112.46	112.03
H ²⁰ -C ¹⁹ -C ¹⁰	110.35	110.33	110.68	110.73
H ²¹ -C ¹⁹ -C ¹⁰	108.45	108.81	109.96	110.55
H ²² -C ¹⁹ -C ¹⁰	111.38	110.94	109.48	109.01
H ²³ -N ¹ -H ²	109.44	106.39	112.20	111.37
H ²⁴ -O ¹⁴ -C ¹²			115.86	115.75
Torsions:				
C ⁴ -N ¹ -H ² -H ³	119.95	121.69	121.65	121.90
H ⁵ -C ⁴ -N ¹ -H ²	-236.66	-176.54	-221.51	-179.77
C ⁶ -C ⁴ -N ¹ -H ²	6.39	64.30	20.15	61.81
N ⁷ -C ⁶ -C ⁴ -N ¹	174.89	155.67	166.98	163.72
O ⁸ -C ⁶ -O ⁷ -C ⁴	181.02	181.54	181.64	180.78
H ⁹ -N ⁷ -C ⁶ -C ⁴	2.74	-1.74	-0.64	-2.84
C ¹⁰ -N ⁷ -C ⁶ -C ⁴	174.77	170.03	176.31	176.19
H ¹¹ -C ¹⁰ -N ⁷ -C ⁶	-51.72	-41.59	-45.18	-26.53
C ¹² -C ¹⁰ -N ⁷ -C ⁶	-167.54	-158.18	-161.87	-143.66
O ¹³ -C ¹² -C ¹⁰ -N ⁷	-1.88	-5.25	-7.78	-12.13
O ¹⁴ -C ¹² -O ¹³ -C ¹⁰	-180.53	-181.12	-180.87	-181.34
C ¹⁵ -C ⁴ -C ⁶ -N ⁷	-65.45	-84.99	-74.30	-76.69
H ¹⁶ -C ¹⁵ -C ⁴ -C ⁶	-56.36	-52.97	-56.13	-55.60
H ¹⁷ -C ¹⁵ -C ⁴ -C ⁶	62.24	68.28	63.21	65.20
H ¹⁸ -C ¹⁵ -C ⁴ -C ⁶	-178.46	-174.12	-178.04	-176.45

Table 3.70: (continued)

Internal Coordinate ^a	Neutral		Acid	
	isolated	2w	isolated	2w
C ¹⁹ -C ¹⁰ -N ⁷ -C ⁶	71.41	79.85	76.56	93.85
H ²⁰ -C ¹⁹ -C ¹⁰ -N ⁷	55.89	57.88	58.54	59.02
H ²¹ -C ²⁰ -C ¹⁰ -N ⁷	-185.75	-183.34	-181.04	-179.95
H ²² -C ²⁰ -C ¹⁰ -N ⁷	-65.35	-62.99	-61.86	-60.63
H ²³ -N ¹ -H ² -C ⁴	119.57	120.28	143.06	-55.71
H ²⁴ -O ¹⁴ -C ¹² -O ¹³			-0.55	-0.59

^aSuperscripted numbers refer to the atom numbering shown in Figures 3.37 and 3.40.

^bOptimized values taken from the Z-matrices, Bond lengths in Å, angles in degrees. Water coordinates are not included in the table.

Figure 3.33: Optimized structures of alanyl-alanine base three water and one water supermolecules. Three water supermolecule (top), one water supermolecule with the water hydrogen bonded to the carbonyl oxygen (middle), and the one water supermolecule with the water hydrogen bonded to the amide hydrogen (bottom).

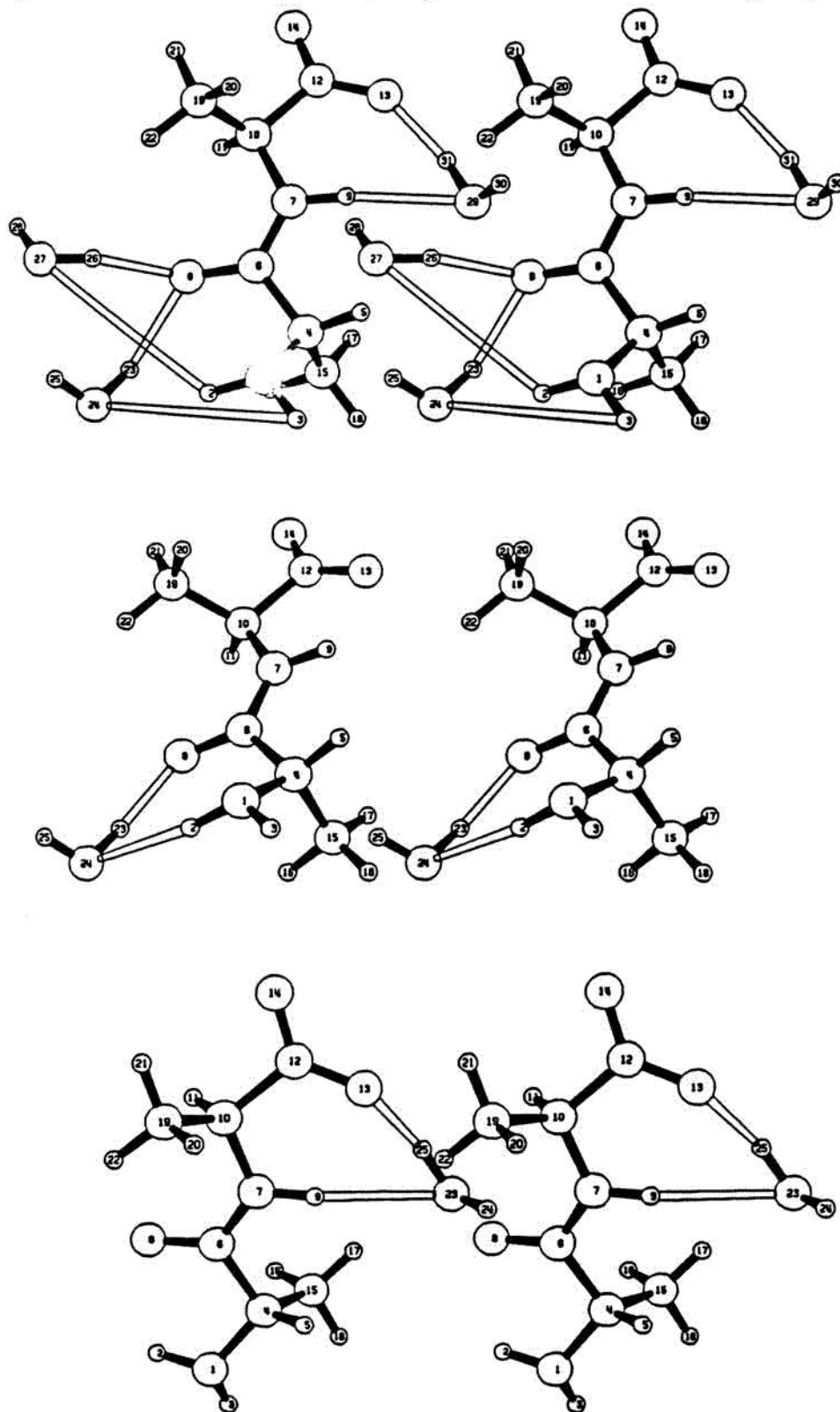


Figure 3.34: Optimized structures of alanyl-alanine base isolated (top) and two water supermolecule (bottom).

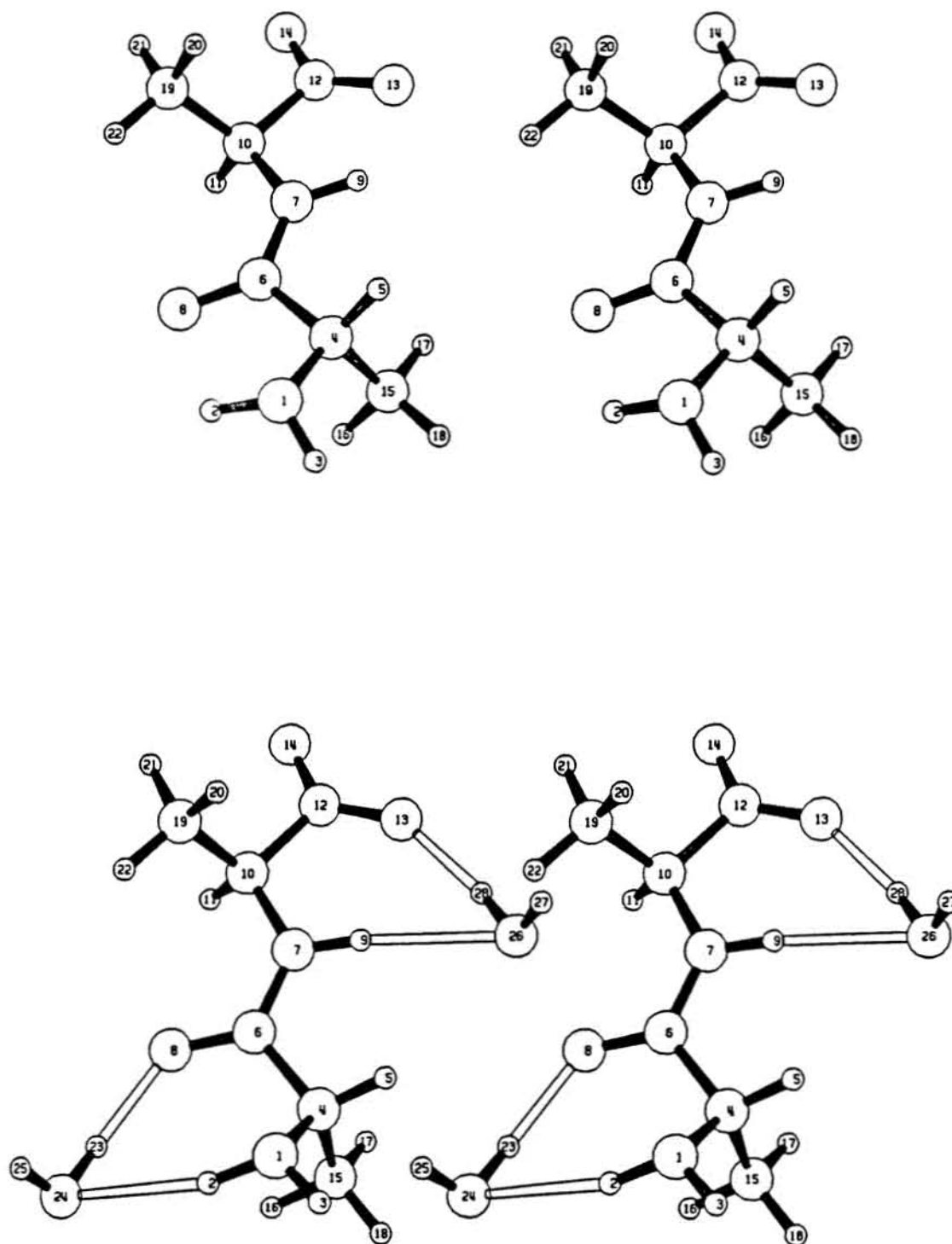


Figure 3.35: Raman spectra of alanyl-alanine in H_2O at $\text{pH}=13$ (top), alanyl-alanine in D_2O at $\text{pD}=13$ (upper middle), alanyl-alanine labelled at the amine α -carbon with deuterium in H_2O at $\text{pH}=13$ (lower middle), and alanyl-alanine labelled with ^{13}C at the carbonyl carbon in H_2O at $\text{pH}=13$ (bottom).

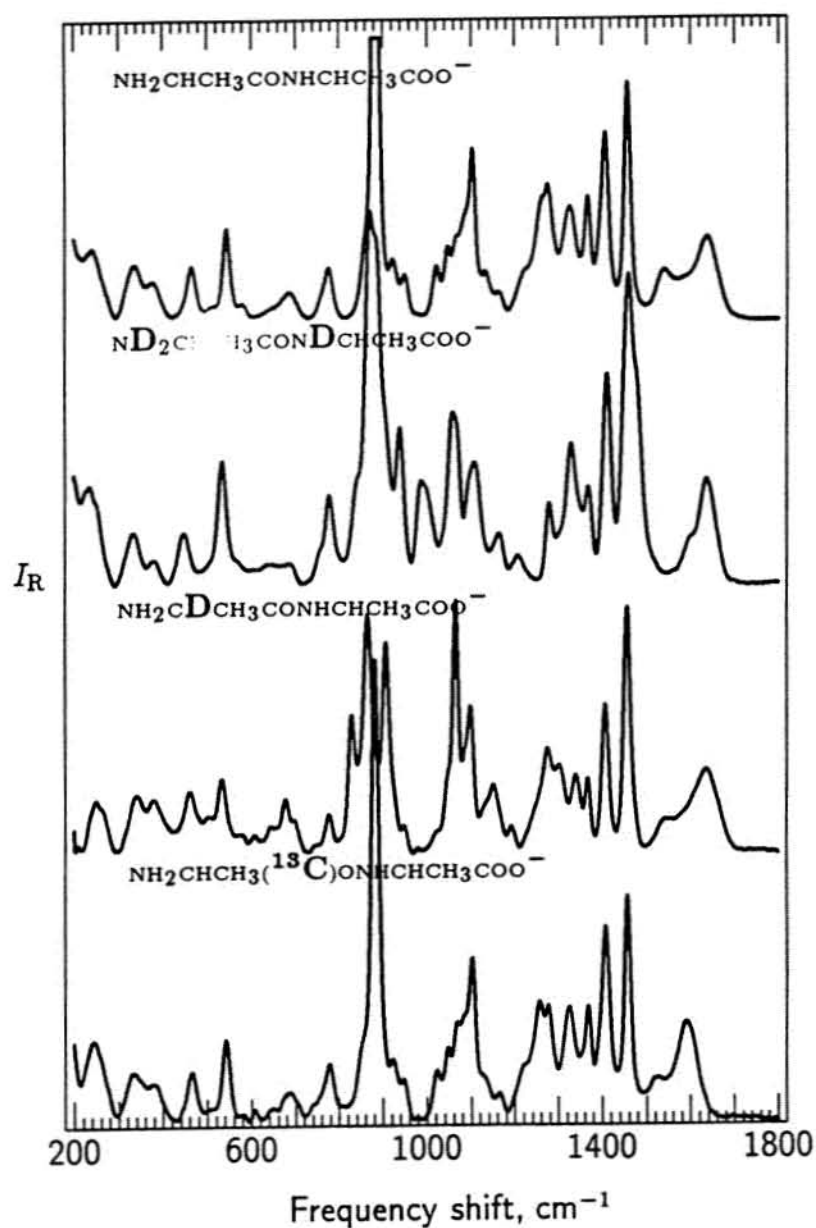


Figure 3.36: Infrared spectra of alanyl-alanine in H_2O at $\text{pH}=13$ (top), alanyl-alanine in D_2O at $\text{pD}=13$ (middle), and alanyl-alanine labelled with ^{13}C at the carbonyl carbon in H_2O at $\text{pH}=13$ (bottom).

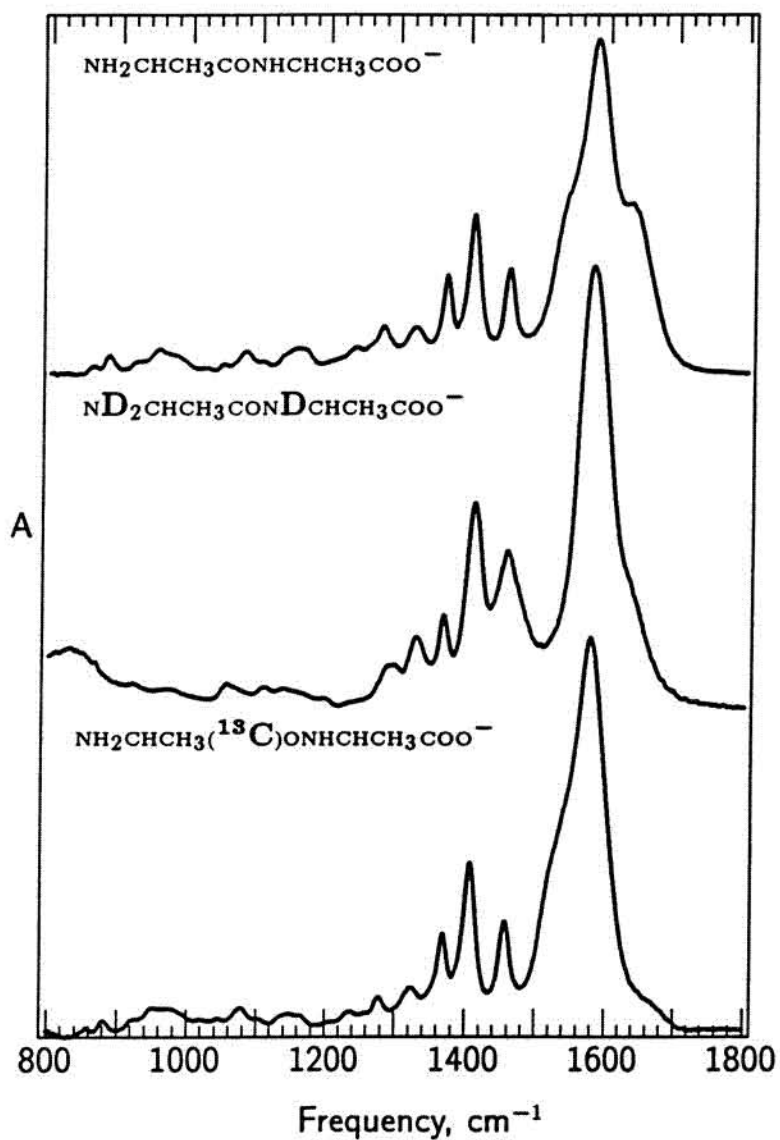


Figure 3.37: Optimized structures of alanyl-alanine zwitterion isolated and two-water supermolecules.

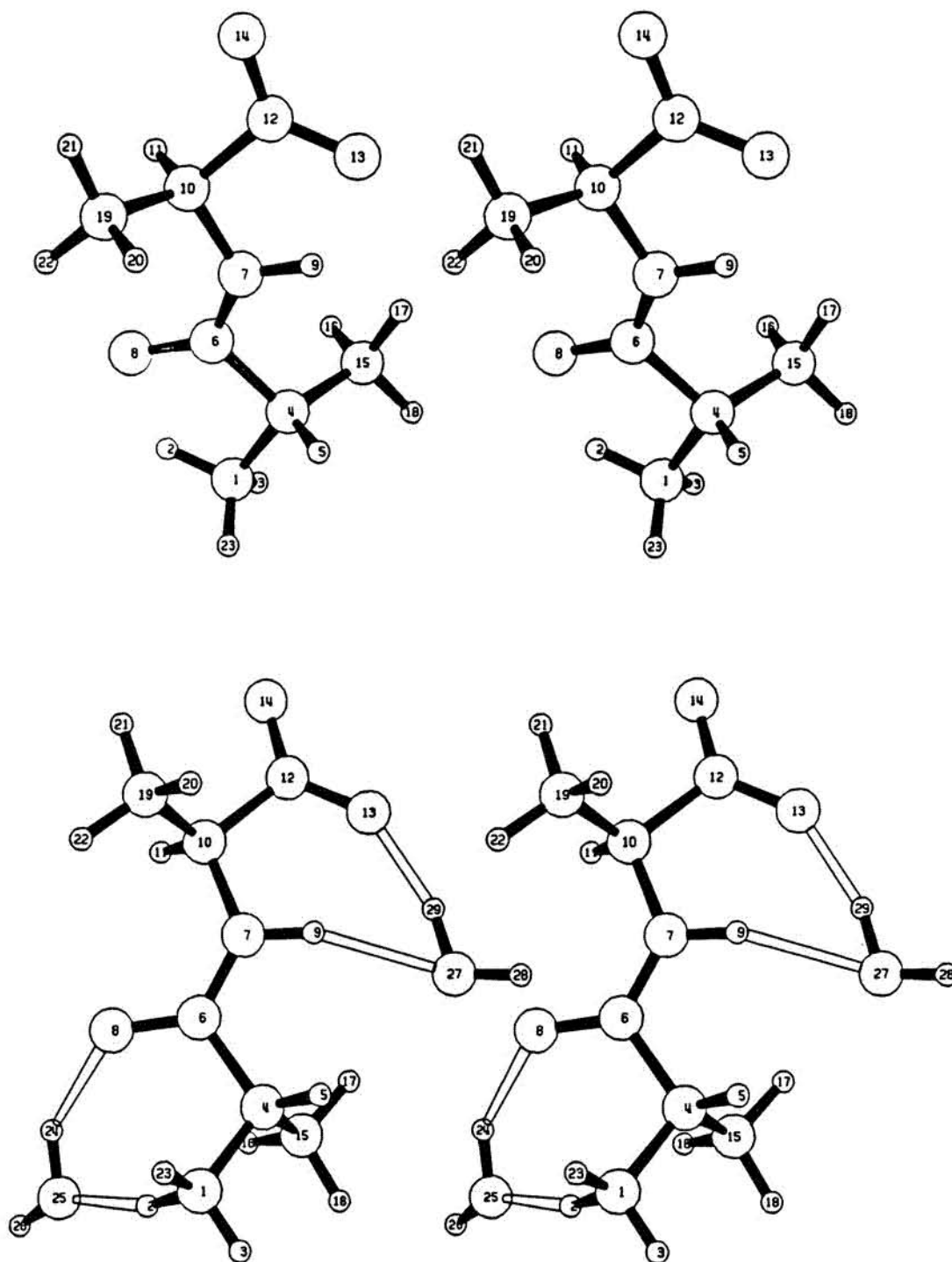


Figure 3.38: Raman spectra of alanyl-alanine in H_2O at $\text{pH}=7$ (top), alanyl-alanine in D_2O at $\text{pD}=7$ (second from top), alanyl-alanine labelled at the amine α -carbon with deuterium in H_2O at $\text{pH}=7$ (third from top), alanyl-alanine labelled with ^{13}C at the carbonyl carbon in H_2O at $\text{pH}=7$ (fourth from top), and alanyl-alanine labelled with ^{13}C at the carbonyl carbon in D_2O at $\text{pD}=7$ (bottom).

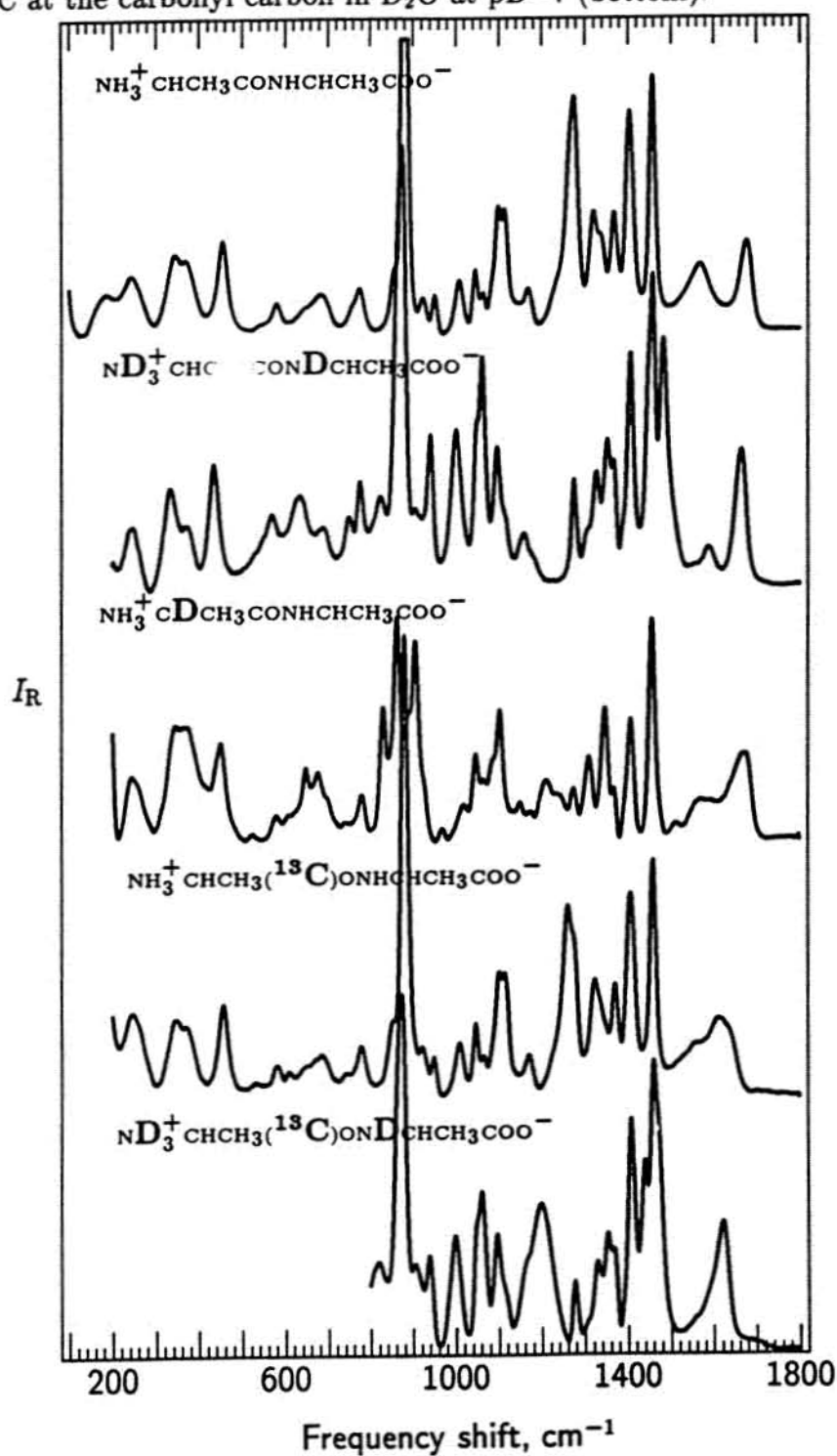


Figure 3.39: Infrared spectra of alanyl-alanine in H_2O at $\text{pH}=7$ (top), and alanyl-alanine in D_2O at $\text{pD}=7$ (bottom).

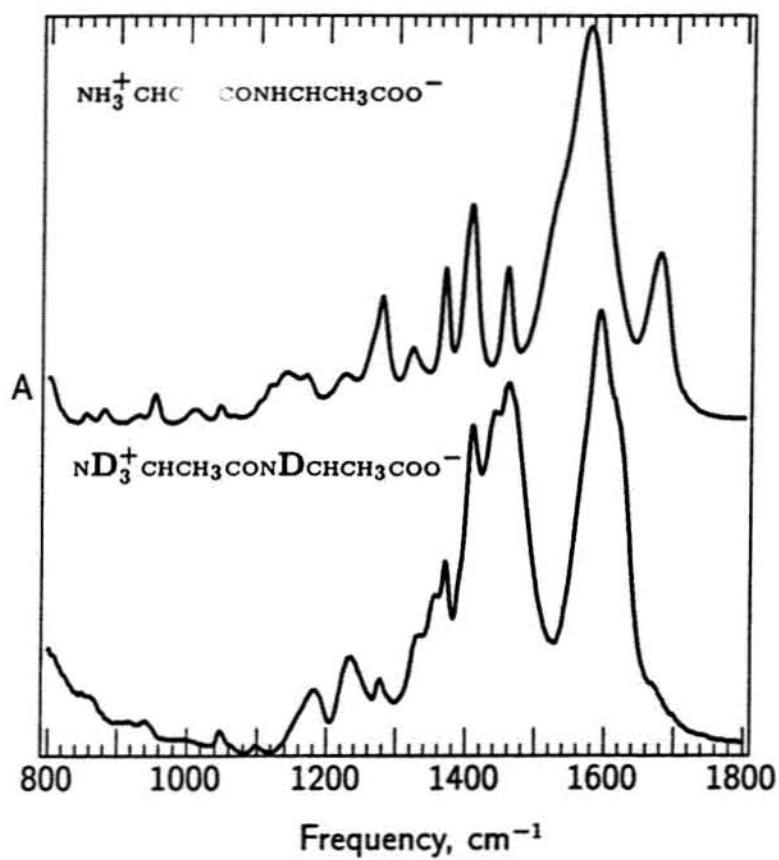


Figure 3.40: Optimized structures of alanyl-alanine at pH=1 isolated and two water supermolecules.

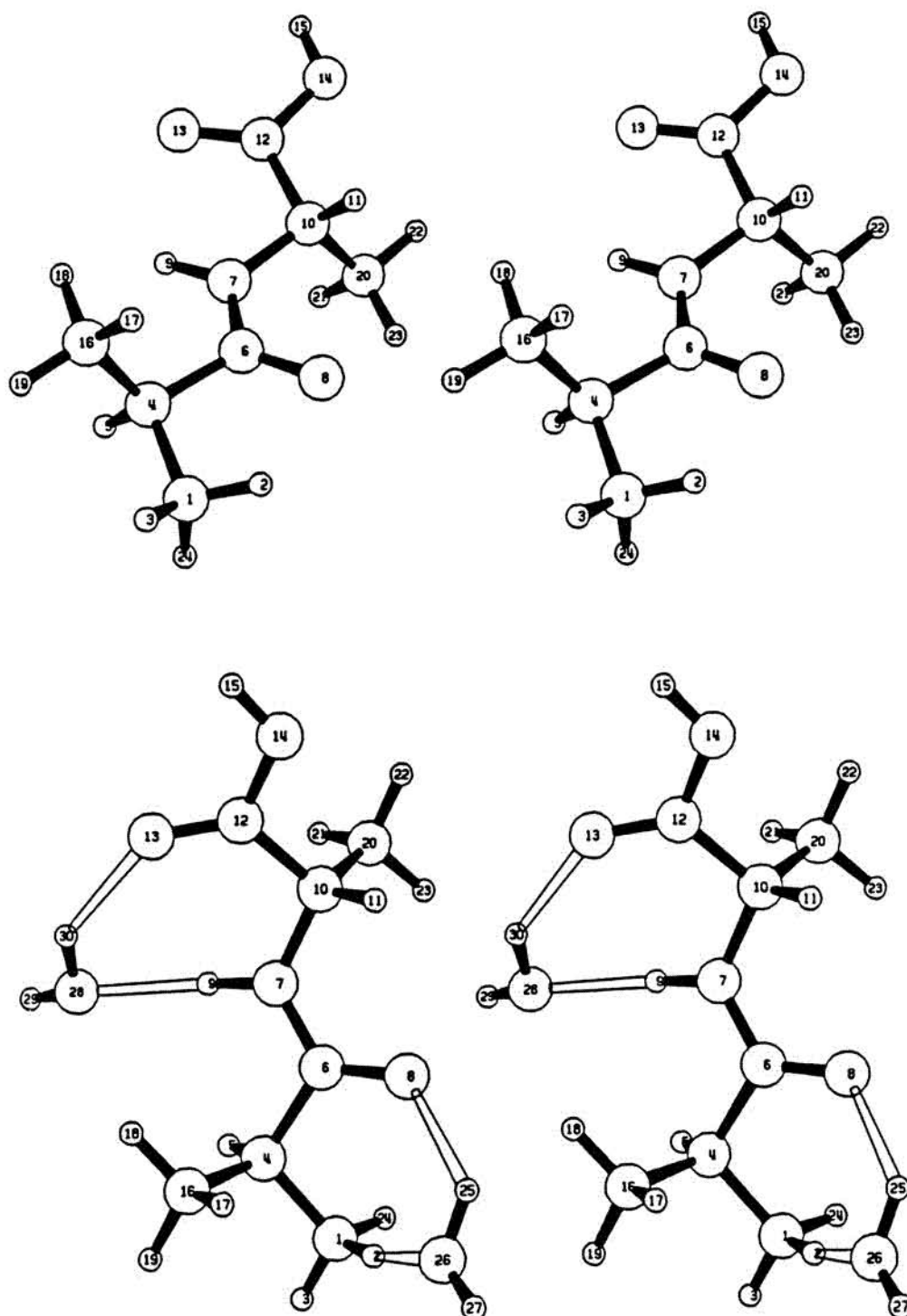


Figure 3.41: Raman spectra of alanyl-alanine in H_2O at $\text{pH}=1$ (top), alanyl-alanine in D_2O at $\text{pD}=1$ (upper middle), alanyl-alanine labelled at the amine α -C with deuterium in H_2O at $\text{pH}=1$ (lower middle), and alanyl-alanine labelled with ^{13}C at the carbonyl carbon in H_2O at $\text{pH}=1$ (bottom).

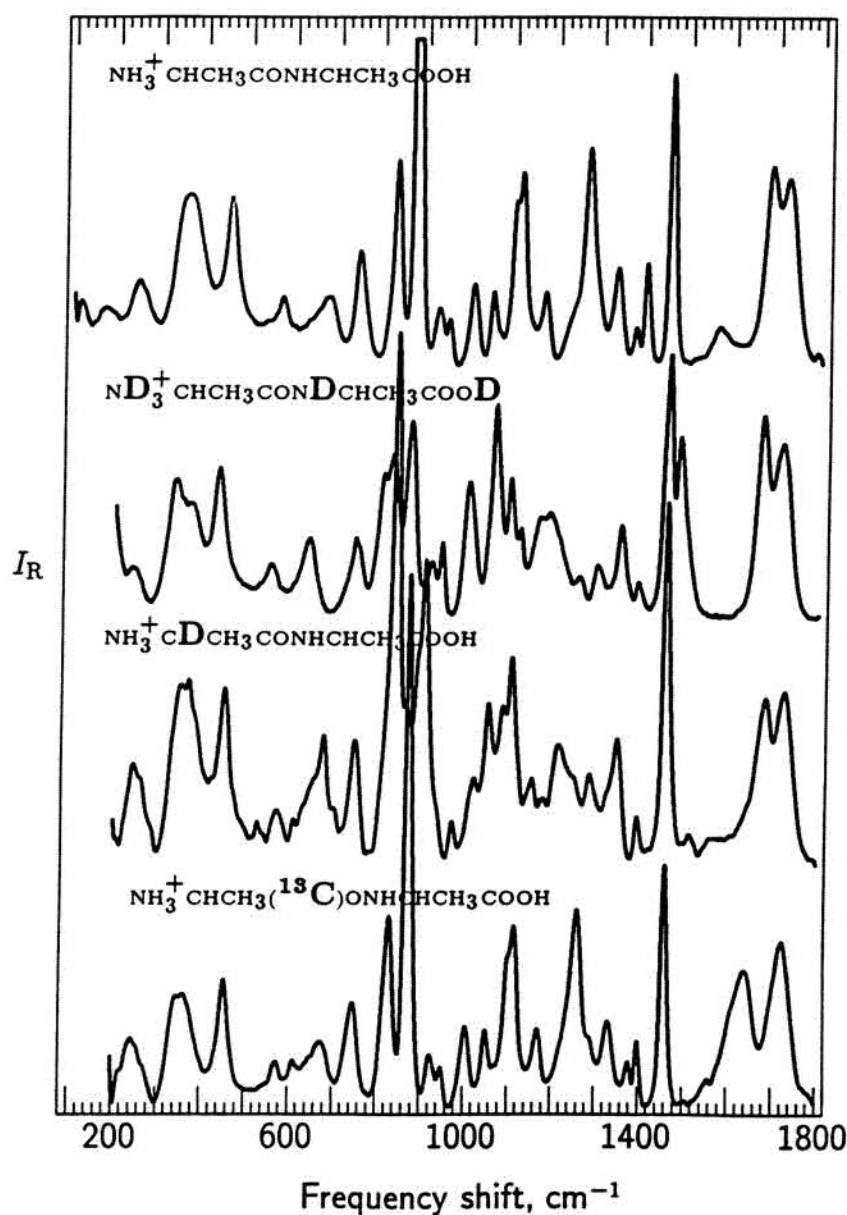


Figure 3.42: Infrared spectra of alanyl-alanine in H_2O at $\text{pH}=1$ (top), alanyl-alanine in D_2O at $\text{pD}=1$ (upper middle), alanyl-alanine labelled at the amine α -C with deuterium in H_2O at $\text{pH}=1$ (lower middle), and alanyl-alanine labelled with ^{13}C at the carbonyl carbon in H_2O at $\text{pH}=1$ (bottom).

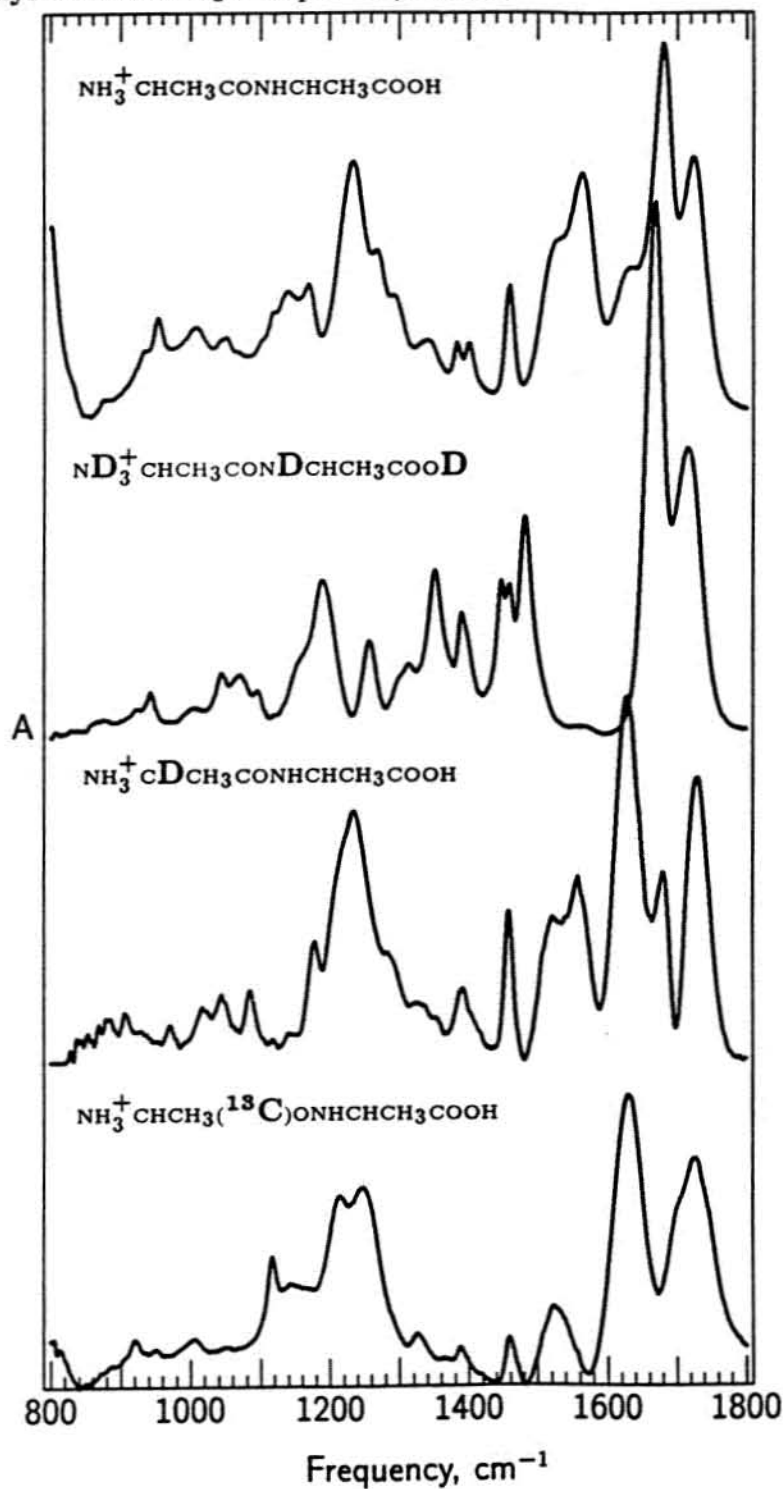


Table 3.71: Alanyl-alanine scale factors for isolated and two-water water-excluded structures.

Coordinate	Base		Neutral		Acid	
	iso	2w	iso	2w	iso	2w
CO ^a s ^a	0.7860	0.8347	0.8660	0.8570	0.7860	0.8347
CN ^a s	0.8870	0.8650	0.7350	0.8350	0.8870	0.8650
CC ^ψ s	0.8380	0.8400	1.0000	0.8500	0.8380	0.8400
NC ^φ s	0.9280	0.8780	0.9510	0.9000	0.9280	0.8780
NH ^a s	0.8100	0.8100	0.8400	0.8100	0.8100	0.6410
C ^{α1} H s	0.8360	0.8360	0.8360	0.8360	0.8360	0.6410
C ^{α2} H s	0.8360	0.8360	0.8360	0.8360	0.8360	0.6410
CC ^c s	0.9980	1.0050	1.0900	1.0000	0.9870	0.9800
CNHC sd	0.8700	0.7700	0.8900	0.7700	0.8700	0.7700
NH ^a ib	0.7500	0.7000	0.8010	0.7200	0.7500	0.7000
NH ^a ob	0.8780	0.6800	0.6100	0.7300	1.0300	0.6800
C ^{α1} H r ¹	0.7990	0.7820	0.8100	0.7890	0.7990	0.7820
C ^{α1} H r ²	0.7245	0.7245	0.7520	0.7450	0.7245	0.7245
C ^{α1} H d ¹	0.9770	0.9500	0.9700	0.9600	0.9770	0.9500
C ^{α1} H d ²	0.8343	0.8100	0.8850	0.8100	0.8343	0.8100
C ^{α1} H d ³	0.9167	0.9450	0.9500	0.9480	0.9167	0.9450
C ^{α2} H r ¹	0.7990	0.7820	0.8100	0.7890	0.7990	0.7820
C ^{α2} H r ²	0.7245	0.7245	0.7520	0.7450	0.7245	0.7245
C ^{α2} H d ¹	0.9770	0.9500	0.9700	0.9600	0.9770	0.9500
C ^{α2} H d ²	0.8343	0.8100	0.8850	0.8100	0.8343	0.8100
C ^{α2} H d ³	0.9167	0.9450	0.9500	0.9480	0.9167	0.9450
CO ^a sd	0.8570	0.7500	0.8500	0.7750	0.8570	0.7500
CO ^a r	0.8730	0.8488	0.7550	0.8620	0.8730	0.8488
CO ^a ob	0.8580	0.7650	0.8550	0.7900	0.8580	0.7650
CC ^c sd	0.8730	0.8770	0.8400	0.8850	0.8440	0.8640
CC ^c r	0.5600	0.6300	0.7500	0.9300	0.9650	0.9600
CC ^c ob	0.9428	0.9500	0.9220	0.9500	0.9260	0.9578
CC ^ψ t	1.0000	1.0000	1.0000	1.0000	1.0000	1.0000
C ^ω N t	0.7250	0.7250	0.7250	0.7250	0.7250	0.7250
NC ^φ t	0.7000	0.7000	0.7000	0.7000	0.7000	0.7000
CO ^c ss	0.9100	0.8860	1.0150	0.9270		
CO ^c as	0.7780	0.7660	0.6800	0.6980		
CO ^c s					0.7750	0.7770

Table 3.71: (continued)

Coordinate	Base		Neutral		Acid	
	iso	2w	iso	2w	iso	2w
CO ^H s					0.9230	0.9682
OH s					0.8000	0.5880
OH b					1.0990	1.1100
CN ⁿ s	0.8730	0.8810	0.9560	0.9020	0.9550	0.8900
NH ₂ ss	0.7000	0.7000				
NH ₂ as	0.7000	0.7000				
NH ₃ ss			0.7000	0.7000	0.6700	0.8000
NH ₃ as ¹			0.7000	0.7000	0.6000	0.8000
NH ₃ as ²			0.7000	0.7000	0.6000	0.8000
NH ₂ sis	0.7505	0.7175				
NH ₂ r	0.7695	0.8000				
NH ₂ w	1.7630	1.5200				
NH ₃ sd			0.7920	0.7190	0.8020	0.7190
NH ₃ ad ¹			0.7700	0.7450	0.7700	0.7550
NH ₃ ad ²			0.7700	0.7450	0.7700	0.7550
NH ₃ r ¹			0.8000	0.8100	0.8300	0.8100
NH ₃ r ²			0.6870	0.6850	0.7150	0.6850
CN ⁿ t	1.8000	1.0000	1.0000	1.0000	4.1000	1.0000
CC ^c t	1.0000	1.0000	1.0000	1.0000	1.0000	1.0000
COH t					1.0000	1.0000
CC ^{me} s	0.9140	0.9310	0.9350	0.9310	0.9140	0.9310
CH ₃ ss	0.8590	0.8489	0.8400	0.8590	0.8590	0.8400
CH ₃ as ^{1,2}	0.8475	0.8460	0.8294	0.8475	0.8467	0.8294
CH ₃ as ^{1,2}	0.8475	0.8460	0.8294	0.8475	0.8467	0.8294
CH ₃ sd	0.7680	0.7657	0.7620	0.7600	0.7680	0.7670
CH ₃ ad ^{1,2}	0.7674	0.7698	0.7700	0.7680	0.7730	0.7719
CH ₃ ad ^{1,2}	0.7674	0.7698	0.7700	0.7680	0.7730	0.7719
CH ₃ r ¹	0.8470	0.8260	0.8600	0.8360	0.8470	0.8260
CH ₃ r ²	0.7760	0.7535	0.7520	0.7620	0.7760	0.7535
CC ^{me} t	0.5000	0.5000	0.5000	0.5000	0.5000	0.5000
CC ^{me} s	0.9140	0.9310	0.9350	0.9310	0.9140	0.9310
CH ₃ ss	0.8590	0.8489	0.8400	0.8590	0.8590	0.8400
CH ₃ as ^{1,2}	0.8475	0.8460	0.8294	0.8475	0.8467	0.8294
CH ₃ as ^{1,2}	0.8475	0.8460	0.8294	0.8475	0.8467	0.8294

Table 3.71: (continued)

Coordinate	Base		Neutral		Acid	
	iso	2w	iso	2w	iso	2w
CH ₃ sd	0.7680	0.7657	0.7620	0.7600	0.7680	0.7670
CH ₃ ad ^{1,2}	0.7674	0.7698	0.7700	0.7680	0.7730	0.7719
CH ₃ ad ^{1,2}	0.7674	0.7698	0.7700	0.7680	0.7730	0.7719
CH ₃ r ¹	0.8470	0.8260	0.8600	0.8360	0.8470	0.8260
CH ₃ r ²	0.7760	0.7535	0.7520	0.7620	0.7760	0.7535
CC ^{me} t	0.5000	0.5000	0.5000	0.5000	0.5000	0.5000

^aAbbreviations: s = stretch, t = torsion, ss = symmetric stretch, as = antisymmetric stretch, d = deformation, sd = symmetric deformation, ad = antisymmetric deformation, r = rock, ib = in plane bend, ob = out of plane bend, w = wag, sis = scissor.

Table 3.72: Scaled 4-31G Frequencies and Potential Energy Distributions for Isolated Alanyl-alanine Structure in Base Conformation.

frequency (cm ⁻¹)			Ala-Ala pH 13 (mean deviation = 12 cm ⁻¹)
obs.	calc.	dev.	
			Potential Energy Distribution
—	34	—	CC ^ψ t(73), NC ^φ t(20)
—	66	—	CC ^c t(65), C ^ω N t(17)
—	73	—	C ^ω N t(44), NC ^φ t(28)
—	103	—	NC ^φ t(25), CC ^c t(22), CC ^ψ t(14), NH ^a ob(12), CNHC sd(9)
—	128	—	CNHC sd(29), CO ^a sd(19), C ^{α2} H d ³ (13), CC ^c t(12), NH ^a ob(10)
—	191	—	CC ^{me} t(96)
—	197	—	CC ^{me} t(94)
245	234	-11	C ^{α2} H d ² (29), C ^{α1} H d ² (12), CNHC sd(9), C ^{α2} H d ¹ (9)
245	249	4	C ^{α1} H d ² (28), CC ^c r(18), C ^{α2} H d ² (14), C ^{α2} H d ³ (9), CO ^a ob(7)
—	312	—	CC ^c r(28), C ^{α1} H d ² (20), CO ^a sd(15)
334	319	-15	C ^{α2} H d ² (23), C ^{α2} H d ³ (14), CC ^c s(12), C ^{α1} H d ³ (9)
334	343	9	CN ⁿ t(47), C ^{α1} H d ³ (13), CO ^a r(13)
377	371	-6	CN ⁿ t(28), C ^{α1} H d ³ (26), CC ^c r(16), CO ^a r(13)
464	445	-19	C ^{α2} H d ¹ (36), C ^ω N t(8)
464	468	4	C ^{α1} H d ¹ (55), C ^{α2} H d ¹ (9)
545	573	28	C ^{α2} H d ¹ (17), C ^{α2} H d ³ (15), CO ^a sd(15), CC ^c r(15), CC ^ψ s(10)
642	647	5	CC ^c sd(41), CC ^c s(21), CO ^a r(10)
688	699	11	CC ^ψ s(23), C ^{α1} H d ³ (19), CO ^a r(16)
761	764	3	CO ^a ob(46), C ^{α1} H d ² (9), C ^ω N t(8)
778	784	6	CC ^c ob(41), CO ^a ob(11), CC ^c sd(9), C ^{α2} H d ² (7)
—	835	—	NH ^a ob(49), NC ^φ t(12), C ^ω N t(11), CC ^c ob(9)
872	853	-19	CC ^c sd(14), CN ⁿ s(12), CC ^{me} s(12), CC ^c s(11), NH ₂ w(8), CO ^c ss(7)
884	885	1	CC ^c s(15), CC ^{me} s(13), CN ⁿ s(12), NH ₂ w(11), CC ^c sd(9), CO ^c ss(7)
920	935	15	CC ^{me} s(24), CH ₃ r ¹ (12), CC ^c s(8), NC ^φ s(7), CNHC sd(7)
952	954	2	CH ₃ r ² (19), CC ^ψ s(16), CH ₃ r ² (12), CO ^a r(11), NC ^φ s(10)
980	982	2	NH ₂ w(56), CH ₃ r ¹ (14), CC ^{me} s(12), CH ₃ r ² (7)
1019	1012	-7	CH ₃ r ² (39), NH ₂ r(19), CC ^{me} s(14), CN ⁿ s(12)
1069	1063	-6	C ^{α2} H r ² (31), CH ₃ r ² (20), CC ^c ob(11)

Table 3.72: (continued)

frequency (cm ⁻¹)			Potential Energy Distribution
obs.	calc.	dev.	
1104	1101	-3	CH ₃ r ¹ (22), CC ^{me} s(18), C ^{α1} H r ² (13), C ^{α1} H d ² (10), CN ⁿ s(9), CO ^a ob(8)
1136	1143	7	CC ^{me} s(22), NC ^φ s(15), C ^{α1} H r ² (13), NH ₂ r(11)
1136	1150	14	NH ₂ r(21), CC ^{me} s(14), CH ₃ r ¹ (13), C ^{α1} H r ² (12), CH ₃ r ¹ (8)
1166	1169	3	NC ^φ s(17), CH ₃ r ¹ (17), CH ₃ r ² (15), C ^{α2} H d ¹ (12), C ^{α2} H r ¹ (7)
1220	1225	5	C ^{α2} H r ² (31), NH ^a ib(24), CH ₃ r ² (8)
1260	1232	-28	CN ⁿ s(34), C ^{α1} H r ¹ (11), NH ₂ w(8), C ^{α1} H d ¹ (7), CH ₃ r ² (7)
1281	1308	27	C ^{α1} H r ² (21), NH ^a ib(12), C ^{α2} H r ² (10), NH ₂ r(9)
1320	1325	5	C ^{α1} H r ² (20), C ^{α1} H r ¹ (19), NH ^a ib(9), C ^{α2} H r ² (9), CH ₃ r ¹ (7)
1335	1341	6	C ^{α2} H r ¹ (66), C ^{α1} H r ¹ (8)
1367	1361	-6	CH ₃ sd(86), CO ^c ss(7)
1367	1374	7	CH ₃ sd(76), C ^{α1} H r ¹ (14)
1407	1383	-24	C ^{α1} H r ¹ (30), CH ₃ sd(20), NH ^a ib(10), NH ₂ r(9)
1407	1409	2	CO ^c ss(54), CC ^c s(13), CC ^c sd(10), CH ₃ sd(9)
1459	1454	-5	CH ₃ ad ^{1,2} (74), CH ₃ ad ^{1,2} (10)
1459	1456	-3	CH ₃ ad ^{1,2} (41), CH ₃ ad ^{1,2} (22), CH ₃ ad ^{1,2} (16), CH ₃ ad ^{1,2} (7)
1459	1460	1	CH ₃ ad ^{1,2} (70), CH ₃ ad ^{1,2} (7), CH ₃ r ¹ (7)
1459	1462	3	CH ₃ ad ^{1,2} (61), CH ₃ ad ^{1,2} (29)
1542	1539	-3	NH ^a ib(32), CN ^a s(20), CO ^a s(17), CC ^ψ s(7)
1578	1573	-5	NH ₂ sis(80), CN ^a s(9)
1602	1603	1	CO ^c as(83)
1638	1652	14	CO ^a s(42), CN ^a s(28), NH ₂ sis(15)
—	2923	—	C ^{α1} H s(95)
—	2940	—	CH ₃ ss(84), CH ₃ as ^{1,2} (10)
—	2941	—	C ^{α2} H s(86), CH ₃ as ^{1,2} (7)
—	2952	—	CH ₃ ss(81), CH ₃ as ^{1,2} (10), C ^{α2} H s(9)
—	2984	—	CH ₃ as ^{1,2} (50), CH ₃ as ^{1,2} (38), CH ₃ ss(10)
—	2998	—	CH ₃ as ^{1,2} (73), CH ₃ as ^{1,2} (13), CH ₃ ss(11)
—	3008	—	CH ₃ as ^{1,2} (58), CH ₃ as ^{1,2} (39)
—	3027	—	CH ₃ as ^{1,2} (87), CH ₃ as ^{1,2} (10)
—	3150	—	NH ₂ ss(99)
—	3250	—	NH ₂ as(100)
—	3355	—	NH ^a s(99)

Table 3.72: (continued)

frequency (cm^{-1})			Potential Energy Distribution
obs.	calc.	dev.	
frequency (cm^{-1})			Ala-Ala in D_2O (mean deviation = 15 cm^{-1})
obs.	calc.	dev.	
—	33	—	$\text{CC}^\psi \text{ t}(73)$, $\text{NC}^\phi \text{ t}(20)$
—	65	—	$\text{CC}^c \text{ t}(62)$, $\text{C}^\omega\text{N} \text{ t}(18)$, $\text{NC}^\phi \text{ t}(7)$
—	72	—	$\text{C}^\omega\text{N} \text{ t}(44)$, $\text{NC}^\phi \text{ t}(28)$
—	101	—	$\text{NC}^\phi \text{ t}(25)$, $\text{CC}^c \text{ t}(24)$, $\text{CC}^\psi \text{ t}(12)$, $\text{CNHC} \text{ sd}(10)$, $\text{NH}^a \text{ ob}(10)$
—	125	—	$\text{CNHC} \text{ sd}(28)$, $\text{CO}^a \text{ sd}(19)$, $\text{CC}^c \text{ t}(14)$, $\text{C}^{\alpha 2}\text{H} \text{ d}^3(13)$, $\text{NH}^a \text{ ob}(9)$
—	191	—	$\text{CC}^{me} \text{ t}(96)$
—	196	—	$\text{CC}^{me} \text{ t}(93)$
225	232	7	$\text{C}^{\alpha 2}\text{H} \text{ d}^2(23)$, $\text{C}^{\alpha 1}\text{H} \text{ d}^2(11)$, $\text{CNHC} \text{ sd}(9)$, $\text{C}^{\alpha 2}\text{H} \text{ d}^1(8)$, $\text{CN}^n \text{ t}(8)$
251	242	−9	$\text{CN}^n \text{ t}(21)$, $\text{CC}^c \text{ r}(19)$, $\text{C}^{\alpha 2}\text{H} \text{ d}^2(17)$, $\text{C}^{\alpha 2}\text{H} \text{ d}^3(12)$, $\text{C}^{\alpha 1}\text{H} \text{ d}^2(9)$
251	260	9	$\text{CN}^n \text{ t}(57)$, $\text{C}^{\alpha 1}\text{H} \text{ d}^2(23)$
—	309	—	$\text{C}^{\alpha 2}\text{H} \text{ d}^2(20)$, $\text{C}^{\alpha 1}\text{H} \text{ d}^3(15)$, $\text{C}^{\alpha 1}\text{H} \text{ d}^2(12)$, $\text{CC}^c \text{ r}(11)$, $\text{C}^{\alpha 2}\text{H} \text{ d}^3(10)$, $\text{CO}^a \text{ sd}(9)$
332	317	−15	$\text{CC}^c \text{ r}(15)$, $\text{CC}^c \text{ s}(10)$, $\text{NC}^\phi \text{ s}(8)$, $\text{CO}^a \text{ sd}(8)$, $\text{C}^{\alpha 1}\text{H} \text{ d}^1(7)$
380	347	−33	$\text{C}^{\alpha 1}\text{H} \text{ d}^3(29)$, $\text{CO}^a \text{ r}(21)$, $\text{CC}^c \text{ r}(14)$, $\text{CNHC} \text{ sd}(9)$
447	424	−23	$\text{C}^{\alpha 2}\text{H} \text{ d}^1(30)$, $\text{C}^\omega\text{N} \text{ t}(12)$, $\text{CC}^c \text{ r}(11)$, $\text{C}^{\alpha 1}\text{H} \text{ d}^1(10)$, $\text{C}^{\alpha 2}\text{H} \text{ d}^3(7)$
447	444	−3	$\text{C}^{\alpha 1}\text{H} \text{ d}^1(45)$, $\text{C}^{\alpha 2}\text{H} \text{ d}^1(15)$
534	552	18	$\text{C}^{\alpha 2}\text{H} \text{ d}^3(16)$, $\text{CC}^c \text{ r}(16)$, $\text{CO}^a \text{ sd}(15)$, $\text{C}^{\alpha 2}\text{H} \text{ d}^1(11)$, $\text{CC}^\psi \text{ s}(8)$
—	625	—	$\text{NH}^a \text{ ob}(49)$, $\text{NC}^\phi \text{ t}(15)$, $\text{C}^\omega\text{N} \text{ t}(9)$, $\text{C}^{\alpha 2}\text{H} \text{ d}^1(8)$
645	636	−9	$\text{CO}^a \text{ r}(22)$, $\text{CC}^c \text{ sd}(19)$, $\text{CC}^c \text{ s}(12)$, $\text{NH}_2 \text{ r}(11)$, $\text{C}^{\alpha 1}\text{H} \text{ d}^3(9)$, $\text{CC}^\psi \text{ s}(7)$
687	665	−22	$\text{CC}^c \text{ sd}(27)$, $\text{CC}^\psi \text{ s}(18)$, $\text{NH}_2 \text{ r}(11)$, $\text{CC}^c \text{ s}(9)$
760	744	−16	$\text{NH}_2 \text{ w}(77)$, $\text{CC}^{me} \text{ s}(7)$
778	780	2	$\text{CO}^a \text{ ob}(59)$, $\text{C}^{\alpha 1}\text{H} \text{ d}^2(9)$
778	786	8	$\text{CC}^c \text{ ob}(54)$, $\text{CC}^c \text{ sd}(10)$, $\text{C}^{\alpha 2}\text{H} \text{ d}^2(7)$
866	855	−11	$\text{CC}^c \text{ sd}(15)$, $\text{CC}^c \text{ s}(13)$, $\text{NH}_2 \text{ r}(11)$, $\text{CO}^a \text{ r}(9)$, $\text{CO}^c \text{ ss}(8)$
884	874	−10	$\text{NH}_2 \text{ r}(37)$, $\text{CC}^{me} \text{ s}(20)$, $\text{CH}_3 \text{ r}^1(12)$

Table 3.72: (continued)

frequency (cm ⁻¹)			Potential Energy Distribution
obs.	calc.	dev.	
904	898	-6	CC ^{me} s(13), CC ^c s(10), CH ₃ r ¹ (9), CH ₃ r ² (8), CN ⁿ s(7)
904	918	14	CC ^{me} s(19), NH ^a ib(18), CH ₃ r ¹ (11), NC ^φ s(10), CC ^c s(10), CH ₃ r ² (7)
938	937	-1	CH ₃ r ² (27), CN ⁿ s(16), CO ^a s(10), CC ^ψ s(8), NH ^a ib(7)
995	997	2	NH ^a ib(39), CH ₃ r ² (21), CC ^ψ s(9), CH ₃ r ² (8)
1066	1068	2	C ^{α2} H r ² (30), CH ₃ r ² (11), CC ^c ob(9)
1066	1075	9	C ^{α1} H r ² (23), CH ₃ r ² (15), C ^{α2} H r ² (8), NH ₂ r(7)
1097	1090	-7	CC ^{me} s(31), NH ₂ sis(20), CH ₃ r ¹ (16), CN ⁿ s(9)
1113	1142	29	CC ^{me} s(33), NC ^φ s(21), CH ₃ r ¹ (12)
1163	1164	1	CH ₃ r ¹ (23), C ^{α2} H d ¹ (15), CH ₃ r ² (15), NC ^φ s(10)
1163	1181	18	NH ₂ sis(62), CH ₃ r ¹ (11)
1209	1210	1	CN ⁿ s(36), C ^{α1} H r ¹ (13), NH ₂ sis(11)
1278	1272	-6	C ^{α2} H r ² (38), CH ₃ r ¹ (10), C ^{α2} H r ¹ (7), CH ₃ r ² (7)
1308	1303	-5	C ^{α1} H r ² (56), CH ₃ r ¹ (10)
1328	1339	11	C ^{α2} H r ¹ (72), C ^{α2} H r ² (8)
1360	1353	-7	C ^{α1} H r ¹ (73)
1365	1361	-4	CH ₃ sd(87)
1371	1375	4	CH ₃ sd(96)
1409	1408	-1	CO ^c ss(56), CC ^c s(13), CC ^c sd(10), CH ₃ sd(9)
1455	1452	-3	CH ₃ ad ^{1,2} (84)
1455	1456	1	CH ₃ ad ^{1,2} (47), CH ₃ ad ^{1,2} (25), CH ₃ ad ^{1,2} (12)
1455	1458	3	CH ₃ ad ^{1,2} (76), CH ₃ r ¹ (8), CH ₃ ad ^{1,2} (7)
1455	1462	7	CH ₃ ad ^{1,2} (58), CH ₃ ad ^{1,2} (31)
1512	1496	-16	CN ^a s(28), CO ^a s(22), CC ^ψ s(11), NC ^φ s(9), NH ^a ib(8), CO ^a r(7)
1596	1597	1	CO ^c as(87)
1638	1637	-1	CO ^a s(48), CN ^a s(35)
—	2274	—	NH ₂ ss(99)
—	2402	—	NH ₂ as(100)
—	2462	—	NH ^a s(98)
—	2923	—	C ^{α1} H s(95)
—	2940	—	CH ₃ ss(84), CH ₃ as ^{1,2} (10)
—	2941	—	C ^{α2} H s(86), CH ₃ as ^{1,2} (7)
—	2952	—	CH ₃ ss(81), CH ₃ as ^{1,2} (10), C ^{α2} H s(9)

Table 3.72: (continued)

frequency (cm ⁻¹)			Potential Energy Distribution
obs.	calc.	dev.	
—	2984	—	CH ₃ as ^{1,2} (50), CH ₃ as ^{1,2} (39), CH ₃ ss(10)
—	2998	—	CH ₃ as ^{1,2} (73), CH ₃ as ^{1,2} (13), CH ₃ ss(11)
—	3008	—	CH ₃ as ^{1,2} (58), CH ₃ as ^{1,2} (39)
—	3027	—	CH ₃ as ^{1,2} (87), CH ₃ as ^{1,2} (10)

frequency (cm ⁻¹)			2-d-Ala-Ala (mean deviation = 15 cm ⁻¹) Potential Energy Distribution
obs.	calc.	dev.	
—	33	—	CC ^ψ t(73), NC ^φ t(20)
—	65	—	CC ^c t(64), C ^ω N t(18)
—	73	—	C ^ω N t(44), NC ^φ t(28)
—	103	—	NC ^φ t(25), CC ^c t(22), CC ^ψ t(14), NH ^a ob(12), CNHC sd(10)
—	127	—	CNHC sd(28), CO ^a sd(19), C ^{α2} H d ³ (13), CC ^c t(13), NH ^a ob(10)
—	191	—	CC ^{me} t(96)
—	197	—	CC ^{me} t(94)
251	234	-17	C ^{α2} H d ² (28), C ^{α1} H d ² (13), CNHC sd(9), C ^{α2} H d ¹ (9)
251	248	-3	C ^{α1} H d ² (28), CC ^c r(18), C ^{α2} H d ² (15), C ^{α2} H d ³ (9), CO ^a ob(7)
—	309	—	CC ^c r(28), C ^{α1} H d ² (20), CO ^a sd(16)
337	319	-18	C ^{α2} H d ² (23), C ^{α2} H d ³ (13), CC ^c s(12), C ^{α1} H d ³ (9)
337	342	5	CN ⁿ t(50), C ^{α1} H d ³ (12), CO ^a r(11)
387	371	-16	C ^{α1} H d ³ (27), CN ⁿ t(27), CC ^c r(16), CO ^a r(13)
460	443	-17	C ^{α2} H d ¹ (35), C ^ω N t(8), C ^{α2} H d ³ (7), CC ^c r(7)
460	465	5	C ^{α1} H d ¹ (55), C ^{α2} H d ¹ (8)
534	567	33	C ^{α2} H d ¹ (18), CC ^c r(15), C ^{α2} H d ³ (14), CO ^a sd(13), CC ^ψ s(11)
640	646	6	CC ^c sd(39), CC ^c s(21), CO ^a r(11)
678	688	10	CC ^ψ s(23), C ^{α1} H d ³ (18), CO ^a r(14)
743	742	-1	CO ^a ob(42), C ^{α1} H r ² (24), C ^{α1} H d ² (9), CH ₃ r ¹ (8)
778	781	3	CC ^c ob(41), CC ^c sd(11), NH ^a ob(8), C ^{α2} H d ² (8), CC ^{me} s(7)
800	813	13	CC ^{me} s(21), NH ^a ob(16), C ^{α1} H r ² (16), CC ^c ob(9), C ^ω N t(7), NC ^φ t(7)

Table 3.72: (continued)

frequency (cm ⁻¹)			Potential Energy Distribution
obs.	calc.	dev.	
829	845	16	NH ^a ob(31), CC ^{me} s(16), NC ^φ t(8)
866	863	-3	CC ^c s(16), CC ^c sd(16), CO ^c ss(9), CC ^{me} s(9), C ^{α1} H r ² (8)
884	912	28	C ^{α1} H r ² (16), C ^{α1} H r ¹ (13), CO ^a ob(10), NH ₂ w(10), CC ^c s(9), CH ₃ r ² (9)
909	927	18	C ^{α1} H r ¹ (45), NH ₂ w(21), CN ⁿ s(18)
927	936	9	CC ^{me} s(22), CH ₃ r ¹ (12), CNHC sd(8)
944	960	16	CH ₃ r ² (16), CH ₃ r ² (15), CC ^ψ s(11), NH ₂ w(10), CO ^a r(9), NC ^φ s(8)
981	1001	20	CH ₃ r ² (41), NH ₂ w(30), CN ⁿ s(10)
1065	1063	-2	C ^{α2} H r ² (30), CH ₃ r ² (18), CC ^c ob(10)
1101	1069	-32	CC ^{me} s(27), NH ₂ r(20), C ^{α1} H r ¹ (15), C ^{α1} H r ² (11), NH ₂ w(7)
1132	1112	-20	CH ₃ r ¹ (43), CC ^{me} s(14), CN ⁿ s(10), C ^{α1} H d ² (8)
1154	1147	-7	CC ^{me} s(35), CH ₃ r ¹ (19), NC ^φ s(14)
1195	1170	-25	NC ^φ s(20), CH ₃ r ¹ (17), CH ₃ r ² (16), C ^{α2} H d ¹ (12), C ^{α2} H r ¹ (8)
1239	1224	-15	C ^{α2} H r ² (31), NH ^a ib(24), CH ₃ r ² (7)
1239	1245	6	CN ⁿ s(27), NH ₂ r(18), CH ₃ r ¹ (15), C ^{α1} H d ³ (9)
1273	1287	14	NH ₂ r(23), CH ₃ r ² (10), NC ^φ s(7)
1304	1329	25	C ^{α2} H r ¹ (27), C ^{α2} H r ² (17), NH ^a ib(15), CH ₃ r ¹ (8)
1343	1348	5	C ^{α2} H r ¹ (43), NH ^a ib(13)
1369	1361	-8	CH ₃ sd(85)
1369	1376	7	CH ₃ sd(92)
1408	1408	0	CO ^c ss(55), CC ^c s(13), CC ^c sd(10), CH ₃ sd(9)
1458	1453	-5	CH ₃ ad ^{1,2} (85)
1458	1456	-2	CH ₃ ad ^{1,2} (44), CH ₃ ad ^{1,2} (23), CH ₃ ad ^{1,2} (22)
1458	1458	0	CH ₃ ad ^{1,2} (63), CH ₃ ad ^{1,2} (13), CH ₃ ad ^{1,2} (7), CH ₃ ad ^{1,2} (7)
1458	1462	4	CH ₃ ad ^{1,2} (61), CH ₃ ad ^{1,2} (29)
1544	1539	-5	NH ^a ib(32), CN ^a s(20), CO ^a s(17), CC ^ψ s(7)
1583	1571	-12	NH ₂ sis(79), CN ^a s(10)
1605	1602	-3	CO ^c as(82)
1644	1649	5	CO ^a s(42), CN ^a s(28), NH ₂ sis(16)
—	2158	—	C ^{α1} H s(98)
—	2939	—	CH ₃ ss(86), CH ₃ as ^{1,2} (11)
—	2941	—	C ^{α2} H s(86), CH ₃ as ^{1,2} (7)
—	2952	—	CH ₃ ss(81), CH ₃ as ^{1,2} (10), C ^{α2} H s(9)

Table 3.72: (continued)

frequency (cm ⁻¹)			Potential Energy Distribution
obs.	calc.	dev.	
—	2983	—	CH ₃ as ^{1,2} (47), CH ₃ as ^{1,2} (43), CH ₃ ss(11)
—	2998	—	CH ₃ as ^{1,2} (73), CH ₃ as ^{1,2} (13), CH ₃ ss(11)
—	3007	—	CH ₃ as ^{1,2} (56), CH ₃ as ^{1,2} (43)
—	3027	—	CH ₃ as ^{1,2} (87), CH ₃ as ^{1,2} (10)
—	3150	—	NH ₂ ss(99)
—	3250	—	NH ₂ as(100)
—	3355	—	NH ^a s(99)

frequency (cm ⁻¹)			Ala-Ala- ¹³ C in amide carbon (mean deviation = 12 cm ⁻¹)
obs.	calc.	dev.	
—	33	—	CC ^ψ t(73), NC ^φ t(20)
—	66	—	CC ^c t(65), C ^ω N t(17)
—	73	—	C ^ω N t(44), NC ^φ t(28)
—	103	—	NC ^φ t(25), CC ^c t(22), CC ^ψ t(14), NH ^a ob(12), CNHC sd(9)
—	127	—	CNHC sd(29), CO ^a sd(19), C ^{α2} H d ³ (13), CC ^c t(12), NH ^a ob(10)
—	191	—	CC ^{me} t(96)
—	197	—	CC ^{me} t(94)
236	234	-2	C ^{α2} H d ² (29), C ^{α1} H d ² (12), CNHC sd(9), C ^{α2} H d ¹ (9)
236	249	13	C ^{α1} H d ² (28), CC ^c r(18), C ^{α2} H d ² (14), C ^{α2} H d ³ (9), CO ^a sd(7), CO ^a ob(7)
—	311	—	CC ^c r(28), C ^{α1} H d ² (20), CO ^a sd(15)
334	319	-15	C ^{α2} H d ² (22), C ^{α2} H d ³ (13), CC ^c s(12), C ^{α1} H d ³ (9)
334	343	9	CN ⁿ t(48), C ^{α1} H d ³ (13), CO ^a r(12)
376	371	-5	CN ⁿ t(28), C ^{α1} H d ³ (26), CC ^c r(16), CO ^a r(13)
467	444	-23	C ^{α2} H d ¹ (36), C ^ω N t(8)
467	467	0	C ^{α1} H d ¹ (54), C ^{α2} H d ¹ (9)
542	572	30	C ^{α2} H d ¹ (17), C ^{α2} H d ³ (15), CO ^a sd(15), CC ^c r(15), CC ^ψ s(10)
644	646	2	CC ^c sd(40), CC ^c s(21), CO ^a r(11)
687	697	10	CC ^ψ s(22), C ^{α1} H d ³ (19), CO ^a r(15)
748	748	0	CO ^a ob(55), C ^{α1} H d ² (11)
778	782	4	CC ^c ob(44), CC ^c sd(11), C ^{α2} H d ² (8), CC ^{me} s(7)

Table 3.72: (continued)

frequency (cm ⁻¹)			Potential Energy Distribution
obs.	calc.	dev.	
—	833	—	NH ^a ob(47), NC ^φ t(12), C ^ω N t(11), CC ^c ob(10)
850	851	1	CC ^c sd(14), CN ⁿ s(12), CC ^{me} s(12), CC ^c s(10), CO ^c ss(7), NH ₂ w(7)
883	885	2	CC ^c s(15), CC ^{me} s(13), CN ⁿ s(11), NH ₂ w(11), CC ^c sd(9), CO ^c ss(7)
920	934	14	CC ^{me} s(22), CH ₃ r ¹ (12), CNHC sd(8), CO ^a r(8)
943	949	6	CH ₃ r ² (21), CC ^ψ s(16), NC ^φ s(12), CH ₃ r ² (11), CO ^a r(9)
980	982	2	NH ₂ w(56), CH ₃ r ¹ (14), CC ^{me} s(12), CH ₃ r ² (7)
1021	1012	-9	CH ₃ r ² (40), NH ₂ r(19), CC ^{me} s(13), CN ⁿ s(12)
1066	1063	-3	C ^{α2} H r ² (31), CH ₃ r ² (20), CC ^c ob(11)
1103	1098	-5	CH ₃ r ¹ (22), CC ^{me} s(19), C ^{α1} H r ² (14), C ^{α1} H d ² (10), CN ⁿ s(10), CO ^a ob(7)
1129	1141	12	CC ^{me} s(23), NC ^φ s(16), C ^{α1} H r ² (10), NH ₂ r(8)
1129	1150	21	NH ₂ r(23), C ^{α1} H r ² (13), CC ^{me} s(11), CH ₃ r ¹ (11), CH ₃ r ¹ (9), C ^{α1} H r ¹ (7)
1166	1168	2	CH ₃ r ¹ (19), CH ₃ r ² (15), NC ^φ s(13), C ^{α2} H d ¹ (12), C ^{α2} H r ¹ (7)
1221	1223	2	C ^{α2} H r ² (30), NH ^a ib(25), CH ₃ r ² (7)
1256	1231	-25	CN ⁿ s(35), C ^{α1} H r ¹ (10), NH ₂ w(9), C ^{α1} H d ¹ (8), CH ₃ r ² (7)
1279	1304	25	C ^{α1} H r ² (15), NH ^a ib(12), C ^{α2} H r ² (12), CN ^a s(8), NC ^φ s(8), NH ₂ r(7)
1321	1324	3	C ^{α1} H r ² (26), C ^{α1} H r ¹ (19), CH ₃ r ¹ (9)
1327	1340	13	C ^{α2} H r ¹ (70)
1368	1361	-7	CH ₃ sd(87), CO ^c ss(7)
1368	1374	6	CH ₃ sd(68), C ^{α1} H r ¹ (18)
1408	1381	-27	C ^{α1} H r ¹ (29), CH ₃ sd(28), NH ₂ r(9)
1408	1408	0	CO ^c ss(55), CC ^c s(13), CC ^c sd(10), CH ₃ sd(9)
1458	1454	-4	CH ₃ ad ^{1,2} (68), CH ₃ ad ^{1,2} (15)
1458	1456	-2	CH ₃ ad ^{1,2} (37), CH ₃ ad ^{1,2} (20), CH ₃ ad ^{1,2} (16), CH ₃ ad ^{1,2} (14)
1458	1460	2	CH ₃ ad ^{1,2} (71), CH ₃ ad ^{1,2} (7), CH ₃ r ¹ (7)
1458	1462	4	CH ₃ ad ^{1,2} (61), CH ₃ ad ^{1,2} (29)
1522	1522	0	NH ^a ib(37), CO ^a s(20), CN ^a s(15)
1560	1563	3	NH ₂ sis(56), CN ^a s(20), CO ^a s(14)
1594	1601	7	CO ^c as(76), NH ₂ sis(7)
1610	1621	11	NH ₂ sis(34), CO ^a s(28), CN ^a s(18), CO ^c as(9)

Table 3.72: (continued)

frequency (cm^{-1})			Potential Energy Distribution
obs.	calc.	dev.	
—	2923	—	$\text{C}^{\alpha 1}\text{H}$ s(95)
—	2940	—	CH_3 ss(84), CH_3 as ^{1,2} (10)
—	2941	—	$\text{C}^{\alpha 2}\text{H}$ s(86), CH_3 as ^{1,2} (7)
—	2952	—	CH_3 ss(81), CH_3 as ^{1,2} (10), $\text{C}^{\alpha 2}\text{H}$ s(9)
—	2984	—	CH_3 as ^{1,2} (50), CH_3 as ^{1,2} (38), CH_3 ss(10)
—	2998	—	CH_3 as ^{1,2} (73), CH_3 as ^{1,2} (13), CH_3 ss(11)
—	3008	—	CH_3 as ^{1,2} (58), CH_3 as ^{1,2} (39)
—	3027	—	CH_3 as ^{1,2} (87), CH_3 as ^{1,2} (10)
—	3150	—	NH_2 ss(99)
—	3250	—	NH_2 as(100)
—	3355	—	NH^a s(99)

Table 3.73: Scaled 4-31G Frequencies and Potential Energy Distribution for Water-Excluded Alanyl-alanine Two-water Supermolecule in Base.

frequency (cm ⁻¹)			Ala-ala pH 13 (mean deviation = 12 cm ⁻¹)
obs.	calc.	dev.	
			Potential Energy Distribution
—	54	—	NC ^φ t(28), CC ^c t(28), CC ^ψ t(23), NH ^a ob(10)
—	93	—	CC ^c t(53), CC ^ψ t(33), C ^ω N t(15)
—	97	—	NC ^φ t(37), C ^ω N t(35), CC ^ψ t(7)
—	133	—	CC ^ψ t(31), NH ^a ob(26), NC ^φ t(17), CC ^c t(15), C ^{α2} H d ¹ (7)
—	170	—	CNHC sd(34), CO ^a sd(19), C ^{α2} H d ³ (17), CC ^{me} t(14), CC ^c r(10)
—	193	—	CC ^{me} t(87)
—	197	—	CC ^{me} t(79)
245	246	1	C ^{α2} H d ² (27), C ^{α1} H d ² (14)
245	264	19	C ^{α1} H d ² (21), C ^{α1} H d ³ (18), C ^{α2} H d ² (16), CO ^a ob(11), CC ^c r(7)
—	284	—	C ^{α1} H d ² (21), CO ^a sd(20), CC ^c r(14), CN ⁿ t(12), CO ^a r(7)
334	316	-18	C ^{α2} H d ² (19), CC ^c s(12), C ^{α1} H d ¹ (8), C ^{α1} H d ³ (8)
334	335	1	CN ⁿ t(33), CC ^c r(19), CNHC sd(9), CO ^a r(8)
377	353	-24	CN ⁿ t(39), C ^{α1} H d ³ (17), CO ^a r(15)
464	447	-17	C ^{α2} H d ¹ (33), CC ^c r(12), C ^{α2} H d ³ (9), C ^{α1} H d ¹ (8)
464	467	3	C ^{α1} H d ¹ (45), C ^{α2} H d ¹ (16)
545	573	28	C ^{α2} H d ¹ (16), C ^{α2} H d ³ (16), CO ^a sd(16), CC ^c r(16), CC ^ψ s(7)
642	646	4	CC ^c sd(40), CC ^c s(18), CO ^a r(13)
688	701	13	CC ^ψ s(18), CO ^a r(16), C ^{α1} H d ³ (11), CC ^c sd(9), C ^{α1} H d ² (8), CH ₃ r ¹ (8)
761	749	-12	CO ^a ob(25), C ^ω N t(20), NH ^a ob(18), NC ^φ t(13)
778	786	8	CO ^a ob(27), CC ^c ob(25)
—	806	—	NH ^a ob(28), CC ^c ob(27), CO ^a ob(11), C ^ω N t(8)
872	860	-12	CC ^c sd(16), CC ^{me} s(14), CN ⁿ s(12), CC ^c s(9), CC ^{me} s(8), NC ^φ s(7), CO ^c ss(7)
884	893	9	CC ^{me} s(15), CN ⁿ s(14), CC ^c s(9), NH ₂ w(8), CC ^{me} s(7), CH ₃ r ¹ (7)
920	929	9	CC ^{me} s(15), CH ₃ r ¹ (11), CC ^c s(9), NC ^φ s(8), CH ₃ r ² (8), CO ^a r(7)
952	952	0	CH ₃ r ² (23), CC ^ψ s(14), NC ^φ s(11), NH ₂ w(11), CO ^a r(9)
980	970	-10	NH ₂ w(51), CH ₃ r ² (34)
1019	1015	-4	CH ₃ r ¹ (25), NH ₂ r(18), CH ₃ r ² (16), CN ⁿ s(12), C ^{α1} H r ² (8)

Table 3.73: (continued)

frequency (cm ⁻¹)			Potential Energy Distribution
obs.	calc.	dev.	
1069	1066	-3	C ^{α2} H r ² (31), CH ₃ r ² (17), CC ^c ob(10), CH ₃ r ¹ (7)
1104	1098	-6	CC ^{me} s(44), CN ⁿ s(18), CH ₃ r ¹ (16)
1136	1136	0	CC ^{me} s(35), NC ^φ s(16), CH ₃ r ¹ (14)
1136	1143	7	NH ₂ r(22), C ^{α1} H r ² (19), C ^{α1} H r ¹ (15), CN ⁿ s(7), CH ₃ r ² (7)
1166	1158	-8	NC ^φ s(21), CH ₃ r ¹ (18), CH ₃ r ² (18), C ^{α2} H d ¹ (13), C ^{α2} H r ¹ (7)
1220	1226	6	NH ^a ib(28), C ^{α2} H r ² (19), CN ^a s(8)
1260	1250	-10	NH ₂ r(19), CN ⁿ s(13), C ^{α2} H r ² (9), C ^{α1} H d ¹ (8), NH ₂ w(8)
1281	1287	6	C ^{α1} H r ² (20), C ^{α2} H r ² (16), NH ^a ib(11), NH ₂ r(8), CH ₃ r ¹ (7)
1320	1315	-5	C ^{α1} H r ² (27), C ^{α1} H r ¹ (19), NH ^a ib(11), C ^{α2} H r ² (9), C ^{α2} H r ¹ (8), CH ₃ r ¹ (7)
1335	1333	-2	C ^{α2} H r ¹ (68), C ^{α1} H r ¹ (7)
1367	1361	-6	CH ₃ sd(88)
1367	1373	6	CH ₃ sd(97)
1407	1399	-8	C ^{α1} H r ¹ (33), CO ^c ss(17), NH ₂ r(11), NH ^a ib(7)
1407	1413	6	CO ^c ss(34), CC ^c s(13), C ^{α1} H r ¹ (11)
1459	1453	-6	CH ₃ ad ^{1,2} (60), CH ₃ ad ^{1,2} (26)
1459	1457	-2	CH ₃ ad ^{1,2} (48), CH ₃ ad ^{1,2} (30), CH ₃ ad ^{1,2} (9)
1459	1461	2	CH ₃ ad ^{1,2} (34), CH ₃ ad ^{1,2} (23), CH ₃ ad ^{1,2} (23)
1459	1463	4	CH ₃ ad ^{1,2} (78), CH ₃ ad ^{1,2} (13)
1542	1542	0	NH ^a ib(29), CN ^a s(26), CO ^a s(12), CC ^ψ s(9)
1578	1573	-5	NH ₂ sis(86), CN ^a s(7)
1602	1598	-4	CO ^c as(81), CO ^c ss(7)
1638	1639	1	CO ^a s(51), CN ^a s(25)
—	2930	—	CH ₃ ss(97)
—	2937	—	CH ₃ ss(87), CH ₃ as ^{1,2} (12)
—	2960	—	C ^{α2} H s(92)
—	2977	—	C ^{α1} H s(80), CH ₃ as ^{1,2} (15)
—	2985	—	CH ₃ as ^{1,2} (92), C ^{α1} H s(7)
—	3000	—	CH ₃ as ^{1,2} (78), CH ₃ ss(8), CH ₃ as ^{1,2} (8)
—	3008	—	CH ₃ as ^{1,2} (84), C ^{α1} H s(13)
—	3028	—	CH ₃ as ^{1,2} (92), CH ₃ as ^{1,2} (7)
—	3137	—	NH ₂ ss(99)
—	3234	—	NH ₂ as(99)
—	3444	—	NH ^a s(100)

Table 3.73: (continued)

frequency (cm ⁻¹)			Potential Energy Distribution
obs.	calc.	dev.	

frequency (cm ⁻¹)			Ala-ala in D ₂ O pD 13 (mean deviation = 15 cm ⁻¹)
obs.	calc.	dev.	
			Potential Energy Distribution
—	52	—	NC ^φ t(28), CC ^c t(26), CC ^ψ t(25), NH ^a ob(10)
—	92	—	CC ^c t(56), CC ^ψ t(35), C ^ω N t(13)
—	96	—	NC ^φ t(40), C ^ω N t(37)
—	131	—	CC ^ψ t(30), NH ^a ob(25), NC ^φ t(18), CC ^c t(17)
—	167	—	CNHC sd(36), CO ^a sd(21), C ^{α2} H d ³ (17), CC ^{me} t(12), CC ^c r(9)
—	192	—	CC ^{me} t(86)
—	197	—	CC ^{me} t(81)
225	228	3	CN ⁿ t(69), C ^{α1} H d ³ (9)
251	246	-5	C ^{α2} H d ² (30), C ^{α1} H d ² (9), CC ^c r(8)
251	265	14	C ^{α1} H d ² (36), CO ^a ob(13), C ^{α1} H d ³ (11), C ^{α2} H d ² (11), CN ⁿ t(7)
—	296	—	CO ^a sd(28), CC ^c r(24), CN ⁿ t(14), C ^{α1} H d ² (9)
332	311	-21	C ^{α2} H d ² (25), C ^{α1} H d ³ (13), C ^{α1} H d ¹ (10), CC ^c s(9)
380	336	-44	CO ^a r(23), CNHC sd(19), C ^{α1} H d ³ (17), CC ^c r(10)
447	431	-16	C ^{α2} H d ¹ (28), CC ^c r(14), C ^{α1} H d ¹ (11), C ^ω N t(10), C ^{α2} H d ³ (7)
447	446	-1	C ^{α1} H d ¹ (39), C ^{α2} H d ¹ (18)
534	548	14	C ^{α2} H d ³ (16), CC ^c r(16), CO ^a sd(13), C ^ω N t(9), NH ^a ob(8)
—	587	—	NH ^a ob(42), C ^{α2} H d ¹ (13), NC ^φ t(13), C ^ω N t(12)
645	629	-16	CO ^a r(25), NH ₂ r(16), CC ^c sd(15), CC ^c s(9), C ^{α1} H d ³ (9), CC ^ψ s(7)
687	666	-21	CC ^c sd(34), CC ^ψ s(13), CC ^c s(10), NH ₂ r(9)
760	756	-4	NH ₂ w(64), CO ^a ob(15)
778	775	-3	CO ^a ob(45), NH ₂ w(15), CC ^{me} s(11), C ^{α1} H d ² (7)
778	789	11	CC ^c ob(58), C ^{α2} H d ² (8), CC ^c sd(7)
866	854	-12	CC ^c sd(15), NC ^φ s(10), CO ^a r(9), CN ⁿ s(9), CC ^{me} s(8), CC ^c s(7)
884	894	10	NH ₂ r(22), CH ₃ r ¹ (12), CC ^{me} s(11), CO ^a r(9), CNHC sd(7)
904	895	-9	CH ₃ r ¹ (26), CC ^{me} s(20), NH ₂ r(15), CN ⁿ s(8)

Table 3.73: (continued)

frequency (cm ⁻¹)			Potential Energy Distribution
obs.	calc.	dev.	
904	907	3	NH ^a ib(25), CC ^c s(21), CH ₃ r ² (16), NC ^φ s(10), CO ^c ss(10), CC ^c sd(9)
938	943	5	CH ₃ r ² (31), CN ⁿ s(14), CC ^ψ s(9), NH ^a ib(8), CO ^a s(7)
995	991	-4	NH ^a ib(43), CH ₃ r ² (21), CC ^ψ s(7)
1066	1064	-2	CC ^{me} s(40), NH ₂ sis(13), CN ⁿ s(12)
1066	1068	2	C ^{α2} H r ² (34), CH ₃ r ² (12), CC ^c ob(9), CH ₃ r ¹ (7)
1097	1094	-3	C ^{α1} H r ² (17), CH ₃ r ² (17), CH ₃ r ¹ (15), C ^{α1} H d ² (9), NH ₂ sis(8), CO ^a s(7)
1113	1130	17	CC ^{me} s(34), NC ^φ s(22), CH ₃ r ¹ (8)
1163	1153	-10	CH ₃ r ¹ (26), C ^{α2} H d ¹ (15), CH ₃ r ² (15), NC ^φ s(9), CC ^{me} s(8)
1163	1180	17	NH ₂ sis(72), CN ⁿ s(17)
1209	1193	-16	CH ₃ r ¹ (17), CN ⁿ s(15), C ^{α1} H d ¹ (13), CH ₃ r ² (9), NC ^φ s(8), C ^{α1} H r ¹ (7)
1278	1268	-10	C ^{α2} H r ² (45), CH ₃ r ¹ (10), CO ^c ss(7)
1308	1304	-4	C ^{α1} H r ² (59), CH ₃ r ¹ (11), C ^{α1} H r ¹ (7)
1328	1330	2	C ^{α2} H r ¹ (75), C ^{α2} H r ² (7)
1360	1360	0	CH ₃ sd(49), C ^{α1} H r ¹ (29), CO ^c ss(7)
1365	1364	-1	C ^{α1} H r ¹ (40), CH ₃ sd(40)
1371	1373	2	CH ₃ sd(98)
1409	1410	1	CO ^c ss(49), CC ^c s(16), CC ^c sd(8), CH ₃ sd(8)
1455	1451	-4	CH ₃ ad ^{1,2} (81), CH ₃ ad ^{1,2} (7)
1455	1456	1	CH ₃ ad ^{1,2} (61), CH ₃ ad ^{1,2} (23)
1455	1458	3	CH ₃ ad ^{1,2} (48), CH ₃ ad ^{1,2} (22), CH ₃ ad ^{1,2} (11)
1455	1463	8	CH ₃ ad ^{1,2} (76), CH ₃ ad ^{1,2} (15)
1512	1506	-6	CN ^a s(32), CO ^a s(19), CC ^ψ s(15), NH ^a ib(8), NC ^φ s(7), CO ^a r(7)
1596	1597	1	CO ^c as(82), CO ^c ss(7)
1638	1630	-8	CO ^a s(52), CN ^a s(31)
—	2266	—	NH ₂ ss(99)
—	2391	—	NH ₂ as(99)
—	2526	—	NH ^a s(99)
—	2930	—	CH ₃ ss(97)
—	2937	—	CH ₃ ss(87), CH ₃ as ^{1,2} (12)
—	2960	—	C ^{α2} H s(92)

Table 3.73: (continued)

frequency (cm^{-1})			Potential Energy Distribution
obs.	calc.	dev.	
—	2977	—	$\text{C}^{\alpha 1}\text{H}$ s(79), CH_3 as ^{1,2} (15)
—	2985	—	CH_3 as ^{1,2} (92), $\text{C}^{\alpha 1}\text{H}$ s(7)
—	3000	—	CH_3 as ^{1,2} (78), CH_3 ss(8), CH_3 as ^{1,2} (8)
—	3008	—	CH_3 as ^{1,2} (83), $\text{C}^{\alpha 1}\text{H}$ s(13)
—	3028	—	CH_3 as ^{1,2} (92), CH_3 as ^{1,2} (7)

frequency (cm^{-1})			2-d Ala-ala pH 13 (mean deviation = 15 cm^{-1})
obs.	calc.	dev.	
—	53	—	NC^{ϕ} t(28), CC^c t(27), CC^{ψ} t(24), NH^a ob(10)
—	93	—	CC^c t(52), CC^{ψ} t(33), $\text{C}^{\omega}\text{N}$ t(16)
—	97	—	NC^{ϕ} t(36), $\text{C}^{\omega}\text{N}$ t(34), CC^{ψ} t(7)
—	133	—	CC^{ψ} t(30), NH^a ob(26), NC^{ϕ} t(18), CC^c t(15), $\text{C}^{\alpha 2}\text{H}$ d ¹ (7)
—	169	—	CNHC sd(34), CO^a sd(20), $\text{C}^{\alpha 2}\text{H}$ d ³ (17), CC^{me} t(13), CC^c r(9)
—	193	—	CC^{me} t(87)
—	197	—	CC^{me} t(80)
251	246	−5	$\text{C}^{\alpha 2}\text{H}$ d ² (27), $\text{C}^{\alpha 1}\text{H}$ d ² (14)
251	264	13	$\text{C}^{\alpha 1}\text{H}$ d ² (21), $\text{C}^{\alpha 1}\text{H}$ d ³ (18), $\text{C}^{\alpha 2}\text{H}$ d ² (16), CO^a ob(11), CC^c r(7)
—	282	—	$\text{C}^{\alpha 1}\text{H}$ d ² (22), CO^a sd(19), CC^c r(15), CN^n t(10), CO^a r(7)
337	315	−22	$\text{C}^{\alpha 2}\text{H}$ d ² (20), CC^c s(11), $\text{C}^{\alpha 1}\text{H}$ d ³ (8), $\text{C}^{\alpha 1}\text{H}$ d ¹ (7)
337	334	−3	CN^n t(35), CC^c r(18), CNHC sd(9), CO^a r(8)
387	353	−34	CN^n t(37), $\text{C}^{\alpha 1}\text{H}$ d ³ (18), CO^a r(15), $\text{C}^{\alpha 1}\text{H}$ d ¹ (7)
460	446	−14	$\text{C}^{\alpha 2}\text{H}$ d ¹ (31), CC^c r(12), $\text{C}^{\alpha 1}\text{H}$ d ¹ (9), $\text{C}^{\alpha 2}\text{H}$ d ³ (9)
460	464	4	$\text{C}^{\alpha 1}\text{H}$ d ¹ (44), $\text{C}^{\alpha 2}\text{H}$ d ¹ (17)
534	568	34	$\text{C}^{\alpha 2}\text{H}$ d ¹ (17), CC^c r(17), $\text{C}^{\alpha 2}\text{H}$ d ³ (16), CO^a sd(15), CC^{ψ} s(7)
640	645	5	CC^c sd(38), CC^c s(17), CO^a r(15)
678	693	15	CC^{ψ} s(18), CO^a r(14), $\text{C}^{\alpha 1}\text{H}$ d ³ (11), CC^c sd(11), $\text{C}^{\alpha 1}\text{H}$ d ² (7), CH_3 r ¹ (7)
743	748	5	CO^a ob(29), $\text{C}^{\omega}\text{N}$ t(19), NH^a ob(15), NC^{ϕ} t(12)
778	780	2	CO^a ob(25), NH^a ob(15), CC^c ob(13), $\text{C}^{\alpha 1}\text{H}$ r ² (9)
—	800	—	CC^c ob(38), NH^a ob(15), $\text{C}^{\alpha 1}\text{H}$ r ² (8)
829	832	3	CC^{me} s(34), $\text{C}^{\alpha 1}\text{H}$ r ² (28), NH^a ob(7)

Table 3.73: (continued)

frequency (cm ⁻¹)			Potential Energy Distribution
obs.	calc.	dev.	
866	865	-1	CC ^c sd(19), CC ^c s(12), CC ^{me} s(11), CC ^ψ s(9), CO ^c ss(9), C ^{α1} H r ² (8), CH ₃ r ¹ (8), NC ^φ s(7)
909	899	-10	C ^{α1} H r ¹ (61), CN ⁿ s(19), NH ₂ w(8), NH ₂ r(7)
909	913	4	C ^{α1} H r ² (15), CN ⁿ s(9), CH ₃ r ² (9), NH ₂ w(8), CC ^c s(7)
927	929	2	CC ^{me} s(15), CC ^c s(10), CH ₃ r ¹ (10), CH ₃ r ² (9), NC ^φ s(8)
944	959	15	NH ₂ w(20), CH ₃ r ² (16), CH ₃ r ² (11), CC ^ψ s(8), NC ^φ s(8), CO ^a r(7)
981	977	-4	CH ₃ r ² (44), NH ₂ w(37), CN ⁿ s(7)
1065	1066	1	C ^{α2} H r ² (31), CH ₃ r ² (17), CC ^c ob(10), CH ₃ r ¹ (7)
1101	1087	-14	CH ₃ r ¹ (44), CC ^{me} s(19), CN ⁿ s(10), NH ₂ r(9)
1132	1128	-4	CC ^{me} s(18), CC ^{me} s(14), NC ^φ s(11), C ^{α1} H r ² (7)
1154	1144	-10	CC ^{me} s(23), CH ₃ r ¹ (17), CC ^{me} s(13)
1195	1160	-35	NC ^φ s(25), CH ₃ r ² (16), CH ₃ r ¹ (13), C ^{α2} H d ¹ (10)
1239	1226	-13	NH ^a ib(25), C ^{α2} H r ² (16), CN ⁿ s(10), CN ^a s(7)
1239	1242	3	NH ₂ r(27), CN ⁿ s(13), CH ₃ r ¹ (11)
1273	1270	-3	NH ₂ r(24), C ^{α2} H r ² (18)
1304	1321	17	C ^{α2} H r ¹ (38), C ^{α2} H r ² (16), NH ^a ib(14), CH ₃ r ¹ (7)
1343	1343	0	C ^{α2} H r ¹ (36), NH ^a ib(19), CC ^ψ s(9), CO ^c ss(7)
1369	1362	-7	CH ₃ sd(88)
1369	1374	5	CH ₃ sd(97)
1408	1410	2	CO ^c ss(49), CC ^c s(17), CC ^c sd(8), CH ₃ sd(8), CO ^c as(7)
1458	1451	-7	CH ₃ ad ^{1,2} (71), CH ₃ ad ^{1,2} (22)
1458	1456	-2	CH ₃ ad ^{1,2} (44), CH ₃ ad ^{1,2} (31), CH ₃ ad ^{1,2} (10)
1458	1458	0	CH ₃ ad ^{1,2} (42), CH ₃ ad ^{1,2} (26), CH ₃ ad ^{1,2} (12), CH ₃ ad ^{1,2} (8)
1458	1463	5	CH ₃ ad ^{1,2} (77), CH ₃ ad ^{1,2} (14)
1544	1541	-3	NH ^a ib(29), CN ^a s(27), CO ^a s(12), CC ^ψ s(9)
1583	1572	-11	NH ₂ sis(85), CN ^a s(8)
1605	1598	-7	CO ^c as(80), CO ^c ss(7)
1644	1632	-12	CO ^a s(52), CN ^a s(25), NH ₂ sis(7)
—	2201	—	C ^{α1} H s(98)
—	2930	—	CH ₃ ss(98)
—	2937	—	CH ₃ ss(87), CH ₃ as ^{1,2} (12)
—	2960	—	C ^{α2} H s(92)
—	2984	—	CH ₃ as ^{1,2} (95)

Table 3.73: (continued)

frequency (cm ⁻¹)			Potential Energy Distribution
obs.	calc.	dev.	
—	3000	—	CH ₃ as ^{1,2} (78), CH ₃ ss(8), CH ₃ as ^{1,2} (8)
—	3004	—	CH ₃ as ^{1,2} (94)
—	3028	—	CH ₃ as ^{1,2} (92), CH ₃ as ^{1,2} (7)
—	3137	—	NH ₂ ss(99)
—	3234	—	NH ₂ as(99)
—	3444	—	NH ^a s(100)

frequency (cm ⁻¹)			Potential Energy Distribution
obs.	calc.	dev.	
—	54	—	NC ^φ t(28), CC ^c t(28), CC ^ψ t(23), NH ^a ob(10)
—	93	—	CC ^c t(53), CC ^ψ t(33), C ^ω N t(15)
—	97	—	NC ^φ t(37), C ^ω N t(36)
—	133	—	CC ^ψ t(31), NH ^a ob(26), NC ^φ t(17), CC ^c t(15), C ^{α2} H d ¹ (7)
—	169	—	CNHC sd(35), CO ^a sd(20), C ^{α2} H d ³ (17), CC ^{me} t(14), CC ^c r(9)
—	193	—	CC ^{me} t(87)
—	197	—	CC ^{me} t(80)
236	246	10	C ^{α2} H d ² (27), C ^{α1} H d ² (13)
236	264	28	C ^{α1} H d ² (21), C ^{α1} H d ³ (18), C ^{α2} H d ² (15), CO ^a ob(11), CO ^a sd(7), CC ^c r(7)
—	283	—	C ^{α1} H d ² (22), CO ^a sd(19), CC ^c r(14), CN ⁿ t(11), CO ^a r(7)
334	316	-18	C ^{α2} H d ² (20), CC ^c s(12), C ^{α1} H d ¹ (8), C ^{α1} H d ³ (8)
334	334	0	CN ⁿ t(34), CC ^c r(19), CNHC sd(9), CO ^a r(8)
376	353	-23	CN ⁿ t(39), C ^{α1} H d ³ (17), CO ^a r(14)
467	446	-21	C ^{α2} H d ¹ (33), CC ^c r(12), C ^{α2} H d ³ (9), C ^{α1} H d ¹ (8)
467	467	0	C ^{α1} H d ¹ (44), C ^{α2} H d ¹ (16)
542	572	30	C ^{α2} H d ³ (16), CO ^a sd(16), CC ^c r(16), C ^{α2} H d ¹ (15), CC ^ψ s(7)
644	646	2	CC ^c sd(39), CC ^c s(17), CO ^a r(14)
687	699	12	CC ^ψ s(17), CO ^a r(15), C ^{α1} H d ³ (10), CC ^c sd(10), C ^{α1} H d ² (9), CH ₃ r ¹ (8)
748	738	-10	CO ^a ob(39), C ^ω N t(16), C ^{α1} H d ³ (10), NC ^φ t(9), NH ^a ob(8)
778	778	0	CC ^c ob(20), NH ^a ob(19), CO ^a ob(18)
—	804	—	CC ^c ob(35), NH ^a ob(25), C ^ω N t(8)

Table 3.73: (continued)

frequency (cm ⁻¹)			Potential Energy Distribution
obs.	calc.	dev.	
850	857	7	CC ^c sd(15), CC ^{me} s(14), CN ⁿ s(12), NC ^φ s(8), CC ^c s(8), CC ^ψ s(7), CO ^c ss(7), CC ^{me} s(7)
883	893	10	CC ^{me} s(14), CN ⁿ s(13), CC ^c s(10), CC ^{me} s(8), CH ₃ r ¹ (8), CC ^c sd(7), NH ₂ w(7)
920	928	8	CC ^{me} s(14), CH ₃ r ¹ (11), CO ^a r(9), CC ^c s(7), CNHC sd(7)
943	947	4	CH ₃ r ² (24), CC ^ψ s(13), NC ^φ s(13), NH ₂ w(9), CC ^c s(7), CO ^a r(7)
980	969	-11	NH ₂ w(52), CH ₃ r ² (33)
1021	1014	-7	CH ₃ r ¹ (26), NH ₂ r(18), CH ₃ r ² (16), CN ⁿ s(11), C ^{α1} H r ² (8)
1066	1066	0	C ^{α2} H r ² (31), CH ₃ r ² (17), CC ^c ob(10), CH ₃ r ¹ (7)
1103	1097	-6	CC ^{me} s(44), CN ⁿ s(19), CH ₃ r ¹ (16)
1129	1135	6	CC ^{me} s(35), NC ^φ s(17), CH ₃ r ¹ (13)
1129	1142	13	NH ₂ r(23), C ^{α1} H r ² (20), C ^{α1} H r ¹ (16), CH ₃ r ² (8), CN ⁿ s(7)
1166	1157	-9	CH ₃ r ¹ (20), NC ^φ s(19), CH ₃ r ² (18), C ^{α2} H d ¹ (13), C ^{α2} H r ¹ (7)
1221	1224	3	NH ^a ib(30), C ^{α2} H r ² (18), CN ^a s(10)
1256	1250	-6	NH ₂ r(20), CN ⁿ s(14), C ^{α1} H d ¹ (9), NH ₂ w(9), C ^{α2} H r ² (7)
1279	1284	5	C ^{α2} H r ² (19), C ^{α1} H r ² (15), NH ^a ib(10), CN ^a s(7), NH ₂ r(7)
1321	1313	-8	C ^{α1} H r ² (33), C ^{α1} H r ¹ (20), NH ^a ib(8), CH ₃ r ¹ (8), C ^{α2} H r ² (7)
1327	1331	4	C ^{α2} H r ¹ (73)
1368	1361	-7	CH ₃ sd(88)
1368	1373	5	CH ₃ sd(97)
1408	1398	-10	C ^{α1} H r ¹ (35), CO ^c ss(16), NH ₂ r(11)
1408	1412	4	CO ^c ss(36), CC ^c s(13), C ^{α1} H r ¹ (11)
1458	1453	-5	CH ₃ ad ^{1,2} (60), CH ₃ ad ^{1,2} (24)
1458	1456	-2	CH ₃ ad ^{1,2} (50), CH ₃ ad ^{1,2} (28), CH ₃ ad ^{1,2} (10)
1458	1461	3	CH ₃ ad ^{1,2} (37), CH ₃ ad ^{1,2} (25), CH ₃ ad ^{1,2} (18)
1458	1463	5	CH ₃ ad ^{1,2} (77), CH ₃ ad ^{1,2} (14)
1522	1523	1	NH ^a ib(34), CN ^a s(24), CO ^a s(13), CC ^ψ s(8)
1560	1567	7	NH ₂ sis(67), CN ^a s(13), CO ^a s(12)
1594	1595	1	CO ^c as(49), CO ^a s(15), NH ₂ sis(14), CN ^a s(7)
1610	1605	-5	CO ^c as(34), CO ^a s(24), NH ₂ sis(14), CN ^a s(12)
—	2930	—	CH ₃ ss(97)
—	2937	—	CH ₃ ss(87), CH ₃ as ^{1,2} (12)
—	2960	—	C ^{α2} H s(92)

Table 3.73: (continued)

frequency (cm ⁻¹)			Potential Energy Distribution
obs.	calc.	dev.	
—	2977	—	C ^α 1H s(80), CH ₃ as ^{1,2} (15)
—	2985	—	CH ₃ as ^{1,2} (92), C ^α 1H s(7)
—	3000	—	CH ₃ as ^{1,2} (78), CH ₃ ss(8), CH ₃ as ^{1,2} (8)
—	3008	—	CH ₃ as ^{1,2} (84), C ^α 1H s(13)
—	3028	—	CH ₃ as ^{1,2} (92), CH ₃ as ^{1,2} (7)
—	3137	—	NH ₂ ss(99)
—	3234	—	NH ₂ as(99)
—	3444	—	NH ^a s(100)

Table 3.74: Scaled 4-31G Frequencies and Potential Energy Distribution for Zwitterionic Alanine-alanine Isolated Structure.

frequency (cm ⁻¹)			NH ₃ ⁺ CH(CH ₃)CONHCH(CH ₃)CO ₂ ⁻ (mean deviation = 12 cm ⁻¹)
obs.	calc.	dev.	Potential Energy Distribution
—	32	—	CC ^ψ t(54), NC ^φ t(36), NH ^a ob(8)
—	57	—	CC ^c t(23), CC ^ψ t(19), NH ^a ob(18), C ^ω N t(16), NC ^φ t(9)
—	77	—	C ^ω N t(33), NC ^φ t(16), CNHC sd(11), CC ^ψ t(8), CO ^a sd(7)
—	97	—	CC ^c t(34), C ^ω N t(18), CNHC sd(15), NC ^φ t(13), CO ^a sd(10)
—	124	—	CC ^c t(35), CNHC sd(22), CO ^a sd(14), NH ^a ob(11), C ^{α2} H d ³ (7)
—	188	—	CC ^{me} t(97)
—	194	—	CC ^{me} t(94)
247	231	-16	C ^{α2} H d ² (26), C ^{α1} H d ² (16), C ^{α2} H d ¹ (10), CNHC sd(8), NC ^φ s(7)
247	262	15	C ^{α2} H d ² (29), C ^{α1} H d ² (24), CC ^c r(13), C ^{α2} H d ³ (8)
—	290	—	CN ⁿ t(80), CC ^ψ t(10)
344	327	-17	C ^{α2} H d ³ (20), C ^{α2} H d ² (13), CC ^c s(11), CN ^a s(10), NC ^φ s(8),
365	350	-15	CC ^c r(28), CO ^a sd(18), C ^{α1} H d ² (11), C ^{α2} H d ³ (11), C ^{α1} H d ³ (8)
—	418	—	C ^{α1} H d ¹ (34), C ^{α1} H d ³ (19), CO ^a r(16), CC ^c r(7)
454	445	-9	C ^{α1} H d ¹ (38), CC ^c r(18), C ^{α1} H d ³ (8)
454	458	4	C ^{α2} H d ¹ (42), C ^{α1} H d ² (11), C ^{α1} H d ³ (10), CO ^a r(9)
579	593	14	CC ^c r(22), C ^{α2} H d ³ (12), C ^{α2} H d ¹ (11), CO ^a sd(11), CC ^ψ s(10)
650	645	-5	CC ^c sd(44), CC ^c s(20), CO ^a r(9)
684	681	-3	CO ^a r(15), CO ^a ob(15), CC ^ψ s(13), C ^{α1} H d ³ (13), CC ^{me} s(9)
758	758	0	CO ^a ob(46), C ^{α1} H d ² (11), CO ^a r(8)
775	776	1	CC ^c ob(47), CC ^c sd(13), C ^{α2} H d ² (9)
855	834	-21	CN ⁿ s(44), CC ^{me} s(13)
—	860	—	NH ^a ob(48), NC ^φ t(20), C ^ω N t(14)
880	883	3	CC ^c s(27), CC ^c sd(16), CO ^c ss(9), CH ₃ r ² (9), CN ⁿ s(8), CC ^{me} s(8), CH ₃ r ¹ (7)
922	927	5	CC ^{me} s(12), CNHC sd(10), CNH ₃ r ² (10), CO ^a r(7), CH ₃ r ² (7), CH ₃ r ¹ (7)

Table 3.74: (continued)

frequency (cm ⁻¹)			Potential Energy Distribution
obs.	calc.	dev.	
952	940	-12	CNH ₃ r ² (17), CH ₃ r ² (15), CH ₃ r ² (15), NC ^φ s(14), CC ^{me} s(8), CC ^c s(7)
952	957	5	CNH ₃ r ² (38), CC ^ψ s(17), CH ₃ r ¹ (8), CH ₃ r ² (8)
1009	1014	5	CNH ₃ r ¹ (23), CC ^{me} s(21), CH ₃ r ¹ (16), C ^{α1} H r ² (13)
1065	1062	-3	C ^{α2} H r ² (32), CH ₃ r ² (14), CC ^c ob(9), CH ₃ r ¹ (7)
1101	1088	-13	CH ₃ r ² (35), CN ⁿ s(14), CC ^{me} s(14), CH ₃ r ² (7)
1114	1122	8	CNH ₃ r ¹ (38), C ^{α1} H r ² (34)
1140	1145	5	NC ^φ s(29), CC ^{me} s(14), CH ₃ r ² (12)
1167	1165	-2	CH ₃ r ¹ (36), CC ^{me} s(24), C ^{α2} H d ¹ (15)
1226	1212	-14	CH ₃ r ¹ (31), CNH ₃ r ² (19), CC ^{me} s(15), C ^{α1} H d ¹ (13)
1235	1228	-7	C ^{α2} H r ² (28), NH ^a ib(20), C ^{α2} H r ¹ (10)
1276	1302	26	C ^{α1} H r ² (34), CNH ₃ r ¹ (8)
1323	1332	9	C ^{α2} H r ² (18), C ^{α2} H r ¹ (15), C ^{α1} H r ¹ (10), NH ^a ib(7), CH ₃ r ¹ (7)
1340	1343	3	C ^{α2} H r ¹ (56), C ^{α1} H r ¹ (11)
1369	1360	-9	C ^{α1} H r ¹ (63)
1369	1370	1	CH ₃ sd(88)
1405	1399	-6	CH ₃ sd(75), CO ^c ss(9)
1405	1402	-3	CO ^c ss(36), CH ₃ sd(18), CO ^c as(14)
1458	1449	-9	CH ₃ ad ^{1,2} (86), CH ₃ r ² (7)
1458	1455	-3	CH ₃ ad ^{1,2} (68), CH ₃ ad ^{1,2} (14)
1458	1461	3	CH ₃ ad ^{1,2} (44), CNH ₃ sd(17), CH ₃ ad ^{1,2} (14), CH ₃ r ¹ (7)
1458	1464	6	CH ₃ ad ^{1,2} (65), CH ₃ ad ^{1,2} (13), CH ₃ r ¹ (8), CH ₃ ad ^{1,2} (7)
—	1468	—	CNH ₃ sd(51), CH ₃ ad ^{1,2} (23), CNH ₃ ad ^{1,2} (8)
1530	1519	-11	NH ^a ib(39), CN ^a s(14), CO ^a s(13), CO ^c ss(9)
1574	1597	23	CO ^c as(54), CO ^c ss(16), NH ^a ib(14)
—	1607	—	CNH ₃ ad ^{1,2} (72), CNH ₃ sd(19)
—	1634	—	CNH ₃ ad ^{1,2} (94)
1680	1689	9	CO ^a s(39), CN ^a s(37)
—	2562	—	NH ₃ as ¹ (57), NH ₃ ss(39)
—	2925	—	CH ₃ ss(91)
—	2929	—	CH ₃ ss(95)
—	2957	—	C ^{α2} H s(49), CH ₃ as ^{1,2} (41), CH ₃ as ^{1,2} (9)
—	2975	—	C ^{α2} H s(50), CH ₃ as ^{1,2} (33), CH ₃ as ^{1,2} (17)

Table 3.74: (continued)

frequency (cm^{-1})			Potential Energy Distribution
obs.	calc.	dev.	
—	2977	—	CH_3 as ^{1,2} (71), CH_3 as ^{1,2} (23)
—	3004	—	CH_3 as ^{1,2} (69), CH_3 as ^{1,2} (14), $\text{C}^{\alpha 1}$ H s(12)
—	3007	—	CH_3 as ^{1,2} (71), CH_3 as ^{1,2} (21), CH_3 ss(7)
—	3014	—	$\text{C}^{\alpha 1}$ H s(82), CH_3 as ^{1,2} (13)
—	3083	—	NH_3 ss(59), NH_3 as ¹ (40)
—	3121	—	NH^a s(97)
—	3145	—	NH_3 as ² (100)

frequency (cm^{-1})			Potential Energy Distribution
obs.	calc.	dev.	
—	32	—	CC^{ψ} t(54), NC^{ϕ} t(36), NH^a ob(8)
—	57	—	CC^c t(22), CC^{ψ} t(19), NH^a ob(18), $\text{C}^{\omega\text{N}}$ t(16), NC^{ϕ} t(9)
—	77	—	$\text{C}^{\omega\text{N}}$ t(33), NC^{ϕ} t(16), CNHC sd(11), CC^{ψ} t(8), CO^a sd(7)
—	97	—	CC^c t(34), $\text{C}^{\omega\text{N}}$ t(18), CNHC sd(15), NC^{ϕ} t(13), CO^a sd(10)
—	123	—	CC^c t(35), CNHC sd(21), CO^a sd(14), NH^a ob(11), $\text{C}^{\alpha 2}$ H d ³ (7)
—	188	—	CC^{me} t(97)
—	194	—	CC^{me} t(94)
236	231	−5	$\text{C}^{\alpha 2}$ H d ² (26), $\text{C}^{\alpha 1}$ H d ² (16), $\text{C}^{\alpha 2}$ H d ¹ (11), CNHC sd(8), NC^{ϕ} s(7)
260	261	1	$\text{C}^{\alpha 2}$ H d ² (29), $\text{C}^{\alpha 1}$ H d ² (24), CC^c r(13), $\text{C}^{\alpha 2}$ H d ³ (8)
—	290	—	CN^n t(80), CC^{ψ} t(10)
344	327	−17	$\text{C}^{\alpha 2}$ H d ³ (20), $\text{C}^{\alpha 2}$ H d ² (14), CC^c s(11), CN^a s(10), NC^{ϕ} s(8),
377	349	−28	CC^c r(28), CO^a sd(18), $\text{C}^{\alpha 1}$ H d ² (11), $\text{C}^{\alpha 2}$ H d ³ (11), $\text{C}^{\alpha 1}$ H d ³ (8)
—	418	—	$\text{C}^{\alpha 1}$ H d ¹ (35), $\text{C}^{\alpha 1}$ H d ³ (18), CO^a r(15), CC^c r(7)
456	444	−12	$\text{C}^{\alpha 1}$ H d ¹ (37), CC^c r(18), $\text{C}^{\alpha 1}$ H d ³ (8)
456	458	2	$\text{C}^{\alpha 2}$ H d ¹ (42), $\text{C}^{\alpha 1}$ H d ² (11), $\text{C}^{\alpha 1}$ H d ³ (10), CO^a r(9)
579	592	13	CC^c r(22), $\text{C}^{\alpha 2}$ H d ³ (12), CC^{ψ} s(11), CO^a sd(11), $\text{C}^{\alpha 2}$ H d ¹ (10)
647	644	−3	CC^c sd(42), CC^c s(19), CO^a r(10), $\text{C}^{\alpha 1}$ H d ³ (7)

Table 3.74: (continued)

frequency (cm ⁻¹)			Potential Energy Distribution
obs.	calc.	dev.	
685	675	-10	CO ^a ob(20), CC ^ψ s(12), CO ^a r(12), C ^{α1} H d ³ (11), CC ^{me} s(8), CC ^c sd(7)
744	746	2	CO ^a ob(42), C ^{α1} H d ² (11), CO ^a r(11)
778	775	-3	CC ^c ob(48), CC ^c sd(14), C ^{α2} H d ² (10)
847	831	-16	CN ⁿ s(43), CC ^{me} s(13)
—	860	—	NH ^a ob(48), NC ^φ t(20), C ^ω N t(14)
881	883	2	CC ^c s(27), CC ^c sd(16), CO ^c ss(9), CN ⁿ s(9), CC ^{me} s(8), CH ₃ r ² (8), CH ₃ r ¹ (7)
922	925	3	CNHC sd(10), CH ₃ r ² (10), CC ^{me} s(10), CNH ₃ r ² (9), CO ^a r(8), CC ^ψ s(7)
951	939	-12	CH ₃ r ² (18), NC ^φ s(17), CH ₃ r ² (13), CC ^{me} s(10), CC ^c s(9), CNH ₃ r ² (8)
951	953	2	CNH ₃ r ² (49), CC ^ψ s(14), CH ₃ r ¹ (10)
1009	1013	4	CNH ₃ r ¹ (23), CC ^{me} s(20), CH ₃ r ¹ (17), C ^{α1} H r ² (14)
1065	1061	-4	C ^{α2} H r ² (32), CH ₃ r ² (14), CC ^c ob(9), CH ₃ r ¹ (7)
1101	1087	-14	CH ₃ r ² (35), CN ⁿ s(14), CC ^{me} s(14), CH ₃ r ² (7)
1117	1119	2	CNH ₃ r ¹ (39), C ^{α1} H r ² (34)
1140	1141	1	NC ^φ s(26), CC ^{me} s(14), CH ₃ r ² (12)
1168	1164	-4	CH ₃ r ¹ (36), CC ^{me} s(24), C ^{α2} H d ¹ (15)
1235	1211	-24	CH ₃ r ¹ (31), CNH ₃ r ² (19), CC ^{me} s(15), C ^{α1} H d ¹ (13)
1235	1225	-10	C ^{α2} H r ² (27), NH ^a ib(20), C ^{α2} H r ¹ (9)
1268	1300	32	C ^{α1} H r ² (31), CNH ₃ r ¹ (7)
1322	1329	7	C ^{α2} H r ² (14), C ^{α1} H r ² (9), NH ^a ib(8), C ^{α1} H r ¹ (8)
1340	1341	1	C ^{α2} H r ¹ (70)
1370	1358	-12	C ^{α1} H r ¹ (74)
1370	1370	0	CH ₃ sd(89)
1401	1399	-2	CH ₃ sd(74), CO ^c ss(9)
1407	1399	-8	CO ^c ss(34), CH ₃ sd(20), CO ^c as(15), CO ^a s(7)
1459	1449	-10	CH ₃ ad ^{1,2} (85), CH ₃ r ² (7)
1459	1455	-4	CH ₃ ad ^{1,2} (55), CH ₃ ad ^{1,2} (14), CNH ₃ sd(11)
1459	1459	0	CH ₃ ad ^{1,2} (27), CH ₃ ad ^{1,2} (26), CNH ₃ sd(23)
1459	1464	5	CH ₃ ad ^{1,2} (67), CH ₃ ad ^{1,2} (12), CH ₃ ad ^{1,2} (8), CH ₃ r ¹ (8)
—	1466	—	CH ₃ ad ^{1,2} (40), CNH ₃ sd(34)
—	1509	—	NH ^a ib(44), CO ^a s(12), CN ^a s(12), CO ^c ss(10)

Table 3.74: (continued)

frequency (cm ⁻¹)			Potential Energy Distribution
obs.	calc.	dev.	
1571	1596	25	CO ^c as(54), CO ^c ss(16), NH ^a ib(13)
1610	1607	-3	CNH ₃ ad ^{1,2} (68), CNH ₃ sd(21)
1636	1634	-2	CNH ₃ ad ^{1,2} (95)
1647	1651	4	CO ^a s(35), CN ^a s(34), CNH ₃ ad ^{1,2} (7)
—	2562	—	NH ₃ as ¹ (57), NH ₃ ss(39)
—	2925	—	CH ₃ ss(91)
—	2929	—	CH ₃ ss(95)
—	2957	—	C ^{α2} H s(49), CH ₃ as ^{1,2} (41), CH ₃ as ^{1,2} (9)
—	2975	—	C ^{α2} H s(50), CH ₃ as ^{1,2} (33), CH ₃ as ^{1,2} (17)
—	2977	—	CH ₃ as ^{1,2} (71), CH ₃ as ^{1,2} (23)
—	3004	—	CH ₃ as ^{1,2} (69), CH ₃ as ^{1,2} (14), C ^{α1} H s(12)
—	3007	—	CH ₃ as ^{1,2} (71), CH ₃ as ^{1,2} (21), CH ₃ ss(7)
—	3014	—	C ^{α1} H s(82), CH ₃ as ^{1,2} (13)
—	3083	—	NH ₃ ss(59), NH ₃ as ¹ (40)
—	3121	—	NH ^a s(97)
—	3145	—	NH ₃ as ² (100)

frequency (cm ⁻¹)			Ala-Ala in D ₂ O: CHNDCH (mean deviation = 14 cm ⁻¹)
obs.	calc.	dev.	
—	31	—	CC ^ψ t(56), NC ^φ t(33), NH ^a ob(8)
—	55	—	CC ^c t(20), NH ^a ob(17), CC ^ψ t(16), NC ^φ t(15), C ^ω N t(13), CN ⁿ t(8)
—	75	—	C ^ω N t(38), NC ^φ t(17), CNHC sd(10)
—	94	—	CC ^c t(38), CNHC sd(16), C ^ω N t(16), CO ^a sd(12), NC ^φ t(9), CN ⁿ t(7)
—	121	—	CC ^c t(37), CNHC sd(21), CO ^a sd(14), NH ^a ob(11), C ^{α2} H d ³ (7)
—	188	—	CC ^{me} t(97)
—	193	—	CC ^{me} t(93)
246	214	-32	CN ⁿ t(64), CC ^ψ t(20)
246	235	-11	C ^{α2} H d ² (29), C ^{α1} H d ² (12), CN ⁿ t(10), C ^{α2} H d ¹ (7)
—	260	—	C ^{α1} H d ² (32), C ^{α2} H d ² (19), CC ^c r(13), C ^{α2} H d ³ (10)

Table 3.74: (continued)

frequency (cm ⁻¹)			Potential Energy Distribution
obs.	calc.	dev.	
333	320	-13	C ^{α2} H d ² (18), C ^{α2} H d ³ (18), CC ^c s(10), CN ^a s(9), C ^{α1} H d ³ (9), C ^{α1} H d ¹ (8)
—	340	—	CC ^c r(21), CO ^a sd(17), C ^{α1} H d ² (13), C ^{α1} H d ³ (10)
367	389	22	C ^{α1} H d ¹ (37), CO ^a r(16), C ^{α1} H d ³ (12)
434	424	-10	C ^{α1} H d ¹ (26), CC ^c r(23), C ^{α1} H d ³ (14)
440	441	1	C ^{α2} H d ¹ (47), C ^{α1} H d ² (12), C ^ω N t(11)
569	576	7	CC ^c r(23), C ^{α2} H d ³ (13), CO ^a sd(12), CC ^ψ s(8), C ^{α2} H d ¹ (7)
635	630	-5	NH ^a ob(21), CO ^a r(16), CC ^c sd(16), CC ^c s(8), NC ^φ t(7)
635	647	12	NH ^a ob(26), CC ^c sd(13), NC ^φ t(12), C ^ω N t(9), CO ^a ob(8), CO ^a r(7)
688	664	-24	CC ^c sd(22), CC ^ψ s(14), CO ^a r(9), CC ^c ob(8)
751	725	-26	CNH ₃ r ² (52), CO ^a ob(27)
—	765	—	CO ^a ob(26), CNH ₃ r ² (17), CC ^{me} s(10), C ^{α1} H d ² (8), CO ^a r(8)
777	777	0	CC ^c ob(52), CC ^c sd(14), C ^{α2} H d ² (9)
825	817	-8	CN ⁿ s(34), CNH ₃ r ¹ (18), CH ₃ r ² (7)
875	872	-3	CNH ₃ r ¹ (31), CN ⁿ s(14), C ^{α1} H d ³ (10), CH ₃ r ¹ (10)
875	881	6	CC ^c s(25), CC ^c sd(15), CC ^{me} s(10), CH ₃ r ¹ (9), CO ^c ss(8), CH ₃ r ² (7)
906	909	3	NH ^a ib(13), CO ^a s(11), CC ^ψ s(9), CNH ₃ r ¹ (9), CC ^{me} s(7), CH ₃ r ¹ (7), CH ₃ r ² (7)
943	925	-18	NC ^φ s(20), CC ^{me} s(17), CH ₃ r ² (15), CC ^c s(13), CH ₃ r ¹ (10), NH ^a ib(7)
1002	1000	-2	NH ^a ib(38), CH ₃ r ² (13), CH ₃ r ² (13), CC ^ψ s(10)
1050	1059	9	C ^{α1} H r ² (25), CC ^{me} s(21), C ^{α1} H d ³ (10), CN ⁿ s(8), CNH ₃ r ¹ (7), CH ₃ r ¹ (7)
1063	1074	11	C ^{α2} H r ² (26), CH ₃ r ² (14), CH ₃ r ² (11), CC ^c ob(7), CNH ₃ sd(7)
1098	1085	-13	CNH ₃ sd(22), CNH ₃ ad ^{1,2} (18), C ^{α2} H r ² (10), C ^{α1} H r ² (9), CH ₃ r ² (8)
1115	1104	-11	CNH ₃ ad ^{1,2} (20), CH ₃ r ² (18), CNH ₃ sd(15), CN ⁿ s(9)
1151	1143	-8	NC ^φ s(32), CH ₃ r ² (15), CC ^{me} s(13)
1160	1164	4	CH ₃ r ¹ (37), CC ^{me} s(27), C ^{α2} H d ¹ (14)
1160	1173	13	CNH ₃ ad ^{1,2} (50), CH ₃ r ¹ (19), CC ^{me} s(12)

Table 3.74: (continued)

frequency (cm ⁻¹)			Potential Energy Distribution
obs.	calc.	dev.	
1176	1182	6	CNH ₃ ad ^{1,2} (51), CNH ₃ sd(44)
1184	1195	11	CNH ₃ ad ^{1,2} (46), CH ₃ r ¹ (16), CC ^{me} s(10), C ^{α1} H d ¹ (9)
1277	1285	8	C ^{α2} H r ² (28), C ^{α2} H r ¹ (11), C ^{α1} H r ² (8), CH ₃ r ¹ (7)
1308	1300	-8	C ^{α1} H r ² (40), CH ₃ r ¹ (8), CC ^ψ s(7)
1329	1339	10	C ^{α2} H r ¹ (71), C ^{α2} H r ² (11)
1354	1345	-9	C ^{α1} H r ¹ (84)
1369	1369	0	CH ₃ sd(88)
1401	1396	-5	CH ₃ sd(95)
1407	1400	-7	CO ^c ss(45), CO ^c as(22), CC ^c s(8), CH ₃ sd(7)
1445	1442	-3	CH ₃ ad ^{1,2} (55), CO ^a s(11), CN ^a s(11)
1459	1456	-3	CH ₃ ad ^{1,2} (76), CH ₃ ad ^{1,2} (11)
1459	1459	0	CH ₃ ad ^{1,2} (24), CH ₃ ad ^{1,2} (24), CH ₃ ad ^{1,2} (15), CO ^a s(9)
1459	1462	3	CH ₃ ad ^{1,2} (42), CH ₃ ad ^{1,2} (35), CH ₃ ad ^{1,2} (8)
1484	1466	-18	CH ₃ ad ^{1,2} (27), CH ₃ ad ^{1,2} (19), CH ₃ ad ^{1,2} (10), CO ^a s(8)
1590	1581	-9	CO ^c as(61), CO ^c ss(24)
1665	1663	-2	CO ^a s(42), CN ^a s(42)
—	1870	—	NH ₃ as ¹ (48), NH ₃ ss(46)
—	2238	—	NH ₃ ss(51), NH ₃ as ¹ (48)
—	2294	—	NH ^a s(95)
—	2321	—	NH ₃ as ² (100)
—	2925	—	CH ₃ ss(91)
—	2929	—	CH ₃ ss(95)
—	2957	—	C ^{α2} H s(49), CH ₃ as ^{1,2} (41), CH ₃ as ^{1,2} (9)
—	2975	—	C ^{α2} H s(50), CH ₃ as ^{1,2} (33), CH ₃ as ^{1,2} (17)
—	2977	—	CH ₃ as ^{1,2} (72), CH ₃ as ^{1,2} (23)
—	3004	—	CH ₃ as ^{1,2} (69), CH ₃ as ^{1,2} (14), C ^{α1} H s(12)
—	3007	—	CH ₃ as ^{1,2} (71), CH ₃ as ^{1,2} (21), CH ₃ ss(7)
—	3014	—	C ^{α1} H s(82), CH ₃ as ^{1,2} (13)

frequency (cm ⁻¹)			Ala-Ala: CDNHCH (mean deviation = 16 cm ⁻¹) Potential Energy Distribution
obs.	calc.	dev.	
—	32	—	CC ^ψ t(55), NC ^φ t(35), NH ^a ob(7)
—	57	—	CC ^c t(23), CC ^ψ t(19), NH ^a ob(18), C ^ω N t(16), NC ^φ t(10)

Table 3.74: (continued)

frequency (cm ⁻¹)			Potential Energy Distribution
obs.	calc.	dev.	
—	77	—	C ^ω N t(33), NC ^φ t(16), CNHC sd(11), CC ^ψ t(8), CO ^a sd(7)
—	97	—	CC ^c t(33), C ^ω N t(18), CNHC sd(15), NC ^φ t(13), CO ^a sd(11)
—	123	—	CC ^c t(36), CNHC sd(21), CO ^a sd(14), NH ^a ob(11), C ^{α2} H d ³ (7)
—	188	—	CC ^{me} t(97)
—	194	—	CC ^{me} t(94)
256	231	-25	C ^{α2} H d ² (26), C ^{α1} H d ² (16), C ^{α2} H d ¹ (10), CNHC sd(8), NC ^φ s(7)
256	261	5	C ^{α2} H d ² (29), C ^{α1} H d ² (25), CC ^c r(12), C ^{α2} H d ³ (8)
—	289	—	CN ⁿ t(80), CC ^ψ t(10)
344	327	-17	C ^{α2} H d ³ (18), C ^{α2} H d ² (13), CC ^c s(11), CN ^a s(10), NC ^φ s(8), CO ^a r(7)
379	346	-33	CC ^c r(28), CO ^a sd(18), C ^{α2} H d ³ (14), C ^{α1} H d ² (11), C ^{α1} H d ³ (9)
—	417	—	C ^{α1} H d ¹ (38), C ^{α1} H d ³ (17), CO ^a r(14)
450	443	-7	C ^{α1} H d ¹ (35), CC ^c r(18), C ^{α1} H d ³ (10)
450	457	7	C ^{α2} H d ¹ (42), C ^{α1} H d ² (10), C ^{α1} H d ³ (10), CO ^a r(10)
579	584	5	CC ^c r(22), CC ^ψ s(13), C ^{α2} H d ¹ (10), C ^{α2} H d ³ (10), CO ^a sd(8), CO ^a r(7)
648	643	-5	CC ^c sd(37), CC ^c s(18), CO ^a r(12), C ^{α1} H d ³ (9)
677	663	-14	CO ^a ob(14), CC ^c sd(12), CC ^ψ s(9), C ^{α1} H r ² (9), C ^{α1} H d ³ (8), CC ^c ob(8), C ^{α2} H d ³ (7)
735	739	4	CO ^a ob(26), C ^{α1} H r ² (16), CO ^a r(11), CH ₃ r ¹ (9), C ^{α1} H d ² (8), C ^{α1} H d ³ (7)
780	775	-5	CC ^c ob(47), CC ^c sd(15), C ^{α2} H d ² (10)
—	809	—	CN ⁿ s(31), CC ^{me} s(23), C ^{α1} H r ² (16), CO ^a ob(7)
831	859	28	NH ^a ob(35), NC ^φ t(16), CN ⁿ s(15), C ^ω N t(11)
863	869	6	C ^{α1} H r ² (16), NH ^a ob(13), C ^{α1} H r ¹ (10), CO ^a ob(8), CNH ₃ r ² (8)
892	875	-17	C ^{α1} H r ¹ (23), CC ^c s(17), CC ^c sd(11), CNH ₃ r ² (8), CN ⁿ s(7)
908	910	2	C ^{α1} H r ¹ (18), C ^{α1} H r ² (14), CC ^c s(9), CH ₃ r ² (9), CO ^a ob(8), CN ⁿ s(7), CNH ₃ r ² (7)
908	928	20	CNHC sd(13), CC ^{me} s(12), CO ^a s(9), CO ^a r(9), CC ^ψ s(8), CH ₃ r ¹ (8)

Table 3.74: (continued)

frequency (cm ⁻¹)			Potential Energy Distribution
obs.	calc.	dev.	
952	943	-9	CH ₃ r ² (18), CH ₃ r ² (16), NC ^φ s(15), CC ^{me} s(9), CC ^c s(7), CNH ₃ r ² (7)
968	992	24	CNH ₃ r ² (27), C ^{α1} H r ¹ (15), CC ^{me} s(15), CNH ₃ r ¹ (13), CC ^ψ s(9)
1069	1061	-8	C ^{α2} H r ² (31), CH ₃ r ² (12), CC ^c ob(9), CH ₃ r ¹ (7)
1087	1075	-12	CNH ₃ r ¹ (28), CH ₃ r ² (25), CH ₃ r ¹ (7), CH ₃ r ² (7)
1105	1131	26	NC ^φ s(17), CNH ₃ r ¹ (13), CH ₃ r ² (12), CC ^{me} s(10), C ^{α1} H r ¹ (8)
1150	1164	14	CH ₃ r ¹ (30), CC ^{me} s(29), C ^{α2} H d ¹ (11)
1150	1169	19	C ^{α1} H r ¹ (15), NC ^φ s(14), CC ^{me} s(12), CH ₃ r ² (7)
1212	1188	-24	CH ₃ r ¹ (43), CNH ₃ r ² (18), C ^{α1} H d ¹ (9), CC ^{me} s(9), CH ₃ ad ^{1,2} (7)
1245	1225	-20	C ^{α2} H r ² (25), NH ^a ib(19), C ^{α2} H r ¹ (8), CO ^a s(7)
1273	1264	-9	CNH ₃ r ¹ (18), CC ^{me} s(12), CC ^ψ s(10), CH ₃ r ² (9), C ^{α1} H r ² (7), C ^{α2} H r ² (7)
1312	1334	22	C ^{α2} H r ¹ (22), C ^{α2} H r ² (22), NH ^a ib(9), CH ₃ r ¹ (9)
1347	1345	-2	C ^{α2} H r ¹ (51), NH ^a ib(8)
1371	1370	-1	CH ₃ sd(90)
1399	1398	-1	CH ₃ sd(78), CO ^c ss(8)
1407	1402	-5	CO ^c ss(37), CH ₃ sd(15), CO ^c as(14)
1458	1448	-10	CH ₃ ad ^{1,2} (88), CH ₃ r ² (7)
1458	1455	-3	CH ₃ ad ^{1,2} (63), CH ₃ ad ^{1,2} (14), CH ₃ ad ^{1,2} (7)
1458	1459	1	CH ₃ ad ^{1,2} (56), CH ₃ ad ^{1,2} (16), CNH ₃ sd(11), CH ₃ r ¹ (7)
1458	1463	5	CH ₃ ad ^{1,2} (69), CH ₃ ad ^{1,2} (11), CH ₃ r ¹ (8), CH ₃ ad ^{1,2} (7)
—	1467	—	CNH ₃ sd(55), CH ₃ ad ^{1,2} (17), CNH ₃ ad ^{1,2} (9)
—	1519	—	NH ^a ib(39), CN ^a s(14), CO ^a s(13), CO ^c ss(9)
1577	1597	20	CO ^c as(54), CO ^c ss(16), NH ^a ib(14)
—	1607	—	CNH ₃ ad ^{1,2} (73), CNH ₃ sd(18)
—	1633	—	CNH ₃ ad ^{1,2} (94)
1673	1687	14	CO ^a s(40), CN ^a s(37)
—	2222	—	C ^{α1} H s(98)
—	2562	—	NH ₃ as ¹ (57), NH ₃ ss(39)
—	2925	—	CH ₃ ss(91)
—	2929	—	CH ₃ ss(95)

Table 3.74: (continued)

frequency (cm ⁻¹)			Potential Energy Distribution
obs.	calc.	dev.	
—	2957	—	C ^{α2} H s(49), CH ₃ as ^{1,2} (41), CH ₃ as ^{1,2} (9)
—	2975	—	C ^{α2} H s(50), CH ₃ as ^{1,2} (33), CH ₃ as ^{1,2} (17)
—	2979	—	CH ₃ as ^{1,2} (73), CH ₃ as ^{1,2} (27)
—	3005	—	CH ₃ as ^{1,2} (69), CH ₃ as ^{1,2} (26)
—	3007	—	CH ₃ as ^{1,2} (71), CH ₃ as ^{1,2} (21), CH ₃ ss(7)
—	3083	—	NH ₃ ss(60), NH ₃ as ¹ (40)
—	3121	—	NH ^a s(97)
—	3145	—	NH ₃ as ² (100)

frequency (cm ⁻¹)			Ala-Ala: CDNDCH (mean deviation = 13 cm ⁻¹) Potential Energy Distribution
obs.	calc.	dev.	
—	30	—	CC ^ψ t(56), NC ^φ t(32), NH ^a ob(7)
—	55	—	CC ^c t(20), NH ^a ob(17), CC ^ψ t(16), NC ^φ t(15), C ^ω N t(13), CN ⁿ t(8)
—	75	—	C ^ω N t(38), NC ^φ t(17), CNHC sd(10)
—	94	—	CC ^c t(37), CNHC sd(17), C ^ω N t(16), CO ^a sd(12), NC ^φ t(9), CN ⁿ t(7)
—	121	—	CC ^c t(38), CNHC sd(20), CO ^a sd(14), NH ^a ob(10), C ^{α2} H d ³ (7)
—	188	—	CC ^{me} t(97)
—	193	—	CC ^{me} t(93)
—	213	—	CN ⁿ t(64), CC ^ψ t(20)
—	235	—	C ^{α2} H d ² (30), C ^{α1} H d ² (12), CN ⁿ t(10), CNHC sd(7), C ^{α2} H d ¹ (7)
—	260	—	C ^{α1} H d ² (33), C ^{α2} H d ² (19), CC ^c r(12), C ^{α2} H d ³ (10)
—	319	—	C ^{α2} H d ² (18), C ^{α2} H d ³ (18), CC ^c s(10), CN ^a s(9), C ^{α1} H d ³ (9), C ^{α1} H d ¹ (8)
—	336	—	CC ^c r(21), CO ^a sd(18), C ^{α1} H d ² (13), C ^{α1} H d ³ (10), C ^{α2} H d ³ (7)
—	388	—	C ^{α1} H d ¹ (40), CO ^a r(14), C ^{α1} H d ³ (11)
—	422	—	C ^{α1} H d ¹ (24), CC ^c r(22), C ^{α1} H d ³ (16), CO ^a r(7)
—	440	—	C ^{α2} H d ¹ (48), C ^ω N t(12), C ^{α1} H d ² (11)
—	570	—	CC ^c r(24), C ^{α2} H d ³ (11), CC ^ψ s(10), CO ^a sd(9), C ^{α2} H d ¹ (7)

Table 3.74: (continued)

frequency (cm ⁻¹)			Potential Energy Distribution
obs.	calc.	dev.	
—	628	—	CO ^a r(22), CC ^c sd(15), NH ^a ob(12), CC ^c s(9), C ^{α1} H d ³ (8)
—	640	—	NH ^a ob(28), NC ^φ t(17), CO ^a ob(14), C ^ω N t(12)
—	658	—	CC ^c sd(35), CC ^c s(12), CC ^c ob(11), NH ^a ob(7)
—	708	—	CNH ₃ r ² (34), CO ^a ob(20), C ^{α1} H r ² (9), CN ⁿ s(8)
—	747	—	CNH ₃ r ² (33), C ^{α1} H r ² (13), CH ₃ r ¹ (9), CO ^a ob(8), CO ^a r(7)
—	777	—	CC ^c ob(53), CC ^c sd(13), C ^{α2} H d ² (9)
—	801	—	CN ⁿ s(33), C ^{α1} H r ² (10), CC ^{me} s(9), CO ^a ob(7), CH ₃ r ² (7)
—	837	—	CNH ₃ r ¹ (40), CC ^{me} s(20), C ^{α1} H r ¹ (12), C ^{α1} H r ² (9)
—	872	—	CC ^c s(19), CC ^c sd(14), CC ^{me} s(9), CC ^ψ s(8), CH ₃ r ¹ (7)
—	893	—	CN ⁿ s(18), NH ^a ib(12), CO ^a s(9), CC ^ψ s(7), C ^{α1} H r ² (7)
—	905	—	C ^{α1} H r ² (15), CC ^c s(13), CH ₃ r ² (10), CO ^a ob(9), C ^{α1} H r ¹ (7)
—	928	—	CC ^{me} s(17), NC ^φ s(15), CH ₃ r ¹ (11), CH ₃ r ² (10), CC ^c s(9)
—	977	—	C ^{α1} H r ¹ (34), NH ^a ib(17), CNH ₃ r ¹ (15), C ^{α1} H d ³ (8)
—	1005	—	CH ₃ r ² (28), NH ^a ib(25), CH ₃ r ² (10), CC ^ψ s(9), C ^{α1} H r ¹ (7)
—	1075	—	C ^{α2} H r ² (38), CH ₃ r ² (13), CC ^c ob(10), NH ^a ib(7)
—	1090	—	CNH ₃ sd(45), CNH ₃ ad ^{1,2} (40)
—	1123	—	NC ^φ s(15), CH ₃ r ² (14), CH ₃ r ² (11), CC ^{me} s(9), C ^{α1} H r ¹ (8)
—	1152	—	CC ^{me} s(28), CH ₃ r ¹ (12), NC ^φ s(11)
—	1164	—	CH ₃ r ¹ (36), CC ^{me} s(27), C ^{α2} H d ¹ (14)
—	1173	—	CH ₃ r ¹ (40), CNH ₃ ad ^{1,2} (9), C ^{α1} H r ¹ (8)
1165	1182	17	CNH ₃ ad ^{1,2} (46), CNH ₃ sd(43), CNH ₃ ad ^{1,2} (7)
1203	1188	-15	CNH ₃ ad ^{1,2} (77), CNH ₃ ad ^{1,2} (7), CH ₃ r ¹ (7)
1203	1235	32	CC ^{me} s(18), CC ^ψ s(17), CH ₃ r ² (14), C ^{α1} H r ² (12), CNH ₃ r ¹ (7)
1279	1288	9	C ^{α2} H r ² (34), C ^{α2} H r ¹ (10), CH ₃ r ¹ (8), CC ^c s(7), CH ₃ r ² (7)
1330	1340	10	C ^{α2} H r ¹ (73), C ^{α2} H r ² (12)
1371	1369	-2	CH ₃ sd(88)
1399	1396	-3	CH ₃ sd(95)
1408	1400	-8	CO ^c ss(45), CO ^c as(22), CC ^c s(8), CH ₃ sd(7)
1450	1441	-9	CH ₃ ad ^{1,2} (55), CO ^a s(11), CN ^a s(11)
1450	1456	6	CH ₃ ad ^{1,2} (69), CH ₃ ad ^{1,2} (7)
1460	1457	-3	CH ₃ ad ^{1,2} (31), CH ₃ ad ^{1,2} (18), CH ₃ ad ^{1,2} (13), CO ^a s(7), CH ₃ ad ^{1,2} (7)

Table 3.74: (continued)

frequency (cm ⁻¹)			Potential Energy Distribution
obs.	calc.	dev.	
1460	1461	1	CH ₃ ad ^{1,2} (42), CH ₃ ad ^{1,2} (27)
1479	1465	-14	CH ₃ ad ^{1,2} (41), CH ₃ ad ^{1,2} (9), CH ₃ ad ^{1,2} (8), CO ^a s(7), CH ₃ ad ^{1,2} (7)
1590	1581	-9	CO ^c as(61), CO ^c ss(24)
1664	1661	-3	CO ^a s(43), CN ^a s(42)
—	1870	—	NH ₃ as ¹ (48), NH ₃ ss(47)
—	2221	—	C ^{α1} H s(97)
—	2238	—	NH ₃ ss(51), NH ₃ as ¹ (48)
—	2294	—	NH ^a s(95)
—	2320	—	NH ₃ as ² (100)
—	2925	—	CH ₃ ss(91)
—	2929	—	CH ₃ ss(95)
—	2957	—	C ^{α2} H s(49), CH ₃ as ^{1,2} (41), CH ₃ as ^{1,2} (9)
—	2975	—	C ^{α2} H s(50), CH ₃ as ^{1,2} (33), CH ₃ as ^{1,2} (17)
—	2979	—	CH ₃ as ^{1,2} (73), CH ₃ as ^{1,2} (27)
—	3005	—	CH ₃ as ^{1,2} (69), CH ₃ as ^{1,2} (25)
—	3007	—	CH ₃ as ^{1,2} (71), CH ₃ as ^{1,2} (21), CH ₃ ss(7)

frequency (cm ⁻¹)			Ala-Ala: CDNHCD (mean deviation = 11 cm ⁻¹) Potential Energy Distribution
obs.	calc.	dev.	
—	32	—	CC ^ψ t(55), NC ^φ t(36), NH ^a ob(7)
—	57	—	CC ^c t(22), CC ^ψ t(19), NH ^a ob(18), C ^ω N t(16), NC ^φ t(10)
—	77	—	C ^ω N t(33), NC ^φ t(16), CNHC sd(11), CC ^ψ t(9), CO ^a sd(7)
—	97	—	CC ^c t(33), C ^ω N t(18), CNHC sd(16), NC ^φ t(13), CO ^a sd(11)
—	122	—	CC ^c t(37), CNHC sd(21), CO ^a sd(14), NH ^a ob(11), C ^{α2} H d ³ (7)
—	188	—	CC ^{me} t(97)
—	194	—	CC ^{me} t(94)
—	231	—	C ^{α2} H d ² (26), C ^{α1} H d ² (16), C ^{α2} H d ¹ (11), CNHC sd(8), NC ^φ s(7)
—	260	—	C ^{α2} H d ² (30), C ^{α1} H d ² (24), CC ^c r(12), C ^{α2} H d ³ (8)
—	289	—	CN ⁿ t(80), CC ^ψ t(10)
—	324	—	C ^{α2} H d ³ (20), C ^{α2} H d ² (14), CN ^a s(10), CC ^c s(10), NC ^φ s(8)

Table 3.74: (continued)

frequency (cm ⁻¹)			Potential Energy Distribution
obs.	calc.	dev.	
—	344	—	CC ^c r(28), CO ^a sd(18), C ^{α1} H d ² (12), C ^{α2} H d ³ (12), C ^{α1} H d ³ (8)
—	416	—	C ^{α1} H d ¹ (32), C ^{α1} H d ³ (18), CO ^a r(14), CC ^c r(8), C ^{α2} H d ¹ (7)
—	440	—	C ^{α1} H d ¹ (40), CC ^c r(15)
—	455	—	C ^{α2} H d ¹ (37), C ^{α1} H d ³ (14), CO ^a r(12), C ^{α1} H d ² (9)
—	576	—	CC ^c r(17), CC ^ψ s(13), C ^{α2} H d ¹ (12), C ^{α2} H d ³ (9), CO ^a sd(8)
—	616	—	CC ^c sd(34), CC ^c s(21), C ^{α2} H r ² (14), CC ^c ob(10), CC ^c r(8)
—	657	—	C ^{α1} H d ³ (15), CO ^a r(15), CO ^a ob(14), C ^{α1} H r ² (9), CC ^ψ s(8), C ^{α2} H d ³ (8)
—	734	—	CO ^a ob(23), C ^{α1} H r ² (14), C ^{α2} H r ² (10), CO ^a r(10)
—	748	—	CC ^c sd(21), CC ^c ob(17), C ^{α2} H r ² (13)
—	806	—	CN ⁿ s(31), CC ^{me} s(21), C ^{α1} H r ² (15)
—	840	—	CC ^{me} s(26), C ^{α2} H r ¹ (15), CC ^c sd(12), C ^{α2} H r ² (9), CH ₃ r ¹ (7)
—	858	—	NH ^a ob(38), NC ^φ t(13), C ^ω N t(10), C ^{α2} H r ² (8), CN ⁿ s(8)
—	868	—	C ^{α1} H r ¹ (23), CN ⁿ s(20), C ^{α1} H r ² (17), CNH ₃ r ² (17), CO ^a ob(7)
—	881	—	CC ^c s(22), CC ^c ob(21), C ^{α2} H r ² (13), CC ^c sd(12), CO ^c ss(7), CH ₃ r ² (7)
—	896	—	C ^{α1} H r ¹ (28), C ^{α1} H r ² (12), C ^{α2} H r ¹ (10), CC ^ψ s(9), CO ^a ob(7)
—	926	—	CH ₃ r ² (19), CN ⁿ s(12), CNH ₃ r ² (11)
—	954	—	CH ₃ r ² (31), NC ^φ s(11), C ^{α2} H r ¹ (9), CC ^c ob(8), CH ₃ r ² (8)
—	991	—	CNH ₃ r ² (25), C ^{α1} H r ¹ (13), CC ^{me} s(13), CNH ₃ r ¹ (12), CC ^ψ s(8)
—	1005	—	C ^{α2} H r ¹ (31), NC ^φ s(17), CNHC sd(7)
—	1077	—	CNH ₃ r ¹ (35), CH ₃ r ² (24), CH ₃ r ¹ (9)
—	1145	—	CH ₃ r ¹ (25), CC ^{me} s(24), C ^{α2} H d ² (8)
1154	1158	4	CH ₃ r ¹ (20), C ^{α1} H r ¹ (18), CC ^{me} s(11), CH ₃ r ¹ (8), CH ₃ r ² (8)
—	1175	—	CH ₃ r ² (27), CC ^c s(14), NH ^a ib(9), C ^{α2} H r ² (7), C ^{α2} H d ¹ (7), CO ^c ss(7), CC ^{me} s(7)
1196	1188	-8	CH ₃ r ¹ (41), CNH ₃ r ² (19), CC ^{me} s(10), C ^{α1} H d ¹ (9)
1218	1195	-23	CH ₃ r ¹ (19), NC ^φ s(10), C ^{α2} H r ¹ (8), CC ^{me} s(8)

Table 3.74: (continued)

frequency (cm^{-1})			Potential Energy Distribution
obs.	calc.	dev.	
1250	1259	9	CNH_3 $r^1(17)$, CC^{me} $s(12)$, NC^ϕ $s(9)$, CH_3 $r^2(9)$, CC^ψ $s(7)$, $\text{C}^{\alpha 1}$ H $r^2(7)$
1336	1327	-9	NH^a $\text{ib}(24)$, CC^ψ $s(12)$
1370	1370	0	CH_3 $\text{sd}(90)$
1401	1398	-3	CH_3 $\text{sd}(79)$, CO^c $\text{ss}(8)$
1406	1402	-4	CO^c $\text{ss}(37)$, CH_3 $\text{sd}(16)$, CO^c $\text{as}(15)$
1458	1448	-10	CH_3 $\text{ad}^{1,2}(88)$, CH_3 $r^2(7)$
1458	1455	-3	CH_3 $\text{ad}^{1,2}(65)$, CH_3 $\text{ad}^{1,2}(14)$
1458	1459	1	CH_3 $\text{ad}^{1,2}(57)$, CH_3 $\text{ad}^{1,2}(14)$, CNH_3 $\text{sd}(12)$, CH_3 $r^1(7)$
1458	1462	4	CH_3 $\text{ad}^{1,2}(75)$, CH_3 $\text{ad}^{1,2}(11)$, CH_3 $r^1(7)$
—	1466	—	CNH_3 $\text{sd}(55)$, CH_3 $\text{ad}^{1,2}(21)$, CNH_3 $\text{ad}^{1,2}(9)$
—	1519	—	NH^a $\text{ib}(39)$, CN^a $s(14)$, CO^a $s(13)$, CO^c $\text{ss}(9)$
1570	1595	25	CO^c $\text{as}(56)$, CO^c $\text{ss}(17)$, NH^a $\text{ib}(14)$
—	1607	—	CNH_3 $\text{ad}^{1,2}(73)$, CNH_3 $\text{sd}(19)$
—	1633	—	CNH_3 $\text{ad}^{1,2}(94)$
1680	1686	6	CO^a $s(40)$, CN^a $s(37)$
—	2186	—	$\text{C}^{\alpha 2}$ H $s(98)$
—	2222	—	$\text{C}^{\alpha 1}$ H $s(98)$
—	2562	—	NH_3 $\text{as}^1(57)$, NH_3 $\text{ss}(39)$
—	2925	—	CH_3 $\text{ss}(91)$
—	2929	—	CH_3 $\text{ss}(95)$
—	2966	—	CH_3 $\text{as}^{1,2}(76)$, CH_3 $\text{as}^{1,2}(23)$
—	2979	—	CH_3 $\text{as}^{1,2}(73)$, CH_3 $\text{as}^{1,2}(27)$
—	3005	—	CH_3 $\text{as}^{1,2}(69)$, CH_3 $\text{as}^{1,2}(26)$
—	3006	—	CH_3 $\text{as}^{1,2}(74)$, CH_3 $\text{as}^{1,2}(19)$, CH_3 $\text{ss}(7)$
—	3083	—	NH_3 $\text{ss}(60)$, NH_3 $\text{as}^1(40)$
—	3121	—	NH^a $s(97)$
—	3145	—	NH_3 $\text{as}^2(100)$

frequency (cm^{-1})			Potential Energy Distribution
obs.	calc.	dev.	
—	30	—	CC^ψ $t(56)$, NC^ϕ $t(33)$, NH^a $\text{ob}(7)$

Table 3.74: (continued)

frequency (cm ⁻¹)			Potential Energy Distribution
obs.	calc.	dev.	
—	55	—	CC ^c t(20), NH ^a ob(17), CC ^ψ t(16), NC ^φ t(15), C ^ω N t(13), CN ⁿ t(8)
—	75	—	C ^ω N t(38), NC ^φ t(17), CNHC sd(10)
—	94	—	CC ^c t(36), CNHC sd(17), C ^ω N t(16), CO ^a sd(12), NC ^φ t(9)
—	120	—	CC ^c t(39), CNHC sd(20), CO ^a sd(13), NH ^a ob(10), C ^{α2} H d ³ (7)
—	188	—	CC ^{me} t(97)
—	193	—	CC ^{me} t(93)
—	213	—	CN ⁿ t(64), CC ^ψ t(20)
—	235	—	C ^{α2} H d ² (29), C ^{α1} H d ² (12), CN ⁿ t(10), CNHC sd(7), C ^{α2} H d ¹ (7)
—	259	—	C ^{α1} H d ² (32), C ^{α2} H d ² (20), CC ^c r(12), C ^{α2} H d ³ (10)
—	317	—	C ^{α2} H d ² (19), C ^{α2} H d ³ (19), CN ^a s(9), CC ^c s(9), C ^{α1} H d ³ (9), C ^{α1} H d ¹ (8)
—	335	—	CC ^c r(20), CO ^a sd(18), C ^{α1} H d ² (13), C ^{α1} H d ³ (9), CO ^a ob(7)
—	387	—	C ^{α1} H d ¹ (37), CO ^a r(15), C ^{α1} H d ³ (12), CC ^c r(7)
—	419	—	C ^{α1} H d ¹ (27), CC ^c r(22), C ^{α1} H d ³ (13)
—	437	—	C ^{α2} H d ¹ (45), C ^{α1} H d ² (11), C ^ω N t(10)
—	561	—	CC ^c r(19), C ^{α2} H d ³ (11), CC ^ψ s(10), CO ^a sd(9), C ^{α2} H d ¹ (8)
—	612	—	CC ^c sd(30), CC ^c s(19), C ^{α2} H r ² (12), CO ^a r(8), CC ^c ob(7)
—	639	—	CO ^a r(21), CC ^ψ s(13), C ^{α1} H d ³ (8), CO ^a ob(8), C ^{α2} H d ³ (7)
—	640	—	NH ^a ob(41), NC ^φ t(17), C ^ω N t(12), CO ^a ob(7)
—	708	—	CNH ₃ r ² (33), CO ^a ob(21), C ^{α1} H r ² (9), CN ⁿ s(8)
—	739	—	C ^{α2} H r ² (16), CNH ₃ r ² (16), CC ^c ob(13), CC ^c sd(10)
—	751	—	CNH ₃ r ² (19), CC ^c sd(13), CC ^c ob(11), C ^{α1} H r ² (8), C ^{α2} H r ² (8)
—	801	—	CN ⁿ s(33), C ^{α1} H r ² (10), CC ^{me} s(9)
—	836	—	CNH ₃ r ¹ (40), CC ^{me} s(18), C ^{α1} H r ¹ (11), C ^{α1} H r ² (8)
—	840	—	CC ^{me} s(31), C ^{α2} H r ² (14), C ^{α2} H r ¹ (11), CC ^c sd(10)
—	878	—	CC ^c s(23), CC ^c ob(19), CC ^c sd(14), C ^{α2} H r ² (13), CO ^c ss(7)
—	886	—	CC ^ψ s(17), C ^{α1} H r ¹ (12), CO ^a s(11), C ^{α2} H r ¹ (9), NH ^a ib(8)
—	898	—	C ^{α1} H r ² (25), CN ⁿ s(19), CO ^a ob(13), CNH ₃ r ¹ (8)

Table 3.74: (continued)

frequency (cm ⁻¹)			Potential Energy Distribution
obs.	calc.	dev.	
—	941	—	CH ₃ r ² (25), C ^{α2} H r ¹ (18), NH ^a ib(12), CC ^c s(10), C ^{α2} H r ² (10), CC ^c ob(10), NC ^φ s(7)
—	975	—	C ^{α1} H r ¹ (24), NH ^a ib(15), CNH ₃ r ¹ (13), C ^{α1} H d ³ (9), NC ^φ s(7)
—	992	—	CH ₃ r ² (27), C ^{α2} H r ¹ (16), C ^{α1} H r ¹ (15), NC ^φ s(13)
—	1018	—	NH ^a ib(28), C ^{α2} H r ¹ (14), CH ₃ r ² (11), CNHC sd(7), CH ₃ r ² (7)
—	1089	—	CNH ₃ sd(46), CNH ₃ ad ^{1,2} (41)
—	1136	—	CC ^{me} s(15), CH ₃ r ² (14), C ^{α1} H r ¹ (13), CC ^{me} s(10)
—	1150	—	CH ₃ r ¹ (29), CC ^{me} s(18), CC ^{me} s(13)
1159	1166	7	CH ₃ r ¹ (38), CNH ₃ ad ^{1,2} (10), C ^{α1} H d ¹ (8), CH ₃ r ¹ (8)
1164	1182	18	CNH ₃ ad ^{1,2} (44), CNH ₃ sd(40), CNH ₃ ad ^{1,2} (9)
1188	1186	-2	CH ₃ r ¹ (15), CH ₃ r ² (15), NC ^φ s(9), C ^{α2} H r ¹ (8), CH ₃ r ¹ (7)
1194	1188	-6	CNH ₃ ad ^{1,2} (76), CNH ₃ ad ^{1,2} (8)
1205	1232	27	CC ^{me} s(19), CH ₃ r ¹ (13), NC ^φ s(11), C ^{α2} H r ² (10)
1245	1243	-2	CC ^ψ s(14), CC ^{me} s(12), CH ₃ r ² (9), C ^{α1} H r ² (8), NH ^a ib(7)
1370	1369	-1	CH ₃ sd(88)
1392	1396	4	CH ₃ sd(94)
1406	1400	-6	CO ^c ss(45), CO ^c as(22), CC ^c s(8), CH ₃ sd(7)
1450	1441	-9	CH ₃ ad ^{1,2} (55), CO ^a s(11), CN ^a s(11)
1450	1455	5	CH ₃ ad ^{1,2} (73), CH ₃ ad ^{1,2} (10)
1458	1457	-1	CH ₃ ad ^{1,2} (30), CH ₃ ad ^{1,2} (20), CH ₃ ad ^{1,2} (16), CO ^a s(7)
1458	1461	3	CH ₃ ad ^{1,2} (40), CH ₃ ad ^{1,2} (35), CH ₃ ad ^{1,2} (8)
1478	1465	-13	CH ₃ ad ^{1,2} (30), CH ₃ ad ^{1,2} (14), CH ₃ ad ^{1,2} (10), CO ^a s(9), CN ^a s(7), CH ₃ ad ^{1,2} (7)
1584	1580	-4	CO ^c as(62), CO ^c ss(24)
1663	1660	-3	CO ^a s(43), CN ^a s(42)
—	1870	—	NH ₃ as ¹ (48), NH ₃ ss(47)
—	2186	—	C ^{α2} H s(98)
—	2221	—	C ^{α1} H s(97)
—	2238	—	NH ₃ ss(51), NH ₃ as ¹ (48)
—	2294	—	NH ^a s(95)
—	2320	—	NH ₃ as ² (100)
—	2925	—	CH ₃ ss(91)

Table 3.74: (continued)

frequency (cm ⁻¹)			Potential Energy Distribution
obs.	calc.	dev.	
—	2929	—	CH ₃ ss(95)
—	2966	—	CH ₃ as ^{1,2} (76), CH ₃ as ^{1,2} (23)
—	2979	—	CH ₃ as ^{1,2} (73), CH ₃ as ^{1,2} (27)
—	3005	—	CH ₃ as ^{1,2} (69), CH ₃ as ^{1,2} (25)
—	3006	—	CH ₃ as ^{1,2} (74), CH ₃ as ^{1,2} (19), CH ₃ ss(7)

frequency (cm ⁻¹)			Potential Energy Distribution
obs.	calc.	dev.	
—	31	—	CC ^ψ t(56), NC ^φ t(33), NH ^a ob(8)
—	55	—	CC ^c t(20), NH ^a ob(17), CC ^ψ t(16), NC ^φ t(15), C ^ω N t(13), CN ⁿ t(8)
—	75	—	C ^ω N t(38), NC ^φ t(17), CNHC sd(10)
—	94	—	CC ^c t(37), CNHC sd(17), C ^ω N t(16), CO ^a sd(12), NC ^φ t(9), CN ⁿ t(7)
—	121	—	CC ^c t(37), CNHC sd(21), CO ^a sd(14), NH ^a ob(11), C ^{α2} H d ³ (7)
—	188	—	CC ^{me} t(97)
—	193	—	CC ^{me} t(93)
—	213	—	CN ⁿ t(64), CC ^ψ t(20)
—	235	—	C ^{α2} H d ² (30), C ^{α1} H d ² (12), CN ⁿ t(10), C ^{α2} H d ¹ (7)
—	260	—	C ^{α1} H d ² (32), C ^{α2} H d ² (19), CC ^c r(13), C ^{α2} H d ³ (10)
—	319	—	C ^{α2} H d ³ (19), C ^{α2} H d ² (18), CC ^c s(10), CN ^a s(9), C ^{α1} H d ³ (9), C ^{α1} H d ¹ (8)
—	339	—	CC ^c r(21), CO ^a sd(17), C ^{α1} H d ² (13), C ^{α1} H d ³ (9), CO ^a ob(7)
—	389	—	C ^{α1} H d ¹ (37), CO ^a r(15), C ^{α1} H d ³ (12)
—	424	—	C ^{α1} H d ¹ (26), CC ^c r(23), C ^{α1} H d ³ (14)
—	441	—	C ^{α2} H d ¹ (47), C ^{α1} H d ² (12), C ^ω N t(11)
—	575	—	CC ^c r(23), C ^{α2} H d ³ (13), CO ^a sd(12), CC ^ψ s(8), C ^{α2} H d ¹ (7)
—	629	—	NH ^a ob(21), CO ^a r(17), CC ^c sd(15), CC ^c s(8), NC ^φ t(7)
—	644	—	NH ^a ob(22), CO ^a ob(13), NC ^φ t(12), CO ^a r(9), CC ^c sd(9), C ^ω N t(9)
—	662	—	CC ^c sd(27), CC ^ψ s(12), CC ^c ob(9), CC ^c s(7), CO ^a r(7)

Table 3.74: (continued)

frequency (cm ⁻¹)			Potential Energy Distribution
obs.	calc.	dev.	
—	718	—	CNH ₃ r ² (41), CO ^a ob(32), NH ^a ob(7)
—	758	—	CNH ₃ r ² (27), CO ^a ob(16), CC ^{me} s(11), CO ^a r(9), CN ⁿ s(7)
—	777	—	CC ^c ob(52), CC ^c sd(14), C ^{α2} H d ² (9)
820	815	-5	CN ⁿ s(32), CNH ₃ r ¹ (18), CNH ₃ r ² (7)
869	872	3	CNH ₃ r ¹ (29), CN ⁿ s(15), C ^{α1} H d ³ (10), CH ₃ r ¹ (10)
874	881	7	CC ^c s(25), CC ^c sd(15), CC ^{me} s(10), CH ₃ r ¹ (9), CO ^c ss(8), CH ₃ r ² (7)
905	908	3	NH ^a ib(12), CO ^a s(10), CNH ₃ r ¹ (10), CC ^ψ s(9), CH ₃ r ¹ (8), CC ^{me} s(7), CH ₃ r ² (7)
940	925	-15	NC ^φ s(20), CC ^{me} s(17), CH ₃ r ² (15), CC ^c s(14), CH ₃ r ¹ (10)
999	992	-7	NH ^a ib(41), CH ₃ r ² (12), CC ^ψ s(11), CH ₃ r ² (11)
1049	1058	9	C ^{α1} H r ² (27), CC ^{me} s(20), C ^{α1} H d ³ (10), CN ⁿ s(8), CNH ₃ r ¹ (7), CH ₃ r ¹ (7)
1060	1074	14	C ^{α2} H r ² (25), CH ₃ r ² (15), CH ₃ r ² (11), CC ^c ob(7), CNH ₃ sd(7)
1096	1083	-13	CNH ₃ sd(20), CNH ₃ ad ^{1,2} (16), C ^{α2} H r ² (11), CH ₃ r ² (11), C ^{α1} H r ² (10)
1112	1102	-10	CNH ₃ ad ^{1,2} (22), CNH ₃ sd(18), CH ₃ r ² (17), CN ⁿ s(9)
1145	1140	-5	NC ^φ s(31), CH ₃ r ² (16), CC ^{me} s(13)
1145	1164	19	CH ₃ r ¹ (37), CC ^{me} s(27), C ^{α2} H d ¹ (14)
1164	1172	8	CNH ₃ ad ^{1,2} (49), CH ₃ r ¹ (20), CC ^{me} s(12)
1181	1182	1	CNH ₃ ad ^{1,2} (51), CNH ₃ sd(44)
1188	1195	7	CNH ₃ ad ^{1,2} (47), CH ₃ r ¹ (15), CC ^{me} s(10), C ^{α1} H d ¹ (9)
1278	1285	7	C ^{α2} H r ² (28), C ^{α2} H r ¹ (11), C ^{α1} H r ² (8), CH ₃ r ¹ (7)
1310	1299	-11	C ^{α1} H r ² (40), CH ₃ r ¹ (8), CC ^ψ s(7)
1331	1339	8	C ^{α2} H r ¹ (71), C ^{α2} H r ² (12)
1354	1345	-9	C ^{α1} H r ¹ (84)
1369	1369	0	CH ₃ sd(88)
1392	1395	3	CH ₃ sd(93)
1409	1400	-9	CO ^c ss(45), CO ^c as(22), CC ^c s(8), CH ₃ sd(7)
1440	1427	-13	CO ^a s(23), CN ^a s(19), CH ₃ ad ^{1,2} (15), NH ^a ib(10), CC ^ψ s(8), NC ^φ s(8)
1461	1453	-8	CH ₃ ad ^{1,2} (74), CH ₃ r ² (7)
1461	1456	-5	CH ₃ ad ^{1,2} (74), CH ₃ ad ^{1,2} (15)

Table 3.74: (continued)

frequency (cm ⁻¹)			Potential Energy Distribution
obs.	calc.	dev.	
1461	1462	1	CH ₃ ad ^{1,2} (70), CH ₃ ad ^{1,2} (11), CH ₃ r ¹ (10)
1472	1464	-8	CH ₃ ad ^{1,2} (61), CH ₃ ad ^{1,2} (13), CH ₃ ad ^{1,2} (10), CH ₃ r ¹ (7)
1592	1581	-11	CO ^c as(61), CO ^c ss(24)
1624	1621	-3	CN ^a s(42), CO ^a s(40)
—	1870	—	NH ₃ as ¹ (48), NH ₃ ss(47)
—	2238	—	NH ₃ ss(51), NH ₃ as ¹ (48)
—	2294	—	NH ^a s(96)
—	2321	—	NH ₃ as ² (100)
—	2925	—	CH ₃ ss(91)
—	2929	—	CH ₃ ss(95)
—	2957	—	C ^{α2} H s(49), CH ₃ as ^{1,2} (41), CH ₃ as ^{1,2} (9)
—	2975	—	C ^{α2} H s(50), CH ₃ as ^{1,2} (33), CH ₃ as ^{1,2} (17)
—	2977	—	CH ₃ as ^{1,2} (72), CH ₃ as ^{1,2} (23)
—	3004	—	CH ₃ as ^{1,2} (69), CH ₃ as ^{1,2} (14), C ^{α1} H s(12)
—	3007	—	CH ₃ as ^{1,2} (71), CH ₃ as ^{1,2} (21), CH ₃ ss(7)
—	3014	—	C ^{α1} H s(82), CH ₃ as ^{1,2} (13)

Table 3.75: Scaled 4-31G Frequencies and Potential Energy Distribution for Water-Excluded Zwitterionic Alanyl-alanine Two-water Supermolecule.

frequency (cm ⁻¹)			Ala-Ala pH 7 (mean deviation = 11 cm ⁻¹)
obs.	calc.	dev.	
			Potential Energy Distribution
—	64	—	CC ^c t(40), NC ^φ t(38), NH ^a ob(14)
—	102	—	C ^ω N t(51), NC ^φ t(42)
—	116	—	CC ^ψ t(55), CC ^c t(32), NH ^a ob(8)
—	125	—	CC ^ψ t(35), CC ^c t(26), NH ^a ob(11)
—	175	—	CC ^{me} t(29), CNHC sd(23), CO ^a sd(16), CC ^{me} t(10)
—	197	—	CC ^{me} t(84)
—	204	—	CC ^{me} t(64), CNHC sd(11), C ^{α2} H d ³ (10), CC ^ψ t(8)
247	234	-13	C ^{α1} H d ² (32), CO ^a sd(18), C ^{α2} H d ¹ (10), CO ^a ob(8)
247	257	10	C ^{α2} H d ² (44), C ^{α2} H d ³ (8), C ^{α1} H d ³ (7), CC ^c r(7), CN ⁿ t(7)
—	310	—	C ^{α1} H d ² (18), C ^{α1} H d ³ (15), C ^{α2} H d ² (15), C ^{α2} H d ³ (15)
344	319	-25	CO ^a sd(16), CO ^a r(11), C ^{α1} H d ¹ (9), CC ^c s(8), CNHC sd(8), C ^{α2} H d ² (8), NC ^φ s(7), C ^{α1} H d ² (7)
365	357	-8	C ^{α2} H d ³ (16), CC ^c r(16), CN ⁿ t(16), CNHC sd(13), CO ^a r(12), C ^{α1} H d ¹ (7)
—	411	—	CN ⁿ t(61), C ^{α1} H d ³ (13)
454	453	-1	C ^{α1} H d ¹ (45), C ^{α2} H d ¹ (12), CN ⁿ s(7)
454	461	7	C ^{α2} H d ¹ (41), C ^{α1} H d ¹ (9), CC ^c r(9), C ^ω N t(7)
579	591	12	CC ^c r(29), C ^{α2} H d ³ (11), C ^{α2} H d ¹ (10), CO ^a sd(10), CC ^ψ s(7)
650	645	-5	CC ^c sd(39), CC ^c s(20), CO ^a r(11)
684	698	14	C ^{α1} H d ³ (24), CC ^ψ s(19), CO ^a r(15)
758	744	-14	CO ^a ob(57), C ^{α1} H d ² (14), C ^ω N t(8)
775	783	8	CC ^c ob(51), C ^{α2} H d ² (9), CC ^c sd(9)
855	834	-21	CN ⁿ s(46), CC ^{me} s(8), NC ^φ s(7), CC ^c sd(7)
—	856	—	NH ^a ob(52), C ^ω N t(17), NC ^φ t(15)
880	885	5	CC ^c s(20), CC ^c sd(17), CN ⁿ s(11), CO ^c ss(10), CC ^{me} s(9), CH ₃ r ¹ (8)
922	926	4	CC ^{me} s(17), CH ₃ r ¹ (12), NC ^φ s(11), CC ^c s(9), CH ₃ r ² (8), CNHC sd(7)
952	943	-9	CNH ₃ r ² (34), CC ^{me} s(22), CH ₃ r ² (22)
952	957	5	CC ^ψ s(18), CNH ₃ r ² (18), CH ₃ r ² (14), CO ^a r(11), CC ^{me} s(9), NC ^φ s(8)
1009	1005	-4	CNH ₃ r ¹ (30), CH ₃ r ¹ (30), C ^{α1} H r ¹ (11), C ^{α1} H r ² (10)

Table 3.75: (continued)

frequency (cm ⁻¹)			Potential Energy Distribution
obs.	calc.	dev.	
1065	1069	4	C ^{α2} H r ² (31), CH ₃ r ² (17), CC ^c ob(10), CH ₃ r ¹ (7)
1101	1094	-7	CC ^{me} s(26), CH ₃ r ² (23), CN ⁿ s(11), CNH ₃ r ¹ (7), CNH ₃ r ² (7)
1114	1112	-2	C ^{α1} H r ² (27), CH ₃ r ² (16), CNH ₃ r ² (15), CNH ₃ r ¹ (12)
1140	1141	1	CC ^{me} s(32), NC ^φ s(27), CH ₃ r ² (7)
1167	1159	-8	CH ₃ r ¹ (29), C ^{α2} H d ¹ (16), CH ₃ r ² (15), NC ^φ s(10), CC ^{me} s(10)
1226	1225	-1	NH ^a ib(19), CH ₃ r ¹ (12), C ^{α2} H r ² (11), C ^{α1} H d ¹ (7), CNH ₃ r ¹ (7)
1235	1238	3	NH ^a ib(15), CH ₃ r ¹ (14), C ^{α2} H r ² (12), CNH ₃ r ¹ (12)
1276	1292	16	C ^{α1} H r ² (24), C ^{α2} H r ² (17), NH ^a ib(9)
1323	1308	-15	C ^{α1} H r ¹ (20), C ^{α1} H r ² (20), C ^{α2} H r ² (9), NH ^a ib(8)
1340	1336	-4	C ^{α2} H r ¹ (74), C ^{α2} H r ² (7)
1369	1365	-4	CH ₃ sd(84), CO ^c ss(10)
1369	1369	0	C ^{α1} H r ¹ (50), NH ^a ib(8), CNH ₃ r ¹ (7)
1405	1390	-15	CH ₃ sd(80), CO ^c ss(7)
1405	1396	-9	CO ^c ss(39), CO ^c as(13), CH ₃ sd(13), CC ^c s(10), CH ₃ sd(10)
1458	1448	-10	CH ₃ ad ^{1,2} (82), CH ₃ r ² (7)
1458	1456	-2	CH ₃ ad ^{1,2} (81)
1458	1460	2	CH ₃ ad ^{1,2} (82), CH ₃ r ¹ (8)
1458	1466	8	CH ₃ ad ^{1,2} (83), CH ₃ r ¹ (11)
—	1504	—	CNH ₃ sd(94)
1530	1535	5	NH ^a ib(32), CO ^a s(21), CN ^a s(18), CC ^ψ s(7)
1574	1590	16	CO ^c as(66), CO ^c ss(15)
—	1606	—	CNH ₃ ad ^{1,2} (79), CNH ₃ r ¹ (13)
—	1630	—	CNH ₃ ad ^{1,2} (82), CN ^a s(7)
1680	1688	8	CO ^a s(38), CN ^a s(37), CNH ₃ ad ^{1,2} (12)
—	2610	—	NH ₃ as ¹ (59), NH ₃ ss(41)
—	2957	—	CH ₃ ss(88), CH ₃ as ^{1,2} (8)
—	2960	—	CH ₃ ss(83), CH ₃ as ^{1,2} (16)
—	2969	—	C ^{α2} H s(89)
—	3002	—	CH ₃ as ^{1,2} (67), CH ₃ as ^{1,2} (23), C ^{α2} H s(8)
—	3009	—	CH ₃ as ^{1,2} (48), C ^{α1} H s(22), CH ₃ as ^{1,2} (22), CH ₃ ss(8)
—	3028	—	C ^{α1} H s(76), CH ₃ as ^{1,2} (11), CH ₃ as ^{1,2} (9)
—	3040	—	CH ₃ as ^{1,2} (73), CH ₃ as ^{1,2} (20), CH ₃ ss(8)

Table 3.75: (continued)

frequency (cm ⁻¹)			Potential Energy Distribution
obs.	calc.	dev.	
—	3062	—	CH ₃ as ^{1,2} (51), CH ₃ as ^{1,2} (42)
—	3071	—	NH ₃ ss(57), NH ₃ as ¹ (39)
—	3135	—	NH ₃ as ² (98)
—	3380	—	NH ^a s(100)

frequency (cm ⁻¹)			Ala-1- ¹³ C-Ala (mean deviation = 11 cm ⁻¹)
obs.	calc.	dev.	
			Potential Energy Distribution
—	64	—	CC ^c t(40), NC ^φ t(38), NH ^a ob(14)
—	102	—	C ^ω N t(51), NC ^φ t(42)
—	116	—	CC ^ψ t(55), CC ^c t(32), NH ^a ob(8)
—	125	—	CC ^ψ t(35), CC ^c t(26), NH ^a ob(10)
—	175	—	CC ^{me} t(29), CNHC sd(23), CO ^a sd(16), CC ^{me} t(10)
—	197	—	CC ^{me} t(84)
—	204	—	CC ^{me} t(64), CNHC sd(11), C ^{α2} H d ³ (10), CC ^ψ t(8)
236	234	-2	C ^{α1} H d ² (32), CO ^a sd(18), C ^{α2} H d ¹ (10), CO ^a ob(8)
260	257	-3	C ^{α2} H d ² (44), C ^{α2} H d ³ (9), C ^{α1} H d ³ (7), CC ^c r(7), CN ⁿ t(7)
—	310	—	C ^{α1} H d ² (19), C ^{α1} H d ³ (15), C ^{α2} H d ³ (15), C ^{α2} H d ² (14)
344	319	-25	CO ^a sd(15), CO ^a r(10), C ^{α1} H d ¹ (9), C ^{α2} H d ² (9), CC ^c s(8), NC ^φ s(7), CNHC sd(7)
377	356	-21	CC ^c r(16), CN ⁿ t(16), C ^{α2} H d ³ (15), CNHC sd(13), CO ^a r(12), C ^{α1} H d ¹ (7)
—	411	—	CN ⁿ t(61), C ^{α1} H d ³ (13)
456	453	-3	C ^{α1} H d ¹ (44), C ^{α2} H d ¹ (13), CN ⁿ s(7)
456	461	5	C ^{α2} H d ¹ (40), C ^{α1} H d ¹ (10), CC ^c r(9), C ^ω N t(7)
579	591	12	CC ^c r(29), C ^{α2} H d ³ (11), C ^{α2} H d ¹ (10), CO ^a sd(10), CC ^ψ s(7)
647	644	-3	CC ^c sd(39), CC ^c s(20), CO ^a r(12)
685	695	10	C ^{α1} H d ³ (23), CC ^ψ s(17), CO ^a r(13), CO ^a ob(10)
744	727	-17	CO ^a ob(53), C ^{α1} H d ² (15)
778	782	4	CC ^c ob(52), C ^{α2} H d ² (10), CC ^c sd(9)
847	831	-16	CN ⁿ s(44), CC ^{me} s(8), NC ^φ s(7), CC ^c sd(7)
—	856	—	NH ^a ob(52), C ^ω N t(17), NC ^φ t(16)

Table 3.75: (continued)

frequency (cm ⁻¹)			Potential Energy Distribution
obs.	calc.	dev.	
881	884	3	CC ^c s(19), CC ^c sd(17), CN ⁿ s(12), CO ^c ss(9), CC ^{me} s(9), CH ₃ r ¹ (8)
922	925	3	CC ^{me} s(16), CH ₃ r ¹ (13), NC ^φ s(9), CNHC sd(8), CO ^a r(8), CC ^c s(7)
951	941	-10	CNH ₃ r ² (24), CH ₃ r ² (23), CC ^{me} s(15), CN ⁿ s(8), CH ₃ r ² (7)
951	952	1	CNH ₃ r ² (29), CC ^{me} s(16), CC ^ψ s(15), CH ₃ r ² (11), CO ^a r(8), NC ^φ s(7)
1009	1005	-4	CH ₃ r ¹ (31), CNH ₃ r ¹ (30), C ^{α1} H r ¹ (11), C ^{α1} H r ² (10)
1065	1069	4	C ^{α2} H r ² (31), CH ₃ r ² (17), CC ^c ob(10), CH ₃ r ¹ (7)
1101	1093	-8	CC ^{me} s(26), CH ₃ r ² (25), CN ⁿ s(12)
1117	1111	-6	C ^{α1} H r ² (28), CNH ₃ r ² (16), CH ₃ r ² (14), CNH ₃ r ¹ (13)
1140	1139	-1	CC ^{me} s(31), NC ^φ s(26), CH ₃ r ² (7)
1168	1159	-9	CH ₃ r ¹ (29), C ^{α2} H d ¹ (16), CH ₃ r ² (14), CC ^{me} s(11), NC ^φ s(8)
1235	1223	-12	NH ^a ib(23), C ^{α2} H r ² (13), CH ₃ r ¹ (9), CO ^a s(7), CN ^a s(7)
1235	1236	1	CH ₃ r ¹ (17), CNH ₃ r ¹ (14), NH ^a ib(12), C ^{α2} H r ² (9), C ^{α1} H d ¹ (7)
1268	1289	21	C ^{α2} H r ² (21), C ^{α1} H r ² (17), NH ^a ib(8)
1322	1306	-16	C ^{α1} H r ² (27), C ^{α1} H r ¹ (18)
1340	1335	-5	C ^{α2} H r ¹ (75), C ^{α2} H r ² (8)
1370	1365	-5	CH ₃ sd(83), CO ^c ss(10)
1370	1367	-3	C ^{α1} H r ¹ (54), CNH ₃ r ¹ (7)
1401	1390	-11	CH ₃ sd(80), CO ^c ss(7)
1407	1396	-11	CO ^c ss(39), CO ^c as(13), CH ₃ sd(13), CC ^c s(10), CH ₃ sd(10)
1459	1448	-11	CH ₃ ad ^{1,2} (81), CH ₃ r ² (7)
1459	1456	-3	CH ₃ ad ^{1,2} (79)
1459	1460	1	CH ₃ ad ^{1,2} (81), CH ₃ r ¹ (8), CH ₃ ad ^{1,2} (7)
1459	1466	7	CH ₃ ad ^{1,2} (83), CH ₃ r ¹ (11)
—	1504	—	CNH ₃ sd(92)
—	1517	—	NH ^a ib(37), CO ^a s(21), CN ^a s(15)
1571	1589	18	CO ^c as(66), CO ^c ss(15)
1610	1605	-5	CNH ₃ ad ^{1,2} (75), CNH ₃ r ¹ (12)
1636	1620	-16	CNH ₃ ad ^{1,2} (44), CN ^a s(24), CO ^a s(18), CNH ₃ ad ^{1,2} (7)
1647	1656	9	CNH ₃ ad ^{1,2} (48), CO ^a s(22), CN ^a s(21)

Table 3.75: (continued)

frequency (cm^{-1})			Potential Energy Distribution
obs.	calc.	dev.	
—	2610	—	NH_3 as ¹ (59), NH_3 ss(41)
—	2957	—	CH_3 ss(88), CH_3 as ^{1,2} (8)
—	2960	—	CH_3 ss(83), CH_3 as ^{1,2} (16)
—	2969	—	$\text{C}^{\alpha 2}$ H s(89)
—	3002	—	CH_3 as ^{1,2} (67), CH_3 as ^{1,2} (23), $\text{C}^{\alpha 2}$ H s(8)
—	3009	—	CH_3 as ^{1,2} (48), $\text{C}^{\alpha 1}$ H s(22), CH_3 as ^{1,2} (22), CH_3 ss(8)
—	3028	—	$\text{C}^{\alpha 1}$ H s(76), CH_3 as ^{1,2} (11), CH_3 as ^{1,2} (9)
—	3040	—	CH_3 as ^{1,2} (73), CH_3 as ^{1,2} (20), CH_3 ss(8)
—	3062	—	CH_3 as ^{1,2} (51), CH_3 as ^{1,2} (42)
—	3071	—	NH_3 ss(57), NH_3 as ¹ (39)
—	3135	—	NH_3 as ² (98)
—	3380	—	NH^a s(100)

frequency (cm ⁻¹)			Ala-Ala in D ₂ O: CHNDCH (mean deviation = 12 cm ⁻¹)
obs.	calc.	dev.	
Potential Energy Distribution			
—	63	—	NC ^ϕ t(40), CC ^c t(37), NH ^a ob(15)
—	101	—	C ^ω N t(51), NC ^ϕ t(42)
—	113	—	CC ^ψ t(64), CC ^c t(29)
—	123	—	CC ^c t(32), CC ^ψ t(29), NH ^a ob(11)
—	169	—	CNHC sd(27), CO ^a sd(21), CC ^{me} t(17), C ^{α1} H d ³ (7), CN ⁿ t(7)
—	196	—	CC ^{me} t(76), CC ^{me} t(7)
—	200	—	CC ^{me} t(70), CC ^{me} t(13)
246	225	-21	C ^{α1} H d ² (23), CN ⁿ t(18), C ^{α1} H d ³ (10), C ^{α2} H d ³ (8), CNHC sd(7), C ^{α2} H d ¹ (7), CO ^a ob(7)
246	241	-5	C ^{α2} H d ² (31), CN ⁿ t(14), CO ^a sd(13)
—	291	—	C ^{α2} H d ² (36), CN ⁿ t(26), C ^{α1} H d ² (13)
333	309	-24	C ^{α1} H d ² (18), CO ^a sd(17), C ^{α1} H d ³ (14), C ^{α2} H d ³ (12), CC ^c r(12), CO ^a r(9)
—	323	—	CN ⁿ t(16), CNHC sd(12), CC ^c s(10), C ^{α1} H d ¹ (8), C ^{α2} H d ³ (8), NC ^ϕ s(7)
367	361	-6	C ^{α1} H d ¹ (16), C ^{α1} H d ³ (15), CO ^a r(14), CC ^c r(14), C ^{α2} H d ³ (12), CNHC sd(7), CN ⁿ t(7)

Table 3.75: (continued)

frequency (cm ⁻¹)			Potential Energy Distribution
obs.	calc.	dev.	
434	431	-3	C ^{α1} H d ¹ (42), CN ⁿ s(9), CC ^c r(7)
440	444	4	C ^{α2} H d ¹ (47), C ^ω N t(13), CC ^c r(8)
569	571	2	CC ^c r(31), C ^{α2} H d ³ (11), CO ^a sd(9)
635	626	-9	CO ^a r(23), CNH ₃ r ² (14), C ^{α1} H d ³ (12), CC ^c sd(11), CC ^ψ s(9), CC ^c s(8), CNH ₃ r ¹ (7)
635	632	-3	NH ^a ob(44), C ^ω N t(16), NC ^φ t(15), CO ^a ob(8)
688	658	-30	CC ^c sd(34), CC ^c s(13), CC ^ψ s(9), CC ^c ob(7), CNH ₃ r ² (7)
751	757	6	CO ^a ob(46), NH ^a ob(10), C ^{α1} H d ² (9), CNH ₃ r ¹ (9), CNH ₃ r ² (9)
—	767	—	CNH ₃ r ² (27), CC ^{me} s(21), CNH ₃ r ¹ (17), CO ^a ob(12)
777	783	6	CC ^c ob(57), C ^{α2} H d ² (8)
825	808	-17	CN ⁿ s(32), CNH ₃ r ² (16), CO ^a r(9), CC ^c sd(8), CH ₃ r ² (7)
875	873	-2	CNH ₃ r ¹ (29), CH ₃ r ¹ (13)
875	881	6	CN ⁿ s(12), CC ^c s(11), CC ^c sd(10), CNH ₃ r ¹ (8), CC ^{me} s(8), CH ₃ r ¹ (8)
906	902	-4	NH ^a ib(21), CC ^c s(18), NC ^φ s(12), CH ₃ r ² (12), CC ^c sd(8), CO ^c ss(p7), CH ₃ r ¹ (7)
943	930	-13	CC ^ψ s(13), CO ^a r(13), CO ^a s(11), NH ^a ib(9), CH ₃ r ² (8), CN ^a s(7), CNHC sd(7)
1002	994	-8	NH ^a ib(43), CH ₃ r ² (18), CC ^ψ s(8)
1050	1052	2	CC ^{me} s(33), C ^{α1} H r ² (22), C ^{α1} H d ³ (7), CN ⁿ s(7)
1063	1071	8	C ^{α2} H r ² (34), CH ₃ r ² (13), CC ^c ob(9), CH ₃ r ¹ (7)
1098	1099	1	CH ₃ r ² (41), C ^{α1} H r ² (10), C ^{α1} H d ² (8), CH ₃ r ¹ (7)
1115	1133	18	CC ^{me} s(25), NC ^φ s(22), CNH ₃ sd(9), CH ₃ r ² (8)
1151	1141	-10	CNH ₃ sd(65), CNH ₃ ad ^{1,2} (19), CN ⁿ s(7)
1160	1151	-9	CNH ₃ ad ^{1,2} (74), CNH ₃ sd(11)
1160	1157	-3	CH ₃ r ¹ (32), C ^{α2} H d ¹ (16), CC ^{me} s(16), CH ₃ r ² (11)
1176	1182	6	CNH ₃ ad ^{1,2} (61), CH ₃ r ¹ (8)
1184	1195	11	CNH ₃ ad ^{1,2} (33), CH ₃ r ¹ (19), CC ^{me} s(11), C ^{α1} H d ¹ (10), CH ₃ r ² (7)
1277	1275	-2	C ^{α2} H r ² (43), CH ₃ r ¹ (9), C ^{α2} H r ¹ (8)
1308	1294	-14	C ^{α1} H r ² (47), C ^{α1} H r ¹ (16), CH ₃ r ¹ (13)
1329	1333	4	C ^{α2} H r ¹ (43), C ^{α1} H r ¹ (32), C ^{α2} H r ² (7)
1354	1339	-15	C ^{α1} H r ¹ (36), C ^{α2} H r ¹ (34)

Table 3.75: (continued)

frequency (cm^{-1})			Potential Energy Distribution
obs.	calc.	dev.	
1369	1365	-4	CH_3 sd(83), CO^c ss(9)
1401	1390	-11	CH_3 sd(82)
1407	1396	-11	CO^c ss(40), CO^c as(13), CH_3 sd(13), CC^c s(10), CH_3 sd(10)
1445	1446	1	CH_3 ad ^{1,2} (82)
1459	1456	-3	CH_3 ad ^{1,2} (81)
1459	1460	1	CH_3 ad ^{1,2} (83), CH_3 r ¹ (8)
1459	1467	8	CH_3 ad ^{1,2} (85), CH_3 r ¹ (11)
1484	1491	7	CO^a s(30), CN^a s(22), CC^ψ s(11), NH^a ib(8)
1590	1586	-4	CO^c as(69), CO^c ss(16)
1665	1677	12	CN^a s(44), CO^a s(43)
—	1911	—	NH_3 ss(50), NH_3 as ¹ (47)
—	2229	—	NH_3 as ¹ (50), NH_3 ss(48)
—	2311	—	NH_3 as ² (99)
—	2479	—	NH^a s(98)
—	2957	—	CH_3 ss(88), CH_3 as ^{1,2} (8)
—	2960	—	CH_3 ss(83), CH_3 as ^{1,2} (16)
—	2969	—	$\text{C}^{\alpha 2}$ H s(89)
—	3002	—	CH_3 as ^{1,2} (67), CH_3 as ^{1,2} (23), $\text{C}^{\alpha 2}$ H s(8)
—	3009	—	CH_3 as ^{1,2} (48), $\text{C}^{\alpha 1}$ H s(22), CH_3 as ^{1,2} (22), CH_3 ss(8)
—	3029	—	$\text{C}^{\alpha 1}$ H s(77), CH_3 as ^{1,2} (11), CH_3 as ^{1,2} (9)
—	3040	—	CH_3 as ^{1,2} (73), CH_3 as ^{1,2} (20), CH_3 ss(8)
—	3062	—	CH_3 as ^{1,2} (51), CH_3 as ^{1,2} (42)

frequency (cm^{-1})			2-d Ala-Ala: CDNHCH (mean deviation = 14 cm^{-1})
obs.	calc.	dev.	
—	64	—	CC^c t(40), NC^ϕ t(38), NH^a ob(14)
—	101	—	C^ωN t(51), NC^ϕ t(42)
—	115	—	CC^ψ t(59), CC^c t(30), NH^a ob(7)
—	125	—	CC^ψ t(32), CC^c t(28), NH^a ob(11)
—	174	—	CC^{me} t(27), CNHC sd(24), CO^a sd(17), CC^{me} t(10)
—	197	—	CC^{me} t(84)
—	203	—	CC^{me} t(66), CNHC sd(10), $\text{C}^{\alpha 2}$ H d ³ (9), CC^ψ t(8)
256	233	-23	$\text{C}^{\alpha 1}$ H d ² (32), CO^a sd(18), $\text{C}^{\alpha 2}$ H d ¹ (10), CO^a ob(8)

Table 3.75: (continued)

frequency (cm ⁻¹)			Potential Energy Distribution
obs.	calc.	dev.	
256	256	0	C ^{α2} H d ² (44), C ^{α2} H d ³ (8), C ^{α1} H d ³ (7), CC ^c r(7), CN ⁿ t(7)
—	309	—	C ^{α1} H d ² (22), C ^{α1} H d ³ (15), C ^{α2} H d ³ (15), C ^{α2} H d ² (11)
344	317	-27	CO ^a sd(14), C ^{α2} H d ² (12), C ^{α1} H d ¹ (10), CC ^c s(9), CO ^a r(8), NC ^φ s(7)
379	357	-22	C ^{α2} H d ³ (16), CC ^c r(16), CN ⁿ t(16), CNHC sd(14), CO ^a r(13)
—	411	—	CN ⁿ t(61), C ^{α1} H d ³ (13)
450	450	0	C ^{α1} H d ¹ (50), C ^{α2} H d ¹ (8), CN ⁿ s(7)
450	460	10	C ^{α2} H d ¹ (45), CC ^c r(8), C ^ω N t(7)
579	587	8	CC ^c r(30), C ^{α2} H d ¹ (10), C ^{α2} H d ³ (10), CC ^ψ s(9), CO ^a sd(9)
648	644	-4	CC ^c sd(38), CC ^c s(20), CO ^a r(13), C ^{α1} H d ³ (7)
677	687	10	C ^{α1} H d ³ (22), CC ^ψ s(18), CO ^a r(11), CC ^c sd(7)
735	729	-6	CO ^a ob(46), C ^{α1} H r ² (14), C ^{α1} H d ² (12), CH ₃ r ¹ (7)
780	782	2	CC ^c ob(50), C ^{α2} H d ² (10), CC ^c sd(10)
—	809	—	C ^{α1} H r ² (25), CN ⁿ s(20), CC ^{me} s(19)
831	840	9	CN ⁿ s(34), C ^{α1} H r ¹ (12), NH ^a ob(10), C ^{α1} H r ² (8)
863	865	2	C ^{α1} H r ¹ (26), NH ^a ob(25), C ^ω N t(7)
892	872	-20	CC ^c sd(13), NH ^a ob(11), CC ^c s(9), CC ^{me} s(9), CC ^ψ s(7), C ^{α1} H r ² (7)
908	911	3	C ^{α1} H r ¹ (20), C ^{α1} H r ² (13), CC ^c s(11), CH ₃ r ² (10)
908	927	19	CC ^{me} s(17), CH ₃ r ¹ (13), NC ^φ s(10), CC ^c s(8), CNHC sd(8), CO ^a r(7), CH ₃ r ² (7)
952	944	-8	CNH ₃ r ² (34), CH ₃ r ² (24), CC ^{me} s(17)
968	973	5	CNH ₃ r ² (26), CC ^ψ s(9), CH ₃ r ² (9), C ^{α1} H r ² (8), CH ₃ r ² (8), CO ^a r(7)
1069	1070	1	C ^{α2} H r ² (31), CH ₃ r ² (18), CC ^c ob(10), CH ₃ r ¹ (7)
1087	1087	0	CH ₃ r ¹ (19), CH ₃ r ² (19), CNH ₃ r ¹ (16), CC ^{me} s(16)
1105	1134	29	CC ^{me} s(20), NC ^φ s(18), CH ₃ r ¹ (10), CH ₃ r ² (8)
1150	1153	3	CC ^{me} s(19), CH ₃ r ¹ (17), CH ₃ r ¹ (11), C ^{α1} H r ¹ (10)
1150	1162	12	NC ^φ s(16), CH ₃ r ¹ (16), CH ₃ r ² (14), C ^{α2} H d ¹ (11)
1212	1217	5	CNH ₃ r ¹ (27), CH ₃ r ¹ (20), NH ^a ib(9), CO ^a s(7)
1245	1229	-16	CNH ₃ r ¹ (16), NH ^a ib(15), CC ^{me} s(12), C ^{α2} H r ² (11), C ^{α1} H d ¹ (7), CNH ₃ r ² (7)

Table 3.75: (continued)

frequency (cm ⁻¹)			Potential Energy Distribution
obs.	calc.	dev.	
1273	1254	-19	C ^{α2} H r ² (17), CNH ₃ r ² (11), CH ₃ r ² (9), CC ^ψ s(8), C ^{α2} H r ¹ (8), CC ^{me} s(8)
1312	1313	1	NH ^a ib(26), C ^{α2} H r ² (21), CC ^ψ s(7), CH ₃ r ¹ (7)
1347	1339	-8	C ^{α2} H r ¹ (73)
1371	1365	-6	CH ₃ sd(84), CO ^c ss(10)
1399	1390	-9	CH ₃ sd(81)
1407	1396	-11	CO ^c ss(40), CO ^c as(13), CH ₃ sd(13), CC ^c s(10), CH ₃ sd(10)
1458	1447	-11	CH ₃ ad ^{1,2} (85), CH ₃ r ² (7)
1458	1456	-2	CH ₃ ad ^{1,2} (82)
1458	1460	2	CH ₃ ad ^{1,2} (81), CH ₃ r ¹ (8), CH ₃ ad ^{1,2} (7)
1458	1465	7	CH ₃ ad ^{1,2} (85), CH ₃ r ¹ (10)
—	1504	—	CNH ₃ sd(94)
—	1534	—	NH ^a ib(33), CO ^a s(21), CN ^a s(18), CC ^ψ s(7)
1577	1590	13	CO ^c as(66), CO ^c ss(15)
—	1604	—	CNH ₃ ad ^{1,2} (80), CNH ₃ r ¹ (12)
—	1630	—	CNH ₃ ad ^{1,2} (81), CN ^a s(8)
1673	1685	12	CO ^a s(39), CN ^a s(37), CNH ₃ ad ^{1,2} (14)
—	2232	—	C ^{α1} H s(98)
—	2610	—	NH ₃ as ¹ (59), NH ₃ ss(41)
—	2957	—	CH ₃ ss(88), CH ₃ as ^{1,2} (8)
—	2960	—	CH ₃ ss(83), CH ₃ as ^{1,2} (16)
—	2969	—	C ^{α2} H s(89)
—	3002	—	CH ₃ as ^{1,2} (67), CH ₃ as ^{1,2} (23), C ^{α2} H s(8)
—	3014	—	CH ₃ as ^{1,2} (58), CH ₃ as ^{1,2} (31), CH ₃ ss(11)
—	3040	—	CH ₃ as ^{1,2} (73), CH ₃ as ^{1,2} (20), CH ₃ ss(8)
—	3062	—	CH ₃ as ^{1,2} (53), CH ₃ as ^{1,2} (41)
—	3071	—	NH ₃ ss(58), NH ₃ as ¹ (40)
—	3135	—	NH ₃ as ² (98)
—	3380	—	NH ^a s(100)
frequency (cm ⁻¹)			2-d Ala-Ala in D ₂ O: CDNDCH (mean deviation = 9 cm ⁻¹)
obs.	calc.	dev.	Potential Energy Distribution
—	62	—	NC ^δ t(40), CC ^c t(37), NH ^a ob(15)

Table 3.75: (continued)

frequency (cm ⁻¹)			Potential Energy Distribution
obs.	calc.	dev.	
—	101	—	C ^ω N t(52), NC ^φ t(41)
—	113	—	CC ^ψ t(67), CC ^c t(27)
—	122	—	CC ^c t(34), CC ^ψ t(26), NH ^a ob(11)
—	168	—	CNHC sd(27), CO ^a sd(22), CC ^{me} t(16), C ^{α1} H d ³ (7), CN ⁿ t(7)
—	196	—	CC ^{me} t(75), CC ^{me} t(8)
—	200	—	CC ^{me} t(70), CC ^{me} t(14)
—	224	—	C ^{α1} H d ² (23), CN ⁿ t(19), C ^{α1} H d ³ (10), C ^{α2} H d ³ (8), CNHC sd(7), C ^{α2} H d ¹ (7), CO ^a ob(7)
—	241	—	C ^{α2} H d ² (31), CO ^a sd(14), CN ⁿ t(14)
—	291	—	C ^{α2} H d ² (36), CN ⁿ t(26), C ^{α1} H d ² (14)
—	306	—	C ^{α1} H d ² (18), CO ^a sd(17), C ^{α1} H d ³ (13), C ^{α2} H d ³ (12), CC ^c r(12), CO ^a r(9)
—	322	—	CN ⁿ t(17), CNHC sd(12), CC ^c s(10), C ^{α2} H d ³ (9), C ^{α1} H d ¹ (8)
—	361	—	C ^{α1} H d ¹ (16), C ^{α1} H d ³ (15), CO ^a r(14), CC ^c r(14), C ^{α2} H d ³ (12), CNHC sd(7), CN ⁿ t(7)
—	428	—	C ^{α1} H d ¹ (44), CN ⁿ s(8), CC ^c r(7)
—	443	—	C ^{α2} H d ¹ (49), C ^ω N t(13), CC ^c r(7)
—	569	—	CC ^c r(32), C ^{α2} H d ³ (11), CO ^a sd(8)
—	621	—	CO ^a r(23), CNH ₃ r ² (14), C ^{α1} H d ³ (13), CC ^ψ s(11), CC ^c sd(8), CNH ₃ r ¹ (8), CC ^c s(7)
—	632	—	NH ^a ob(43), C ^ω N t(16), NC ^φ t(15), CO ^a ob(8)
—	657	—	CC ^c sd(37), CC ^c s(15), CC ^ψ s(8), CC ^c ob(7)
—	735	—	CO ^a ob(40), C ^{α1} H r ² (23), NH ^a ob(10), C ^{α1} H d ² (8)
—	751	—	CNH ₃ r ¹ (31), CNH ₃ r ² (23), CN ⁿ s(16), C ^{α1} H r ¹ (11), CC ^{me} s(8)
—	781	—	CC ^c ob(49), C ^{α2} H d ² (7), CNH ₃ r ² (7)
—	795	—	CNH ₃ r ² (25), CN ⁿ s(15), CC ^c ob(9), CC ^c sd(7)
—	820	—	CC ^{me} s(27), C ^{α1} H r ² (16), C ^{α1} H r ¹ (15), CH ₃ r ¹ (8), CO ^a ob(7)
—	865	—	C ^{α1} H r ² (15), CC ^c sd(14), CC ^{me} s(12), CH ₃ r ¹ (9), CC ^ψ s(8), NC ^φ s(8), CC ^c s(8)
—	895	—	CN ⁿ s(18), C ^{α1} H r ² (17), CC ^c s(10), CNH ₃ r ¹ (9), CH ₃ r ² (8)

Table 3.75: (continued)

frequency (cm ⁻¹)			Potential Energy Distribution
obs.	calc.	dev.	
—	902	—	NH ^a ib(23), CC ^c s(12), NC ^φ s(11), CH ₃ r ¹ (10), CC ^{me} s(8), CH ₃ r ² (8)
—	921	—	CO ^a r(15), CC ^ψ s(10), CO ^a s(9), CNHC sd(8), NH ^a ib(7)
—	986	—	NH ^a ib(30), C ^{α1} H r ¹ (14), CNH ₃ r ¹ (12), CH ₃ r ² (8)
—	1013	—	CH ₃ r ² (28), C ^{α1} H r ¹ (21), NH ^a ib(13), CNH ₃ r ¹ (8), CH ₃ r ² (8)
—	1071	—	C ^{α2} H r ² (35), CH ₃ r ² (13), CC ^c ob(9), CH ₃ r ¹ (7)
—	1121	—	CH ₃ r ² (14), CC ^{me} s(13), CC ^{me} s(12), C ^{α1} H r ¹ (11), NC ^φ s(10), CH ₃ r ² (8)
—	1135	—	CNH ₃ sd(30), CC ^{me} s(14), CC ^{me} s(13), NC ^φ s(10)
—	1142	—	CNH ₃ sd(43), CNH ₃ ad ^{1,2} (31), CN ⁿ s(7)
—	1153	—	CNH ₃ ad ^{1,2} (59), CNH ₃ sd(10), CNH ₃ r ¹ (9)
—	1157	—	CH ₃ r ¹ (31), C ^{α2} H d ¹ (16), CC ^{me} s(15), CH ₃ r ² (10)
1165	1172	7	CH ₃ r ¹ (42), CNH ₃ ad ^{1,2} (13)
1203	1189	-14	CNH ₃ ad ^{1,2} (79), CH ₃ r ¹ (13)
1203	1226	23	CH ₃ r ² (19), CC ^ψ s(15), CC ^{me} s(13), C ^{α1} H r ² (12), C ^{α1} H d ¹ (7)
1279	1277	-2	C ^{α2} H r ² (44), CH ₃ r ¹ (10)
1330	1336	6	C ^{α2} H r ¹ (77), C ^{α2} H r ² (8)
1371	1365	-6	CH ₃ sd(83), CO ^c ss(9)
1399	1390	-9	CH ₃ sd(80)
1408	1396	-12	CO ^c ss(40), CH ₃ sd(15), CO ^c as(12), CC ^c s(10), CH ₃ sd(10)
1450	1446	-4	CH ₃ ad ^{1,2} (84)
1450	1456	6	CH ₃ ad ^{1,2} (82)
1460	1460	0	CH ₃ ad ^{1,2} (83), CH ₃ r ¹ (8)
1460	1465	5	CH ₃ ad ^{1,2} (87), CH ₃ r ¹ (10)
1479	1490	11	CO ^a s(29), CN ^a s(24), CC ^ψ s(11), NH ^a ib(9), NC ^φ s(7)
1590	1586	-4	CO ^c as(69), CO ^c ss(16)
1664	1673	9	CN ^a s(45), CO ^a s(44)
—	1909	—	NH ₃ ss(51), NH ₃ as ¹ (47)
—	2229	—	NH ₃ as ¹ (46), NH ₃ ss(44), C ^{α1} H s(9)
—	2232	—	C ^{α1} H s(89)
—	2311	—	NH ₃ as ² (99)
—	2479	—	NH ^a s(98)

Table 3.75: (continued)

frequency (cm ⁻¹)			Potential Energy Distribution
obs.	calc.	dev.	
—	2957	—	CH ₃ ss(88), CH ₃ as ^{1,2} (8)
—	2960	—	CH ₃ ss(83), CH ₃ as ^{1,2} (16)
—	2969	—	C ^{α2} H s(89)
—	3002	—	CH ₃ as ^{1,2} (67), CH ₃ as ^{1,2} (23), C ^{α2} H s(8)
—	3014	—	CH ₃ as ^{1,2} (58), CH ₃ as ^{1,2} (31), CH ₃ ss(11)
—	3040	—	CH ₃ as ^{1,2} (73), CH ₃ as ^{1,2} (20), CH ₃ ss(8)
—	3062	—	CH ₃ as ^{1,2} (53), CH ₃ as ^{1,2} (41)

frequency (cm ⁻¹)			CDNHCD (mean deviation = 12 cm ⁻¹) Potential Energy Distribution
obs.	calc.	dev.	
—	63	—	CC ^c t(40), NC ^φ t(39), NH ^a ob(14)
—	101	—	C ^ω N t(52), NC ^φ t(41)
—	115	—	CC ^ψ t(58), CC ^c t(31), NH ^a ob(7)
—	124	—	CC ^ψ t(33), CC ^c t(27), NH ^a ob(11)
—	174	—	CC ^{me} t(26), CNHC sd(24), CO ^a sd(17), CC ^{me} t(9)
—	197	—	CC ^{me} t(84)
—	203	—	CC ^{me} t(67), CNHC sd(9), C ^{α2} H d ³ (9), CC ^ψ t(8)
—	233	—	C ^{α1} H d ² (32), CO ^a sd(19), C ^{α2} H d ¹ (10), CO ^a ob(8), C ^{α1} H d ³ (7)
—	256	—	C ^{α2} H d ² (45), C ^{α2} H d ³ (8), C ^{α1} H d ³ (7), CC ^c r(7), CN ⁿ t(7)
—	308	—	C ^{α1} H d ² (20), C ^{α2} H d ³ (16), C ^{α1} H d ³ (15), C ^{α2} H d ² (12)
—	315	—	CO ^a sd(15), C ^{α2} H d ² (11), C ^{α1} H d ¹ (9), CO ^a r(9), CC ^c s(8), NC ^φ s(7), CNHC sd(7)
—	355	—	CC ^c r(16), CN ⁿ t(16), C ^{α2} H d ³ (15), CNHC sd(14), CO ^a r(13), C ^{α1} H d ¹ (7)
—	411	—	CN ⁿ t(61), C ^{α1} H d ³ (13)
—	449	—	C ^{α1} H d ¹ (47), C ^{α2} H d ¹ (12), CN ⁿ s(7)
—	455	—	C ^{α2} H d ¹ (40), C ^{α1} H d ¹ (9), CC ^c r(8)
—	575	—	CC ^c r(22), C ^{α2} H d ¹ (11), CC ^ψ s(8), C ^{α2} H d ³ (8), CO ^a sd(8)
—	619	—	CC ^c sd(30), CC ^c s(18), C ^{α2} H r ² (11), CC ^c r(10), CC ^c ob(9), CO ^a r(7)
—	681	—	C ^{α1} H d ³ (26), CO ^a r(19), CC ^ψ s(15)
—	728	—	CO ^a ob(47), C ^{α1} H r ² (15), C ^{α1} H d ² (12), CH ₃ r ¹ (7)

Table 3.75: (continued)

frequency (cm ⁻¹)			Potential Energy Distribution
obs.	calc.	dev.	
—	747	—	C ^{α2} H r ² (25), CC ^c ob(24), CC ^c sd(16), CH ₃ r ¹ (9), C ^{α2} H d ² (8)
—	806	—	C ^{α1} H r ² (22), CN ⁿ s(22), CC ^{me} s(18)
—	836	—	CC ^{me} s(19), CC ^c sd(12), CN ⁿ s(12)
—	846	—	CN ⁿ s(26), C ^{α1} H r ¹ (13), CC ^{me} s(13), C ^{α2} H r ¹ (8), C ^{α2} H r ² (7)
—	863	—	NH ^a ob(35), C ^ω N t(10), C ^{α1} H r ¹ (8), C ^{α1} H r ² (8), NC ^φ t(8), CC ^{me} s(7)
—	882	—	C ^{α1} H r ¹ (26), CC ^ψ s(14), C ^{α2} H r ¹ (13), C ^{α1} H r ² (12), CO ^a r(9)
—	891	—	CC ^c ob(19), CC ^c s(18), CC ^c sd(16), C ^{α2} H r ² (10), CO ^c ss(9), CH ₃ r ² (7)
—	936	—	CH ₃ r ² (22), C ^{α1} H r ¹ (9), CNH ₃ r ² (9), CN ⁿ s(8), CC ^{me} s(8), C ^{α2} H r ¹ (7)
—	949	—	CNH ₃ r ² (33), CH ₃ r ² (12), CC ^{me} s(10), CC ^c ob(7)
—	976	—	CNH ₃ r ² (20), CH ₃ r ² (19), CC ^ψ s(9), CH ₃ r ² (8), NC ^φ s(7)
—	1013	—	C ^{α2} H r ¹ (35), NC ^φ s(16), CNHC sd(10)
—	1088	—	CH ₃ r ¹ (21), CH ₃ r ² (18), CNH ₃ r ¹ (16), CC ^{me} s(15), CN ⁿ s(7)
—	1136	—	CH ₃ r ¹ (36), CC ^{me} s(27), C ^{α2} H d ² (7)
1154	1149	-5	CH ₃ r ¹ (22), C ^{α1} H r ¹ (18), CH ₃ r ² (11), CH ₃ r ¹ (8), CC ^{me} s(7)
—	1180	—	CH ₃ r ² (31), CC ^c s(11), C ^{α2} H d ¹ (9), NH ^a ib(8), CO ^c ss(8)
1196	1192	-4	CH ₃ r ¹ (19), NC ^φ s(13), CC ^{me} s(12)
1218	1220	2	CNH ₃ r ¹ (40), CH ₃ r ¹ (22)
1250	1242	-8	CNH ₃ r ² (16), CC ^{me} s(15), CH ₃ r ² (11), C ^{α1} H d ¹ (8)
1336	1303	-33	NH ^a ib(42), CC ^ψ s(14), CO ^a s(7)
1370	1365	-5	CH ₃ sd(84), CO ^c ss(9)
1401	1389	-12	CH ₃ sd(81)
1406	1396	-10	CO ^c ss(40), CH ₃ sd(14), CO ^c as(13), CC ^c s(10), CH ₃ sd(10)
1458	1447	-11	CH ₃ ad ^{1,2} (85), CH ₃ r ² (7)
1458	1455	-3	CH ₃ ad ^{1,2} (83)
1458	1459	1	CH ₃ ad ^{1,2} (84), CH ₃ r ¹ (7)
1458	1465	7	CH ₃ ad ^{1,2} (86), CH ₃ r ¹ (10)
—	1504	—	CNH ₃ sd(94)
—	1534	—	NH ^a ib(33), CO ^a s(21), CN ^a s(18), CC ^ψ s(7)

Table 3.75: (continued)

frequency (cm^{-1})			Potential Energy Distribution
obs.	calc.	dev.	
1570	1588	18	CO^c as(67), CO^c ss(16)
—	1604	—	CNH_3 ad ^{1,2} (80), CNH_3 r ¹ (12)
—	1630	—	CNH_3 ad ^{1,2} (81), CN^a s(8)
1680	1684	4	CO^a s(38), CN^a s(37), CNH_3 ad ^{1,2} (14)
—	2190	—	$\text{C}^{\alpha 2}$ H s(98)
—	2232	—	$\text{C}^{\alpha 1}$ H s(98)
—	2610	—	NH_3 as ¹ (59), NH_3 ss(41)
—	2957	—	CH_3 ss(91)
—	2960	—	CH_3 ss(83), CH_3 as ^{1,2} (16)
—	2999	—	CH_3 as ^{1,2} (75), CH_3 as ^{1,2} (23)
—	3014	—	CH_3 as ^{1,2} (58), CH_3 as ^{1,2} (31), CH_3 ss(11)
—	3040	—	CH_3 as ^{1,2} (74), CH_3 as ^{1,2} (19), CH_3 ss(8)
—	3062	—	CH_3 as ^{1,2} (53), CH_3 as ^{1,2} (41)
—	3071	—	NH_3 ss(58), NH_3 as ¹ (40)
—	3135	—	NH_3 as ² (98)
—	3380	—	NH^a s(100)

frequency (cm^{-1})			CDND CD (mean deviation = 6 cm^{-1})
obs.	calc.	dev.	
—	62	—	NC^ϕ t(41), CC^c t(37), NH^a ob(15)
—	100	—	C^ωN t(52), NC^ϕ t(40)
—	113	—	CC^ψ t(66), CC^c t(28)
—	122	—	CC^c t(34), CC^ψ t(26), NH^a ob(11), NC^ϕ t(7)
—	168	—	CNHC sd(27), CO^a sd(21), CC^{me} t(15), $\text{C}^{\alpha 1}$ H d ³ (7), CN^n t(7)
—	195	—	CC^{me} t(74), CC^{me} t(9)
—	200	—	CC^{me} t(69), CC^{me} t(15)
—	224	—	$\text{C}^{\alpha 1}$ H d ² (22), CN^n t(19), $\text{C}^{\alpha 1}$ H d ³ (10), $\text{C}^{\alpha 2}$ H d ³ (8), CNHC sd(7), $\text{C}^{\alpha 2}$ H d ¹ (7), CO^a ob(7)
—	241	—	$\text{C}^{\alpha 2}$ H d ² (31), CO^a sd(14), CN^n t(14)
—	291	—	$\text{C}^{\alpha 2}$ H d ² (38), CN^n t(25), $\text{C}^{\alpha 1}$ H d ² (13)
—	305	—	$\text{C}^{\alpha 1}$ H d ² (19), CO^a sd(17), $\text{C}^{\alpha 1}$ H d ³ (13), $\text{C}^{\alpha 2}$ H d ³ (12), CC^c r(12), CO^a r(8)

Table 3.75: (continued)

frequency (cm ⁻¹)			Potential Energy Distribution
obs.	calc.	dev.	
—	321	—	CN ⁿ t(18), CNHC sd(13), CC ^c s(10), C ^{α2} H d ³ (10), C ^{α1} H d ¹ (7)
—	360	—	C ^{α1} H d ¹ (16), C ^{α1} H d ³ (16), CO ^a r(14), CC ^c r(14), C ^{α2} H d ³ (11), CNHC sd(7), CN ⁿ t(7)
—	428	—	C ^{α1} H d ¹ (44), CN ⁿ s(8), CC ^c r(7)
—	439	—	C ^{α2} H d ¹ (48), C ^ω N t(12), CC ^c r(8)
—	558	—	CC ^c r(26), C ^{α2} H d ³ (9), CO ^a sd(8), CC ^ψ s(7), C ^{α2} H d ¹ (7)
—	612	—	CC ^c sd(22), CO ^a r(16), CC ^c s(15), C ^{α2} H r ² (8)
—	628	—	NH ^a ob(27), C ^ω N t(13), NC ^φ t(12), CO ^a ob(9), CC ^ψ s(8), CNH ₃ r ² (8)
—	637	—	NH ^a ob(16), CC ^c sd(10), CC ^ψ s(7), CNH ₃ r ² (7)
—	733	—	CO ^a ob(39), C ^{α1} H r ² (22), NH ^a ob(8), C ^{α1} H d ² (8)
—	745	—	C ^{α2} H r ² (20), CC ^c ob(18), CN ⁿ s(15), CNH ₃ r ¹ (10), CC ^c sd(8)
—	752	—	CNH ₃ r ² (26), CNH ₃ r ¹ (21), C ^{α1} H r ¹ (8), CC ^c ob(7), CN ⁿ s(7)
—	793	—	CNH ₃ r ² (30), CN ⁿ s(18), CO ^a r(8), CH ₃ r ² (7)
—	820	—	CC ^{me} s(24), C ^{α1} H r ¹ (15), C ^{α1} H r ² (15), CH ₃ r ¹ (8)
—	835	—	CC ^{me} s(32), C ^{α2} H r ² (12), C ^{α2} H r ¹ (8), CC ^c sd(8), CH ₃ r ¹ (7)
—	875	—	C ^{α1} H r ² (28), C ^{α2} H r ¹ (14), CC ^ψ s(11), C ^{α1} H r ¹ (8)
—	884	—	CC ^c s(25), CC ^c sd(22), CC ^c ob(12), CO ^c ss(12), C ^{α2} H r ² (7), CH ₃ r ² (7)
—	907	—	CN ⁿ s(19), CH ₃ r ² (12), CO ^a r(10), NH ^a ib(9), CNH ₃ r ¹ (9), CC ^ψ s(7)
—	931	—	NH ^a ib(27), C ^{α2} H r ² (19), CC ^c ob(17), CH ₃ r ² (10), NC ^φ s(9)
—	983	—	NH ^a ib(19), CH ₃ r ² (19), C ^{α1} H r ¹ (15), C ^{α2} H r ¹ (13), CNH ₃ r ¹ (10)
—	1003	—	C ^{α2} H r ¹ (28), NC ^φ s(14), CO ^a s(8), CNHC sd(8), CO ^a sd(7)
—	1014	—	CH ₃ r ² (28), C ^{α1} H r ¹ (20), NH ^a ib(14), CH ₃ r ² (8), CNH ₃ r ¹ (7)
—	1126	—	CC ^{me} s(26), C ^{α1} H r ¹ (16), CH ₃ r ² (13), CNH ₃ sd(9)
—	1135	—	CH ₃ r ¹ (25), CNH ₃ sd(23), CC ^{me} s(20)
—	1142	—	CNH ₃ sd(45), CNH ₃ ad ^{1,2} (29)
1159	1153	-6	CNH ₃ ad ^{1,2} (60), CNH ₃ sd(10), CNH ₃ r ¹ (7)

Table 3.75: (continued)

frequency (cm ⁻¹)			Potential Energy Distribution
obs.	calc.	dev.	
1164	1168	4	CH ₃ r ¹ (31), CNH ₃ ad ^{1,2} (14), CNH ₃ r ¹ (8), C ^{α1} H d ¹ (7)
1188	1184	-4	CH ₃ r ¹ (21), CH ₃ r ² (14), NC ^φ s(9), C ^{α2} H r ¹ (7), CH ₃ r ¹ (7)
1194	1189	-5	CNH ₃ ad ^{1,2} (77)
1205	1208	3	CC ^{me} s(21), CH ₃ r ¹ (15), C ^{α2} H r ² (14), CC ^c s(8), C ^{α2} H d ³ (8), CH ₃ r ² (8)
1245	1234	-11	CC ^ψ s(16), CH ₃ r ² (15), C ^{α1} H r ² (10), CC ^{me} s(10), NC ^φ s(9)
1370	1365	-5	CH ₃ sd(83), CO ^c ss(10)
1392	1389	-3	CH ₃ sd(79), CO ^c ss(7)
1406	1396	-10	CO ^c ss(39), CH ₃ sd(17), CO ^c as(12), CC ^c s(10), CH ₃ sd(10)
1450	1446	-4	CH ₃ ad ^{1,2} (84)
1450	1455	5	CH ₃ ad ^{1,2} (84)
1458	1459	1	CH ₃ ad ^{1,2} (85), CH ₃ r ¹ (7)
1458	1465	7	CH ₃ ad ^{1,2} (87), CH ₃ r ¹ (10)
1478	1490	12	CO ^a s(29), CN ^a s(24), CC ^ψ s(11), NH ^a ib(9), NC ^φ s(7)
1584	1584	0	CO ^c as(70), CO ^c ss(17)
1663	1672	9	CN ^a s(45), CO ^a s(44)
—	1909	—	NH ₃ ss(51), NH ₃ as ¹ (47)
—	2189	—	C ^{α2} H s(98)
—	2229	—	NH ₃ as ¹ (46), NH ₃ ss(44), C ^{α1} H s(9)
—	2232	—	C ^{α1} H s(89)
—	2311	—	NH ₃ as ² (99)
—	2479	—	NH ^a s(98)
—	2957	—	CH ₃ ss(91)
—	2960	—	CH ₃ ss(83), CH ₃ as ^{1,2} (16)
—	2999	—	CH ₃ as ^{1,2} (75), CH ₃ as ^{1,2} (23)
—	3014	—	CH ₃ as ^{1,2} (58), CH ₃ as ^{1,2} (31), CH ₃ ss(11)
—	3040	—	CH ₃ as ^{1,2} (74), CH ₃ as ^{1,2} (19), CH ₃ ss(8)
—	3062	—	CH ₃ as ^{1,2} (53), CH ₃ as ^{1,2} (41)

frequency (cm ⁻¹)			Ala-1- ¹³ C-Ala in D ₂ O (mean deviation = 9 cm ⁻¹)
obs.	calc.	dev.	
—	62	—	NC ^φ t(40), CC ^c t(37), NH ^a ob(15)
—	101	—	C ^ω N t(52), NC ^φ t(42)

Table 3.75: (continued)

frequency (cm ⁻¹)			Potential Energy Distribution
obs.	calc.	dev.	
—	113	—	CC ^ψ t(64), CC ^c t(29)
—	123	—	CC ^c t(32), CC ^ψ t(29), NH ^a ob(10)
—	168	—	CNHC sd(27), CO ^a sd(21), CC ^{me} t(17), C ^{α1} H d ³ (7), CN ⁿ t(7)
—	196	—	CC ^{me} t(76), CC ^{me} t(7)
—	200	—	CC ^{me} t(70), CC ^{me} t(13)
—	225	—	C ^{α1} H d ² (22), CN ⁿ t(18), C ^{α1} H d ³ (10), C ^{α2} H d ³ (8), CNHC sd(7), C ^{α2} H d ¹ (7), CO ^a ob(7)
—	241	—	C ^{α2} H d ² (31), CN ⁿ t(14), CO ^a sd(13)
—	291	—	C ^{α2} H d ² (36), CN ⁿ t(27), C ^{α1} H d ² (13)
—	308	—	C ^{α1} H d ² (18), CO ^a sd(17), C ^{α1} H d ³ (14), C ^{α2} H d ³ (12), CC ^c r(12), CO ^a r(8)
—	323	—	CN ⁿ t(16), CNHC sd(12), CC ^c s(11), C ^{α1} H d ¹ (8), C ^{α2} H d ³ (8), NC ^φ s(7)
—	361	—	C ^{α1} H d ¹ (16), C ^{α1} H d ³ (15), CO ^a r(14), CC ^c r(14), C ^{α2} H d ³ (12), CNHC sd(7), CN ⁿ t(7)
—	431	—	C ^{α1} H d ¹ (42), CN ⁿ s(9), CC ^c r(7)
—	443	—	C ^{α2} H d ¹ (47), C ^ω N t(13), CC ^c r(8)
—	571	—	CC ^c r(31), C ^{α2} H d ³ (11), CO ^a sd(9)
—	624	—	CO ^a r(22), CNH ₃ r ² (15), C ^{α1} H d ³ (13), CC ^ψ s(10), CC ^c sd(10), CC ^c s(8), CNH ₃ r ¹ (7)
—	629	—	NH ^a ob(40), C ^ω N t(15), NC ^φ t(15), CO ^a ob(9)
—	658	—	CC ^c sd(34), CC ^c s(13), CC ^ψ s(9), CC ^c ob(7), CNH ₃ r ² (7)
—	741	—	CO ^a ob(55), NH ^a ob(15), C ^{α1} H d ² (11)
—	765	—	CNH ₃ r ² (35), CNH ₃ r ¹ (24), CC ^{me} s(20), CN ⁿ s(8)
—	783	—	CC ^c ob(57), C ^{α2} H d ² (8)
820	806	-14	CN ⁿ s(29), CNH ₃ r ² (16), CO ^a r(10), CC ^c sd(9), CH ₃ r ² (7)
869	873	4	CNH ₃ r ¹ (28), CH ₃ r ¹ (13)
874	881	7	CN ⁿ s(13), CC ^c s(11), CC ^c sd(10), CNH ₃ r ¹ (9), CC ^{me} s(8), CH ₃ r ² (7), CH ₃ r ¹ (7)
905	902	-3	NH ^a ib(21), CC ^c s(17), NC ^φ s(12), CH ₃ r ² (11), CC ^c sd(7), CC ^{me} s(7), CH ₃ r ¹ (7)
940	927	-13	CC ^ψ s(14), CO ^a r(13), CO ^a s(9), CH ₃ r ² (9), CNHC sd(7), NH ^a ib(7)

Table 3.75: (continued)

frequency (cm ⁻¹)			Potential Energy Distribution
obs.	calc.	dev.	
999	988	-11	NH ^a ib(45), CH ₃ r ² (16), CC ^ψ s(7)
1049	1052	3	CC ^{me} s(32), C ^{α1} H r ² (22), C ^{α1} H d ³ (7), CN ⁿ s(7)
1060	1071	11	C ^{α2} H r ² (34), CH ₃ r ² (14), CC ^c ob(9), CH ₃ r ¹ (7)
1096	1097	1	CH ₃ r ² (41), C ^{α1} H r ² (10), CH ₃ r ¹ (8), C ^{α1} H d ² (7), CC ^{me} s(7)
1112	1131	19	CC ^{me} s(25), NC ^φ s(23), CH ₃ r ² (10)
1145	1141	-4	CNH ₃ sd(69), CNH ₃ ad ^{1,2} (17), CN ⁿ s(7)
1145	1150	5	CNH ₃ ad ^{1,2} (75), CNH ₃ sd(11)
1164	1157	-7	CH ₃ r ¹ (32), C ^{α2} H d ¹ (16), CC ^{me} s(16), CH ₃ r ² (11)
1181	1181	0	CNH ₃ ad ^{1,2} (59), CH ₃ r ¹ (9)
1188	1195	7	CNH ₃ ad ^{1,2} (35), CH ₃ r ¹ (19), CC ^{me} s(11), C ^{α1} H d ¹ (9), CH ₃ r ² (8)
1278	1274	-4	C ^{α2} H r ² (43), CH ₃ r ¹ (9), C ^{α2} H r ¹ (8)
1310	1294	-16	C ^{α1} H r ² (47), C ^{α1} H r ¹ (16), CH ₃ r ¹ (14)
1331	1332	1	C ^{α2} H r ¹ (45), C ^{α1} H r ¹ (30), C ^{α2} H r ² (7)
1354	1339	-15	C ^{α1} H r ¹ (38), C ^{α2} H r ¹ (32)
1369	1365	-4	CH ₃ sd(83), CO ^c ss(9)
1392	1389	-3	CH ₃ sd(81)
1409	1396	-13	CO ^c ss(40), CH ₃ sd(14), CO ^c as(13), CC ^c s(10), CH ₃ sd(10)
1440	1444	4	CH ₃ ad ^{1,2} (67), CO ^a s(9), CN ^a s(7)
1461	1456	-5	CH ₃ ad ^{1,2} (77)
1461	1461	0	CH ₃ ad ^{1,2} (84), CH ₃ r ¹ (8)
1461	1467	6	CH ₃ ad ^{1,2} (56), CO ^a s(8), CN ^a s(7), CH ₃ r ¹ (7)
1472	1471	-1	CH ₃ ad ^{1,2} (29), CO ^a s(16), CH ₃ ad ^{1,2} (12), CN ^a s(9)
1592	1586	-6	CO ^c as(69), CO ^c ss(16)
1624	1633	9	CN ^a s(45), CO ^a s(41)
—	1911	—	NH ₃ ss(50), NH ₃ as ¹ (47)
—	2229	—	NH ₃ as ¹ (50), NH ₃ ss(48)
—	2311	—	NH ₃ as ² (99)
—	2479	—	NH ^a s(98)
—	2957	—	CH ₃ ss(88), CH ₃ as ^{1,2} (8)
—	2960	—	CH ₃ ss(83), CH ₃ as ^{1,2} (16)
—	2969	—	C ^{α2} H s(89)
—	3002	—	CH ₃ as ^{1,2} (67), CH ₃ as ^{1,2} (23), C ^{α2} H s(8)

Table 3.75: (continued)

frequency (cm^{-1})			Potential Energy Distribution
obs.	calc.	dev.	
—	3009	—	CH_3 as ^{1,2} (48), $\text{C}^{\alpha 1}$ H s(22), CH_3 as ^{1,2} (22), CH_3 ss(8)
—	3029	—	$\text{C}^{\alpha 1}$ H s(77), CH_3 as ^{1,2} (11), CH_3 as ^{1,2} (9)
—	3040	—	CH_3 as ^{1,2} (73), CH_3 as ^{1,2} (20), CH_3 ss(8)
—	3062	—	CH_3 as ^{1,2} (51), CH_3 as ^{1,2} (42)

Table 3.76: Scaled 4-31G Frequencies and Potential Energy Distribution for Isolated Alanyl-alanine in acid.

frequency (cm^{-1})			Ala-Ala pH 1 (mean deviation = 13 cm^{-1})
obs.	calc.	dev.	
			Potential Energy Distribution
—	37	—	$\text{NC}^\phi \text{ t}(55)$, $\text{CC}^\psi \text{ t}(39)$
—	68	—	$\text{CC}^c \text{ t}(45)$, $\text{C}^\omega\text{N} \text{ t}(33)$
—	78	—	$\text{CC}^\psi \text{ t}(35)$, $\text{C}^\omega\text{N} \text{ t}(21)$, $\text{NC}^\phi \text{ t}(15)$, $\text{CNHC} \text{ sd}(7)$
—	98	—	$\text{CC}^c \text{ t}(30)$, $\text{CC}^\psi \text{ t}(17)$, $\text{NC}^\phi \text{ t}(17)$, $\text{CNHC} \text{ sd}(12)$, $\text{CO}^a \text{ sd}(8)$
—	131	—	$\text{CNHC} \text{ sd}(24)$, $\text{CC}^c \text{ t}(19)$, $\text{CO}^a \text{ sd}(17)$, $\text{C}^{\alpha 2}\text{H} \text{ d}^3(10)$, $\text{C}^\omega\text{N} \text{ t}(9)$
—	187	—	$\text{CC}^{me} \text{ t}(48)$, $\text{CC}^{me} \text{ t}(46)$
—	190	—	$\text{CC}^{me} \text{ t}(48)$, $\text{CC}^{me} \text{ t}(46)$
237	232	-5	$\text{C}^{\alpha 2}\text{H} \text{ d}^2(28)$, $\text{C}^{\alpha 1}\text{H} \text{ d}^2(13)$, $\text{CNHC} \text{ sd}(9)$, $\text{C}^{\alpha 2}\text{H} \text{ d}^1(7)$
237	244	7	$\text{C}^{\alpha 1}\text{H} \text{ d}^2(32)$, $\text{C}^{\alpha 2}\text{H} \text{ d}^2(14)$, $\text{C}^{\alpha 2}\text{H} \text{ d}^3(14)$, $\text{CC}^c \text{ sd}(11)$, $\text{CO}^a \text{ sd}(7)$
—	314	—	$\text{C}^{\alpha 2}\text{H} \text{ d}^2(25)$, $\text{C}^{\alpha 2}\text{H} \text{ d}^3(20)$, $\text{CC}^c \text{ s}(9)$, $\text{CC}^c \text{ r}(8)$, $\text{CC}^c \text{ ob}(8)$, $\text{C}^{\alpha 1}\text{H} \text{ d}^3(7)$
344	327	-17	$\text{CC}^c \text{ sd}(26)$, $\text{CO}^a \text{ sd}(17)$, $\text{C}^{\alpha 1}\text{H} \text{ d}^2(14)$, $\text{C}^{\alpha 1}\text{H} \text{ d}^1(8)$
372	402	30	$\text{CN}^n \text{ t}(38)$, $\text{C}^{\alpha 1}\text{H} \text{ d}^3(14)$, $\text{C}^{\alpha 1}\text{H} \text{ d}^1(12)$, $\text{CO}^a \text{ r}(8)$
—	409	—	$\text{CN}^n \text{ t}(46)$, $\text{C}^{\alpha 1}\text{H} \text{ d}^3(25)$, $\text{CO}^a \text{ r}(13)$
456	438	-18	$\text{C}^{\alpha 1}\text{H} \text{ d}^1(37)$, $\text{C}^{\alpha 2}\text{H} \text{ d}^1(15)$, $\text{CC}^c \text{ sd}(14)$, $\text{C}^\omega\text{N} \text{ t}(7)$
456	452	-4	$\text{C}^{\alpha 2}\text{H} \text{ d}^1(30)$, $\text{C}^{\alpha 1}\text{H} \text{ d}^1(17)$, $\text{C}^{\alpha 1}\text{H} \text{ d}^3(9)$
571	576	5	$\text{CC}^c \text{ sd}(24)$, $\text{C}^{\alpha 2}\text{H} \text{ d}^1(12)$, $\text{CO}^a \text{ sd}(12)$, $\text{CC}^\psi \text{ s}(11)$, $\text{C}^{\alpha 2}\text{H} \text{ d}^3(8)$
650	633	-17	$\text{CO}^H \text{ t}(32)$, $\text{CC}^c \text{ r}(30)$, $\text{CC}^c \text{ ob}(10)$, $\text{CC}^{me} \text{ s}(7)$
—	662	—	$\text{CO}^H \text{ t}(45)$, $\text{CC}^c \text{ r}(20)$, $\text{CO}^a \text{ r}(11)$
681	696	15	$\text{CC}^\psi \text{ s}(16)$, $\text{C}^{\alpha 1}\text{H} \text{ d}^3(14)$, $\text{CO}^a \text{ ob}(11)$, $\text{CO}^a \text{ r}(10)$, $\text{CC}^c \text{ r}(9)$
749	734	-15	$\text{CO}^a \text{ ob}(27)$, $\text{NH}^a \text{ ob}(18)$, $\text{C}^\omega\text{N} \text{ t}(9)$, $\text{C}^{\alpha 1}\text{H} \text{ d}^2(7)$
—	772	—	$\text{CC}^c \text{ ob}(38)$, $\text{CO}^H \text{ t}(13)$, $\text{CO}^a \text{ ob}(11)$, $\text{CC}^{me} \text{ s}(9)$
818	817	-1	$\text{NH}^a \text{ ob}(57)$, $\text{CO}^a \text{ ob}(13)$
834	828	-6	$\text{CN}^n \text{ s}(29)$, $\text{CC}^{me} \text{ s}(11)$, $\text{CC}^c \text{ s}(10)$
876	869	-7	$\text{CN}^n \text{ s}(24)$, $\text{CC}^c \text{ s}(14)$, $\text{CC}^{me} \text{ s}(8)$
927	930	3	$\text{CC}^{me} \text{ s}(21)$, $\text{CCH}_3 \text{ r}^1(12)$, $\text{CNHC} \text{ sd}(8)$, $\text{CO}^a \text{ r}(8)$
953	952	-1	$\text{CNH}_3 \text{ r}^2(37)$, $\text{CCH}_3 \text{ r}^2(17)$, $\text{CC}^{me} \text{ s}(12)$, $\text{CCH}_3 \text{ r}^2(7)$
953	961	8	$\text{CCH}_3 \text{ r}^2(21)$, $\text{CNH}_3 \text{ r}^2(16)$, $\text{CC}^\psi \text{ s}(15)$, $\text{NC}^\phi \text{ s}(10)$, $\text{CC}^{me} \text{ s}(8)$, $\text{CO}^a \text{ r}(7)$

Table 3.76: (continued)

frequency (cm ⁻¹)			Potential Energy Distribution
obs.	calc.	dev.	
1009	1018	9	CCH ₃ r ¹ (27), CNH ₃ r ¹ (17), CN ⁿ s(11), CC ^{me} s(11), C ^{α1} H r ² (10)
1055	1086	31	C ^{α2} H r ² (21), CCH ₃ r ² (11), CC ^{me} s(8), CCH ₃ r ² (7)
1101	1095	-6	CCH ₃ r ² (28), CCH ₃ r ² (11), CC ^{me} s(10), CN ⁿ s(9), C ^{α2} H r ² (8)
1119	1115	-4	CNH ₃ r ¹ (39), C ^{α1} H r ² (34), C ^{α1} H r ¹ (7)
1140	1141	1	CC ^{me} s(31), CCH ₃ r ¹ (19), NC ^φ s(18)
1166	1166	0	CCH ₃ r ¹ (18), NC ^φ s(17), CCH ₃ r ² (17), C ^{α2} H d ¹ (12), CO ^H s(9)
1239	1216	-23	CNH ₃ r ² (24), CCH ₃ r ¹ (23), C ^{α1} H d ¹ (16), CC ^{me} s(12), CCH ₃ r ² (8)
1239	1236	-3	C ^{α2} H r ² (22), CO ^H s(20), OH b(14), C ^{α2} H r ¹ (9)
1270	1269	-1	NH ^a ib(23), OH b(13), C ^{α1} H r ² (8), CN ^a s(7), C ^{α2} H r ² (7), CO ^H s(7)
1295	1289	-6	C ^{α1} H r ² (28), C ^{α2} H r ² (13), OH b(7), CCH ₃ r ¹ (7)
1295	1307	12	C ^{α2} H r ¹ (21), NH ^a ib(14), C ^{α2} H r ² (14), C ^{α1} H r ¹ (8), C ^{α1} H r ² (7), CCH ₃ r ¹ (7)
1338	1353	15	C ^{α2} H r ¹ (38), C ^{α1} H r ¹ (34), OH b(8)
1381	1375	-6	C ^{α1} H r ¹ (38), C ^{α2} H r ¹ (14)
1381	1388	7	CCH ₃ sd(97)
1404	1403	-1	CCH ₃ sd(92)
1459	1452	-7	CCH ₃ ad ^{1,2} (79), CCH ₃ ad ^{1,2} (9), CCH ₃ r ² (7)
1459	1455	-4	CCH ₃ ad ^{1,2} (71), CCH ₃ ad ^{1,2} (8)
1459	1460	1	CCH ₃ ad ^{1,2} (83), CCH ₃ r ¹ (12)
1459	1467	8	CCH ₃ ad ^{1,2} (81), CCH ₃ r ¹ (9), CCH ₃ ad ^{1,2} (7)
1525	1519	-6	CNH ₃ sd(41), CO ^H s(12), OH b(11), CN ^a s(7)
1525	1520	-5	CNH ₃ sd(33), CO ^H s(15), OH b(11), CO ^a s(9)
1564	1566	2	NH ^a ib(44), CO ^a s(12), CN ^a s(12)
1625	1611	-14	CNH ₃ ad ^{1,2} (56), CNH ₃ sd(21), CNH ₃ ad ^{1,2} (20)
1625	1648	23	CNH ₃ ad ^{1,2} (67), CNH ₃ ad ^{1,2} (26)
1679	1677	-2	CO ^a s(40), CN ^a s(36)
1726	1731	5	CO ^c s(68), OH b(12), CC ^c s(8)
—	2662	—	NH ₃ as ¹ (78), NH ₃ ss(21)
—	2880	—	NH ₃ as ² (99)

Table 3.76: (continued)

frequency (cm^{-1})			Potential Energy Distribution
obs.	calc.	dev.	
—	2937	—	NH_3 ss(78), NH_3 as ¹ (21)
—	2970	—	CH_3 ss(96)
—	2975	—	CH_3 ss(80), CH_3 as ^{1,2} (11), $\text{C}^{\alpha 2}\text{H}$ s(10)
—	2986	—	$\text{C}^{\alpha 2}\text{H}$ s(88), CH_3 ss(12)
—	3004	—	$\text{C}^{\alpha 1}\text{H}$ s(85), CH_3 as ^{1,2} (13)
—	3026	—	CH_3 as ^{1,2} (53), CH_3 as ^{1,2} (34), $\text{C}^{\alpha 1}\text{H}$ s(13)
—	3034	—	CH_3 as ^{1,2} (89), CH_3 ss(8)
—	3039	—	CH_3 as ^{1,2} (62), CH_3 as ^{1,2} (33)
—	3050	—	CH_3 as ^{1,2} (100)
—	3409	—	NH^a s(100)
—	3531	—	OH s(100)

frequency (cm^{-1})			Ala-Ala in D_2O (mean deviation = 14 cm^{-1})
obs.	calc.	dev.	
—	36	—	NC^ϕ t(54), CC^ψ t(40)
—	66	—	CC^c t(43), C^ωN t(33)
—	75	—	CC^ψ t(34), C^ωN t(22), NC^ϕ t(17), CNHC sd(7)
—	95	—	CC^c t(32), NC^ϕ t(16), CNHC sd(14), CC^ψ t(14), CO^a sd(9)
—	128	—	CNHC sd(22), CC^c t(21), CO^a sd(16), C^ωN t(10), $\text{C}^{\alpha 2}\text{H}$ d ³ (9)
—	187	—	CC^{me} t(53), CC^{me} t(42)
—	189	—	CC^{me} t(52), CC^{me} t(42)
—	229	—	$\text{C}^{\alpha 2}\text{H}$ d ² (36), CNHC sd(9), $\text{C}^{\alpha 2}\text{H}$ d ³ (7)
240	239	-1	$\text{C}^{\alpha 1}\text{H}$ d ² (39), $\text{C}^{\alpha 2}\text{H}$ d ³ (11), CO^a sd(11), CC^c sd(9), CO^a ob(7)
—	289	—	CN^n t(69), $\text{C}^{\alpha 1}\text{H}$ d ² (7)
335	305	-30	$\text{C}^{\alpha 2}\text{H}$ d ² (23), $\text{C}^{\alpha 2}\text{H}$ d ³ (14), CC^c s(9), $\text{C}^{\alpha 1}\text{H}$ d ³ (9), CC^c ob(7)
335	323	-12	CC^c sd(24), CN^n t(16), CO^a sd(13), $\text{C}^{\alpha 1}\text{H}$ d ² (11), $\text{C}^{\alpha 1}\text{H}$ d ¹ (9)
376	378	2	$\text{C}^{\alpha 1}\text{H}$ d ³ (32), CO^a r(19), $\text{C}^{\alpha 1}\text{H}$ d ¹ (15), CNHC sd(9)
435	405	-30	$\text{C}^{\alpha 2}\text{H}$ d ¹ (27), $\text{C}^{\alpha 1}\text{H}$ d ¹ (15), C^ωN t(15), CC^c sd(12)
435	422	-13	$\text{C}^{\alpha 1}\text{H}$ d ¹ (30), $\text{C}^{\alpha 2}\text{H}$ d ¹ (15), $\text{C}^{\alpha 1}\text{H}$ d ³ (11), CN^n s(7)
—	494	—	CO^H t(85)

Table 3.76: (continued)

frequency (cm ⁻¹)			Potential Energy Distribution
obs.	calc.	dev.	
548	546	-2	CC ^c sd(22), CO ^a sd(12), C ^{α2} H d ³ (8), CC ^ψ s(7), C ^{α2} H d ¹ (7)
602	604	2	NH ^a ob(50), CO ^a ob(9), C ^{α2} H d ¹ (8)
—	624	—	CC ^c r(46), CO ^a r(11), CO ^H s(7)
638	662	24	CC ^ψ s(22), CO ^a r(21), CNH ₃ r ¹ (14), C ^{α1} H d ³ (7)
746	746	0	CNH ₃ r ² (32), CC ^c ob(17), CN ⁿ s(8), CC ^{me} s(8), CC ^{me} s(7)
755	753	-2	CC ^c ob(30), CNH ₃ r ² (27)
755	775	20	CO ^a ob(42), CC ^{me} s(12), NH ^a ob(11), C ^{α1} H d ² (8), CNH ₃ r ² (8)
803	808	5	CN ⁿ s(18), CC ^c s(12), CC ^c ob(11), CNH ₃ r ² (8), CNH ₃ r ¹ (7)
829	855	26	CN ⁿ s(29), CC ^c s(14), CCH ₃ r ² (11), CCH ₃ r ² (7)
871	883	12	CNH ₃ r ¹ (47), CCH ₃ r ¹ (16), C ^{α1} H d ³ (9)
920	910	-10	CC ^{me} s(20), NH ^a ib(18), NC ^φ s(17), CCH ₃ r ¹ (12), CCH ₃ r ² (11), CC ^c s(7)
942	933	-9	CO ^a r(12), CO ^a s(11), CC ^ψ s(11), CNHC sd(9), NH ^a ib(9), CCH ₃ r ² (8), CN ^a s(7)
1003	1013	10	NH ^a ib(46), CCH ₃ r ² (17), CC ^ψ s(7)
1045	1046	1	C ^{α1} H r ² (26), CC ^{me} s(22), CN ⁿ s(9), C ^{α1} H d ³ (8), CNH ₃ r ¹ (7)
1067	1066	-1	OH b(43), CO ^H s(15), C ^{α2} H r ² (7)
1098	1090	-8	CCH ₃ r ² (37), CC ^{me} s(8), C ^{α1} H d ² (7)
1098	1099	1	C ^{α2} H r ² (23), OH b(13), CO ^c s(10), CO ^H s(8), CCH ₃ r ² (8)
1119	1133	14	CNH ₃ ad ^{1,2} (45), CNH ₃ sd(24), CNH ₃ ad ^{1,2} (10)
1152	1140	-12	CC ^{me} s(24), NC ^φ s(15), CCH ₃ r ¹ (13)
1152	1164	12	CCH ₃ r ¹ (19), CCH ₃ r ² (14), C ^{α2} H d ¹ (12), NC ^φ s(9), CCH ₃ r ¹ (8)
1162	1176	14	CCH ₃ r ¹ (23), CNH ₃ ad ^{1,2} (18), NC ^φ s(7), CNH ₃ ad ^{1,2} (7)
1185	1190	5	CNH ₃ sd(63), CNH ₃ ad ^{1,2} (30)
1190	1196	6	CNH ₃ ad ^{1,2} (56), CCH ₃ r ² (8), C ^{α1} H d ¹ (7)
1259	1270	11	C ^{α2} H r ² (45), CCH ₃ r ¹ (12), CO ^H s(7)
1301	1286	-15	C ^{α1} H r ² (46), CCH ₃ r ¹ (10)
1314	1330	16	C ^{α2} H r ¹ (71), CO ^H s(7)
1352	1346	-6	C ^{α1} H r ¹ (83)
1390	1386	-4	CCH ₃ sd(94)
1395	1400	5	CCH ₃ sd(98)
1447	1444	-3	CCH ₃ ad ^{1,2} (60), CO ^H s(12), CCH ₃ ad ^{1,2} (8)

Table 3.76: (continued)

frequency (cm ⁻¹)			Potential Energy Distribution
obs.	calc.	dev.	
1447	1450	3	CCH ₃ ad ^{1,2} (86)
1459	1460	1	CCH ₃ ad ^{1,2} (85), CCH ₃ r ¹ (12)
1459	1466	7	CCH ₃ ad ^{1,2} (63), CCH ₃ ad ^{1,2} (20), CCH ₃ r ¹ (7)
1481	1481	0	CO ^H s(19), CCH ₃ ad ^{1,2} (18), CC ^c s(14), CCH ₃ ad ^{1,2} (10), CC ^c r(7)
—	1496	—	CO ^a s(25), CN ^a s(20), NH ^a ib(11), CC ^ψ s(8), NC ^φ s(8)
1670	1660	-10	CO ^a s(45), CN ^a s(39)
1717	1713	-4	CO ^c s(76), CC ^c s(7)
—	1951	—	NH ₃ as ¹ (64), NH ₃ ss(34)
—	2119	—	NH ₃ ss(49), NH ₃ as ² (26), NH ₃ as ¹ (25)
—	2129	—	NH ₃ as ² (73), NH ₃ ss(16), NH ₃ as ¹ (9)
—	2503	—	NH ^a s(98)
—	2572	—	OH s(100)
—	2970	—	CH ₃ ss(96)
—	2975	—	CH ₃ ss(80), CH ₃ as ^{1,2} (11), C ^{α2} H s(10)
—	2986	—	C ^{α2} H s(88), CH ₃ ss(12)
—	3004	—	C ^{α1} H s(85), CH ₃ as ^{1,2} (13)
—	3026	—	CH ₃ as ^{1,2} (53), CH ₃ as ^{1,2} (34), C ^{α1} H s(13)
—	3034	—	CH ₃ as ^{1,2} (89), CH ₃ ss(8)
—	3039	—	CH ₃ as ^{1,2} (62), CH ₃ as ^{1,2} (33)
—	3050	—	CH ₃ as ^{1,2} (100)

frequency (cm ⁻¹)			2-D Ala-Ala (mean deviation = 19 cm ⁻¹)
obs.	calc.	dev.	
—	37	—	NC ^φ t(55), CC ^ψ t(40)
—	68	—	CC ^c t(45), C ^ω N t(33)
—	77	—	CC ^ψ t(35), C ^ω N t(21), NC ^φ t(15), CNHC sd(7)
—	98	—	CC ^c t(30), CC ^ψ t(17), NC ^φ t(17), CNHC sd(13), CO ^a sd(8)
—	131	—	CNHC sd(23), CC ^c t(19), CO ^a sd(17), C ^{α2} H d ³ (10), C ^ω N t(8)
—	187	—	CC ^{me} t(47), CC ^{me} t(47)
—	190	—	CC ^{me} t(47), CC ^{me} t(47)
243	232	-11	C ^{α2} H d ² (28), C ^{α1} H d ² (13), CNHC sd(9), C ^{α2} H d ¹ (7)

Table 3.76: (continued)

frequency (cm ⁻¹)			Potential Energy Distribution
obs.	calc.	dev.	
243	243	0	C ^{α1} H d ² (32), C ^{α2} H d ² (14), C ^{α2} H d ³ (14), CC ^c sd(11), CO ^a sd(7)
—	314	—	C ^{α2} H d ² (24), C ^{α2} H d ³ (21), CC ^c s(8), CC ^c r(8), CC ^c ob(8), C ^{α1} H d ³ (7)
363	323	-40	CC ^c sd(26), CO ^a sd(16), C ^{α1} H d ² (13), C ^{α1} H d ¹ (8)
363	401	38	CN ⁿ t(36), C ^{α1} H d ³ (15), C ^{α1} H d ¹ (14), CO ^a r(8)
—	409	—	CN ⁿ t(49), C ^{α1} H d ³ (23), CO ^a r(12)
451	436	-15	C ^{α1} H d ¹ (39), CC ^c sd(15), C ^{α2} H d ¹ (13)
451	450	-1	C ^{α2} H d ¹ (31), C ^{α1} H d ¹ (14), C ^{α1} H d ³ (10)
572	570	-2	CC ^c sd(25), CC ^ψ s(13), C ^{α2} H d ¹ (12), CO ^a sd(10), C ^{α2} H d ³ (8)
648	632	-16	CC ^c r(31), CO ^H t(28), CC ^c ob(9), CO ^a r(7), CC ^{me} s(7)
648	656	8	CO ^H t(40), CO ^a r(12), CC ^c r(10), CC ^ψ s(7)
677	685	8	CC ^c r(16), CO ^H t(16), CO ^a ob(10), CC ^ψ s(9), C ^{α1} H d ³ (8), C ^{α2} H d ³ (7)
702	723	21	CO ^a ob(24), C ^{α1} H r ² (12), CO ^a r(9), C ^{α1} H d ² (8), CCH ₃ r ¹ (8), NH ^a ob(7)
—	762	—	CC ^c ob(23), NH ^a ob(15), C ^{α1} H r ² (13), CO ^H t(8), CC ^{me} s(8)
748	787	39	NH ^a ob(21), CC ^c ob(21), C ^{α1} H r ² (15), CC ^{me} s(8), CO ^H t(7)
816	822	6	NH ^a ob(22), CN ⁿ s(19), CC ^{me} s(14), CC ^c s(9)
838	851	13	CC ^c s(13), CO ^a ob(9), CC ^ψ s(8), NH ^a ob(8), CC ^{me} s(8), CC ^c ob(7)
869	883	14	C ^{α1} H r ¹ (39), CN ⁿ s(29), CNH ₃ r ² (8), C ^{α1} H r ² (7)
904	921	17	C ^{α1} H r ¹ (21), C ^{α1} H r ² (12), CN ⁿ s(11), CCH ₃ r ² (9), CO ^a ob(7), CCH ₃ r ² (7)
933	931	-2	CC ^{me} s(22), CCH ₃ r ¹ (13), CNHC sd(10), CO ^a r(9)
969	953	-16	CNH ₃ r ² (19), CCH ₃ r ² (16), CCH ₃ r ² (15), NC ^φ s(9), CC ^{me} s(8)
1018	979	-39	CNH ₃ r ² (27), CC ^{me} s(14), CC ^ψ s(9), CCH ₃ r ² (8), C ^{α1} H r ¹ (7), C ^{α1} H r ² (7)
1052	1083	31	CCH ₃ r ² (21), CNH ₃ r ¹ (16), CCH ₃ r ¹ (10), C ^{α2} H r ² (9)
1084	1091	7	C ^{α2} H r ² (20), CCH ₃ r ² (16), CNH ₃ r ¹ (8), CCH ₃ r ¹ (7), CCH ₃ r ² (7)
1107	1134	27	CC ^{me} s(23), NC ^φ s(16), CCH ₃ r ¹ (11), CCH ₃ r ¹ (9)

Table 3.76: (continued)

frequency (cm ⁻¹)			Potential Energy Distribution
obs.	calc.	dev.	
1149	1155	6	CCH ₃ r ¹ (17), C ^{α1} H r ¹ (12), CC ^{me} s(11), CCH ₃ r ¹ (10), C ^{α2} H d ¹ (7), CC ^{me} s(7)
1178	1170	-8	NC ^φ s(20), CCH ₃ r ² (12), CCH ₃ r ¹ (9), C ^{α2} H d ¹ (8), CO ^H s(8), C ^{α1} H r ¹ (7), CC ^{me} s(7)
1211	1200	-11	CCH ₃ r ¹ (26), CNH ₃ r ² (21), CNH ₃ r ¹ (14), C ^{α1} H d ¹ (12), CC ^{me} s(9)
1234	1234	0	C ^{α2} H r ² (18), CO ^H s(14), OH b(10), NH ^a ib(8)
1243	1245	2	CNH ₃ r ¹ (15), CO ^H s(9), CCH ₃ r ² (8), NC ^φ s(7), OH b(7)
1285	1279	-6	C ^{α2} H r ² (22), OH b(17), NH ^a ib(14), CC ^c s(7)
1327	1311	-16	C ^{α2} H r ¹ (28), NH ^a ib(20), C ^{α2} H r ² (13), CCH ₃ r ¹ (8)
1350	1363	13	C ^{α2} H r ¹ (45), OH b(14)
1391	1388	-3	CCH ₃ sd(97)
1401	1403	2	CCH ₃ sd(94)
1458	1451	-7	CCH ₃ ad ^{1,2} (86), CCH ₃ r ² (7)
1458	1454	-4	CCH ₃ ad ^{1,2} (75)
1458	1458	0	CCH ₃ ad ^{1,2} (84), CCH ₃ r ¹ (10)
1458	1467	9	CCH ₃ ad ^{1,2} (81), CCH ₃ r ¹ (9), CCH ₃ ad ^{1,2} (7)
1509	1519	10	CNH ₃ sd(48), CO ^H s(10), OH b(9), CN ^a s(7)
1521	1520	-1	CNH ₃ sd(26), CO ^H s(17), OH b(13), CO ^a s(9), CC ^c r(7)
1559	1566	7	NH ^a ib(44), CO ^a s(12), CN ^a s(12)
1628	1610	-18	CNH ₃ ad ^{1,2} (56), CNH ₃ sd(21), CNH ₃ ad ^{1,2} (20)
1628	1645	17	CNH ₃ ad ^{1,2} (65), CNH ₃ ad ^{1,2} (27)
1680	1675	-5	CO ^a s(40), CN ^a s(36)
1730	1731	1	CO ^c s(68), OH b(12), CC ^c s(8)
—	2220	—	C ^{α1} H s(98)
—	2662	—	NH ₃ as ¹ (78), NH ₃ ss(21)
—	2880	—	NH ₃ as ² (99)
—	2937	—	NH ₃ ss(78), NH ₃ as ¹ (21)
—	2970	—	CH ₃ ss(96)
—	2975	—	CH ₃ ss(80), CH ₃ as ^{1,2} (11), C ^{α2} H s(10)
—	2986	—	C ^{α2} H s(88), CH ₃ ss(12)
—	3023	—	CH ₃ as ^{1,2} (71), CH ₃ as ^{1,2} (29)
—	3034	—	CH ₃ as ^{1,2} (89), CH ₃ ss(8)
—	3038	—	CH ₃ as ^{1,2} (69), CH ₃ as ^{1,2} (28)

Table 3.76: (continued)

frequency (cm ⁻¹)			Potential Energy Distribution
obs.	calc.	dev.	
—	3050	—	CH ₃ as ^{1,2} (100)
—	3409	—	NH ^a s(100)
—	3531	—	OH s(100)

frequency (cm ⁻¹)			¹³ C Ala-Ala (mean deviation = 15 cm ⁻¹)
obs.	calc.	dev.	
—	37	—	NC ^φ t(55), CC ^ψ t(39)
—	68	—	CC ^c t(45), C ^ω N t(33)
—	77	—	CC ^ψ t(35), C ^ω N t(21), NC ^φ t(15), CNHC sd(7)
—	98	—	CC ^c t(30), CC ^ψ t(17), NC ^φ t(17), CNHC sd(12), CO ^a sd(8)
—	131	—	CNHC sd(23), CC ^c t(19), CO ^a sd(17), C ^{α2} H d ³ (10), C ^ω N t(9)
—	187	—	CC ^{me} t(49), CC ^{me} t(46)
—	190	—	CC ^{me} t(48), CC ^{me} t(46)
241	232	-9	C ^{α2} H d ² (29), C ^{α1} H d ² (12), CNHC sd(9), C ^{α2} H d ¹ (7)
241	243	2	C ^{α1} H d ² (32), C ^{α2} H d ³ (14), C ^{α2} H d ² (13), CC ^c sd(11), CO ^a sd(7)
340	313	-27	C ^{α2} H d ² (25), C ^{α2} H d ³ (21), CC ^c s(9), CC ^c r(8), CC ^c ob(8), C ^{α1} H d ³ (7)
340	326	-14	CC ^c sd(26), CO ^a sd(16), C ^{α1} H d ² (14), C ^{α1} H d ¹ (8)
368	401	33	CN ⁿ t(38), C ^{α1} H d ³ (14), C ^{α1} H d ¹ (13), CO ^a r(8)
—	409	—	CN ⁿ t(46), C ^{α1} H d ³ (24), CO ^a r(12)
454	438	-16	C ^{α1} H d ¹ (37), C ^{α2} H d ¹ (15), CC ^c sd(14), C ^ω N t(7)
454	451	-3	C ^{α2} H d ¹ (29), C ^{α1} H d ¹ (17), C ^{α1} H d ³ (10)
571	576	5	CC ^c sd(24), C ^{α2} H d ¹ (12), CO ^a sd(12), CC ^ψ s(11), C ^{α2} H d ³ (8)
616	632	16	CO ^H t(31), CC ^c r(30), CC ^c ob(10), CC ^{me} s(7)
—	661	—	CO ^H t(43), CC ^c r(18), CO ^a r(11)
671	691	20	CO ^a ob(17), CC ^ψ s(12), C ^{α1} H d ³ (11), CC ^c r(10), CO ^H t(9)
747	727	-20	CO ^a ob(27), NH ^a ob(12), C ^{α1} H d ² (9), CO ^a r(9), C ^ω N t(7)
—	769	—	CC ^c ob(38), CO ^H t(13), CC ^{me} s(10), CO ^a ob(8)
819	813	-6	NH ^a ob(61), CO ^a ob(9)
833	825	-8	CN ⁿ s(28), CC ^c s(10), CC ^{me} s(10)

Table 3.76: (continued)

frequency (cm ⁻¹)			Potential Energy Distribution
obs.	calc.	dev.	
872	869	-3	CN ⁿ s(25), CC ^c s(14), CC ^{me} s(8), CCH ₃ r ² (7)
921	928	7	CC ^{me} s(21), CCH ₃ r ¹ (12), CNHC sd(10), CO ^a r(10)
951	950	-1	CNH ₃ r ² (20), CCH ₃ r ² (17), CCH ₃ r ² (16), NC ^φ s(10)
951	957	6	CNH ₃ r ² (33), CC ^{me} s(16), CCH ₃ r ² (13), CC ^ψ s(11)
1005	1018	13	CCH ₃ r ¹ (28), CNH ₃ r ¹ (17), C ^{α1} H r ² (11), CN ⁿ s(11), CC ^{me} s(11)
1052	1085	33	C ^{α2} H r ² (20), CCH ₃ r ² (13), CC ^{me} s(7)
1102	1094	-8	CCH ₃ r ² (26), CCH ₃ r ² (12), CC ^{me} s(10), C ^{α2} H r ² (9), CN ⁿ s(8)
1118	1113	-5	CNH ₃ r ¹ (40), C ^{α1} H r ² (33)
1141	1139	-2	CC ^{me} s(30), NC ^φ s(18), CCH ₃ r ¹ (17)
1169	1165	-4	CCH ₃ r ¹ (19), CCH ₃ r ² (17), NC ^φ s(14), C ^{α2} H d ¹ (13), CO ^H s(8)
1247	1215	-32	CNH ₃ r ² (24), CCH ₃ r ¹ (23), C ^{α1} H d ¹ (16), CC ^{me} s(12), CCH ₃ r ² (8)
1247	1236	-11	C ^{α2} H r ² (22), CO ^H s(19), OH b(13), C ^{α2} H r ¹ (9)
1260	1265	5	NH ^a ib(24), OH b(12), CN ^a s(9), CO ^a s(8), CO ^H s(8), NC ^φ s(7)
1290	1289	-1	C ^{α1} H r ² (28), C ^{α2} H r ² (14), OH b(7), CCH ₃ r ¹ (7)
1290	1304	14	C ^{α2} H r ¹ (17), C ^{α2} H r ² (16), NH ^a ib(10), C ^{α1} H r ² (8), C ^{α1} H r ¹ (7), CCH ₃ r ¹ (7)
1331	1351	20	C ^{α2} H r ¹ (46), C ^{α1} H r ¹ (24), OH b(10)
1384	1371	-13	C ^{α1} H r ¹ (49), C ^{α2} H r ¹ (10)
1384	1388	4	CCH ₃ sd(97)
1401	1403	2	CCH ₃ sd(95)
1459	1452	-7	CCH ₃ ad ^{1,2} (77), CCH ₃ ad ^{1,2} (11), CCH ₃ r ² (7)
1459	1454	-5	CCH ₃ ad ^{1,2} (70), CCH ₃ ad ^{1,2} (10)
1459	1460	1	CCH ₃ ad ^{1,2} (83), CCH ₃ r ¹ (12)
1459	1467	8	CCH ₃ ad ^{1,2} (80), CCH ₃ r ¹ (9), CCH ₃ ad ^{1,2} (7)
1510	1514	4	CNH ₃ sd(18), CO ^H s(16), CO ^a s(14), OH b(12), NH ^a ib(9)
1526	1516	-10	CNH ₃ sd(50), CN ^a s(9), CO ^H s(8), OH b(7), CNH ₃ ad ^{1,2} (7)
1552	1556	4	NH ^a ib(41), CO ^a s(9), CN ^a s(8), CO ^H s(8)
1611	1609	-2	CNH ₃ ad ^{1,2} (50), CNH ₃ sd(26), CNH ₃ ad ^{1,2} (17)
1628	1639	11	CN ^a s(34), CO ^a s(33), CNH ₃ ad ^{1,2} (12)

Table 3.76: (continued)

frequency (cm^{-1})			Potential Energy Distribution
obs.	calc.	dev.	
1641	1648	7	CNH_3 ad ^{1,2} (72), CNH_3 ad ^{1,2} (21)
1731	1730	-1	CO^c s(69), OH b(12), CC^c s(8)
—	2662	—	NH_3 as ¹ (78), NH_3 ss(21)
—	2880	—	NH_3 as ² (99)
—	2937	—	NH_3 ss(78), NH_3 as ¹ (21)
—	2970	—	CH_3 ss(96)
—	2975	—	CH_3 ss(80), CH_3 as ^{1,2} (11), $\text{C}^{\alpha 2}\text{H}$ s(10)
—	2986	—	$\text{C}^{\alpha 2}\text{H}$ s(88), CH_3 ss(12)
—	3004	—	$\text{C}^{\alpha 1}\text{H}$ s(85), CH_3 as ^{1,2} (13)
—	3026	—	CH_3 as ^{1,2} (53), CH_3 as ^{1,2} (34), $\text{C}^{\alpha 1}\text{H}$ s(13)
—	3034	—	CH_3 as ^{1,2} (89), CH_3 ss(8)
—	3039	—	CH_3 as ^{1,2} (62), CH_3 as ^{1,2} (33)
—	3050	—	CH_3 as ^{1,2} (100)
—	3409	—	NH^a s(100)
—	3531	—	OH s(100)

Table 3.77: Scaled 4-31G Frequencies and Potential Energy Distribution for Water-Excluded Alanyl-alanine Two-water Supramolecule in Acid.

frequency (cm ⁻¹)			Ala-Ala pH 1 (mean deviation = 11 cm ⁻¹)
obs.	calc.	dev.	Potential Energy Distribution
—	78	—	NC ^φ t(79), NH ^a ob(24)
—	93	—	C ^ω N t(40), CC ^c t(35), NC ^φ t(10), NH ^a ob(7)
—	98	—	CC ^c t(53), C ^ω N t(11), NH ^a ob(10), CC ^ψ t(9)
—	134	—	CC ^ψ t(78)
—	172	—	CC ^{me} t(32), CNHC sd(18), CO ^a sd(18), C ^{α2} H d ³ (9), CC ^ψ t(9), CC ^{me} t(8)
—	192	—	CC ^{me} t(85)
—	208	—	CC ^{me} t(59), C ^{α2} H d ³ (11), CC ^ψ t(11), CNHC sd(8)
237	229	-8	C ^{α2} H d ² (30), C ^{α1} H d ² (16), CNHC sd(9), CO ^a sd(9)
237	234	-3	C ^{α1} H d ² (23), C ^{α2} H d ³ (16), C ^{α2} H d ² (14), CC ^c sd(10), C ^{α1} H d ³ (7)
—	310	—	C ^{α1} H d ² (20), C ^{α1} H d ³ (14), C ^{α2} H d ² (12), C ^{α2} H d ³ (8)
344	320	-24	CC ^c sd(15), CO ^a sd(14), C ^{α1} H d ¹ (11), C ^{α2} H d ² (9), CC ^c s(8)
372	348	-24	CO ^a r(19), CNHC sd(18), CN ⁿ t(17), C ^{α1} H d ³ (12)
—	423	—	CN ⁿ t(62), C ^{α1} H d ³ (13), CC ^c sd(7)
456	450	-6	C ^{α1} H d ¹ (48), C ^{α2} H d ¹ (17)
456	456	0	C ^{α2} H d ¹ (35), C ^{α1} H d ¹ (14), C ^ω N t(8)
571	563	-8	CC ^c sd(28), CO ^a sd(12), C ^{α2} H d ¹ (10), CC ^ψ s(9), C ^{α2} H d ³ (9)
650	639	-11	CC ^c r(34), CO ^H t(16), CO ^a r(12)
—	663	—	CO ^H t(58), CO ^a r(8), CC ^c r(7)
681	691	10	C ^{α1} H d ³ (17), CC ^c r(16), CC ^ψ s(12), CO ^a ob(12), CO ^H t(7)
749	740	-9	CO ^a ob(44), C ^{α1} H d ² (14), C ^ω N t(8), CO ^a r(7)
—	786	-14	CC ^c ob(45), CO ^H t(18), CC ^{me} s(10)
818	819	1	NH ^a ob(36), C ^ω N t(17), NC ^φ t(11), CC ^c s(7)
834	828	-6	CN ⁿ s(21), NH ^a ob(12), C ^ω N t(7)
876	878	2	CN ⁿ s(26), CC ^c s(13), CC ^{me} s(7), CH ₃ r ² (7), CH ₃ r ¹ (7), CH ₃ r ² (7)
927	923	-4	CH ₃ r ¹ (16), CC ^{me} s(14), CNHC sd(8), CO ^a r(7), CH ₃ r ² (7)
953	948	-5	CNH ₃ r ² (34), CH ₃ r ² (24), CC ^{me} s(19)
953	961	8	CH ₃ r ² (20), CC ^ψ s(15), CNH ₃ r ² (15), CC ^{me} s(11), NC ^φ s(9), CO ^a r(7)
1009	1010	1	CH ₃ r ¹ (31), CNH ₃ r ¹ (26), C ^{α1} H r ² (13), C ^{α1} H r ¹ (10)
1055	1083	28	C ^{α2} H r ² (22), CH ₃ r ² (15), CC ^{me} s(13), CC ^c s(7), C ^{α2} H d ³ (7)

Table 3.77: (continued)

frequency (cm ⁻¹)			Potential Energy Distribution
obs.	calc.	dev.	
1101	1099	-2	CH ₃ r ² (29), CC ^{me} s(18), CN ⁿ s(14), C ^{α1} H d ² (7)
1119	1114	-5	C ^{α1} H r ² (27), CNH ₃ r ² (20), CNH ₃ r ¹ (19)
1140	1134	-6	CC ^{me} s(33), CH ₃ r ¹ (22), NC ^φ s(12), CC ^c ob(7)
1166	1163	-3	NC ^φ s(27), CH ₃ r ² (16), CH ₃ r ¹ (12), C ^{α2} H d ¹ (11), CO ^H s(9)
1239	1230	-9	CH ₃ r ¹ (25), CNH ₃ r ¹ (19), C ^{α1} H d ¹ (12), CH ₃ r ² (7)
1239	1245	6	C ^{α2} H r ² (27), CO ^H s(23), OH b(14), C ^{α2} H r ¹ (9)
1270	1279	9	C ^{α1} H r ² (33), CN ^a s(10), NH ^a ib(10), CH ₃ r ¹ (7)
1295	1290	-5	C ^{α2} H r ² (31), OH b(16), C ^{α2} H r ¹ (12), CH ₃ r ¹ (7)
1295	1310	15	NH ^a ib(21), C ^{α1} H r ¹ (19), CN ^a s(9), C ^{α1} H r ² (8), C ^{α2} H r ¹ (7)
1338	1344	6	C ^{α2} H r ¹ (46), C ^{α1} H r ¹ (18), OH b(12)
1381	1382	1	C ^{α1} H r ¹ (34), CH ₃ sd(9), CC ^ψ s(7), NH ^a ib(7), C ^{α2} H r ¹ (7)
1381	1386	5	CH ₃ sd(91)
1404	1402	-2	CH ₃ sd(86)
1459	1452	-7	CH ₃ ad ^{1,2} (61), CH ₃ ad ^{1,2} (28)
1459	1454	-5	CH ₃ ad ^{1,2} (54), CH ₃ ad ^{1,2} (29)
1459	1461	2	CH ₃ ad ^{1,2} (87), CH ₃ r ¹ (8)
1459	1466	7	CH ₃ ad ^{1,2} (82), CH ₃ r ¹ (10)
1525	1518	-7	CNH ₃ sd(40), CO ^H s(18), OH b(14), CC ^c r(7)
1525	1523	-2	CNH ₃ sd(52), CO ^H s(14), OH b(10)
1564	1570	6	NH ^a ib(50), CN ^a s(23)
1625	1616	-9	CNH ₃ ad ^{1,2} (75), CNH ₃ r ¹ (14)
1625	1633	8	CNH ₃ ad ^{1,2} (65), CO ^a s(18), CN ^a s(7)
1679	1677	-2	CO ^a s(44), CNH ₃ ad ^{1,2} (29), CN ^a s(15)
1726	1730	4	CO ^c s(66), OH b(14), CC ^c s(9)
—	2628	—	C ^{α2} H s(100)
—	2629	—	C ^{α1} H s(99)
—	2707	—	NH ₃ as ¹ (60), NH ₃ ss(39)
—	2923	—	NH ^a s(99)
—	2938	—	CH ₃ ss(90), CH ₃ as ^{1,2} (9)
—	2940	—	CH ₃ ss(93)
—	2990	—	CH ₃ as ^{1,2} (61), CH ₃ as ^{1,2} (35)
—	2996	—	CH ₃ as ^{1,2} (88), CH ₃ as ^{1,2} (7)
—	3013	—	CH ₃ as ^{1,2} (93)
—	3028	—	CH ₃ as ^{1,2} (55), CH ₃ as ^{1,2} (39)

Table 3.77: (continued)

frequency (cm ⁻¹)			Potential Energy Distribution
obs.	calc.	dev.	
—	3029	—	OH s(99)
—	3272	—	NH ₃ ss(60), NH ₃ as ¹ (39)
—	3338	—	NH ₃ as ² (99)

frequency (cm ⁻¹)			Ala-Ala in D ₂ O pD 1 (mean deviation = 13 cm ⁻¹)
obs.	calc.	dev.	
—	75	—	NC ^φ t(76), NH ^a ob(25)
—	92	—	C ^ω N t(43), CC ^c t(27), NC ^φ t(14)
—	97	—	CC ^c t(59), CC ^ψ t(9), NH ^a ob(8), C ^ω N t(8)
—	131	—	CC ^ψ t(81)
—	166	—	CNHC sd(21), CO ^a sd(21), CC ^{me} t(20), C ^{α2} H d ³ (9), CC ^ψ t(9)
—	191	—	CC ^{me} t(86)
—	204	—	CC ^{me} t(72), C ^{α2} H d ³ (7), CC ^ψ t(7)
—	219	—	C ^{α2} H d ³ (19), CN ⁿ t(18), C ^{α2} H d ² (14), C ^{α1} H d ² (10), CC ^c sd(9), C ^{α1} H d ³ (7)
240	227	-13	C ^{α2} H d ² (22), C ^{α1} H d ² (21), CO ^a sd(11), CNHC sd(9)
—	281	—	CN ⁿ t(43), C ^{α2} H d ² (16), C ^{α1} H d ² (7)
335	303	-32	C ^{α1} H d ² (21), CO ^a sd(16), CC ^c sd(12), C ^{α1} H d ³ (11)
335	322	-13	CNHC sd(16), CN ⁿ t(12), CC ^c s(11), C ^{α2} H d ² (8), CO ^a r(8), C ^{α2} H d ³ (7)
376	360	-16	C ^{α1} H d ³ (26), CO ^a r(15), CN ⁿ t(15), C ^{α1} H d ¹ (11), CC ^c sd(8)
435	425	-10	C ^{α1} H d ¹ (53), CC ^c sd(11)
435	430	-5	C ^{α2} H d ¹ (44), C ^ω N t(13), CO ^H t(10), C ^{α1} H d ² (7)
—	503	—	CO ^H t(81)
548	538	-10	CC ^c sd(26), CO ^a sd(11), C ^{α2} H d ¹ (10), C ^{α2} H d ³ (8)
602	602	0	NH ^a ob(33), C ^ω N t(23), NC ^φ t(11)
600	619	19	CC ^c r(31), CO ^a r(17), NH ^a ob(10)
638	645	7	CC ^c r(22), CNH ₃ r ² (13), CC ^ψ s(11), C ^{α1} H d ³ (8)
746	746	0	CO ^a ob(55), C ^{α1} H d ² (11), NH ^a ob(10)
755	764	9	CC ^c ob(31), CC ^{me} s(14), CC ^c s(9), CN ⁿ s(7)
755	773	18	CNH ₃ r ² (37), CNH ₃ r ¹ (17), CC ^{me} s(16), CC ^c ob(9)
803	796	-7	CC ^c ob(17), CN ⁿ s(17), CNH ₃ r ² (15), CO ^a r(9), CC ^c s(7)

Table 3.77: (continued)

frequency (cm ⁻¹)			Potential Energy Distribution
obs.	calc.	dev.	
829	853	24	CC ^c s(15), CN ⁿ s(15), CH ₃ r ² (8), CH ₃ r ¹ (8), CH ₃ r ² (8)
871	881	10	CNH ₃ r ¹ (36), CH ₃ r ¹ (21), CN ⁿ s(11)
920	906	-14	CH ₃ r ¹ (17), CC ^{me} s(15), NC ^φ s(13), CH ₃ r ² (9), NH ^a ib(8)
942	936	-6	CC ^ψ s(14), CH ₃ r ² (12), CH ₃ r ² (11), CO ^a r(10), NH ^a ib(9), CO ^a s(7), NC ^φ s(7)
1003	1024	21	NH ^a ib(53), CH ₃ r ² (10)
1045	1053	8	CC ^{me} s(22), C ^{α1} H r2(21), C ^{α1} H d ³ (7), CN ⁿ s(7)
1067	1067	0	OH b(26), C ^{α2} H r2(12), CH ₃ r ² (11), CC ^{me} s(9)
1098	1095	-3	CH ₃ r ² (35), CC ^{me} s(10), C ^{α1} H d ² (7)
1098	1101	3	OH b(29), CO ^c s(15), CO ^H s(15), C ^{α2} H r2(9)
1119	1135	16	CC ^{me} s(26), CH ₃ r ¹ (17), NC ^φ s(10), CC ^c ob(7)
1152	1152	0	CNH ₃ ad ^{1,2} (69), CNH ₃ sd(22)
1152	1159	7	CNH ₃ sd(58), CNH ₃ ad ^{1,2} (18)
1162	1160	-2	NC ^φ s(17), CH ₃ r ¹ (16), CH ₃ r ² (15), C ^{α2} H d ¹ (12)
1185	1183	-2	CNH ₃ ad ^{1,2} (27), CH ₃ r ¹ (15), NC ^φ s(9), CNH ₃ r ¹ (9), CC ^{me} s(7)
1190	1196	6	CNH ₃ ad ^{1,2} (66), CH ₃ r ¹ (10)
1259	1265	6	C ^{α2} H r2(54), CH ₃ r ¹ (11), CO ^H s(7)
1301	1282	-19	C ^{α1} H r2(49), CH ₃ r ¹ (13)
1314	1320	6	C ^{α2} H r1(51), C ^{α1} H r1(26)
1352	1341	-11	C ^{α1} H r1(52), C ^{α2} H r1(19)
1390	1384	-6	CH ₃ sd(93)
1395	1401	6	CH ₃ sd(96)
1447	1445	-2	CH ₃ ad ^{1,2} (65), CO ^H s(13)
1447	1451	4	CH ₃ ad ^{1,2} (83)
1459	1459	0	CH ₃ ad ^{1,2} (68), CH ₃ ad ^{1,2} (13), CH ₃ r ¹ (7)
1459	1466	7	CH ₃ ad ^{1,2} (84), CH ₃ r ¹ (10)
1481	1476	-5	CO ^H s(21), CH ₃ ad ^{1,2} (16), CC ^c s(12), CH ₃ ad ^{1,2} (11), CC ^c r(8)
1500	1497	-3	CN ^a s(30), CO ^a s(12), CC ^ψ s(10), NH ^a ib(10), NC ^φ s(7)
1670	1657	-13	CO ^a s(62), CN ^a s(24)
1717	1711	-6	CO ^c s(75), CC ^c s(8)
—	1982	—	NH ₃ as ¹ (50), NH ₃ ss(47)
—	2155	—	NH ^a s(97)

Table 3.77: (continued)

frequency (cm ⁻¹)			Potential Energy Distribution
obs.	calc.	dev.	
—	2208	—	OH s(99)
—	2373	—	NH ₃ ss(52), NH ₃ as ¹ (47)
—	2460	—	NH ₃ as ² (99)
—	2628	—	C ^{α2} H s(99)
—	2630	—	C ^{α1} H s(99)
—	2938	—	CH ₃ ss(91), CH ₃ as ^{1,2} (9)
—	2940	—	CH ₃ ss(94)
—	2990	—	CH ₃ as ^{1,2} (61), CH ₃ as ^{1,2} (35)
—	2996	—	CH ₃ as ^{1,2} (88), CH ₃ as ^{1,2} (7)
—	3013	—	CH ₃ as ^{1,2} (94)
—	3028	—	CH ₃ as ^{1,2} (55), CH ₃ as ^{1,2} (39)

frequency (cm ⁻¹)			Potential Energy Distribution
obs.	calc.	dev.	
—	77	—	NC ^φ t(80), NH ^a ob(23)
—	93	—	C ^ω N t(40), CC ^c t(34), NC ^φ t(9), NH ^a ob(7)
—	98	—	CC ^c t(53), C ^ω N t(11), NH ^a ob(10), CC ^ψ t(9)
—	133	—	CC ^ψ t(79)
—	171	—	CC ^{me} t(29), CO ^a sd(19), CNHC sd(18), C ^{α2} H d ³ (9), CC ^ψ t(9), CC ^{me} t(8)
—	192	—	CC ^{me} t(85)
—	207	7	CC ^{me} t(61), C ^{α2} H d ³ (11), CC ^ψ t(10), CNHC sd(7)
243	228	-15	C ^{α2} H d ² (29), C ^{α1} H d ² (16), CNHC sd(10), CO ^a sd(9)
243	234	-9	C ^{α1} H d ² (23), C ^{α2} H d ³ (16), C ^{α2} H d ² (15), CC ^c sd(9), C ^{α1} H d ³ (7)
—	308	—	C ^{α1} H d ² (22), C ^{α1} H d ³ (13), CO ^a sd(10), C ^{α2} H d ² (8), CC ^c sd(8), C ^{α2} H d ³ (7)
363	318	-45	C ^{α2} H d ² (13), CC ^c sd(12), C ^{α1} H d ¹ (11), CO ^a sd(10), CC ^c s(9)
363	348	-15	CO ^a r(20), CNHC sd(18), CN ⁿ t(16), C ^{α1} H d ³ (12)
—	423	—	CN ⁿ t(61), C ^{α1} H d ³ (14), CC ^c sd(7)
451	447	-4	C ^{α1} H d ¹ (57), C ^{α2} H d ¹ (10)
451	454	3	C ^{α2} H d ¹ (42), C ^ω N t(8), C ^{α1} H d ¹ (7), C ^{α1} H d ² (7)

Table 3.77: (continued)

frequency (cm ⁻¹)			Potential Energy Distribution
obs.	calc.	dev.	
572	558	-14	CC ^c sd(29), CO ^a sd(11), CC ^ψ s(10), C ^{α2} H d ¹ (9), C ^{α2} H d ³ (9)
648	637	-11	CC ^c r(33), CO ^a r(16), CO ^H t(11), C ^{α1} H d ³ (8)
648	658	10	CO ^H t(53), C ^{α1} H d ³ (9), CO ^a ob(7), CC ^c ob(7)
677	682	5	CC ^c r(23), CO ^H t(17), CO ^a ob(10), C ^{α1} H d ³ (8), CC ^ψ s(7)
702	724	22	CO ^a ob(30), C ^{α1} H r ₂ (13), C ^{α1} H d ² (12), CH ₃ r ¹ (9), CO ^a r(7)
—	784	—	CC ^c ob(38), CO ^H t(16), CC ^{me} s(9)
748	799	51	C ^{α1} H r ₂ (22), NH ^a ob(13), C ^ω N t(12), CC ^{me} s(12), CC ^c ob(10), CN ⁿ s(7)
816	819	3	NH ^a ob(18), CN ⁿ s(14), CC ^c s(10), C ^ω N t(8), CC ^{me} s(7)
838	852	14	C ^{α1} H r ₂ (15), NH ^a ob(14), CO ^a ob(10)
869	864	-5	C ^{α1} H r ₁ (38), CN ⁿ s(31), CNH ₃ r ¹ (8)
904	914	10	C ^{α1} H r ₁ (15), C ^{α1} H r ₂ (12), CH ₃ r ¹ (11), CNHC sd(9), CO ^a r(7)
933	926	-7	CH ₃ r ² (15), CC ^{me} s(12), NC ^φ s(10), CH ₃ r ¹ (9), CC ^c s(8), C ^{α1} H r ₁ (7)
969	949	-20	CNH ₃ r ² (32), CH ₃ r ² (26), CC ^{me} s(14)
1018	975	-43	CNH ₃ r ² (27), CH ₃ r ² (12), CC ^ψ s(9), CC ^{me} s(9), C ^{α1} H r ₂ (7)
1052	1083	31	C ^{α2} H r ₂ (20), CC ^{me} s(13), CH ₃ r ² (12)
1084	1091	7	CH ₃ r ¹ (22), CH ₃ r ² (13), CNH ₃ r ¹ (11), CC ^{me} s(10)
1107	1130	23	CC ^{me} s(31), CH ₃ r ¹ (18), NC ^φ s(13), CC ^c ob(7)
1149	1152	3	CH ₃ r ¹ (16), CH ₃ r ¹ (12), C ^{α1} H r ₁ (10), CH ₃ r ² (8), C ^{α2} H d ¹ (7), CH ₃ r ² (7)
1178	1170	-8	NC ^φ s(24), CH ₃ r ² (9), CH ₃ r ¹ (8), C ^{α1} H r ₁ (7)
1211	1224	13	CNH ₃ r ¹ (45), CH ₃ r ¹ (16)
1234	1237	3	CNH ₃ r ² (22), CC ^{me} s(18), CH ₃ r ² (12), C ^{α1} H d ¹ (10)
1243	1245	2	C ^{α2} H r ₂ (26), CO ^H s(23), OH b(14), C ^{α2} H r ₁ (9)
1285	1289	4	C ^{α2} H r ₂ (34), OH b(18), C ^{α2} H r ₁ (13), CC ^c s(7), CH ₃ r ¹ (7)
1327	1322	-5	NH ^a ib(32), C ^{α2} H r ₁ (23), CN ^a s(10)
1350	1360	10	C ^{α2} H r ₁ (37), OH b(12), CN ^a s(9), CC ^ψ s(8)
1391	1386	-5	CH ₃ sd(97)
1401	1401	0	CH ₃ sd(93)
1458	1452	-6	CH ₃ ad ^{1,2} (50), CH ₃ ad ^{1,2} (39)
1458	1453	-5	CH ₃ ad ^{1,2} (51), CH ₃ ad ^{1,2} (36)
1458	1461	3	CH ₃ ad ^{1,2} (87), CH ₃ r ¹ (8)

Table 3.77: (continued)

frequency (cm ⁻¹)			Potential Energy Distribution
obs.	calc.	dev.	
1458	1464	6	CH ₃ ad ^{1,2} (84), CH ₃ r ¹ (9)
1509	1518	9	CNH ₃ sd(40), CO ^H s(18), OH b(14), CC ^c r(7)
1521	1523	2	CNH ₃ sd(52), CO ^H s(15), OH b(10)
1559	1570	11	NH ^a ib(50), CN ^a s(23)
1628	1613	-15	CNH ₃ ad ^{1,2} (76), CNH ₃ r ¹ (13)
1628	1632	4	CNH ₃ ad ^{1,2} (62), CO ^a s(20), CN ^a s(7)
1680	1676	-4	CO ^a s(43), CNH ₃ ad ^{1,2} (32), CN ^a s(14)
1730	1730	0	CO ^c s(66), OH b(14), CC ^c s(9)
—	1946	—	C ^{α1} H s(96)
—	2628	—	C ^{α2} H s(100)
—	2706	—	NH ₃ as ¹ (60), NH ₃ ss(39)
—	2923	—	NH ^a s(99)
—	2938	—	CH ₃ ss(90), CH ₃ as ^{1,2} (9)
—	2940	—	CH ₃ ss(93)
—	2990	—	CH ₃ as ^{1,2} (61), CH ₃ as ^{1,2} (35)
—	2996	—	CH ₃ as ^{1,2} (88), CH ₃ as ^{1,2} (7)
—	3013	—	CH ₃ as ^{1,2} (93)
—	3028	—	CH ₃ as ^{1,2} (55), CH ₃ as ^{1,2} (39)
—	3029	—	OH s(99)
—	3272	—	NH ₃ ss(60), NH ₃ as ¹ (39)
—	3338	—	NH ₃ as ² (99)

frequency (cm ⁻¹)			Ala-Ala-13C in amide carbon pH 1 (mean deviation = 14 cm ⁻¹)
obs.	calc.	dev.	Potential Energy Distribution
—	78	—	NC ^φ t(79), NH ^a ob(24)
—	93	—	C ^ω N t(40), CC ^c t(33), NC ^φ t(10), NH ^a ob(7)
—	98	—	CC ^c t(55), C ^ω N t(11), NH ^a ob(9), CC ^ψ t(9)
—	134	—	CC ^ψ t(78)
—	172	—	CC ^{me} t(31), CNHC sd(18), CO ^a sd(18), C ^{α2} H d ³ (9), CC ^ψ t(9), CC ^{me} t(8)
—	192	—	CC ^{me} t(85)
—	208	—	CC ^{me} t(59), C ^{α2} H d ³ (11), CC ^ψ t(11), CNHC sd(8)

Table 3.77: (continued)

frequency (cm ⁻¹)			Potential Energy Distribution
obs.	calc.	dev.	
241	228	-13	C ^{α2} H d ² (30), C ^{α1} H d ² (15), CNHC sd(9), CO ^a sd(9)
241	234	-7	C ^{α1} H d ² (23), C ^{α2} H d ³ (16), C ^{α2} H d ² (14), CC ^c sd(10), C ^{α1} H d ³ (7)
340	309	-31	C ^{α1} H d ² (21), C ^{α1} H d ³ (13), C ^{α2} H d ² (11), C ^{α2} H d ³ (8), CO ^a sd(7)
340	320	-20	CC ^c sd(14), CO ^a sd(13), C ^{α1} H d ¹ (11), C ^{α2} H d ² (10), CC ^c s(8)
368	348	-20	CO ^a r(19), CNHC sd(18), CN ⁿ t(17), C ^{α1} H d ³ (12)
—	423	—	CN ⁿ t(62), C ^{α1} H d ³ (13), CC ^c sd(7)
454	449	-5	C ^{α1} H d ¹ (46), C ^{α2} H d ¹ (19)
454	455	1	C ^{α2} H d ¹ (33), C ^{α1} H d ¹ (16), C ^ω N t(7)
571	562	-9	CC ^c sd(28), CO ^a sd(12), CC ^ψ s(9), C ^{α2} H d ¹ (9), C ^{α2} H d ³ (9)
616	639	23	CC ^c r(34), CO ^H t(15), CO ^a r(13)
—	661	—	CO ^H t(54), C ^{α1} H d ³ (8), CO ^a r(8)
671	686	15	CO ^a ob(18), CC ^c r(17), C ^{α1} H d ³ (12), CO ^H t(11), CC ^ψ s(9)
747	728	-19	CO ^a ob(36), C ^{α1} H d ² (14), CO ^a r(9)
—	785	—	CC ^c ob(45), CO ^H t(18), CC ^{me} s(10)
819	818	-1	NH ^a ob(31), C ^ω N t(15), NC ^φ t(10), CC ^c s(8), CN ⁿ s(7)
833	825	-8	NH ^a ob(18), CN ⁿ s(18), C ^ω N t(10)
872	878	6	CN ⁿ s(25), CC ^c s(13), CC ^{me} s(7), CH ₃ r ² (7), CH ₃ r ¹ (7), CH ₃ r ² (7)
921	922	1	CH ₃ r ¹ (16), CC ^{me} s(13), CNHC sd(8), CO ^a r(8)
951	947	-4	CNH ₃ r ² (26), CH ₃ r ² (25), CC ^{me} s(14), CH ₃ r ² (9), CN ⁿ s(7)
951	957	6	CNH ₃ r ² (23), CH ₃ r ² (17), CC ^{me} s(16), CC ^ψ s(13), NC ^φ s(8)
1005	1009	4	CH ₃ r ¹ (31), CNH ₃ r ¹ (26), C ^{α1} H r ² (13), C ^{α1} H r ¹ (10)
1052	1083	31	C ^{α2} H r ² (22), CH ₃ r ² (14), CC ^{me} s(13), CC ^c s(7), C ^{α2} H d ³ (7)
1102	1097	-5	CH ₃ r ² (30), CC ^{me} s(18), CN ⁿ s(14)
1118	1113	-5	C ^{α1} H r ² (27), CNH ₃ r ² (20), CNH ₃ r ¹ (19)
1141	1132	-9	CC ^{me} s(33), CH ₃ r ¹ (22), NC ^φ s(12), CC ^c ob(7)
1169	1163	-6	NC ^φ s(25), CH ₃ r ² (16), CH ₃ r ¹ (13), C ^{α2} H d ¹ (11), CO ^H s(9)
1247	1230	-17	CH ₃ r ¹ (24), CNH ₃ r ¹ (19), C ^{α1} H d ¹ (12), CH ₃ r ² (7)
1247	1245	-2	C ^{α2} H r ² (27), CO ^H s(23), OH b(13), C ^{α2} H r ¹ (9)
1260	1275	15	C ^{α1} H r ² (27), CN ^a s(15), NH ^a ib(13), CO ^a s(7), CH ₃ r ¹ (7)
1290	1290	0	C ^{α2} H r ² (32), OH b(16), C ^{α2} H r ¹ (12), CC ^c s(7), CH ₃ r ¹ (7)

Table 3.77: (continued)

frequency (cm ⁻¹)			Potential Energy Distribution
obs.	calc.	dev.	
1290	1305	15	C ^α 1H r1(17), NH ^a ib(16), C ^α 1H r2(15), CN ^a s(9)
1331	1343	12	C ^α 2H r1(51), OH b(14), C ^α 1H r1(12)
1384	1377	-7	C ^α 1H r1(44), CC ^ψ s(7)
1384	1386	2	CH ₃ sd(96)
1401	1401	0	CH ₃ sd(91)
1459	1452	-7	CH ₃ ad ^{1,2} (65), CH ₃ ad ^{1,2} (25)
1459	1454	-5	CH ₃ ad ^{1,2} (58), CH ₃ ad ^{1,2} (26)
1459	1461	2	CH ₃ ad ^{1,2} (87), CH ₃ r ¹ (8)
1459	1466	7	CH ₃ ad ^{1,2} (83), CH ₃ r ¹ (10)
1510	1516	6	CNH ₃ sd(30), CO ^H s(20), OH b(16), CC ^c r(8)
1526	1522	-4	CNH ₃ sd(61), CO ^H s(11), OH b(8)
1552	1559	7	NH ^a ib(52), CN ^a s(19)
1611	1607	-4	CO ^a s(40), CNH ₃ ad ^{1,2} (21), CN ^a s(14), CNH ₃ ad ^{1,2} (10)
1628	1618	-10	CNH ₃ ad ^{1,2} (70), CNH ₃ r ¹ (13), CO ^a s(8)
1641	1657	16	CNH ₃ ad ^{1,2} (74), CO ^a s(15)
1731	1730	-1	CO ^c s(67), OH b(14), CC ^c s(9)
—	2628	—	C ^α 2H s(100)
—	2629	—	C ^α 1H s(99)
—	2707	—	NH ₃ as ¹ (60), NH ₃ ss(39)
—	2923	—	NH ^a s(99)
—	2938	—	CH ₃ ss(90), CH ₃ as ^{1,2} (9)
—	2940	—	CH ₃ ss(93)
—	2990	—	CH ₃ as ^{1,2} (61), CH ₃ as ^{1,2} (35)
—	2996	—	CH ₃ as ^{1,2} (88), CH ₃ as ^{1,2} (7)
—	3013	—	CH ₃ as ^{1,2} (93)
—	3028	—	CH ₃ as ^{1,2} (55), CH ₃ as ^{1,2} (39)
—	3029	—	OH s(99)
—	3272	—	NH ₃ ss(60), NH ₃ as ¹ (39)
—	3338	—	NH ₃ as ² (99)

Scale factors for the two-water supermolecule acid and base structures are identical except where affected by the addition of protons (the carboxy terminal stretch and bends and the amine terminal stretch and torsion). The methyl defor-

mations, which are nearly pure modes, were allowed to optimize freely to determine the amount of variation in scale factors expected between structures. All other scale factors were fixed. The isolated structure scale factors for acid and base structures were also identical, except for the same coordinates and the also the NH amide out-of-plane bend (*ob*). Scale factors for all of the non-polar groups remained relatively constant for all structures, isolated and supermolecule, as expected. The scale factors for the zwitterion are not the same as those for the acid and base structures, neither isolated nor two-water water-excluded conformations. However, the non-polar coordinate scale factors remain similar.

Additional supermolecule structures for the basic conformation of dialanine were scaled; two different one-water supermolecules, one with the water hydrogen bonded to the amide hydrogen, the other with the water hydrogen bonded to the carbonyl oxygen, and the three-water supermolecule. scale factors for these three structures are listed in Table 3.78. Observed and calculated frequencies and PED predictions are listed in Tables 3.79, 3.80, and 3.81, respectively. The one-water supermolecule structures can be considered as half “isolated”, half “two-water” structures. Scale factors for the portion of the structure that is “isolated” are similar to those for the isolated molecule while the scale factors for the hydrated portion are similar to the two-water supermolecule scale factors. This consistency in hydration state is also observed in the optimized internal coordinates. The one-water supermolecule structures represent the internal hydrogen bonding observed at the beginning and end of helices where only one part of the peptide bond, either the carbonyl oxygen or the amide hydrogen, participate in hydrogen bond formation. The three-water supermolecule models the observed structure of crystalline tri-alanine [Qian *et al*, 1991] where two hydrogen bonds are formed to the carboxy terminal oxygens. Since the structure of crystalline tri-alanine is well defined, it can be used to test our scale factors. In order to be a valid test, the effects of the additional hydrogen bond had to be determined.

Table 3.78: Water-Excluded Alanyl-alanine One- and Three-water Supermolecule Scale Factors.

Coordinate	1w-H	1w-O	3w
CO ^a s ^a	78.40	83.67	88.20
CN ^a s	91.65	85.60	84.70
CC ^ψ s	83.80	81.48	84.30
NC ^φ s	90.43	91.50	88.90
NH ^a s	81.00	81.00	70.00
C ^{α1} H s	83.60	83.60	83.60
C ^{α2} H s	83.60	83.60	83.60
CC ^c s	97.49	100.50	100.90
CNHC sd	86.00	86.20	72.10
NH ^a ib	72.70	73.20	70.70
NH ^a ob	85.50	69.00	69.00
C ^{α1} H r ¹	80.46	79.40	78.12
C ^{α1} H r ²	72.80	74.62	73.00
C ^{α1} H d ¹	97.85	95.50	96.00
C ^{α1} H d ²	83.43	81.20	81.40
C ^{α1} H d ³	91.67	94.50	94.50
C ^{α2} H r ¹	80.46	79.40	78.12
C ^{α2} H r ²	72.80	74.62	73.00
C ^{α2} H d ¹	97.85	95.50	96.00
C ^{α2} H d ²	83.43	81.20	81.40
C ^{α2} H d ³	91.67	94.50	94.50
CO ^a sd	87.30	74.50	72.00
CO ^a r	90.00	87.42	90.00
CO ^a ob	86.80	76.50	75.70
CC ^c sd	90.33	85.80	88.40
CC ^c r	61.11	55.80	62.00
CC ^c ob	92.60	97.20	92.15
CC ^ψ t	100.00	100.00	100.00
C ^ω N t	72.50	72.50	72.50
NC ^φ t	70.00	70.00	70.00
CO ^c ss	88.60	91.20	88.60
CO ^c as	77.10	77.10	76.60
CN ⁿ s	87.50	86.80	86.00
NH ₂ ss	70.00	77.00	77.00

Table 3.78: (continued)

Coordinate	1w-H	1w-O	3w
NH ₂ as	70.00	70.00	70.00
NH ₂ sis	74.55	71.59	72.00
NH ₂ r	76.80	81.70	79.40
NH ₂ w	164.80	154.70	161.70
CN ⁿ t	230.00	100.00	100.00
CC ^c t	100.00	100.00	100.00
CC ^{me} s	92.30	91.70	93.50
CH ₃ ss	84.89	84.89	85.90
CH ₃ as ^{1,2}	84.60	84.60	84.75
CH ₃ as ^{1,2}	84.60	84.60	84.75
CH ₃ sd	76.00	76.72	76.18
CH ₃ ad ^{1,2}	76.60	76.97	76.89
CH ₃ ad ^{1,2}	76.60	76.97	76.89
CH ₃ r ¹	82.30	82.30	82.60
CH ₃ r ²	75.27	75.80	76.10
CC ^{me} t	50.00	50.00	50.00
CC ^{me} s	92.30	91.70	93.50
CH ₃ ss	84.89	84.89	85.90
CH ₃ as ^{1,2}	84.60	84.60	84.75
CH ₃ as ^{1,2}	84.60	84.60	84.75
CH ₃ sd	76.00	76.72	76.18
CH ₃ ad ^{1,2}	76.60	76.97	76.89
CH ₃ ad ^{1,2}	76.60	76.97	76.89
CH ₃ r ¹	82.30	82.30	82.60
CH ₃ r ²	75.27	75.80	76.10
CC ^{me} t	50.00	50.00	50.00

^aAbbreviations: s = stretch, t = torsion, ss = symmetric stretch, as = antisymmetric stretch, d = deformation, sd = symmetric deformation, ad = antisymmetric deformation, r = rock, ib = in plane bend, ob = out of plane bend, sis = scissor, w = wag.

Table 3.79: Scaled 4-31G Frequencies and Potential Energy Distribution for Water-Excluded Alanyl-alanine One-water Supermolecule, the Water Hydrogen Bonded to the Amide Hydrogen in Base.

frequency (cm ⁻¹)			Ala-ala pH 13 (mean deviation = 11 cm ⁻¹)
obs.	calc.	dev.	
			Potential Energy Distribution
—	46	—	CC ^ψ t(56), NC ^φ t(27), CC ^c t(18)
—	80	—	C ^ω N t(49), NC ^φ t(41)
—	82	—	CC ^ψ t(44), CC ^c t(33), C ^ω N t(9)
—	126	—	CC ^c t(41), NH ^a ob(25), NC ^φ t(9)
—	156	—	CNHC sd(41), CO ^a sd(19), C ^{α2} H d ³ (13), CC ^c t(8)
—	195	—	CC ^{me} t(92)
—	202	—	CC ^{me} t(92)
245	245	0	C ^{α1} H d ² (40), CO ^a sd(16), CO ^a ob(9), C ^{α2} H d ¹ (7)
245	247	2	C ^{α2} H d ² (33), CC ^c r(24), C ^{α2} H d ³ (17)
—	316	—	C ^{α2} H d ² (32), C ^{α1} H d ² (10), CO ^a sd(9), C ^{α2} H d ³ (8), CC ^c r(8), CC ^c ob(7)
334	321	-13	CN ⁿ t(15), C ^{α1} H d ¹ (13), C ^{α1} H d ² (11), CC ^c r(11), CO ^a sd(10)
334	344	10	CN ⁿ t(36), C ^{α1} H d ³ (15), CO ^a r(14)
377	388	11	CN ⁿ t(29), C ^{α1} H d ³ (25), CC ^c r(13), CO ^a r(12)
464	457	-7	C ^{α2} H d ¹ (46), C ^ω N t(8), C ^{α1} H d ² (7)
464	474	10	C ^{α1} H d ¹ (57), CN ⁿ t(9)
545	571	26	C ^{α2} H d ³ (18), CC ^c r(17), C ^{α2} H d ¹ (14), CO ^a sd(13), CC ^ψ s(9)
642	650	8	CC ^c sd(38), CC ^c s(20), CO ^a r(12)
688	699	11	CC ^ψ s(23), C ^{α1} H d ³ (19), CO ^a r(14)
761	752	-9	CO ^a ob(27), NH ^a ob(17), C ^ω N t(16), NC ^φ t(11), C ^{α1} H d ² (7)
778	784	6	CC ^c ob(37), CO ^a ob(17), C ^{α2} H d ² (7), CH ₃ r ¹ (7)
—	811	—	NH ^a ob(37), CO ^a ob(15), CC ^c ob(15), C ^ω N t(7), NC ^φ t(7)
872	857	-15	CC ^c sd(16), CN ⁿ s(14), CC ^{me} s(11), NH ₂ w(9), CC ^c s(7), CO ^c ss(7)
884	890	6	CC ^c s(12), CN ⁿ s(11), NH ₂ w(11), CC ^{me} s(11), CC ^c sd(10), CO ^c ss(7), CC ^{me} s(7), CH ₃ r ¹ (7)
920	935	15	CC ^{me} s(21), CH ₃ r ¹ (12), CC ^c s(9), CH ₃ r ² (9), NC ^φ s(8)
952	955	3	CH ₃ r ² (20), CC ^ψ s(15), CO ^a r(12), CH ₃ r ² (12), NC ^φ s(9)
980	986	6	NH ₂ w(54), CH ₃ r ¹ (14), CC ^{me} s(12), CH ₃ r ² (11)
1019	1012	-7	CH ₃ r ² (35), NH ₂ r(20), CC ^{me} s(16), CN ⁿ s(10)
1069	1069	0	C ^{α2} H r ² (29), CH ₃ r ² (18), CC ^c ob(10)

Table 3.79: (continued)

frequency (cm ⁻¹)			Potential Energy Distribution
obs.	calc.	dev.	
1104	1104	0	CH ₃ r ¹ (25), CC ^{me} s(19), C ^{α1} H r ² (11), C ^{α1} H d ² (10), CO ^a ob(9), CN ⁿ s(8)
1136	1140	4	CC ^{me} s(38), CH ₃ r ¹ (19), NC ^φ s(14)
1136	1154	18	NH ₂ r(28), C ^{α1} H r ² (21), CC ^{me} s(7)
1166	1167	1	NC ^φ s(21), CH ₃ r ² (13), NH ₂ r(9), CH ₃ r ¹ (9), C ^{α2} H d ¹ (8)
1220	1224	4	CN ⁿ s(29), NH ₂ w(8), NC ^φ s(7), NH ^a ib(7), C ^{α1} H d ¹ (7), CH ₃ r ² (7)
1260	1232	-28	NH ^a ib(24), C ^{α2} H r ² (22), CO ^a s(7), CN ⁿ s(7)
1281	1299	18	C ^{α2} H r ² (23), NH ^a ib(18), CN ^a s(8), C ^{α1} H r ² (7)
1320	1322	2	C ^{α1} H r ² (35), C ^{α1} H r ¹ (22), CH ₃ r ¹ (10), NH ₂ r(7)
1335	1348	13	C ^{α2} H r ¹ (69), C ^{α1} H r ¹ (7)
1367	1357	-10	CH ₃ sd(86)
1367	1376	9	CH ₃ sd(78), C ^{α1} H r ¹ (12)
1407	1380	-27	C ^{α1} H r ¹ (31), CH ₃ sd(17), NH ^a ib(9), NH ₂ r(9)
1407	1410	3	CO ^c ss(46), CC ^c s(15), CC ^c sd(9), CO ^c as(7), CH ₃ ad ^{1,2} (7)
1459	1451	-8	CH ₃ ad ^{1,2} (77), CH ₃ ad ^{1,2} (10)
1459	1454	-5	CH ₃ ad ^{1,2} (60), CH ₃ ad ^{1,2} (15), CH ₃ ad ^{1,2} (10)
1459	1460	1	CH ₃ ad ^{1,2} (74), CH ₃ ad ^{1,2} (17)
1459	1467	8	CH ₃ ad ^{1,2} (87), CH ₃ r ¹ (8)
1542	1544	2	NH ^a ib(33), CN ^a s(25), CO ^a s(13), CC ^ψ s(7)
1578	1571	-7	NH ₂ sis(82), CO ^a s(7), CN ^a s(7)
1602	1600	-2	CO ^c as(80), CO ^c ss(7)
1638	1651	13	CO ^a s(44), CN ^a s(26), NH ₂ sis(15)
—	2920	—	CH ₃ ss(89), CH ₃ as ^{1,2} (11)
—	2927	—	C ^{α1} H s(95)
—	2936	—	CH ₃ ss(84), CH ₃ as ^{1,2} (13)
—	2952	—	C ^{α2} H s(93)
—	2974	—	CH ₃ as ^{1,2} (61), CH ₃ as ^{1,2} (31)
—	2999	—	CH ₃ as ^{1,2} (80), CH ₃ ss(9), CH ₃ as ^{1,2} (7)
—	3026	—	CH ₃ as ^{1,2} (93)
—	3028	—	CH ₃ as ^{1,2} (58), CH ₃ as ^{1,2} (35), CH ₃ ss(7)
—	3149	—	NH ₂ ss(99)
—	3247	—	NH ₂ as(100)
—	3446	—	NH ^a s(100)

Table 3.79: (continued)

frequency (cm ⁻¹)			Potential Energy Distribution
obs.	calc.	dev.	

frequency (cm ⁻¹)			Ala-ala pD 13 (mean deviation = 11 cm ⁻¹) Potential Energy Distribution
obs.	calc.	dev.	
—	45	—	CC ^ψ t(58), NC ^φ t(26), CC ^c t(16)
—	79	—	NC ^φ t(50), CC ^ψ t(26), C ^ω N t(17)
—	80	—	C ^ω N t(42), CC ^c t(28), CC ^ψ t(18), NH ^a ob(7)
—	124	—	CC ^c t(43), NH ^a ob(23), NC ^φ t(8)
—	153	—	CNHC sd(41), CO ^a sd(19), C ^{α2} H d ³ (11), CC ^c t(9)
—	195	—	CC ^{me} t(92)
—	201	—	CC ^{me} t(91)
225	239	14	C ^{α1} H d ² (22), CN ⁿ t(19), CO ^a sd(13), CC ^c r(10), C ^{α2} H d ³ (7)
251	245	-6	C ^{α2} H d ² (30), CC ^c r(18), C ^{α2} H d ³ (14)
251	264	13	CN ⁿ t(62), C ^{α1} H d ² (19)
—	311	—	C ^{α2} H d ² (32), C ^{α1} H d ² (12), C ^{α1} H d ³ (11), CO ^a sd(8), C ^{α2} H d ³ (7), CC ^c ob(7)
332	327	-5	CO ^a sd(15), CC ^c r(13), CC ^c s(10), NC ^φ s(8), CO ^a r(8)
380	355	-25	C ^{α1} H d ³ (34), CO ^a r(18), CC ^c r(11), CNHC sd(10), C ^{α1} H d ¹ (7)
447	434	-13	C ^{α2} H d ¹ (33), C ^ω N t(14), CC ^c r(9), C ^{α1} H d ¹ (8)
447	448	1	C ^{α1} H d ¹ (46), C ^{α2} H d ¹ (14)
534	546	12	C ^{α2} H d ³ (18), CC ^c r(17), CO ^a sd(13), NH ^a ob(7)
—	599	—	NH ^a ob(45), C ^{α2} H d ¹ (12), NC ^φ t(12), C ^ω N t(11)
645	638	-7	CO ^a r(24), CC ^c sd(18), CC ^c s(11), C ^{α1} H d ³ (10), NH ₂ r(10), CC ^ψ s(7)
687	668	-19	CC ^c sd(27), CC ^ψ s(19), CC ^c s(10), NH ₂ r(10), CC ^c ob(7)
760	744	-16	NH ₂ w(77)
778	780	2	CO ^a ob(56), C ^{α1} H d ² (8)
778	786	8	CC ^c ob(52), C ^{α2} H d ² (8), CC ^c sd(8)
866	861	-5	CC ^c sd(17), NH ₂ r(10), CC ^{me} s(9), NC ^φ s(8), CC ^c s(8), CH ₃ r ¹ (8), CO ^a r(7), CO ^c ss(7)
884	877	-7	NH ₂ r(41), CC ^{me} s(20), CH ₃ r ¹ (12)
904	905	1	CC ^{me} s(12), CN ⁿ s(10), CH ₃ r ¹ (9), CH ₃ r ² (8), CC ^c s(7)

Table 3.79: (continued)

frequency (cm ⁻¹)			Potential Energy Distribution
obs.	calc.	dev.	
904	910	6	NH ^a ib(23), CC ^c s(14), CC ^{me} s(10), CH ₃ r ² (10), NC ^φ s(9), CH ₃ r ¹ (8), CO ^c ss(7)
938	943	5	CH ₃ r ² (28), CN ⁿ s(15), CO ^a s(10), CC ^ψ s(9)
995	997	2	NH ^a ib(42), CH ₃ r ² (22), CC ^ψ s(7), CH ₃ r ² (7)
1066	1070	4	C ^{α2} H r ² (25), CH ₃ r ² (10), CC ^c ob(8)
1066	1076	10	C ^{α1} H r ² (21), CH ₃ r ² (13), C ^{α2} H r ² (8)
1097	1095	-2	CC ^{me} s(33), NH ₂ sis(21), CH ₃ r ¹ (14), CN ⁿ s(9)
1113	1136	23	CC ^{me} s(36), NC ^φ s(17), CH ₃ r ¹ (14)
1163	1158	-5	CH ₃ r ¹ (20), CH ₃ r ² (16), NC ^φ s(14), C ^{α2} H d ¹ (14)
1163	1178	15	NH ₂ sis(58), CH ₃ r ¹ (12)
1209	1208	-1	CN ⁿ s(37), NH ₂ sis(14), C ^{α1} H r ¹ (11), CH ₃ r ² (7)
1278	1272	-6	C ^{α2} H r ² (47), CH ₃ r ¹ (10)
1308	1304	-4	C ^{α1} H r ² (58), CH ₃ r ¹ (10)
1328	1346	18	C ^{α2} H r ¹ (66), C ^{α1} H r ¹ (13)
1360	1352	-8	C ^{α1} H r ¹ (59), CH ₃ sd(8), C ^{α2} H r ¹ (7)
1365	1358	-7	CH ₃ sd(80), C ^{α2} H r ¹ (7)
1371	1376	5	CH ₃ sd(94)
1409	1409	0	CO ^c ss(49), CC ^c s(16), CC ^c sd(9), CO ^c as(8)
1455	1449	-6	CH ₃ ad ^{1,2} (85)
1455	1454	-1	CH ₃ ad ^{1,2} (67), CH ₃ ad ^{1,2} (16)
1455	1460	5	CH ₃ ad ^{1,2} (74), CH ₃ ad ^{1,2} (17)
1455	1465	10	CH ₃ ad ^{1,2} (88), CH ₃ r ¹ (8)
1512	1500	-12	CN ^a s(31), CO ^a s(20), CC ^ψ s(12), NH ^a ib(9), NC ^φ s(8), CO ^a r(8)
1596	1598	2	CO ^c as(82), CO ^c ss(8)
1638	1635	-3	CO ^a s(51), CN ^a s(32)
—	2274	—	NH ₂ ss(99)
—	2400	—	NH ₂ as(100)
—	2528	—	NH ^a s(98)
—	2920	—	CH ₃ ss(89), CH ₃ as ^{1,2} (11)
—	2927	—	C ^{α1} H s(95)
—	2936	—	CH ₃ ss(84), CH ₃ as ^{1,2} (13)
—	2952	—	C ^{α2} H s(93)
—	2974	—	CH ₃ as ^{1,2} (61), CH ₃ as ^{1,2} (31)

Table 3.79: (continued)

frequency (cm ⁻¹)			Potential Energy Distribution
obs.	calc.	dev.	
—	2999	—	CH ₃ as ^{1,2} (80), CH ₃ ss(9), CH ₃ as ^{1,2} (7)
—	3026	—	CH ₃ as ^{1,2} (93)
—	3028	—	CH ₃ as ^{1,2} (58), CH ₃ as ^{1,2} (35), CH ₃ ss(7)

frequency (cm ⁻¹)			Potential Energy Distribution
obs.	calc.	dev.	
—	46	—	CC ^ψ t(57), NC ^φ t(27), CC ^c t(17)
—	80	—	C ^ω N t(56), NC ^φ t(31)
—	81	—	CC ^ψ t(48), CC ^c t(30), NC ^φ t(10)
—	126	—	CC ^c t(40), NH ^a ob(25), NC ^φ t(9)
—	156	—	CNHC sd(40), CO ^a sd(19), C ^{α2} H d ³ (12), CC ^c t(9)
—	195	—	CC ^{me} t(92)
—	202	—	CC ^{me} t(92)
251	245	-6	C ^{α1} H d ² (40), CO ^a sd(16), CO ^a ob(9), C ^{α2} H d ¹ (7)
251	247	-4	C ^{α2} H d ² (33), CC ^c r(23), C ^{α2} H d ³ (17)
—	314	—	C ^{α2} H d ² (25), C ^{α1} H d ² (15), CO ^a sd(15), CC ^c r(13)
337	320	-17	C ^{α1} H d ¹ (12), CN ⁿ t(12), C ^{α2} H d ² (10), CC ^c s(9)
337	343	6	CN ⁿ t(40), C ^{α1} H d ³ (14), CO ^a r(13)
387	387	0	CN ⁿ t(28), C ^{α1} H d ³ (26), CC ^c r(13), CO ^a r(12)
460	456	-4	C ^{α2} H d ¹ (45), C ^ω N t(8)
460	471	11	C ^{α1} H d ¹ (57), CN ⁿ t(9)
534	564	30	CC ^c r(18), C ^{α2} H d ³ (17), C ^{α2} H d ¹ (14), CC ^ψ s(11), CO ^a sd(11)
640	649	9	CC ^c sd(36), CC ^c s(19), CO ^a r(13)
678	686	8	CC ^ψ s(22), C ^{α1} H d ³ (17), CO ^a r(11), CO ^a ob(7)
743	739	-4	CO ^a ob(34), C ^{α1} H r ² (17), C ^{α1} H d ² (9), C ^ω N t(9), CH ₃ r ¹ (9)
778	772	-6	NH ^a ob(26), CC ^c ob(19), C ^{α1} H r ² (11), NC ^φ t(8), C ^ω N t(7)
—	797	—	CC ^c ob(36), NH ^a ob(17), C ^{α1} H r ² (7)
829	840	11	CC ^{me} s(29), CN ⁿ s(11), NH ^a ob(10), C ^{α1} H r ² (8)
866	871	5	CC ^c sd(19), CC ^c s(13), CC ^{me} s(12), CO ^c ss(10), C ^{α1} H r ² (7), CH ₃ r ¹ (7)
909	919	10	C ^{α1} H r ² (16), NH ₂ w(15), CO ^a ob(12), CH ₃ r ² (10), CC ^c s(7)
909	930	21	C ^{α1} H r ¹ (45), NH ₂ w(14), CN ⁿ s(13)

Table 3.79: (continued)

frequency (cm ⁻¹)			Potential Energy Distribution
obs.	calc.	dev.	
927	937	10	CC ^{me} s(18), CH ₃ r ¹ (11), C ^{α1} H r ¹ (10), CH ₃ r ² (8), NC ^φ s(7), CC ^c s(7)
944	962	18	CH ₃ r ² (17), CH ₃ r ² (15), CC ^ψ s(10), C ^{α1} H r ¹ (10), CO ^a r(8), NH ₂ w(7)
981	1001	20	CH ₃ r ² (40), NH ₂ w(31), CN ⁿ s(10)
1065	1068	3	CC ^{me} s(24), NH ₂ r(22), C ^{α1} H r ¹ (13), C ^{α1} H r ² (10), NH ₂ w(9)
1101	1069	-32	C ^{α2} H r ² (27), CH ₃ r ² (18), CC ^c ob(10)
1132	1113	-19	CH ₃ r ¹ (45), CC ^{me} s(15), CN ⁿ s(9), C ^{α1} H d ² (8)
1154	1141	-13	CC ^{me} s(37), CH ₃ r ¹ (23), NC ^φ s(10), C ^{α2} H d ¹ (7)
1195	1167	-28	NC ^φ s(29), CH ₃ r ² (17), CH ₃ r ¹ (11), C ^{α2} H d ¹ (10)
1239	1228	-11	NH ^a ib(28), C ^{α2} H r ² (24)
1239	1243	4	CN ⁿ s(25), NH ₂ r(16), CH ₃ r ¹ (12), C ^{α1} H d ³ (9)
1273	1281	8	NH ₂ r(23), C ^{α2} H r ² (16), CH ₃ r ² (7)
1304	1322	18	NH ^a ib(21), C ^{α2} H r ² (14), C ^{α2} H r ¹ (13), NH ₂ r(10), CC ^ψ s(8)
1343	1352	9	C ^{α2} H r ¹ (48), CH ₃ sd(19), CO ^c ss(9)
1369	1358	-11	CH ₃ sd(71), C ^{α2} H r ¹ (17)
1369	1377	8	CH ₃ sd(94)
1408	1409	1	CO ^c ss(49), CC ^c s(16), CC ^c sd(9), CO ^c as(8)
1458	1449	-9	CH ₃ ad ^{1,2} (89)
1458	1453	-5	CH ₃ ad ^{1,2} (68), CH ₃ ad ^{1,2} (16)
1458	1460	2	CH ₃ ad ^{1,2} (74), CH ₃ ad ^{1,2} (17)
1458	1465	7	CH ₃ ad ^{1,2} (89), CH ₃ r ¹ (7)
1544	1543	-1	NH ^a ib(33), CN ^a s(25), CO ^a s(13), CC ^ψ s(7)
1583	1569	-14	NH ₂ sis(81), CN ^a s(8), CO ^a s(7)
1605	1600	-5	CO ^c as(80), CO ^c ss(7)
1644	1647	3	CO ^a s(45), CN ^a s(25), NH ₂ sis(16)
—	2160	—	C ^{α1} H s(98)
—	2921	—	CH ₃ ss(90), CH ₃ as ^{1,2} (11)
—	2936	—	CH ₃ ss(84), CH ₃ as ^{1,2} (13)
—	2952	—	C ^{α2} H s(93)
—	2972	—	CH ₃ as ^{1,2} (66), CH ₃ as ^{1,2} (31)
—	2999	—	CH ₃ as ^{1,2} (80), CH ₃ ss(9), CH ₃ as ^{1,2} (7)
—	3026	—	CH ₃ as ^{1,2} (93)
—	3027	—	CH ₃ as ^{1,2} (59), CH ₃ as ^{1,2} (35), CH ₃ ss(7)

Table 3.79: (continued)

frequency (cm ⁻¹)			Potential Energy Distribution
obs.	calc.	dev.	
—	3149	—	NH ₂ ss(99)
—	3247	—	NH ₂ as(100)
—	3446	—	NH ^a s(100)

frequency (cm ⁻¹)			Ala-1- ¹³ C-Ala pH 13 (mean deviation = 12 cm ⁻¹)
obs.	calc.	dev.	
			Potential Energy Distribution
—	46	—	CC ^ψ t(56), NC ^φ t(27), CC ^c t(18)
—	80	—	C ^ω N t(49), NC ^φ t(41)
—	82	—	CC ^ψ t(44), CC ^c t(33), C ^ω N t(9)
—	126	—	CC ^c t(41), NH ^a ob(25), NC ^φ t(9)
—	156	—	CNHC sd(41), CO ^a sd(19), C ^{α2} H d ³ (12), CC ^c t(8)
—	195	—	CC ^{me} t(92)
—	202	—	CC ^{me} t(92)
236	245	9	C ^{α1} H d ² (39), CO ^a sd(15), CO ^a ob(9), C ^{α2} H d ¹ (7)
236	247	11	C ^{α2} H d ² (33), CC ^c r(22), C ^{α2} H d ³ (16)
—	315	—	C ^{α2} H d ² (31), C ^{α1} H d ² (11), CO ^a sd(11), CC ^c r(9), C ^{α2} H d ³ (8), CC ^c ob(7)
334	321	-13	CN ⁿ t(14), C ^{α1} H d ¹ (12), C ^{α1} H d ² (9), CO ^a sd(9), CC ^c r(9), CC ^c s(7)
334	344	10	CN ⁿ t(36), C ^{α1} H d ³ (15), CO ^a r(14)
376	388	12	CN ⁿ t(29), C ^{α1} H d ³ (25), CC ^c r(13), CO ^a r(12)
467	457	-10	C ^{α2} H d ¹ (46), C ^ω N t(8), C ^{α1} H d ² (7)
467	473	6	C ^{α1} H d ¹ (57), CN ⁿ t(9)
542	570	28	C ^{α2} H d ³ (18), CC ^c r(17), C ^{α2} H d ¹ (13), CO ^a sd(13), CC ^ψ s(9)
644	649	5	CC ^c sd(37), CC ^c s(20), CO ^a r(13)
687	696	9	CC ^ψ s(22), C ^{α1} H d ³ (18), CO ^a r(12), CO ^a ob(9)
748	743	-5	CO ^a ob(36), C ^ω N t(13), C ^{α1} H d ² (10), NH ^a ob(9), NC ^φ t(8)
778	779	1	CC ^c ob(34), NH ^a ob(11), CO ^a ob(11), C ^{α2} H d ² (8), CH ₃ r ¹ (7)
—	808	—	NH ^a ob(37), CC ^c ob(21), CO ^a ob(8), C ^ω N t(8), NC ^φ t(7)
850	854	4	CC ^c sd(15), CN ⁿ s(14), CC ^{me} s(12), NH ₂ w(8), NC ^φ s(7)
883	890	7	CC ^c s(12), CN ⁿ s(11), NH ₂ w(11), CC ^{me} s(11), CC ^c sd(10), CO ^c ss(8), CC ^{me} s(7), CH ₃ r ¹ (7)

Table 3.79: (continued)

frequency (cm ⁻¹)			Potential Energy Distribution
obs.	calc.	dev.	
920	934	14	CC ^{me} s(20), CH ₃ r ¹ (12), CC ^c s(8), CNHC sd(7), CO ^a r(7), CH ₃ r ² (7)
943	949	6	CH ₃ r ² (22), CC ^ψ s(14), CH ₃ r ² (11), NC ^φ s(10), CO ^a r(10)
980	986	6	NH ₂ w(54), CH ₃ r ¹ (14), CC ^{me} s(12), CH ₃ r ² (10)
1021	1011	-10	CH ₃ r ² (37), NH ₂ r(19), CC ^{me} s(15), CN ⁿ s(10)
1066	1069	3	C ^{α2} H r ² (29), CH ₃ r ² (18), CC ^c ob(10)
1103	1101	-2	CH ₃ r ¹ (25), CC ^{me} s(20), C ^{α1} H r ² (11), C ^{α1} H d ² (10), CO ^a ob(8), CN ⁿ s(8)
1129	1139	10	CC ^{me} s(37), CH ₃ r ¹ (17), NC ^φ s(15)
1129	1154	25	NH ₂ r(26), C ^{α1} H r ² (20), CH ₃ r ¹ (8)
1166	1166	0	NC ^φ s(18), CH ₃ r ² (13), NH ₂ r(11), CH ₃ r ¹ (9), C ^{α2} H d ¹ (8)
1221	1224	3	CN ⁿ s(27), NH ^a ib(9), C ^{α2} H r ² (8), NH ₂ w(8), NC ^φ s(7), CH ₃ r ² (7)
1256	1229	-27	NH ^a ib(24), C ^{α2} H r ² (18), CN ⁿ s(10), CO ^a s(8)
1279	1294	15	C ^{α2} H r ² (25), NH ^a ib(15), CN ^a s(9), CH ₃ r ¹ (7)
1321	1321	0	C ^{α1} H r ² (36), C ^{α1} H r ¹ (21), CH ₃ r ¹ (10), NH ₂ r(8)
1327	1347	20	C ^{α2} H r ¹ (72)
1368	1357	-11	CH ₃ sd(87)
1368	1376	8	CH ₃ sd(62), C ^{α1} H r ¹ (20)
1408	1379	-29	CH ₃ sd(33), C ^{α1} H r ¹ (25), NH ₂ r(8)
1408	1409	1	CO ^c ss(48), CC ^c s(15), CC ^c sd(9), CO ^c as(7)
1458	1450	-8	CH ₃ ad ^{1,2} (69), CH ₃ ad ^{1,2} (16)
1458	1453	-5	CH ₃ ad ^{1,2} (53), CH ₃ ad ^{1,2} (17), CH ₃ ad ^{1,2} (14)
1458	1460	2	CH ₃ ad ^{1,2} (73), CH ₃ ad ^{1,2} (18)
1458	1467	9	CH ₃ ad ^{1,2} (87), CH ₃ r ¹ (8)
1522	1526	4	NH ^a ib(38), CN ^a s(20), CO ^a s(15), NC ^φ s(7)
1560	1560	0	NH ₂ sis(58), CO ^a s(18), CN ^a s(16)
1594	1600	6	CO ^c as(75), CO ^c ss(7)
1610	1619	9	NH ₂ sis(35), CO ^a s(29), CN ^a s(17)
—	2920	—	CH ₃ ss(89), CH ₃ as ^{1,2} (11)
—	2927	—	C ^{α1} H s(95)
—	2936	—	CH ₃ ss(84), CH ₃ as ^{1,2} (13)
—	2952	—	C ^{α2} H s(93)
—	2974	—	CH ₃ as ^{1,2} (61), CH ₃ as ^{1,2} (31)

Table 3.79: (continued)

frequency (cm ⁻¹)			Potential Energy Distribution
obs.	calc.	dev.	
—	2999	—	CH ₃ as ^{1,2} (80), CH ₃ ss(9), CH ₃ as ^{1,2} (7)
—	3026	—	CH ₃ as ^{1,2} (93)
—	3028	—	CH ₃ as ^{1,2} (58), CH ₃ as ^{1,2} (35), CH ₃ ss(7)
—	3149	—	NH ₂ ss(99)
—	3247	—	NH ₂ as(100)
—	3446	—	NH ^a s(100)

Table 3.80: Scaled 4-31G Frequencies and Potential Energy Distribution for Water-Excluded Alanyl-alanine One-water Supermolecule, The Water Hydrogen Bonded to the Carbonyl Oxygen, in Base.

frequency (cm ⁻¹)			Ala-ala pH 13 (mean deviation = 13 cm ⁻¹)
obs.	calc.	dev.	
			Potential Energy Distribution
—	52	—	NC ^φ t(38), CC ^ψ t(32), NH ^a ob(14), CC ^c t(10)
—	75	—	CC ^c t(67), C ^ω N t(23), CC ^ψ t(19)
—	94	—	C ^ω N t(37), NC ^φ t(27), NH ^a ob(7), CC ^c t(7)
—	124	—	CC ^ψ t(25), NC ^φ t(17), CNHC sd(15), NH ^a ob(12), CO ^a sd(9), C ^{α2} H d ³ (8)
—	142	—	CO ^a sd(20), CNHC sd(17), CC ^ψ t(15), C ^{α2} H d ³ (14), CC ^c t(10), NH ^a ob(7)
—	189	—	CC ^{me} t(95)
—	196	—	CC ^{me} t(90)
245	241	-4	C ^{α2} H d ² (25), C ^{α1} H d ² (19), CNHC sd(10), C ^{α2} H d ¹ (9)
245	262	17	C ^{α2} H d ² (26), C ^{α1} H d ² (18), C ^{α1} H d ³ (14), CO ^a ob(9), CC ^c r(9)
—	286	—	C ^{α1} H d ² (20), CC ^c r(19), CN ⁿ t(15), CO ^a sd(13), CO ^a r(8)
334	314	-20	C ^{α1} H d ³ (15), CN ⁿ t(12), C ^{α2} H d ² (11), CC ^c s(9), CC ^ψ s(7)
334	336	2	CN ⁿ t(50), CC ^c r(16), C ^{α2} H d ² (7)
377	353	-24	CO ^a r(24), C ^{α1} H d ³ (20), CNHC sd(14), CN ⁿ t(11), CC ^c r(8)
464	437	-27	C ^{α2} H d ¹ (31), CC ^c r(11), C ^{α2} H d ³ (9), C ^{α1} H d ¹ (7), C ^ω N t(7)
464	467	3	C ^{α1} H d ¹ (47), C ^{α2} H d ¹ (14)
545	572	27	C ^{α2} H d ¹ (19), CO ^a sd(17), C ^{α2} H d ³ (15), CC ^c r(14), CC ^ψ s(8)
642	647	5	CC ^c sd(42), CC ^c s(19), CO ^a r(11)
688	701	13	CC ^ψ s(20), CO ^a r(16), C ^{α1} H d ³ (13), CH ₃ r ¹ (9), C ^{α1} H d ² (8)
761	760	-1	CO ^a ob(43), C ^ω N t(11), NC ^φ t(8), C ^{α1} H d ³ (7), CC ^c ob(7)
778	784	6	CC ^c ob(27), CO ^a ob(17), NH ^a ob(11), CC ^c sd(8)
—	815	—	NH ^a ob(38), CC ^c ob(22), C ^ω N t(12), NC ^φ t(11)
872	853	-19	CC ^c sd(16), CC ^c s(14), CC ^{me} s(12), CN ⁿ s(10), CO ^c ss(8)
884	888	4	CC ^{me} s(18), CN ⁿ s(16), CC ^c s(11), NH ₂ w(8), CH ₃ r ² (7)
920	931	11	CC ^{me} s(23), CH ₃ r ¹ (13), NC ^φ s(11), CC ^c s(10), CH ₃ r ² (10)
952	953	1	CC ^ψ s(17), CH ₃ r ² (16), CO ^a r(15), CH ₃ r ² (10), NC ^φ s(8), NH ₂ w(8)
980	971	-9	NH ₂ w(59), CH ₃ r ² (26)
1019	1014	-5	CH ₃ r ² (21), CH ₃ r ¹ (20), NH ₂ r(15), CN ⁿ s(13), C ^{α1} H r ² (8), CC ^{me} s(8)

Table 3.80: (continued)

frequency (cm ⁻¹)			Potential Energy Distribution
obs.	calc.	dev.	
1069	1063	-6	C ^{α2} H r ² (27), CH ₃ r ² (20), CC ^c ob(11), CH ₃ r ¹ (7)
1104	1095	-9	CC ^{me} s(40), CH ₃ r ¹ (21), CN ⁿ s(19)
1136	1138	2	CC ^{me} s(28), CH ₃ r ¹ (13), NC ^φ s(11)
1136	1140	4	NH ₂ r(22), C ^{α1} H r ² (19), C ^{α1} H r ¹ (15), CC ^{me} s(10)
1166	1157	-9	NC ^φ s(20), CH ₃ r ¹ (18), CH ₃ r ² (17), C ^{α2} H d ¹ (12), C ^{α2} H r ¹ (8)
1220	1224	4	NH ^a ib(27), C ^{α2} H r ² (27)
1260	1249	-11	NH ₂ r(19), CN ⁿ s(17), C ^{α1} H d ¹ (9), NH ₂ w(9), CH ₃ r ² (7)
1281	1301	20	C ^{α1} H r ² (33), CH ₃ r ¹ (10), C ^{α2} H r ² (7), NH ₂ r(7)
1320	1323	3	C ^{α1} H r ¹ (17), C ^{α2} H r ² (16), NH ^a ib(14), C ^{α1} H r ² (14)
1335	1337	2	C ^{α2} H r ¹ (67)
1367	1361	-6	CH ₃ sd(86), CO ^c ss(8)
1367	1374	7	CH ₃ sd(97)
1407	1399	-8	C ^{α1} H r ¹ (34), CO ^c ss(16), NH ₂ r(13), NH ^a ib(7)
1407	1408	1	CO ^c ss(41), CC ^c s(11), C ^{α1} H r ¹ (9), CC ^c sd(7), CH ₃ sd(7)
1459	1452	-7	CH ₃ ad ^{1,2} (51), CH ₃ ad ^{1,2} (39)
1459	1457	-2	CH ₃ ad ^{1,2} (47), CH ₃ ad ^{1,2} (24), CH ₃ ad ^{1,2} (14)
1459	1460	1	CH ₃ ad ^{1,2} (36), CH ₃ ad ^{1,2} (29), CH ₃ ad ^{1,2} (14)
1459	1463	4	CH ₃ ad ^{1,2} (53), CH ₃ ad ^{1,2} (36)
1542	1541	-1	NH ^a ib(26), CO ^a s(20), CN ^a s(20), CC ^ψ s(8)
1578	1572	-6	NH ₂ sis(85), CN ^a s(8)
1602	1600	-2	CO ^c as(83)
1638	1644	6	CO ^a s(45), CN ^a s(32)
—	2927	—	CH ₃ ss(94)
—	2937	—	CH ₃ ss(87), CH ₃ as ^{1,2} (10)
—	2950	—	C ^{α1} H s(51), C ^{α2} H s(43)
—	2950	—	C ^{α2} H s(50), C ^{α1} H s(43)
—	2981	—	CH ₃ as ^{1,2} (97)
—	2997	—	CH ₃ as ^{1,2} (78), CH ₃ as ^{1,2} (12)
—	3008	—	CH ₃ as ^{1,2} (93)
—	3026	—	CH ₃ as ^{1,2} (88), CH ₃ as ^{1,2} (10)
—	3234	—	NH ₂ as(98)
—	3294	—	NH ₂ ss(98)
—	3342	—	NH ^a s(99)

Table 3.80: (continued)

frequency (cm ⁻¹)			Potential Energy Distribution
obs.	calc.	dev.	
frequency (cm ⁻¹)			Ala-ala pD 13 (mean deviation = 15 cm ⁻¹)
obs.	calc.	dev.	Potential Energy Distribution
—	51	—	NC ^φ t(37), CC ^ψ t(33), NH ^a ob(14), CC ^c t(8)
—	74	—	CC ^c t(66), C ^ω N t(24), CC ^ψ t(20)
—	94	—	C ^ω N t(36), NC ^φ t(28), NH ^a ob(7), CC ^c t(7)
—	121	—	CC ^ψ t(21), NC ^φ t(18), CNHC sd(15), NH ^a ob(11), CO ^a sd(11), C ^{α2} H d ³ (7)
—	140	—	CO ^a sd(19), CC ^ψ t(17), CNHC sd(16), C ^{α2} H d ³ (13), CC ^c t(11)
—	189	—	CC ^{me} t(95)
—	195	—	CC ^{me} t(90)
225	224	-1	CN ⁿ t(69)
251	242	-9	C ^{α2} H d ² (30), C ^{α1} H d ² (13), CNHC sd(9)
251	262	11	C ^{α1} H d ² (31), C ^{α2} H d ² (17), CO ^a ob(11), C ^{α1} H d ³ (10), CN ⁿ t(8)
—	296	—	CC ^c r(31), CO ^a sd(21), C ^{α1} H d ² (9), CN ⁿ t(8)
332	310	-22	C ^{α1} H d ³ (23), C ^{α2} H d ² (19), C ^{α2} H d ³ (8), CC ^ψ s(7), C ^{α1} H d ¹ (7)
380	345	-35	CO ^a r(23), CNHC sd(20), CC ^c r(15), C ^{α1} H d ³ (11), C ^{α2} H d ³ (7)
447	422	-25	C ^{α2} H d ¹ (28), CC ^c r(13), C ^ω N t(12), C ^{α1} H d ¹ (9), C ^{α2} H d ³ (8)
447	446	-1	C ^{α1} H d ¹ (44), C ^{α2} H d ¹ (15)
534	549	15	CO ^a sd(16), C ^{α2} H d ³ (15), CC ^c r(14), C ^{α2} H d ¹ (10), CC ^ψ s(7), NH ^a ob(7), C ^ω N t(7)
—	604	—	NH ^a ob(45), NC ^φ t(15), C ^{α2} H d ¹ (11), C ^ω N t(10)
645	634	-11	CO ^a r(22), CC ^c sd(17), NH ₂ r(14), CC ^c s(10), C ^{α1} H d ³ (9), CC ^ψ s(7)
687	663	-24	CC ^c sd(31), CC ^ψ s(15), CC ^c s(10), NH ₂ r(10)
760	756	-4	NH ₂ w(64), CO ^a ob(15)
778	769	-9	CO ^a ob(47), NH ₂ w(16), CC ^{me} s(11), C ^{α1} H d ² (7)
778	790	12	CC ^c ob(57), CC ^c sd(10), C ^{α2} H d ² (7), CC ^{me} s(7)
866	850	-16	CC ^c sd(14), CC ^c s(11), CO ^a r(9), NC ^φ s(7), CO ^c ss(7), CN ⁿ s(7), CH ₃ r ¹ (7)

Table 3.80: (continued)

frequency (cm ⁻¹)			Potential Energy Distribution
obs.	calc.	dev.	
884	889	5	CC ^{me} s(17), CH ₃ r ¹ (15), CC ^c s(11), CN ⁿ s(9), CH ₃ r ² (7)
904	892	-12	NH ₂ r(32), CH ₃ r ¹ (13), NH ^a ib(10), CC ^{me} s(7)
904	913	9	CC ^{me} s(18), NH ^a ib(15), CH ₃ r ¹ (13), NC ^φ s(11), CC ^c s(9), CH ₃ r ² (7)
938	938	0	CH ₃ r ² (26), CN ⁿ s(15), NH ^a ib(10), CO ^a s(8), NH ₂ r(7)
995	987	-8	NH ^a ib(36), CH ₃ r ² (21), CC ^ψ s(11), CH ₃ r ² (9), NC ^φ s(7)
1066	1061	-5	CC ^{me} s(40), CN ⁿ s(12), NH ₂ sis(12), C ^{α1} H d ³ (7), NH ₂ r(7)
1066	1072	6	C ^{α2} H r ² (34), CH ₃ r ² (13), CC ^c ob(11)
1097	1087	-10	C ^{α1} H r ² (18), CH ₃ r ² (17), CH ₃ r ¹ (15), C ^{α1} H d ² (9), CO ^a s(7), NH ₂ sis(7)
1113	1135	22	CC ^{me} s(35), NC ^φ s(21), CH ₃ r ¹ (10)
1163	1153	-10	CH ₃ r ¹ (25), C ^{α2} H d ¹ (15), CH ₃ r ² (15), NC ^φ s(10)
1163	1178	15	NH ₂ sis(74), CN ⁿ s(12)
1209	1196	-13	CN ⁿ s(21), CH ₃ r ¹ (14), C ^{α1} H d ¹ (12), CH ₃ r ² (9), NC ^φ s(8), C ^{α1} H r ¹ (8)
1278	1276	-2	C ^{α2} H r ² (38), C ^{α2} H r ¹ (11), CO ^c ss(7), CH ₃ r ¹ (7)
1308	1308	0	C ^{α1} H r ² (59), CH ₃ r ¹ (11), C ^{α1} H r ¹ (7)
1328	1335	7	C ^{α2} H r ¹ (71), C ^{α2} H r ² (12)
1360	1360	0	C ^{α1} H r ¹ (44), CH ₃ sd(31)
1365	1362	-3	CH ₃ sd(56), C ^{α1} H r ¹ (27)
1371	1373	2	CH ₃ sd(98)
1409	1407	-2	CO ^c ss(55), CC ^c s(13), CC ^c sd(10), CH ₃ sd(10)
1455	1452	-3	CH ₃ ad ^{1,2} (71), CH ₃ ad ^{1,2} (19)
1455	1456	1	CH ₃ ad ^{1,2} (56), CH ₃ ad ^{1,2} (17), CH ₃ ad ^{1,2} (12)
1455	1458	3	CH ₃ ad ^{1,2} (36), CH ₃ ad ^{1,2} (32), CH ₃ ad ^{1,2} (15)
1455	1463	8	CH ₃ ad ^{1,2} (54), CH ₃ ad ^{1,2} (35)
1512	1507	-5	CN ^a s(28), CO ^a s(25), CC ^ψ s(13), NH ^a ib(8), NC ^φ s(7), CO ^a r(7)
1596	1596	0	CO ^c as(87)
1638	1636	-2	CO ^a s(47), CN ^a s(36)
—	2376	—	NH ₂ ss(91), NH ₂ as(8)
—	2394	—	NH ₂ as(91), NH ₂ ss(8)
—	2453	—	NH ^a s(98)
—	2927	—	CH ₃ ss(94)

Table 3.80: (continued)

frequency (cm ⁻¹)			Potential Energy Distribution
obs.	calc.	dev.	
—	2937	—	CH ₃ ss(87), CH ₃ as ^{1,2} (10)
—	2950	—	C ^{α2} H s(72), C ^{α1} H s(21)
—	2951	—	C ^{α1} H s(73), C ^{α2} H s(21)
—	2981	—	CH ₃ as ^{1,2} (97)
—	2997	—	CH ₃ as ^{1,2} (78), CH ₃ as ^{1,2} (12)
—	3008	—	CH ₃ as ^{1,2} (93)
—	3026	—	CH ₃ as ^{1,2} (88), CH ₃ as ^{1,2} (10)

frequency (cm ⁻¹)			Potential Energy Distribution
obs.	calc.	dev.	
—	52	—	NC ^φ t(38), CC ^ψ t(33), NH ^a ob(14), CC ^c t(9)
—	75	—	CC ^c t(67), C ^ω N t(23), CC ^ψ t(19)
—	94	—	C ^ω N t(37), NC ^φ t(27), NH ^a ob(8), CC ^c t(7)
—	123	—	CC ^ψ t(23), NC ^φ t(17), CNHC sd(15), NH ^a ob(11), CO ^a sd(10), C ^{α2} H d ³ (8)
—	141	—	CO ^a sd(20), CNHC sd(16), CC ^ψ t(16), C ^{α2} H d ³ (13), CC ^c t(11), NH ^a ob(7)
—	189	—	CC ^{me} t(96)
—	195	—	CC ^{me} t(90)
251	241	-10	C ^{α2} H d ² (24), C ^{α1} H d ² (19), CNHC sd(10), C ^{α2} H d ¹ (9)
251	261	10	C ^{α2} H d ² (27), C ^{α1} H d ² (17), C ^{α1} H d ³ (14), CC ^c r(10), CO ^a ob(9)
—	285	—	C ^{α1} H d ² (21), CC ^c r(19), CO ^a sd(13), CN ⁿ t(13), CO ^a r(7)
337	313	-24	C ^{α1} H d ³ (15), CN ⁿ t(14), C ^{α2} H d ² (11), CC ^c s(9), CC ^ψ s(7)
337	335	-2	CN ⁿ t(51), CC ^c r(13), C ^{α2} H d ² (7)
387	353	-34	CO ^a r(24), C ^{α1} H d ³ (20), CNHC sd(14), CC ^c r(9), CN ⁿ t(9)
460	436	-24	C ^{α2} H d ¹ (30), CC ^c r(12), C ^{α2} H d ³ (9), C ^{α1} H d ¹ (8), C ^ω N t(7)
460	464	4	C ^{α1} H d ¹ (48), C ^{α2} H d ¹ (13)
534	567	33	C ^{α2} H d ¹ (20), CO ^a sd(16), C ^{α2} H d ³ (15), CC ^c r(14), CC ^ψ s(8)
640	646	6	CC ^c sd(41), CC ^c s(19), CO ^a r(12)
678	692	14	CC ^ψ s(20), CO ^a r(14), C ^{α1} H d ³ (13), CH ₃ r ¹ (9), C ^{α1} H d ² (7), CC ^c sd(7)
743	755	12	CO ^a ob(49), C ^{α1} H d ³ (8), C ^ω N t(8)

Table 3.80: (continued)

frequency (cm ⁻¹)			Potential Energy Distribution
obs.	calc.	dev.	
778	780	2	CC ^c ob(24), NH ^a ob(19), CO ^a ob(7), CC ^c sd(7)
—	806	—	CC ^c ob(24), NH ^a ob(18), C ^{α1} H r ² (14), CC ^{me} s(9), C ^ω N t(8)
829	830	1	CC ^{me} s(29), C ^{α1} H r ² (19), NH ^a ob(17)
866	857	-9	CC ^c sd(18), CC ^c s(17), CO ^c ss(10), CH ₃ r ¹ (9), CC ^{me} s(8), CC ^ψ s(7), C ^{α1} H r ² (7)
909	903	-6	C ^{α1} H r ¹ (63), NH ₂ r(7)
909	911	2	CN ⁿ s(23), NH ₂ w(17), CH ₃ r ² (10), C ^{α1} H r ² (9), CC ^c s(8)
927	933	6	CC ^{me} s(23), CH ₃ r ¹ (14), NC ^φ s(7), CNHC sd(7), CO ^a sd(7), CO ^a r(7)
944	959	15	NH ₂ w(19), CH ₃ r ² (13), CH ₃ r ² (12), CO ^a r(11), CC ^ψ s(10), NC ^φ s(7)
981	979	-2	CH ₃ r ² (43), NH ₂ w(39), CN ⁿ s(7)
1065	1064	-1	C ^{α2} H r ² (27), CH ₃ r ² (20), CC ^c ob(11), CH ₃ r ¹ (7)
1101	1087	-14	CH ₃ r ¹ (42), CC ^{me} s(21), CN ⁿ s(11), NH ₂ r(7)
1132	1122	-10	CC ^{me} s(21), C ^{α1} H r ² (12), C ^{α1} H r ¹ (9), NH ₂ r(8)
1154	1142	-12	CC ^{me} s(33), CH ₃ r ¹ (22), NC ^φ s(7), C ^{α2} H d ¹ (7)
1195	1160	-35	NC ^φ s(25), CH ₃ r ² (16), CH ₃ r ¹ (12), C ^{α2} H d ¹ (10), C ^{α2} H r ¹ (7)
1239	1224	-15	NH ^a ib(26), C ^{α2} H r ² (26)
1239	1243	4	NH ₂ r(20), CN ⁿ s(19), CH ₃ r ¹ (12), NH ₂ w(8), C ^{α1} H d ¹ (7)
1273	1284	11	NH ₂ r(32), C ^{α2} H r ² (8)
1304	1330	26	C ^{α2} H r ¹ (41), C ^{α2} H r ² (22), CH ₃ r ¹ (9), NH ^a ib(8)
1343	1348	5	C ^{α2} H r ¹ (28), NH ^a ib(22), CC ^ψ s(9), CO ^c ss(7)
1369	1361	-8	CH ₃ sd(84)
1369	1374	5	CH ₃ sd(96)
1408	1406	-2	CO ^c ss(56), CC ^c s(13), CH ₃ sd(10), CC ^c sd(9)
1458	1451	-7	CH ₃ ad ^{1,2} (59), CH ₃ ad ^{1,2} (34)
1458	1456	-2	CH ₃ ad ^{1,2} (34), CH ₃ ad ^{1,2} (27), CH ₃ ad ^{1,2} (19), CH ₃ ad ^{1,2} (11)
1458	1458	0	CH ₃ ad ^{1,2} (28), CH ₃ ad ^{1,2} (23), CH ₃ ad ^{1,2} (23), CH ₃ ad ^{1,2} (15)
1458	1463	5	CH ₃ ad ^{1,2} (57), CH ₃ ad ^{1,2} (34)
1544	1540	-4	NH ^a ib(26), CO ^a s(20), CN ^a s(20), CC ^ψ s(8), NH ₂ sis(7)
1583	1571	-12	NH ₂ sis(83), CN ^a s(9)
1605	1600	-5	CO ^c as(82)
1644	1638	-6	CO ^a s(47), CN ^a s(31), NH ₂ sis(7)
—	2178	—	C ^{α1} H s(98)

Table 3.80: (continued)

frequency (cm ⁻¹)			Potential Energy Distribution
obs.	calc.	dev.	
—	2927	—	CH ₃ ss(96)
—	2937	—	CH ₃ ss(87), CH ₃ as ^{1,2} (10)
—	2950	—	C ^{α2} H s(93)
—	2981	—	CH ₃ as ^{1,2} (97)
—	2997	—	CH ₃ as ^{1,2} (78), CH ₃ as ^{1,2} (12)
—	3006	—	CH ₃ as ^{1,2} (96)
—	3026	—	CH ₃ as ^{1,2} (88), CH ₃ as ^{1,2} (10)
—	3233	—	NH ₂ as(98)
—	3294	—	NH ₂ ss(98)
—	3342	—	NH ^a s(99)

frequency (cm ⁻¹)			Ala-1- ¹³ C-Ala pH 13 (mean deviation = 14 cm ⁻¹)
obs.	calc.	dev.	
—	52	—	NC ^φ t(37), CC ^ψ t(32), NH ^a ob(14), CC ^c t(9)
—	75	—	CC ^c t(67), C ^ω N t(23), CC ^ψ t(19)
—	94	—	C ^ω N t(37), NC ^φ t(27), NH ^a ob(7), CC ^c t(7)
—	124	—	CC ^ψ t(24), NC ^φ t(17), CNHC sd(15), NH ^a ob(12), CO ^a sd(10), C ^{α2} H d ³ (8)
—	141	—	CO ^a sd(20), CNHC sd(17), CC ^ψ t(15), C ^{α2} H d ³ (13), CC ^c t(10), NH ^a ob(7)
—	189	—	CC ^{me} t(95)
—	196	—	CC ^{me} t(90)
236	241	5	C ^{α2} H d ² (25), C ^{α1} H d ² (19), CNHC sd(10), C ^{α2} H d ¹ (9)
236	261	25	C ^{α2} H d ² (26), C ^{α1} H d ² (18), C ^{α1} H d ³ (14), CC ^c r(10), CO ^a ob(9)
—	286	—	C ^{α1} H d ² (21), CC ^c r(18), CN ⁿ t(14), CO ^a sd(13), CO ^a r(7)
334	314	-20	C ^{α1} H d ³ (15), C ^{α2} H d ² (11), CN ⁿ t(11), CC ^c s(10), CC ^ψ s(7)
334	336	2	CN ⁿ t(51), CC ^c r(15), C ^{α2} H d ² (7)
376	353	-23	CO ^a r(24), C ^{α1} H d ³ (20), CNHC sd(14), CN ⁿ t(11), CC ^c r(8)
467	436	-31	C ^{α2} H d ¹ (30), CC ^c r(12), C ^{α2} H d ³ (9), C ^{α1} H d ¹ (7), C ^ω N t(7)
467	467	0	C ^{α1} H d ¹ (47), C ^{α2} H d ¹ (14)
542	572	30	C ^{α2} H d ¹ (18), CO ^a sd(17), C ^{α2} H d ³ (15), CC ^c r(14), CC ^ψ s(8)
644	646	2	CC ^c sd(42), CC ^c s(19), CO ^a r(11)

Table 3.80: (continued)

frequency (cm ⁻¹)			Potential Energy Distribution
obs.	calc.	dev.	
687	700	13	CC ^ψ s(19), CO ^a r(16), C ^{α1} H d ³ (12), C ^{α1} H d ² (9), CH ₃ r ¹ (9)
748	743	-5	CO ^a ob(56), C ^{α1} H d ³ (10), C ^ω N t(7)
778	781	3	CC ^c ob(30), NH ^a ob(17), CC ^c sd(9), CC ^{me} s(7)
—	814	—	NH ^a ob(37), CC ^c ob(24), C ^ω N t(12), NC ^φ t(11)
850	851	1	CC ^c sd(15), CC ^{me} s(13), CC ^c s(12), CN ⁿ s(10), CO ^c ss(8)
883	887	4	CC ^{me} s(17), CN ⁿ s(14), CC ^c s(12), CC ^c sd(7), NH ₂ w(7), CH ₃ r ² (7)
920	931	11	CC ^{me} s(23), CH ₃ r ¹ (13), NC ^φ s(10), CC ^c s(9), CH ₃ r ² (9)
943	946	3	CC ^ψ s(17), CH ₃ r ² (16), CO ^a r(13), CH ₃ r ² (10), NC ^φ s(8), NH ₂ w(7)
980	971	-9	NH ₂ w(60), CH ₃ r ² (26)
1021	1013	-8	CH ₃ r ¹ (21), CH ₃ r ² (21), NH ₂ r(15), CN ⁿ s(13), C ^{α1} H r ² (8), CC ^{me} s(7)
1066	1063	-3	C ^{α2} H r ² (27), CH ₃ r ² (20), CC ^c ob(11), CH ₃ r ¹ (7)
1103	1093	-10	CC ^{me} s(41), CN ⁿ s(20), CH ₃ r ¹ (20)
1129	1137	8	CC ^{me} s(34), NC ^φ s(16), CH ₃ r ¹ (14)
1129	1139	10	NH ₂ r(27), C ^{α1} H r ² (22), C ^{α1} H r ¹ (19), CH ₃ r ² (7)
1166	1155	-11	CH ₃ r ¹ (22), CH ₃ r ² (17), NC ^φ s(16), C ^{α2} H d ¹ (13), C ^{α2} H r ¹ (7)
1221	1223	2	NH ^a ib(28), C ^{α2} H r ² (26), NC ^φ s(7)
1256	1249	-7	NH ₂ r(19), CN ⁿ s(18), C ^{α1} H d ¹ (10), NH ₂ w(10), CH ₃ r ² (7)
1279	1298	19	C ^{α1} H r ² (27), C ^{α2} H r ² (10), CH ₃ r ¹ (8), NH ^a ib(7)
1321	1320	-1	C ^{α1} H r ¹ (21), C ^{α1} H r ² (20), NH ^a ib(12), C ^{α2} H r ² (11)
1327	1336	9	C ^{α2} H r ¹ (71), C ^{α2} H r ² (9)
1368	1361	-7	CH ₃ sd(86), CO ^c ss(8)
1368	1374	6	CH ₃ sd(97)
1408	1398	-10	C ^{α1} H r ¹ (36), CO ^c ss(14), NH ₂ r(14), CH ₃ ad ^{1,2} (7)
1408	1408	0	CO ^c ss(43), CC ^c s(11), C ^{α1} H r ¹ (8), CC ^c sd(8), CH ₃ sd(8)
1458	1452	-6	CH ₃ ad ^{1,2} (51), CH ₃ ad ^{1,2} (38)
1458	1456	-2	CH ₃ ad ^{1,2} (49), CH ₃ ad ^{1,2} (24), CH ₃ ad ^{1,2} (12)
1458	1460	2	CH ₃ ad ^{1,2} (37), CH ₃ ad ^{1,2} (29), CH ₃ ad ^{1,2} (13)
1458	1463	5	CH ₃ ad ^{1,2} (53), CH ₃ ad ^{1,2} (35)
1522	1522	0	NH ^a ib(32), CO ^a s(22), CN ^a s(17), CC ^ψ s(7)
1560	1567	7	NH ₂ sis(71), CN ^a s(14)
1594	1597	3	CO ^c as(55), CO ^a s(11), NH ₂ sis(11), CN ^a s(10)

Table 3.80: (continued)

frequency (cm^{-1})			Potential Energy Distribution
obs.	calc.	dev.	
1610	1610	0	CO^c as(31), CO^a s(26), CN^a s(17), NH_2 sis(12)
—	2927	—	CH_3 ss(94)
—	2937	—	CH_3 ss(87), CH_3 as ^{1,2} (10)
—	2950	—	$\text{C}^{\alpha 1}\text{H}$ s(52), $\text{C}^{\alpha 2}\text{H}$ s(42)
—	2950	—	$\text{C}^{\alpha 2}\text{H}$ s(51), $\text{C}^{\alpha 1}\text{H}$ s(42)
—	2981	—	CH_3 as ^{1,2} (97)
—	2997	—	CH_3 as ^{1,2} (78), CH_3 as ^{1,2} (12)
—	3008	—	CH_3 as ^{1,2} (93)
—	3026	—	CH_3 as ^{1,2} (88), CH_3 as ^{1,2} (10)
—	3234	—	NH_2 as(98)
—	3294	—	NH_2 ss(98)
—	3342	—	NH^a s(99)

Table 3.81: Scaled 4-31G Frequencies and Potential Energy Distribution for Water-Excluded Alanyl-alanine Three-water Supermolecule, Two Waters Hydrogen Bonded to the Carbonyl Oxygen, in Base.

frequency (cm ⁻¹)			Ala-Ala pH 13 (mean deviation = 12 cm ⁻¹)
obs.	calc.	dev.	Potential Energy Distribution
—	57	—	CC ^c t(33), NC ^φ t(31), CC ^ψ t(16), NH ^a ob(10)
—	96	—	CC ^c t(41), CC ^ψ t(23), C ^ω N t(23), NC ^φ t(11)
—	109	—	C ^ω N t(27), CC ^c t(19), NH ^a ob(13), NC ^φ t(13), CO ^a ob(9), C ^{α1} H d ² (7)
—	149	—	CC ^ψ t(44), NC ^φ t(24), NH ^a ob(19), C ^{α2} H d ¹ (7), CC ^c t(7)
—	169	—	CNHC sd(41), C ^{α2} H d ³ (19), CO ^a sd(16), CC ^{me} t(11), CC ^c r(10)
—	188	—	CC ^{me} t(91)
—	200	—	CC ^{me} t(83)
245	245	0	C ^{α2} H d ² (34), CNHC sd(7), CC ^c r(7)
245	264	19	C ^{α1} H d ² (19), C ^{α1} H d ³ (18), CO ^a sd(12), CO ^a ob(10), CC ^c r(8), CN ⁿ t(8)
—	295	—	C ^{α1} H d ² (29), CN ⁿ t(16), CO ^a sd(13), CC ^c r(9)
334	316	-18	C ^{α2} H d ² (13), CC ^c s(9), CO ^a sd(9), CC ^c r(9), CN ⁿ t(9), C ^{α1} H d ¹ (8), C ^{α1} H d ³ (8), NC ^φ s(7)
334	326	-8	CN ⁿ t(32), CC ^c r(15), C ^{α2} H d ² (12), CNHC sd(8), C ^{α2} H d ³ (7)
377	348	-29	CN ⁿ t(26), C ^{α1} H d ³ (24), CO ^a r(18)
464	451	-13	C ^{α2} H d ¹ (29), C ^{α2} H d ³ (11), CC ^c r(11), C ^{α1} H d ¹ (10)
464	469	5	C ^{α1} H d ¹ (43), C ^{α2} H d ¹ (19)
545	567	22	C ^{α2} H d ¹ (16), CO ^a sd(16), CC ^c r(16), C ^{α2} H d ³ (15), CC ^ψ s(7)
642	650	8	CC ^c sd(40), CC ^c s(17), CO ^a r(13)
688	704	16	CC ^ψ s(18), CO ^a r(16), C ^{α1} H d ³ (11), CC ^c sd(9), CH ₃ r ¹ (8), C ^{α1} H d ² (7)
761	757	-4	CO ^a ob(37), C ^ω N t(16), CC ^c ob(9), NH ^a ob(7), C ^{α1} H d ³ (7), NC ^φ t(7)
778	783	5	CC ^c ob(42), CO ^a ob(15), C ^{α2} H d ² (7), CC ^c sd(7)
—	821	—	NH ^a ob(43), C ^ω N t(14), CO ^a ob(11), NC ^φ t(11), CC ^c ob(9)
872	860	-12	CC ^c sd(15), CC ^{me} s(15), CN ⁿ s(13), CC ^c s(8), CC ^{me} s(8), NC ^φ s(7), CO ^c ss(7)
884	891	7	CN ⁿ s(15), CC ^{me} s(14), CC ^c s(9), CC ^{me} s(9), CH ₃ r ¹ (8), CC ^c sd(7), NH ₂ w(7)

Table 3.81: (continued)

frequency (cm ⁻¹)			Potential Energy Distribution
obs.	calc.	dev.	
920	927	7	CC ^{me} s(13), CC ^c s(10), CH ₃ r ¹ (10), CH ₃ r ² (9), NC ^φ s(7), CO ^a r(7)
952	955	3	CH ₃ r ² (22), CC ^ψ s(13), NC ^φ s(12), NH ₂ w(12), CO ^a r(10)
980	975	-5	NH ₂ w(50), CH ₃ r ² (35)
1019	1015	-4	CH ₃ r ¹ (25), NH ₂ r(20), CH ₃ r ² (14), CN ⁿ s(12), C ^{α1} H r ² (7)
1069	1065	-4	C ^{α2} H r ² (31), CH ₃ r ² (17), CC ^c ob(9), CH ₃ r ¹ (8)
1104	1098	-6	CC ^{me} s(44), CN ⁿ s(18), CH ₃ r ¹ (16)
1136	1134	-2	CC ^{me} s(34), NC ^φ s(17), CH ₃ r ¹ (12)
1136	1142	6	NH ₂ r(21), C ^{α1} H r ² (19), C ^{α1} H r ¹ (14), CC ^ψ s(7), CH ₃ r ² (7)
1166	1160	-6	NC ^φ s(20), CH ₃ r ¹ (20), CH ₃ r ² (18), C ^{α2} H d ¹ (13), C ^{α2} H r ¹ (7)
1220	1230	10	NH ^a ib(21), C ^{α2} H r ² (14), CN ⁿ s(9), CN ^a s(7)
1260	1247	-13	NH ₂ r(17), C ^{α2} H r ² (15), CN ⁿ s(9), NH ^a ib(7)
1281	1289	8	C ^{α1} H r ² (20), C ^{α2} H r ² (16), NH ^a ib(13), CN ^a s(7)
1320	1317	-3	C ^{α1} H r ² (28), C ^{α1} H r ¹ (20), C ^{α2} H r ¹ (10), NH ^a ib(9), C ^{α2} H r ² (8), CH ₃ r ¹ (7)
1335	1333	-2	C ^{α2} H r ¹ (64), C ^{α1} H r ¹ (10)
1367	1364	-3	CH ₃ sd(87), CO ^c ss(7)
1367	1371	4	CH ₃ sd(97)
1407	1397	-10	C ^{α1} H r ¹ (31), CO ^c ss(17), NH ₂ r(10), NH ^a ib(9), CH ₃ ad ^{1,2} (7)
1407	1412	5	CO ^c ss(34), CC ^c s(12), C ^{α1} H r ¹ (10), CH ₃ ad ^{1,2} (7)
1459	1452	-7	CH ₃ ad ^{1,2} (68), CH ₃ ad ^{1,2} (18)
1459	1457	-2	CH ₃ ad ^{1,2} (59), CH ₃ ad ^{1,2} (20), CH ₃ ad ^{1,2} (8)
1459	1461	2	CH ₃ ad ^{1,2} (59), CH ₃ ad ^{1,2} (15), CH ₃ ad ^{1,2} (7)
1459	1462	3	CH ₃ ad ^{1,2} (73)
1542	1554	12	NH ^a ib(27), CN ^a s(22), CO ^a s(13), NH ₂ sis(12), CC ^ψ s(8)
1578	1574	-4	NH ₂ sis(79), CN ^a s(11)
1602	1601	-1	CO ^c as(81)
1638	1640	2	CO ^a s(52), CN ^a s(25)
—	2949	—	CH ₃ ss(97)
—	2958	—	CH ₃ ss(73), CH ₃ as ^{1,2} (16), C ^{α2} H s(10)
—	2968	—	C ^{α2} H s(84), CH ₃ ss(15)
—	2980	—	C ^{α1} H s(84), CH ₃ as ^{1,2} (12)
—	2991	—	CH ₃ as ^{1,2} (95)
—	3007	—	CH ₃ as ^{1,2} (73), CH ₃ as ^{1,2} (13), CH ₃ ss(9)

Table 3.81: (continued)

frequency (cm ⁻¹)			Potential Energy Distribution
obs.	calc.	dev.	
—	3012	—	CH ₃ as ^{1,2} (84), C ^{α1} H s(12)
—	3032	—	CH ₃ as ^{1,2} (87), CH ₃ as ^{1,2} (10)
—	3188	—	NH ^a s(100)
—	3239	—	NH ₂ as(96)
—	3300	—	NH ₂ ss(96)

frequency (cm ⁻¹)			Ala-Ala in D ₂ O pD 13 (mean deviation = 16 cm ⁻¹)
obs.	calc.	dev.	
—	56	—	NC ^φ t(32), CC ^c t(30), CC ^ψ t(17), NH ^a ob(10)
—	95	—	CC ^c t(43), CC ^ψ t(24), C ^ω N t(23), NC ^φ t(9)
—	107	—	C ^ω N t(28), CC ^c t(18), NC ^φ t(15), NH ^a ob(12), CO ^a ob(9), C ^{α1} H d ² (7)
—	145	—	CC ^ψ t(40), NC ^φ t(25), NH ^a ob(18), CC ^c t(9)
—	167	—	CNHC sd(42), C ^{α2} H d ³ (19), CO ^a sd(17), CC ^c r(10), CC ^{me} t(10)
—	188	—	CC ^{me} t(91)
—	200	—	CC ^{me} t(84)
225	221	-4	CN ⁿ t(73), C ^{α1} H d ³ (9)
251	244	-7	C ^{α2} H d ² (34), CC ^c r(9), CNHC sd(7), C ^{α2} H d ³ (7)
251	270	19	C ^{α1} H d ² (31), CN ⁿ t(11), C ^{α1} H d ³ (9), CO ^a ob(9), CC ^ψ t(7)
—	302	—	CO ^a sd(28), CC ^c r(26), C ^{α1} H d ² (17)
332	312	-20	C ^{α2} H d ² (23), C ^{α1} H d ³ (16), C ^{α1} H d ¹ (11), CC ^c s(8), CC ^ψ s(7)
380	332	-48	CO ^a r(24), C ^{α1} H d ³ (17), CNHC sd(15), C ^{α2} H d ² (7)
447	435	-12	C ^{α2} H d ¹ (25), C ^{α1} H d ¹ (13), CC ^c r(13), C ^ω N t(11), C ^{α2} H d ³ (9)
447	449	2	C ^{α1} H d ¹ (38), C ^{α2} H d ¹ (21)
534	546	12	CC ^c r(17), C ^{α2} H d ³ (16), CO ^a sd(15), C ^{α2} H d ¹ (10)
—	604	—	NH ^a ob(46), C ^ω N t(18), NC ^φ t(14), C ^{α2} H d ¹ (9)
645	631	-14	CO ^a r(25), NH ₂ r(18), CC ^c sd(13), C ^{α1} H d ³ (9), CC ^ψ s(8), CC ^c s(8)
687	668	-19	CC ^c sd(35), CC ^ψ s(12), CC ^c s(10), NH ₂ r(9)
760	758	-2	NH ₂ w(71), CO ^a ob(8), CN ⁿ s(7)
778	774	-4	CO ^a ob(48), CC ^{me} s(9), C ^{α1} H d ² (7), NH ₂ w(7)

Table 3.81: (continued)

frequency (cm ⁻¹)			Potential Energy Distribution
obs.	calc.	dev.	
778	783	5	CC ^c ob(56), C ^{α2} H d ² (9), CC ^c sd(7)
866	855	-11	CC ^c sd(15), NC ^φ s(10), CO ^a r(9), CN ⁿ s(9), CC ^{me} s(9), CC ^c s(7)
884	891	7	NH ₂ r(18), CH ₃ r ¹ (14), CC ^{me} s(12), CO ^a r(10), CNHC sd(7)
904	894	-10	CH ₃ r ¹ (27), CC ^{me} s(20), NH ₂ r(19), CN ⁿ s(7)
904	910	6	CC ^c s(22), NH ^a ib(21), CH ₃ r ² (17), NC ^φ s(10), CO ^c ss(10), CC ^c sd(9)
938	944	6	CH ₃ r ² (30), CN ⁿ s(14), CC ^ψ s(9), NH ^a ib(9), CO ^a s(8)
995	998	3	NH ^a ib(44), CH ₃ r ² (21), CC ^ψ s(7)
1066	1065	-1	CC ^{me} s(36), NH ₂ sis(12), CN ⁿ s(10)
1066	1067	1	C ^{α2} H r ² (28), CH ₃ r ² (10), CC ^{me} s(8), CC ^c ob(7), CH ₃ r ¹ (7)
1097	1097	0	CH ₃ r ² (19), C ^{α1} H r ² (18), CH ₃ r ¹ (14), C ^{α1} H d ² (9), CO ^a s(8), CC ^ψ s(7)
1113	1129	16	CC ^{me} s(35), NC ^φ s(22), CH ₃ r ¹ (8)
1163	1155	-8	CH ₃ r ¹ (26), C ^{α2} H d ¹ (15), CH ₃ r ² (15), NC ^φ s(9), CC ^{me} s(8)
1163	1179	16	NH ₂ sis(72), CN ⁿ s(20)
1209	1190	-19	CH ₃ r ¹ (18), C ^{α1} H d ¹ (13), CN ⁿ s(10), CH ₃ r ² (9), NC ^φ s(8), C ^{α1} H r ¹ (7)
1278	1268	-10	C ^{α2} H r ² (45), CH ₃ r ¹ (9), CO ^c ss(7)
1308	1308	0	C ^{α1} H r ² (59), CH ₃ r ¹ (10), C ^{α1} H r ¹ (8)
1328	1330	2	C ^{α2} H r ¹ (73), C ^{α2} H r ² (7)
1360	1359	-1	C ^{α1} H r ¹ (53), CH ₃ sd(15)
1365	1365	0	CH ₃ sd(73), C ^{α1} H r ¹ (13)
1371	1371	0	CH ₃ sd(98)
1409	1409	0	CO ^c ss(49), CC ^c s(16), CC ^c sd(8), CH ₃ sd(8)
1455	1450	-5	CH ₃ ad ^{1,2} (87)
1455	1456	1	CH ₃ ad ^{1,2} (84), CH ₃ r ¹ (8)
1455	1461	6	CH ₃ ad ^{1,2} (80)
1455	1462	7	CH ₃ ad ^{1,2} (90), CH ₃ r ¹ (7)
1512	1518	6	CN ^a s(32), CO ^a s(20), CC ^ψ s(15), NH ^a ib(8), CO ^a r(8)
1596	1600	4	CO ^c as(83)
1638	1631	-7	CO ^a s(53), CN ^a s(31)
—	2340	—	NH ^a s(98)
—	2378	—	NH ₂ ss(86), NH ₂ as(14)

Table 3.81: (continued)

frequency (cm ⁻¹)			Potential Energy Distribution
obs.	calc.	dev.	
—	2400	—	NH ₂ as(86), NH ₂ ss(14)
—	2949	—	CH ₃ ss(97)
—	2958	—	CH ₃ ss(73), CH ₃ as ^{1,2} (16), C ^{α2} H s(10)
—	2968	—	C ^{α2} H s(84), CH ₃ ss(15)
—	2980	—	C ^{α1} H s(84), CH ₃ as ^{1,2} (13)
—	2991	—	CH ₃ as ^{1,2} (95)
—	3007	—	CH ₃ as ^{1,2} (73), CH ₃ as ^{1,2} (13), CH ₃ ss(9)
—	3012	—	CH ₃ as ^{1,2} (84), C ^{α1} H s(12)
—	3032	—	CH ₃ as ^{1,2} (87), CH ₃ as ^{1,2} (10)

frequency (cm ⁻¹)			Potential Energy Distribution
obs.	calc.	dev.	
—	57	—	CC ^c t(32), NC ^φ t(31), CC ^ψ t(16), NH ^a ob(10)
—	95	—	CC ^c t(41), CC ^ψ t(24), C ^ω N t(23), NC ^φ t(10)
—	109	—	C ^ω N t(27), CC ^c t(19), NH ^a ob(13), NC ^φ t(13), CO ^a ob(9), C ^{α1} H d ² (7)
—	148	—	CC ^ψ t(42), NC ^φ t(24), NH ^a ob(19), CC ^c t(8), C ^{α2} H d ¹ (7)
—	168	—	CNHC sd(40), C ^{α2} H d ³ (19), CO ^a sd(17), CC ^{me} t(11), CC ^c r(10)
—	188	—	CC ^{me} t(91)
—	200	0	CC ^{me} t(83)
251	245	-6	C ^{α2} H d ² (34), CNHC sd(7), CO ^a sd(7)
251	263	12	C ^{α1} H d ² (18), C ^{α1} H d ³ (18), CO ^a sd(12), CO ^a ob(9), CC ^c r(9), CN ⁿ t(8)
—	294	—	C ^{α1} H d ² (31), CO ^a sd(13), CN ⁿ t(13), CC ^c r(10)
337	315	-22	C ^{α2} H d ² (13), CN ⁿ t(13), CC ^c r(10), C ^{α1} H d ³ (9), CO ^a sd(9), CC ^c s(8), C ^{α1} H d ¹ (7)
337	326	-11	CN ⁿ t(32), C ^{α2} H d ² (14), CC ^c r(13), CNHC sd(8), C ^{α2} H d ³ (7)
387	347	-40	C ^{α1} H d ³ (25), CN ⁿ t(24), CO ^a r(18), C ^{α1} H d ¹ (7)
460	450	-10	C ^{α2} H d ¹ (27), C ^{α1} H d ¹ (12), CC ^c r(12), C ^{α2} H d ³ (11)
460	466	6	C ^{α1} H d ¹ (42), C ^{α2} H d ¹ (20)
534	563	29	C ^{α2} H d ¹ (17), CC ^c r(17), C ^{α2} H d ³ (15), CO ^a sd(15), CC ^ψ s(7)

Table 3.81: (continued)

frequency (cm ⁻¹)			Potential Energy Distribution
obs.	calc.	dev.	
640	649	9	CC ^c sd(37), CC ^c s(17), CO ^a r(15)
678	696	18	CC ^ψ s(19), CO ^a r(14), C ^{α1} H d ³ (11), CC ^c sd(11), C ^{α1} H d ² (7), CH ₃ r ¹ (7)
743	754	11	CO ^a ob(42), C ^ω N t(14), C ^{α1} H d ³ (8), CC ^c ob(7)
778	781	3	CC ^c ob(40), CO ^a ob(11), C ^{α2} H d ² (8), CC ^c sd(7)
—	809	—	NH ^a ob(26), C ^{α1} H r ² (19), C ^ω N t(11), CC ^c ob(10), NC ^φ t(8)
829	838	9	CC ^{me} s(30), C ^{α1} H r ² (18), NH ^a ob(16), CO ^a ob(7)
866	867	1	CC ^c sd(20), CC ^{me} s(14), CC ^c s(12), CO ^c ss(10), CH ₃ r ¹ (9), CC ^ψ s(8), C ^{α1} H r ² (8), NC ^φ s(7)
884	897	13	C ^{α1} H r ¹ (62), CN ⁿ s(20), NH ₂ r(7)
909	914	5	C ^{α1} H r ² (18), CN ⁿ s(9), NH ₂ w(7)
927	928	1	CC ^c s(12), CC ^{me} s(12), CH ₃ r ² (11), NC ^φ s(9), CH ₃ r ¹ (9)
944	962	18	NH ₂ w(21), CH ₃ r ² (17), NC ^φ s(9), CC ^ψ s(8), CO ^a r(8), CH ₃ r ² (8)
981	980	-1	CH ₃ r ² (45), NH ₂ w(37)
1065	1065	0	C ^{α2} H r ² (31), CH ₃ r ² (17), CC ^c ob(9), CH ₃ r ¹ (8)
1101	1086	-15	CH ₃ r ¹ (43), CC ^{me} s(19), CN ⁿ s(10), NH ₂ r(10)
1132	1126	-6	CC ^{me} s(19), CC ^{me} s(14), NC ^φ s(11)
1154	1143	-11	CC ^{me} s(22), CC ^{me} s(15), CH ₃ r ¹ (13)
1195	1161	-34	NC ^φ s(23), CH ₃ r ² (17), CH ₃ r ¹ (16), C ^{α2} H d ¹ (12)
1239	1229	-10	CN ⁿ s(17), NH ^a ib(15), C ^{α2} H r ² (9), NH ₂ w(8), CH ₃ r ¹ (7), CH ₃ r ² (7)
1239	1240	1	NH ₂ r(26), NH ^a ib(12), C ^{α2} H r ² (12), CH ₃ r ¹ (9)
1273	1268	-5	NH ₂ r(21), C ^{α2} H r ² (19)
1304	1321	17	C ^{α2} H r ¹ (42), C ^{α2} H r ² (16), NH ^a ib(13), CH ₃ r ¹ (7)
1343	1347	4	C ^{α2} H r ¹ (30), NH ^a ib(22), CC ^ψ s(10), CO ^c ss(7)
1369	1364	-5	CH ₃ sd(86)
1369	1372	3	CH ₃ sd(95)
1408	1409	1	CO ^c ss(49), CC ^c s(16), CH ₃ sd(9), CC ^c sd(8)
1458	1450	-8	CH ₃ ad ^{1,2} (82), CH ₃ ad ^{1,2} (11)
1458	1456	-2	CH ₃ ad ^{1,2} (77), CH ₃ ad ^{1,2} (9), CH ₃ r ¹ (7)
1458	1460	2	CH ₃ ad ^{1,2} (81)
1458	1462	4	CH ₃ ad ^{1,2} (89), CH ₃ r ¹ (7)
1544	1553	9	NH ^a ib(27), CN ^a s(22), CO ^a s(13), NH ₂ sis(13), CC ^ψ s(8)

Table 3.81: (continued)

frequency (cm ⁻¹)			Potential Energy Distribution
obs.	calc.	dev.	
1583	1573	-10	NH ₂ sis(76), CN ^a s(13)
1605	1601	-4	CO ^c as(81)
1644	1633	-11	CO ^a s(53), CN ^a s(24), NH ₂ sis(8)
—	2203	—	C ^{α1} H s(98)
—	2950	—	CH ₃ ss(97)
—	2958	—	CH ₃ ss(73), CH ₃ as ^{1,2} (16), C ^{α2} H s(10)
—	2968	—	C ^{α2} H s(84), CH ₃ ss(15)
—	2991	—	CH ₃ as ^{1,2} (95)
—	3007	—	CH ₃ as ^{1,2} (69), CH ₃ as ^{1,2} (12), CH ₃ ss(8)
—	3008	—	CH ₃ as ^{1,2} (90)
—	3032	—	CH ₃ as ^{1,2} (87), CH ₃ as ^{1,2} (10)
—	3188	—	NH ^a s(100)
—	3239	—	NH ₂ as(96)
—	3300	—	NH ₂ ss(96)

frequency (cm ⁻¹)			Ala-1- ¹³ C-Ala pH 13 (mean deviation = 14 cm ⁻¹)
obs.	calc.	dev.	
—	57	—	CC ^c t(33), NC ^φ t(31), CC ^ψ t(16), NH ^a ob(10)
—	96	—	CC ^c t(41), CC ^ψ t(23), C ^ω N t(23), NC ^φ t(11)
—	109	—	C ^ω N t(27), CC ^c t(19), NH ^a ob(13), NC ^φ t(13), CO ^a ob(9), C ^{α1} H d ² (7)
—	149	—	CC ^ψ t(44), NC ^φ t(24), NH ^a ob(19), C ^{α2} H d ¹ (7), CC ^c t(7)
—	169	—	CNHC sd(41), C ^{α2} H d ³ (19), CO ^a sd(17), CC ^{me} t(11), CC ^c r(10)
—	188	—	CC ^{me} t(91)
—	200	—	CC ^{me} t(83)
236	245	9	C ^{α2} H d ² (34), CNHC sd(7), CC ^c r(7)
236	263	27	C ^{α1} H d ² (19), C ^{α1} H d ³ (18), CO ^a sd(12), CO ^a ob(10), CC ^c r(9), CN ⁿ t(8)
—	294	—	C ^{α1} H d ² (30), CN ⁿ t(15), CO ^a sd(13), CC ^c r(9)
334	316	-18	C ^{α2} H d ² (13), CC ^c s(9), CO ^a sd(9), CC ^c r(9), CN ⁿ t(9), C ^{α1} H d ¹ (8), C ^{α1} H d ³ (8), NC ^φ s(7)

Table 3.81: (continued)

frequency (cm ⁻¹)			Potential Energy Distribution
obs.	calc.	dev.	
334	326	-8	CN ⁿ t(33), CC ^c r(14), C ^{α2} H d ² (13), CNHC sd(8), C ^{α2} H d ³ (7)
376	348	-28	CN ⁿ t(26), C ^{α1} H d ³ (24), CO ^a r(18)
467	451	-16	C ^{α2} H d ¹ (29), C ^{α2} H d ³ (11), CC ^c r(11), C ^{α1} H d ¹ (10)
467	469	2	C ^{α1} H d ¹ (43), C ^{α2} H d ¹ (19)
542	567	25	CO ^a sd(16), CC ^c r(16), C ^{α2} H d ¹ (15), C ^{α2} H d ³ (15)
644	650	6	CC ^c sd(39), CC ^c s(17), CO ^a r(14)
687	703	16	CC ^ψ s(18), CO ^a r(16), C ^{α1} H d ³ (10), CC ^c sd(9), C ^{α1} H d ² (8), CH ₃ r ¹ (8)
748	742	-6	CO ^a ob(50), C ^ω N t(13), C ^{α1} H d ³ (11)
778	780	2	CC ^c ob(45), C ^{α2} H d ² (9), CC ^c sd(7), CH ₃ r ¹ (7)
—	818	—	NH ^a ob(44), C ^ω N t(17), NC ^φ t(12), CC ^c ob(11)
850	858	8	CC ^c sd(15), CC ^{me} s(15), CN ⁿ s(13), CC ^c s(8), NC ^φ s(7), CC ^{me} s(7)
883	891	8	CN ⁿ s(13), CC ^{me} s(13), CC ^c s(9), CC ^{me} s(9), CH ₃ r ¹ (9), CC ^c sd(7)
920	926	6	CC ^{me} s(12), CH ₃ r ¹ (10), CO ^a r(9), CC ^c s(8), CH ₃ r ² (7)
943	951	8	CH ₃ r ² (24), CC ^ψ s(13), NC ^φ s(13), NH ₂ w(10), CO ^a r(8), CC ^c s(7)
980	974	-6	NH ₂ w(52), CH ₃ r ² (34)
1021	1015	-6	CH ₃ r ¹ (26), NH ₂ r(20), CH ₃ r ² (14), CN ⁿ s(12), C ^{α1} H r ² (7)
1066	1065	-1	C ^{α2} H r ² (31), CH ₃ r ² (17), CC ^c ob(9), CH ₃ r ¹ (8)
1103	1096	-7	CC ^{me} s(45), CN ⁿ s(19), CH ₃ r ¹ (16)
1129	1133	4	CC ^{me} s(35), NC ^φ s(18), CH ₃ r ¹ (12)
1129	1141	12	NH ₂ r(22), C ^{α1} H r ² (20), C ^{α1} H r ¹ (15), CH ₃ r ² (8), CC ^ψ s(7)
1166	1159	-7	CH ₃ r ¹ (21), NC ^φ s(18), CH ₃ r ² (18), C ^{α2} H d ¹ (14), C ^{α2} H r ¹ (7)
1221	1229	8	NH ^a ib(24), C ^{α2} H r ² (14), CN ^a s(9), CN ⁿ s(8)
1256	1247	-9	NH ₂ r(18), C ^{α2} H r ² (12), CN ⁿ s(10), C ^{α1} H d ¹ (7)
1279	1285	6	C ^{α2} H r ² (19), C ^{α1} H r ² (15), NH ^a ib(12), CN ^a s(8)
1321	1315	-6	C ^{α1} H r ² (34), C ^{α1} H r ¹ (21), CH ₃ r ¹ (8), NH ^a ib(7)
1327	1331	4	C ^{α2} H r ¹ (69)
1368	1364	-4	CH ₃ sd(87), CO ^c ss(7)
1368	1371	3	CH ₃ sd(97)
1408	1397	-11	C ^{α1} H r ¹ (33), CO ^c ss(14), NH ₂ r(10), NH ^a ib(8), CH ₃ ad ^{1,2} (7)

Table 3.81: (continued)

frequency (cm ⁻¹)			Potential Energy Distribution
obs.	calc.	dev.	
1408	1411	3	CO ^c ss(37), CC ^c s(13), C ^{α1} H r ¹ (9), CC ^c sd(7)
1458	1452	-6	CH ₃ ad ^{1,2} (68), CH ₃ ad ^{1,2} (18)
1458	1457	-1	CH ₃ ad ^{1,2} (55), CH ₃ ad ^{1,2} (24)
1458	1461	3	CH ₃ ad ^{1,2} (59), CH ₃ ad ^{1,2} (12), CH ₃ ad ^{1,2} (8)
1458	1462	4	CH ₃ ad ^{1,2} (81), CH ₃ r ¹ (7)
1522	1535	13	NH ^a ib(34), CN ^a s(23), CO ^a s(13), CC ^ψ s(8)
1560	1567	7	NH ₂ sis(65), CN ^a s(15), CO ^a s(11)
1594	1597	3	CO ^c as(42), CO ^a s(19), NH ₂ sis(17), CN ^a s(8)
1610	1607	-3	CO ^c as(41), CO ^a s(21), NH ₂ sis(12), CN ^a s(10)
—	2949	—	CH ₃ ss(97)
—	2958	—	CH ₃ ss(73), CH ₃ as ^{1,2} (16), C ^{α2} H s(10)
—	2968	—	C ^{α2} H s(84), CH ₃ ss(15)
—	2980	—	C ^{α1} H s(84), CH ₃ as ^{1,2} (12)
—	2991	—	CH ₃ as ^{1,2} (95)
—	3007	—	CH ₃ as ^{1,2} (73), CH ₃ as ^{1,2} (13), CH ₃ ss(9)
—	3012	—	CH ₃ as ^{1,2} (84), C ^{α1} H s(12)
—	3032	—	CH ₃ as ^{1,2} (87), CH ₃ as ^{1,2} (10)
—	3188	—	NH ^a s(100)
—	3239	—	NH ₂ as(96)
—	3300	—	NH ₂ ss(96)

In order to examine the effects of incorporating incorrect geometries in the G matrix, several altered geometries were created and normal mode analyses were performed using the optimized scale factors and force constants. For the first two, the bond lengths of the carbonyl oxygen or the amide hydrogen were increased by ten percent. No other changes were incorporated. The results of the normal mode analyses are listed in Tables 3.82 and 3.83. The final structure was that of isolated alanyl-alanine in base. The scale factors and force constants were from the two-water water-excluded calculations. The results of the normal mode analysis are in Table 3.84. Small changes in the structure, a 10% increase in bond length, did not affect frequency predictions nor PED predictions. Gross change in structure, the isolated geometry, leads to large changes in frequency predictions and predicted PED assignments. This means that for testing hypothetical structures by prediction of their vibrational spectra, the scale factors and force constants are accurate. If the hypothetical structure is nearly correct, experimentally determined frequencies will be accurately predicted. If the hypothetical structure is inaccurate, the predicted frequencies will not match experimental spectra.

Table 3.82: Alanyl-alanine Two-water Supramolecule Structure with the CO Stretch Coordinate Increased 10%, Water-Excluded Force Constants and Scale Factors used for the Normal Mode Analysis.

frequency (cm ⁻¹)			Ala-ala pH 13 (mean deviation = 12 cm ⁻¹)
obs.	calc.	dev.	
			Potential Energy Distribution
—	54	—	NC ^φ t(28), CC ^c t(28), CC ^ψ t(24), NH ^a ob(9)
—	93	—	CC ^c t(51), CC ^ψ t(32), C ^ω N t(17)
—	98	—	NC ^φ t(36), C ^ω N t(32), CC ^ψ t(8)
—	134	—	CC ^ψ t(31), NH ^a ob(26), NC ^φ t(18), CC ^c t(15), C ^{α2} H d ¹ (7)
—	169	—	CNHC sd(35), CO ^a sd(19), C ^{α2} H d ³ (17), CC ^{me} t(14), CC ^c r(10)
—	193	—	CC ^{me} t(87)
—	197	—	CC ^{me} t(79)
245	247	2	C ^{α2} H d ² (28), C ^{α1} H d ² (13)
245	265	20	C ^{α1} H d ² (21), C ^{α1} H d ³ (18), C ^{α2} H d ² (15), CO ^a ob(10), CO ^a sd(7), CC ^c r(7)
—	285	—	C ^{α1} H d ² (23), CO ^a sd(19), CC ^c r(14), CN ⁿ t(11)
334	316	-18	C ^{α2} H d ² (20), CC ^c s(12), C ^{α1} H d ¹ (8), C ^{α1} H d ³ (8)
334	335	1	CN ⁿ t(36), CC ^c r(19), CNHC sd(9), CO ^a r(7)
377	353	-24	CN ⁿ t(37), C ^{α1} H d ³ (18), CO ^a r(15), CNHC sd(7)
464	447	-17	C ^{α2} H d ¹ (32), CC ^c r(12), C ^{α2} H d ³ (9), C ^{α1} H d ¹ (8)
464	467	3	C ^{α1} H d ¹ (45), C ^{α2} H d ¹ (16)
545	573	28	C ^{α2} H d ¹ (16), C ^{α2} H d ³ (16), CO ^a sd(16), CC ^c r(16), CC ^ψ s(7)
642	646	4	CC ^c sd(40), CC ^c s(17), CO ^a r(14)
688	700	12	CC ^ψ s(18), CO ^a r(16), C ^{α1} H d ³ (11), CC ^c sd(9), C ^{α1} H d ² (8), CH ₃ r ¹ (8)
761	755	-6	CO ^a ob(34), C ^ω N t(18), NH ^a ob(12), NC ^φ t(8), CC ^c ob(7)
778	787	9	CC ^c ob(34), CO ^a ob(19), CC ^c sd(7)
—	815	—	NH ^a ob(38), CC ^c ob(18), CO ^a ob(11), C ^ω N t(10), NC ^φ t(9)
872	860	-12	CC ^c sd(16), CC ^{me} s(14), CN ⁿ s(12), CC ^c s(9), CC ^{me} s(8), NC ^φ s(7), CO ^c ss(7)
884	893	9	CN ⁿ s(15), CC ^{me} s(15), CC ^c s(10), NH ₂ w(8), CC ^c sd(7), CC ^{me} s(7), CH ₃ r ¹ (7)
920	929	9	CC ^{me} s(15), CH ₃ r ¹ (11), CC ^c s(9), NC ^φ s(8), CH ₃ r ² (8), CO ^a r(7)
952	952	0	CH ₃ r ² (22), CC ^ψ s(14), NC ^φ s(11), NH ₂ w(11), CO ^a r(10)
980	970	-10	NH ₂ w(51), CH ₃ r ² (34)

Table 3.82: (continued)

frequency (cm ⁻¹)			Potential Energy Distribution
obs.	calc.	dev.	
1019	1015	-4	CH ₃ r ¹ (25), NH ₂ r(18), CH ₃ r ² (16), CN ⁿ s(12), C ^{α1} H r ² (8)
1069	1066	-3	C ^{α2} H r ² (31), CH ₃ r ² (17), CC ^c ob(10), CH ₃ r ¹ (7)
1104	1098	-6	CC ^{me} s(43), CN ⁿ s(18), CH ₃ r ¹ (17)
1136	1136	0	CC ^{me} s(33), NC ^φ s(16), CH ₃ r ¹ (13)
1136	1143	7	NH ₂ r(22), C ^{α1} H r ² (19), C ^{α1} H r ¹ (14), CH ₃ r ² (7)
1166	1158	-8	NC ^φ s(21), CH ₃ r ¹ (19), CH ₃ r ² (18), C ^{α2} H d ¹ (13), C ^{α2} H r ¹ (7)
1220	1226	6	NH ^a ib(28), C ^{α2} H r ² (18), CN ^a s(9)
1260	1250	-10	NH ₂ r(19), CN ⁿ s(13), C ^{α2} H r ² (9), C ^{α1} H d ¹ (8), NH ₂ w(8)
1281	1288	7	C ^{α1} H r ² (20), C ^{α2} H r ² (16), NH ^a ib(11), NH ₂ r(8), CH ₃ r ¹ (7)
1320	1315	-5	C ^{α1} H r ² (27), C ^{α1} H r ¹ (19), NH ^a ib(11), C ^{α2} H r ² (9), C ^{α2} H r ¹ (8), CH ₃ r ¹ (7)
1335	1333	-2	C ^{α2} H r ¹ (68), C ^{α1} H r ¹ (7)
1367	1361	-6	CH ₃ sd(88)
1367	1373	6	CH ₃ sd(97)
1407	1399	-8	C ^{α1} H r ¹ (33), CO ^c ss(17), NH ₂ r(11), NH ^a ib(7)
1407	1413	6	CO ^c ss(34), CC ^c s(13), C ^{α1} H r ¹ (11)
1459	1453	-6	CH ₃ ad ^{1,2} (60), CH ₃ ad ^{1,2} (26)
1459	1457	-2	CH ₃ ad ^{1,2} (48), CH ₃ ad ^{1,2} (30), CH ₃ ad ^{1,2} (8)
1459	1461	2	CH ₃ ad ^{1,2} (33), CH ₃ ad ^{1,2} (24), CH ₃ ad ^{1,2} (23)
1459	1463	4	CH ₃ ad ^{1,2} (79), CH ₃ ad ^{1,2} (12)
1542	1542	0	NH ^a ib(29), CN ^a s(26), CO ^a s(12), CC ^ψ s(9)
1578	1573	-5	NH ₂ sis(87), CN ^a s(7)
1602	1598	-4	CO ^c as(81), CO ^c ss(7)
1638	1639	1	CO ^a s(51), CN ^a s(25)
—	2930	—	CH ₃ ss(97)
—	2937	—	CH ₃ ss(87), CH ₃ as ^{1,2} (12)
—	2960	—	C ^{α2} H s(92)
—	2977	—	C ^{α1} H s(80), CH ₃ as ^{1,2} (14)
—	2985	—	CH ₃ as ^{1,2} (92), C ^{α1} H s(7)
—	3001	—	CH ₃ as ^{1,2} (78), CH ₃ ss(8), CH ₃ as ^{1,2} (8)
—	3008	—	CH ₃ as ^{1,2} (84), C ^{α1} H s(13)
—	3028	—	CH ₃ as ^{1,2} (92), CH ₃ as ^{1,2} (7)
—	3137	—	NH ₂ ss(99)
—	3234	—	NH ₂ as(99)

Table 3.82: (continued)

frequency (cm ⁻¹)			Potential Energy Distribution
obs.	calc.	dev.	
—	3444	—	NH ^a s(100)

frequency (cm ⁻¹)			Ala-ala in D ₂ O pD 13 (mean deviation = 15 cm ⁻¹)
obs.	calc.	dev.	
—	53	—	NC ^φ t(28), CC ^c t(26), CC ^ψ t(25), NH ^a ob(9)
—	92	—	CC ^c t(54), CC ^ψ t(34), C ^ω N t(15)
—	97	—	NC ^φ t(40), C ^ω N t(34)
—	132	—	CC ^ψ t(29), NH ^a ob(24), NC ^φ t(19), CC ^c t(17)
—	167	—	CNHC sd(36), CO ^a sd(21), C ^{α2} H d ³ (17), CC ^{me} t(11), CC ^c r(9)
—	192	—	CC ^{me} t(86)
—	197	—	CC ^{me} t(81)
225	228	3	CN ⁿ t(69), C ^{α1} H d ³ (9)
251	246	-5	C ^{α2} H d ² (30), C ^{α1} H d ² (9), CC ^c r(8)
251	266	15	C ^{α1} H d ² (36), CO ^a ob(12), C ^{α1} H d ³ (11), C ^{α2} H d ² (11), CN ⁿ t(8)
—	296	—	CO ^a sd(28), CC ^c r(24), CN ⁿ t(13), C ^{α1} H d ² (10)
332	311	-21	C ^{α2} H d ² (25), C ^{α1} H d ³ (13), C ^{α1} H d ¹ (10), CC ^c s(9)
380	336	-44	CO ^a r(22), CNHC sd(20), C ^{α1} H d ³ (18), CC ^c r(10)
447	431	-16	C ^{α2} H d ¹ (28), CC ^c r(14), C ^{α1} H d ¹ (11), C ^ω N t(10), C ^{α2} H d ³ (7)
447	446	-1	C ^{α1} H d ¹ (39), C ^{α2} H d ¹ (18)
534	549	15	CC ^c r(17), C ^{α2} H d ³ (16), CO ^a sd(14), C ^{α2} H d ¹ (8), C ^ω N t(7)
—	597	—	NH ^a ob(45), C ^ω N t(13), NC ^φ t(13), C ^{α2} H d ¹ (11)
645	629	-16	CO ^a r(26), NH ₂ r(16), CC ^c sd(15), CC ^c s(9), C ^{α1} H d ³ (9), CC ^ψ s(7)
687	666	-21	CC ^c sd(35), CC ^ψ s(13), CC ^c s(10), NH ₂ r(9)
760	757	-3	NH ₂ w(66), CO ^a ob(13)
778	775	-3	CO ^a ob(46), NH ₂ w(13), CC ^{me} s(10), C ^{α1} H d ² (7)
778	789	11	CC ^c ob(58), C ^{α2} H d ² (8), CC ^c sd(7)
866	854	-12	CC ^c sd(15), NC ^φ s(10), CO ^a r(9), CN ⁿ s(9), CC ^{me} s(8), CC ^c s(7)
884	894	10	NH ₂ r(19), CH ₃ r ¹ (13), CC ^{me} s(11), CO ^a r(10), CNHC sd(7)

Table 3.82: (continued)

frequency (cm ⁻¹)			Potential Energy Distribution
obs.	calc.	dev.	
904	895	-9	CH ₃ r ¹ (27), CC ^{me} s(21), NH ₂ r(17), CN ⁿ s(8)
904	907	3	NH ^a ib(25), CC ^c s(21), CH ₃ r ² (16), NC ^φ s(10), CO ^c ss(10), CC ^c sd(9)
938	943	5	CH ₃ r ² (31), CN ⁿ s(14), CC ^ψ s(9), CO ^a s(8), NH ^a ib(8)
995	991	-4	NH ^a ib(43), CH ₃ r ² (21), CC ^ψ s(7)
1066	1064	-2	CC ^{me} s(41), NH ₂ sis(13), CN ⁿ s(12), C ^{α1} H d ³ (7)
1066	1068	2	C ^{α2} H r ² (34), CH ₃ r ² (12), CC ^c ob(9), CH ₃ r ¹ (7)
1097	1094	-3	CH ₃ r ² (18), C ^{α1} H r ² (17), CH ₃ r ¹ (14), C ^{α1} H d ² (9), NH ₂ sis(8), CO ^a s(7)
1113	1130	17	CC ^{me} s(34), NC ^φ s(22), CH ₃ r ¹ (8)
1163	1153	-10	CH ₃ r ¹ (27), C ^{α2} H d ¹ (15), CH ₃ r ² (14), NC ^φ s(8), CC ^{me} s(8)
1163	1179	16	NH ₂ sis(72), CN ⁿ s(18)
1209	1193	-16	CH ₃ r ¹ (17), C ^{α1} H d ¹ (13), CN ⁿ s(13), CH ₃ r ² (9), NC ^φ s(8), C ^{α1} H r ¹ (7)
1278	1268	-10	C ^{α2} H r ² (45), CH ₃ r ¹ (10), CO ^c ss(7)
1308	1304	-4	C ^{α1} H r ² (59), CH ₃ r ¹ (11), C ^{α1} H r ¹ (7)
1328	1331	3	C ^{α2} H r ¹ (75), C ^{α2} H r ² (7)
1360	1360	0	CH ₃ sd(49), C ^{α1} H r ¹ (29), CO ^c ss(7)
1365	1364	-1	C ^{α1} H r ¹ (40), CH ₃ sd(40)
1371	1373	2	CH ₃ sd(98)
1409	1410	1	CO ^c ss(49), CC ^c s(16), CC ^c sd(8), CH ₃ sd(8)
1455	1451	-4	CH ₃ ad ^{1,2} (82), CH ₃ ad ^{1,2} (7)
1455	1456	1	CH ₃ ad ^{1,2} (63), CH ₃ ad ^{1,2} (21)
1455	1458	3	CH ₃ ad ^{1,2} (50), CH ₃ ad ^{1,2} (21), CH ₃ ad ^{1,2} (11)
1455	1463	8	CH ₃ ad ^{1,2} (77), CH ₃ ad ^{1,2} (14)
1512	1506	-6	CN ^a s(32), CO ^a s(19), CC ^ψ s(14), NC ^φ s(7), NH ^a ib(7), CO ^a r(7)
1596	1597	1	CO ^c as(82), CO ^c ss(7)
1638	1630	-8	CO ^a s(52), CN ^a s(31)
—	2266	—	NH ₂ ss(99)
—	2391	—	NH ₂ as(99)
—	2526	—	NH ^a s(99)
—	2930	—	CH ₃ ss(97)
—	2937	—	CH ₃ ss(87), CH ₃ as ^{1,2} (12)

Table 3.82: (continued)

frequency (cm ⁻¹)			Potential Energy Distribution
obs.	calc.	dev.	
—	2960	—	C ^{α2} H s(92)
—	2977	—	C ^{α1} H s(79), CH ₃ as ^{1,2} (15)
—	2985	—	CH ₃ as ^{1,2} (92), C ^{α1} H s(7)
—	3000	—	CH ₃ as ^{1,2} (78), CH ₃ ss(8), CH ₃ as ^{1,2} (8)
—	3008	—	CH ₃ as ^{1,2} (83), C ^{α1} H s(13)
—	3028	—	CH ₃ as ^{1,2} (92), CH ₃ as ^{1,2} (7)

frequency (cm ⁻¹)			Potential Energy Distribution
obs.	calc.	dev.	
—	54	—	NC ^φ t(28), CC ^c t(28), CC ^ψ t(24), NH ^a ob(9)
—	93	—	CC ^c t(51), CC ^ψ t(32), C ^ω N t(18)
—	98	—	NC ^φ t(36), C ^ω N t(32), CC ^ψ t(9)
—	134	—	CC ^ψ t(30), NH ^a ob(26), NC ^φ t(19), CC ^c t(15), C ^{α2} H d ¹ (7)
—	169	—	CNHC sd(35), CO ^a sd(20), C ^{α2} H d ³ (17), CC ^{me} t(13), CC ^c r(9)
—	193	—	CC ^{me} t(87)
—	197	—	CC ^{me} t(80)
251	246	-5	C ^{α2} H d ² (27), C ^{α1} H d ² (13)
251	264	13	C ^{α1} H d ² (20), C ^{α1} H d ³ (19), C ^{α2} H d ² (15), CO ^a ob(10), CC ^c r(8), CO ^a sd(7)
200	283	83	C ^{α1} H d ² (24), CO ^a sd(19), CC ^c r(15), CN ⁿ t(10)
337	315	-22	C ^{α2} H d ² (20), CC ^c s(12), C ^{α1} H d ³ (8), C ^{α1} H d ¹ (7)
337	335	-2	CN ⁿ t(38), CC ^c r(18), CNHC sd(9), CO ^a r(7)
387	352	-35	CN ⁿ t(35), C ^{α1} H d ³ (19), CO ^a r(15), CNHC sd(7), C ^{α1} H d ¹ (7)
460	446	-14	C ^{α2} H d ¹ (31), CC ^c r(12), C ^{α1} H d ¹ (9), C ^{α2} H d ³ (9)
460	464	4	C ^{α1} H d ¹ (44), C ^{α2} H d ¹ (17)
534	569	35	C ^{α2} H d ¹ (17), CC ^c r(17), C ^{α2} H d ³ (16), CO ^a sd(15), CC ^ψ s(7)
640	644	4	CC ^c sd(37), CC ^c s(17), CO ^a r(16)
678	693	15	CC ^ψ s(18), CO ^a r(14), C ^{α1} H d ³ (11), CC ^c sd(11), C ^{α1} H d ² (7), CH ₃ r ¹ (7)
743	753	10	CO ^a ob(39), C ^ω N t(16), NH ^a ob(9), C ^{α1} H d ³ (7)
778	783	5	CC ^c ob(26), CO ^a ob(16), NH ^a ob(11)

Table 3.82: (continued)

frequency (cm ⁻¹)			Potential Energy Distribution
obs.	calc.	dev.	
—	805	—	CC ^c ob(24), NH ^a ob(21), C ^{α1} H r ² (15), C ^ω N t(8)
829	835	6	CC ^{me} s(31), C ^{α1} H r ² (23), NH ^a ob(13), CO ^a ob(7)
866	865	-1	CC ^c sd(19), CC ^c s(12), CC ^{me} s(12), CC ^ψ s(9), CO ^c ss(9), C ^{α1} H r ² (8), CH ₃ r ¹ (8), NC ^φ s(7)
909	898	-11	C ^{α1} H r ¹ (61), CN ⁿ s(19), NH ₂ w(8), NH ₂ r(7)
909	913	4	C ^{α1} H r ² (15), CN ⁿ s(9), CH ₃ r ² (9), NH ₂ w(8), CC ^c s(7)
927	929	2	CC ^{me} s(15), CC ^c s(10), CH ₃ r ¹ (10), CH ₃ r ² (9), NC ^φ s(8), CO ^a r(7)
944	959	15	NH ₂ w(19), CH ₃ r ² (16), CH ₃ r ² (11), CC ^ψ s(8), NC ^φ s(8), CO ^a r(8)
981	977	-4	CH ₃ r ² (44), NH ₂ w(38)
1065	1066	1	C ^{α2} H r ² (31), CH ₃ r ² (17), CC ^c ob(10), CH ₃ r ¹ (7)
1101	1088	-13	CH ₃ r ¹ (43), CC ^{me} s(19), CN ⁿ s(10), NH ₂ r(9)
1132	1128	-4	CC ^{me} s(17), CC ^{me} s(14), NC ^φ s(10), C ^{α1} H r ² (7)
1154	1144	-10	CC ^{me} s(24), CH ₃ r ¹ (16), CC ^{me} s(13)
1195	1160	-35	NC ^φ s(24), CH ₃ r ² (17), CH ₃ r ¹ (14), C ^{α2} H d ¹ (11)
1239	1226	-13	NH ^a ib(25), C ^{α2} H r ² (16), CN ⁿ s(10), CN ^a s(7)
1239	1242	3	NH ₂ r(26), CN ⁿ s(12), CH ₃ r ¹ (11)
1273	1270	-3	NH ₂ r(25), C ^{α2} H r ² (18)
1304	1321	17	C ^{α2} H r ¹ (38), C ^{α2} H r ² (16), NH ^a ib(14), CH ₃ r ¹ (7)
1343	1343	0	C ^{α2} H r ¹ (37), NH ^a ib(19), CC ^ψ s(9), CO ^c ss(7)
1369	1362	-7	CH ₃ sd(88)
1369	1374	5	CH ₃ sd(97)
1408	1410	2	CO ^c ss(49), CC ^c s(17), CC ^c sd(8), CH ₃ sd(8), CO ^c as(7)
1458	1451	-7	CH ₃ ad ^{1,2} (71), CH ₃ ad ^{1,2} (22)
1458	1456	-2	CH ₃ ad ^{1,2} (46), CH ₃ ad ^{1,2} (29), CH ₃ ad ^{1,2} (11)
1458	1458	0	CH ₃ ad ^{1,2} (45), CH ₃ ad ^{1,2} (24), CH ₃ ad ^{1,2} (11), CH ₃ ad ^{1,2} (8)
1458	1463	5	CH ₃ ad ^{1,2} (78), CH ₃ ad ^{1,2} (14)
1544	1541	-3	NH ^a ib(29), CN ^a s(27), CO ^a s(12), CC ^ψ s(9)
1583	1572	-11	NH ₂ sis(85), CN ^a s(8)
1605	1598	-7	CO ^c as(80), CO ^c ss(7)
1644	1632	-12	CO ^a s(52), CN ^a s(25), NH ₂ sis(8)
—	2201	—	C ^{α1} H s(98)
—	2930	—	CH ₃ ss(98)

Table 3.82: (continued)

frequency (cm^{-1})			Potential Energy Distribution
obs.	calc.	dev.	
—	2937	—	CH_3 ss(87), CH_3 as ^{1,2} (12)
—	2960	—	$\text{C}^{\alpha 2}\text{H}$ s(92)
—	2984	—	CH_3 as ^{1,2} (95)
—	3001	—	CH_3 as ^{1,2} (78), CH_3 ss(8), CH_3 as ^{1,2} (8)
—	3004	—	CH_3 as ^{1,2} (94)
—	3028	—	CH_3 as ^{1,2} (92), CH_3 as ^{1,2} (7)
—	3137	—	NH_2 ss(99)
—	3234	—	NH_2 as(99)
—	3444	—	NH^a s(100)

frequency (cm^{-1})			Ala-1- ¹³ C-Ala pH 13 (mean deviation = 14 cm^{-1})
obs.	calc.	dev.	
—	54	—	NC^ϕ t(28), CC^c t(28), CC^ψ t(24), NH^a ob(9)
—	93	—	CC^c t(51), CC^ψ t(32), C^ωN t(16)
—	98	—	NC^ϕ t(37), C^ωN t(32), CC^ψ t(8)
—	134	—	CC^ψ t(31), NH^a ob(25), NC^ϕ t(18), CC^c t(15), $\text{C}^{\alpha 2}\text{H}$ d ¹ (7)
—	169	—	CNHC sd(35), CO^a sd(20), $\text{C}^{\alpha 2}\text{H}$ d ³ (17), CC^{me} t(14), CC^c r(9)
—	193	—	CC^{me} t(87)
—	197	—	CC^{me} t(80)
236	247	11	$\text{C}^{\alpha 2}\text{H}$ d ² (28), $\text{C}^{\alpha 1}\text{H}$ d ² (13)
236	264	28	$\text{C}^{\alpha 1}\text{H}$ d ² (20), $\text{C}^{\alpha 1}\text{H}$ d ³ (18), $\text{C}^{\alpha 2}\text{H}$ d ² (14), CO^a ob(10), CO^a sd(8), CC^c r(8)
—	284	—	$\text{C}^{\alpha 1}\text{H}$ d ² (24), CO^a sd(19), CC^c r(14), CN^n t(10)
334	316	-18	$\text{C}^{\alpha 2}\text{H}$ d ² (20), CC^c s(12), $\text{C}^{\alpha 1}\text{H}$ d ¹ (8), $\text{C}^{\alpha 1}\text{H}$ d ³ (7)
334	335	1	CN^n t(36), CC^c r(19), CNHC sd(9), CO^a r(7)
376	353	-23	CN^n t(37), $\text{C}^{\alpha 1}\text{H}$ d ³ (18), CO^a r(14), CNHC sd(7)
467	447	-20	$\text{C}^{\alpha 2}\text{H}$ d ¹ (32), CC^c r(12), $\text{C}^{\alpha 2}\text{H}$ d ³ (9), $\text{C}^{\alpha 1}\text{H}$ d ¹ (8)
467	467	0	$\text{C}^{\alpha 1}\text{H}$ d ¹ (44), $\text{C}^{\alpha 2}\text{H}$ d ¹ (16)
542	572	30	$\text{C}^{\alpha 2}\text{H}$ d ¹ (16), $\text{C}^{\alpha 2}\text{H}$ d ³ (16), CO^a sd(16), CC^c r(16), CC^ψ s(7)
644	645	1	CC^c sd(39), CC^c s(17), CO^a r(15)
687	699	12	CC^ψ s(17), CO^a r(16), $\text{C}^{\alpha 1}\text{H}$ d ³ (10), CC^c sd(10), $\text{C}^{\alpha 1}\text{H}$ d ² (9), CH_3 r ¹ (8)

Table 3.82: (continued)

frequency (cm ⁻¹)			Potential Energy Distribution
obs.	calc.	dev.	
748	741	-7	CO ^a ob(47), C ^ω N t(14), C ^{α1} H d ³ (10)
778	782	4	CC ^c ob(33), NH ^a ob(12), CO ^a ob(10), C ^{α2} H d ² (7), CC ^c sd(7)
—	813	—	NH ^a ob(37), CC ^c ob(22), C ^ω N t(12), NC ^φ t(9)
850	857	7	CC ^c sd(15), CC ^{me} s(15), CN ⁿ s(12), NC ^φ s(8), CC ^c s(8), CO ^c ss(7), CC ^{me} s(7)
883	892	9	CC ^{me} s(14), CN ⁿ s(13), CC ^c s(10), CC ^{me} s(8), CH ₃ r ¹ (8), CC ^c sd(7), NH ₂ w(7)
920	928	8	CC ^{me} s(15), CH ₃ r ¹ (11), CO ^a r(9), CC ^c s(7), CNHC sd(7)
943	947	4	CH ₃ r ² (24), CC ^ψ s(13), NC ^φ s(12), NH ₂ w(9), CO ^a r(8), CC ^c s(7)
980	969	-11	NH ₂ w(53), CH ₃ r ² (33)
1021	1014	-7	CH ₃ r ¹ (26), NH ₂ r(18), CH ₃ r ² (16), CN ⁿ s(12), C ^{α1} H r ² (8)
1066	1066	0	C ^{α2} H r ² (31), CH ₃ r ² (17), CC ^c ob(10), CH ₃ r ¹ (7)
1103	1097	-6	CC ^{me} s(44), CN ⁿ s(19), CH ₃ r ¹ (16)
1129	1135	6	CC ^{me} s(34), NC ^φ s(18), CH ₃ r ¹ (12)
1129	1142	13	NH ₂ r(23), C ^{α1} H r ² (20), C ^{α1} H r ¹ (15), CN ⁿ s(7), CH ₃ r ² (7)
1166	1157	-9	CH ₃ r ¹ (20), NC ^φ s(18), CH ₃ r ² (18), C ^{α2} H d ¹ (14), C ^{α2} H r ¹ (7)
1221	1224	3	NH ^a ib(30), C ^{α2} H r ² (18), CN ^a s(10)
1256	1250	-6	NH ₂ r(20), CN ⁿ s(14), C ^{α1} H d ¹ (9), NH ₂ w(9), C ^{α2} H r ² (8)
1279	1284	5	C ^{α2} H r ² (19), C ^{α1} H r ² (15), NH ^a ib(10), CN ^a s(7), NH ₂ r(7)
1321	1313	-8	C ^{α1} H r ² (33), C ^{α1} H r ¹ (20), NH ^a ib(8), CH ₃ r ¹ (8), C ^{α2} H r ² (7)
1327	1331	4	C ^{α2} H r ¹ (72)
1368	1361	-7	CH ₃ sd(88)
1368	1373	5	CH ₃ sd(97)
1408	1398	-10	C ^{α1} H r ¹ (35), CO ^c ss(15), NH ₂ r(12)
1408	1412	4	CO ^c ss(36), CC ^c s(13), C ^{α1} H r ¹ (10)
1458	1453	-5	CH ₃ ad ^{1,2} (60), CH ₃ ad ^{1,2} (25)
1458	1456	-2	CH ₃ ad ^{1,2} (50), CH ₃ ad ^{1,2} (28), CH ₃ ad ^{1,2} (10)
1458	1461	3	CH ₃ ad ^{1,2} (36), CH ₃ ad ^{1,2} (24), CH ₃ ad ^{1,2} (20)
1458	1463	5	CH ₃ ad ^{1,2} (78), CH ₃ ad ^{1,2} (14)
1522	1523	1	NH ^a ib(34), CN ^a s(24), CO ^a s(12), CC ^ψ s(8)
1560	1567	7	NH ₂ sis(67), CN ^a s(13), CO ^a s(12)
1594	1595	1	CO ^c as(49), CO ^a s(15), NH ₂ sis(15), CN ^a s(7)

Table 3.82: (continued)

frequency (cm ⁻¹)			Potential Energy Distribution
obs.	calc.	dev.	
1610	1605	-5	CO ^c as(33), CO ^a s(25), NH ₂ sis(14), CN ^a s(12)
—	2930	—	CH ₃ ss(97)
—	2937	—	CH ₃ ss(87), CH ₃ as ^{1,2} (12)
—	2960	—	C ^{α2} H s(92)
—	2977	—	C ^{α1} H s(80), CH ₃ as ^{1,2} (14)
—	2985	—	CH ₃ as ^{1,2} (92), C ^{α1} H s(7)
—	3000	—	CH ₃ as ^{1,2} (78), CH ₃ ss(8), CH ₃ as ^{1,2} (8)
—	3008	—	CH ₃ as ^{1,2} (84), C ^{α1} H s(13)
—	3028	—	CH ₃ as ^{1,2} (92), CH ₃ as ^{1,2} (7)
—	3137	—	NH ₂ ss(99)
—	3234	—	NH ₂ as(99)
—	3444	—	NH ^a s(100)

Table 3.83: Alanyl-alanine Two-water Supermolecule Structure with the NH Stretch Coordinate Increased 10%, Water-Excluded Force Constants and Scale Factors used in the Normal Mode Analysis.

frequency (cm^{-1})			Ala-ala pH 13 (mean deviation = 12 cm^{-1})
obs.	calc.	dev.	
			Potential Energy Distribution
—	54	—	$\text{NC}^\phi \text{ t}(28)$, $\text{CC}^c \text{ t}(28)$, $\text{CC}^\psi \text{ t}(24)$, $\text{NH}^a \text{ ob}(9)$
—	93	—	$\text{CC}^c \text{ t}(52)$, $\text{CC}^\psi \text{ t}(33)$, $\text{C}^\omega\text{N} \text{ t}(14)$
—	98	—	$\text{C}^\omega\text{N} \text{ t}(36)$, $\text{NC}^\phi \text{ t}(36)$, $\text{CC}^\psi \text{ t}(8)$
—	135	—	$\text{CC}^\psi \text{ t}(30)$, $\text{NH}^a \text{ ob}(26)$, $\text{NC}^\phi \text{ t}(17)$, $\text{CC}^c \text{ t}(15)$, $\text{C}^{\alpha 2}\text{H} \text{ d}^1(7)$
—	170	—	$\text{CNHC} \text{ sd}(34)$, $\text{CO}^a \text{ sd}(19)$, $\text{C}^{\alpha 2}\text{H} \text{ d}^3(17)$, $\text{CC}^{me} \text{ t}(14)$, $\text{CC}^c \text{ r}(9)$
—	193	—	$\text{CC}^{me} \text{ t}(87)$
—	197	—	$\text{CC}^{me} \text{ t}(80)$
245	246	1	$\text{C}^{\alpha 2}\text{H} \text{ d}^2(27)$, $\text{C}^{\alpha 1}\text{H} \text{ d}^2(13)$
245	264	19	$\text{C}^{\alpha 1}\text{H} \text{ d}^2(21)$, $\text{C}^{\alpha 1}\text{H} \text{ d}^3(18)$, $\text{C}^{\alpha 2}\text{H} \text{ d}^2(16)$, $\text{CO}^a \text{ ob}(11)$, $\text{CC}^c \text{ r}(7)$
—	284	—	$\text{C}^{\alpha 1}\text{H} \text{ d}^2(22)$, $\text{CO}^a \text{ sd}(19)$, $\text{CC}^c \text{ r}(14)$, $\text{CN}^n \text{ t}(12)$, $\text{CO}^a \text{ r}(7)$
334	316	-18	$\text{C}^{\alpha 2}\text{H} \text{ d}^2(19)$, $\text{CC}^c \text{ s}(12)$, $\text{C}^{\alpha 1}\text{H} \text{ d}^1(8)$, $\text{C}^{\alpha 1}\text{H} \text{ d}^3(8)$
334	335	1	$\text{CN}^n \text{ t}(34)$, $\text{CC}^c \text{ r}(19)$, $\text{CNHC} \text{ sd}(9)$, $\text{CO}^a \text{ r}(8)$
377	353	-24	$\text{CN}^n \text{ t}(39)$, $\text{C}^{\alpha 1}\text{H} \text{ d}^3(17)$, $\text{CO}^a \text{ r}(15)$
464	447	-17	$\text{C}^{\alpha 2}\text{H} \text{ d}^1(32)$, $\text{CC}^c \text{ r}(12)$, $\text{C}^{\alpha 2}\text{H} \text{ d}^3(9)$, $\text{C}^{\alpha 1}\text{H} \text{ d}^1(8)$
464	467	3	$\text{C}^{\alpha 1}\text{H} \text{ d}^1(44)$, $\text{C}^{\alpha 2}\text{H} \text{ d}^1(16)$
545	573	28	$\text{C}^{\alpha 2}\text{H} \text{ d}^1(16)$, $\text{C}^{\alpha 2}\text{H} \text{ d}^3(16)$, $\text{CO}^a \text{ sd}(16)$, $\text{CC}^c \text{ r}(16)$, $\text{CC}^\psi \text{ s}(7)$
642	646	4	$\text{CC}^c \text{ sd}(40)$, $\text{CC}^c \text{ s}(18)$, $\text{CO}^a \text{ r}(13)$
688	701	13	$\text{CC}^\psi \text{ s}(18)$, $\text{CO}^a \text{ r}(16)$, $\text{C}^{\alpha 1}\text{H} \text{ d}^3(11)$, $\text{CC}^c \text{ sd}(9)$, $\text{C}^{\alpha 1}\text{H} \text{ d}^2(8)$, $\text{CH}_3 \text{ r}^1(8)$
761	752	-9	$\text{CO}^a \text{ ob}(31)$, $\text{C}^\omega\text{N} \text{ t}(17)$, $\text{NH}^a \text{ ob}(13)$, $\text{NC}^\phi \text{ t}(11)$, $\text{C}^{\alpha 1}\text{H} \text{ d}^3(7)$, $\text{CC}^c \text{ ob}(7)$
778	788	10	$\text{CC}^c \text{ ob}(34)$, $\text{CO}^a \text{ ob}(20)$, $\text{CC}^c \text{ sd}(7)$
—	815	—	$\text{NH}^a \text{ ob}(37)$, $\text{CC}^c \text{ ob}(18)$, $\text{CO}^a \text{ ob}(12)$, $\text{C}^\omega\text{N} \text{ t}(9)$, $\text{NC}^\phi \text{ t}(7)$
872	860	-12	$\text{CC}^c \text{ sd}(15)$, $\text{CC}^{me} \text{ s}(14)$, $\text{CN}^n \text{ s}(12)$, $\text{CC}^c \text{ s}(9)$, $\text{NC}^\phi \text{ s}(7)$, $\text{CO}^c \text{ ss}(7)$, $\text{CC}^{me} \text{ s}(7)$
884	893	9	$\text{CN}^n \text{ s}(15)$, $\text{CC}^{me} \text{ s}(14)$, $\text{CC}^c \text{ s}(10)$, $\text{NH}_2 \text{ w}(8)$, $\text{CC}^c \text{ sd}(7)$, $\text{CC}^{me} \text{ s}(7)$, $\text{CH}_3 \text{ r}^1(7)$
920	929	9	$\text{CC}^{me} \text{ s}(15)$, $\text{CH}_3 \text{ r}^1(11)$, $\text{CC}^c \text{ s}(9)$, $\text{NC}^\phi \text{ s}(8)$, $\text{CH}_3 \text{ r}^2(8)$, $\text{CO}^a \text{ r}(7)$
952	952	0	$\text{CH}_3 \text{ r}^2(23)$, $\text{CC}^\psi \text{ s}(14)$, $\text{NC}^\phi \text{ s}(11)$, $\text{NH}_2 \text{ w}(11)$, $\text{CO}^a \text{ r}(10)$

Table 3.83: (continued)

frequency (cm ⁻¹)			Potential Energy Distribution
obs.	calc.	dev.	
980	970	-10	NH ₂ w(51), CH ₃ r ² (34)
1019	1015	-4	CH ₃ r ¹ (25), NH ₂ r(18), CH ₃ r ² (16), CN ⁿ s(12), C ^{α1} H r ² (8)
1069	1066	-3	C ^{α2} H r ² (30), CH ₃ r ² (17), CC ^c ob(10), CH ₃ r ¹ (7)
1104	1098	-6	CC ^{me} s(44), CN ⁿ s(18), CH ₃ r ¹ (17)
1136	1136	0	CC ^{me} s(33), NC ^φ s(16), CH ₃ r ¹ (13)
1136	1143	7	NH ₂ r(22), C ^{α1} H r ² (19), C ^{α1} H r ¹ (15), CH ₃ r ² (7)
1166	1158	-8	NC ^φ s(21), CH ₃ r ¹ (19), CH ₃ r ² (18), C ^{α2} H d ¹ (13), C ^{α2} H r ¹ (7)
1220	1226	6	NH ^a ib(28), C ^{α2} H r ² (18), CN ^a s(9)
1260	1250	-10	NH ₂ r(19), CN ⁿ s(13), C ^{α2} H r ² (9), C ^{α1} H d ¹ (8), NH ₂ w(8)
1281	1287	6	C ^{α1} H r ² (19), C ^{α2} H r ² (17), NH ^a ib(11), NH ₂ r(7), CH ₃ r ¹ (7)
1320	1314	-6	C ^{α1} H r ² (28), C ^{α1} H r ¹ (20), NH ^a ib(10), C ^{α2} H r ² (8), C ^{α2} H r ¹ (7), CH ₃ r ¹ (7)
1335	1333	-2	C ^{α2} H r ¹ (69)
1367	1361	-6	CH ₃ sd(88)
1367	1373	6	CH ₃ sd(97)
1407	1399	-8	C ^{α1} H r ¹ (33), CO ^c ss(18), NH ₂ r(11), NH ^a ib(7)
1407	1413	6	CO ^c ss(33), CC ^c s(12), C ^{α1} H r ¹ (11)
1459	1453	-6	CH ₃ ad ^{1,2} (60), CH ₃ ad ^{1,2} (26)
1459	1457	-2	CH ₃ ad ^{1,2} (48), CH ₃ ad ^{1,2} (29), CH ₃ ad ^{1,2} (9)
1459	1461	2	CH ₃ ad ^{1,2} (34), CH ₃ ad ^{1,2} (23), CH ₃ ad ^{1,2} (22)
1459	1463	4	CH ₃ ad ^{1,2} (78), CH ₃ ad ^{1,2} (14)
1542	1541	-1	NH ^a ib(29), CN ^a s(27), CO ^a s(12), CC ^ψ s(9)
1578	1573	-5	NH ₂ sis(87)
1602	1598	-4	CO ^c as(81), CO ^c ss(7)
1638	1639	1	CO ^a s(51), CN ^a s(25)
—	2930	—	CH ₃ ss(97)
—	2937	—	CH ₃ ss(87), CH ₃ as ^{1,2} (12)
—	2960	—	C ^{α2} H s(92)
—	2977	—	C ^{α1} H s(80), CH ₃ as ^{1,2} (15)
—	2985	—	CH ₃ as ^{1,2} (92), C ^{α1} H s(7)
—	3000	—	CH ₃ as ^{1,2} (78), CH ₃ ss(8), CH ₃ as ^{1,2} (8)
—	3008	—	CH ₃ as ^{1,2} (84), C ^{α1} H s(13)
—	3028	—	CH ₃ as ^{1,2} (92), CH ₃ as ^{1,2} (7)
—	3137	—	NH ₂ ss(99)

Table 3.83: (continued)

frequency (cm^{-1})			Potential Energy Distribution
obs.	calc.	dev.	
—	3234	—	NH ₂ as(99)
—	3444	—	NH ^a s(100)

frequency (cm^{-1})			Ala-ala in D ₂ O pD 13 (mean deviation = 15 cm^{-1})
obs.	calc.	dev.	
—	53	—	NC ^φ t(28), CC ^c t(26), CC ^ψ t(25), NH ^a ob(9)
—	92	—	CC ^c t(55), CC ^ψ t(36), C ^ω N t(12)
—	96	—	NC ^φ t(39), C ^ω N t(38)
—	132	—	CC ^ψ t(29), NH ^a ob(24), NC ^φ t(18), CC ^c t(17)
—	167	—	CNHC sd(35), CO ^a sd(21), C ^{α2} H d ³ (17), CC ^{me} t(12), CC ^c r(9)
—	192	—	CC ^{me} t(86)
—	197	—	CC ^{me} t(81)
225	228	3	CN ⁿ t(69), C ^{α1} H d ³ (9)
251	246	−5	C ^{α2} H d ² (30), C ^{α1} H d ² (9), CC ^c r(8)
251	265	14	C ^{α1} H d ² (37), CO ^a ob(12), C ^{α2} H d ² (11), C ^{α1} H d ³ (10), CN ⁿ t(8)
200	296	96	CO ^a sd(28), CC ^c r(24), CN ⁿ t(13), C ^{α1} H d ² (9)
332	311	−21	C ^{α2} H d ² (25), C ^{α1} H d ³ (13), C ^{α1} H d ¹ (10), CC ^c s(9)
380	336	−44	CO ^a r(23), CNHC sd(19), C ^{α1} H d ³ (17), CC ^c r(10)
447	431	−16	C ^{α2} H d ¹ (28), CC ^c r(14), C ^{α1} H d ¹ (11), C ^ω N t(10), C ^{α2} H d ³ (7)
447	446	−1	C ^{α1} H d ¹ (39), C ^{α2} H d ¹ (19)
534	549	15	C ^{α2} H d ³ (16), CC ^c r(16), CO ^a sd(15), C ^{α2} H d ¹ (8), C ^ω N t(7)
—	595	—	NH ^a ob(46), NC ^φ t(14), C ^ω N t(13), C ^{α2} H d ¹ (11)
645	629	−16	CO ^a r(25), NH ₂ r(16), CC ^c sd(15), CC ^c s(9), C ^{α1} H d ³ (9), CC ^ψ s(7)
687	666	−21	CC ^c sd(34), CC ^ψ s(13), CC ^c s(10), NH ₂ r(9)
760	756	−4	NH ₂ w(66), CO ^a ob(12)
778	776	−2	CO ^a ob(46), NH ₂ w(12), CC ^{me} s(10), C ^{α1} H d ² (7)
778	789	11	CC ^c ob(58), C ^{α2} H d ² (8), CC ^c sd(7)
866	853	−13	CC ^c sd(15), NC ^φ s(10), CO ^a r(9), CN ⁿ s(9), CC ^{me} s(8), CC ^c s(7)

Table 3.83: (continued)

frequency (cm ⁻¹)			Potential Energy Distribution
obs.	calc.	dev.	
884	894	10	NH ₂ r(16), CH ₃ r ¹ (14), CC ^{me} s(12), CO ^a r(10), CNHC sd(8)
904	895	-9	CH ₃ r ¹ (28), NH ₂ r(21), CC ^{me} s(21), CN ⁿ s(7)
904	907	3	NH ^a ib(24), CC ^c s(21), CH ₃ r ² (16), NC ^φ s(10), CO ^c ss(10), CC ^c sd(9)
938	943	5	CH ₃ r ² (31), CN ⁿ s(14), CC ^ψ s(9), NH ^a ib(8), CO ^a s(7)
995	991	-4	NH ^a ib(43), CH ₃ r ² (21), CC ^ψ s(7)
1066	1064	-2	CC ^{me} s(41), NH ₂ sis(13), CN ⁿ s(12), C ^{α1} H d ³ (7)
1066	1068	2	C ^{α2} H r ² (34), CH ₃ r ² (12), CC ^c ob(9), CH ₃ r ¹ (7)
1097	1094	-3	CH ₃ r ² (18), C ^{α1} H r ² (17), CH ₃ r ¹ (14), C ^{α1} H d ² (9), NH ₂ sis(8), CO ^a s(7)
1113	1130	17	CC ^{me} s(34), NC ^φ s(22), CH ₃ r ¹ (8)
1163	1153	-10	CH ₃ r ¹ (27), C ^{α2} H d ¹ (15), CH ₃ r ² (14), NC ^φ s(8), CC ^{me} s(8)
1163	1179	16	NH ₂ sis(72), CN ⁿ s(18)
1209	1193	-16	CH ₃ r ¹ (17), C ^{α1} H d ¹ (13), CN ⁿ s(13), CH ₃ r ² (9), NC ^φ s(8), C ^{α1} H r ¹ (7)
1278	1268	-10	C ^{α2} H r ² (45), CH ₃ r ¹ (10), CO ^c ss(7)
1308	1304	-4	C ^{α1} H r ² (59), CH ₃ r ¹ (11), C ^{α1} H r ¹ (7)
1328	1331	3	C ^{α2} H r ¹ (75), C ^{α2} H r ² (7)
1360	1360	0	CH ₃ sd(50), C ^{α1} H r ¹ (28), CO ^c ss(7)
1365	1364	-1	C ^{α1} H r ¹ (40), CH ₃ sd(39)
1371	1373	2	CH ₃ sd(98)
1409	1410	1	CO ^c ss(49), CC ^c s(16), CC ^c sd(8), CH ₃ sd(8)
1455	1451	-4	CH ₃ ad ^{1,2} (82), CH ₃ ad ^{1,2} (7)
1455	1456	1	CH ₃ ad ^{1,2} (62), CH ₃ ad ^{1,2} (22)
1455	1458	3	CH ₃ ad ^{1,2} (49), CH ₃ ad ^{1,2} (21), CH ₃ ad ^{1,2} (11)
1455	1463	8	CH ₃ ad ^{1,2} (76), CH ₃ ad ^{1,2} (15)
1512	1506	-6	CN ^a s(32), CO ^a s(19), CC ^ψ s(15), NH ^a ib(8), NC ^φ s(7), CO ^a r(7)
1596	1597	1	CO ^c as(82), CO ^c ss(7)
1638	1631	-7	CO ^a s(52), CN ^a s(31)
—	2266	—	NH ₂ ss(99)
—	2391	—	NH ₂ as(99)
—	2526	—	NH ^a s(99)
—	2930	—	CH ₃ ss(97)

Table 3.83: (continued)

frequency (cm ⁻¹)			Potential Energy Distribution
obs.	calc.	dev.	
—	2937	—	CH ₃ ss(87), CH ₃ as ^{1,2} (12)
—	2960	—	C ^{α2} H s(92)
—	2977	—	C ^{α1} H s(79), CH ₃ as ^{1,2} (15)
—	2985	—	CH ₃ as ^{1,2} (92), C ^{α1} H s(7)
—	3000	—	CH ₃ as ^{1,2} (78), CH ₃ ss(8), CH ₃ as ^{1,2} (8)
—	3008	—	CH ₃ as ^{1,2} (83), C ^{α1} H s(13)
—	3028	—	CH ₃ as ^{1,2} (92), CH ₃ as ^{1,2} (7)

frequency (cm ⁻¹)			Potential Energy Distribution
obs.	calc.	dev.	
—	54	—	NC ^φ t(28), CC ^c t(28), CC ^ψ t(24), NH ^a ob(9)
—	93	—	CC ^c t(52), CC ^ψ t(33), C ^ω N t(15)
—	97	—	C ^ω N t(36), NC ^φ t(35), CC ^ψ t(8)
—	134	—	CC ^ψ t(29), NH ^a ob(26), NC ^φ t(17), CC ^c t(15), C ^{α2} H d ¹ (7)
—	169	—	CNHC sd(34), CO ^a sd(20), C ^{α2} H d ³ (17), CC ^{me} t(13), CC ^c r(9)
—	193	—	CC ^{me} t(87)
—	197	—	CC ^{me} t(80)
251	246	-5	C ^{α2} H d ² (27), C ^{α1} H d ² (14), C ^{α2} H d ¹ (7)
251	264	13	C ^{α1} H d ² (20), C ^{α1} H d ³ (18), C ^{α2} H d ² (16), CO ^a ob(11), CC ^c r(7)
—	282	—	C ^{α1} H d ² (23), CO ^a sd(19), CC ^c r(15), CN ⁿ t(10), CO ^a r(7)
337	315	-22	C ^{α2} H d ² (19), CC ^c s(11), C ^{α1} H d ³ (8), C ^{α1} H d ¹ (7)
337	334	-3	CN ⁿ t(35), CC ^c r(18), CNHC sd(9), CO ^a r(8)
387	353	-34	CN ⁿ t(37), C ^{α1} H d ³ (18), CO ^a r(15), C ^{α1} H d ¹ (7)
460	446	-14	C ^{α2} H d ¹ (31), CC ^c r(12), C ^{α1} H d ¹ (10), C ^{α2} H d ³ (9)
460	464	4	C ^{α1} H d ¹ (44), C ^{α2} H d ¹ (17)
534	569	35	C ^{α2} H d ¹ (17), CC ^c r(17), C ^{α2} H d ³ (16), CO ^a sd(15), CC ^ψ s(7)
640	645	5	CC ^c sd(38), CC ^c s(17), CO ^a r(15)
678	693	15	CC ^ψ s(18), CO ^a r(14), C ^{α1} H d ³ (11), CC ^c sd(11), C ^{α1} H d ² (7), CH ₃ r ¹ (7)
743	750	7	CO ^a ob(35), C ^ω N t(16), NH ^a ob(10), NC ^φ t(10), C ^{α1} H d ³ (7)
778	783	5	CC ^c ob(24), CO ^a ob(18), NH ^a ob(11), C ^{α1} H r ² (7)

Table 3.83: (continued)

frequency (cm ⁻¹)			Potential Energy Distribution
obs.	calc.	dev.	
—	805	—	CC ^c ob(26), NH ^a ob(20), C ^{α1} H r ² (14), C ^ω N t(7)
829	835	6	CC ^{me} s(31), C ^{α1} H r ² (23), NH ^a ob(13), CO ^a ob(7)
866	865	-1	CC ^c sd(19), CC ^c s(12), CC ^{me} s(11), CC ^ψ s(9), CO ^c ss(9), C ^{α1} H r ² (8), CH ₃ r ¹ (8), NC ^φ s(7)
909	898	-11	C ^{α1} H r ¹ (61), CN ⁿ s(19), NH ₂ w(8), NH ₂ r(7)
909	913	4	C ^{α1} H r ² (15), CN ⁿ s(9), CH ₃ r ² (9), CC ^c s(7), NH ₂ w(7)
927	929	2	CC ^{me} s(15), CC ^c s(10), CH ₃ r ¹ (10), CH ₃ r ² (9), NC ^φ s(8)
944	959	15	NH ₂ w(19), CH ₃ r ² (16), CH ₃ r ² (11), CC ^ψ s(8), NC ^φ s(8), CO ^a r(7)
981	977	-4	CH ₃ r ² (44), NH ₂ w(38)
1065	1066	1	C ^{α2} H r ² (31), CH ₃ r ² (17), CC ^c ob(10), CH ₃ r ¹ (7)
1101	1087	-14	CH ₃ r ¹ (43), CC ^{me} s(19), CN ⁿ s(10), NH ₂ r(9)
1132	1128	-4	CC ^{me} s(17), CC ^{me} s(15), NC ^φ s(10), C ^{α1} H r ² (7)
1154	1144	-10	CC ^{me} s(24), CH ₃ r ¹ (16), CC ^{me} s(13)
1195	1160	-35	NC ^φ s(24), CH ₃ r ² (16), CH ₃ r ¹ (14), C ^{α2} H d ¹ (11)
1239	1226	-13	NH ^a ib(25), C ^{α2} H r ² (16), CN ⁿ s(10), CN ^a s(7)
1239	1242	3	NH ₂ r(27), CN ⁿ s(13), CH ₃ r ¹ (11)
1273	1270	-3	NH ₂ r(23), C ^{α2} H r ² (19)
1304	1321	17	C ^{α2} H r ¹ (38), C ^{α2} H r ² (15), NH ^a ib(14), CH ₃ r ¹ (7)
1343	1343	0	C ^{α2} H r ¹ (36), NH ^a ib(18), CC ^ψ s(9), CO ^c ss(7)
1369	1362	-7	CH ₃ sd(88)
1369	1374	5	CH ₃ sd(97)
1408	1410	2	CO ^c ss(50), CC ^c s(17), CC ^c sd(8), CH ₃ sd(8), CO ^c as(7)
1458	1451	-7	CH ₃ ad ^{1,2} (71), CH ₃ ad ^{1,2} (22)
1458	1456	-2	CH ₃ ad ^{1,2} (45), CH ₃ ad ^{1,2} (30), CH ₃ ad ^{1,2} (11)
1458	1458	0	CH ₃ ad ^{1,2} (44), CH ₃ ad ^{1,2} (24), CH ₃ ad ^{1,2} (11), CH ₃ ad ^{1,2} (9)
1458	1463	5	CH ₃ ad ^{1,2} (77), CH ₃ ad ^{1,2} (14)
1544	1540	-4	NH ^a ib(30), CN ^a s(27), CO ^a s(12), CC ^ψ s(9)
1583	1572	-11	NH ₂ sis(85), CN ^a s(8)
1605	1598	-7	CO ^c as(80), CO ^c ss(7)
1644	1632	-12	CO ^a s(52), CN ^a s(25), NH ₂ sis(7)
—	2201	—	C ^{α1} H s(98)
—	2930	—	CH ₃ ss(98)
—	2937	—	CH ₃ ss(87), CH ₃ as ^{1,2} (12)

Table 3.83: (continued)

frequency (cm ⁻¹)			Potential Energy Distribution
obs.	calc.	dev.	
—	2960	—	C ^{α2} H s(92)
—	2984	—	CH ₃ as ^{1,2} (95)
—	3000	—	CH ₃ as ^{1,2} (78), CH ₃ ss(8), CH ₃ as ^{1,2} (8)
—	3004	—	CH ₃ as ^{1,2} (94)
—	3028	—	CH ₃ as ^{1,2} (92), CH ₃ as ^{1,2} (7)
—	3137	—	NH ₂ ss(99)
—	3234	—	NH ₂ as(99)
—	3444	—	NH ^a s(100)

frequency (cm ⁻¹)			Ala-1- ¹³ C-Ala pH 13 (mean deviation = 14 cm ⁻¹)
obs.	calc.	dev.	
—	54	—	NC ^φ t(28), CC ^c t(28), CC ^ψ t(24), NH ^a ob(9)
—	93	—	CC ^c t(52), CC ^ψ t(33), C ^ω N t(14)
—	97	—	C ^ω N t(37), NC ^φ t(36), CC ^ψ t(7)
—	134	—	CC ^ψ t(30), NH ^a ob(26), NC ^φ t(17), CC ^c t(15), C ^{α2} H d ¹ (7)
—	169	—	CNHC sd(35), CO ^a sd(20), C ^{α2} H d ³ (17), CC ^{me} t(14), CC ^c r(9)
—	193	—	CC ^{me} t(87)
—	197	—	CC ^{me} t(80)
236	246	10	C ^{α2} H d ² (27), C ^{α1} H d ² (13)
236	264	28	C ^{α1} H d ² (21), C ^{α1} H d ³ (18), C ^{α2} H d ² (15), CO ^a ob(11), CO ^a sd(7), CC ^c r(7)
—	283	—	C ^{α1} H d ² (22), CO ^a sd(19), CC ^c r(14), CN ⁿ t(11), CO ^a r(7)
334	316	-18	C ^{α2} H d ² (19), CC ^c s(12), C ^{α1} H d ¹ (8), C ^{α1} H d ³ (8)
334	334	0	CN ⁿ t(34), CC ^c r(19), CNHC sd(9), CO ^a r(8)
376	353	-23	CN ⁿ t(39), C ^{α1} H d ³ (17), CO ^a r(14)
467	447	-20	C ^{α2} H d ¹ (32), CC ^c r(12), C ^{α2} H d ³ (9), C ^{α1} H d ¹ (8)
467	467	0	C ^{α1} H d ¹ (44), C ^{α2} H d ¹ (16)
542	572	30	C ^{α2} H d ¹ (16), C ^{α2} H d ³ (16), CO ^a sd(16), CC ^c r(16), CC ^ψ s(7)
644	646	2	CC ^c sd(39), CC ^c s(17), CO ^a r(14)
687	699	12	CC ^ψ s(17), CO ^a r(15), C ^{α1} H d ³ (10), CC ^c sd(10), C ^{α1} H d ² (9), CH ₃ r ¹ (8)
748	739	-9	CO ^a ob(44), C ^ω N t(13), C ^{α1} H d ³ (11), NC ^φ t(8)

Table 3.83: (continued)

frequency (cm ⁻¹)			Potential Energy Distribution
obs.	calc.	dev.	
778	782	4	CC ^c ob(32), NH ^a ob(13), CO ^a ob(12), C ^{α2} H d ² (7), CC ^c sd(7)
—	812	—	NH ^a ob(36), CC ^c ob(24), C ^ω N t(11), NC ^φ t(8)
850	857	7	CC ^c sd(15), CC ^{me} s(15), CN ⁿ s(12), NC ^φ s(8), CC ^c s(8), CC ^ψ s(7), CO ^c ss(7), CC ^{me} s(7)
883	892	9	CC ^{me} s(14), CN ⁿ s(13), CC ^c s(10), CC ^{me} s(8), CH ₃ r ¹ (8), CC ^c sd(7), NH ₂ w(7)
920	928	8	CC ^{me} s(14), CH ₃ r ¹ (11), CO ^a r(9), CC ^c s(7), CNHC sd(7)
943	947	4	CH ₃ r ² (24), CC ^ψ s(13), NC ^φ s(13), NH ₂ w(9), CC ^c s(7), CO ^a r(7)
980	969	-11	NH ₂ w(53), CH ₃ r ² (33)
1021	1014	-7	CH ₃ r ¹ (26), NH ₂ r(18), CH ₃ r ² (16), CN ⁿ s(12), C ^{α1} H r ² (8)
1066	1066	0	C ^{α2} H r ² (30), CH ₃ r ² (17), CC ^c ob(10), CH ₃ r ¹ (7)
1103	1097	-6	CC ^{me} s(44), CN ⁿ s(19), CH ₃ r ¹ (16)
1129	1135	6	CC ^{me} s(34), NC ^φ s(18), CH ₃ r ¹ (12)
1129	1142	13	NH ₂ r(23), C ^{α1} H r ² (20), C ^{α1} H r ¹ (15), CN ⁿ s(7), CH ₃ r ² (7)
1166	1157	-9	CH ₃ r ¹ (20), NC ^φ s(18), CH ₃ r ² (18), C ^{α2} H d ¹ (14), C ^{α2} H r ¹ (7)
1221	1224	3	NH ^a ib(30), C ^{α2} H r ² (18), CN ^a s(10)
1256	1250	-6	NH ₂ r(20), CN ⁿ s(14), C ^{α1} H d ¹ (9), NH ₂ w(9), C ^{α2} H r ² (7)
1279	1283	4	C ^{α2} H r ² (20), C ^{α1} H r ² (14), NH ^a ib(10), CN ^a s(7), NH ₂ r(7)
1321	1313	-8	C ^{α1} H r ² (34), C ^{α1} H r ¹ (21), CH ₃ r ¹ (9), NH ^a ib(8)
1327	1331	4	C ^{α2} H r ¹ (73)
1368	1361	-7	CH ₃ sd(88)
1368	1373	5	CH ₃ sd(97)
1408	1398	-10	C ^{α1} H r ¹ (34), CO ^c ss(16), NH ₂ r(11)
1408	1412	4	CO ^c ss(35), CC ^c s(13), C ^{α1} H r ¹ (11)
1458	1453	-5	CH ₃ ad ^{1,2} (60), CH ₃ ad ^{1,2} (25)
1458	1456	-2	CH ₃ ad ^{1,2} (50), CH ₃ ad ^{1,2} (27), CH ₃ ad ^{1,2} (10)
1458	1460	2	CH ₃ ad ^{1,2} (37), CH ₃ ad ^{1,2} (24), CH ₃ ad ^{1,2} (18)
1458	1463	5	CH ₃ ad ^{1,2} (77), CH ₃ ad ^{1,2} (15)
1522	1522	0	NH ^a ib(35), CN ^a s(24), CO ^a s(12), CC ^ψ s(8)
1560	1567	7	NH ₂ sis(67), CN ^a s(13), CO ^a s(12)
1594	1595	1	CO ^c as(49), CO ^a s(15), NH ₂ sis(15), CN ^a s(7)
1610	1605	-5	CO ^c as(33), CO ^a s(25), NH ₂ sis(14), CN ^a s(12)

Table 3.83: (continued)

frequency (cm ⁻¹)			Potential Energy Distribution
obs.	calc.	dev.	
—	2930	—	CH ₃ ss(97)
—	2937	—	CH ₃ ss(87), CH ₃ as ^{1,2} (12)
—	2960	—	C ^{α2} H s(92)
—	2977	—	C ^{α1} H s(80), CH ₃ as ^{1,2} (15)
—	2985	—	CH ₃ as ^{1,2} (92), C ^{α1} H s(7)
—	3000	—	CH ₃ as ^{1,2} (78), CH ₃ ss(8), CH ₃ as ^{1,2} (8)
—	3008	—	CH ₃ as ^{1,2} (84), C ^{α1} H s(13)
—	3028	—	CH ₃ as ^{1,2} (92), CH ₃ as ^{1,2} (7)
—	3137	—	NH ₂ ss(99)
—	3234	—	NH ₂ as(99)
—	3444	—	NH ^a s(100)

Table 3.84: Alanyl-alanine Isolated Structure, Two-water Water-Excluded Force Constants and Scale Factors used for the Normal Mode Analysis.

frequency (cm ⁻¹)			Ala-ala pH 13 (mean deviation = 16 cm ⁻¹)
obs.	calc.	dev.	
			Potential Energy Distribution
—	53	—	NC ^φ t(25), CC ^c t(24), CC ^ψ t(22), CO ^c ss(7)
—	89	—	CC ^ψ t(35), CC ^c t(35)
—	101	—	C ^ω N t(39), NC ^φ t(23), C ^{α2} H d ¹ (7)
—	131	—	NC ^φ t(31), NH ^a ob(27), CC ^c t(11), C ^{α2} H d ¹ (7)
—	169	—	CNHC sd(32), C ^{α2} H d ³ (17), CO ^a sd(15), CC ^c r(11)
—	198	—	CC ^{me} t(75), CH ₃ r ² (7)
—	202	—	CC ^{me} t(69), CH ₃ ss(9)
245	219	-26	C ^{α2} H d ² (26), CN ^a s(10), NC ^φ s(8), CO ^a sd(8), CC ^ψ s(7), CC ^{me} t(7)
245	270	25	C ^{α1} H d ³ (19), C ^{α2} H d ² (13), C ^{α1} H d ² (11), CC ^c r(9)
—	282	—	C ^{α1} H d ² (17), CC ^c r(15), CO ^a sd(9), C ^{α2} H d ² (7), CC ^{me} s(7)
334	308	-26	C ^{α2} H d ² (18), C ^{α2} H d ³ (16), CC ^c s(12), C ^{α1} H d ¹ (8), C ^{α1} H d ² (7), C ^{α1} H d ³ (7)
334	341	7	CN ⁿ t(22), C ^{α1} H d ¹ (11), CO ^a r(10), CNHC sd(9), C ^{α1} H d ³ (9), CC ^c r(9), CO ^a sd(8)
377	355	-22	CN ⁿ t(59), CO ^a r(13), CNHC sd(8)
464	456	-8	C ^{α2} H d ¹ (17), CC ^c r(14), C ^{α1} H d ¹ (13), C ^ω N t(13), NC ^φ s(10), CC ^ψ t(10), C ^{α2} H d ² (7)
464	461	-3	C ^{α1} H d ¹ (33), C ^{α2} H d ¹ (20), C ^{α1} H d ³ (11), CC ^{me} s(9)
545	552	7	CC ^c r(18), CO ^a sd(17), C ^ω N t(13), C ^{α2} H d ³ (10), C ^{α2} H d ² (9)
642	650	8	CC ^c sd(19), CC ^c s(16), CO ^a r(14), C ^{α1} H d ³ (10)
688	688	0	CC ^ψ s(23), C ^{α1} H d ³ (10), NC ^φ t(9), CO ^c as(9), CO ^a r(8), CC ^c sd(7), CC ^c ob(7)
761	744	-17	CO ^a ob(42), NC ^φ t(20), NH ^a ob(7)
778	772	-6	CC ^c ob(28), CC ^c sd(22), C ^{α2} H d ² (9), CC ^{me} s(7)
800	820	20	NH ^a ob(43), NH ^a ib(16), CO ^a ob(10), C ^ω N t(7)
872	859	-13	CNHC sd(19), CN ⁿ s(17), CC ^{me} s(17), CO ^a s(9), C ^{α1} H d ² (8)
884	875	-9	CH ₃ r ¹ (15), CC ^{me} s(13), NC ^φ s(11), C ^{α2} H d ³ (9), CO ^a ob(9), CO ^a sd(7), CC ^c t(7)
920	916	-4	CNHC sd(15), CC ^c s(10), CN ⁿ s(8), CC ^{me} s(8), CH ₃ r ² (8), CO ^a s(7), NC ^φ s(7), CH ₃ r ² (7)
952	944	-8	CH ₃ r ² (25), CH ₃ r ² (13), CC ^c s(8), CNHC sd(7)
980	987	7	NH ₂ w(67), CH ₃ r ² (11)

Table 3.84: (continued)

frequency (cm ⁻¹)			Potential Energy Distribution
obs.	calc.	dev.	
1019	1014	-5	CH ₃ r ² (20), NH ₂ r(19), CN ⁿ s(16), CC ^{me} s(12), CH ₃ r ¹ (11)
1069	1080	11	C ^{α1} H d ² (20), C ^{α2} H r ² (12), C ^{α2} H d ³ (10), CC ^{me} s(9), CH ₃ r ¹ (8)
1104	1089	-15	C ^{α2} H r ² (22), C ^{α1} H d ² (14), CN ⁿ s(9), CC ^{me} s(9), CH ₃ r ¹ (8), CH ₃ r ² (8), C ^{α2} H d ³ (7)
1136	1135	-1	NH ₂ r(17), C ^{α1} H r ² (16), CN ⁿ s(13), CH ₃ r ² (10), C ^{α1} H r ¹ (8)
1136	1140	4	NC ^φ s(24), CC ^{me} s(19), CH ₃ r ² (10), C ^{α2} H d ¹ (9)
1166	1158	-8	C ^{α2} H d ¹ (32), CH ₃ r ¹ (21), CC ^{me} s(10), CH ₃ r ² (10)
1220	1206	-14	NH ^a ib(14), C ^{α2} H r ² (11), CN ⁿ s(9), CN ^a s(8)
1260	1265	5	NH ₂ r(14), C ^{α2} H r ¹ (10), CN ⁿ s(8), NH ₂ w(8)
1281	1291	10	C ^{α2} H r ¹ (31), CO ^c ss(15), C ^{α2} H s(7), NH ₂ r(7)
1320	1311	-9	C ^{α2} H r ² (21), C ^{α2} H r ¹ (13), CC ^{me} s(8)
1335	1346	11	CH ₃ sd(33), C ^{α1} H r ¹ (13), CH ₃ sd(10), C ^{α1} H r ² (7)
1367	1357	-10	CH ₃ sd(36), CH ₃ sd(32)
1367	1384	17	CH ₃ sd(15), C ^{α1} H r ¹ (12), CH ₃ sd(12), C ^{α2} H r ¹ (10)
1407	1406	-1	CH ₃ ad ^{1,2} (28), C ^{α1} H r ¹ (14), C ^{α1} H r ² (10), NH ₂ r(10)
1407	1422	15	CO ^c ss(15), C ^{α1} H r ¹ (14), CH ₃ ad ^{1,2} (12), CC ^c t(9), CH ₃ sd(9)
1459	1449	-10	CH ₃ ad ^{1,2} (17), CH ₃ ad ^{1,2} (14), CH ₃ ad ^{1,2} (14), CH ₃ ad ^{1,2} (12), CH ₃ sd(8)
1459	1455	-4	CH ₃ ad ^{1,2} (33), CH ₃ ad ^{1,2} (23), CH ₃ r ¹ (15), CH ₃ ad ^{1,2} (8)
1459	1457	-2	CH ₃ ad ^{1,2} (35), CH ₃ ad ^{1,2} (17), CH ₃ as ^{1,2} (9), CH ₃ ad ^{1,2} (9)
1459	1476	17	CH ₃ ad ^{1,2} (26), CH ₃ ad ^{1,2} (21), CH ₃ as ^{1,2} (9), CH ₃ ad ^{1,2} (7)
1542	1540	-2	CN ^a s(35), NH ^a ib(20), NH ^a ob(12), CO ^a r(9), CO ^a ob(7)
1578	1571	-7	NH ₂ sis(92)
1602	1632	30	CO ^a s(54), CO ^a sd(10), CN ^a s(9), CO ^a r(8)
1638	1683	45	CO ^c as(48), CC ^c ob(28), CO ^c ss(8), CC ^c sd(7)
—	2781	—	CH ₃ ss(51), CH ₃ ss(11), CH ₃ as ^{1,2} (8), CC ^{me} t(8), CH ₃ r ¹ (7)
—	2853	—	CH ₃ ss(45), CH ₃ ss(20), CH ₃ r ¹ (12)
—	2901	—	C ^{α1} H s(41), CH ₃ as ^{1,2} (17), C ^{α1} H r ² (12), CH ₃ ss(10)
—	2923	—	C ^{α2} H s(46), C ^{α2} H r ¹ (19), CH ₃ as ^{1,2} (16), C ^{α1} H s(8)
—	2956	—	CH ₃ as ^{1,2} (25), CH ₃ as ^{1,2} (22), CH ₃ as ^{1,2} (17), C ^{α1} H s(7)
—	2982	—	CH ₃ as ^{1,2} (43), CH ₃ as ^{1,2} (15), CH ₃ as ^{1,2} (9), C ^{α2} H s(8), CH ₃ ss(8)
—	2988	—	CH ₃ as ^{1,2} (30), CH ₃ as ^{1,2} (17), CH ₃ as ^{1,2} (15), C ^{α1} H s(8)

Table 3.84: (continued)

frequency (cm ⁻¹)			Potential Energy Distribution
obs.	calc.	dev.	
—	3004	—	CH ₃ as ^{1,2} (50), CH ₃ as ^{1,2} (10), C ^{α1} H s(9), C ^{α2} H s(7), CH ₃ ad ^{1,2} (7)
—	3139	—	NH ₂ ss(99)
—	3236	—	NH ₂ as(99)
—	3402	—	NH ^a s(86), NH ^a ib(12)

frequency (cm ⁻¹)			Potential Energy Distribution
obs.	calc.	dev.	
—	52	—	NC ^φ t(26), CC ^ψ t(23), CC ^c t(23)
—	88	—	CC ^ψ t(35), CC ^c t(35)
—	99	—	C ^ω N t(39), NC ^φ t(24), C ^{α2} H d ¹ (7)
—	128	—	NC ^φ t(32), NH ^a ob(25), CC ^c t(12)
—	167	—	CNHC sd(33), C ^{α2} H d ³ (16), CO ^a sd(15), CC ^c r(10)
—	197	—	CC ^{me} t(66), CH ₃ r ² (7)
—	201	—	CC ^{me} t(65), CH ₃ ss(8)
225	210	-15	CN ⁿ t(26), CC ^{me} t(16), C ^{α2} H d ² (12), CC ^{me} t(7)
251	245	-6	CN ⁿ t(34), C ^{α2} H d ² (23), CC ^c r(9), C ^{α1} H d ³ (7)
251	269	18	C ^{α1} H d ² (25), C ^{α1} H d ³ (14), CN ⁿ t(10), CO ^a ob(9), C ^ω N t(8), C ^{α2} H d ¹ (7), CC ^{me} s(7)
—	292	—	CO ^a sd(20), CC ^c r(15), CN ⁿ t(15), C ^{α2} H d ² (11), CN ^a s(7)
332	305	-27	C ^{α2} H d ² (17), C ^{α2} H d ³ (14), C ^{α1} H d ² (11), CC ^c s(8), C ^{α1} H d ¹ (7)
380	336	-44	CNHC sd(21), CO ^a r(20), C ^{α1} H d ¹ (13), C ^{α1} H d ³ (9)
447	439	-8	C ^ω N t(21), C ^{α2} H d ¹ (15), C ^{α1} H d ¹ (14), CC ^c r(14), NC ^φ s(10), CC ^ψ t(7)
447	442	-5	C ^{α1} H d ¹ (29), C ^{α2} H d ¹ (21), C ^{α1} H d ³ (11), CC ^{me} s(8)
534	536	2	C ^ω N t(21), CC ^c r(20), CO ^a sd(18), C ^{α2} H d ² (11), C ^{α2} H d ³ (10)
—	593	—	NH ^a ob(46), NC ^φ t(22), NH ^a ib(20)
645	621	-24	CO ^a r(22), CC ^ψ s(20), NH ₂ r(17), C ^{α1} H d ³ (13)
687	673	-14	CC ^c sd(23), CC ^c s(14), CO ^c as(14), CC ^c ob(11), CC ^ψ s(10)
760	762	2	NH ₂ w(37), CO ^a ob(26)
778	769	-9	CC ^c ob(24), CC ^c sd(19), NH ₂ w(15), C ^{α2} H d ² (8), CC ^{me} s(7)

Table 3.84: (continued)

frequency (cm ⁻¹)			Potential Energy Distribution
obs.	calc.	dev.	
778	784	6	NH ₂ w(28), CO ^a ob(26), CC ^{me} s(10), CC ^c ob(7)
866	838	-28	NH ₂ r(27), NC ^φ s(10), CH ₃ r ¹ (8), CNHC sd(7)
884	854	-30	CNHC sd(14), CC ^{me} s(14), CN ⁿ s(13), CH ₃ r ¹ (10), CO ^a s(9), C ^{α1} H d ² (9)
904	887	-17	NC ^φ s(13), CNHC sd(12), NH ₂ r(12), CH ₃ r ¹ (12), CC ^{me} s(10)
904	918	14	CC ^c s(22), CH ₃ r ² (16), CC ^c sd(11), C ^{α2} H d ³ (8), CO ^c ss(7), CC ^c t(7)
938	939	1	CH ₃ r ² (30), CN ⁿ s(17), CNHC sd(10), CO ^a s(7), NH ₂ r(7)
995	991	-4	NH ^a ib(30), CH ₃ r ² (16), NH ^a ob(15), NH ^a s(9)
1066	1052	-14	CC ^{me} s(29), C ^{α1} H d ² (28), NH ₂ sis(14), CN ⁿ s(11)
1066	1082	16	C ^{α2} H r ² (33), C ^{α2} H d ³ (17), CC ^c ob(8), NC ^φ s(7), CH ₃ r ² (7)
1097	1096	-1	CH ₃ r ² (18), C ^{α1} H r ² (17), CC ^ψ s(11), CO ^a s(8), CH ₃ r ¹ (8)
1113	1133	20	NC ^φ s(22), CC ^{me} s(19), CH ₃ r ² (15), C ^{α2} H d ¹ (8), C ^{α2} H d ² (7)
1163	1155	-8	C ^{α2} H d ¹ (34), CH ₃ r ¹ (22), CC ^{me} s(11), CH ₃ r ² (11)
1163	1179	16	NH ₂ sis(73), CN ⁿ s(12)
1209	1195	-14	CN ⁿ s(20), C ^{α1} H d ³ (16), CH ₃ r ¹ (12), CH ₃ r ² (7)
1278	1279	1	C ^{α2} H r ¹ (35), CO ^c ss(12), C ^{α2} H r ² (8), C ^{α2} H s(7)
1308	1303	-5	C ^{α2} H r ² (27), C ^{α2} H r ¹ (16), CC ^c s(12), CC ^{me} s(8), CO ^c ss(7), CH ₃ r ¹ (7)
1328	1333	5	C ^{α1} H r ² (27), C ^{α1} H r ¹ (13), C ^{α1} H s(10), CC ^{me} s(7)
1360	1355	-5	CH ₃ sd(52), CH ₃ sd(21)
1365	1363	-2	CH ₃ sd(21), CH ₃ sd(20), CH ₃ ad ^{1,2} (14), C ^{α1} H r ¹ (9)
1371	1380	9	C ^{α1} H r ¹ (37), CH ₃ sd(14)
1409	1419	10	CO ^c ss(18), CH ₃ ad ^{1,2} (12), CC ^c t(10), C ^{α1} H r ¹ (8), CH ₃ sd(8), CO ^c as(7)
1455	1439	-16	CH ₃ ad ^{1,2} (41), CH ₃ ad ^{1,2} (19), CH ₃ sd(10)
1455	1453	-2	CH ₃ ad ^{1,2} (39), CH ₃ ad ^{1,2} (30), CH ₃ r ¹ (9)
1455	1455	0	CH ₃ ad ^{1,2} (36), CH ₃ ad ^{1,2} (19), CH ₃ r ¹ (14), CH ₃ as ^{1,2} (9)
1455	1475	20	CH ₃ ad ^{1,2} (24), CH ₃ ad ^{1,2} (23), CH ₃ as ^{1,2} (10), CH ₃ ad ^{1,2} (8)
1512	1503	-9	CN ^a s(35), CO ^a r(15), CC ^ψ s(9), CO ^a ob(8)
1596	1624	28	CO ^a s(57), CN ^a s(11), CO ^a sd(11), CO ^a r(7)
1638	1680	42	CO ^c as(49), CC ^c ob(29), CC ^c sd(8), CO ^c ss(8)
—	2266	—	NH ₂ ss(99)

Table 3.84: (continued)

frequency (cm ⁻¹)			Potential Energy Distribution
obs.	calc.	dev.	
—	2392	—	NH ₂ as(99)
—	2496	—	NH ^a s(85), NH ^a ib(12)
—	2781	—	CH ₃ ss(52), CH ₃ ss(11), CH ₃ as ^{1,2} (8), CC ^{me} t(8), CH ₃ r ¹ (7)
—	2853	—	CH ₃ ss(46), CH ₃ ss(19), CH ₃ r ¹ (12)
—	2900	—	C ^{α1} H s(41), CH ₃ as ^{1,2} (17), C ^{α1} H r ² (12), CH ₃ ss(10)
—	2923	—	C ^{α2} H s(47), C ^{α2} H r ¹ (20), CH ₃ as ^{1,2} (16), C ^{α1} H s(7)
—	2956	—	CH ₃ as ^{1,2} (25), CH ₃ as ^{1,2} (22), CH ₃ as ^{1,2} (17), C ^{α1} H s(7)
—	2982	—	CH ₃ as ^{1,2} (42), CH ₃ as ^{1,2} (16), CH ₃ as ^{1,2} (9), C ^{α2} H s(8), CH ₃ ss(8)
—	2988	—	CH ₃ as ^{1,2} (30), CH ₃ as ^{1,2} (19), CH ₃ as ^{1,2} (16), C ^{α1} H s(8)
—	3006	—	CH ₃ as ^{1,2} (49), CH ₃ as ^{1,2} (11), C ^{α1} H s(9), C ^{α2} H s(8)

frequency (cm ⁻¹)			2-d Ala-ala pH 13 (mean deviation = 18 cm ⁻¹)
obs.	calc.	dev.	
—	53	—	NC ^φ t(26), CC ^c t(24), CC ^ψ t(22)
—	89	—	CC ^ψ t(35), CC ^c t(35), C ^ω N t(7)
—	100	—	C ^ω N t(38), NC ^φ t(23), C ^{α2} H d ¹ (7)
—	130	—	NC ^φ t(32), NH ^a ob(27), CC ^c t(11), C ^{α2} H d ¹ (7)
—	168	—	CNHC sd(32), C ^{α2} H d ³ (17), CO ^a sd(16), CC ^c r(10)
—	198	—	CC ^{me} t(75), CH ₃ r ² (7)
—	202	—	CC ^{me} t(70), CH ₃ ss(9)
251	219	-32	C ^{α2} H d ² (25), CN ^a s(10), NC ^φ s(8), CO ^a sd(8), CC ^ψ s(7), CC ^{me} t(7)
251	269	18	C ^{α1} H d ³ (19), C ^{α2} H d ² (13), C ^{α1} H d ² (10), CC ^c r(9)
—	280	—	C ^{α1} H d ² (19), CC ^c r(15), CO ^a sd(9), CC ^{me} s(7)
337	307	-30	C ^{α2} H d ² (19), C ^{α2} H d ³ (16), CC ^c s(12), C ^{α1} H d ¹ (9), C ^{α1} H d ³ (7), CC ^c sd(7)
337	341	4	CN ⁿ t(24), C ^{α1} H d ¹ (10), C ^{α1} H d ³ (9), CO ^a r(9), CC ^c r(9), CNHC sd(8), CO ^a sd(8)
387	354	-33	CN ⁿ t(58), CO ^a r(13), CNHC sd(8)
460	454	-6	C ^{α1} H d ¹ (24), CC ^c r(14), NC ^φ s(10), C ^ω N t(10), C ^{α2} H d ¹ (9), CC ^ψ t(9), C ^{α2} H d ² (7)
460	459	-1	C ^{α2} H d ¹ (28), C ^{α1} H d ¹ (23), CC ^{me} s(11), C ^{α1} H d ³ (10)

Table 3.84: (continued)

frequency (cm ⁻¹)			Potential Energy Distribution
obs.	calc.	dev.	
534	549	15	CC ^c r(19), CO ^a sd(16), C ^ω N t(13), C ^{α2} H d ² (10), C ^{α2} H d ³ (10)
640	645	5	CO ^a r(16), CC ^c sd(15), CC ^c s(14), C ^{α1} H d ³ (12), CC ^ψ s(8)
678	682	4	CC ^ψ s(20), CC ^c sd(11), CO ^c as(11), CC ^c ob(9), NC ^φ t(9), C ^{α1} H d ³ (7)
743	743	0	CO ^a ob(42), NC ^φ t(20)
778	771	-7	CC ^c ob(28), CC ^c sd(21), C ^{α2} H d ² (9), CC ^{me} s(7)
—	802	—	NH ^a ob(28), C ^{α1} H r ² (17), C ^{α1} H r ¹ (8), C ^{α1} H d ² (8), NH ^a ib(7), CO ^a r(7), CC ^{me} s(7)
829	830	1	CC ^{me} s(18), C ^ω N t(16), NH ^a ob(13), NH ^a ib(10), CO ^a ob(10), C ^{α1} H r ² (7)
866	866	0	NC ^φ s(13), CC ^c sd(12), CC ^ψ s(10), CO ^a ob(10), CH ₃ r ¹ (9), CO ^a s(7), CNHC sd(7), CC ^{me} s(7)
909	897	-12	C ^{α1} H r ² (23), C ^{α1} H r ¹ (14), CO ^a s(10), CNHC sd(8), C ^{α1} H s(7)
909	905	-4	C ^{α1} H r ¹ (34), CNHC sd(16), CN ⁿ s(10), NH ₂ r(8)
927	922	-5	CH ₃ r ² (18), CC ^c s(14), CN ⁿ s(13), NH ₂ w(7)
944	956	12	CH ₃ r ² (30), CH ₃ r ² (15), CN ⁿ s(14)
981	993	12	NH ₂ w(67), CH ₃ r ² (11)
1065	1077	12	C ^{α1} H d ² (21), CH ₃ r ¹ (13), C ^{α2} H r ² (10), C ^{α2} H d ³ (9)
1101	1089	-12	C ^{α2} H r ² (25), C ^{α1} H d ² (11), CN ⁿ s(9), CH ₃ r ² (9), C ^{α2} H d ³ (8), CC ^{me} s(7), CH ₃ r ¹ (7)
1132	1110	-22	NH ₂ r(14), CH ₃ r ² (11), C ^{α1} H r ¹ (10), CC ^{me} s(10), CH ₃ r ¹ (7)
1154	1149	-5	CC ^{me} s(24), C ^{α2} H d ¹ (18), NC ^φ s(15)
1195	1158	-37	C ^{α2} H d ¹ (24), CH ₃ r ¹ (19), CH ₃ r ² (18), NC ^φ s(12)
1239	1222	-17	CN ⁿ s(13), C ^{α2} H r ² (12), NH ^a ib(11)
1239	1261	22	NH ₂ r(18), CN ⁿ s(11), NH ₂ w(8), CH ₃ r ¹ (7)
1273	1285	12	NH ₂ r(30), C ^{α2} H r ¹ (16)
1304	1303	-1	C ^{α2} H r ¹ (32), C ^{α2} H r ² (16), CO ^c ss(12), C ^{α2} H s(9), CC ^c s(7)
1343	1341	-2	CH ₃ sd(29), NH ^a ib(9), CH ₃ sd(9)
1369	1357	-12	CH ₃ sd(37), CH ₃ sd(31)
1369	1384	15	CH ₃ sd(15), CH ₃ sd(15), CH ₃ ad ^{1,2} (13), NH ^a ib(9), C ^{α2} H r ¹ (9)

Table 3.84: (continued)

frequency (cm ⁻¹)			Potential Energy Distribution
obs.	calc.	dev.	
1408	1414	6	CO ^c ss(20), CC ^c t(12), CH ₃ ad ^{1,2} (12), CH ₃ ad ^{1,2} (12), CO ^c as(9), CH ₃ sd(7)
1458	1442	-16	CH ₃ ad ^{1,2} (42), CH ₃ sd(15), CH ₃ ad ^{1,2} (10), CH ₃ ad ^{1,2} (10)
1458	1451	-7	CH ₃ ad ^{1,2} (44), CH ₃ ad ^{1,2} (19), CH ₃ r ¹ (14)
1458	1454	-4	CH ₃ ad ^{1,2} (36), CH ₃ ad ^{1,2} (21), CH ₃ ad ^{1,2} (17)
1458	1474	16	CH ₃ ad ^{1,2} (23), CH ₃ ad ^{1,2} (23), CH ₃ as ^{1,2} (10), CH ₃ ad ^{1,2} (9)
1544	1539	-5	CN ^a s(37), NH ^a ib(21), NH ^a ob(12), CO ^a r(9)
1583	1569	-14	NH ₂ sis(90)
1605	1624	19	CO ^a s(55), CO ^a sd(10), CO ^a r(9), CN ^a s(8), NH ₂ sis(7)
1644	1683	39	CO ^c as(48), CC ^c ob(28), CO ^c ss(8), CC ^c sd(7)
—	2159	—	C ^{α1} H s(73), C ^{α1} H r ² (24)
—	2782	—	CH ₃ ss(53), CH ₃ ss(11), CC ^{me} t(8), CH ₃ as ^{1,2} (7), CH ₃ r ¹ (7)
—	2854	—	CH ₃ ss(51), CH ₃ ss(18), CH ₃ r ¹ (12)
—	2919	—	C ^{α2} H s(39), CH ₃ as ^{1,2} (20), C ^{α2} H r ¹ (16), CH ₃ as ^{1,2} (7)
—	2948	—	CH ₃ as ^{1,2} (47), CH ₃ as ^{1,2} (13), CH ₃ sd(9), CH ₃ as ^{1,2} (9)
—	2977	—	CH ₃ as ^{1,2} (24), C ^{α2} H s(20), CH ₃ as ^{1,2} (13), CH ₃ as ^{1,2} (12), C ^{α2} H r ¹ (9)
—	2982	—	CH ₃ as ^{1,2} (53), CH ₃ ss(11), CH ₃ as ^{1,2} (10)
—	2998	—	CH ₃ as ^{1,2} (68), CH ₃ ad ^{1,2} (9)
—	3138	—	NH ₂ ss(99)
—	3236	—	NH ₂ as(99)
—	3402	—	NH ^a s(86), NH ^a ib(12)

frequency (cm ⁻¹)			Potential Energy Distribution
obs.	calc.	dev.	
—	53	—	NC ^φ t(25), CC ^c t(24), CC ^ψ t(22), CO ^c ss(7)
—	89	—	CC ^ψ t(35), CC ^c t(35)
—	100	—	C ^ω N t(39), NC ^φ t(24), C ^{α2} H d ¹ (7)
—	131	—	NC ^φ t(31), NH ^a ob(27), CC ^c t(11), C ^{α2} H d ¹ (7)
—	169	—	CNHC sd(32), C ^{α2} H d ³ (17), CO ^a sd(15), CC ^c r(10)
—	198	—	CC ^{me} t(75), CH ₃ r ² (7)
—	202	—	CC ^{me} t(70), CH ₃ ss(9)

Table 3.84: (continued)

frequency (cm ⁻¹)			Potential Energy Distribution
obs.	calc.	dev.	
236	219	-17	C ^{α2} H d ² (26), CN ^a s(10), NC ^φ s(8), CO ^a sd(8), CC ^ψ s(7), CC ^{me} t(7)
236	269	33	C ^{α1} H d ³ (19), C ^{α2} H d ² (13), C ^{α1} H d ² (10), CC ^c r(9)
—	281	—	C ^{α1} H d ² (18), CC ^c r(14), CO ^a sd(9), CN ^a s(7), CC ^{me} s(7)
334	307	-27	C ^{α2} H d ² (19), C ^{α2} H d ³ (16), CC ^c s(12), C ^{α1} H d ¹ (8), C ^{α1} H d ² (7), C ^{α1} H d ³ (7), CC ^c sd(7)
334	341	7	CN ⁿ t(22), C ^{α1} H d ¹ (11), CO ^a r(10), CNHC sd(9), C ^{α1} H d ³ (9), CC ^c r(9), CO ^a sd(8)
376	355	-21	CN ⁿ t(59), CO ^a r(13), CNHC sd(8)
467	455	-12	C ^{α2} H d ¹ (17), C ^{α1} H d ¹ (14), CC ^c r(14), C ^ω N t(13), NC ^φ s(10), CC ^ψ t(10), C ^{α2} H d ² (7)
467	460	-7	C ^{α1} H d ¹ (32), C ^{α2} H d ¹ (20), C ^{α1} H d ³ (11), CC ^{me} s(9)
542	552	10	CC ^c r(18), CO ^a sd(17), C ^ω N t(12), C ^{α2} H d ³ (10), C ^{α2} H d ² (9)
644	649	5	CC ^c sd(18), CC ^c s(16), CO ^a r(14), C ^{α1} H d ³ (11)
687	688	1	CC ^ψ s(22), C ^{α1} H d ³ (11), NC ^φ t(10), CO ^a r(9), CO ^c as(9), CC ^c sd(8), CC ^c ob(7)
748	729	-19	CO ^a ob(49), NC ^φ t(16), CC ^{me} s(7)
778	771	-7	CC ^c ob(27), CC ^c sd(23), C ^{α2} H d ² (9), CC ^{me} s(7)
—	815	—	NH ^a ob(45), NH ^a ib(17), C ^ω N t(8)
850	855	5	CNHC sd(20), CC ^{me} s(16), CN ⁿ s(15), CO ^a s(10), C ^{α1} H d ² (7), C ^ω N t(7)
883	873	-10	CH ₃ r ¹ (15), CC ^{me} s(13), NC ^φ s(11), C ^{α2} H d ³ (9), CO ^a sd(7), CO ^a ob(7), CC ^c t(7)
920	915	-5	CNHC sd(15), CN ⁿ s(9), CH ₃ r ² (9), CC ^c s(8), CC ^{me} s(8), CO ^a s(7), NC ^φ s(7)
943	941	-2	CH ₃ r ² (26), CH ₃ r ² (12), CC ^c s(10)
980	986	6	NH ₂ w(67), CH ₃ r ² (12)
1021	1013	-8	CH ₃ r ² (20), NH ₂ r(19), CN ⁿ s(15), CC ^{me} s(11), CH ₃ r ¹ (11), C ^{α1} H r ¹ (7)
1066	1079	13	C ^{α1} H d ² (22), C ^{α2} H r ² (10), CC ^{me} s(10), C ^{α2} H d ³ (9), CH ₃ r ¹ (9), CN ⁿ s(7)
1103	1089	-14	C ^{α2} H r ² (24), C ^{α1} H d ² (12), CN ⁿ s(9), CH ₃ r ² (9), C ^{α2} H d ³ (8), CC ^{me} s(8), CH ₃ r ¹ (7)
1129	1135	6	NH ₂ r(16), C ^{α1} H r ² (15), CN ⁿ s(13), CH ₃ r ² (10), C ^{α1} H r ¹ (8)

Table 3.84: (continued)

frequency (cm ⁻¹)			Potential Energy Distribution
obs.	calc.	dev.	
1129	1136	7	NC ^φ s(23), CC ^{me} s(18), CH ₃ r ² (10), C ^{α2} H d ¹ (8)
1166	1158	-8	C ^{α2} H d ¹ (33), CH ₃ r ¹ (21), CC ^{me} s(11), CH ₃ r ² (9)
1221	1205	-16	NH ^a ib(14), C ^{α2} H r ² (10), CN ^a s(8), CN ⁿ s(8)
1256	1265	9	NH ₂ r(15), C ^{α2} H r ¹ (9), CN ⁿ s(9), NH ₂ w(8)
1279	1289	10	C ^{α2} H r ¹ (31), CO ^c ss(14), C ^{α2} H s(7), NH ₂ r(7)
1321	1310	-11	C ^{α2} H r ² (23), C ^{α2} H r ¹ (15), CC ^{me} s(9), CC ^c s(7)
1327	1344	17	CH ₃ sd(29), C ^{α1} H r ¹ (14), CH ₃ sd(10), C ^{α1} H r ² (9)
1368	1357	-11	CH ₃ sd(35), CH ₃ sd(34)
1368	1382	14	CH ₃ sd(17), CH ₃ sd(13), C ^{α2} H r ¹ (10), C ^{α1} H r ¹ (9)
1408	1404	-4	CH ₃ ad ^{1,2} (26), C ^{α1} H r ¹ (17), NH ₂ r(11), C ^{α1} H r ² (10)
1408	1422	14	CO ^c ss(15), C ^{α1} H r ¹ (14), CH ₃ ad ^{1,2} (12), CC ^c t(9), CH ₃ sd(9)
1458	1449	-9	CH ₃ ad ^{1,2} (16), CH ₃ ad ^{1,2} (14), CH ₃ ad ^{1,2} (14), CH ₃ ad ^{1,2} (12), CH ₃ sd(8)
1458	1455	-3	CH ₃ ad ^{1,2} (34), CH ₃ ad ^{1,2} (23), CH ₃ r ¹ (15)
1458	1457	-1	CH ₃ ad ^{1,2} (36), CH ₃ ad ^{1,2} (19), CH ₃ as ^{1,2} (9), CH ₃ ad ^{1,2} (7)
1458	1475	17	CH ₃ ad ^{1,2} (26), CH ₃ ad ^{1,2} (20), CH ₃ as ^{1,2} (9), CH ₃ ad ^{1,2} (8)
1522	1522	0	CN ^a s(32), NH ^a ib(24), NH ^a ob(13), CO ^a r(7)
1560	1567	7	NH ₂ sis(71), CO ^a s(14)
1594	1595	1	CO ^a s(42), NH ₂ sis(26), CO ^a sd(8)
1610	1682	72	CO ^c as(48), CC ^c ob(29), CC ^c sd(8), CO ^c ss(8)
—	2781	—	CH ₃ ss(51), CH ₃ ss(11), CH ₃ as ^{1,2} (8), CC ^{me} t(8), CH ₃ r ¹ (7)
—	2853	—	CH ₃ ss(45), CH ₃ ss(20), CH ₃ r ¹ (12)
—	2900	—	C ^{α1} H s(41), CH ₃ as ^{1,2} (17), C ^{α1} H r ² (12), CH ₃ ss(10)
—	2923	—	C ^{α2} H s(46), C ^{α2} H r ¹ (19), CH ₃ as ^{1,2} (16), C ^{α1} H s(8)
—	2956	—	CH ₃ as ^{1,2} (25), CH ₃ as ^{1,2} (22), CH ₃ as ^{1,2} (17), C ^{α1} H s(7)
—	2982	—	CH ₃ as ^{1,2} (43), CH ₃ as ^{1,2} (15), CH ₃ as ^{1,2} (9), C ^{α2} H s(8), CH ₃ ss(8)
—	2988	—	CH ₃ as ^{1,2} (30), CH ₃ as ^{1,2} (17), CH ₃ as ^{1,2} (15), C ^{α1} H s(8)
—	3004	—	CH ₃ as ^{1,2} (50), CH ₃ as ^{1,2} (10), C ^{α1} H s(9), C ^{α2} H s(7), CH ₃ ad ^{1,2} (7)
—	3139	—	NH ₂ ss(99)
—	3236	—	NH ₂ as(99)
—	3402	—	NH ^a s(86), NH ^a ib(12)

Chapter 4

DISCUSSION

4.1 Comparison of Hydration Models

Scale factors for calculated vapor phase structures have been shown to be transferable between molecules [Fogarasi and Pulay, 1985]. A single set of scale factors has also been shown to accurately predict vibrational spectra for different conformations of the same molecule [Williams, 1992; Mirkin and Krimm, 1990]. The scale factors determined in these studies show, because of their transferability, that they can correct the systematic errors due to the approximations made in solving the Schrödinger equation (1.10).

In the methanol work [second section of the results, and Williams *et al*, 1995], one goal was to determine a model of hydration so that a single set of scale factors could accurately predict both vapor and aqueous phase spectra. If this was achieved, the effort required to determine scale factors for aqueous spectra would be considerably reduced. However, no model of hydration was found which could directly apply vapor phase scale factors to accurately predict experimental aqueous spectra.

Several models of hydration were studied: force constants calculated from the isolated geometry scaled to aqueous frequencies; self consistent reaction field theory (SCRF, modeling the effect of hydration through a solvent field with a uniform

dielectric); and force constants calculated from supermolecule structures scaled to aqueous frequencies. Scale factors for nonpolar coordinates vary little among the various hydration models. This was expected since nonpolar coordinates are minimally affected by formation of hydrogen bonds. For this report, the models were compared using methanol and ethanol.

Experimental frequencies shift down 15 cm^{-1} for the CO *s*, and up 70 cm^{-1} for the OH *b* for methanol in aqueous solution compared to vapor phase [Williams *et al*, 1995]. Except for the CH₃ rocks ($r^{1,2}$) the nonpolar coordinate scale factors, for all models of solvation of methanol [Williams *et al*, 1995] and ethanol (table 3.4), were similar.

The first model considered was isolated geometry force constants scaled to aqueous frequencies. Scale factors for various polar coordinates using this model had already been shown to be different from vapor phase scale factors [Williams and Lowrey, 1991; Lowrey and Williams, 1992a and b; Williams 1992; Williams *et al*, 1995]. It was not anticipated that this model be consistent with the vapor phase, the same unscaled force constants were used to predict two sets of experimental frequencies. Comparison of scale factors for vapor and aqueous phases does, however, provide a basis for the anticipated changes between force constants for vapor versus solvated models. For methanol and ethanol, the polar CO *s* and OH *b* coordinates differed from the methanol vapor phase scale factors but were consistent between methanol and ethanol.

Most scale factors for methanol and ethanol using the SCRF model are similar to the scale factors developed for the isolated methanol or ethanol geometry scaled to aqueous frequencies. The CO *s* for methanol is closer to the vapor phase CO *s* scale factor, however, for ethanol it is not. This is also seen in the geometries, the SCRF geometries do not differ from the isolated geometries. Anticipated effects on geometry due to solvation are not seen. The conclusion is that the SCRF model is no better than the isolated structure. In addition, due to the additional calculation

involved in determining the molecular volume, SCRF requires greater computational time.

The final model considered was the supermolecule model. In a study of *N*-methylacetamide (NMA) [Williams, 1992], scale factors for isolated NMA (the vacuum NMA structure scaled to experimental frequencies from NMA isolated in a frozen N₂ matrix) were similar to scale factors determined for the three water NMA supermolecule scaled to aqueous NMA spectra. This result suggested that supermolecule structures might be an adequate model of the effects of solvation on molecular structure.

The CO and OH stretch (*s*) coordinates of methanol were most affected by formation of hydrogen bonds in supermolecule models. The CO *s* was predicted to increase upon formation of a hydrogen bond to the oxygen and decrease upon formation of a hydrogen bond to the hydroxyl hydrogen. In the two and three water supermolecules, where hydrogen bonds are made to both the oxygen and hydroxyl hydrogen of methanol, the net result is that the CO *s* decreases [Williams *et al*, 1995]. The OH *s* increases with formation of hydrogen bonds. Differences in ethanol geometry (see table 3.3) between the solvation models, are only observed for the O–C and O–H bond lengths and the H–O–C bond angle. The two water supermolecule predicts the O–C bond length to be shorter, the O–H bond length longer, and the H–O–C bond angle larger than the isolated and SCRF models, just as was seen in methanol [Williams *et al*, 1995].

Supermolecule scale factors for methanol [Williams *et al*, 1995] and ethanol [thesis], unlike NMA, were not similar to scale factors for vapor phase methanol. The CO *s* vapor phase scale factor accurately predicted the aqueous frequency when a single hydrogen bond was formed between water and the methanol oxygen in a one-water supermolecule model. However, the vapor phase OH *b* scale factor predicted a greater than observed shift in frequencies. Conversely, when a single hydrogen bond was formed between water and the methanol hydroxyl hydrogen, the OH *b* vapor

phase scale factor accurately predicted the aqueous phase frequency, but the CO *s* vapor phase scale factor was too high. As the number of waters was increased, the scale factors for both the CO *s* and the OH *b* approached the values for the vapor phase. In the four-water supermolecule, the scale factors for both CO *s* and OH *b* were more similar to the vapor phase than the two- and three-water supermolecules but were still significantly different from the vapor phase scale factors [Williams *et al*, 1995]. The supermolecule model for methanol does not predict the changes due to solvation as well as it did for NMA.

The ethanol two-water supermolecule scale factor for the OH *b* was similar to the vapor phase scale factor, unlike the methanol two-water supermolecule scale factor. However, the ethanol CO *s* scale factor was not the same as the vapor phase scale factor. The polar scale factors for the two-water methanol and ethanol supermolecules were not similar to each other. The ethanol supermolecule scale factor for the OH *b* matched the methanol vapor phase scale factor better than the isolated or SCRF model, but the CO *s* was not as good.

None of the models adequately describe the effects of solvation because none yielded a set of scale factors that correctly predicted frequencies for both vapor and aqueous phase spectra. Supermolecule models incorporating large numbers of water molecules approach the ability to predict force constants so that one set of scale factors may be used for both vapor and aqueous phase structures [Williams *et al*, 1995].

A disadvantage of supermolecule models is the greatly increased computation time required for the water molecules. In addition, some other problems were noted with the use of supermolecules as a model of solvation. When ring structures were formed in supermolecule structures, redundant coordinates were introduced. These extra coordinates were omitted. Choosing a different set of coordinates to omit had no effect on frequencies except for the hydrogen-bonded water molecules [Williams and Lowrey, 1991; Lowrey *et al*, 1993]. This was not true for methanol

[Williams *et al*, 1995]. Different calculations, with different sets of redundant internal coordinates omitted from the calculation, led to artifacts. Calculated frequencies and potential energy distributions for methanol changed because of coupling between water and methanol coordinates. The coupling was not observed in the *ab initio* calculations performed in Cartesian coordinates. To avoid these artifacts the Cartesian coordinates and force constants associated with water were removed after geometry optimization and prior to conversion to internal coordinates [Williams *et al*, 1995].

4.2 Water-Excluded Scale Factors

None of the three models of hydration compared above satisfied the desire to have one set of scale factors that could be used for both isolated and aqueous phases. The difficulties with supermolecules and the ineffectiveness of SCRF suggested the explicit modeling of solvation effects through incorporation into the scale factors was the best alternative. This left one difficulty. Protein secondary structures often contain distinct hydrogen bonds. In order to fully model protein solution structures, the influences of hydrogen bond formation on internal coordinates must be determined. With small molecules, intramolecular hydrogen bonds cannot be formed.

Formation of hydrogen bonded structures using water supermolecules is not the same as modeling the effects of solvation. Solvation is not well modeled by supermolecules and to try to add sufficient waters explicitly would be prohibitively expensive—addition of water molecules adds considerable time to computational calculations. The number of molecules required to model solvation is not known [Williams *et al*, 1995] and the model, a static set of water molecules surrounding the solute, does not mimic the constantly changing structure of liquid water. The effects of solvation are, instead, implicitly incorporated into the model by scaling to experimental aqueous frequencies. Incorporated water molecules can be used to model the effects of hydrogen bonding. To avoid the ring redundancies and coupling artifacts the water

coordinates and force constants can be deleted from the calculations prior to conversion to internal coordinates for scaling. This preserves the effect of the hydrogen bond on the geometry [Williams *et al*, 1995].

The validity of this model must be proven. This can be done by demonstrating transferability of the scale factors between different molecular geometries using this model.

Transferability of Water-Excluded Scale Factors

In this section only the transferability of scale factors developed for small molecules (methylamine, acetate, glycine, glycinate, and *N*-methylacetamide) are considered. Larger molecules will be considered in the sections on alanine and alanyl-alanine. Comparison of scale factors for hydrogen bonded coordinates must be done carefully, the number and location of hydrogen bonds strongly affects the choice of scale factor. The scale factors for the water-excluded models are listed in tables 3.18 and 3.29.

Most nonpolar coordinate scale factors transferred between different structures well. Hydrogen stretch coordinates transfer less well than scale factors for other nonpolar coordinates. This is partly due to limitations in the harmonic approximation; hydrogen stretches are affected more by anharmonicity than are the heavy atom stretches. Not all hydrogen stretch coordinates were scaled, either because their spectra were not measured for all isotopic species or because of ambiguity in their assignments.

The CC *s* coordinate scale factor transferred between the acid and base forms of glycine, but not to NMA (see tables 3.18 and 3.29). This may be due to differences in the electronic structure of the CC bonds: one of the glycine carbons is bound to two oxygen atoms that share a negative charge, the NMA equivalent is bound to an oxygen atom and a nitrogen atom neither being charged.

The CN *s* scale factor does not transfer between basic and acidic conforma-

tions of methylamine or glycine. The addition of the proton and charge is sufficient to change the CN *s* scale factor. There is also a change in the degree of hydration state for methylamine. The scale factor does not transfer from the acid structure of methylamine to the acid form of glycine, probably due to the difference in hydration states of the amine groups. The CN *s* scale factor does transfer from methylamine in base to glycinate even though the glycinate amine group does not form an explicit hydrogen bond.

The scale factors for methyl and methylene group deformations transfer relatively well with the exception of the CH₃ *r* scale factors. The CH₂ hydrogen stretch coordinate scale factors transfer between the two glycine conformations but the CH₃ *ss* and *as* scale factors transfer less well. There seems to be better transferability of NCH₃ stretch scale factors than CCH₃ stretch scale factors.

The COO *ss* and *as* transfer well between acetate and glycinate. The CCOO *sd* and *r* differ by about four percent, slightly greater than the three percent used as our criterion for good transferability. The CCOO *w* did not transfer well. The amine group scale factors can not be compared; the protonated states and hydrated structures, in glycine or glycinate and methylamine acid or base, are different. Part of this difference is the preference of the carboxyl group of glycinate to form hydrogen bonds compared to the amine group.

Retention of Electronic Effects of Hydrogen Bonding

The effects of hydrogen bonding on molecular structure are observed as changes in the optimized internal coordinates. The effects on electronic distribution are seen as consistent trends in the scale factors associated with coordinates affected by the formation of new hydrogen bonds. These effects are observed in glycinate over the one, two, and four water supermolecule calculations (see tables 3.18 and 3.17) and the NMA one, two, and three water supermolecule calculations (see tables 3.29 and 3.28).

For glycinate (see table 3.17), C^3O^4 stretch coordinate increases with the addition of water molecules. The C^3O^5 stretch does not change consistently. One of the CH stretch coordinates increases, while the other decreases. Both of the NH stretch coordinates decrease as do the CN and CC stretches. Consistent increases are observed for both of the OCN angle bends and both of the HNC angle bends: the carbonyl oxygen and the amine hydrogens are getting closer together.

Consistent changes in the internal coordinates are reflected in several of the scale factors for glycinate. The CO *ss* scale factor decreases with increasing numbers of hydrogen bonds while the CO *as* increases. Four of the CH₂ deformations (scissor, rock, wag and twist) decrease with an increase in hydrogen bonding. The NH₂ scissors decreases and the NH₂ twist and wag both increase with the addition of water molecules. Finally, the CCOO *r* decreases. Other scale factors change, but not consistently as hydrogen bonds are added.

It is interesting to note that the nonpolar CH₂ deformation scale factors change consistently. This may be attributable to coincidence: nonpolar groups are not expected to be reactive with water. However, consistent changes are observed in the calculated structures at the CH, CC, and CN stretches which may reflect consistent changes in the electronic structure for these nonpolar coordinates.

The five different NMA supermolecule structures allow us to examine the effect of adding a hydrogen bond to either the amide hydrogen or to the carbonyl oxygen. The CO *s* internal coordinate and scale factor increase with an increase in hydrogen bonding. Both the CN *s* internal coordinate and scale factor decrease with an increase in the number of hydrogen bonds. Changes to the CNHC *sd* scale factor reflect consistent changes in internal coordinates for the HNC and CNC bond angles. These changes are observed regardless of the placement of the water.

The CC *s* internal coordinate decreases with formation of hydrogen bonds to the oxygen, and increases only slightly (0.0002 Å), but consistently, with addition of hydrogen bonds to the amide hydrogen (see table 3.28). The CC *s* scale factor

increases with addition of hydrogen bonds to the oxygen. A very large decrease in the scale factor is observed upon formation of a hydrogen bond with the amide hydrogen (see table 3.29), certainly much larger than might be expected from the very small change in the calculated bond lengths.

The NC *s* internal coordinate increases with hydrogen bond formation to the oxygen and decreases with formation to the amide hydrogen. The scale factor increases with bond formation to the oxygen but is not consistent upon hydrogen bond formation with the hydrogen.

The NH *s* internal coordinate increases with formation of hydrogen bonds. With hydrogen bond formation to oxygen the change is small. The NH *s* scale factor increases only with formation of a hydrogen bond to the amide hydrogen, but in contrast to what was observed with a small change in the CC *s*, it is insensitive to the formation of a hydrogen bond with oxygen. The NCH₃ *r* scale factor increases with formation of a hydrogen bond to the amide hydrogen, as do the HCN bond angles. None of the other NCH₃ deformations change consistently.

Finally, the OCC bond angle decreases with the formation of hydrogen bonds. The CO *sd* scale factor decreases with formation of hydrogen bonds only with the carbonyl oxygen. The CO *r*, however, changes consistently only with formation of hydrogen bonds to the amide hydrogen. Consistent changes to the CO *ob* scale factor are not observed.

The difference in the responses of the internal coordinates to hydrogen bond formation compared to the scale factor responses for those coordinates cannot be predicted by considering the magnitude of the change in internal coordinates. Neither can the direction of the shifts of the scale factors be predicted from the direction of change in the internal coordinate.

4.3 C $^{\alpha}$ Coordinates

The principle goal in scaling alanine was the development of scale factors for the C $^{\alpha}$ coordinates: the C $^{\alpha}$ H deformations ($d^{1,2,3}$), C $^{\alpha}$ H $r^{1,2}$, and the side chain CC me stretch (s). Our calculations show that the C $^{\alpha}$ H $d^{1,2,3}$ contribute to the PED at 415, 343, and 279 cm $^{-1}$ in base, and at 409, 335, and 275 cm $^{-1}$ in acid, in good agreement with previous studies [Susi and Byler, 1980; Diem *et al*, 1982; and Srivastava and Gupta, 1972]. For the C $^{\alpha}$ H r coordinates of alaninate, the shift in frequency due to deuteration of the C $^{\alpha}$ hydrogen (alaninate- d_4) is more obvious in D $_2$ O (Figure 3.28) than in H $_2$ O (Figure 3.27). In figure 3.28, the shift of peaks from 1334 and 1292 cm $^{-1}$ (alaninate, bottom), and from 1332 and 1282 cm $^{-1}$ (alaninate- d_3 , middle), to 940 and 893 cm $^{-1}$ (alaninate- d_4 , top), is clearly seen. At pH=1 in H $_2$ O (figure 3.29) peak shifts are observed from 1364 and 1328 cm $^{-1}$ (alanine, bottom) and 1364 and 1322 cm $^{-1}$ (alanine- d_3 , middle) to one peak at 879 cm $^{-1}$ (alanine- d_4 , top).

Frequencies with contributions from CC me s and CN ter s have been determined from the difference spectra shown in Figures 3.31 (alaninate, pH=13) and 3.32 (alanine, pH=1). Difference spectra shown at the top of Figures 3.31 and 3.32 were generated by subtracting the normalized spectrum of $^{13}\text{C}^{me}$ substituted alaninate or alanine at pH=1 from that of the spectrum of the normal isotopic species. Our calculations on both supermolecule structures of alaninate (Table 3.53 for the CO $_2$ bridged structure, and Table 3.57 for the NH-OC bridged structure) show contributions from the CC me s at 1368, 1140, 1020, 957, 853, 785, and 622 cm $^{-1}$ (there is less than 4% difference between the two structures for the CC me s coordinate at each frequency). Difference peaks (see figure 3.31) are observed at all but the 957, and 622 cm $^{-1}$ frequencies. Our calculations on alanine at pH=1 (Table 3.59) show CC me s contributions at 1328, 1214, 1117, 1008, 951, 920, and 746 cm $^{-1}$. Difference peaks are observed at all but the 1328, 1214, and 951 cm $^{-1}$ frequencies. Widely varying the scale factor for the CC me s did not eliminate contributions to these frequencies. Difference peaks are observed in Figure 3.31, top, at 1072 and 927 cm $^{-1}$ and in Fig-

ure 3.32, top, at 823 cm^{-1} , where there are no calculated contributions by the CC^{me} s to the PED. There is a substantial CH_3 r^2 contribution calculated at these frequencies that we believe accounts for the differences in the experimental spectra.

The spectra at the bottom of Figures 3.31 and 3.32 were generated by subtracting the normalized spectrum of ^{15}N substituted alaninate or ^{15}N substituted alanine at $\text{pH}=1$ from that of alaninate, or alanine at $\text{pH}=1$, respectively. Our calculations for alaninate (Table 3.53) show contributions from the CN^{ter} s at 1238, 1140, 927, 853, 785, and 539 cm^{-1} , all of which are observed in Figure 3.31, bottom. As with the CC^{me} s, there is less than 4% difference at each frequency between the two supermolecule structures. Other observed frequencies in Figure 3.31 bottom, at 1020, 1353, and 1368 cm^{-1} , contain calculated contributions from NH_2 twist (tw). For alanine at $\text{pH}=1$ we calculate CN^{ter} s contributions at 1117, 1008, 951, 920, 823, 746, 603, and 528 cm^{-1} . We see difference peaks at all but the 951, 746, and 603 cm^{-1} frequencies. The predicted contributions at these unobserved frequencies is less than eight percent.

Our assignments of the NH_2 scissor ($scis$) and COO^- antisymmetric stretch (as) in alaninate disagree with those by Venyaminov and Kalnin [1990] who assign a COO^- stretch to the higher frequency (1595 cm^{-1}) and an NH_2 deformation to the lower frequency (1556 cm^{-1}). Comparing Figures 3.27 and 3.28 for all six isotopic species, the peak at about 1600 cm^{-1} shifts upon solvation in D_2O , which implies a strong contribution from the NH_2 $scis$ coordinate. The peak at 1564 cm^{-1} (Figure 3.27, bottom) does not shift in D_2O , indicating the principle contribution is from the COO^- as coordinate. Our *ab initio* calculations for the isotopic species in D_2O support our interpretation. When the scale factors are adjusted to agree with the Venyaminov and Kalnin [1990] interpretation, shifting the COO^- as in H_2O to the higher frequency, the calculated frequencies for the COO^- as in D_2O no longer match the experimental data. In addition, scale factors adjusted to match the Venyaminov and Kalnin [1990] assignments differ by more than 3% from results for glycinate

[Lowrey *et al*, 1993] and acetate [Williams and Lowrey, 1991].

A Fermi resonance analysis [Krimm and Dwivedi, 1982] was performed on the alaninate spectrum which indicates that the observed peak at 590 cm^{-1} is an overtone of a combination of the 279 and 343 cm^{-1} bands in resonance with a fundamental calculated to be at 622 cm^{-1} , which is shifted to the observed 654 cm^{-1} . A Fermi resonance was suspected because of the necessity of fitting the CN^{ter} s and CC^{me} s coordinates to the modes predicted by the difference spectra of Figure 3.31. We could not obtain a good fit if all five observed frequencies between 900 and 500 cm^{-1} were included. Removing one observed frequency provided a good fit of the coordinates to the difference spectra with one predicted frequency between the 590 and 654 observed peaks. Adjusting scale factors did not correct the predicted frequency to either observed peak. The Fermi resonance calculation provides a good match of the coordinates to the difference spectra as well as a good match to the predicted frequency. A resonance in all of the alaninate isotopic species at about 600 cm^{-1} is suggested by our calculations. The fundamental and overtone frequencies for each isotopic species are labeled in the legends to Figures 3.27 and 3.28.

The CCOO wag coordinate in glycinate [Lowrey *et al*, 1993] and acetate [Williams and Lowrey, 1991] contributes to modes at about 620 cm^{-1} . If the CCOO wag force constant in alaninate is scaled so that it contributes to frequencies at about 620 cm^{-1} , the scale factor (45.09%) is only half of that for glycinate [Lowrey *et al*, 1993] (85%) or acetate [Williams and Lowrey, 1991] (83.62%). If, instead, the scale factor from glycinate is used as a starting point, the CCOO wag contributes at 785 cm^{-1} . Diem *et al* [1982] and Barron *et al* [1991] both predict that the CCOO wag contributes most to the 785 cm^{-1} mode. However, Kettle *et al* [1990] and Srivastava and Gupta [1972] predict the CCOO wag contributes most to the band at 654 cm^{-1} .

To investigate whether assignment to the lower or higher frequency for the CCOO wag is more appropriate, we calculated scale factors for acetate using the 6-31G** basis set using information from earlier work [Williams and Lowrey, 1991].

These scale factors (see Table 3.42) were transferred unchanged to alaninate. Calculations using these transferred scale factors predict that the CCOO *wag* makes its primary contribution at 785 cm^{-1} . Results using the 4-31G* and 6-31+G** basis sets also support the assignment of the CCOO *wag* to 785 cm^{-1} . The scaled diagonal force constants for the CCOO *wag*, assigned to 785 cm^{-1} , for the four different basis sets, and for both alanine and acetate, have the same value, about $0.495\text{ mdyne \AA rad}^{-2}$.

Scale factors from the 6-31G** calculations on acetate at a low 0.64 for the CO *as* and at a high 1.05 for the CO *r* are slightly unusual. These unusual scale factors could indicate misassignments of frequencies to the functional groups represented in the PED. However, the assignments are consistent across numerous other calculations performed at different levels and on different molecules containing the carboxylate group. The CCOO *wag* coordinate assignment is unaffected by these unusual scale factors, and all of the assignments with the 6-31G** basis are consistent with previous results [Williams and Lowrey, 1991].

When scale factors are compared it must be between similarly hydrogen bonded supermolecule structures. The water-excluded scale factors for acetate and glycinate transfer well to the CO₂ bridged alaninate. (The CO–HN bridged alaninate polar coordinates are expected to be different because of the differences in supermolecule structures.) The only scale factors that show more than three percent differences are for the acetate CCOO bends. The acetate CCOO *wag* scale factor is smaller than either the glycinate or alaninate scale factors by about 12%. The acetate and alaninate CCOO *r* scale factors differ by about 6% with glycine falling directly between. Finally, the acetate and glycinate CCOO *sd* differ by about 4% with alaninate being between them. This is better agreement for these coordinates and for the NH₂ deformations (all within 3%) than for our isolated molecule and supermolecule calculations [Williams *et al*, 1995; Williams and Lowrey, 1991; Lowrey and Williams, 1992; Williams, 1992; Lowrey *et al*, 1993; Williams *et al*, 1993] where water is not

excluded from the transformation to internal coordinates.

A comparison of scale factors for molecules at different values of pH indicates moderately good transferability. For the glycine four water supermolecule [Lowrey *et al*, 1993; Williams *et al*, 1993], only one scale factor, CN^{ter} s , differs by more than 5% between basic and acidic forms. In the glycine and alanine water-excluded models only the C^α d^1 and d^2 exceed a 5% difference in scale factors. Eighteen of twenty-two scale factors for the water-excluded models are within 3%.

The effect of using non-stationary geometries in normal mode calculations was examined by calculating frequencies for several different model geometries of ala-ala using the same force constant matrix. Increasing the C=O amide stretch or the NH amide stretch in alanyl-alanine by 10% changed no frequencies by more than 2 cm^{-1} or PEDs by more than 3% over four isotopomers (compare table 3.73 with 3.82 and 3.83). All calculated frequencies were positive. Substantially different model geometries resulted in substantially larger changes in the calculated frequencies and PEDs (see table 3.84), as was expected, but no negative frequencies were obtained.

4.4 Peptide Bond Coordinates

Scale factors from alanine and NMA were transferred to alanyl-alanine to serve as starting points for optimizing the frequency calculations. All comparable scale factors from alanine (see tables 3.51 and 3.58) agree with the alanyl-alanine results within three percent, except for the CC^c sd and rock (r), the CN^n s and the NH_2 wag (w), which may be due to end effects, and the C^α deformations. The alanyl-alanine acid and base scale factors for the c^α deformations are between the scale factors for the acid and base forms of alanine. The one-water alanine supermolecule in base scale factor for the non-polar CC^{me} s is more than three percent higher than the isolated alanyl-alanine scale factors, however, this may be related to a trend for that scale factor to increase as more waters are added to the alanyl-alanine structures.

Agreement between the alanyl-alanine scale factors and the NMA structures (see table 3.29) is good with the exception of the three-water CO^a deformations and the one-water supermolecule scale factors. The problems with the one-water scale factors may be related to NMA structural deformations. The scale factors developed for alanyl-alanine show good transferability for similar structures within the different alanyl-alanine hydration states and between acid and base conformations. Frequency predictions are also good, the average standard deviation is about 12 cm^{-1} .

The scale factors for the acid and base conformations of alanyl-alanine were developed simultaneously for similar hydration states to maximize transferability. All of the scale factors for the acid and base forms of the two-water supermolecules are identical except for the CC^c *s* and bends, and the CN^n *s*, probably due to the differences in protonation states. The CN^n torsion (*t*) scale factor is also different between the acid and base isolated structures.

Two different one-water supermolecules were scaled, the “1wn” has a water hydrogen bonded from the amide hydrogen to one of the carboxyl oxygens, the “1wo” water bridges between the amide carbonyl oxygen to one of the amine hydrogens. These two structures can be considered hybrids of the two-water supermolecules and the isolated structures. The 1wn structure carboxy terminus is similar to the carboxy terminal portion of the two-water supermolecule and its amine terminus is similar to the isolated structure. The 1wo one-water supermolecule has its water hydrogen bonded like the amine terminal portion of the two-water supermolecule. We found, as we had expected, that the scale factors for the hydrated portions of the one-water supermolecules are similar to the related portion of the two-water supermolecules and the nonhydrated scale factors are similar to the isolated molecule scale factors (see tables 3.71, and 3.78). The non-polar coordinates are not strongly affected by the addition of water. All of the scale factors for the C^α bends, the CC^{me} *s*, and the CH_3 bends vary by less than three percent. The CH_3 anti-symmetric deformations ($ad^{1,2}$), which were allowed to optimize freely, vary by less than one percent. The assignment

of these coordinates is unambiguous and all authors agree on their assignment [Sutton and Koenig, 1970; Moore and Krimm, 1976; Gupta and Gupta, 1978; Diem *et al*, 1984; Dwivedi and Krimm, 1984; Freedman *et al*, 1988; Cheam and Krimm, 1989b; and Balázs, 1990]. In addition, the modes are nearly pure, there is minimal mixing with other coordinates.

The transferability of these scale factors are a good indication that the SQMFF method is capable of correcting the systematic errors in the calculated force constants due both to the approximations used in solving the Schrödinger equation and to solvation effects. Solvation effects are implicitly incorporated into the scale factors of all of the structures modeled by scaling the model structures to aqueous frequencies. The different supermolecule models were designed to reflect intramolecular hydrogen bonded structures of proteins in solution. The peptide carbonyl and amide hydrogen form intramolecular hydrogen bonds of known geometry between residues within helical and sheet structures. In solution effects due to both solvation and hydrogen bonding are present. The supermolecule structures represent hydrogen bonded peptide bonds. The peptide groups at the beginning and end of helices form only a single intramolecular hydrogen bond, internal peptide groups form two hydrogen bonds. The two-water supermolecules reflect the internal helical hydrogen bonding patterns, while the one-water supermolecules reflect peptide bonds at the the beginning and end of helical segments. These supermolecule structure scale factors can be used for modeling the corresponding internal hydrogen bonds of a protein in solution.

Consistent changes are seen in some scale factors as increasing numbers of waters are added to the supermolecule as was observed in smaller molecules. This finding confirms conclusions made earlier that electronic structure changes are modeled by water-excluded supermolecule structures. The CNHC symmetric deformation (*sd*) scale factors decrease with increasing waters of hydration while the NH₂ scissor (*sis*) scale factors increase. The CN^a and CO^a *s* scale factors decrease when waters

of hydration are added to the carbonyl oxygen and increase when they are added to the amide hydrogen. The CO^a *sd* scale factors increase with addition of water to the oxygen and decrease as water is added to the amide hydrogen.

Our PED assignments agree with most previous work on ala-ala [Freedman *et al*, 1988; Oboodi *et al*, 1984; Roberts *et al*, 1988; Diem *et al*, 1984; Gupta and Gupta, 1978; Sutton and Koenig, 1970], alanyl dipeptide [Balázs, 1990; Cheam and Krimm, 1989b], and poly-ala [Moore and Krimm, 1976; Dwivedi and Krimm, 1984]. Krimm and co-workers [Cheam and Krimm, 1989a, b; Moore and Krimm, 1976; Dwivedi and Krimm, 1984] assign less of the CN^a *s* to the amide I mode and more in the skeletal stretch region at about 900 cm^{-1} in the polypeptide and the dipeptide. If we were to change our current assignments to agree with the assignments of Krimm and co-workers, we would have to change scale factors for CO^a *s*, NH^a in-plane bend (*ib*), and CN^a *s*. This would cause our alanyl-alanine scale factors to be quite different from the scale factors developed for NMA. The other analyses of alanyl-alanine do not address the percent contribution by these coordinates.

Chapter 5

CONCLUSIONS

The work with methanol and ethanol demonstrated that there are no models for solvation currently available that meet the criterion of using the same scale factors for both vapor and solvated states. Out of problems with ring formation in supermolecules, a new method, water-excluded, was discovered that has proved quite useful.

Small molecules were used to build a set of scale factors that have been successfully applied to alanine and alanyl-alanine. In building this set of scale factors it has been demonstrated that the transferability of these new scale factors is very good. This is especially evident among the various alanyl-alanine supermolecule structures. This demonstrates that not only can the systematic errors due to approximations in solving Schrödinger's equation be corrected, but the effects of solvation can also be corrected. Consistency in scale factor and internal coordinate changes with addition of water to supermolecule structures also illustrates that electronic structure changes are incorporated into the water-excluded model. PED and frequency predictions are very good.

For alanine, a Fermi resonance analysis explains observed peaks well. The different basis sets used in the alanine analyses also demonstrates that the 4-31G basis set is as good at predicting frequencies and PED as larger basis sets that are

more computationally intense.

This set of scale factors can predict peptide frequencies accurately. They are free of the influence of transition dipole coupling (TDC). The next step in the development of a set of scale factors and force constants for peptides and proteins in water is to apply these scale factors to systems where TDC effects are present so that these effects can be determined. These scale factors will predict frequencies expected if there were no TDC present. Differences between the observed and calculated spectra will be due to TDC. Then, using equation 1.22, the effects due to TDC can be understood and incorporated.

Bibliography

- [1] Allen, Wesley E., and Attila G. Császár, (1993) On the *ab initio* determination of higher-order force constants at nonstationary reference geometries, *Journal of Chemical Physics* 98, 2983-3015.
- [2] Balázs, András, (1990) Ab Initio Study of the Force Field and Vibrational Assignment of *N*-Acetyl-*N'*-methylalaninamide, *Journal of Physical Chemistry* 94, 2754-2763.
- [3] Bandekar, Jagdeesh, (1992) Amide modes and protein conformation, *Biochimica et Biophysica Acta* 1120, 123-143.
- [4] Barron, L. D., A. R. Gargaro, L. Hecht, P. L. Polavarapu, (1991) Experimental and *ab initio* theoretical vibrational Raman optical activity of alanine, *Spectrochimica Acta* 47A, 1001-1016.
- [5] Blom, C. E., P. J. Slingerland and C. Altona, (1976a) Application of self-consistent-field *ab initio* calculations to organic molecules I. Equilibrium structure and force constants of hydrocarbons, *Molecular Physics* 31, 1359-1376.
- [6] Blom, C. E., C. Altona, (1976b) Application of self-consistent-field *ab initio* calculations to organic molecules II. Scale factor method for the calculations of vibrational frequencies from *ab initio* force constants: ethane, propane, and cyclopropane, *Molecular Physics* 31, 1377-1391.

- [7] Chang, Chi-Deu, and Johannes Meienhofer, (1978) Solid-Phase Peptide Synthesis Using Mild Base Cleavage of N^α -Fluorenylmethyloxycarbonylamino Acids, Exemplified by a Synthesis of Dihydrosomatostatin, *International Journal of Peptide and Protein Research* 11, 246-249.
- [8] Cheam, T. C., and S. Krimm, (1985) Infrared Intensities of amide modes in N -methylacetamide and poly(glycine I) from *ab initio* calculations of dipole moment derivatives of N -methylacetamide, *Journal of Chemical Physics* 82, 1631-1641.
- [9] Cheam, T. C., and S. Krimm, (1989a) Ab Initio Force Fields of Glycine Dipeptide in C_5 and C_7 Conformations, *Journal of Molecular Structure* 193, 1-34.
- [10] Cheam, T. C., and S. Krimm, (1989b) Ab Initio Force Fields of Alanine Dipeptide in C_5 and C_7 Conformations, *Journal of Molecular Structure (Theochem)* 188, 15-43.
- [11] Diem, M., P. L. Polavarapu, M. Oboodi, L. A. Nafie, (1982) Vibrational Circular Dichroism in Amino Acids and Peptides. 4. Vibrational Analysis, Assignments, and Solution-Phase Raman Spectra of Deuterated Isotopomers of Alanine, *Journal of the American Chemical Society* 104, 3329-3336.
- [12] Diem, Max, M. Reza Oboodi, and Carlos Alva, (1984) Determination of Peptide Conformation via Vibrational Coupling: Application to Diastereoisomeric Alanine Dipeptides, *Biopolymers* 23, 1917-1930.
- [13] Ditchfield, R., W. J. Hehre, and J. A. Pople, (1971) Self-Consistent Molecular-Orbital Methods. IX. An Extended Gaussian-Type Basis for Molecular-Orbital Studies of Organic Molecules, *The Journal of Chemical Physics* 54, 724-728.
- [14] Dwivedi, Anil M., and S. Krimm, (1984) Vibrational Analysis of Peptides, Polypeptides, and Proteins. XVIII. Conformational Sensitivity of the α -Helix Spectrum: α_I - and α_{II} -Poly(L-alanine), *Biopolymers* 23, 923-943.

- [15] Elliot, A. and E. J. Ambrose, (1950) Structure of Synthetic Polypeptides, *Nature* 165, 921-922.
- [16] Fogarasi, Géza, and András Balázs, (1985) A Comparative ab initio Study of Amides Part I. Force fields and vibrational assignments for formamide, acetamide and *N*-methylformamide, *Journal of Molecular Structure (Theochem)* 133, 105-123.
- [17] Fogarasi, Géza, and Péter Pulay, (1984) Ab Initio Vibrational Force Fields *Annual Review of Physical Chemistry* 35, 191-213.
- [18] Fogarasi, Geza, and Peter Pulay, (1985) in *Vibrational Spectra*, 14, Chapter 3, Ab Initio Calculation of Force Fields and Vibrational Spectra, 125-219.
- [19] Fogarasi, Geza, Xuefeng Zhou, Patterson W. Taylor, and Peter Pulay, (1992) The Calculation of ab Initio Molecular Geometries: Efficient Optimization by Natural Internal Coordinates and Empirical Correction by Offset Forces *Journal of the American Chemical Society* 114, 8191-8201.
- [20] Foresman, James B., and Æleen Frisch, (1993) *Exploring Chemistry with Electronic Structure Methods: A Guide to Using Gaussian*, Gaussian, Inc., Pittsburgh.
- [21] Freedman, T. B., A. C. Chernovitz, W. M. Auk, M. G. Paterlini, and L. A. Nafie, (1988) Vibrational Circular Dichroism in the Methine Bending Modes of Amino Acids and Dipeptides, *Journal of the American Chemical Society* 110, 6970-6974.
- [22] Gaussian 92/DFT, Revision G.2, M. J. Frisch, G. W. Trucks, H. B. Schlegel, P. M. W. Gill, B. G. Johnson, M. W. Wong, J. B. Foresman, M. A. Robb, M. Head-Gordon, E. S. Replogle, R. Gomperts, J. L. Andres, K. Raghavachari, J. S. Binkley, C. Gonzalez, R. L. Martin, D. J. Fox, D. J. Defrees, J. Baker, J. J. P. Stewart, and J. A. Pople, Gaussian, Inc., Pittsburgh PA, 1993.

- [23] Gupta, M. K., and V. D. Gupta, (1978) Normal Mode Analysis of L-Alanyl-L-Alanine, *Indian Journal of Biochemistry and Biophysics* 15, 413-416.
- [24] Hamada, Yoshiaki, Naoki Tanaka, Yoko Sugawara, Akiko Y. Hirakawa, Mamichi Tsuboi, Shigeki Kato, and Keiji Morokuma, (1982) Force Field in the Methy-lamine Molecule from Ab Initio MO Calculation, *Journal of Molecular Spec-troscopy* 96, 313-330.
- [25] Haris, Parvez I., George T. Robillard, Alard A. van Dijk, and Dennis Chap-man, (1992) Potential of ^{13}C and ^{15}N Labeling for Studying Protein-Protein Interactions Using Fourier Transform Infrared Spectroscopy, *Biochemistry* 31, 6279-6284.
- [26] Henderson, R., J. M. Baldwin, T. A. Ceska, T. Zemlin, E. Beckmann, and K. H. Downing, (1990) Model for the Structure of Bacteriorhodopsin Based on High-resolution Electron Cryo-microscopy, *Journal of Molecular Biology* 213, 899-929.
- [27] Johnson, C. K., (1976) "ORTEP-II: A FORTRAN Thermal-Ellipsoid Plot Program for Crystal Structure Illustrations", Oak Ridge National Laboratory ORNL-5138.
- [28] Kettle, s. F. A., E. Lugwisha, P. Vorderwisch, J. Eckert, (1990) Intermolecu-lar vibrational coupling in DL- α alanine and its N-deutero isotopomer, *Spec-trochimica Acta* 46A, 921-926.
- [29] Krimm, S., and Yasuaki Abe, (1972) Intermolecular Interaction Effects in the Amide I Vibrations of β Polypeptides, *Proceedings of the National Academy of Sciences, USA* 69, 2788-2792.
- [30] Krimm, S., and Jagdeesh Bandekar, (1986) Vibrational Spectroscopy and Con-formation of Peptides, Polypeptides, and Proteins, *Advances in Protein Chem-istry* 38, 181-365.

- [31] Krimm, S., and Anil M. Dwivedi, (1982) Vibrational Analysis of Peptides, Polypeptides and Proteins XII—Fermi Resonance Analysis of the Unperturbed ND Stretching Fundamental in Polypeptides, *Journal of Raman Spectroscopy* 12, 133-137.
- [32] Latajka, Z., H. Ratajczak, W. B. Person, (1989) On the Reliability of SCF ab initio Calculations of Vibrational Frequencies and Intensities of Hydrogen-Bonded Systems, *Journal of Molecular Structure* 194, 89-105.
- [33] Lord, Richard C., (1977) Strategy and Tactics in the Raman Spectroscopy of Biomolecules, *Applied Spectroscopy* 31, 187-194.
- [34] Lowrey, Alfred H., and Robert W. Williams, (1992a) Effects of hydration on scale factors for ab initio force constants II, *Journal of Molecular Structure (Theochem)* 253, 35-56.
- [35] Lowrey, Alfred H., and Robert W. Williams, (1992b), Effects of hydration on scale factors for ab initio force constants III: Supermolecules, *Journal of Molecular Structure (Theochem)* 253, 57-72.
- [36] Lowrey, Alfred H., Victor Kalasinsky, and Robert W. Williams, (1993) Scaled Quantum Mechanical Force Field for Glycine in Basic Solution, *Structural Chemistry* 4, 289-297.
- [37] Ludlam, Cheryl F. C., Sanjay Sonar, Chan-Ping Lee, Matthew Coleman, Judith Herzfeld, Urram L. RajBhandayr, and Kenneth J. Rothschild, (1995) Site-Directed Isotope Labeling and ATR-FTIR Difference Spectroscopy of Bacteriorhodopsin: The Peptide Carbonyl Group of Tyr 185 Is Structurally Active During the bR \rightarrow N Transition, *Biochemistry* 34, 2-6.
- [38] Lugtenburg, Johan, Richard A. Mathies, Robert G. Griffin, and Judith Herzfeld, (1988) Structure and function of rhodopsins from solid state NMR and reso-

- nance Raman spectroscopy of isotopic retinal derivatives, *Trends in Biochemical Sciences* 13, 388-393.
- [39] Mirkin, Noemi E., and Samuel Krimm, (1990) Vibrational Dynamics of the Cis Peptide Group, *Journal of the American Chemical Society* 112, 9016-9017.
- [40] Miyazawa, Tatsuo, (1960) Perturbation Treatment of the Characteristic Vibrations of Polypeptide Chains in Various Configurations, *The Journal of Chemical Physics* 32, 1647-1656.
- [41] Møller, Chr., and M. S. Plesset, (1934) Note on an Approximation Treatment for Many-Electron Systems, *Physical Review* 46, 618-622.
- [42] Moore, Walter J., (1955) Physical Chemistry, 2nd ed., Prentice-Hall, Inc., Englewood Cliffs, N. J.
- [43] Moore, W. H., and S. Krimm, (1976) Vibrational Analysis of Peptides, Polypeptides, and Proteins. II. β -Poly(L-alanine) and β -Poly(L-alanylglycine), *Biopolymers* 15, 2465-2483.
- [44] Morrison, Robert T., and Robert N. Boyd, (1983) Organic Chemistry, 4th ed., Allyn and Bacon, Inc., Boston.
- [45] Naik, Vaman M., and S. Krimm, (1986) Vibrational Analysis of the Structure of Gramicidin A. I. Normal Mode Analysis, *Biophysical Journal* 49, 1131-1145.
- [46] Oboodi, M. Reza, Carlos Alva, and Max Diem (1984), Solution-Phase Raman Studies of Alanyl Dipeptides and Various Isotopomers: A Reevaluation of the Amide III Vibrational Assignment, *Journal of Physical Chemistry* 88, 501-505.
- [47] Palmö, K., L.-O. Pietilä, and S. Krimm, (1991) Construction of Molecular Mechanics Energy Functions by Mathematical Transformation of *Ab Initio* Force Fields and Structures, *Journal of Computational Chemistry* 12, 385-390.

- [48] Pulay, P., (1969) *Ab initio* calculation of force constants and equilibrium geometries in polyatomic molecules. I. Theory, *Molecular Physics* 17, 197-204.
- [49] Pulay, Peter, Geza Fogarasi, Gabor Pongor, James E. Boggs, and Anna Vargha, (1983) Combination of Theoretical *ab Initio* and Experimental Information to Obtain Reliable Harmonic Force Constants. Scaled Quantum Mechanical (SQM) Force Fields for Glyoxal, Acrolein, Butadiens, Formaldehyde, and Ethylene, *Journal of the American Chemical Society* 105, 7037-7047.
- [50] Pulay, Peter, and Wilfried Meyer, (1974) Comparison of the *ab initio* Force Constants of Ethane, Ethylene and Acetylene, *Molecular Physics* 27, 473-490.
- [51] Pulay, Peter, and Ferenc Török, (1975) Force Constants, Vibrational Assignment and Geometry of Methyl Amine from Hartree-Fock Calculations, *Journal of Molecular Structure* 29, 239-246.
- [52] Pulay, Peter, Geza Fogarasi, Frank Pang, and James E. Boggs, (1979) Systematic *ab Initio* Gradient Calculation of Molecular Geometries, Force Constants, and Dipole Moment Derivatives, *Journal of the American Chemical Society* 101, 2550-2560.
- [53] Qian, Weili, Jagdeesh Bandekar, and Samuel Krimm, (1991) Vibrational Analysis of Crystalline Tri-L-Alanine, *Biopolymers* 31, 193-210.
- [54] Raman, C. V., (1928) A Change of Wave-length in Light Scattering, *Nature* 121, 619.
- [55] Raman, C. V., and K. S. Krishnan, (1928a) A New Type of Secondary Radiation, *Nature* 121, 501-502.
- [56] Raman, C. V., and K. S. Krishnan, (1928b) The Optical Analogue of the Compton Effect, *Nature* 121, 711.

- [57] Raman, C. V., and K. S. Krishnan, (1928c) Molecular Spectra in the Extreme Infra-Red, *Nature* 122, 278.
- [58] Roberts, G. M., O. Lee, J. Calienne, and M. Diem, (1988) Infrared Vibrational Circular Dichroism in the Amide III Spectral Region of Peptides, *Journal of the American Chemical Society* 110, 1749-1752.
- [59] Roothaan, C. C. J., (1951) New Developments in Molecular Orbital Theory, *Reviews of Modern Physics* 23, 69-89.
- [60] Rothschild, Kenneth J., (1992) FTIR Difference Spectroscopy of Bacteriorhodopsin: Toward a Molecular Model, *Journal of Bioenergetics and Biomembranes* 24, 147-167.
- [61] Schrödinger, Erwin, (1926) *Annals Physik* 79, 361-.
- [62] Sengupta, Pradeep K., and S. Krimm, (1985) Vibrational Analysis of Peptides, Polypeptides, and Proteins. XXXII. α -Poly(L-Glutamic Acid), *Biopolymers* 24, 1479-1491.
- [63] Spiro, Thomas G., and Bruce P. Gabor, (1977) Laser Raman Scattering as a Probe of Protein Structure, *Annual Review of Biochemistry* 46, 553-572.
- [64] Srivastava, R. B., and V. D. Gupta, (1972) Normal Modes of Vibration in L-Alanine, *Indian Journal of Pure and Applied Physics* 10, 596-598.
- [65] Susi, H., and D. M. Byler, (1980) Vibrational Analysis of L-Alanine and Deuterated Analogs, *Journal of Molecular Structure* 63, 1-11.
- [66] Sutherland, G. B. B. M., (1952) Infrared Analysis of the Structure of Amino Acids, Polypeptides, and Proteins, *Advances in Protein Chemistry* 7, 291-318.
- [67] Sutton, P., and J. L. Koenig, (1970) Raman Spectra of L-Alanine Oligomers, *Biopolymers* 6, 615-634.

- [68] Tadesse, Lema, Ramina Nazarbaghi, and Lee Walters, (1991) Isotopically Enhanced Infrared Spectroscopy: A Novel Method for Examining Secondary Structure at Specific Sites in Conformationally Heterogeneous Peptides, *Journal of the American Chemical Society* 113, 7036-7037.
- [69] Takei, Hiro, Yahaloma Gat, Zvi Rothman, Aaron Lewis, and Mordechai Sheves, (1994) Active Site Lysine Backbone Undergoes Conformational Changes in the Bacteriorhodopsin Photocycle, *The Journal of Biological Chemistry* 269, 7387-7389.
- [70] Tapia, O., (1991), On the Theory of Solvent-Effect Representation Part I. A Generalized Self-consistent Reaction Field Theory, *Journal of Molecular Structure (Theochem)* 226, 59-72.
- [71] Tobin, Marvin C., (1968) Raman Spectra of Crystalline Lysozyme, Pepsin, and Alpha Chymotrypsin, *Science* 161, 68-69.
- [72] Torii, Hajime, and Mitsuo Tasumi, (1992) Model Calculations on the Amide-I Infrared Bands of Globular Proteins, *Journal of Chemical Physics* 96, 3379-3387.
- [73] Venyaminov, S. Yu., and N. N. Kalnin, (1990) Quantitative IR Spectrophotometry of Peptide Compounds in Water (H₂O) Solutions. I. Spectral Parameters of Amino Acid Residue Absorption Bands, *Biopolymers* 30, 1243-1257.
- [74] Wallach, D. F. H., J. M. Graham, and A. R. Oseroff, (1970) Application of Laser Raman Spectroscopy to the Structural Analysis of Polypeptides in Dilute Aqueous Solution, *FEBS Letters* 7, 330-334.
- [75] Weaver, James L. and Robert W. Williams, (1990) Amide III Frequencies for Ala-X Peptides Depend on the X Amino Acid Size, *Biopolymers* 30, 593-598.

- [76] Weir, Alan F., Alfred H. Lowrey, and Robert W. Williams, (1996) Transferable Quantum Mechanical Scale Factors for Alanine, *Journal of Molecular Structure (Theochem)* 362, 339-354.
- [77] Williams, Robert W., (1983) Estimation of Protein Secondary Structure from the Laser Raman Amide I Spectrum, *Journal of Molecular Biology* 166, 581-603.
- [78] Williams, Robert W., (1986) Protein Secondary Structure Analysis Using Raman Amide I and Amide III Spectra, *Methods in Enzymology* 130, 311-331.
- [79] Williams, Robert W., (1992) Effects of Hydration on Scale Factors for ab initio Force Constants. IV. *trans* and *cis* N-Methylacetamide, *Biopolymers* 32, 829-847.
- [80] Williams, R. W. (1994) "Determination of Membrane Protein Secondary Structure Using Vibrational and CD Spectroscopies" in *Membrane Protein Structure: Experimental Approaches* (Stephen White, ed.) pp 181-205, Oxford University Press, New York.
- [81] Williams, Robert W., Terry Cutrera, A. Keith Dunker, and Warner L. Petricolas, (1980) The Estimation of Protein Secondary Structure by Laser Raman Spectroscopy from the Amide III' Intensity Distribution, *FEBS Letters* 115, 306-308.
- [82] Williams, Robert W., Victor F. Kalasinsky, Alfred H. Lowrey, (1993) Scaled quantum mechanical force field for *cis*- and *trans*-glycine in acidic solution, *Journal of Molecular Structure (Theochem)* 281, 157-171.
- [83] Williams, Robert W., and Alfred H. Lowrey, (1991) Effects of Hydration on Scale Factors for Ab Initio Force Constants, *Journal of Computational Chemistry* 12, 761-777.

- [84] Williams, Robert W., James L. Weaver, and Alfred H. Lowrey, (1990) Relation between Calculated Amide Frequencies and Solution Structure in Ala-X Peptides, *Biopolymers* 30, 599-608.
- [85] Williams, Robert W., James L. Cheh, Alfred H. Lowrey, and Alan F. Weir, (1995) Effects of Hydration on Scale Factors for *ab Initio* Force Constants. 9. Methanol, *Journal of Physical Chemistry* 99, 5299-5307.
- [86] Wilson, E. Bright, Jr., (1939) A Method of Obtaining the Expanded Secular Equation for the Vibration Frequencies of a Molecule, *Journal of Chemical Physics* 7, 1047-1052.
- [87] Yu, Nai-Teng, (1977) Raman Spectroscopy: A Conformational Probe in Biochemistry, *CRC Critical Reviews in Biochemistry* , 229-280.
- [88] Zhang, Yuan-Peng, Ruthven N. A. H. Lewis, Robert S. Hodges, and Ronald N. McElhaney, (1995) Peptide Models of Helical Hydrophobic Transmembrane Segments of Membrane Proteins. 2. Differential Scanning Calorimetric and FTIR Spectroscopic Studies of the Interaction of Ac-K₂-(LA)₁₂-K₂- Amide with Phosphatidylcholine Bilayer, *Biochemistry* 34, 2362-2371.